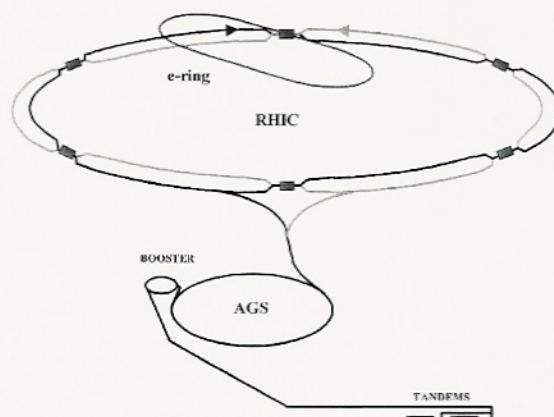


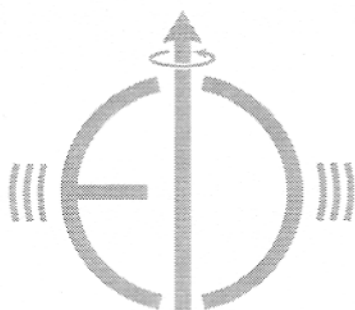


Proceedings of the Electron Ion Collider Workshops
February 26 - March 2, 2002
Brookhaven National Laboratory

VOLUME 1

Accelerator Concepts





Proceedings of the Electron Ion Collider Workshops
February 26 - March 2, 2002
Brookhaven National Laboratory

VOLUME I

Accelerator Concepts

Edited by:

M.S. Davis

A. Deshpande

S. Ozaki

R. Venugopalan

Disclaimer

This report was prepared as an account of work sponsored by an agency of the United States Government. Neither the United States Government nor any agency thereof, nor any employees, nor any of their contractors, subcontractors or their employees, makes any warranty, express or implied, or assumes any legal liability or responsibility for the accuracy, completeness, or any third party's use or the results of such use of any information, apparatus, product or process disclosed, or represents that its use would not infringe privately owned rights. Reference herein to any specific commercial product, process, or service by trade name, trademark, manufacturer, or otherwise does not necessarily constitute or imply its endorsement, recommendation, or favoring by the United States Government or any agency thereof or its contractors or subcontractors. The views and opinions of authors expressed herein do not necessarily state or reflect those of the United States Government or any agency thereof.

Table of Contents

Volume I: Accelerator Concepts

Preface

Agenda

First Plenary Session

Goal of the Workshop (S. Ozaki, BNL)

EIC Status and Considerations (S. Peggs, BNL)

Ring-Ring Collider Scheme (Y. Shatunov, BINP)

Exploration of the Derbenev-Kondratenko Equation in the MIT Bates South Hall Ring
(T. Zwart, MIT Bates)

Advanced Concepts for EIC (Ya. Derbenev, TJNAF)

EIC: An Electron-Light Ion Collider Based at CEBAF (L. Merminga, TJNAF)

RHIC Accelerator Performance and Status (T. Roser, BNL)

Ring-Ring, Linac-Ring Joint Working Group Session

Electron Cooling at RHIC (Y. Shatunov, BNL)

Electron Cooling Facility for RHIC (D. Wang, MIT Bates)

Linac Ring Working Group

Polarized Electron Sources for a Linac-Ring EIC (M. Farkhondeh, MIT-Bates)

Energy Recovering Linac Issues (L. Merminga, TJNAF)

RF Issues in Energy Recovery Linacs (J. Delayen, TJNAF)

Analysis and Simulation of Beam-Beam Effects in a Linac-Ring Collider
(L. Merminga, TJNAF)

Ring-Ring Working Group

Electrons are not Protons: (D. Barber, DESY)

Self Polarization Tests at Bates (D. Wang, MIT-Bates)

Interaction Region Working Group

HERA ep Interaction Regions (U. Schneekloth, DESY)

The PEP-II Interaction Region (U. Wienands, SLAC-PEP II)

Luminosity Scaling with IR Parameters (S. Peggs, BNL)
Spin Rotators with the Energy Range from 2 GeV to 10 GeV for eRHIC
(J. Kewisch, BNL)
Building the Detector-Accelerator Interface (B. Parker, BNL)
Toy Model of a Detector for EIC (E. Barrelet, in2p3/cnrs)
Shielding Against Synchrotron Radiation at HERA (D. Pitzl, DESY)
Luminosity Study (D.K. Hassell, MIT-Bates)
A 3 Beams Insertion Preliminary Consideration (A. Verdier, CERN)

Second Plenary Session

IR Group Summary Talk (W. Krasny, CERN)
Ring-Ring Working Group Summary (C. Tschalaer, MIT-Bates)
Linac Ring Working Group (I. Ben-Zvi, BNL)

Participants

Volume II: Physics Opportunities and Detector Issues

Preface

Agenda

First Plenary Session

Collider Summary of EIC Accelerator Workshop (S. Ozaki and T.Roser, BNL)
Physics of Nucleon Spin (R. Jaffe, MIT)
Recent Excitement from RHIC (G.Bunce, BNL)
Experimental Status of Spin DIS (G.K.Mallot, CERN)
Experimental Status of eA, μ A, and ep Physics (J. Moss, LANL)
Physics of Saturation: AA, eA, pA (D. Kharzeev, BNL)
Nonperturbative Structure of the Nucleon (T.Thomas, Univ. Adelaide)
Recent RHIC Results with AA (M. Baker, BNL)
Lessons from HERA Collider Program on Physics and Detectors
(A. Caldwell, Columbia, Univ.)
About the Workshop (A. Deshpande, BNL)

Second Plenary Session

Experimental Observables in eA and Polarized ep at Future Colliders
(A. De Roeck, CERN)

eA Physics: Theoretical Issues (M. Strikman, Penn State)

pA Physics at RHIC (J.C Peng, LANL)

Parallel Session I: eA Physics at EIC

e-A Parallel Session Summaries (J. Marian-Jalilian, BNL)

e-A Parallel Session Summaries (A. Bruell, MIT)

Single Hadron Transverse Momentum Distribution as a Probe of Gluon Saturation
(J. Qiu, Iowa State)

Hard Diffraction in eA Collisions (Y. Kovchegov, Univ. Washington)

Phenomenology of Generalized Parton Distributions (A.V. Belitsky, Univ. Maryland)

Energy Dependence of QCD Cross Sections. Saturation Effects from HERA to RHIC to LHC
(H. Weigert, Univ. Regensburg, Germany)

High Partonic Density Effects QCD Expected at EIC (K. Tuchin, Univ. Washington)

Exclusive Processes at EIC: Feasibility Study (A. Sandacz, SINS, Poland)

Nuclear Shadowing in DIS on Nuclei: Leading Twist vs. Eikonal Approaches
(V. Guzey, Univ. of Adelaide)

Analysis of HERA Data at Low x (K. Kowalski, Columbia, BNL and DESY)

Higher Twist Effects in Nuclei (R. Fries, Duke Univ.)

Nuclear Shadowing in Non-linear Small x pQCD (A. Freund, Univ. Regensburg)

Parallel Session II: ep Physics at EIC

Polarized ep Physics: Summary (A. Deshpande, BNL/RBRC and W. Vogelsang, BNL)

Polarized Gluon Distribution from Present and Prospective future g_1
Measurements (J. Lichtenstedt, Tel Aviv Univ.)

g_1 at Low x and Low Q^2 with Polarized ep Colliders (S. Bass, ECT, Italy)

Probing the Spin Structure of the Photon at the EIC (M. Stratman, Regensburg Univ.,
Germany)

The Case for a Large Polarized Anitquark Flavor Asymmetry $\Delta\bar{u}(x) - \Delta\bar{d}(x)$
(C. Weiss, Regensburg Univ., Germany)

What Do We Learn from Lambda Polarization in SIDIS (M. Anselmino, Univ. di Torino
and INFN, Italy)

Conditional Parton Distribution Functions and Nucleon Structure (M. Strikman, Penn State)

Accurate Tests of QCD Factorization at Electron Ion Collider (P. Nadolsky, SMU)

Deep Virtual Compton Scattering: Experimental Aspects (B. Fox, RBRC and BNL)

Quark-Hadron Duality in Electron-Nucleon Scattering (W. Melnitchouk, TJNAF)

Future Transversity Measurement (M. Grosse-Pederkamp, RBRC)

An Initial Study on Measuring F_2^p at the EIC (A. Vogt, NIHKEF, Netherlands)

Fragmentation Functions from Semi-Inclusive DIS Pion Production and

Implications for the Polarized Parton Densities (S. Kretzer, Michigan State Univ.)

Parallel Session III: Detector and IR Design for EIC

Overview (N. Saito, Kyoto Univ., Japan)

Recent R&D Activities on an Accordion-type Calorimeter (E. Kistenev, BNL)

Rear Detection Systems and Luminosity Measurement at H1 and Zeus (U. Schneekloth, DESY,)

Constraints on the H1/Zeus Interaction Regions from the HERA Luminosity Upgrade (U. Schneekloth, DESY)

Forward Physics and Detection Systems at HERA (H. Kowalski, Columbia, BNL and DESY)

Particle Identification at H1 (D. Milstead, Univ. Liverpool, England)

Particle Identification at Belle (T. Iijima, KEK, Japan)

EIC Detector Studies (J. Chwastowski, Institute Of Nuclear Physics, Poland)

Silicon Tracking for PHENIX Upgrade (Y. Goto, RBRC)

Discussion: Detector Design Working Group (B. Surrow, BNL)

Third Plenary Session

12 GeV Upgrade at Jefferson Lab (R. Ent, TJNAF)

The Future of Lepton-Nucleon Scattering: A Brief Summary of the Durham (HERA-3) Workshop, December 2001 (M. Klein, DESY, Zeuthen)

Tesla-N Plans (V. Korotkov, DESY, Zeuthen)

Final Plenary Session

Plans and Discussion (R. Milner, MIT Bates)

QCD and other Fundamental Interactions (V. Hughes, Yale Univ.)

New Directions in QCD and the Electron Ion Collider (S. Brodsky, SLAC)

Participants

Preface

Electron Ion Collider Workshop

February 26 to March 2, 2002
Brookhaven National Laboratory

The fifth in the series of Electron Ion Collider Workshops was held at Brookhaven National Laboratory on February 26 – March 2, 2002. The first two days, Feb. 26th & 27th, were dedicated to the accelerator and the interaction point design issues (hence forth called the EIC Accelerator Workshop). On February 28th, March 1st and 2nd the focus shifted to the physics of polarized e-p scattering, un-polarized e-A scattering, and the detector issues (from now on called the EIC Physics Workshop). The aim of the Workshop was to refine the physics goals of this proposed collider facility identified in previous meetings (see list below) and to begin dedicated efforts on the design of the accelerator, interaction region, and proposals for detectors in view of the physics case.

In the EIC Accelerator Workshop feasibility of various collider options, including the ring-ring geometry and linac-ring geometry for the electron-ion and polarized electron-proton collisions along with their implications for the interaction point (IP) design, were studied. The performance potentials for various options were considered, and technical risks involved were evaluated. The EIC Physics Workshop advanced the physics discussions started in previous EIC workshops (listed below), along with many new ideas for measurements that could be pursued with a Collider at BNL. Finally, working groups were formed to focus on various tasks, namely, the accelerator and IP development, detailed studies of various physics processes of interest in conjunction with realistic Monte Carlo simulations and Detector studies. The goal of this effort is to move towards a collaboration that will fully develop an electron-hadron collider design within the next 3 years.

In all ~50 people attended the Accelerator Workshop (Feb. 26-27, 2002), while ~130 people attended the EIC Physics workshop (Feb. 28 – March 2, 2002). Both had plenary as well as parallel sessions. For the Accelerator Workshop Chris Tschalaer (MIT/Bates) convened the group dedicated to the Ring-Ring collider design, Ilan Ben-Zvi (BNL) convened the group for the Linac-Ring design, while Witek Krasny (CERN/in2p3) convened a group focused on the interaction point design. For the EIC Physics Workshop Jamal J. Marian (BNL), Antje Bruell (MIT) & Raju Venugopalan (BNL) convened the e-A physics working group (WG), Abhay Deshpande (RBRC) and Werner Vogelsang (BNL/RBRC) convened the polarized e-p physics WG, while Naohito Saito (RIKEN/Kyoto U.), Bernd Surrow (BNL) and Abhay Deshpande (RBRC) convened the WG dedicated to the detector issues.

The Workshop proceedings are separated into two volumes. Volume I includes the summaries and slides from the presentations of the Accelerator Workshop, while Volume II includes summaries and selected slides from the EIC Physics Workshop. The authors were requested to summarize their presentations in two or three pages and to include a selection of the most important slides from their presentation. In a few cases, when the authors did not oblige, the responsibility of selection of slides was borne by the editors of these volumes. In addition to the

paper volumes, the proceedings are also available on CDs as PDF files and will be available in the near future on the EIC web pages at <http://www.bnl.gov/eic>.

This Workshop benefited immensely from the enthusiastic support and active involvement in the scientific organization and program development by the Electron Ion Collider Steering Committee and the Local Organizing Committees. Doris Rueger, the Workshop Secretary, was instrumental for the success of these workshops. She was well supported by Marcy Chaloupka. Sue Davis did an incredible job of putting together the EIC White Paper in time for the workshop and getting these proceedings in order and in their final form. We would also like to thank Pat Yalden of BNL's Photography and Graphic Arts department for doing a wonderful job on the Workshop posters and the cover pages of the proceedings. Last but not least, we appreciate the financial support from Brookhaven Science Associates without which this workshop would not have been possible.

Abhay Deshpande & Satoshi Ozaki
May, 2002

Electron Ion Collider Steering Committee:

J. Cameron (IUCF), R. Holt (ANL), V. W. Hughes (Yale), P. Jacobs (LBNL), R. Milner (MIT/Bates), G. Garvey (LANL), P. Paul(BNL), J. C. Peng (UIUC).

Local Organizing Committee for EIC Accelerator Workshop:

S. Ozaki (Chair), S. Peggs, T. Roser, C. Tschalaer(MIT-Bates)

Local Organizing Committee for EIC Workshop:

A. Deshpande (Chair), W. Guryan, J. J. Marian, L. McLerran, B. Surrow, R. Venugopalan (Co-Chair), W. Vogelsang

Previous Electron Ion Collider Workshops:

1. Physics with a High Luminosity Polarized Electron Ion Collider, EPIC 99, April 1999, IUCF, Bloomington, IN
2. The eRHIC Workshop, April 2000, Yale University, New Haven, CT
3. The eRHIC Workshop, July 2001, BNL, Upton, NY
4. Physics with an Electron Polarized Ion Collider, EPIC 2000, September 2000, MIT, Boston, MA

EIC Accelerator Concepts Workshop Program (Overall)

February 26-27, 2002
Brookhaven National Laboratory

Tuesday, February 26

8:30	Registration	<i>Physics Seminar Lounge</i>			
9:00	Plenary Session	<i>Physics Seminar Room</i>	S. Ozaki	BNL	Chairman
9:00	Welcome Greeting		P. Paul	BNL	
	Goal of the Workshop		S. Ozaki	BNL	
9:15	Present Status of EIC		S. Peggs	BNL	
	Collider Considerations				
9:35	Ring-Ring Collider Scheme		Y. Shatunov	BINP	
9:55	Bates R&D on Self-Polarization		T. Zwart	MIT Bates	
10:15	Linac-Ring Collider Scheme		Ya. Derbenev	TJNAF	
10:35	Coffee Break	<i>Physics Seminar Lounge</i>			
10:50	Plenary Session	<i>Physics Seminar Room</i>	R. Milner	MIT Bates	Chairman
10:50	An Electron-Ion Collider based at CEBAF		L. Merminga	TJNAF	
11:10	Interaction Region Consideration		W. Krasny	CERN	
11:30	RHIC Performance Parameters and Cooling		T. Roser	BNL	
11:50	Working Group Organization		S. Ozaki	BNL	
12:00	Lunch				
13:00	Working Group Meetings	RR Group	R. Milner	MIT Bates	Convener
		LR Group	I. Ben-Zvi,	BNL	Convener
		IR Group	W. Krasny	CERN	Convener
15:00	Coffee Break	<i>Physics Seminar Lounge</i>			
15:30	Working Group Meetings				

Wednesday, February 27

8:30	Plenary Session: WG Intermediate reports		S. Peggs	BNL	Chairman
		<i>Physics Seminar Room</i>			
9:00	Joint Session of Working Group RR, LR & IR		W. Krasny	CERN	Chairman
		<i>Physics Seminar Room</i>			
10:30	Coffee Break	<i>Physics Seminar Lounge</i>			
10:50	Working Group Meetings				
15:30	Coffee Break	<i>Physics Seminar Lounge</i>			
16:00	Plenary: Working Group Summary Reports		J. Delayen	TJNAF	Chairman
	RR Working Group		C. Tschalaer	MIT Bates	
	LR Working Group		I. Ben-Zvi	BNL	
	IR Working Group		W. Krasny	CERN	
		<i>Physics Seminar Room</i>			
17:30	Adjourn				

EIC Accelerator Concepts Workshop Program (Ring-Ring Group)
 February 26-27, 2002
 Brookhaven national laboratory

Tuesday, February 26

13:00 RR-LR Joint Working Group *Physics Small Seminar Room*
 (Richard Milner/Ilan Ben-Zvi, Convener)

13:00 EIC luminosity limits, e-cooling feasibility	Ya. Derbenev	TJNAF
13:40 Electron cooling at RHIC	Y. Shatunov	BINP
14:20 Electron cooling beam dynamics	D. Wang	MIT Bates

15:00 Coffee Break *Physics Seminar Lounge*

15:30 RR Working Group *Physics Small Seminar Room (tentative)*
 (Richard Milner, Convener)

15:30 Introduction to ring-ring group		
15:50 "Electrons are not protons: electron polarization in rings, spin	D. Barber	DESY
16:30		
17:00		
17:30 End of Session		

Wednesday, February 27

8:30 Plenary Session: WG Intermediate reports
 Steve Peggs, Chairman *Physics Seminar Room*

9:00 Joint Session of Working Group RR, LR & IR
 (Witek Krasny, Chairman) *Physics Seminar Room*

10:30 Coffee Break *Physics Seminar Lounge*

10:50 RR Working Group *Physics Small Seminar Room (tentative)*
 (Chris Tschalaer, Convener)

10:50 EIC e-ring size considerations, self-polarization, wigglers, spin transparency	Ya. Shatunov	BINP
11:30 Discussion		

12:00 Lunch

13:00 Self polarization test at Bates	F. Wang	MIT Bates
14:00 Discussion		
14:30 Working Group summary writing		

15:30 Coffee Break *Physics Seminar Lounge*

16:00 Plenary: Working Group Summary Reports
 (Jean Delayen, Chairman) *Physics Seminar Room*

17:30 Adjourn

EIC Accelerator Concepts Workshop Program (Linac-Ring Group)

February 26-27, 2002

Brookhaven National Laboratory

Tuesday, February 26

13:00 RR-LR Joint Working Group *Physics Small Seminar Room*
(Richard Milner/Ilan Ben-Zvi, Convener)

13:00 EIC luminosity limits, e-cooling feasibility	Ya. Derbenev	TJNAF
13:40 Electron cooling at RHIC	Y. Shatunov	BINP
14:20 Electron cooling beam dynamics	D. Wang	BNL

15:00 Coffee Break *Physics Seminar Lounge*

15:30 LR Working Group *Physics Orange Room (tentative)*
(Ilan Ben-Zvi, Convener)

15:30 Polarized electron source for Linac Ring Collider	M. Farkhondeh	MIT Bates
16:10 Energy recovering linac issues	L. Merminga	TJNAF
16:50 Discussion		
17:30 End of Session		

Wednesday, February 27

8:30 Plenary Session: WG Intermediate reports
Steve Peggs, Chairman *Physics Seminar Room*

9:00 Joint Session of Working Group RR, LR & IR
(Witek Krasny, Chairman) *Physics Seminar Room*

10:30 Coffee Break *Physics Seminar Lounge*

10:50 LR Working Group *Physics Orange Room (tentative)*
(Ilan Ben-Zvi, Convener)

10:50 Beam-Beam stability in linac-ring collisions	R. Li	TJNAF
11:30 Circulator Rings for ERL-based EIC	Ya. Derbenev	TJNAF

12:00 Lunch

13:00 RF issues in ERLs	J. Delayen	TJNAF
13:40 Luminosity limitations in Linac-ring Colliders	L. Merminga	TJNAF
14:30 Working Group summary writing		

15:30 Coffee Break *Physics Seminar Lounge*

16:00 Plenary: Working Group Summary Reports
(Jean Delayen, Chairman) *Physics Seminar Room*

17:30 Adjourn

EIC Accelerator Concepts Workshop Program (Interaction Region Group)
 February 26-27
 Brookhaven National Laboratory

Tuesday, February 26

- 13:00 IR Working Group** **Physics Room 2-160**
(Witek Krasny, Convener)
- 13:00 Introduction and Organization of Working Group
- 13:20 Review of the existing designs of the interaction regions relevant for the EIC Project
- | | | |
|------------------------------------|----------------|------|
| IP design for the HERA ep collider | U. Schneekloth | DESY |
| IP design for the SLAC B-factory | U. Wienands | SLAC |
- 14:30 Luminosity of EIC and its dependence on the available space for the detector. Luminosity vs. beta* trade-off S. Peggs BNL
- 15:00 Coffee Break** **Physics Seminar Lounge**
- 15:40 Constraints on the IP design and the e momentum range imposed by spin rotator magnets, ion beam momentum range, & eRHIC J. Kewisch BNL
- 16:20 Detector-accelerator interface issues: Integration of accelerator & detector components, dual role magnets, beam separation B. Parker BNL
- 17:10 A toy model of a 4-pi detector for EIC E. Barrelet in2p3/cnrs

Wednesday, February 27

- 8:30 Plenary Session: WG Intermediate reports**
Steve Peggs, Chairman **Physics Seminar Room**
- 9:00 Joint Session of Working Group RR, LR & IR**
(Witek Krasny, Chairman) **Physics Seminar Room**
- 10:30 Coffee Break** **Physics Seminar Lounge**
- 10:50 IR Working Group** **Physics Room 2-160 (tentative)**
(Witek Krasny, Convener)
- 10:50 Shielding against synchrotron radiation D. Pitzl DESY
- 11:30 Luminosity & polarization requirements as a function of center of mass energy. Physics cases for highest achievable ep & eA D. Hasell MIT
- 12:10 Lunch
- 13:10 Feasibility of a design of a unique "three-beam interaction zone" A. Verdier CERN
- 13:40 Possibilities of low beta* crab crossing and traveling ion focus for EIC
- 14:10 Working Group summary writing Ya.Derbenev TJNAF
- 15:30 Coffee Break** **Physics Seminar Lounge**
- 16:00 Plenary: Working Group Summary Reports**
(Jean Delaysen, Chairman) **Physics Seminar Room**
- 17:30 Adjourn**

Goal of the Workshop

Satoshi Ozaki

EIC Accelerator Workshop

February 26-27, 2002

Brookhaven National Laboratory

Purpose of the Workshop

Study feasibility of various collider options for the electron-ion and polarized electron-proton collisions,

- Ring on Ring Option
- Ring on Ring Option with Top-off Linac
- Energy-Recovery-Linac on Ring Option

Assess their performance potentials, and evaluate technical risks involved.

Now is the time to review the options, with an idea that future R&D efforts can be focused on a promising few options.

The Facility Requirements

- Collider geometry capable of e-A and polarized e-p Collisions
- Range of $s^{1/2}$ for e-A as high as possible: (~ 63 GeV/u)
- Range of variable $s^{1/2}$ for e-p: 30 – 100 GeV
 - ◀ (Beam Energy)_{Max}: (E_e) 10 GeV, (E_p) 250 GeV, (E_A) 100 GeV/u
- E_p/E_e , E_A/E_e : preferably independent of $s^{1/2}$ for detector geometry?
- Range of Ion Species: As wide as possible, p to U?
- Polarization: 70% \times 70%
- Luminosity: 10^{33} cm⁻²s⁻¹ per nucleon
- Integrated Luminosity for Significant Physics:
 - For inclusive physics (Yale workshop): ~ 2 fb⁻¹
 - For exclusive and semi-inclusive: ~ 5 – 10 times more
- e⁺p, in addition to e⁻p, requirement?
 - To be addressed by Electron Ion Collider Workshop

Questions to be Answered by Working Groups

Each working group should answer the following questions.

- What is the likely performance achievable with each option?
- What are advantages and disadvantages of each option?
- What is the impact of each option on the IR design?
- What is a showstopper, if any?
- What is the path forward?

Expectations

- The output of this Workshop can provide several options on which to build physics cases in the workshop that immediately follows.
- This workshop should act as a catalyst to begin the R&D collaborations towards the realization of an electron-ion collider.
- The work here should lead to other future workshops, most likely scheduled in conjunction with the next EIC Workshops.

EIC Status & Considerations – The White Paper

S. Peggs, BNL

Table of Contents

- 1 Introduction
- 2 Status of the Partonic Structure of Hadrons & Nuclei
- 3 Scientific Opportunities with an EIC

- 4 **Accelerator Design**
 - 4.1 **Overview**
 - 4.2 **Electron Ring on Proton Ring Colliders**
 - 4.2.1 **The Low Energy Green Field Option**
 - 4.2.2 **The High Energy eRHIC Ring-Ring Option**
 - 4.3 **Electron Linac on Proton Ring Colliders**
 - 4.3.1 **Luminosity**
 - 4.3.2 **Conceptual Point Design Parameters**
 - 4.4 **The EIC Electron Cooling System**
 - 4.5 **Interaction Region**

- 5 **A Prototype Detector for the EIC**

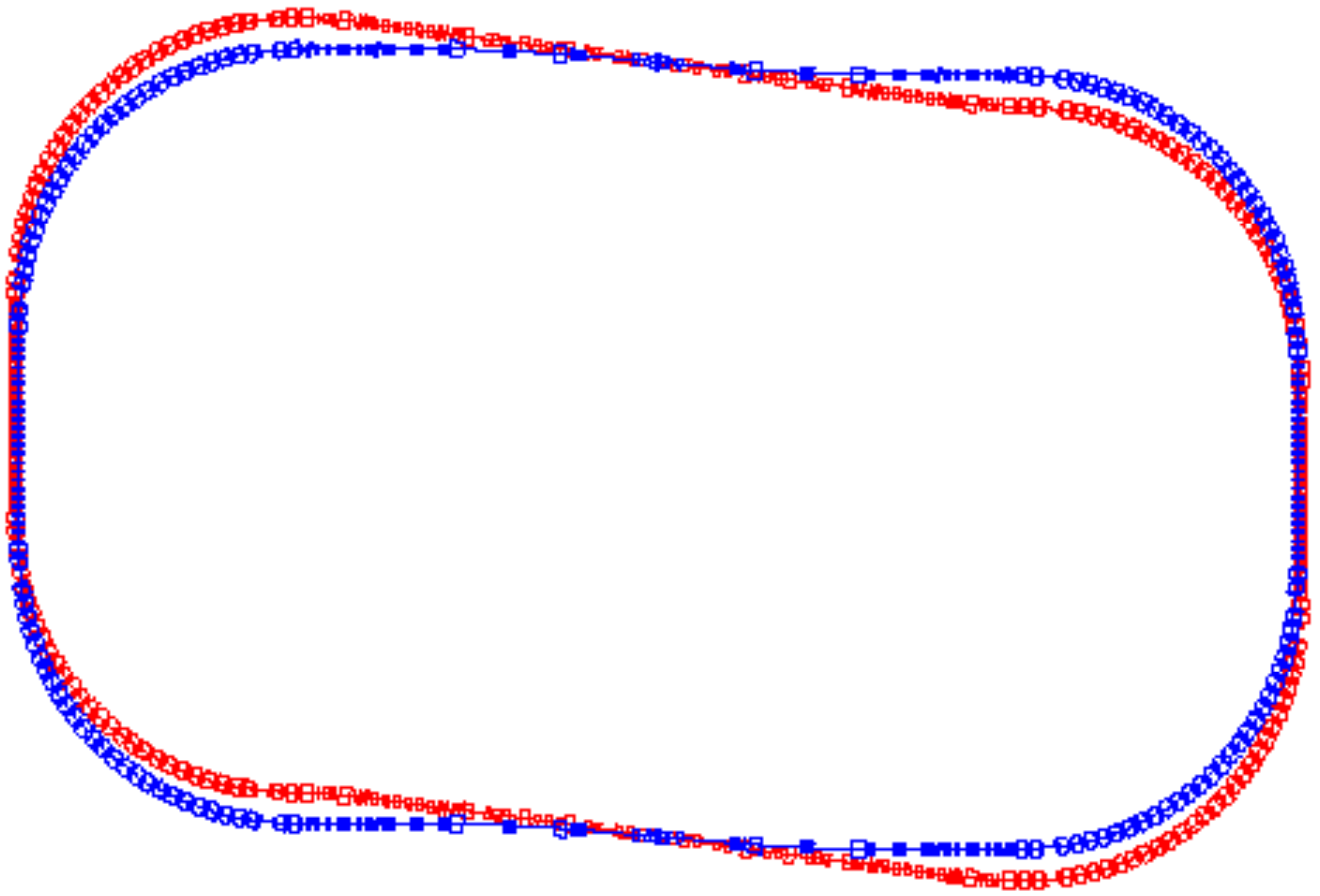
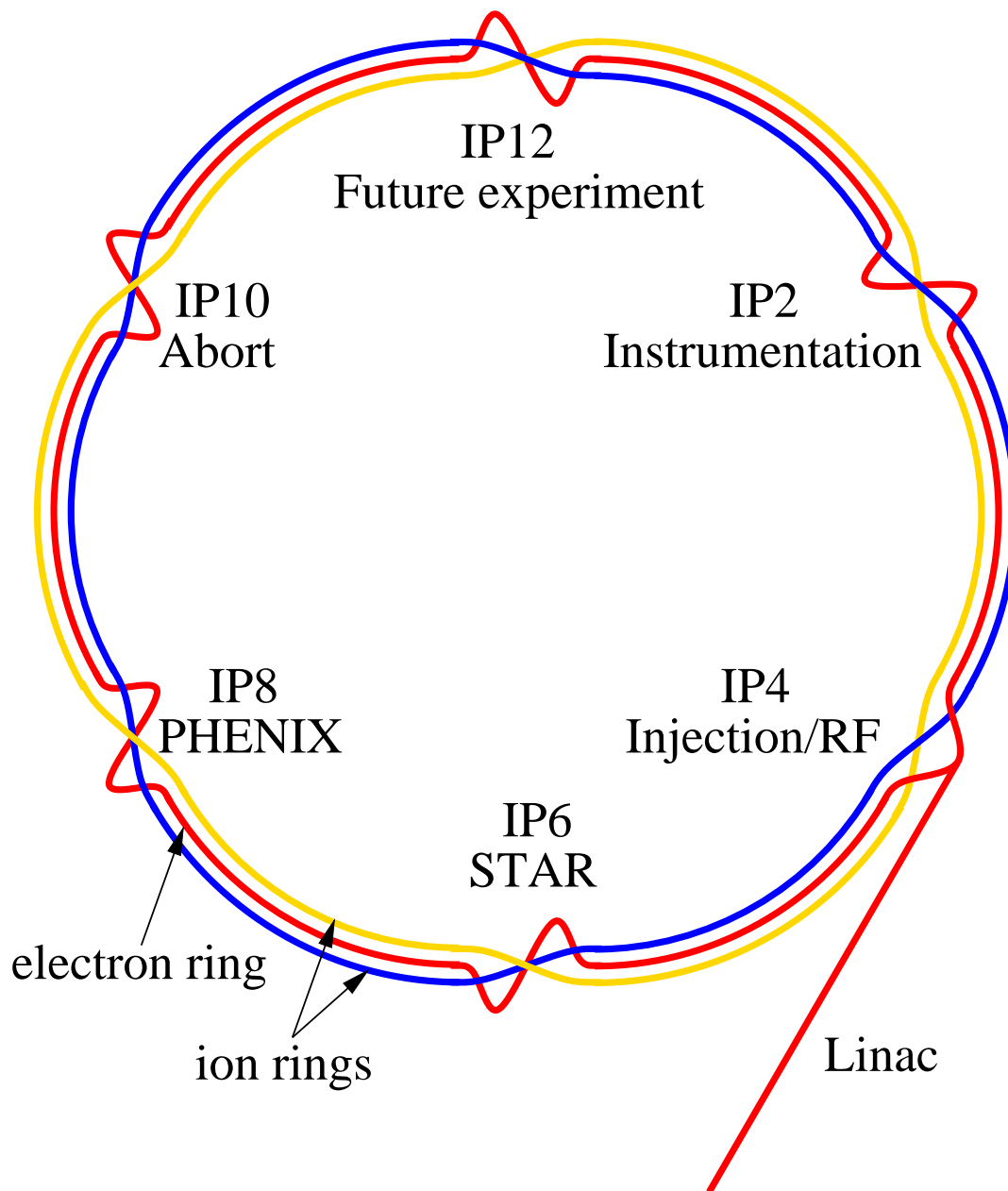


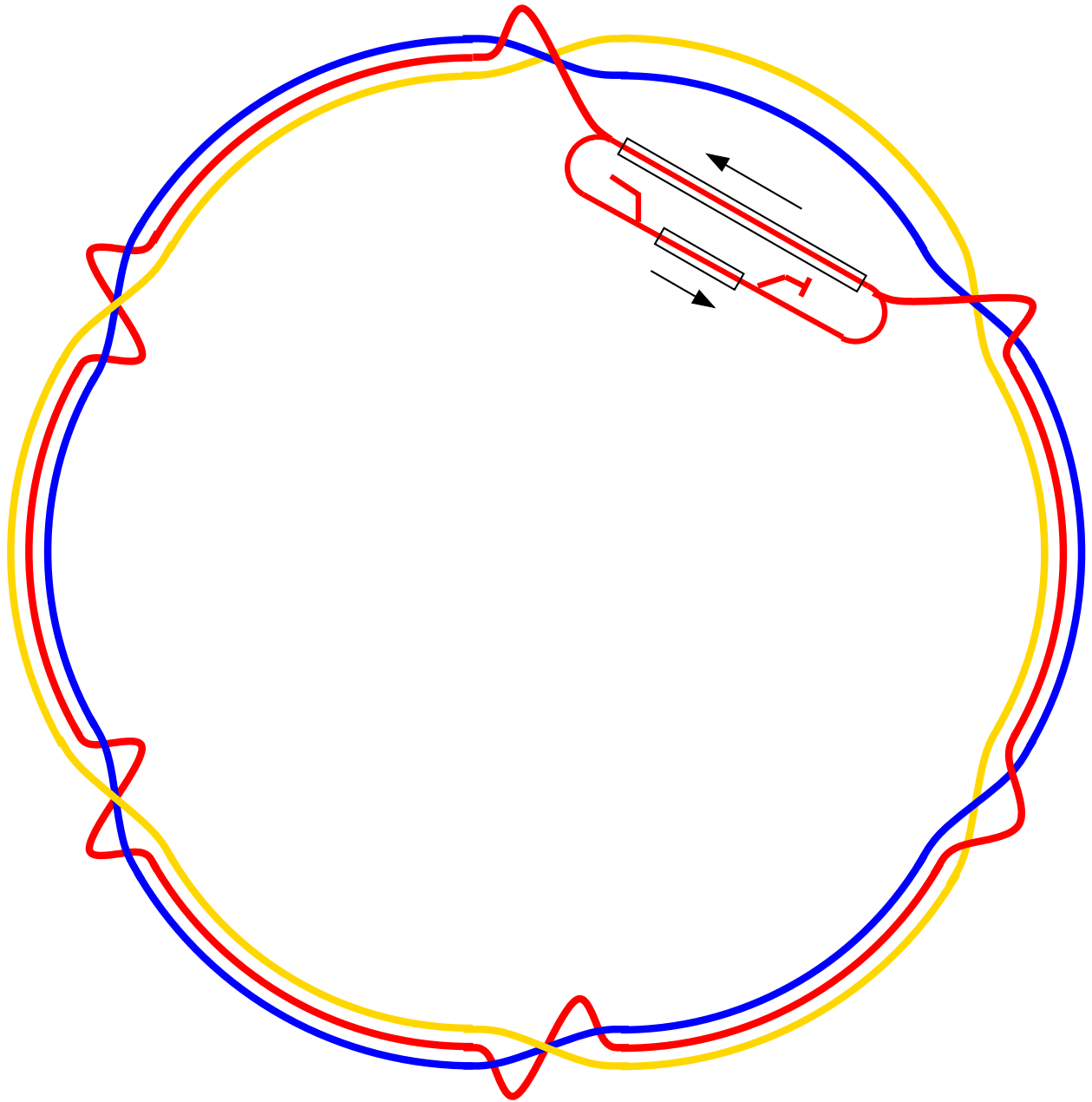
FIGURE 2. Layout of e-p collider.

We chosen the scheme of two intersecting in two points rings. Both rings have approximately equal circumferences 1388 m. Each ring has two experimental straight sections, two technical straights and four identical arcs. The rings are separated vertically about 1 m outside the interaction areas.

MIT-Bates **ring-ring** scenario
(Koop et al, 2nd EPIC Workshop)



eRHIC **ring-ring** scenario



eRHIC **linac-ring** scenario, with Energy Recovery Linac

ULTIMATE PERFORMANCE

Beam-beam parameters (round beams):

$$\xi_e = \frac{N_i}{\epsilon_e} \left(\frac{r_e Z}{4\pi\gamma_e} \right) \quad (1)$$

$$\xi_i = \frac{N_e}{\epsilon_i} \left(\frac{r_i(v/c)_i}{4\pi Z} \right) \quad (2)$$

Emittance subscripts are correct! For example, e-cooling reduces ϵ_i and allows N_e to be reduced.

Electron-ion luminosity can be written

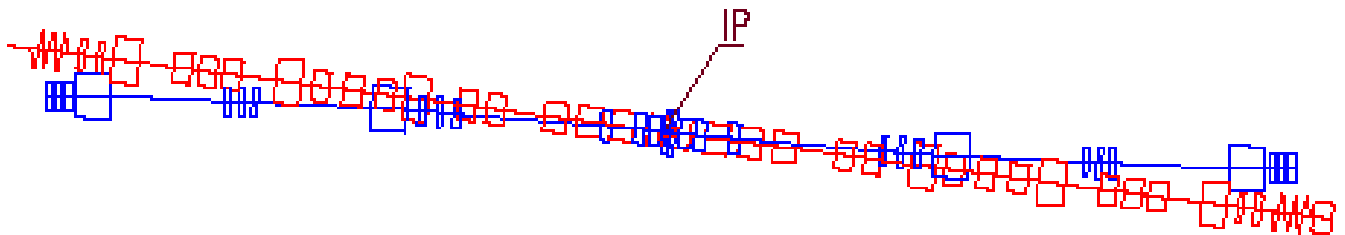
$$L = F_c \xi_e \xi_i \sigma_e'^* \sigma_i'^* \left(\frac{4\pi\gamma_e\gamma_i}{r_e r_i} \right) \quad (3)$$

- When beam-beam limits and angular apertures have been met, $\xi_e \xi_i \sigma_e'^* \sigma_i'^*$ is fixed.
- Then the **only way to increase the luminosity is to increase the collision frequency F_c** (more bunches)
- Linac-ring collisions allow the usual $\xi_e \approx 0.06$ limit to be violated.

	THERA	EPIC 2	eRHIC	eRHIC	HER
Scenario	linac-ring	linac-ring	linac-ring	ring-ring	(SLAC)
Ion specie	protons	protons	protons/gold	protons/gold	–
Luminosity , [$10^{32}\text{cm}^{-2}\text{s}^{-1}$]	.041	21	4.6/.036	3.5/.086	–
Dipole bend radius, [m]	608	~ 50	243	243	165
RMS beam size, σ^* [μm]	10	25	21/60	40/50	157
Bunch spacing, [ns]	211	6.7	35.5	35.5	4.2
IONS					
Ion energy, [GeV/u]	1,000	50	100/250	250/100	–
Ion rms emittance, [μm]	1.0	2.0	0.8/1.0	0.8/1.0	–
Ion average current, [A]	.071	2.4	.14/.68	.42/.42	–
Ion IP beta, β_e^* [m]	.10	.10	.15/.39	.53/.27	–
Ion b-b parameter, ξ_i	.0023	.004	.0046/.0015	.004/.004	–
Laslett SC tune shift	.0003	.024	.001/.003	.003/.003	–
ELECTRONS					
Electron energy, [GeV]	250	5	10	10	9
Electron emittance, [nm]	.2	6	3	18	49
Electron beam current, [A]	.000084	.264	.135/.135	.12/.37	1.5
Electron beam power, [GW]	.023	1.32	1.35/1.35	1.2/3.7	13.5
Synch. rad. power, [MW]	–	\sim .29	.49/.49	.43/1.3	7.2
Electron IP beta, β_e^* [m]	.50	.10	.15/1.2	.089/.139	.05/.50
Electron b-b parameter, ξ_e	.23	.35	.11/.57	.06/.06	.055

ION STORAGE RING ISSUES

Long range beam-beam. Early beam separation is easy with very unequal rigidities. EPIC:



Electron cloud. Ionized electrons are accelerated by the next ion bunches, possibly with runaway, threatening **cryogenic heat load, instabilities.**

- A paucity of data from **superconducting** rings (Tev, HERA, RHIC, LHC). More work required ...

Intra-Beam Scattering, electron cooling. RHIC expects the gold rms emittance to grow from $2 \mu\text{m}$ to $7 \mu\text{m}$ in 10 hours. With electron cooling it should shrink to about $1 \mu\text{m}$ in 1 hour.

Laslett space charge tune shift.

$$\Delta Q_{\text{sc}} \approx -\frac{N_i}{\epsilon_i} \frac{C}{\sigma_L \beta \gamma^2} \left(\frac{r_i}{2(2\pi)^{3/2}} \right) \quad (4)$$

Strong dependence on circumference C , RMS bunch length σ_L , and the Lorentz factor $\beta\gamma^2$.

- Make the bunch **longer at injection** (eRHIC: 28 MHz to inject, 197 MHz to collide).
- The bunch must be **shorter than β^*** in collision (hourglass effect).

ELECTRON STORAGE RING ISSUES

Synchrotron radiation. The total synchrotron power is

$$P \text{ [MW]} = 0.0885 \frac{E^4 \text{ [GeV}^4\text{]}}{\rho \text{ [m]}} I \text{ [A]} \quad (5)$$

- The SLAC HER serves as a natural “ruler” to compare prospective electron rings. (See Table).

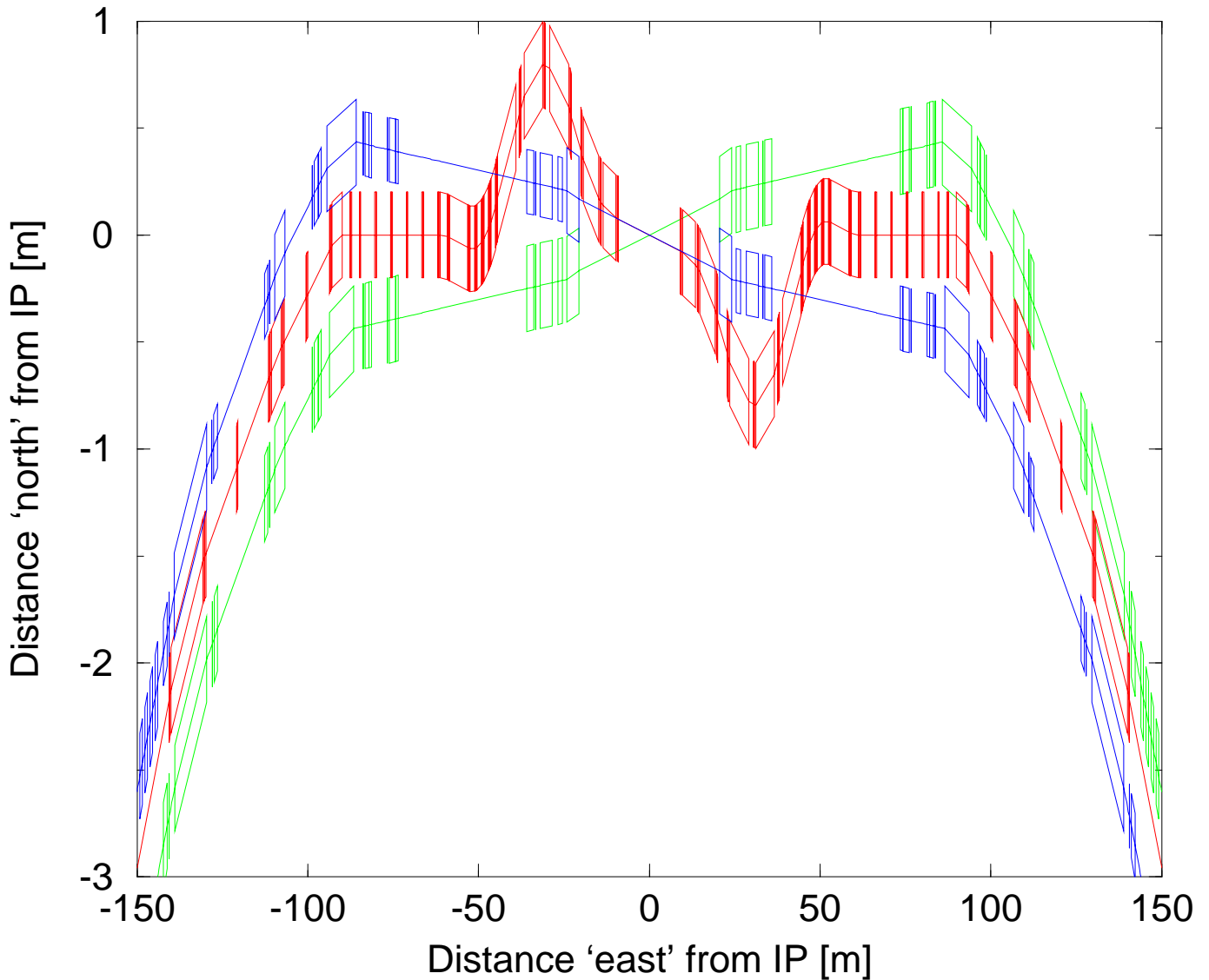
Polarization. The natural polarization time

$$T_{\text{pol}} \text{ [s]} = 15.8 \frac{C \rho^2 \text{ [m}^3\text{]}}{E_e^5 \text{ [GeV}^5\text{]}} \quad (6)$$

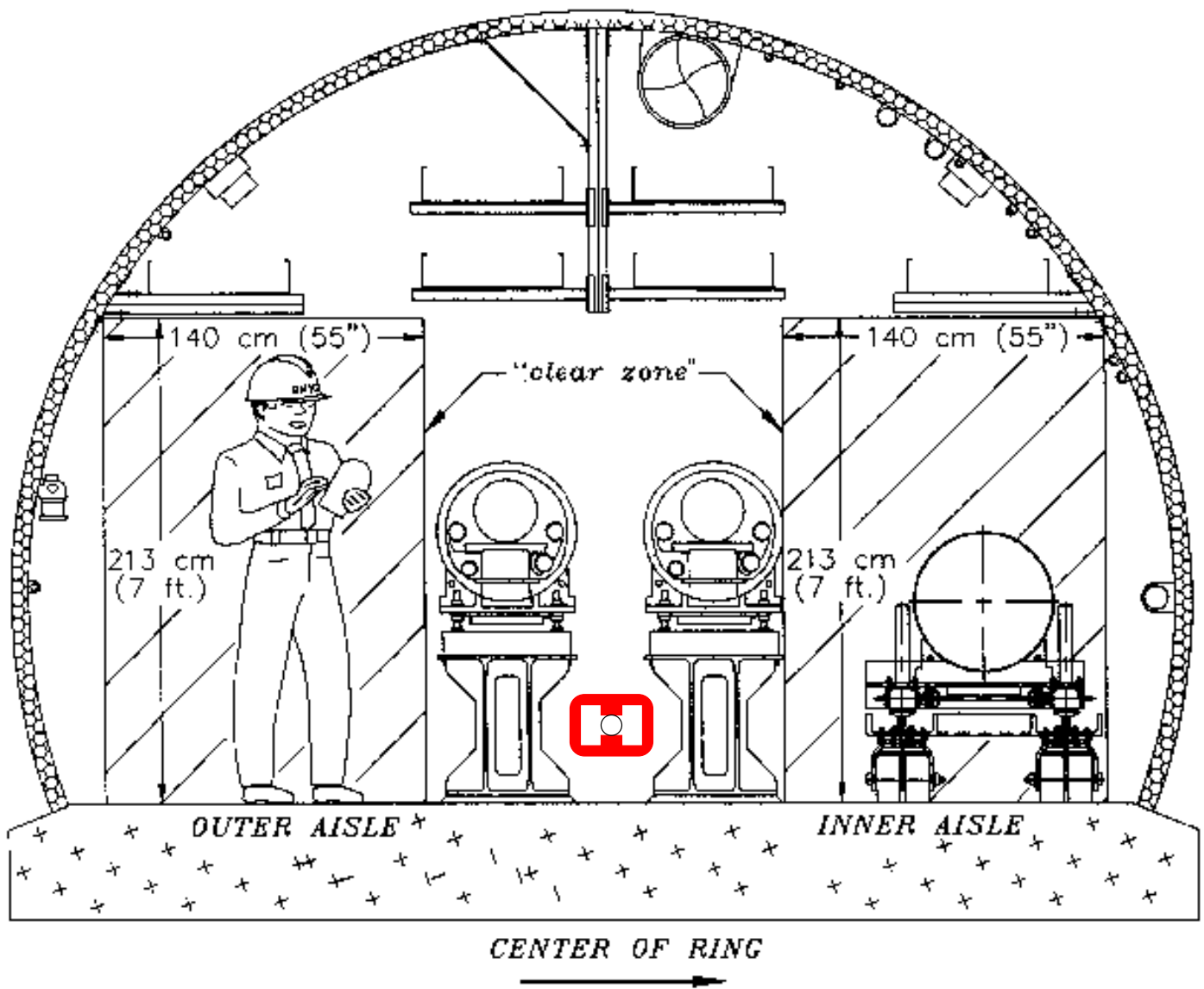
can be too long (9.9 hours in eRHIC) – may have to inject pre-polarized!

- Acceleration through intrinsic spin resonances probably impossible ($E = J 0.441 \text{ [GeV]}$).
- Permanent magnets?

Interaction Region optics – spin rotators.



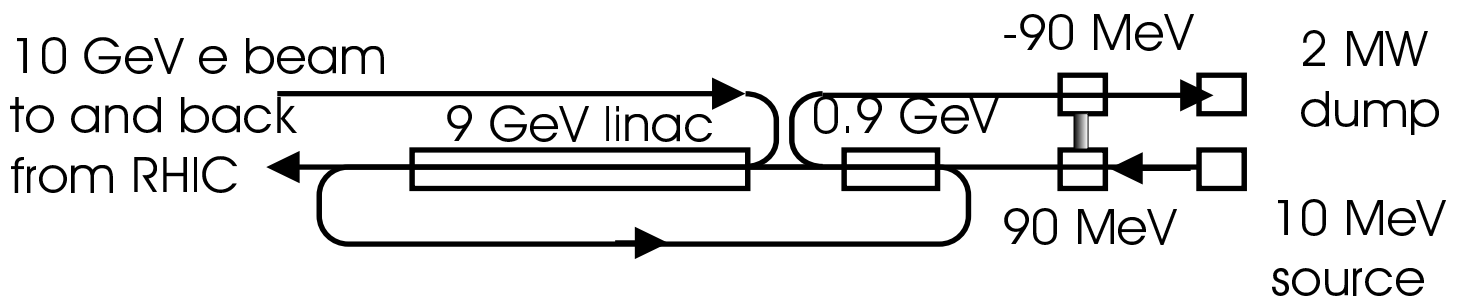
- Spin rotator dipoles tend to be stronger than arc dipoles – must keep linear synchrotron radiation load to less than 15 kW/m.
- The vertical displacement is useful ...



eRHIC tunnel cross section, with an electron magnet between the ion rings.

ENERGY RECOVERY LINAC ISSUES

A four stage Energy Recovery Linac



- Linac must be superconducting.
- Accelerating and decelerating beams must go in the same direction.
- Each stage has an energy range of about a factor of 10 – or much more? (Bazarov, PAC 01).

Beam transport. The electrons must circulate once with little synchrotron energy loss.

- Use a “full radius” recirculator, even with collisions at only one IP?

Energy recuperation. Electron beam power is ~ 1 GW, so recuperation must be very efficient.

- JLAB IR-FEL (250 kW, 5 mA, 50 MeV) reports a beam loss upper limit of $2\mu\text{A}$, or $\leq 4 \times 10^{-4}$
- Losses in a high power ERL at this upper limit could be unacceptable. Very little power can be lost at cryogenic temperatures.
- More work is required to understand both the origin of ERL beam losses, and their possible cures.

Higher Order Mode power dissipation.

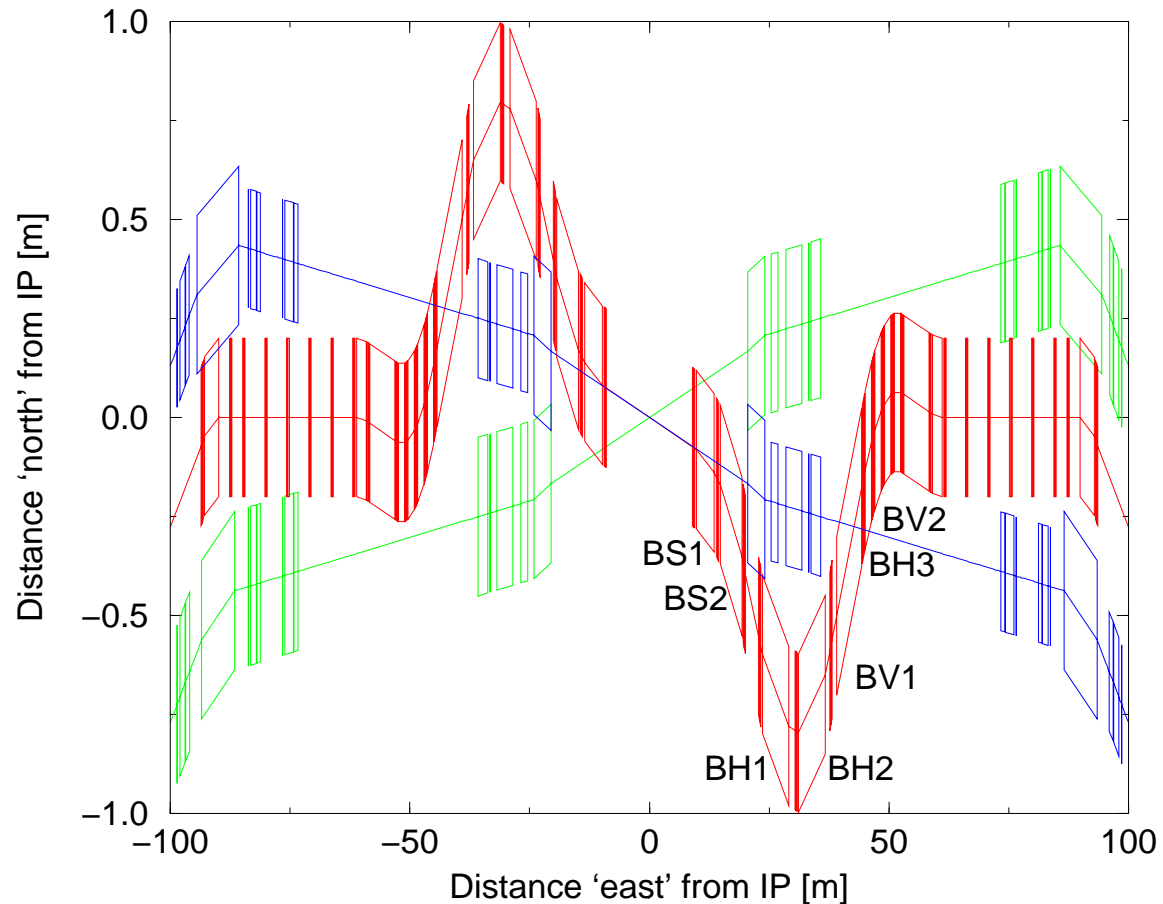
Collective instabilities can be driven by HOMs in the superconducting cavities.

- EPIC 2 predicts about 8 kW of HOM power dissipated per cavity, primarily in longitudinal modes, with **only a few Watts at cryogenic temperatures.**
- More studies & operating experience are required.

Beam Break Up. Collective BBU phenomena are longitudinal and transverse, single and multi-bunch, and single and multi-pass.

- Calculated EPIC 2 and eRHIC thresholds are somewhat below nominal currents. **Use feedback.**

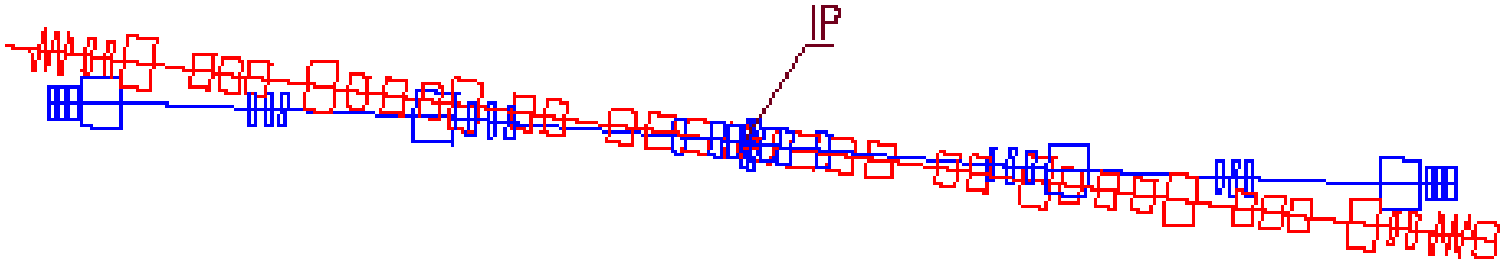
INTERACTION REGION ISSUES



The “NIM” ring-ring IR optics

- with 3 beams
- electron ring in the RHIC tunnel
- geometrically constrained spin rotators

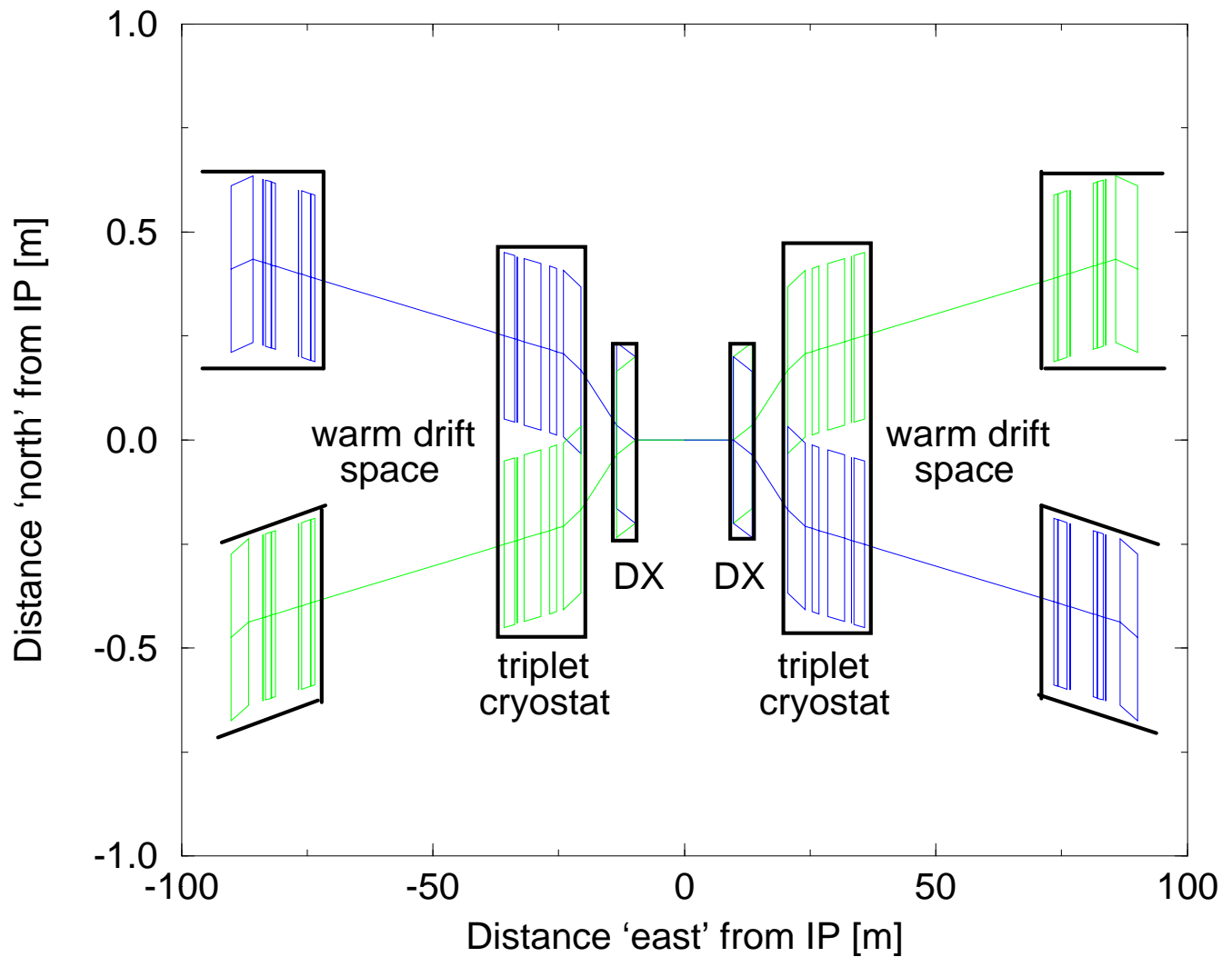
works, but is inferior to “green field” solutions ...



... such as that of **MIT-Bates**.

- **eRHIC** now foresees **collisions only at IP12**
- **An electron ring** can therefore be **outside the RHIC tunnel**.
- **Linac-ring** IR optics **do not require a spin rotator**
- **The experiment** would like to **integrate IR magnets into the detector**

CONVERGE ON AN IR DESIGN?



The existing RHIC geometric constraints are FULLY negotiable for collisions at IP12 ...

... with either ring-ring or linac-ring schemes.

SUMMARY

1. It is now possible to **merge the electron ring designs** – if we agree that this is desirable.
2. The **linac-ring scenario continues to evolve**, in addressing its challenges
3. The time is ripe to begin merging ring-ring, linac-ring, and detector perspectives, on a **common IR optics design**.
4. The White Paper describes the status of a work in progress. **How do we collaborate from here?**

Ring–Ring Collider Scheme

Yu.M.Shatunov, BINP, Novosibirsk

EIC Accelerator Workshop 2002

Radiative polarization

$$P_{eq} = -\frac{8}{5\sqrt{3}} \frac{\langle |k|^3 \vec{b} (\vec{n}_s - \vec{d}) \rangle}{\langle |k|^3 [1 - \frac{2}{9}(\vec{n} \cdot \vec{v})^2 + \frac{11}{18} \vec{d}^2] \rangle}$$

\vec{n}_s - "spin closed orbit"

$\vec{d} = \gamma \frac{\partial \vec{n}_s}{\partial \gamma}$ - spin orbit coupling

$$\vec{b} = \frac{\vec{B}}{B}; \quad k = \frac{B}{B_0}; \quad B_0 = \frac{1}{2\pi} \int B d\theta$$

$\tau_p \sim \gamma^{-5}$ - polarization time

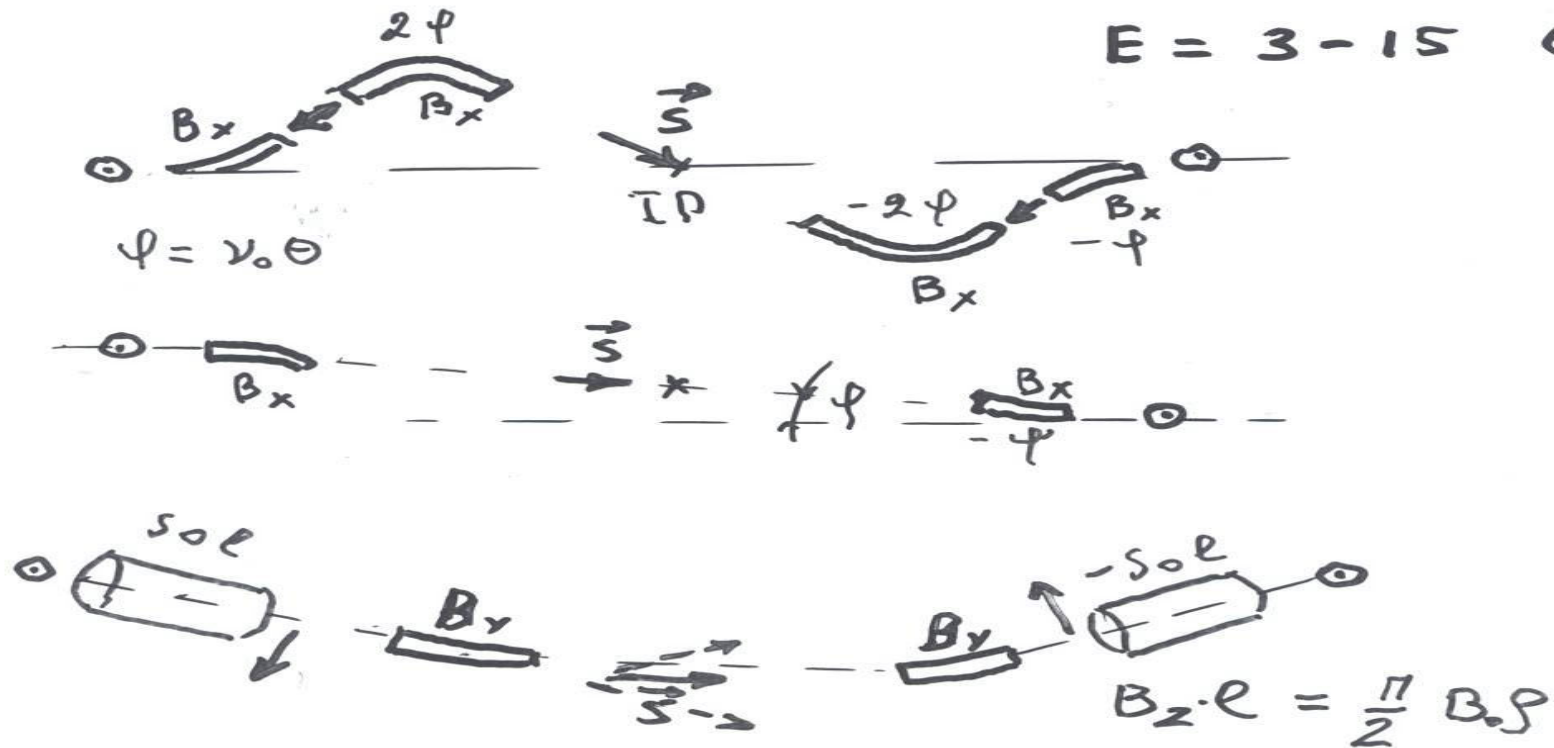
polarizing wigglers

$$\tau_p^{-1} \sim B^3 \gamma^2$$

$\Delta E \sim B^2 \gamma^2$ - energy losses

Spin Rotators

$E = 3 - 15 \text{ GeV}$



For high energy

$$B_x + B_y$$

HERA "mini rotator"

Closed orbit displacements

Spin transparency

$$\vec{S}' = [\vec{w} \times \vec{S}] \quad \text{- BMT equation}$$

$$\vec{w} = \vec{w}_0 + \vec{w}$$

$$\underline{I = \int_{\theta_1}^{\theta_2} (\vec{w} \cdot \vec{e}_z) d\theta = 0}$$

$$\begin{cases} w_x = v_0 y'' + K_x \frac{\Delta\delta}{\delta} \\ w_y = -v_0 x'' + K_y \frac{\Delta\delta}{\delta} \\ w_z = K_z \frac{\Delta\delta}{\delta} \end{cases}$$

$$T_x = \begin{pmatrix} 0 & -2\Gamma \\ (2\Gamma)^{-1} & 0 \end{pmatrix}; \quad T_z = \begin{pmatrix} 0 & 2\Gamma \\ -(2\Gamma)^{-1} & 0 \end{pmatrix} \quad \text{- transfer matrix along solenoidal section}$$

$$\Gamma = \frac{B \cdot p}{B_y}$$

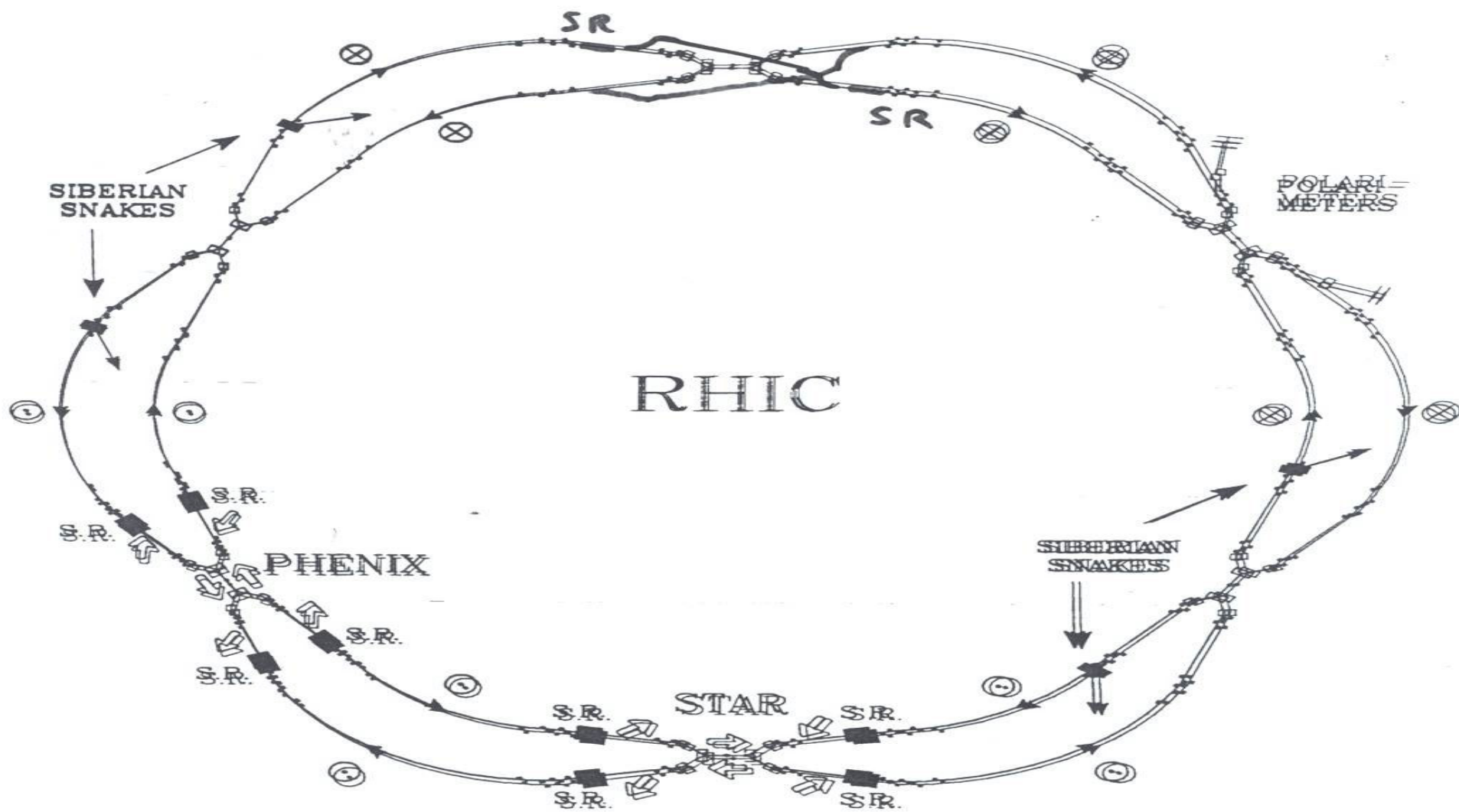


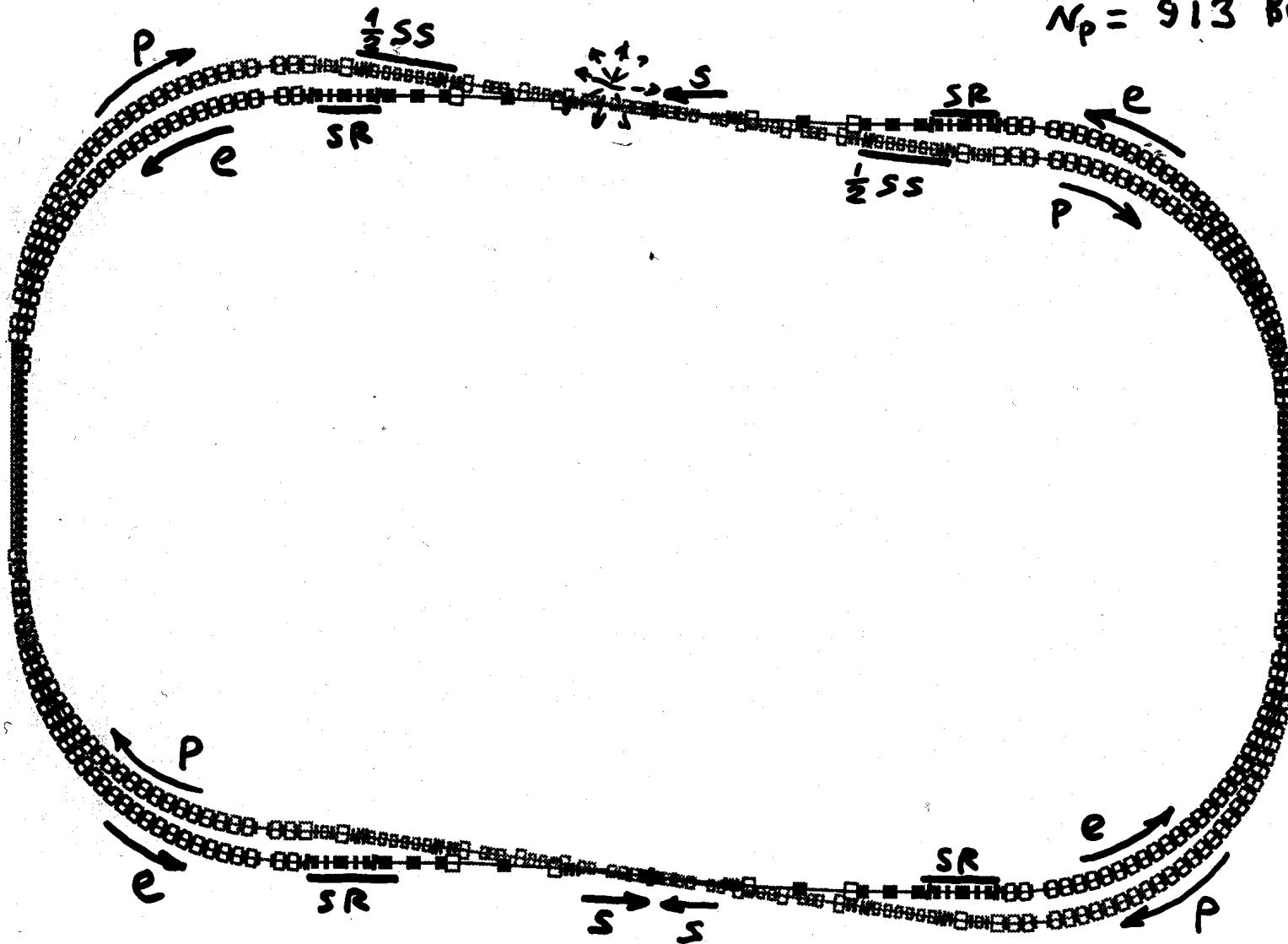
Figure 2

Collider layout

$$L = 1388 \text{ m}$$

$$f_{RF} = 197 \text{ MHz}$$

$$N_p = 913 \text{ Bunches} = N_p$$



**CONCEPTUAL DESIGN STUDY
OF $e - p$ RING-RING COLLIDER
WITH POLARIZED BEAMS**

MIT Bates – BINP collaboration

Yu.M. Shatunov

FEATURES of PROJECT

Head-on ~~bunch-to-bunch~~ collision

Multi bunch operation

Low and equal β^*

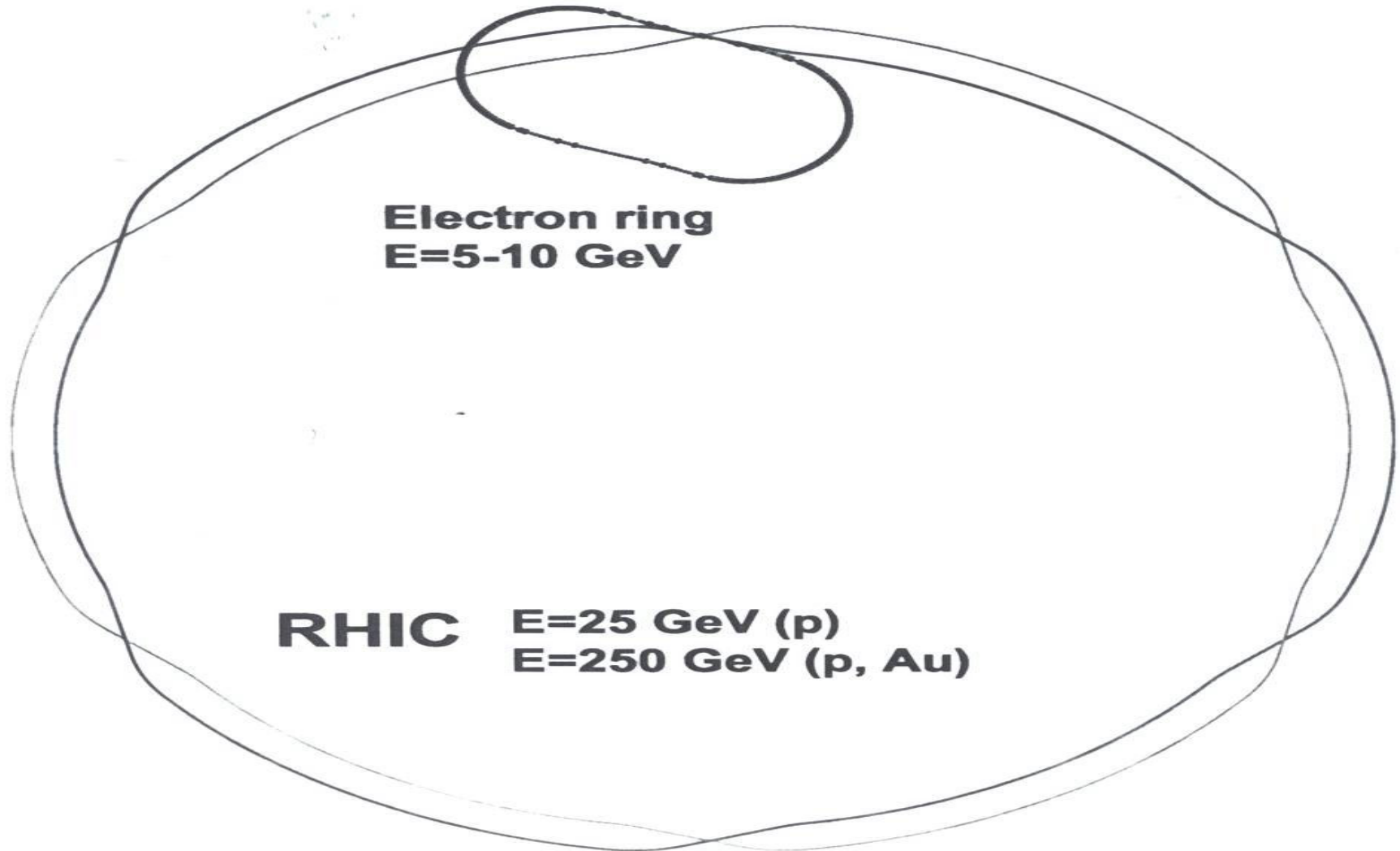
Round beams

Electron cooling of protons (injection)

+ SR
Siberian snakes in proton ring

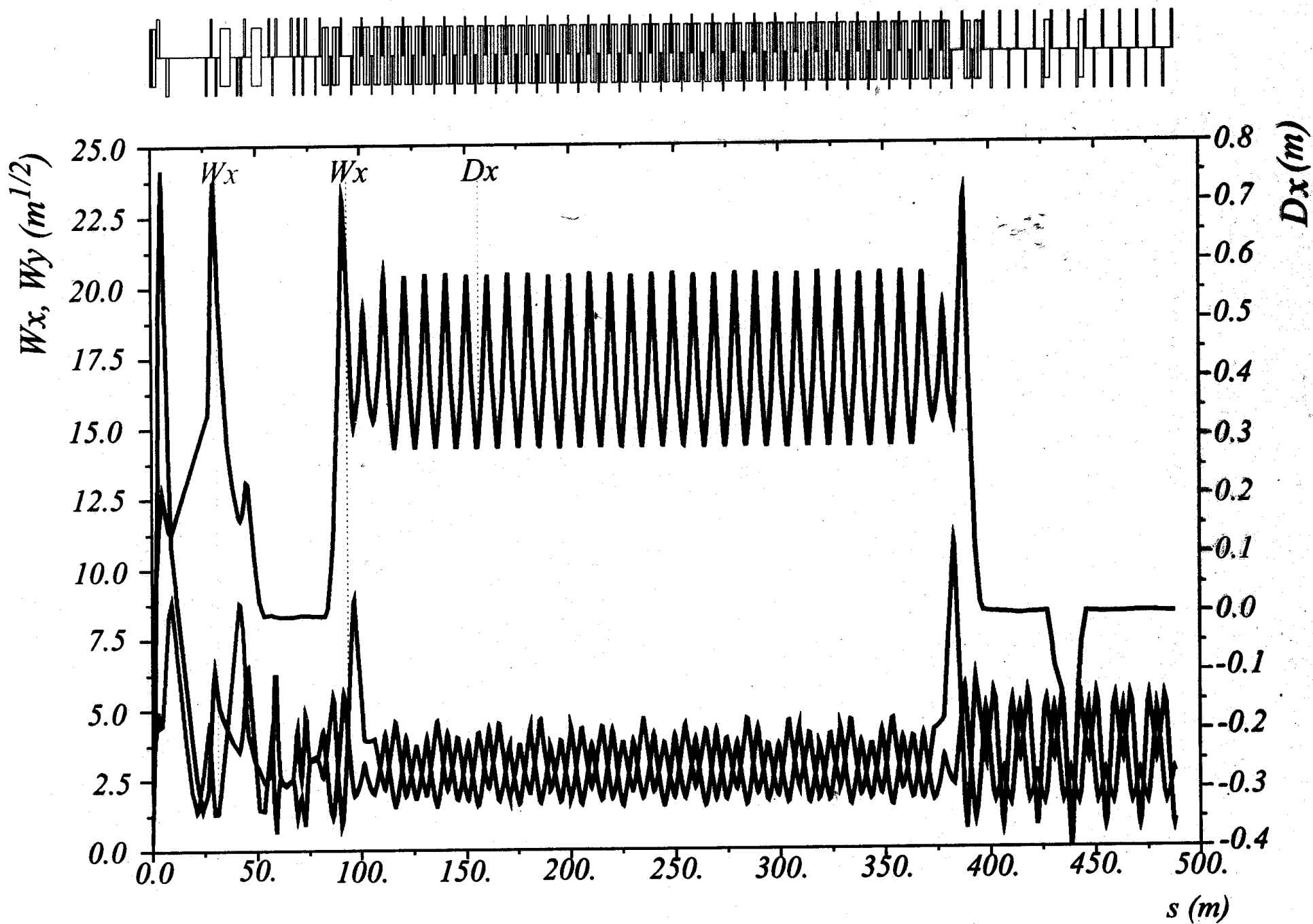
Spin rotators in electron ring

eRHIC

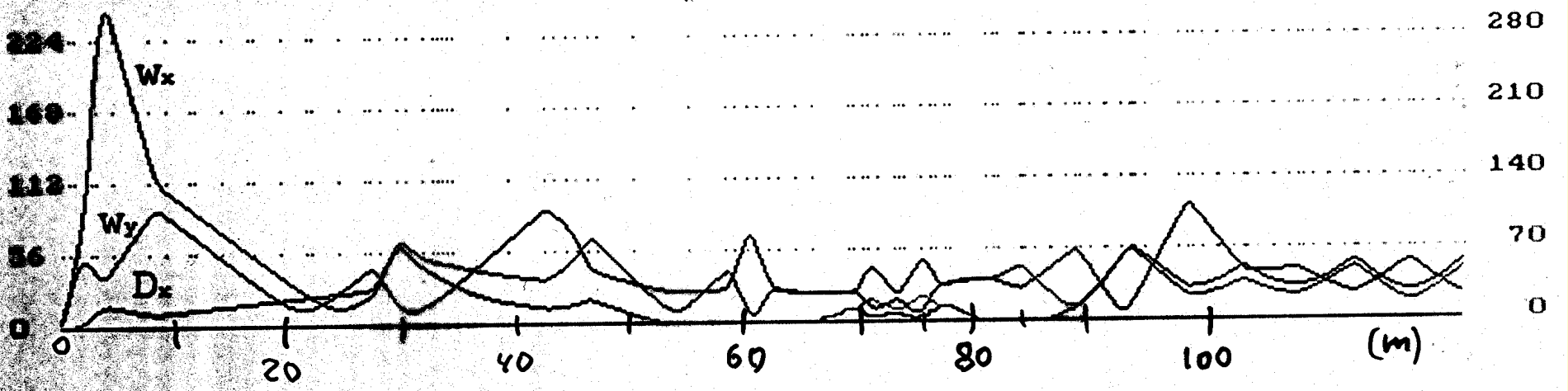


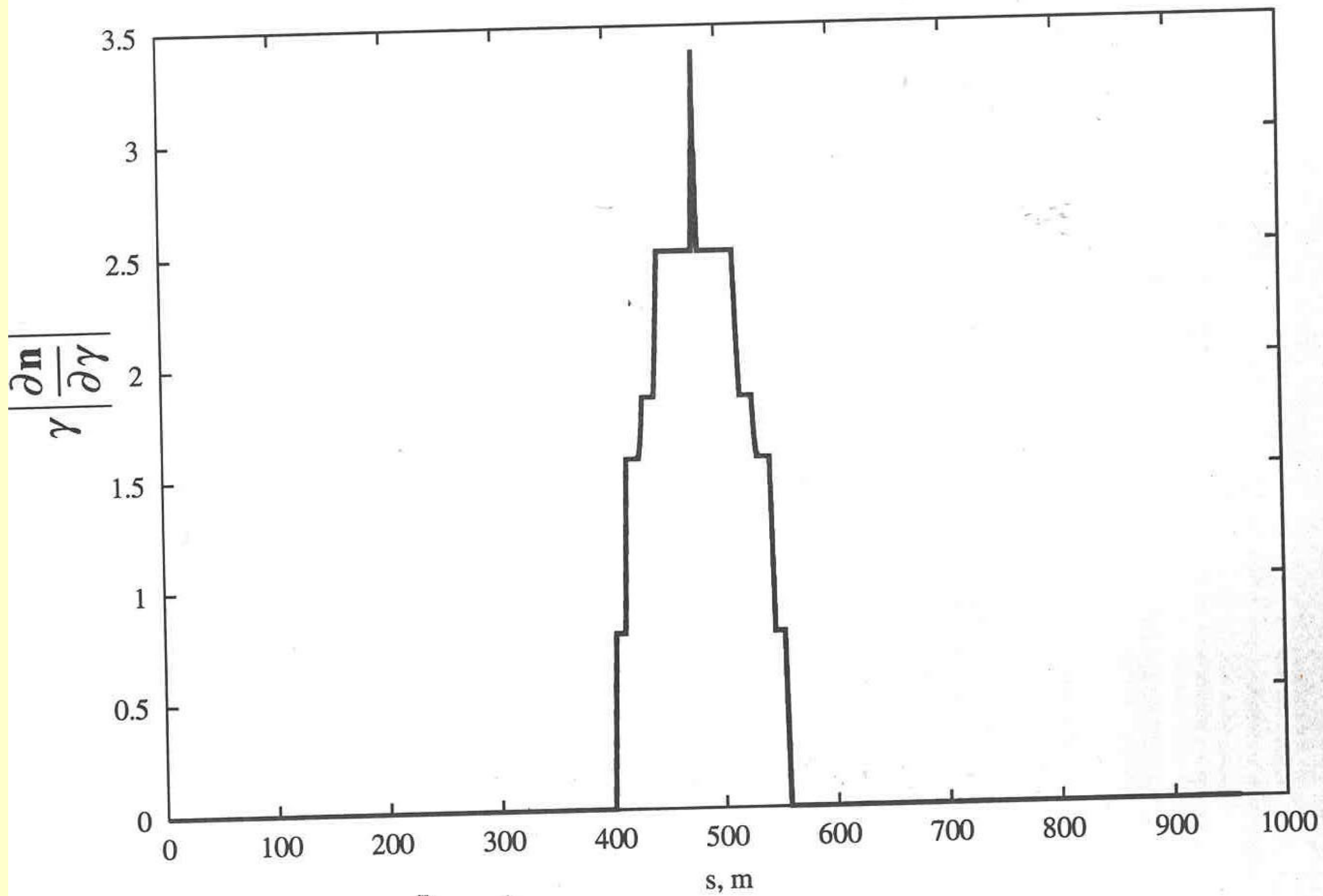
Electron ring
E=5-10 GeV

RHIC **E=25 GeV (p)**
 E=250 GeV (p, Au)

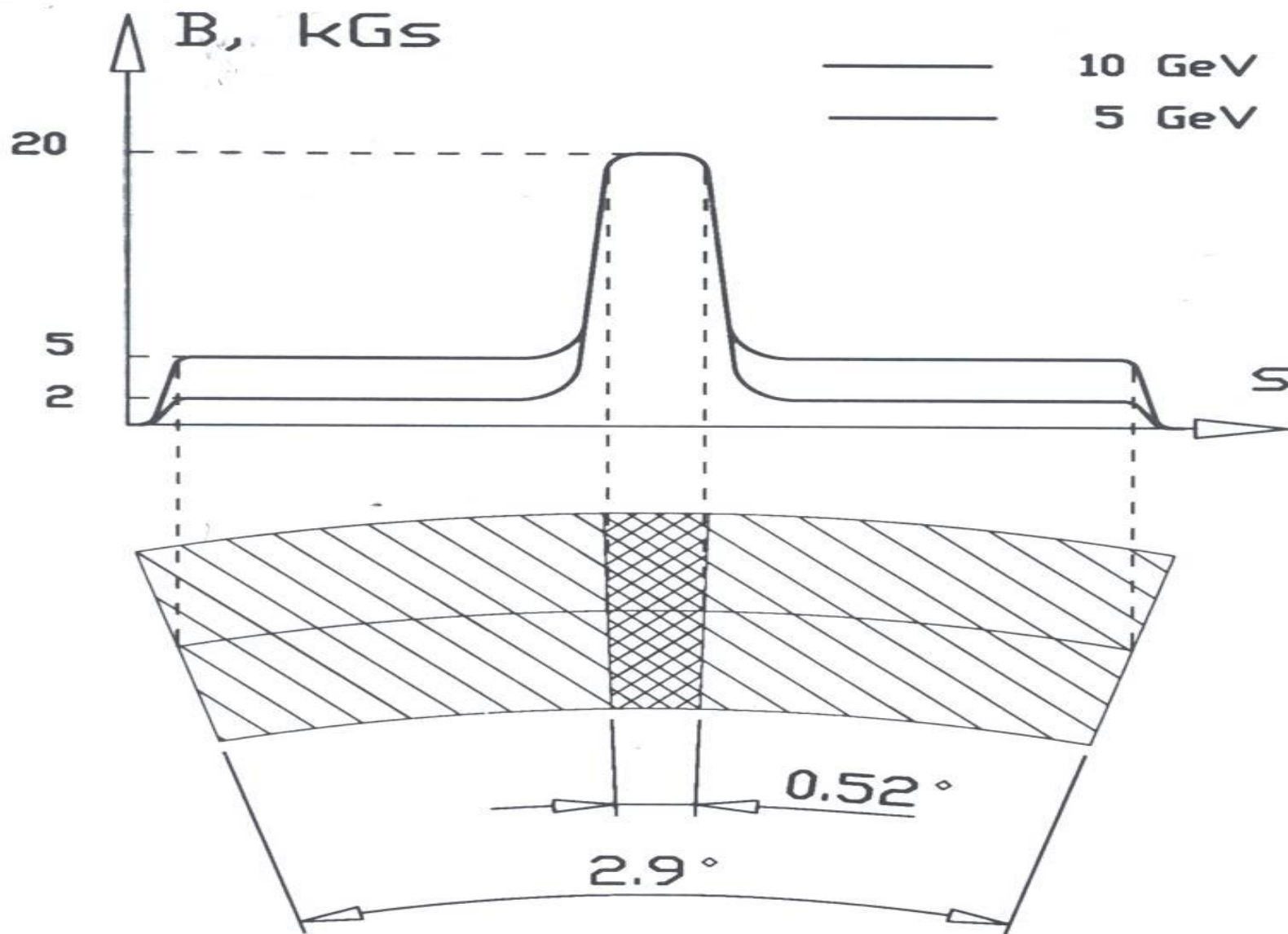


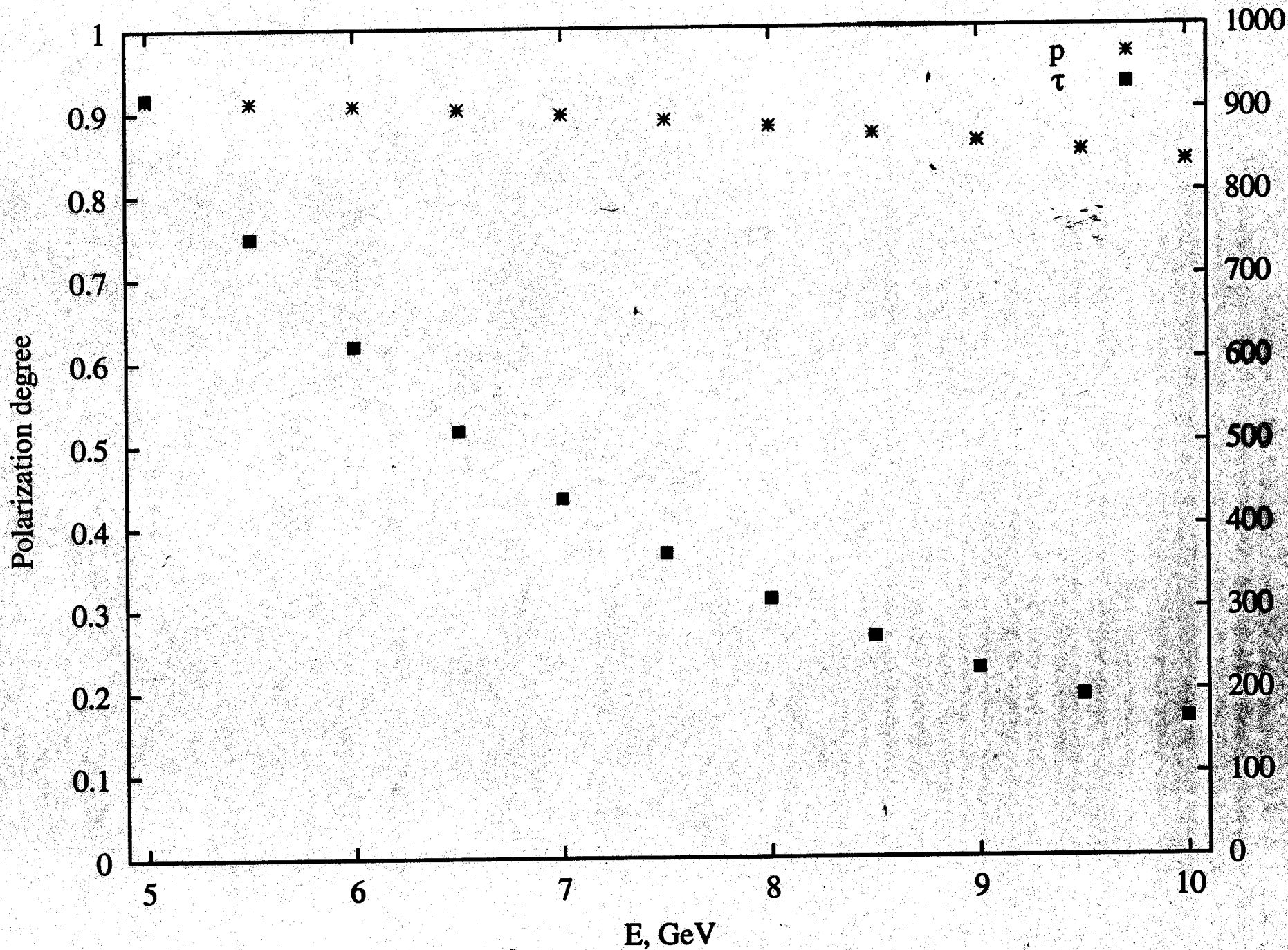
sol. 26 Txm



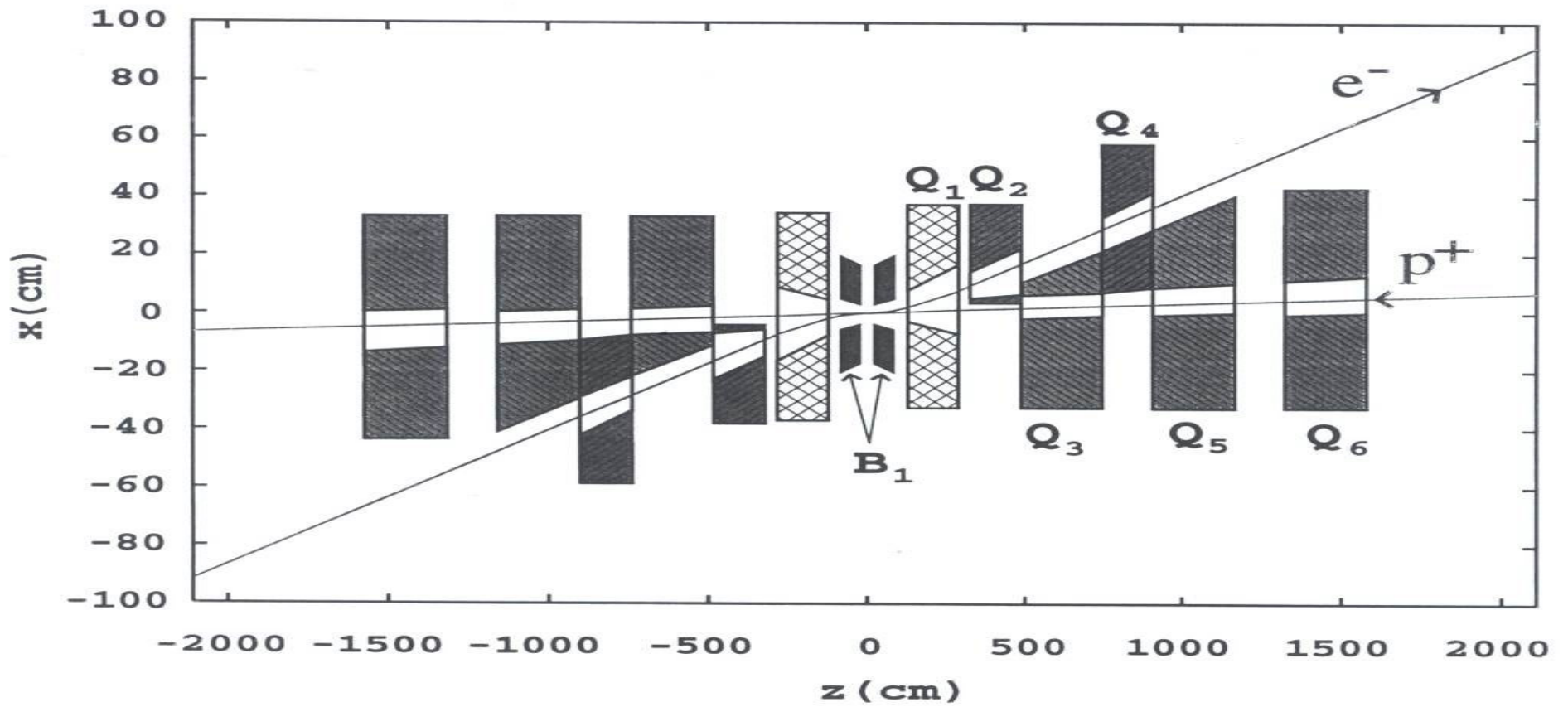


Super Bend





$$\beta^* = \beta^* = 10 \text{ cm}$$



Electron cooling

$$1) \delta_e = \delta_p$$



$$\tau = \frac{l_{cool}}{\gamma \beta c}$$

$$\omega_L \tau \gg 1$$

$$S_{max} = v_{tr} \tau \gg S_L$$

rest frame;

"magnetized cooling"

3) l_{cool} as long as possible

$$4) \beta_x \approx \beta_z \approx l_{cool}$$

5) to avoid "electron heating"

$$\tau_{cool} = \frac{v_{tr}^3}{4\pi e \Gamma_p c^3} \cdot \frac{\delta_p^2}{L_c n_e R}$$

$$\left. \begin{array}{l} l_{cool} = 30 \text{ m} \\ \beta_{cool} = 60 \text{ m} \\ n_e = 1 \cdot 10^9 \\ B = 1 \text{ T} \\ \gamma = 25 \end{array} \right\}$$

$$\tau_{cool} \approx 1600 \text{ sec}$$

against IBS
and beam-beam

Electron Ring $E = 5-10 \text{ GeV}$

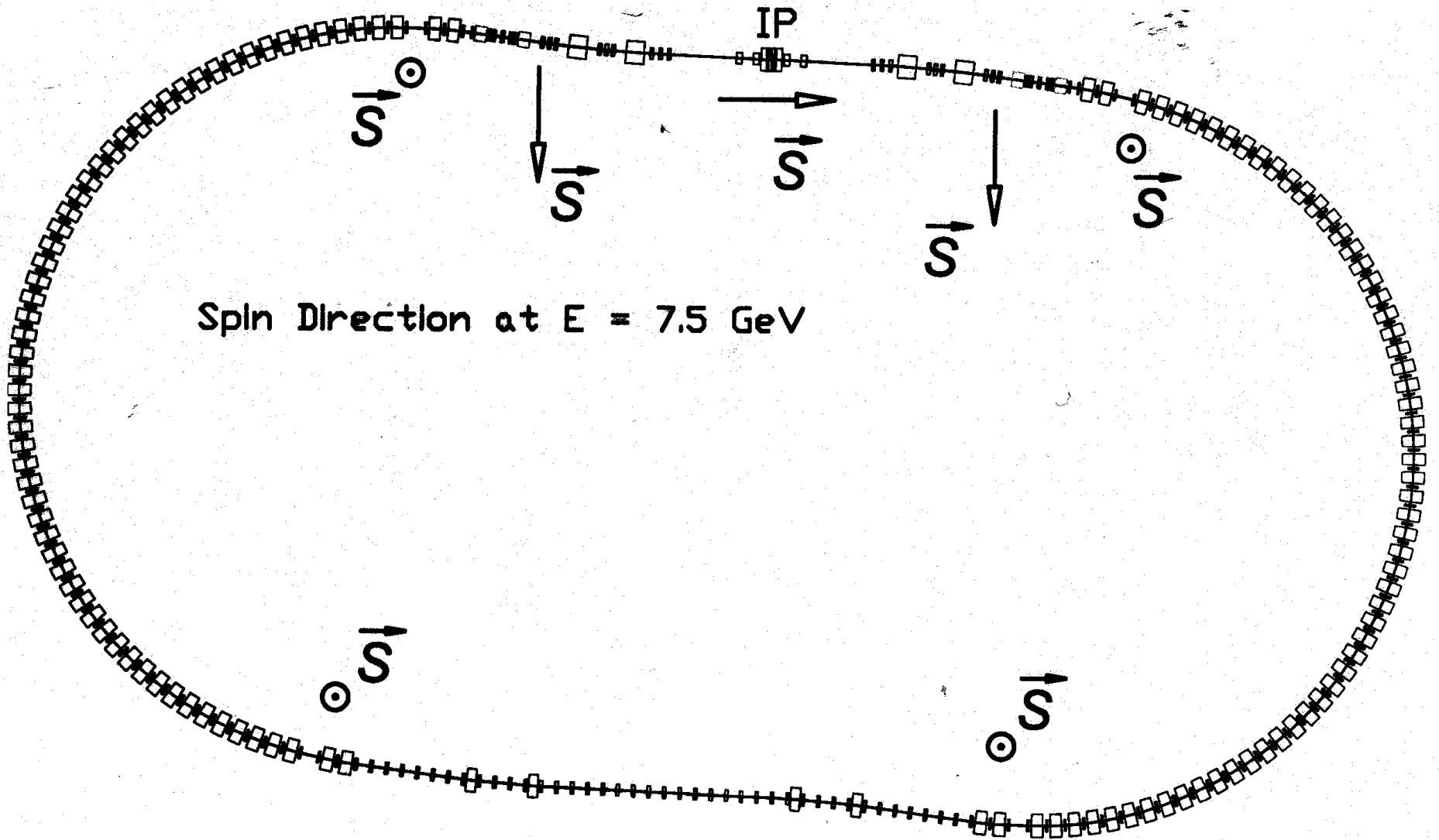
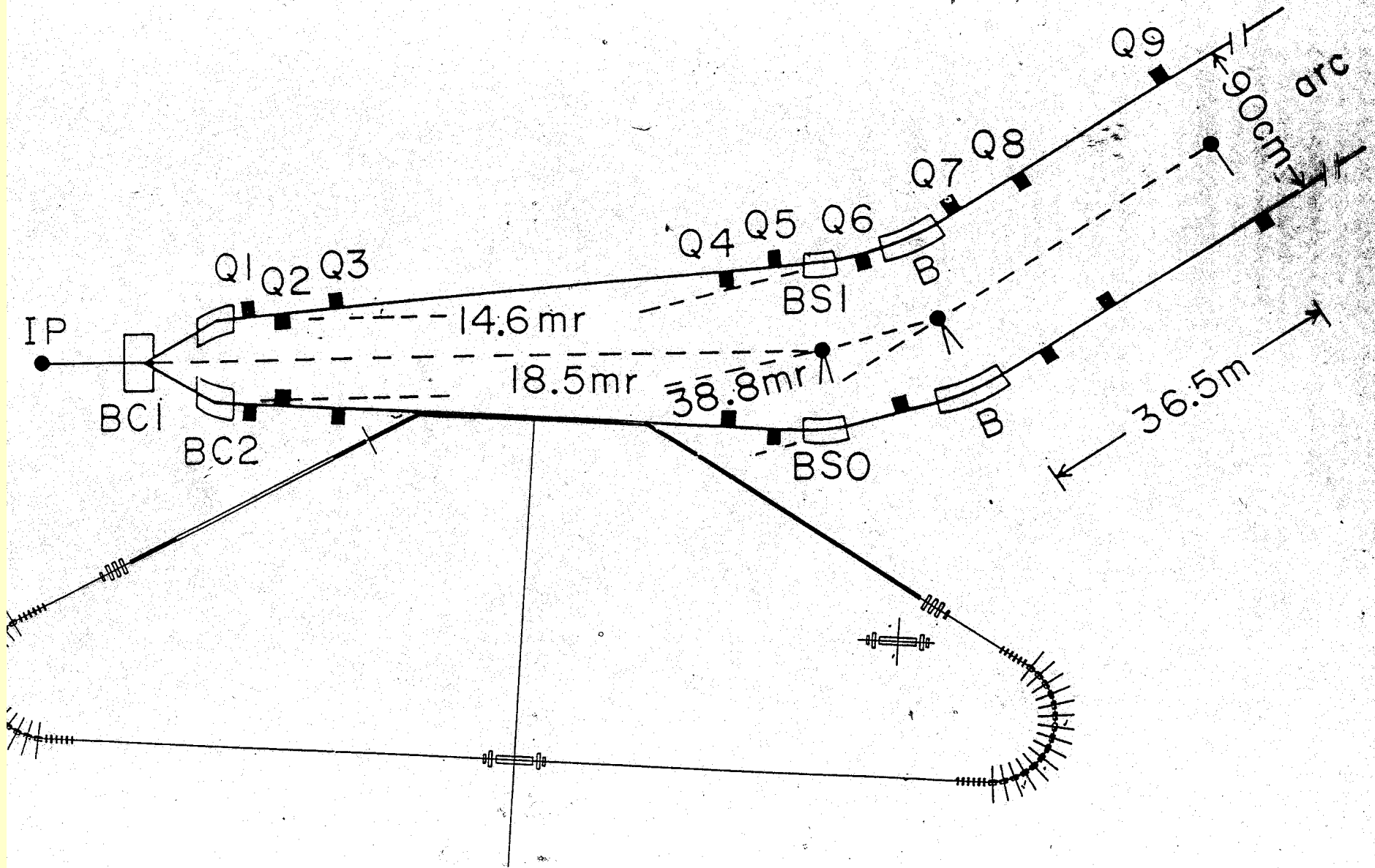


Fig. IV.2-3. RHIC half-insertion at 6 o'clock.



General parameters of the electron-proton collider

	Units	Electron ring	Proton ring
Circumferences	<i>m</i>	958.25	3833
Energy	<i>GeV</i>	5–10	25–200
Arc radius	<i>m</i>	97.98	610
Bending radius	<i>m</i>	63.59	243
Number of bunches		90	<u>360</u>
Bunch spacing	<i>m</i>	10.65	10.65
Bunch population		<u>$1 \cdot 10^{11}$</u>	$1 \cdot 10^{11}$
Beam currents	<i>A</i>	0.45	0.45
Harmonic number		1170	2520
RF frequency	<i>MHz</i>	365.7	196.9
Accelerating voltage	<i>MV</i>	30	1.5
Energy losses/turn	<i>MeV</i>	2.83– <u>21.26</u>	
Total radiated power	<i>MW</i>	<u>1.27–9.57</u>	
Beam emittances, $\epsilon_{x,z}$	$\mu m \cdot mrad$	43–65	48–6
Beta function at IP	<i>cm</i>	10	10
Beam size at IP, $\sigma_{x,z}^*$	μm	65–80	68–24
Momentum spread		$1.0-1.6 \cdot 10^{-3}$	$1.1-0.4 \cdot 10^{-3}$:
Bunch length, σ_l	<i>cm</i>	1–2	10–5
Beam-beam parameter, ξ		0.046–0.023	0.009–0.002
Lasslett tune shift, $\Delta\nu$			0.2–0.009
Luminosity	$cm^{-2}s^{-1}$		$0.45-1 \cdot 10^{33}$

Exploration of the Derbenev Kondratenko Equation in the MIT Bates South Hall Ring

Townsend Zwart
EIC Workshop
February 2002

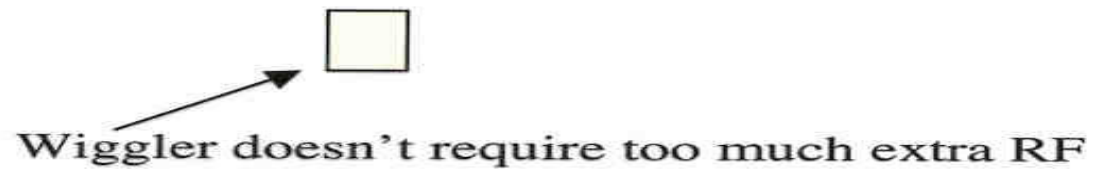
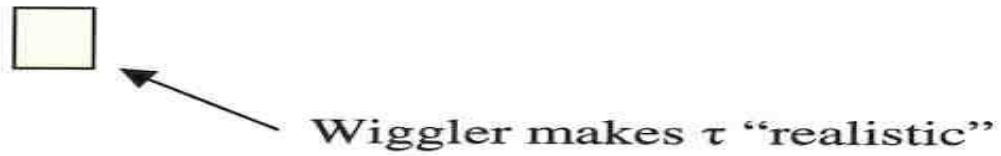
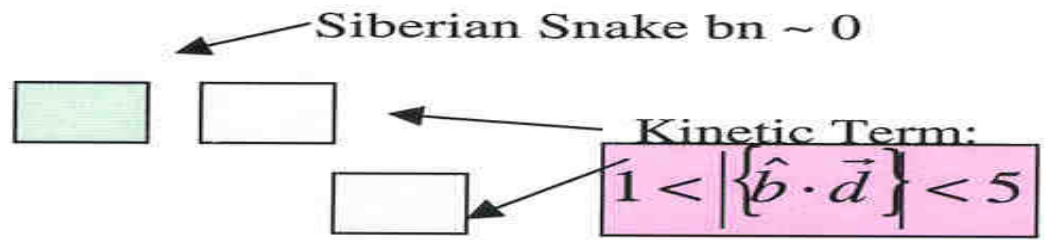
E. Booth, K. Dow, M. Farkhondeh, W. Franklin, E. Ihloff,
K. Jacobs, J. Matthews, R. Milner, T. Smith, E. Tsentalovich,
W. Turchinets, J. van der Laan, F. Wang
&
The BLAST Collaboration

Special Thanks to
D. Barber, A. Krisch & Y. Shatunov



Talk Outline

- **What:** Map out the DK formula for radiative polarization with a special emphasis on the “kinetic” term.
- **Why:** Benchmark test of the accuracy of the DK formula and stringent test of codes (ASPIRIN, SLIM) which predict the equilibrium polarization in storage rings. This should build confidence in the design and feasibility of a spin transparent rotator for the electron ring of an EIC ring-ring machine.
- **How:** Use the Bates infrastructure including:
 - Polarized Electron Source
 - South Hall Ring
 - Siberian Snake
 - Laser Back-scattering Polarimeter
 - RF Spin Flipper
- **Add:**
 - Wiggler
 - One additional RF cavity (new lattice)



Derbenev Kondratenko Mane Formula

$$P_{eq} = \frac{8}{5\sqrt{3}} \frac{\left\{ \frac{1}{|\rho|^3} \hat{b} \cdot \left(\hat{n} - \gamma \frac{\partial \hat{n}}{\partial \gamma} \right) \right\}}{\left\{ \frac{1}{|\rho|^3} \left(1 - \frac{2}{9} (\hat{n} \cdot \hat{v})^2 + \frac{11}{18} \left(\gamma \frac{\partial \hat{n}}{\partial \gamma} \right)^2 \right) \right\}}$$

Time Constant

$$\tau^{-1} = \frac{5\sqrt{3}\gamma^5 \hbar e^2}{8\rho^3 m^2 c^2} \left(1 - \frac{2}{9} (\hat{n} \cdot \hat{v})^2 + \frac{11}{18} \left(\gamma \frac{\partial \hat{n}}{\partial \gamma} \right)^2 \right)$$

Synchrotron Radiation Power

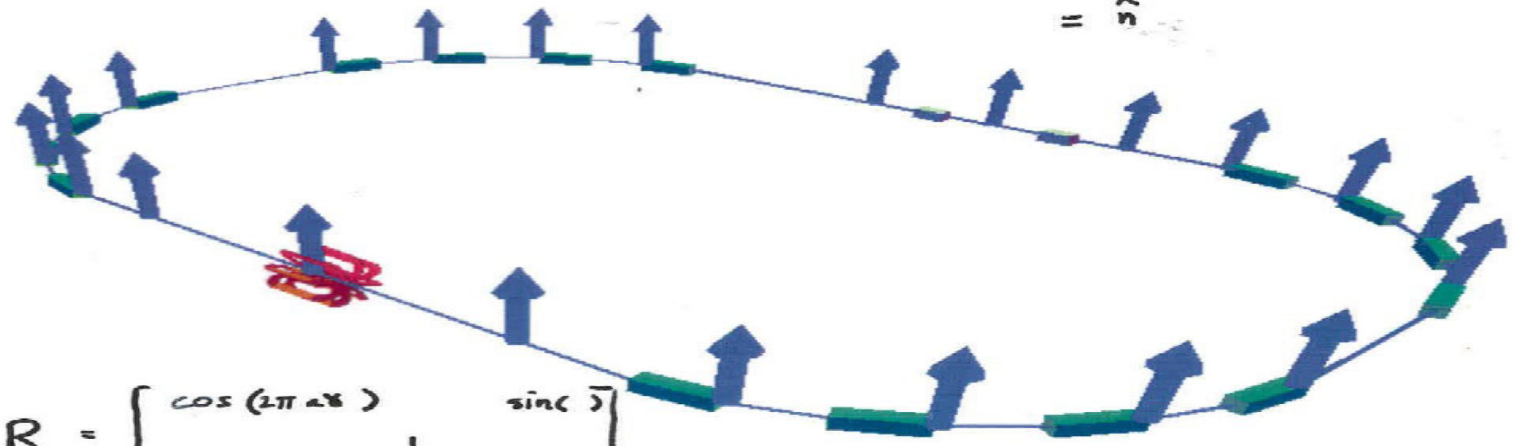
$$P = C_{\gamma} \gamma^4 R \left\langle \frac{1}{\rho^2} \right\rangle$$

CLOSED SPIN ORBIT

FLAT RING

$$\hat{n}(\phi) = (n_x, n_y, n_z)$$

$$R \hat{n} = Y \hat{n}$$
$$= \hat{n}$$



$$R = \begin{bmatrix} \cos(2\pi \alpha) & \sin(\alpha) \\ -\sin(\alpha) & \cos(\alpha) \end{bmatrix}$$

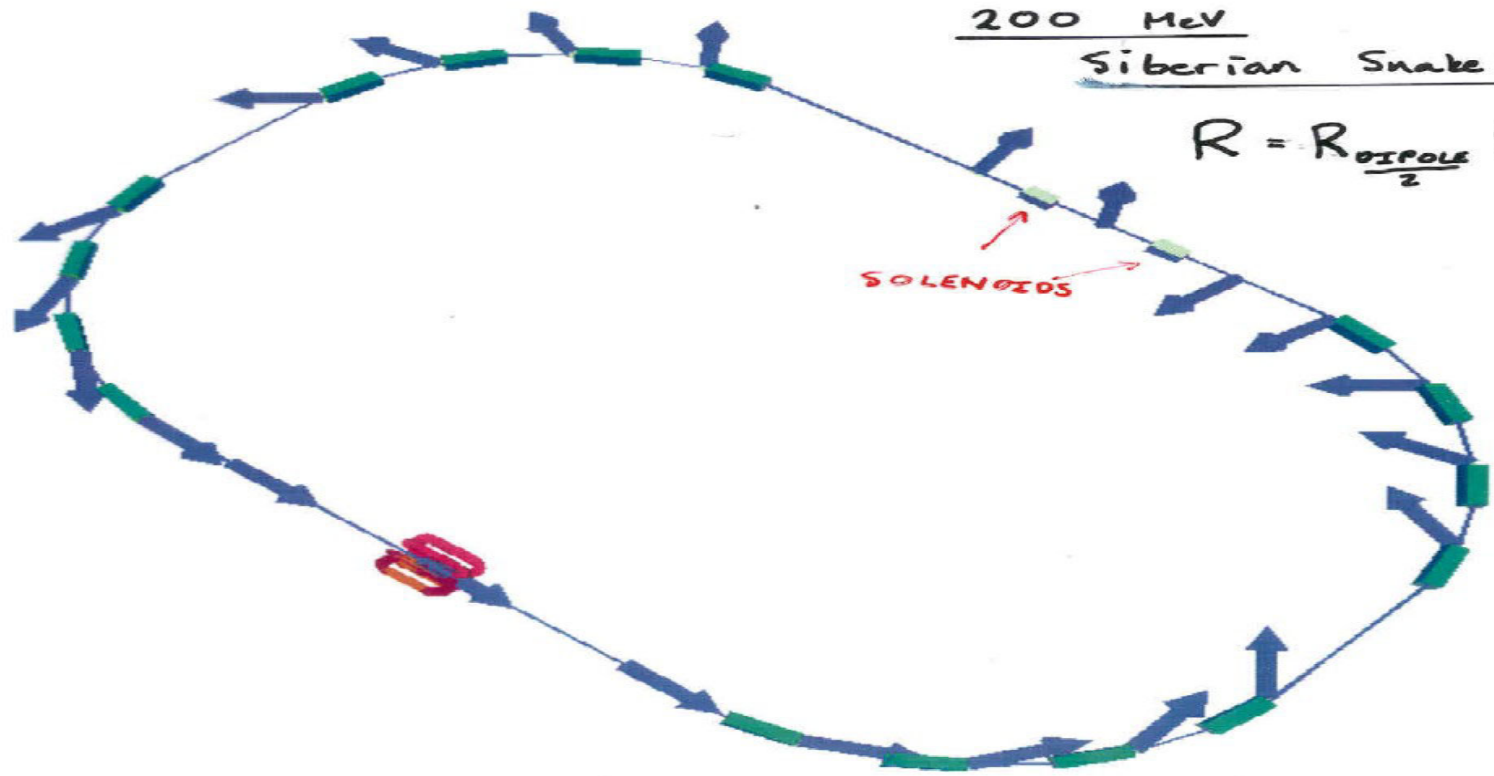
$$\hat{n} \neq \hat{p} ! ! ! !$$

200 MeV

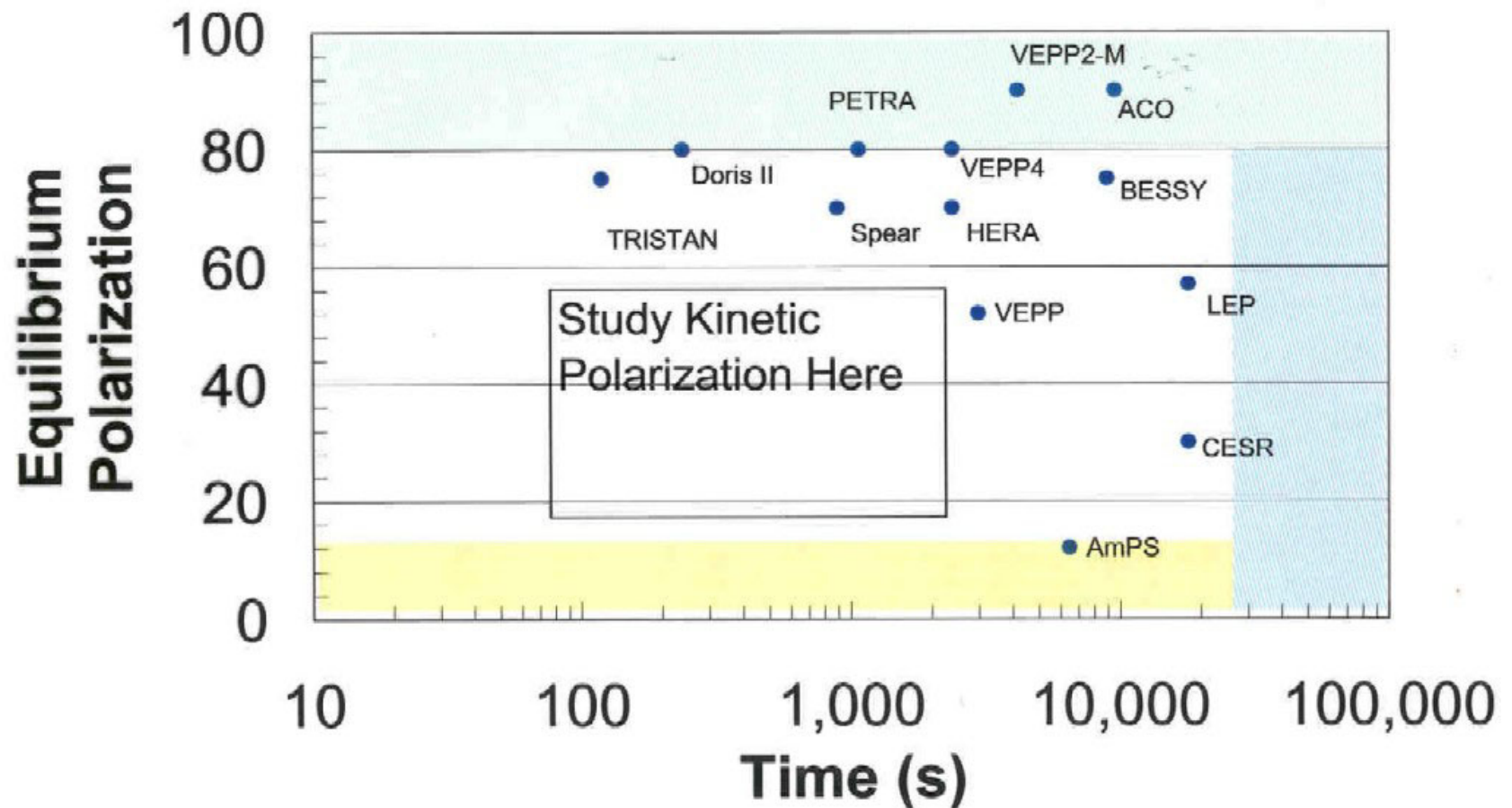
Siberian Snake Ring

$$R = R_{\frac{DISPOLE}{2}} S R_{\frac{DISPOLE}{2}}$$

SOLENOIDS



World Polarization vs. Time



From Buon, CERN Acc. School 5th Advanced Acc. Physics Course. CERN 95-06 22 Nov 1995

The MIT Bates Facility

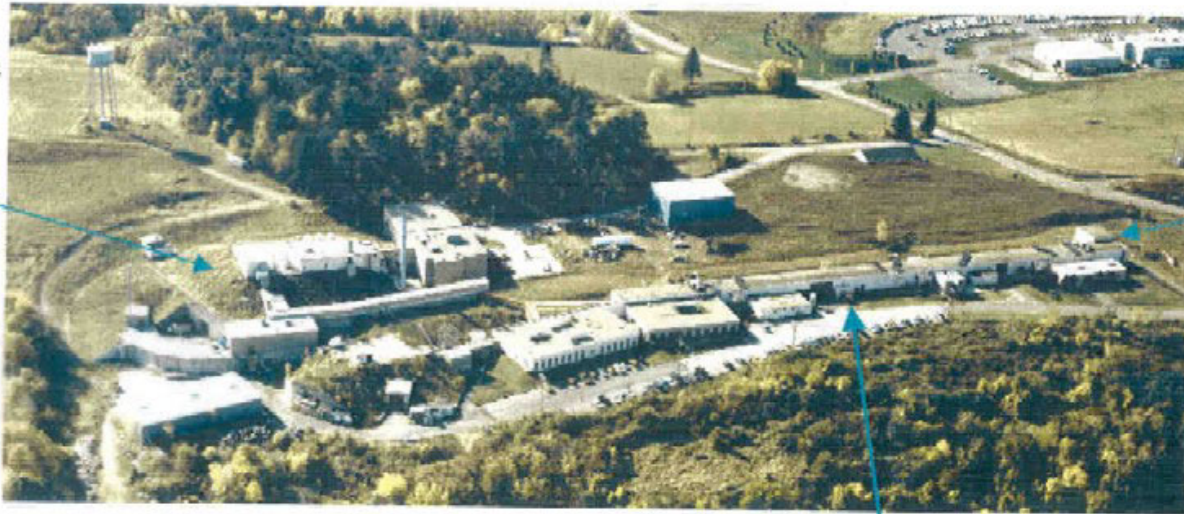
South Hall
Ring

BLAST
Detector

Siberian
Snake

Compton
Polarimeter

RF Spin
Flipper



Polarized
Injector

Diode Laser
200 W

$I_e \sim 10 \text{ mA}$

$P > 65\%$

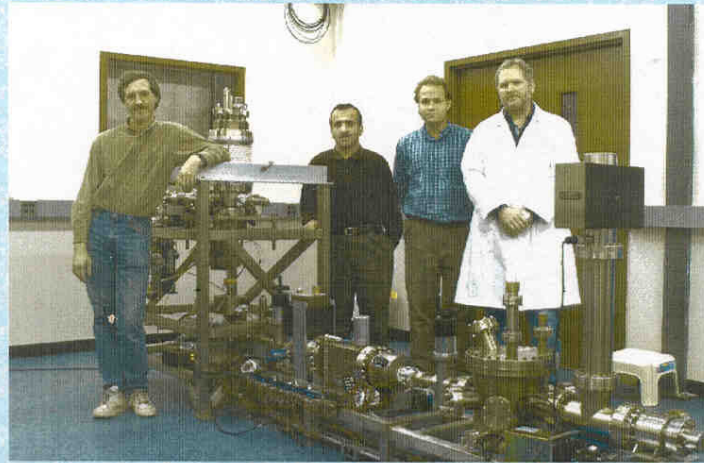
$DF \sim 1\%$

180 m LINAC

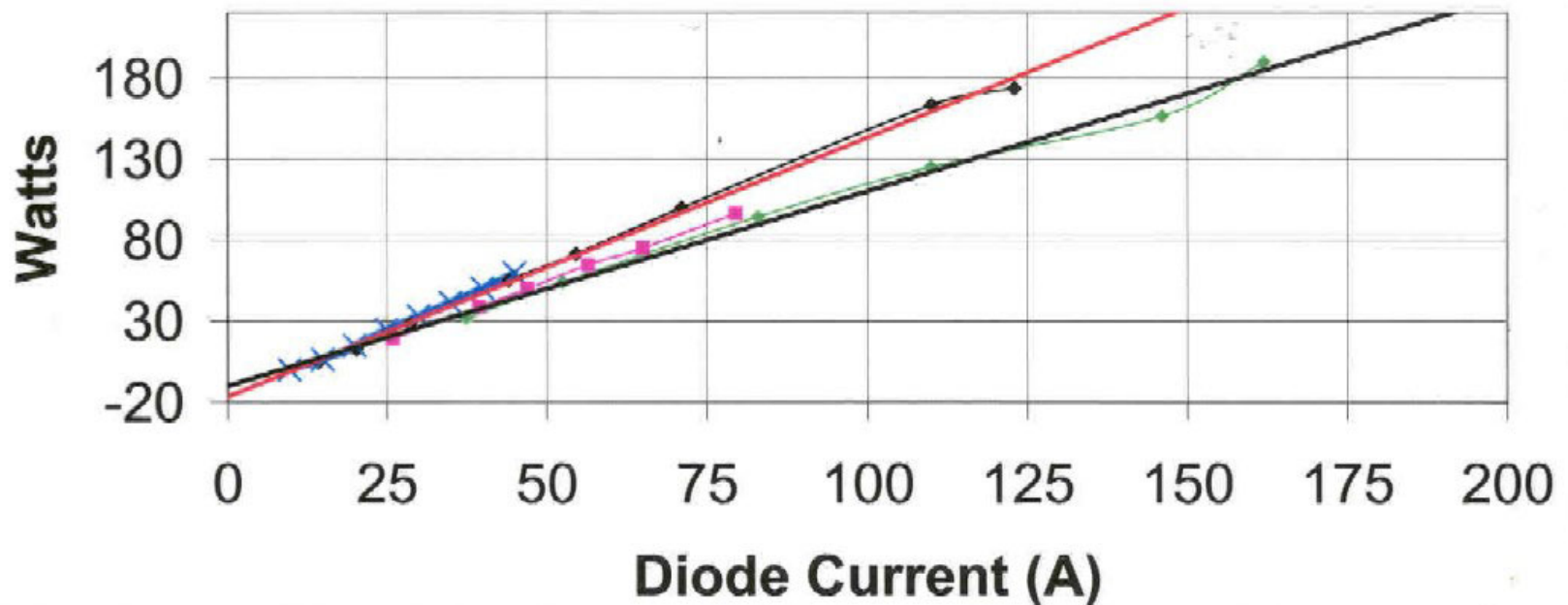
1.1 GeV w/ two
pass recirculation

Polarized Source Group at Work on the Test Beam Setup

Goto talk by M. Farkhondeh

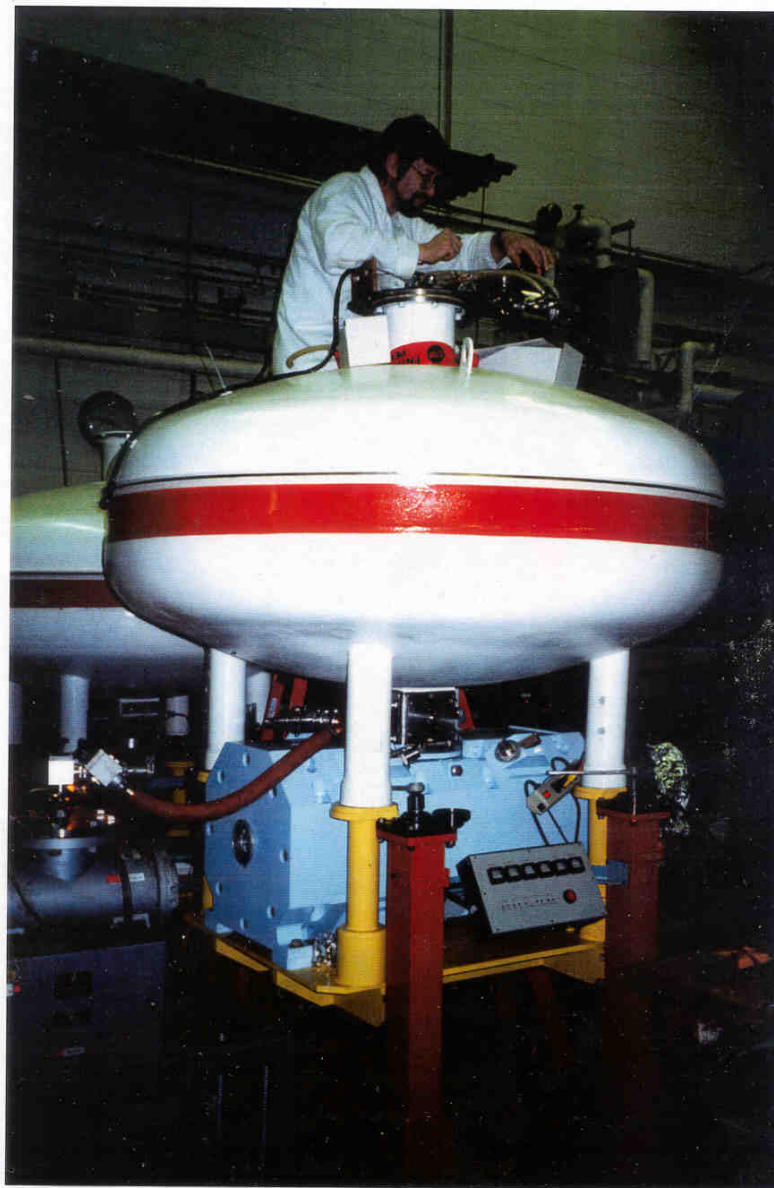


OPTOPower Laser Diode (Spectra Physics)



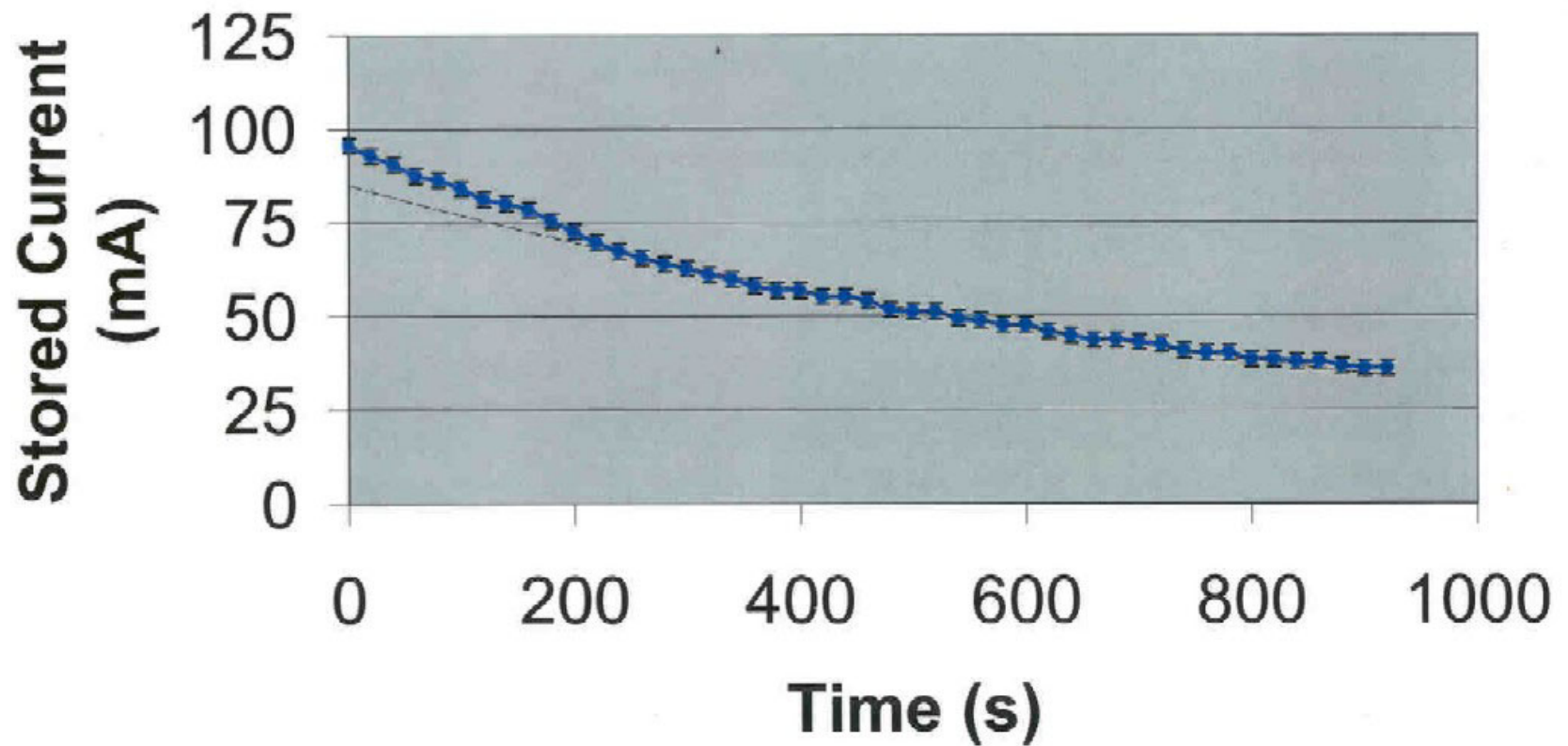
- ◆ Long Pulse (2 ms)
- ◆ Short Pulse (6us)
- ✕ Calibration Data
- Long Pulse (25 us)
- Linear (Long Pulse (2 ms))
- Linear (Short Pulse (6us))

M/Zwart/diodedata/diodep



Manufactured in Novosibirsk
7.0 TESLA

Stored Polarized Electrons 669 MeV - Snake On



Compton Polarimeter

Bill Franklin et. al.



Coherent Verdi

LBO doubled Nd:YV04 (Vanadate)

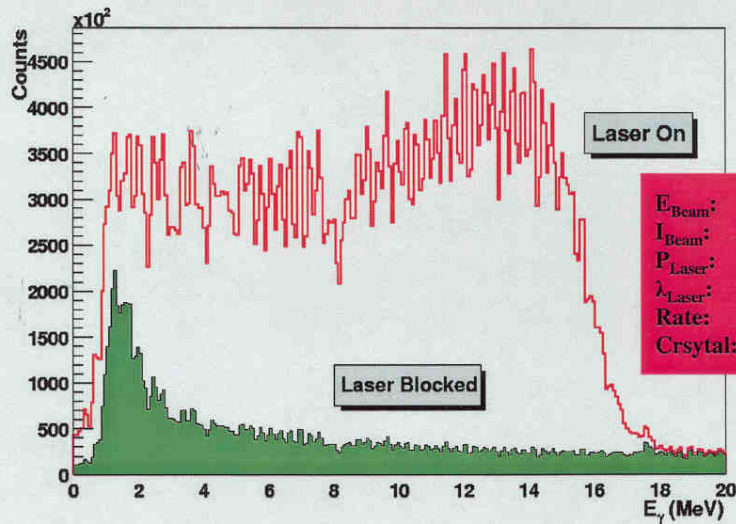
Power: 5W λ : 532 nm ϵ : 2.25 mm x 0.5 mm

Single Mode

Excellent Power and Pointing Stability

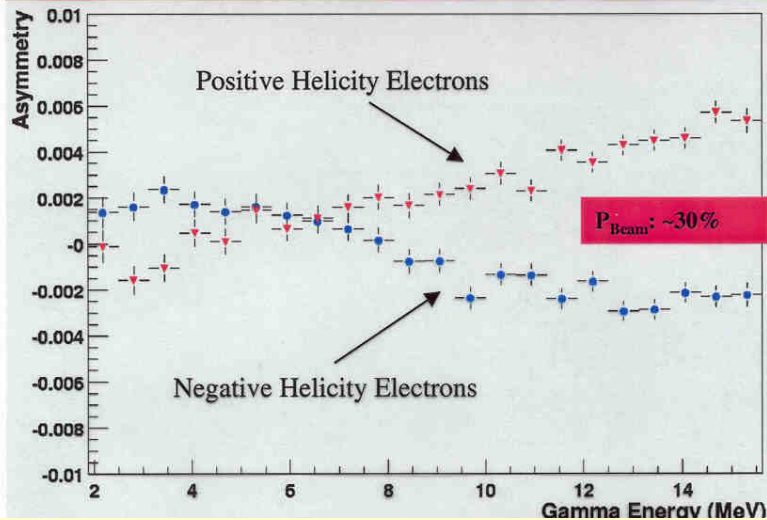
Frequency Doubling Possible (~2W of 266 nm)

Backscattered Photon Spectrum

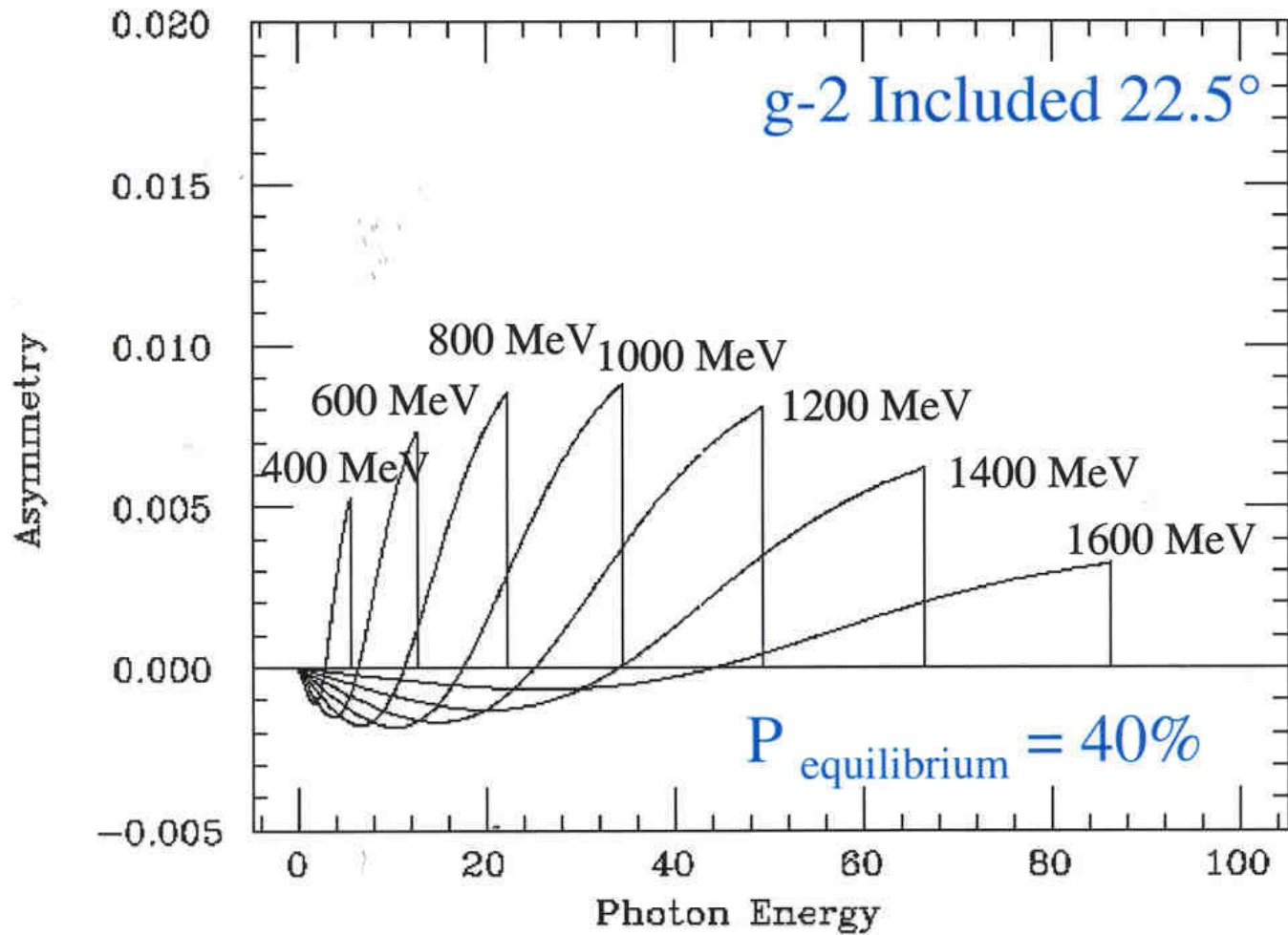


E_{Beam} : 669 MeV
 I_{Beam} : 50 mA
 P_{Laser} : 5 W
 λ_{Laser} : 532 nm
Rate: 250 kHz
Crystal: CsI

Measured Asymmetry

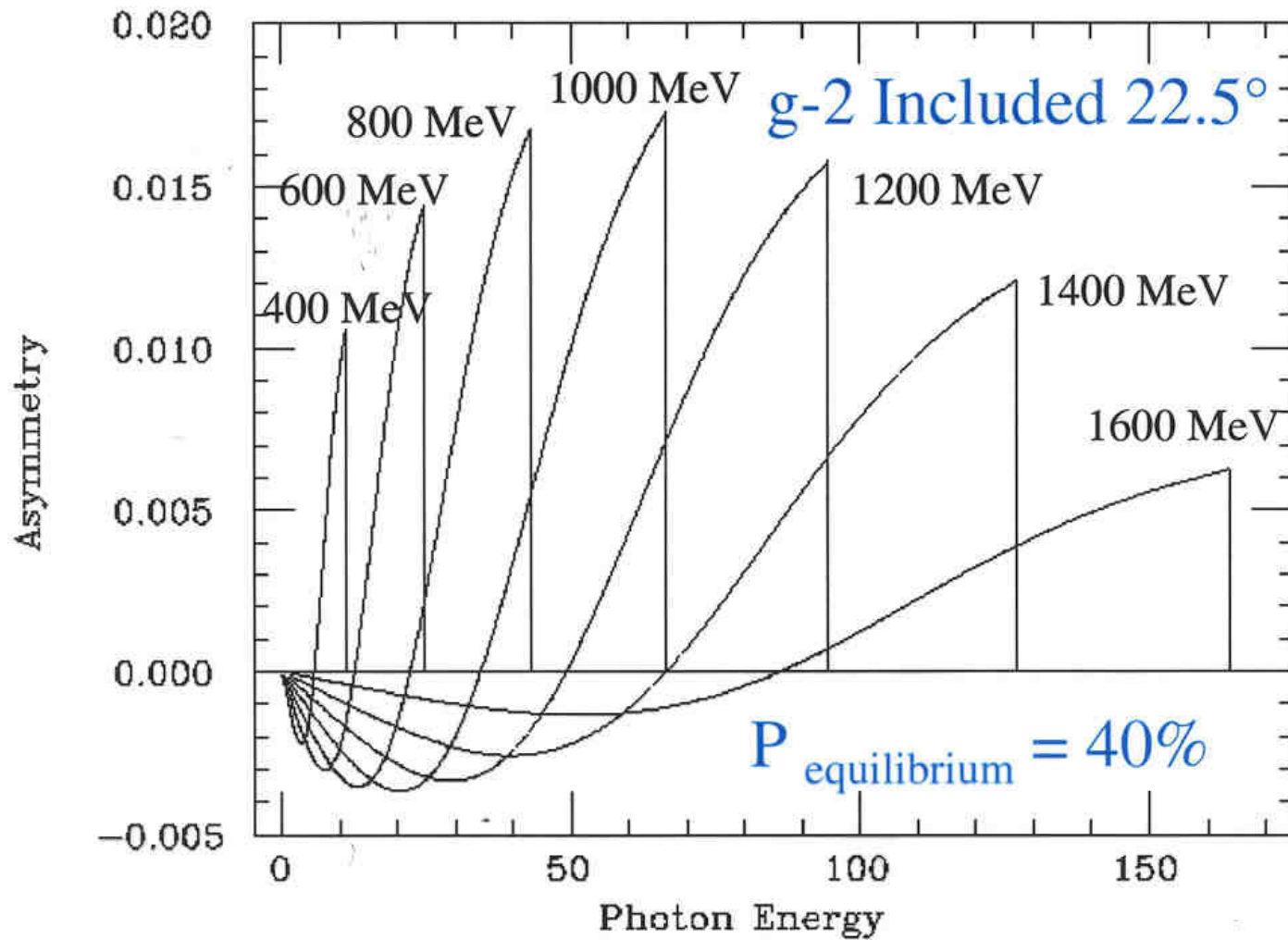


Compton Asymmetry



$\lambda = 532 \text{ nm}$

Compton Asymmetry

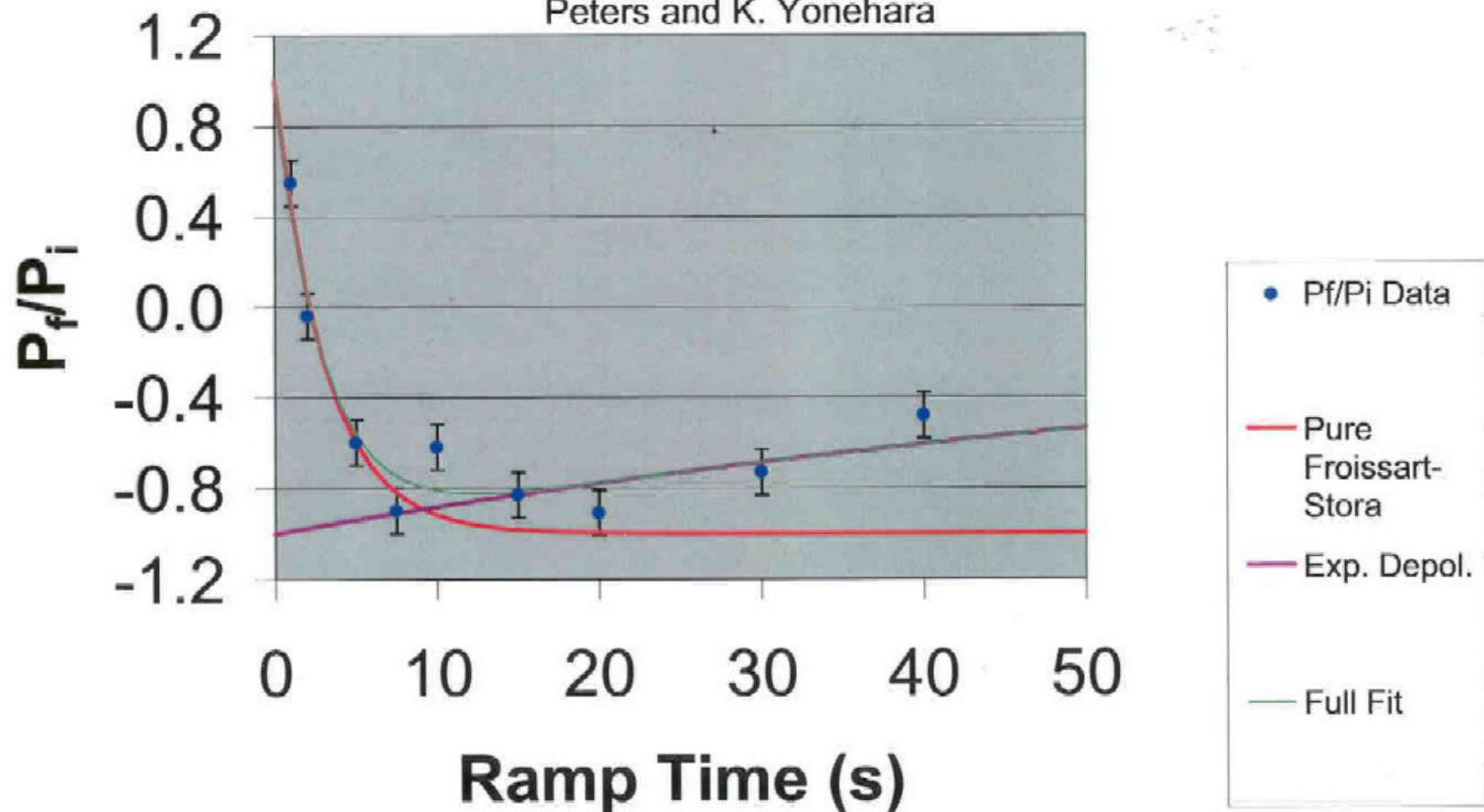


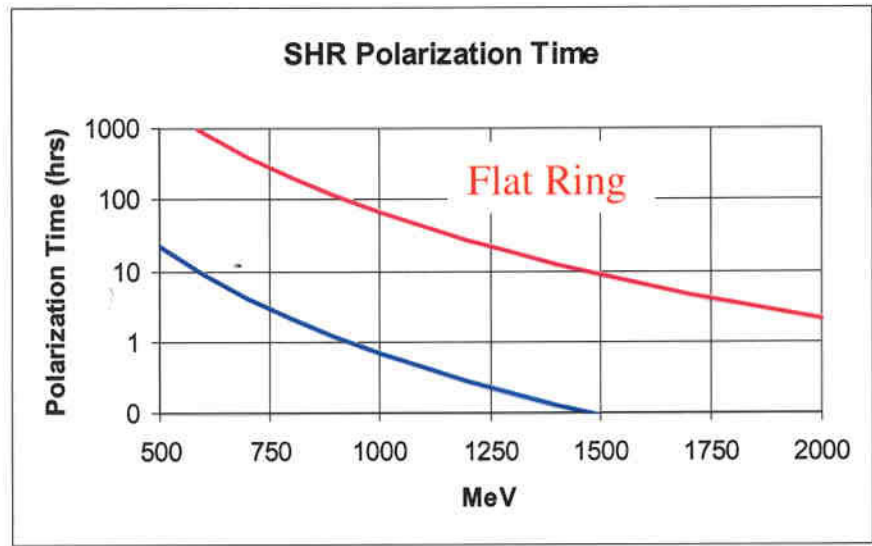
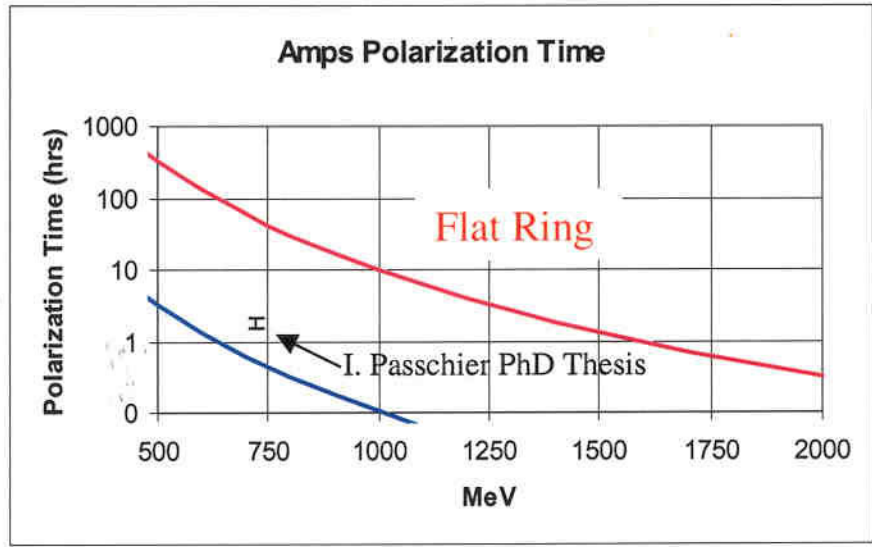
$\lambda = 266 \text{ nm} !$

Froissart-Stora Spin Flipper

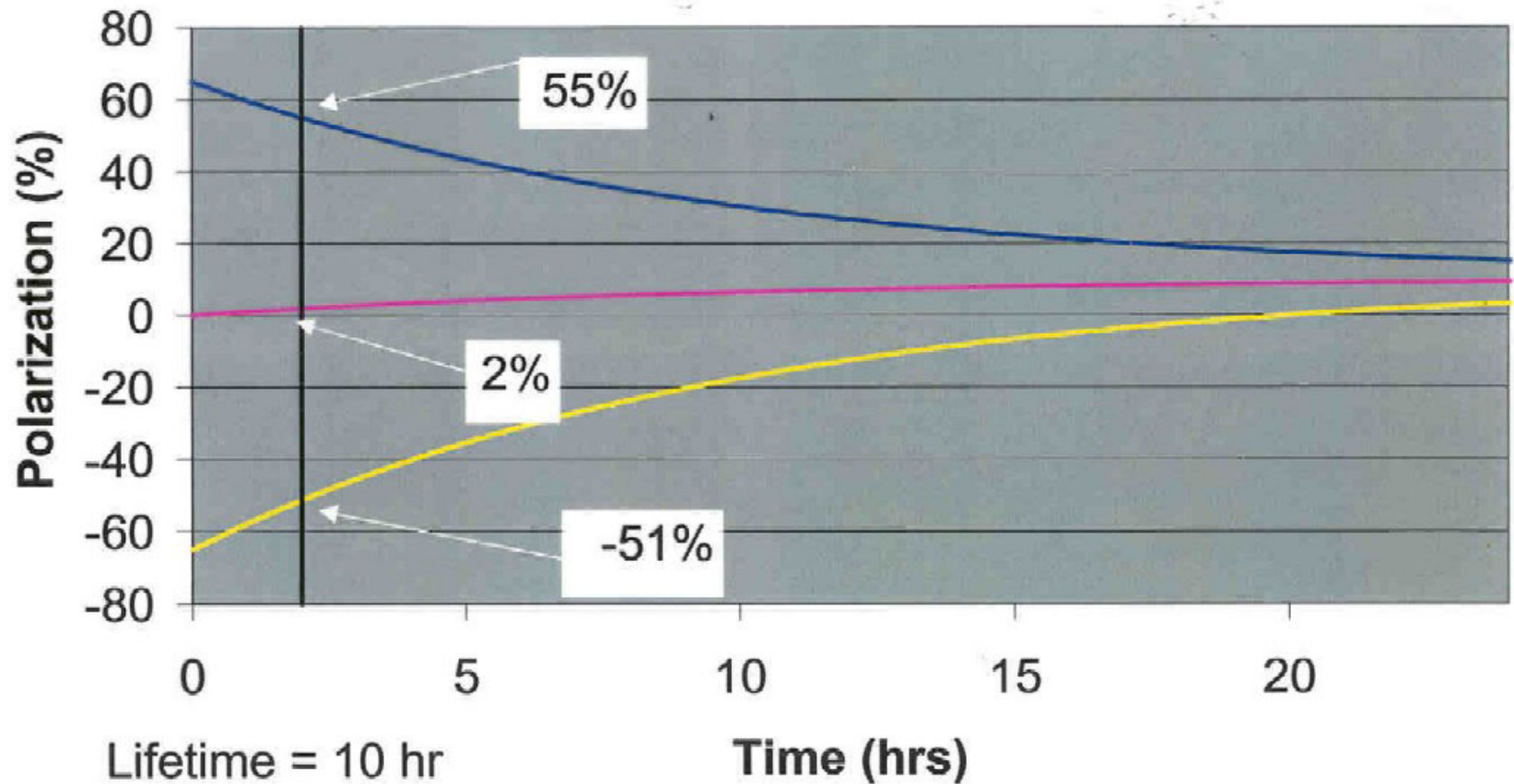
V.A. Anferov, B.B. Blinov, A.D. Krisch, W. Lorenzon, V.S. Morozov, C.C.

Peters and K. Yonehara

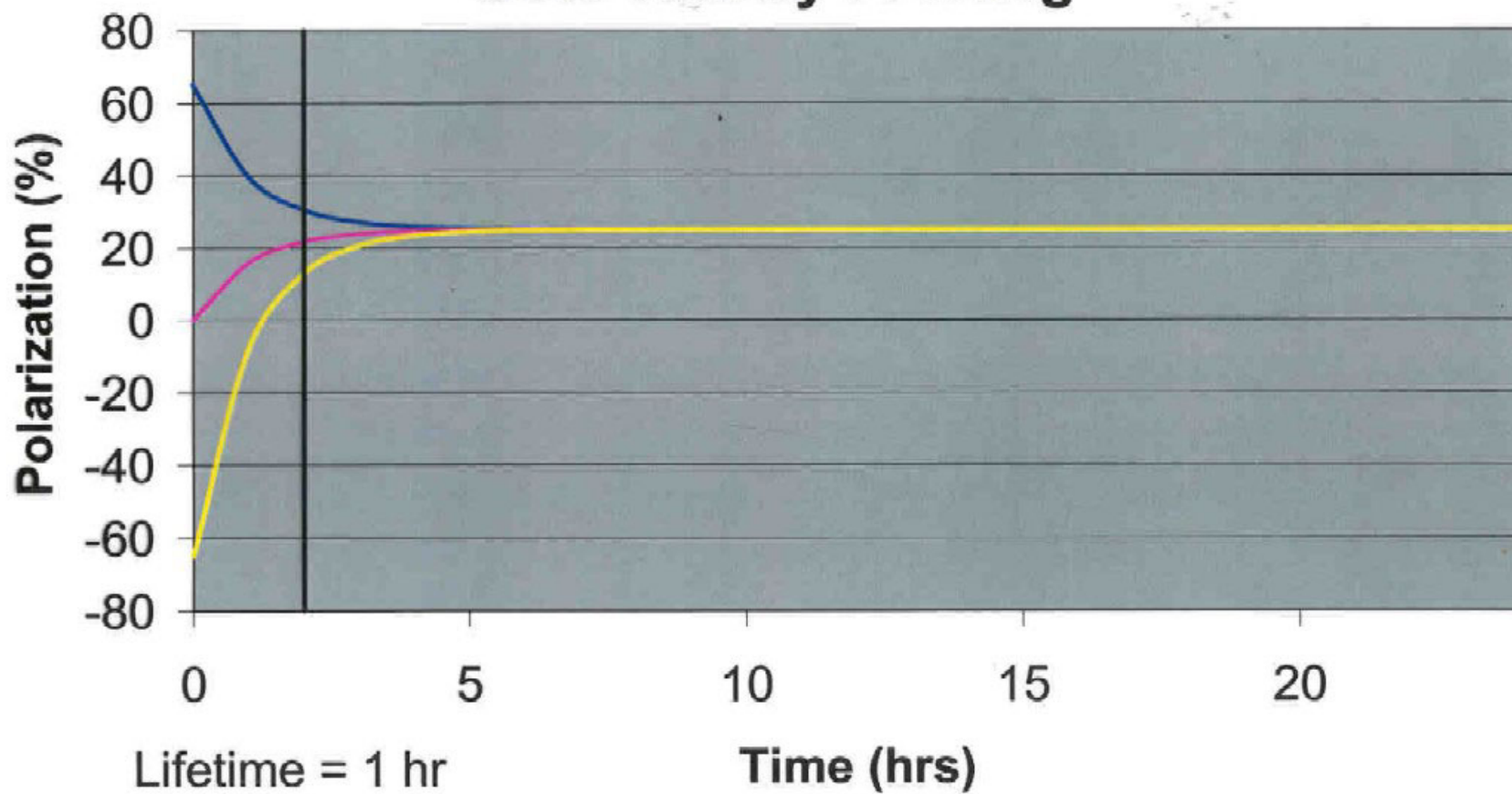




Radiative Polarization Today (Shatunov suggestion)



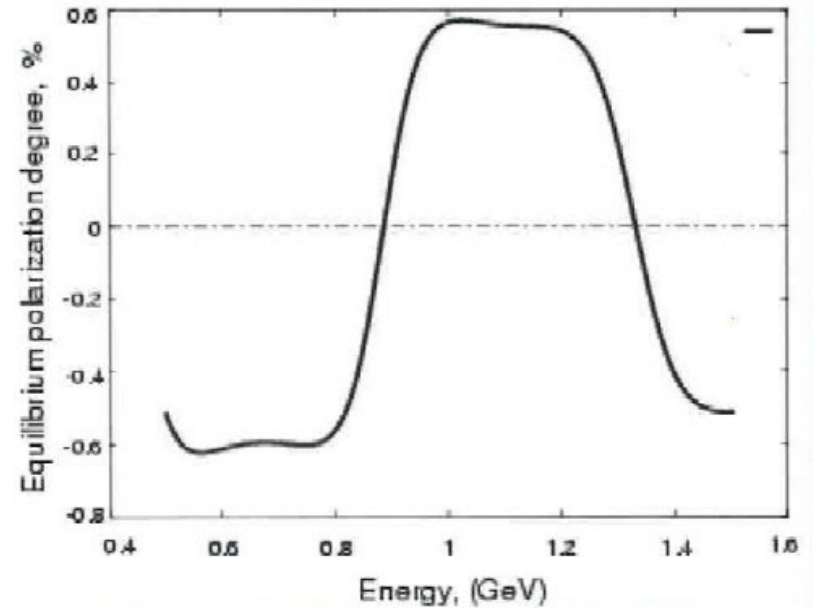
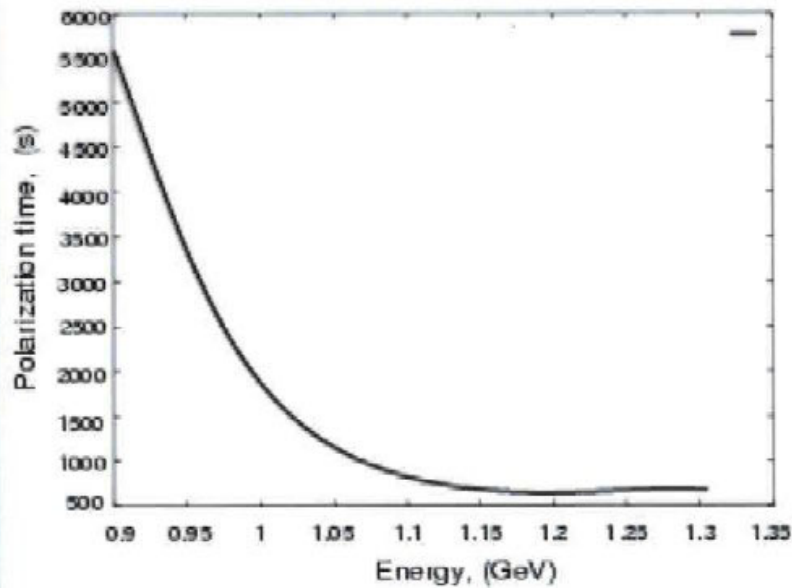
Kinetic Radiative Polarization Tomorrow Wiggler(s) ! Goto Talk by F. Wang



Shatunov Proposal

Goto Y.M. Shatunov talk

Add Wiggler + RF to SHR



Conclusions

1) Bates is in a good position to make definitive measurements of the electron radiative polarization and rigorously test the Derbenev Kondratenko formula, particularly the “Kinetic” term. This will also provide a stringent test of computer programs used to predict equilibrium polarization in electron rings.

2) Bates has the manpower and most of the infrastructure to achieve this goal. The addition of a superconducting Wiggler magnet and one additional RF cavity in the SHR are necessary to best realize program.

Advanced Concepts for EIC

Ya. Derbenev

Jefferson Laboratory

EIC Accelerator Workshop

BNL

February 26-27, 2002



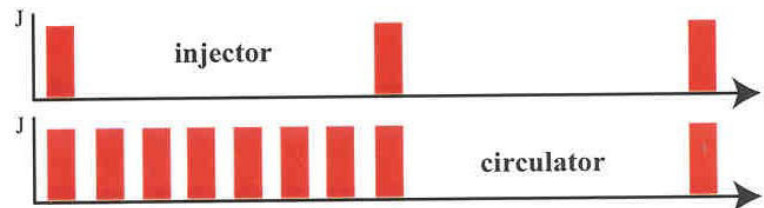
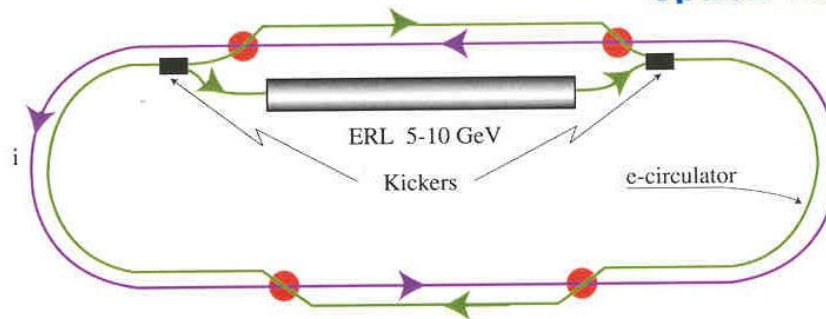
Contents

- **Electron Beam:**
 - **Electron Circulator**
 - **Scanned Photocathode**
 - **Hollow Beam Injector with Beam Concentrator**
- **Ion Beam:**
 - **Smoky Beam Injection in Booster**
 - **Optimizing the Electron Cooling**
 - **Very Short Bunches**
- **Interaction Point:**
 - **Low Beta***
 - **Crab Crossing**
 - **Traveling Ion Focus**
 - **Circular Colliding Beams**
- **Spin:**
 - **Solenoid Snakes for Electrons**
 - **Twisted Orbits**
 - **Longitudinal Snakes for Protons**
 - **Spin Control for d and He**
 - **Flipping Spin**



Circulator Rings for LR Collider, or LCR option

- Macropulse source regime (high pulse / low average value)
- Number of revolutions in CR = macro-duty factor
- High circulating current = macropulse value
- Still ERL CW, although:
- Pulse SRF linac in alliance with CR as damping accumulator might be an interesting option
- Naturally convertible to pure LR option when beneficial



LCR features

Respectively the RR option:

- Easy spin (no crossing resonances, no quantum depolarization)
- Emittance determined by the photoinjector (CR regime)
- Easily variable energy
- Easier interaction point (no depolarization of bends to appear)
- Larger admissible beam-beam tune shift (higher lumi)
- Larger accessible circulating current

Respectively the LR option:

- Photoinjector released of high average current
- Reduction of BBU in SRF linac
- Reduction of HOM

Issues:

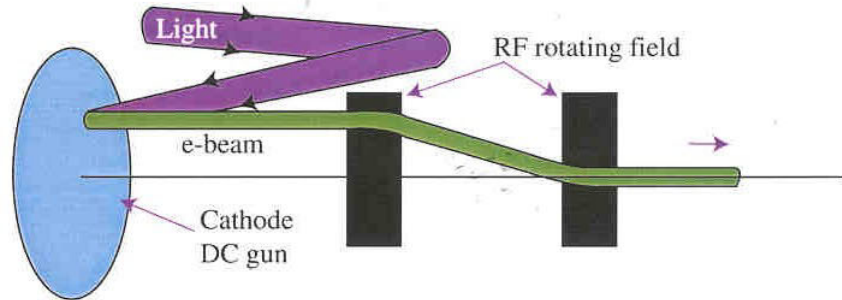
- Fast ejection-injection (develop best kickers)
- Microwave stability of short bunches in CR
- CSR effect
- SRF in CR to maintain short bunches



Possible Advances In Photo Injector

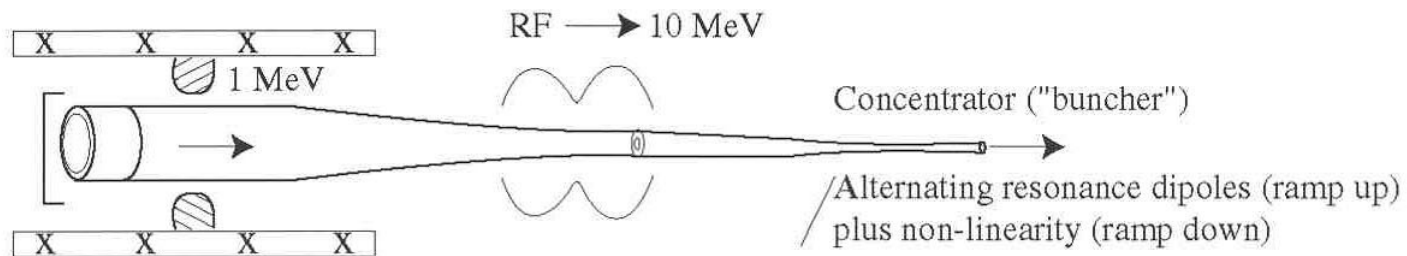
Scanned Cathode Photogun

The goal: To extend cathode lifetime while emittance is still reduced



Hollow Beam Injector with Beam Concentrator

The goal: Reduction of space-charge effect on emittance

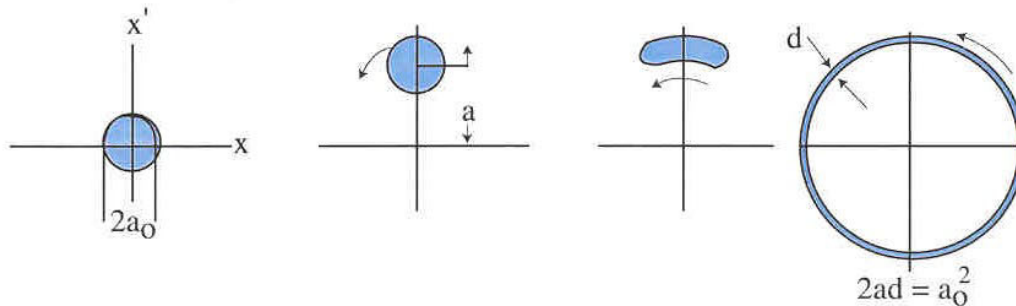


Smoky Ion Beam Injection in Booster

/ how to stack ion beam in booster over space charge limit maintaining beam emittance/

- Halo transformation of ion beam in phase space after linac

/process similar to beam debunching in a ring: after beam kick, an introduced resonance dipole field (static) drops adiabatically along the beam path /



/Similar gymnastics in y-plane/

Beam stacking:

- Focus the smoky beam to stripping foil
- Use beam raster applying an RF dipole field (compensated)

Turning the smoky beam back to the true size:

- After beam longitudinal bunching/acceleration to a large gamma in booster, make the reverse halo gymnastics in phase space by resonance RF dipoles



Electron Cooling and Luminosity

Optimizing the Electron Cooling

Measures to undertake:

- **Equalize cooling rates using the *dispersive mechanism***
- **This allows to avoid beam extension, hence, relax of the *alignment demands***
- ***Reduce x-y coupling outside the cooling section to a minimum***

Then, one gets a minimum critical electron current and ion equilibrium (flat beam) against IBS

Very Short Ion Bunches

- *Electron cooling in cooperation with a strong SRF allows to obtain very short ion bunches (1cm or even shorter)*

Circulators for Electron Cooling

- **Cooling of intense ion beams (up to a few Amps) requires a high electron current (hundreds of mA), in order to defeat the IBS**

This request can be satisfied at ERL incorporated with Circulator

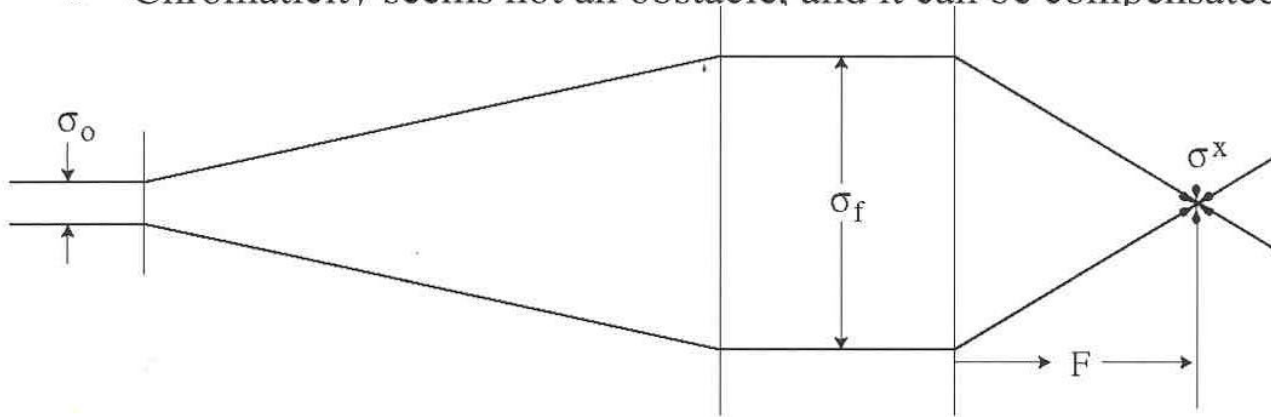


Low Beta-star for Ion Beam

Small transverse and longitudinal beam size (both after cooling) allow one to design quite a strong final focus:

β^* about 1 cm or even shorter

- Chromaticity seems not an obstacle, and it can be compensated if needed



$$\beta^* = \frac{F^2}{\beta_f} = \frac{F^2}{\beta_0} \left(\frac{\sigma_0}{\sigma_f} \right)^2 = \frac{F^2}{\gamma \sigma_f^2} \epsilon_n$$

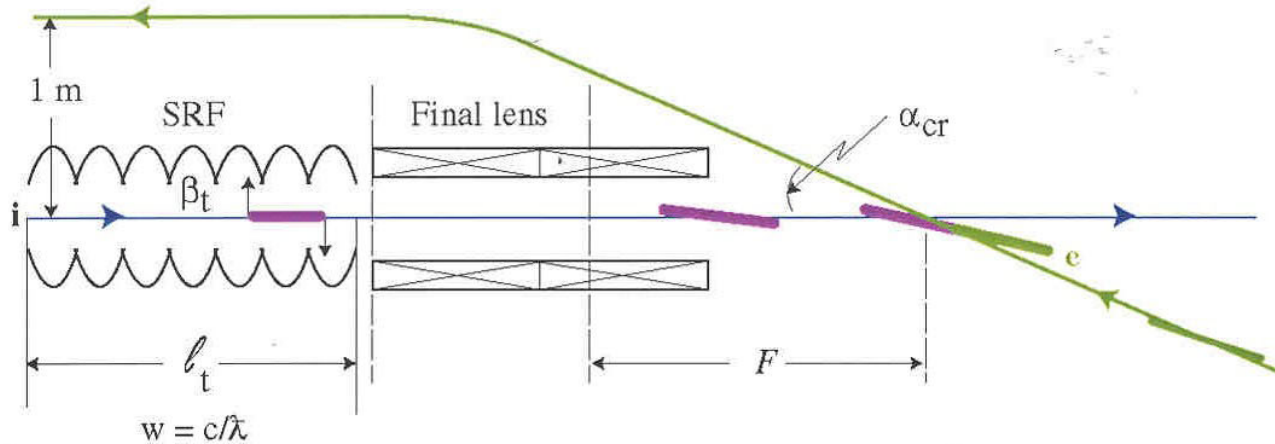
Parameter	Units	Value
γ		100
F	m	3
σ_f	mm	2
ϵ_n	4×10^{-5} cm	1

$\beta^* = 1$ cm



Crab Crossing for Interaction Point

- Short bunches also make feasible the Crab Crossing:
- SRF deflectors 1.5 GHz can be used to create a proper bunch tilt



$$\alpha_{cr} = 2\alpha_f = 2\theta_t \frac{F}{\lambda}$$

$$\theta_t = \frac{eB_t l_t}{E}$$

$$E = 100 \text{ GeV}$$

$$F = 3 \text{ m}$$

$$\lambda = 20 \text{ cm} \quad (1.5 \text{ GHz})$$

$$B_t = 600 \text{ G} \quad (= 20 \text{ MV/m})$$

$$l_t = 4 \text{ m}$$

$$\sigma_f = 1 \text{ mm}$$

$$\alpha_{cr} = 0.1$$

$$\theta_t = 5 \cdot 10^{-4}$$

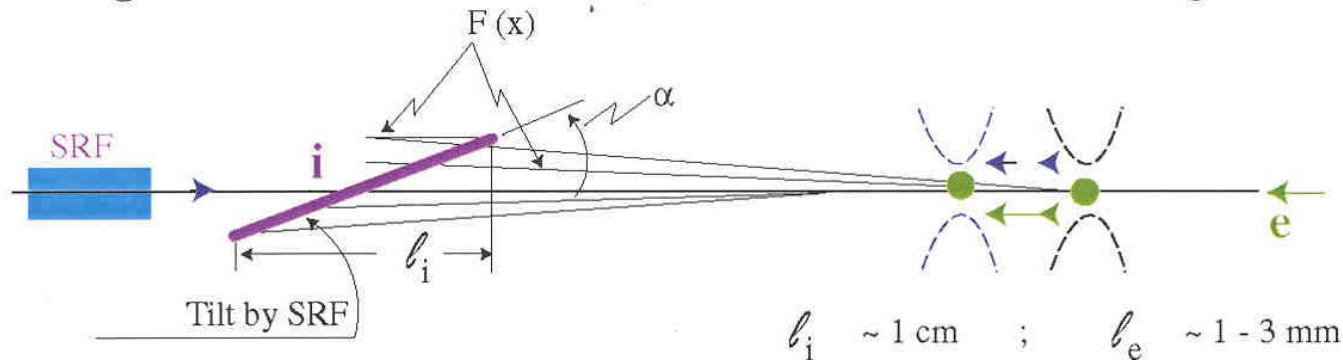


Traveling Ion Focus

/R. Brinkmann, 1995, general idea/

SRF deflectors (same) also can be used for arrangement of Traveling Focus (at $l_i \gg l_e$), in cooperation with sextupole non-linearity introduced in the final focusing magnets

- Traveling Focus allows one to decrease N_i or use bunches of a larger ϵ_i



$$\varphi = \frac{\omega}{c} s \quad \alpha = \frac{dx}{ds} \quad \beta_i^* \ll l_i$$

Matching condition: $\frac{dF}{ds} = \frac{1}{2}$ hence, $\frac{dF}{dx} = \frac{1}{2\alpha}$

$$\Delta F_b \sim \frac{1}{2} l_i \quad (\text{over the bunch})$$

ΔF over the aperture:

$$\Delta F_A = \frac{A}{2\alpha}$$

The feasibility condition:

$$\Delta F_A \ll F \Rightarrow \alpha \gg \frac{A}{2F}$$

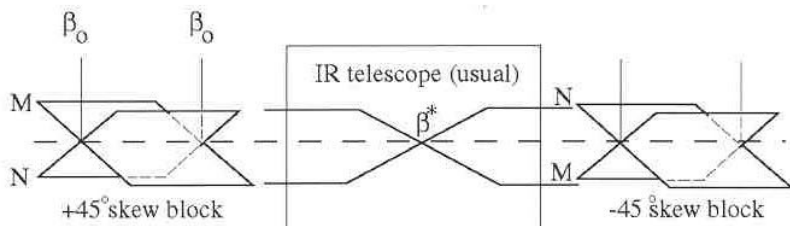
Ease to satisfy



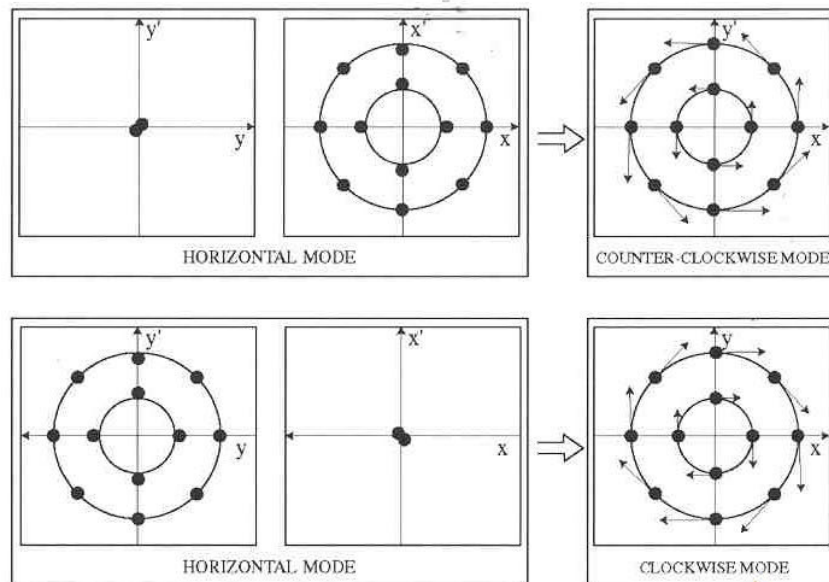
Circular Colliding Beams

- Arrangement of Circular Modes at interaction point improves the beam-beam stability

IR with Beam Rounders

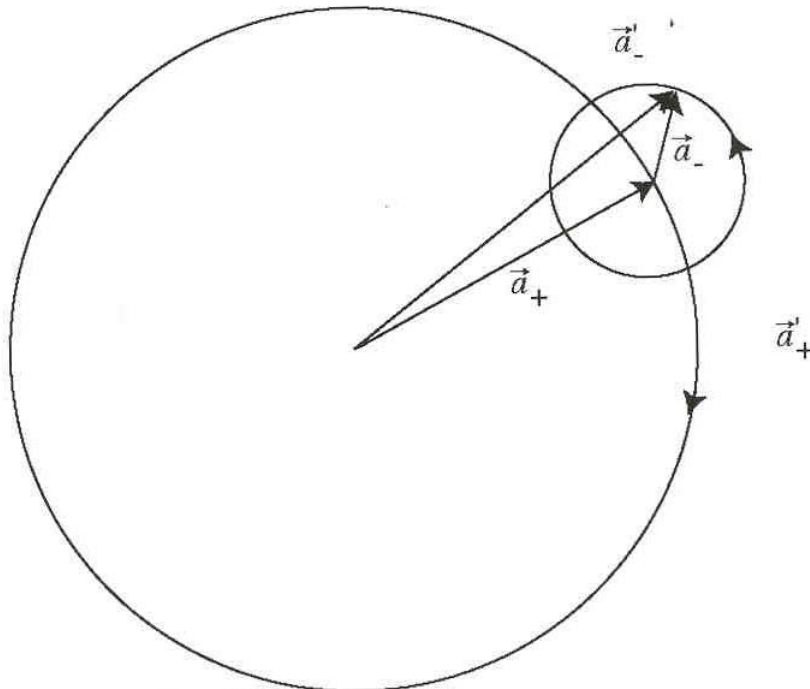


Planar to Circular Modes Transformation



Circular Colliding Beams

- Circular modes seem especially effective at a large aspect ratio ($\epsilon_x \gg \epsilon_y$), due to a strong reduction of particle radial oscillations (i.e. effective linearization of bb interaction)



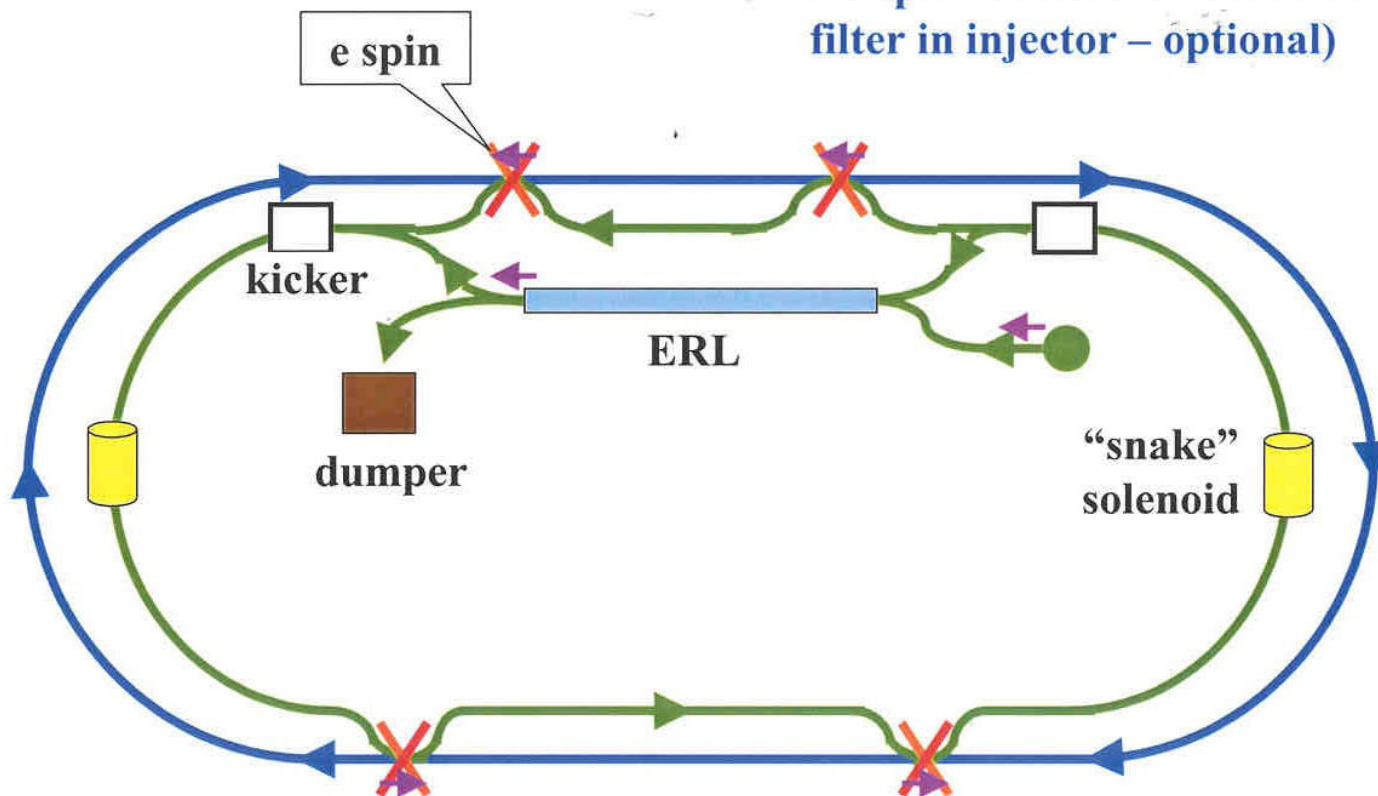
- Flat ion beams can be obtained with help of electron cooling
- Flat e-beams can be delivered to CR from a magnetized e-gun
- e-beams in storage rings are inherently flat
- a rotating electron beam at IP in CR can be delivered from a magnetized e-source



Spin Trends

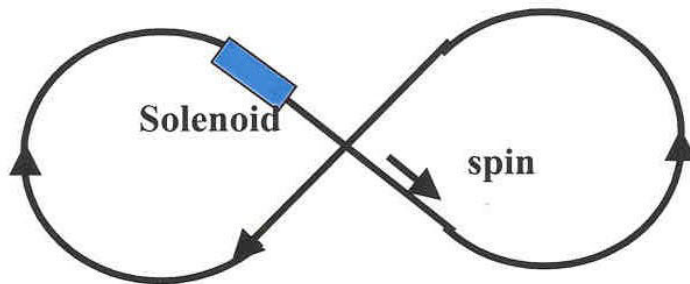
- Solenoid Snakes for electrons in CR

- Full solenoid snake at 5 GeV: 60 TM
- 10 : 120
- No spin rotators is needed in CR (Wien filter in injector – optional)



Spin Trends

Twisted Spin Synchrotrons



Spin features:

- zero spin tune
- No resonance crossing
- Intrinsic spin resonance stay away
- Longitudinal either transverse polarization is easily organized, stabilized and controlled for all the particle species (p, d, He, ..., and electrons)
- No spin rotators are needed
- Convenient for circulator, booster and collider rings suited for EPIC
- Easy longitudinal snakes for protons can be introduced (instead of 45 degree snake axis of RHIC), to make $\frac{1}{2}$ spin tune value
- Polarized beam acceleration problem is gone

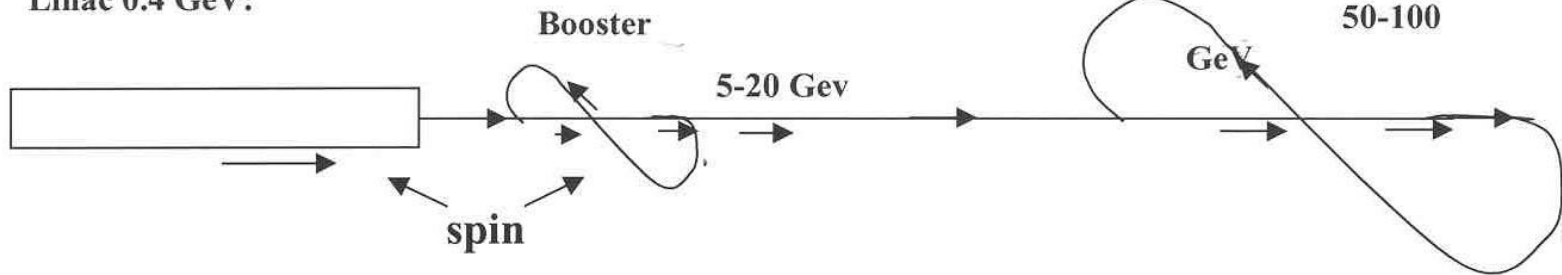


Spin Trends

Twisted Spin EIC rings

Ion spin track:

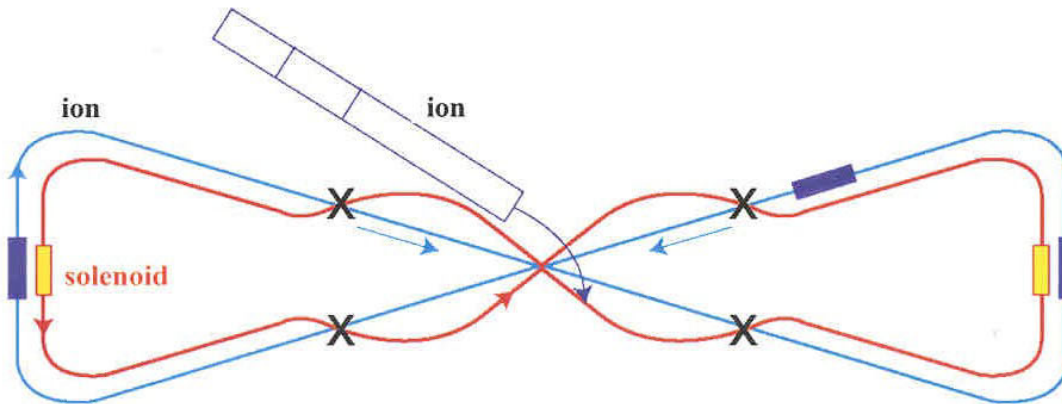
Linac 0.4 GeV:



• Longitudinal Snakes for Protons (ease)

- e – circulator could be used as ion booster

- 2 or 4 IP



Spin Trends

Spin control for D and He³

- Longitudinal spin can be stabilized by small solenoids
- Transverse (horizontal and longitudinal) spin both can be stabilized and controlled by horizontal dipoles distributed around arcs

Flipping spin

- Protons: all the possibilities that are available in conventional rings
- D and He: varying adiabatically the controlling dipoles field strengths and signs



Conclusion & Outlook

1. The SRF ERL technology provide a potential for
 - realization of high luminosity EIC (33-35 level), related to two major elements:
 - - polarized 5-10 GeV electron beam
 - - high quality e-beam for cooling of ion beam
2. Incorporation with circulator ring raises drastically the utilization efficiency of ERL
3. Improvements of the Interaction Region (crab crossing,...) seem easily compatible with the LR version of EIC (compatibility with the RR to be studied)
4. Possible new solutions for polarized ion beam transport (twisted rings) seem to raise essentially the EIC capabilities
5. A consistent concept of EIC luminosity level 34 seems possible to compose today basing on the existing state of art of accelerator and polarized sources technology
6. Luminosity level 35 seems possible at increase of a polarized electron source peak current by a factor of 10 (to 25 A)
7. Other approaches to efficient utilization of e-beam accelerated in SRF linac should be examined, as well (say, SRF linac incorporated with electron circulator in the regime of damping ring)



ELIC: An Electron - Light Ion Collider based at CEBAF

L. Merminga, K. Beard, Y. Chao, J. Delayen, Ya. Derbenev, J. Grames, A. Hutton, G. Krafft, R. Li, M. Poelker, B. Yunn, Y. Zhang

Jefferson Lab

EIC Accelerator Workshop
Brookhaven National Laboratory
February 26-27, 2002



Outline

- Nuclear Physics Requirements
- Basis of Proposal / Concept
- ELIC Layout
- Parameter Choices / Table
- Accelerator Technology issues
 - Polarized Electron Source, RF, SRF, Cryogenics
- Accelerator Physics Issues
 - Proton Ring
 - Energy Recovering Linacs
 - Electron-Ion Collisions
- Integration with 25 GeV Fixed Target Program
- R&D Topics and Conclusions



Nuclear Physics Requirements

- An electron - light ion collider with the following requirements has been proposed as a means for studying hadronic structure:
 - Center-of-mass energy between 20 GeV and 30 GeV with energy asymmetry of ~ 10 , which yields $E_e \sim 3 \text{ GeV}$ on $E_i \sim 30 \text{ GeV}$ up to $E_e \sim 5 \text{ GeV}$ on $E_i \sim 50 \text{ GeV}$
 - CW Luminosity from 10^{33} to $10^{35} \text{ cm}^{-2} \text{ sec}^{-1}$
 - Ion species of interest: protons, deuterons, He^3
 - Longitudinal polarization of both beams in the interaction region $\geq 50\%$ -80%
 - Spin-flip of both beams extremely desirable for exclusive measurements



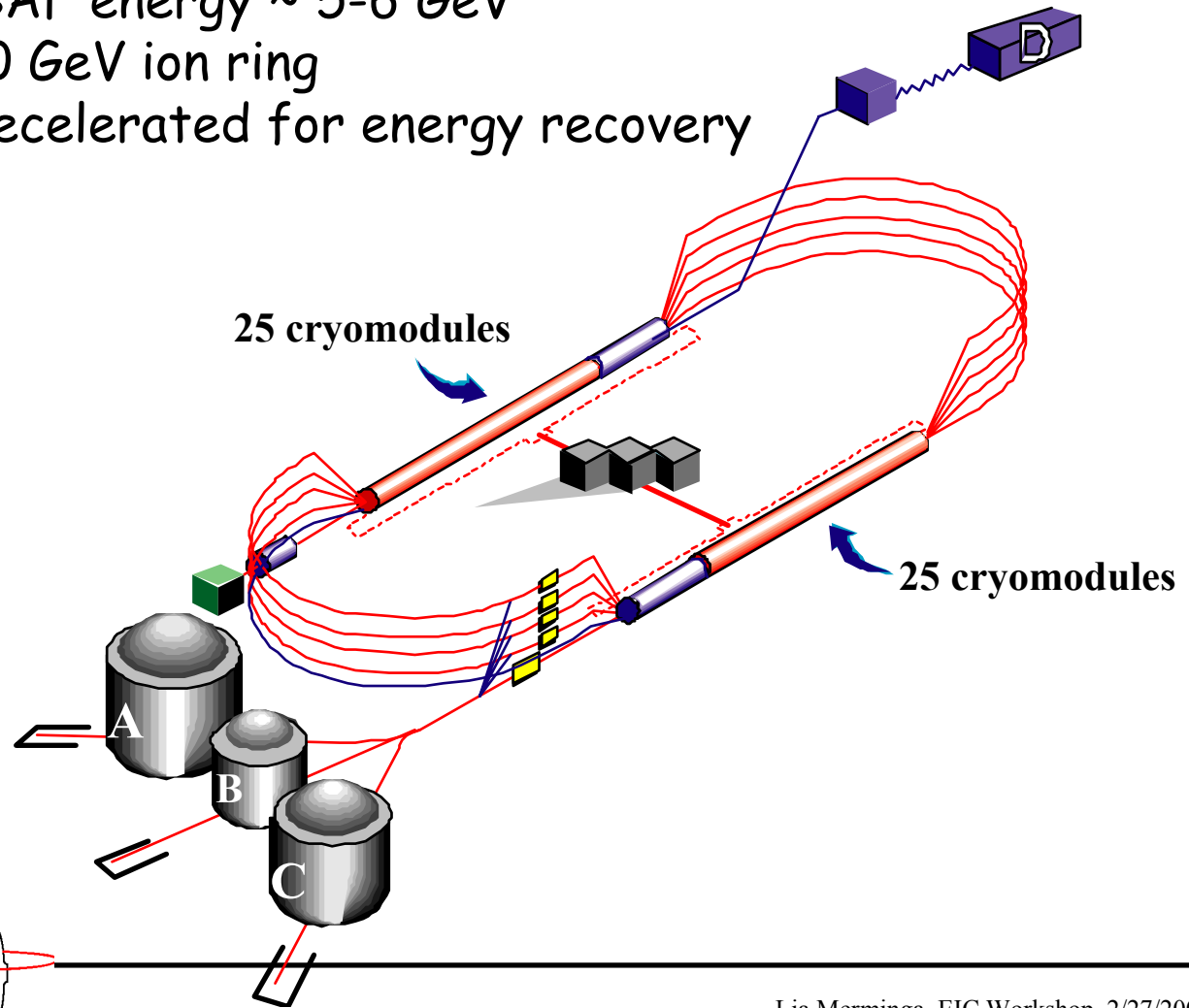
Basis of Proposal

- **CEBAF** is used for the acceleration of electrons
- **Energy recovery** is used for rf power savings and beam dump requirements
- **"Figure-8" storage ring** is used for the ions for flexible spin manipulations of all light-ion species of interest
- **Circulator ring** for the electrons may be used to ease high current polarized photoinjector requirements



CEBAF with Energy Recovery

- Install 50 Upgrade CEBAF cryomodules at ~ 20 MV/m in both linacs
- Single-pass CEBAF energy ~ 5 -6 GeV
- Collision with 50 GeV ion ring
- Electrons are decelerated for energy recovery



Jefferson Lab

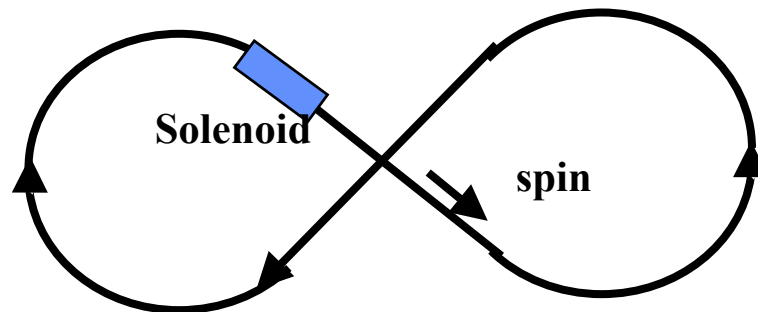
Thomas Jefferson National Accelerator Facility

Lia Merminga EIC Workshop 2/27/2002

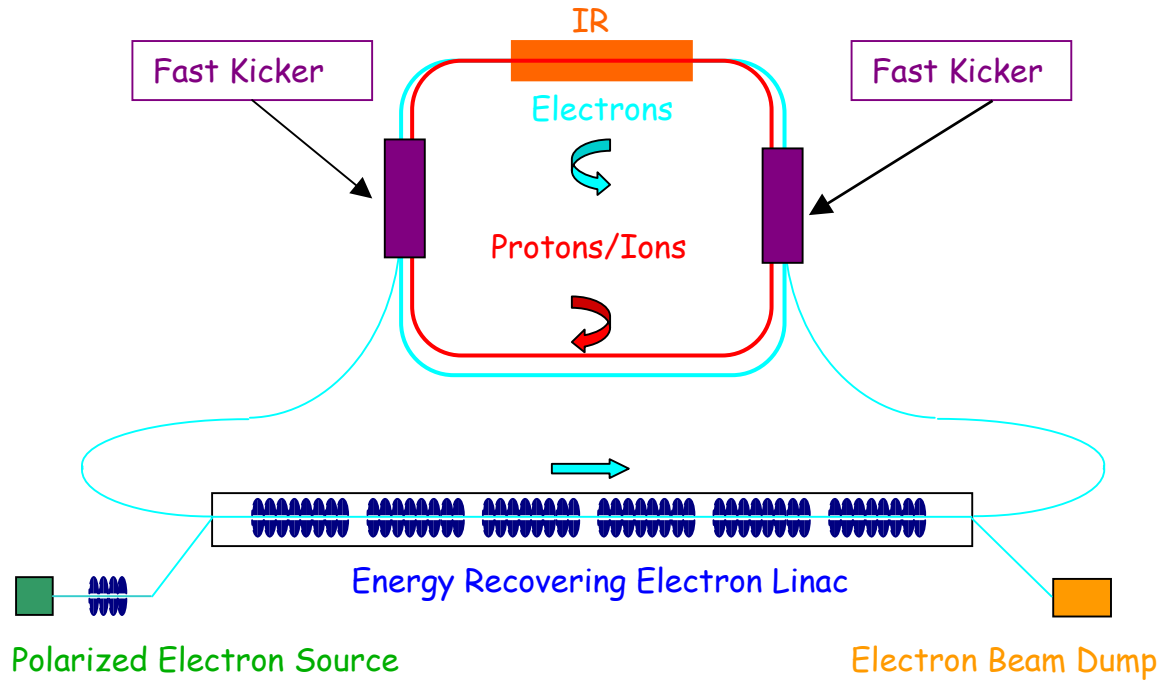
Operated by the Southeastern Universities Research Association for the U. S. Department of Energy

"Figure-8" Ion Ring

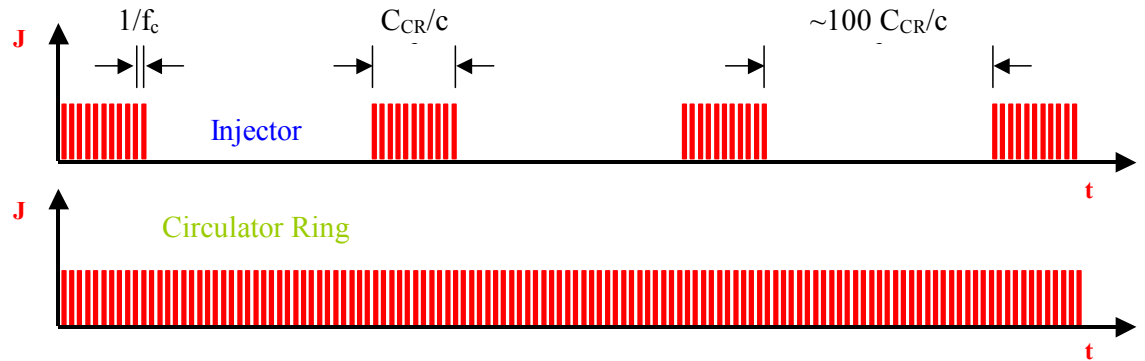
- Zero spin tune avoids intrinsic spin resonances
- No spin rotators are needed
- Can get longitudinal polarization for all ion species at all energies continuously



Circulator Ring



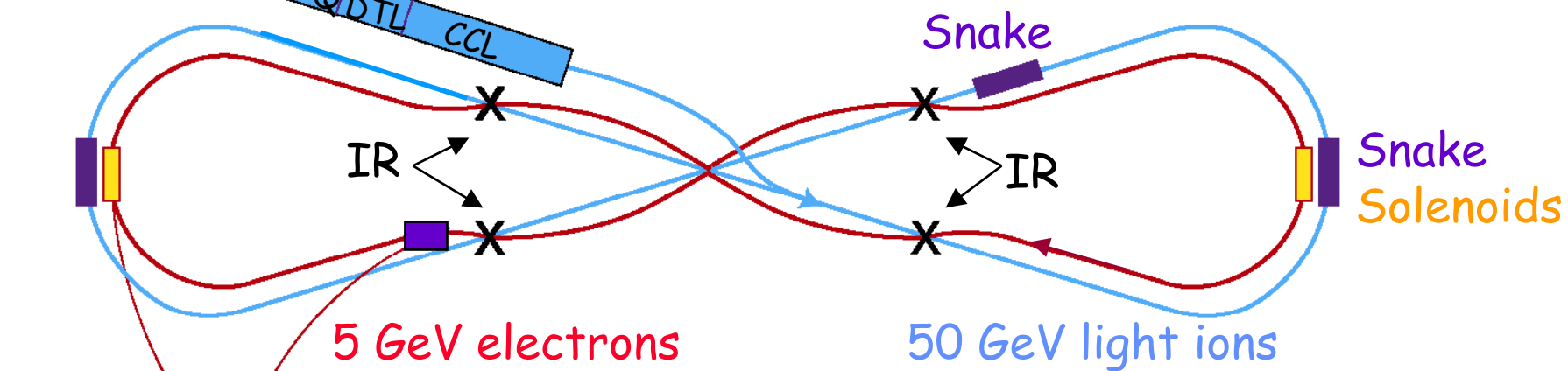
Different filling patterns are being explored (Hutton, Litvinenko)



ELIC Layout

Ion Source

RFQ DTL CCL



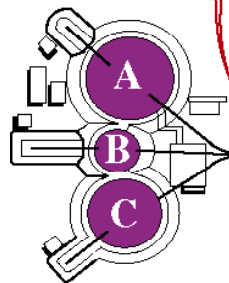
5 GeV electrons

50 GeV light ions

Injector



CEBAF with Energy Recovery



Beam Dump

Jefferson Lab

Lia Merminga EIC Workshop 2/27/2002

Parameter Choices

- We have developed self-consistent parameters for 4 point designs (PDs):
 - PD0: Max peak luminosity *without cooling* and parameters based on demonstrated performance to date
 - PD1: Max luminosity of $1 \times 10^{33} \text{ cm}^{-2} \text{ sec}^{-1}$
Electron cooling required
 - PD2: Max luminosity of $1 \times 10^{34} \text{ cm}^{-2} \text{ sec}^{-1}$
Electron cooling required -> short ion bunches
Circulator ring
Crab crossing
 - PD3: Max achievable luminosity
Electron cooling required -> short ion bunches
Circulator ring
Crab crossing
Traveling focus ?
- Assumptions
 $E_e = 5 \text{ GeV}$, $E_i = 50 \text{ GeV}$, $\epsilon_n^e = 10 \text{ } \mu\text{m}$, $\epsilon_n^i = 2 \text{ } \mu\text{m}$ (w/out cooling)
Equal beam sizes for electrons and ions are assumed at the IP



Parameter Table

Parameter	Units	Point Design 0		Point Design 1		Point Design 2		Point Design 3	
		e^-	Ions	e^-	Ions	e^-	Ions	e^-	Ions
Energy	GeV	5	50	5	50	5	50	5	50
Cooling	-	-	No	-	Yes	-	Yes	-	Yes
Lumi	$\text{cm}^{-2} \text{sec}^{-1}$	1×10^{32}		1×10^{33}		1×10^{34}		6×10^{34}	
N_{bunch}	ppb	1×10^{10}	2.5×10^{10}	1×10^{10}	2.5×10^{10}	2×10^{10}	5×10^9	1×10^{10}	1×10^{10}
f_c	MHz	150		150		500		1500	
I_{ave}	A	0.24	0.6	0.24	0.6	1.6	0.4	2.5	2.5
σ^*	μm	45	45	14	14	6	6	4.5	4.5
ϵ_n	μm	10	2	10	0.2	10	0.2	10	0.1
β^*	cm	200	5	20	5	4	1	2	1
σ_z	cm	0.1	5	0.1	5	0.1	1	0.1	1
ξ_e / ξ_i	-	0.5	.0006	0.5	0.006	0.1	0.01	0.2	0.01
Δv_L	-	-	0.005	-	0.05	-	0.05	-	0.09



Accelerator Technology Issues

■ Electron Source

→ State of the art in high average current, polarized sources:
~1 mA at 80% polarization [C. Sinclair, JLab]

Circulator ring appears promising

■ RF Issues

ERLs favor high Q_{ext} for rf power savings, increased system efficiency
For 25 Hz amplitude of microphonic noise, optimum $Q_{\text{ext}} \sim 3 \times 10^7$

→ RF Control becomes more difficult with high Q_{ext} at high gradient
(See J. Delayen, "RF Issues in Energy Recovering Linacs" L/R WG)

■ Superconducting RF Issues

→ Demonstrate high CW gradient (18 MV/m) at high Q_0 (1×10^{10})

■ Cryogenics

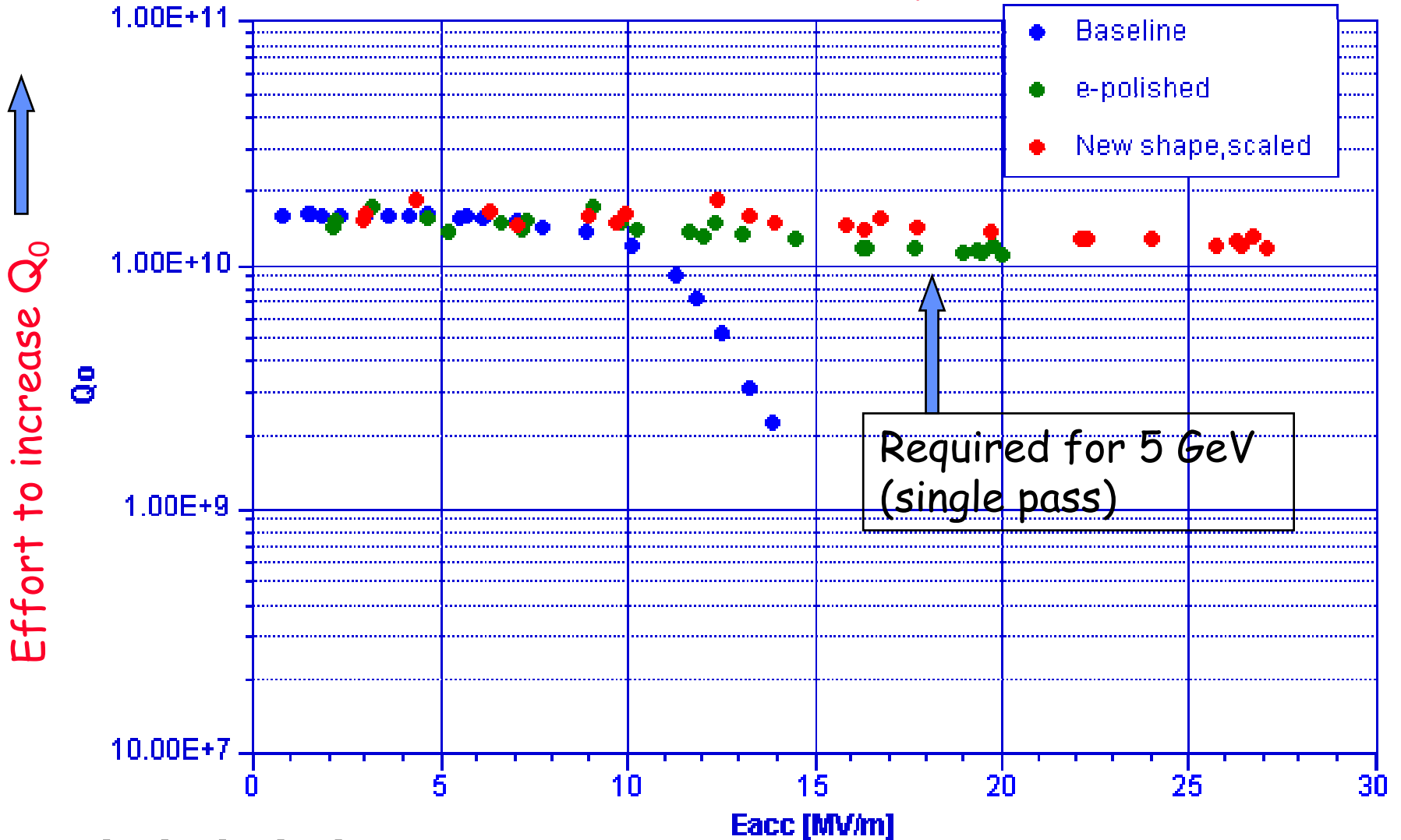
→ At $Q_0 = 1 \times 10^{10}$ dynamic load ~10 kW, installed ~20 kW (x2 Upgrade CEBAF)



Jefferson Lab 7-cell Cavity



Jefferson Lab 7-cell Cavity Performance



Accelerator Physics Issues of the Proton Ring

- Intrabeam scattering: Transverse and longitudinal
⇒ For luminosity $>10^{33} \text{ cm}^{-2}\text{sec}^{-1}$ electron cooling is required
- Collective Effects
 - Longitudinal mode coupling
 - Transverse mode coupling instability



Accelerator Physics Issues of the ERL

- Accelerator Transport
 - Demonstrate energy recovery with large energy ratio
 - An energy recovery experiment at CEBAF has been proposed and is being planned (D. Douglas)
- Beam Loss
 - Is 4×10^{-6} relative loss achievable?
- Collective Effects
 - Single-bunch effects
 - Emittance growth and energy spread due to wakes
 - Multipass, Multibunch Beam Breakup (BBU) Instability
 - $I_{th} \sim 200$ mA, growth rate ~ 2 msec \Rightarrow feedback ?
- HOM Power Dissipation
 - \sim kW per cavity
 - JLab FEL and the ERL Prototype (Cornell/JLab) to address several of these issues



Accelerator Physics Issues of the Electron-Ion Collisions

- IR design integrated with real detector geometry
- Crab crossing tolerances and resonance excitation effects
- Emittance growth of the electrons (which have to be recirculated and energy recovered) due to a single collision with the protons $\Rightarrow N_p < 1.5 \times 10^{12}$
- Beam-beam kink instability



Beam-Beam Kink Instability

- The beam-beam force due to the relative offset between the head of the proton bunch and the electron beam will deflect the electrons. The deflected electrons subsequently interact with the tail of the proton bunch through beam-beam kick.
- The electron beam acts as a transverse impedance to the proton bunch, and can lead to an instability.
- In the linear approximation, and disregarding the evolution of the wake within the proton bunch, a stability criterion has been derived [Li, Lebedev, Bisognano, Yunn, PAC 2001]

$$D_e \xi_p \leq 4\nu_s$$

- For the case of equal bunches and linear beam-beam force, chromaticity appears to increase the threshold of the instability [Perevedentsev, Valishev, PRST '01].
- The instability has been observed in numerical simulations [R. Li, J. Bisognano, Phys. Rev. E (1993)] during the beam-beam studies of linac-ring B-Factory. The code is presently being used to simulate unequal bunches and a nonlinear force. We also expect chromaticity to be beneficial in this case

* See Rui Li, "Beam-beam stability in Linac-Ring colliders" L/R WG



Beam-Beam in Linac-Ring Colliders

PHYSICAL REVIEW E

VOLUME 48, NUMBER 5

NOVEMBER 1993

Strong-strong simulation on the beam-beam effect in a linac-ring *B* factory

Rui Li and Joseph J. Bisognano

Continuous Electron Beam Accelerator Facility, 12000 Jefferson Avenue, Newport News, Virginia 23606

(Received 16 April 1993)

Since the inherently low emittance required by the linac-ring *B* factory implies high disruption for the linac bunch, previous investigations of the beam-beam tune-shift limit may not apply. A strong-strong simulation scheme was developed based on a macroparticle model to simulate beam-beam interaction in this situation self-consistently. Included in the ring dynamics are linear betatron oscillations and synchrotron motion, as well as transverse and longitudinal damping and quantum excitation. As a benchmarking test, the coherent quadrupole effect in a ring-ring collider was observed by the simulation. The code was then used to study the stability of the storage-ring bunch in a linac-ring collider and yielded strong synchrotron coupling due to the deep envelope modulation of the linac bunch. It was, however, observed that when initial conditions for the linac beam were properly chosen to match the focusing provided by the ring beam at IP, the beam-beam tune-shift limit of the ring beam could be comparable to that of a ring-ring collider.

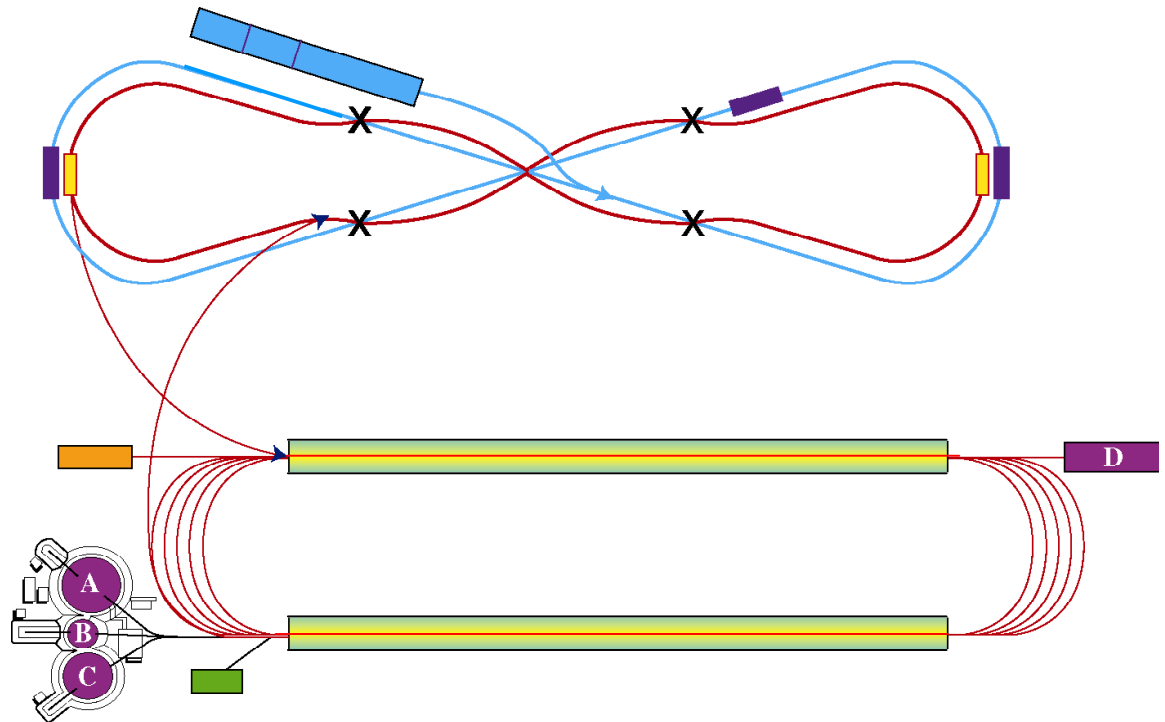
PACS number(s): 41.85.-p, 41.75.-i



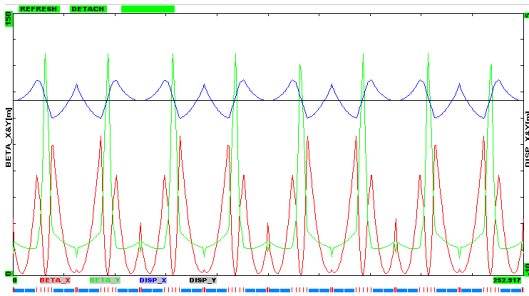
Integration with 25 GeV Fixed Target Program

- Five accelerating passes through CEBAF
⇒ 25 GeV Fixed Target (FT) Program
- One accelerating/one decelerating pass through CEBAF
⇒ 30 GeV CM Collider Program

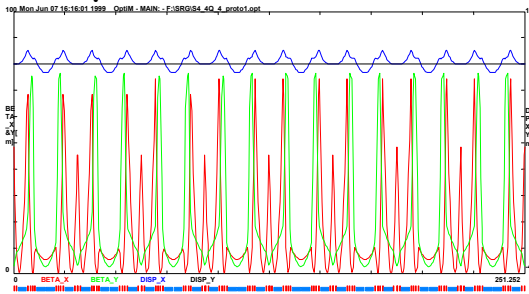
Exploring whether
collider and fixed
target modes can run
simultaneously or in
alternating mode



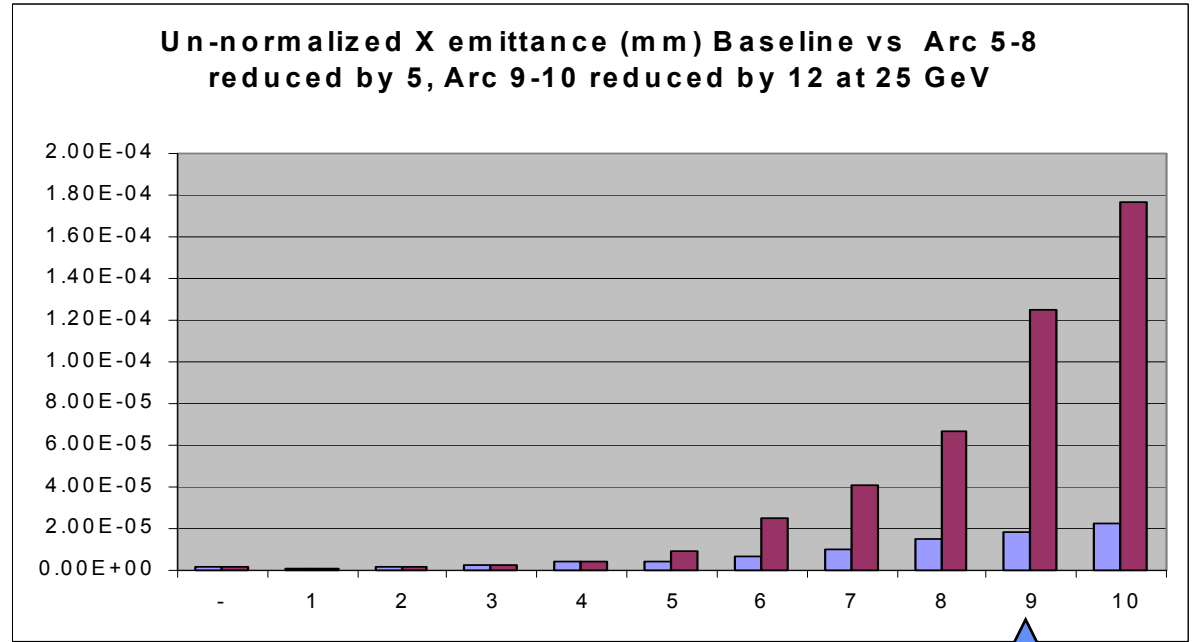
Feasibility of 25 GeV FT Program at CEBAF



Optics for arcs 5-8



Optics for arcs 9, 10



Arc 9 β -functions ~ 70 m

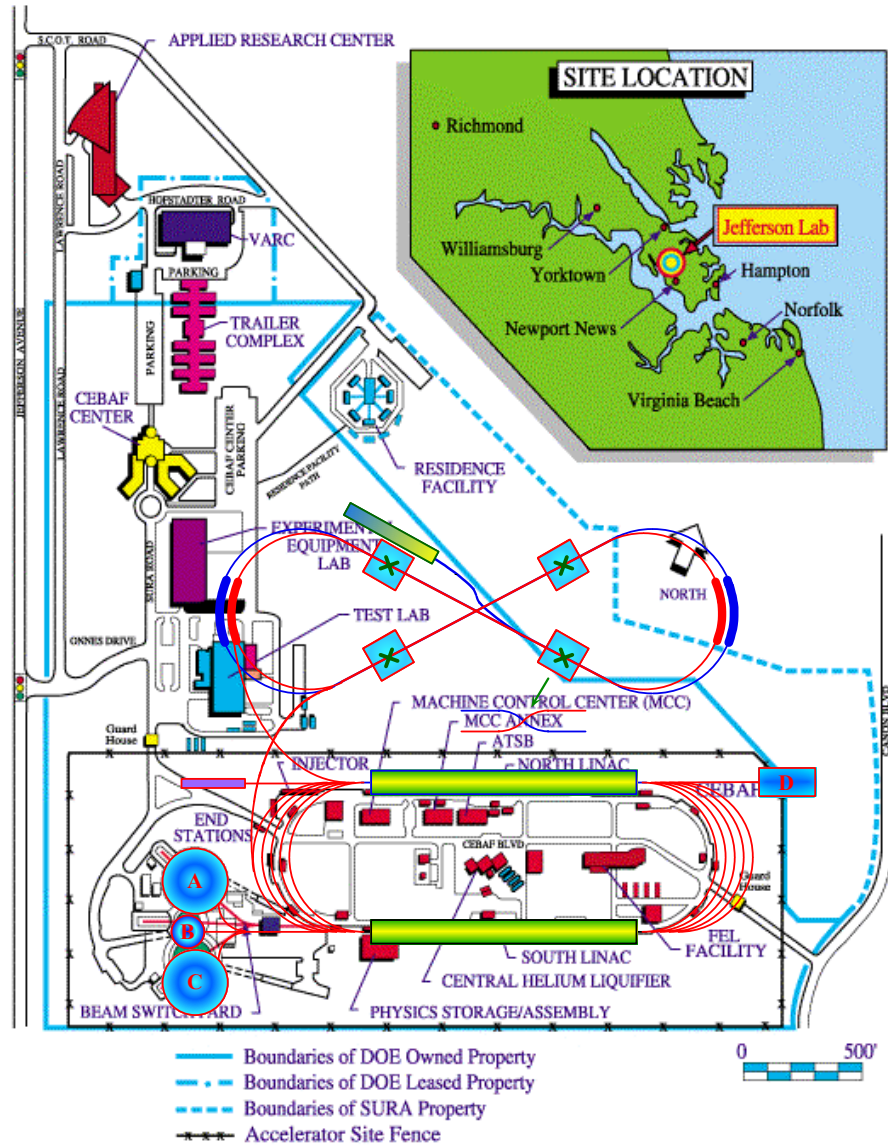
Emittance incl. SR at arc 9: 2×10^{-8} m rad

SR leads to spot sizes at the IP of 0.3-0.5 mm at 25 GeV

See Y. Chao, Jlab TN 99-037



Site Map



Conclusions / R&D Strategy

- The feasibility of an electron-light ion collider based at CEBAF has been examined
- Self-consistent sets of parameters have been developed
- Luminosities of 10^{33} to several 10^{34} appear feasible. Electron cooling is required
- "Circulator ring" concept promises to ease polarized electron source requirements significantly
- Additional conceptual luminosity improvements are being explored
- **ERL Prototype** to address high average current issues of EIC colliders
- **Energy Recovery experiment at CEBAF** to address high input/output energy issues of EIC colliders
- An integrated electron-ion collider program (CM energy 20-30 GeV) and fixed target program (at 25 GeV) based at CEBAF appears feasible

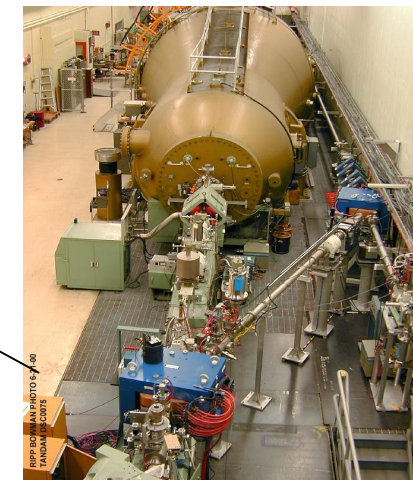
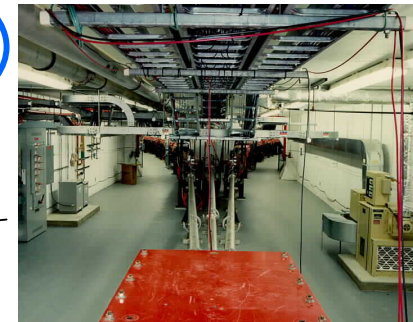
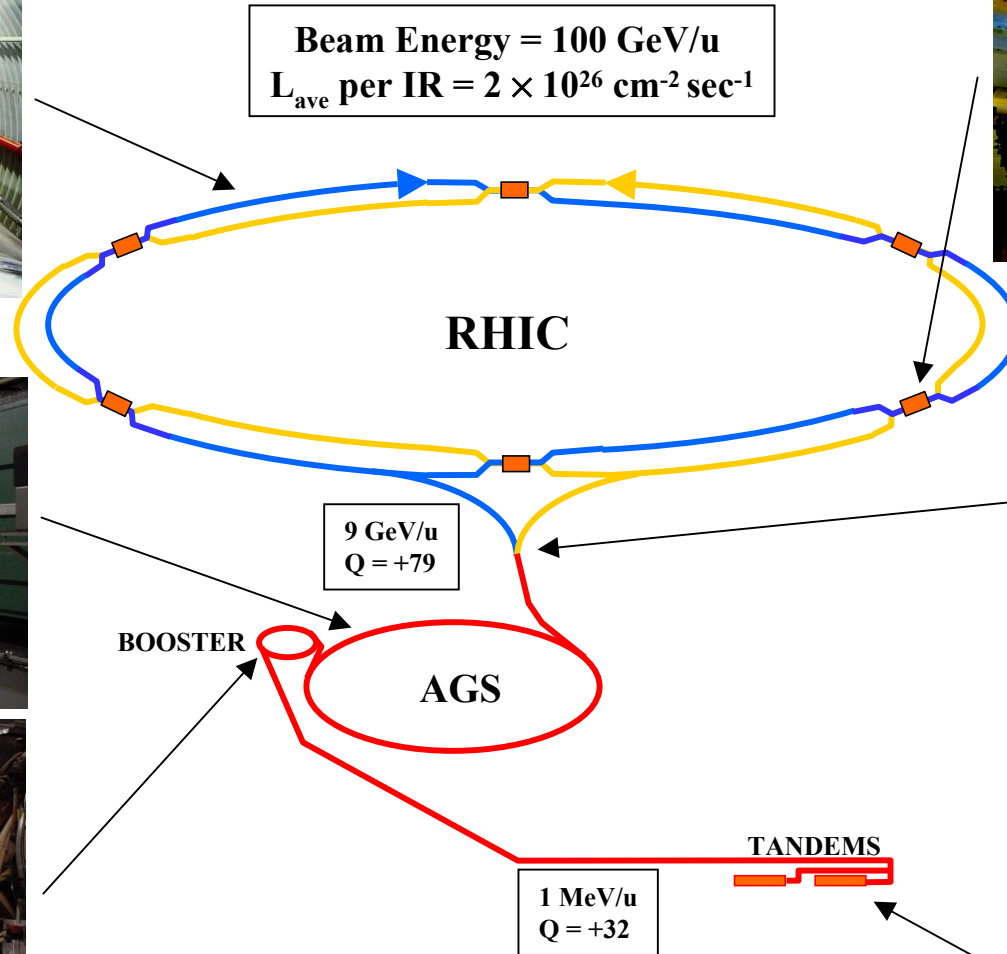


RHIC Performance and Plans

RHIC accelerator performance and status

Plans and upgrades

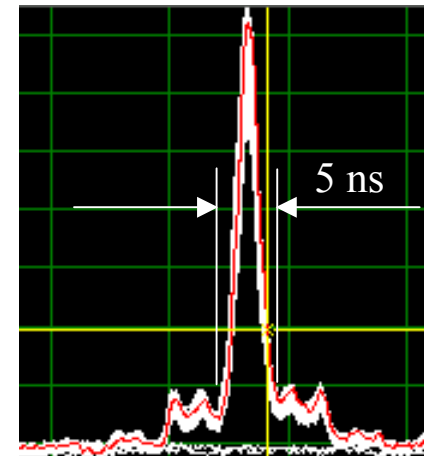
Gold Ion Collisions in RHIC



RFPF BOMMAN PHOTO 5/2/00
TANDEM 03/2005

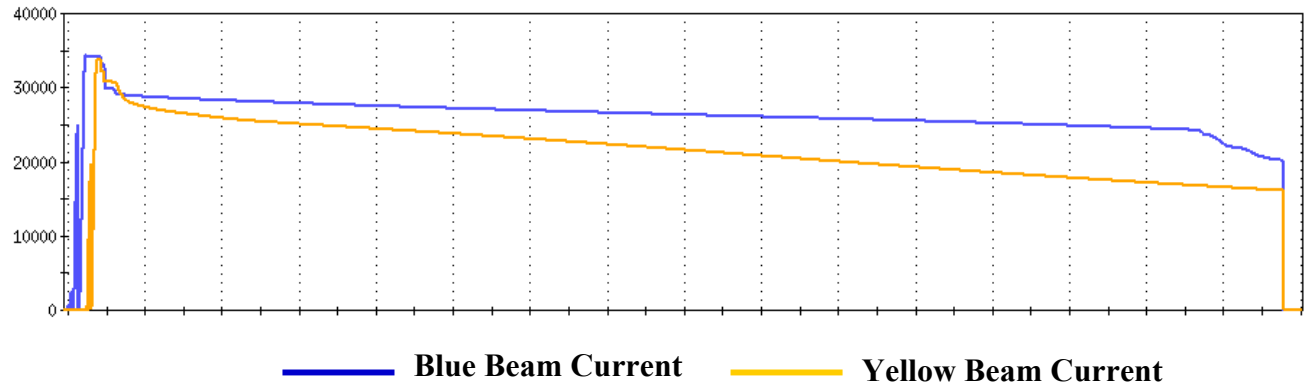
FY2001 - 02 RHIC Gold Parameters

- **55 - 56 bunches** per ring ✓ (110 bunches per ring tested, intensity limited)
- **7.5×10^8 Au/bunch @ storage energy** (intensity limited during acceleration)
- **1×10^9 Au/bunch achieved @ injection** ✓
- **Longitudinal emittance:** 0.5 eVs/nucleon/bunch (0.3-0.6 Design) ✓
- **Transverse emittance at storage:** $15 \pi \mu\text{m}$ (norm, 95%) ✓
- **Storage energy:** 100 GeV/ amu ($\gamma = 107.4$) ✓ 10 GeV / amu ($\gamma=10.5$) ✓
- **Lattice with β^* squeeze during acceleration ramp:**
 - $\beta^* = 3 \text{ m}$ and 10m @ all IP at injection ✓
 - $\beta^* = 1 \text{ m}$ @ 8 and 2 m @ 2, 6 and 10 o'clock at storage ✓
- **Peak Luminosity:** $5 \times 10^{26} \text{ cm}^{-2} \text{ s}^{-1}$ ($2.5 \times$ design average) ✓
- **Bunch length: 5ns** with 200 MHz storage rf system
(diamond length: $\sigma = 25 \text{ cm}$) ✓

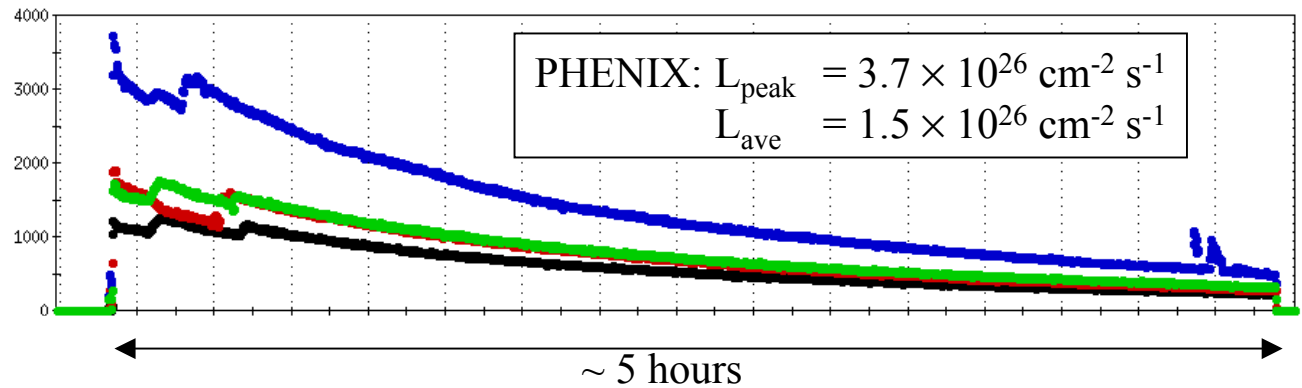


“Typical Store” # 1812

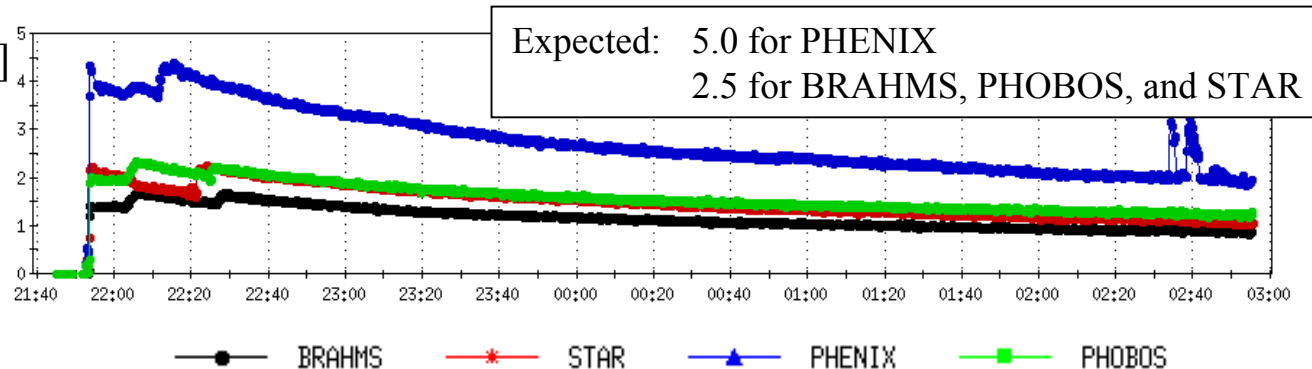
Beam currents [$\times 10^6$ ions]



Collision rate [Hz]

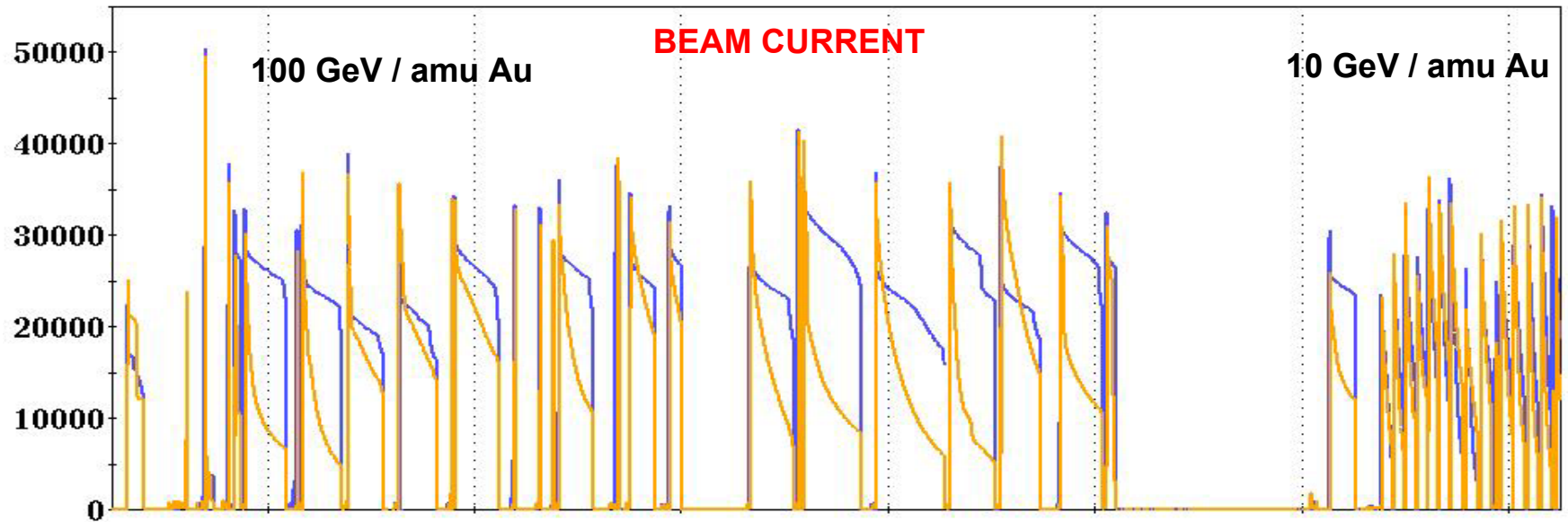


Specific luminosity [$\text{Hz}/10^{18}$]



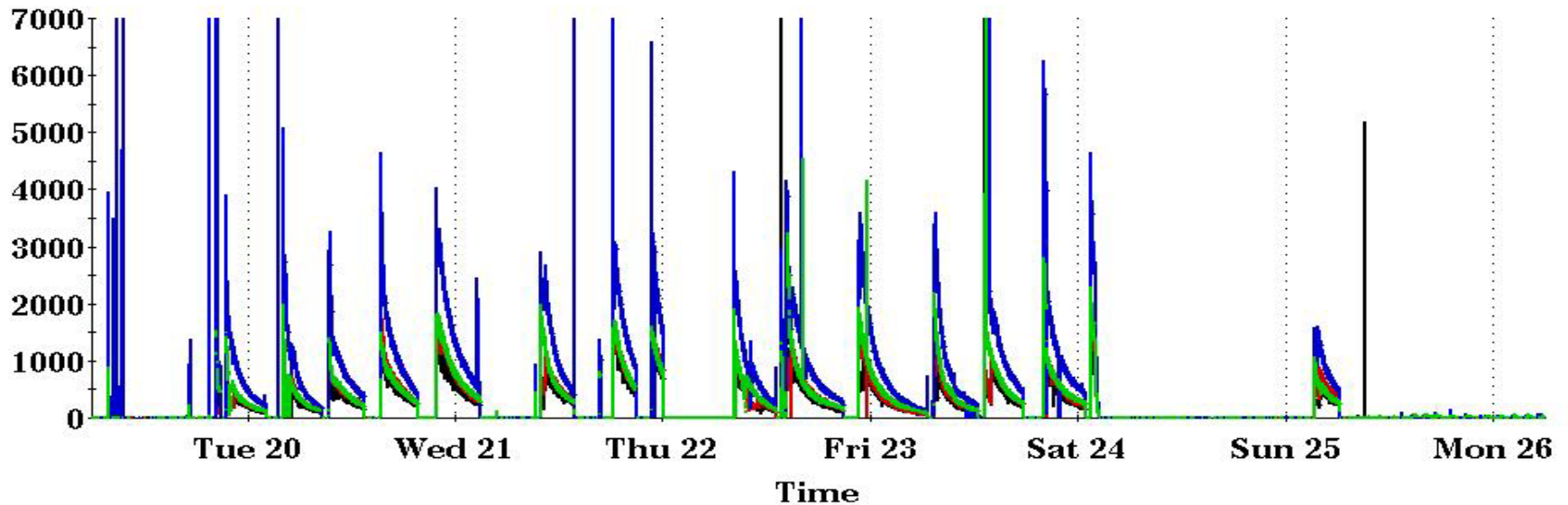
RHIC Performance

$\times 10^6$ Au

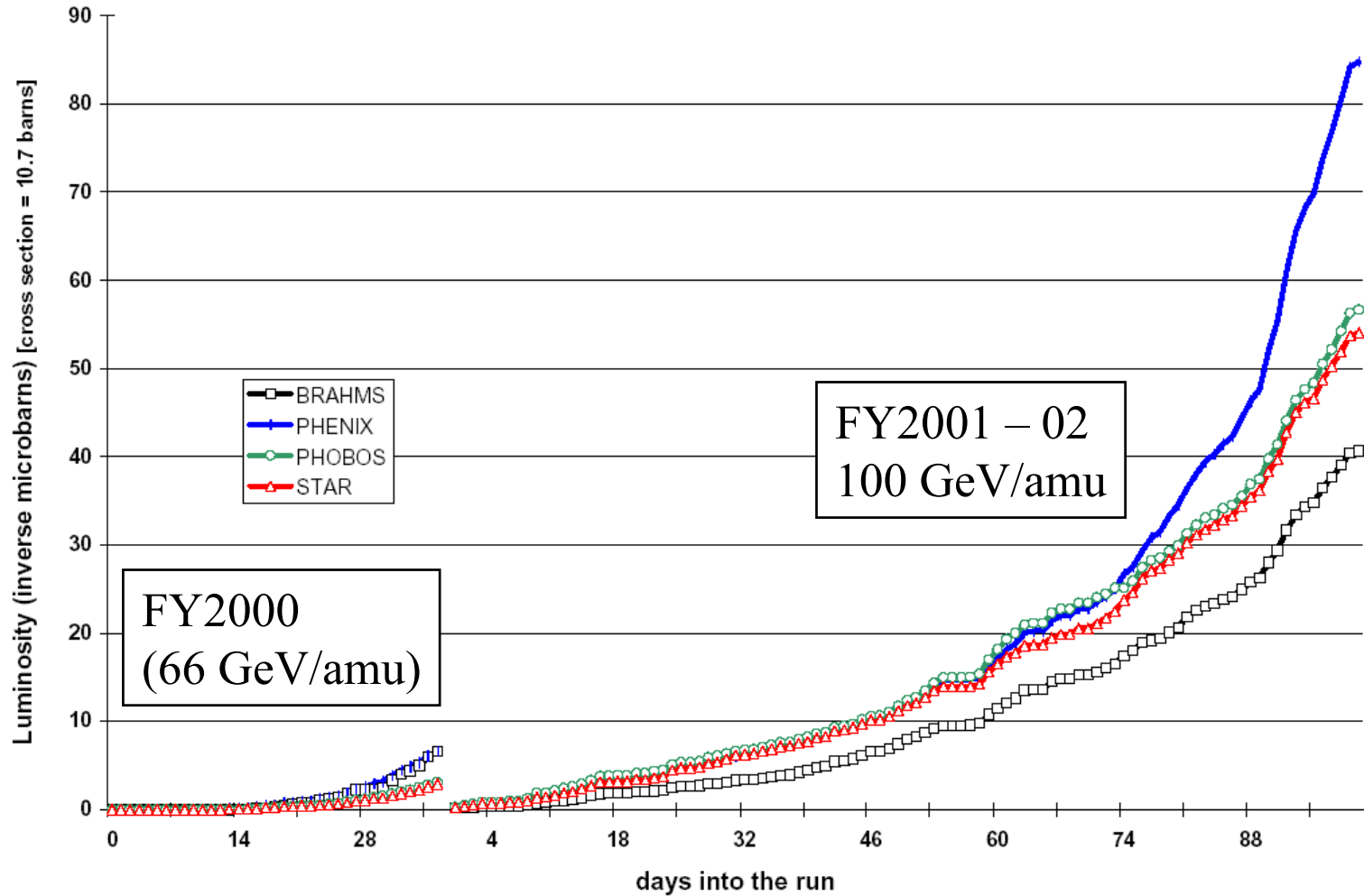


$\times 10^{23}$ cm⁻² sec⁻¹

LUMINOSITY



Integrated Au-Au luminosity



RHIC commissioning and challenges

- Single- and multi-bunch instabilities
 - Effect of vacuum chamber impedance, electron cloud (?)
- Intensity limitation for gold due to vacuum break-down
 - Limited to about 40×10^9 Au/ring
 - Electron cloud ? Ion or electron desorption ?
- Intra-Beam Scattering (IBS)
 - Transverse and longitudinal emittance growth
 - Determines RHIC Au performance
 - Eventually will need electron cooling (see below)
- Beam-beam tune shift and spread
 - First strong-strong hadron collider (after ISR)

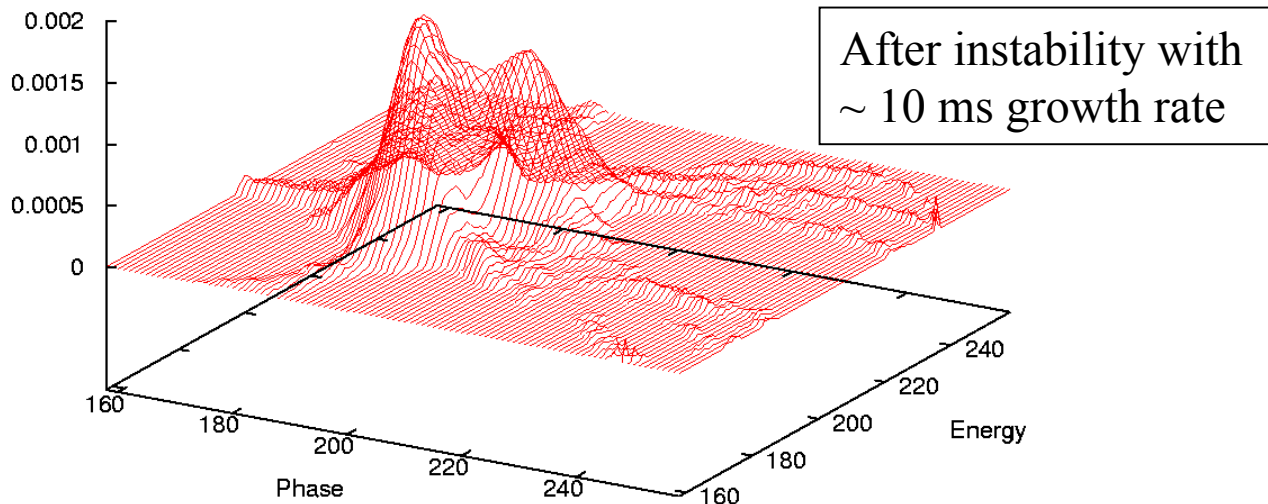
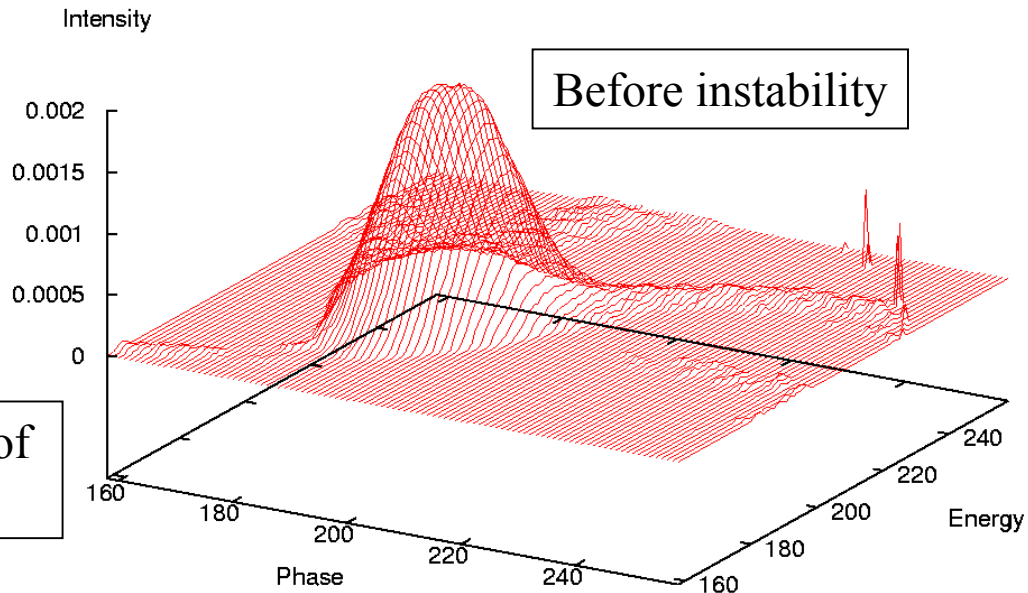
Transverse instabilities in RHIC

High sensitivity around transition

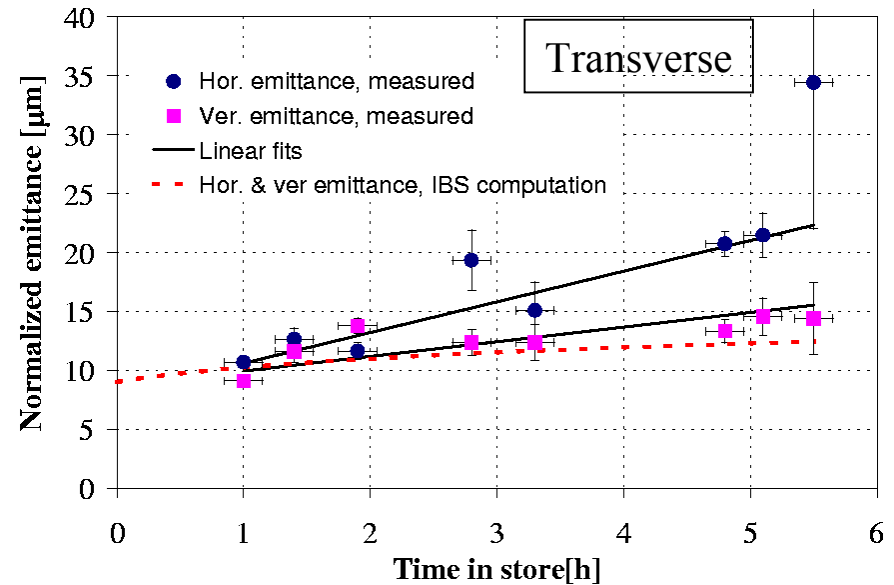
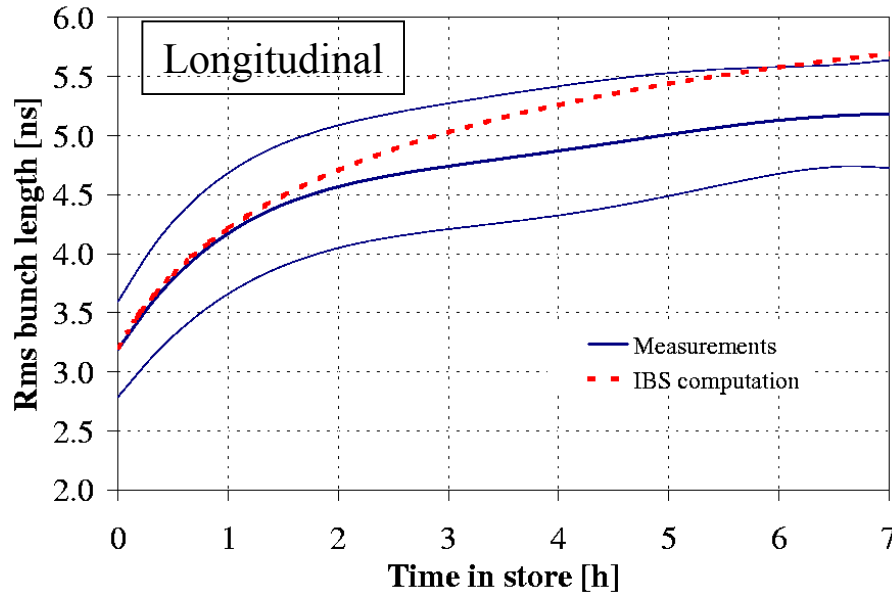
Effect of vacuum chamber impedance, electron cloud (?)

Cures: beam-beam tune spread, **octupoles**, transverse dampers, rf quad, ...

Tomographic reconstruction of 2D bunch density



Intra-Beam Scattering (IBS) in RHIC



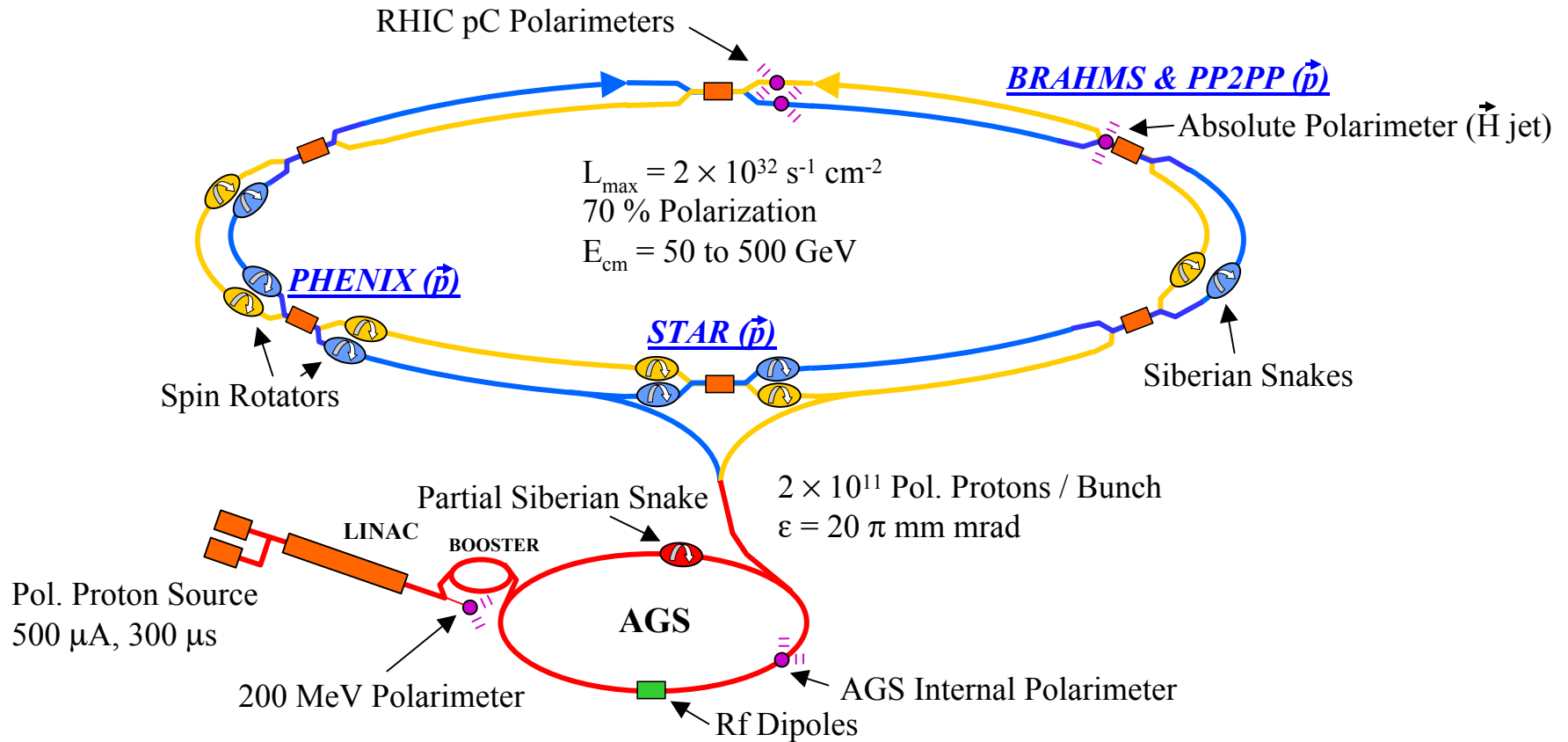
Longitudinal emittance growth agrees well with model

Additional source of transverse emittance growth (Beam-beam, dynamic apert.)

IBS determines RHIC Au performance

Eventually will need electron cooling (see below)

Polarized Proton Collisions in RHIC



High intensity polarized H⁻ source



KEK OPPIS
upgraded at TRIUMF

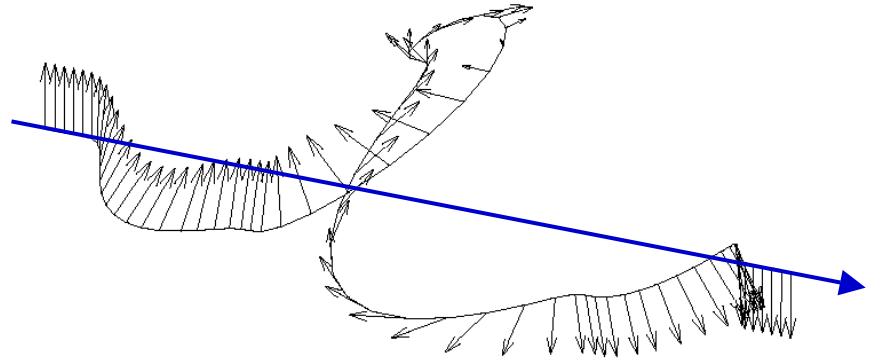
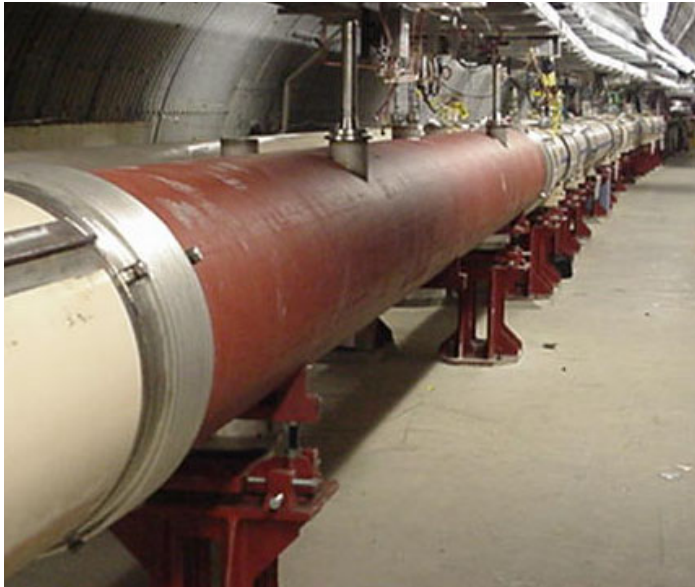
70 - 80 % Polarization

15×10^{11} protons/pulse
at source

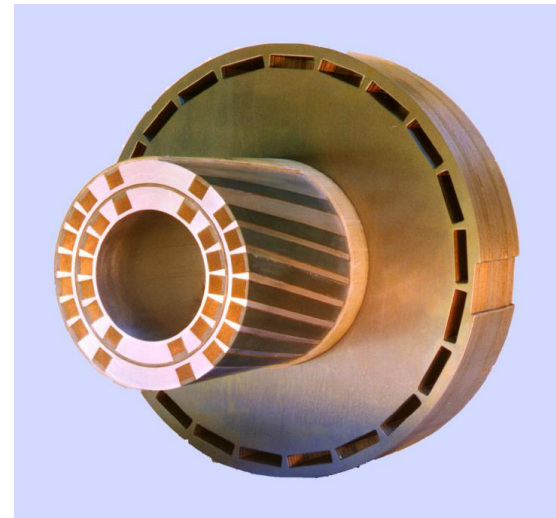
6×10^{11} protons/pulse
at end of LINAC

First Siberian Snake in RHIC Tunnel

Siberian Snake: 4 superconducting helical dipoles, 4 Tesla,
2.4 m long with full 360° twist

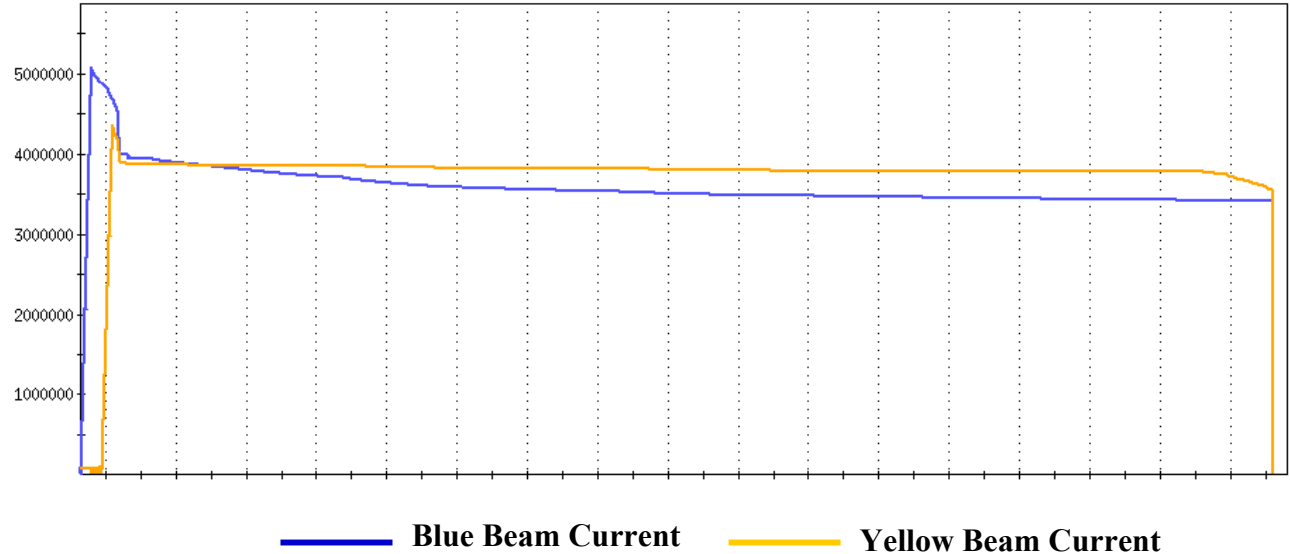


Funded by RIKEN, Japan
Designed and constructed at BNL

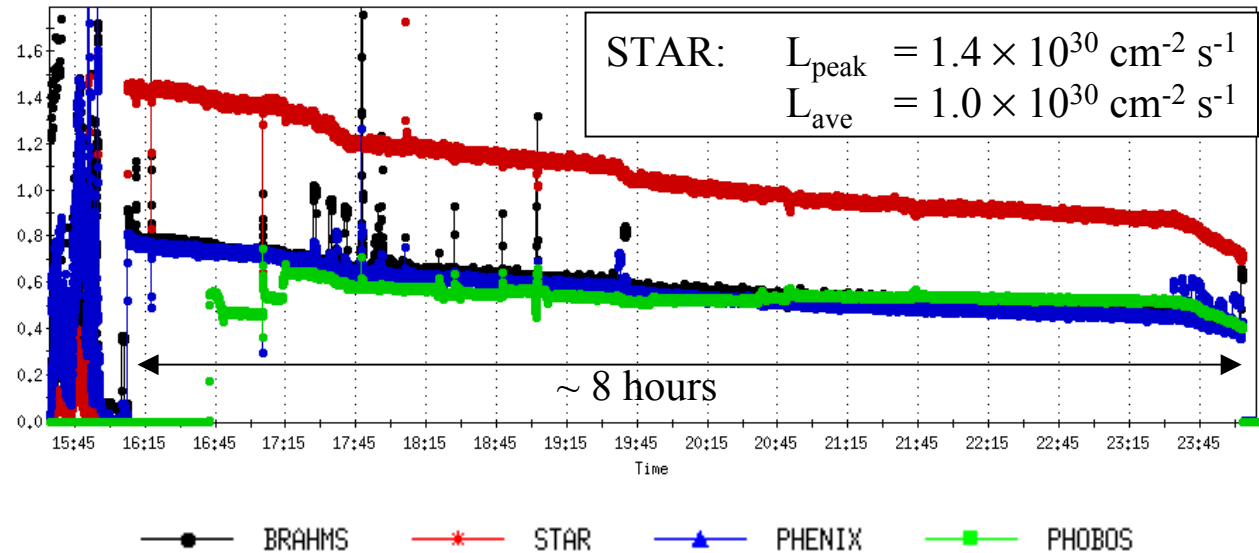


“Typical Store” # 2304

Beam currents [$\times 10^6$ ions]



Luminosity [$\times 10^{30} \text{ cm}^{-2} \text{ s}^{-1}$]



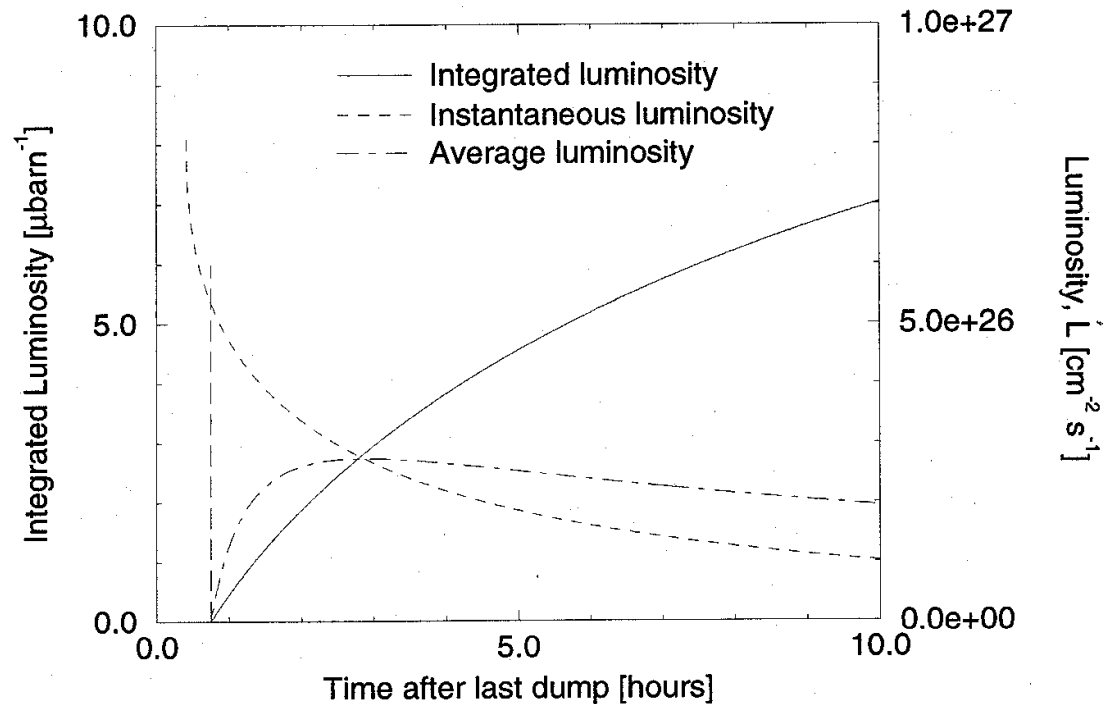
Results from first RHIC polarized proton run

- 55 bunches per ring with 0.8×10^{11} p^\uparrow /bunch
- Charge/bunch and total charge higher than with gold beams
- Lattice with constant β^* of 3 m during ramp
- Peak luminosity at beginning of store: $1.5 \times 10^{30} \text{ cm}^{-2} \text{ s}^{-1}$
- Energy/beam: 100 GeV
- Beam polarization $\sim 25 \%$
RHIC polarimeters work reliably
- Little if any depolarization in RHIC during acceleration and store
Siberian Snakes work
- $\sim 60 \%$ polarization loss in AGS; aggravated by lower ramp-rate from back-up Westinghouse motor-generator
- **Strong Siberian snake in AGS ($\sim 30 \%$ of full snake) could avoid all depolarization in the AGS**

RHIC design luminosity

$$L = \frac{3 f_{rev} \gamma}{2} \frac{N_b N^2}{\epsilon \beta^*} = 9 \text{ to } 1 \times 10^{26} \text{ cm}^{-2} \text{ s}^{-1} \text{ over 10 hours}$$

$$N_b = 56; N = 1 \times 10^9; \epsilon = 15 \text{ to } 40 \pi \mu\text{m}; \beta^* = 2 \text{ m}$$



RHIC luminosity upgrade (RHIC II)

- ‘Enhanced’ luminosity (x4) possible with existing machine:
 - Double the number of bunches to 112
 - Decrease β^* from 2 m to 1m
- Further luminosity upgrades can be achieved by:
 - Decreasing β^* further with modified optics
 - Increasing bunch intensity
 - Decreasing beam emittance
- All options are limited by intra-beam scattering and require beam cooling at full energy!
- Feasibility study on RHIC electron cooling shows that luminosity can be increased ten times.

Heavy Ion Luminosity Upgrades

	RDM	RDM+	RHIC II
Initial emittance(95%) $\pi\mu\text{m}$	15	15	15
Final emittance (95%) $\pi\mu\text{m}$	40	40	3
Beta function at IR [m]	2.0	1.0	1.0 \rightarrow 0.5
Number of bunches	56	112	112
Bunch population [10^9]	1	1	1
Beam-beam parameter per IR	0.0016	0.0016	0.004
Angular size at IR [μrad]	108	153	95
RMS beam size at IR [μm]	216	150	95
Peak luminosity [$10^{26} \text{ cm}^{-2} \text{ s}^{-1}$]	8	32	83
Average luminosity [$10^{26} \text{ cm}^{-2} \text{ s}^{-1}$]	2	8	70

RDM and RDM+ assume 10 hr stores

RHIC II includes electron beam cooling and assumes 5 hr stores since burn-off is high

Proton Luminosity Upgrades

	RHIC Spin	RHIC II	Future Upgrade
Emittance(95%) $\pi\mu\text{m}$	20	12	12
Beta function at IR [m]	1	1	0.3
Number of bunches	112	112	336
Bunch population [10^{11}]	2	2	2
Beam-beam parameter per IR	0.007	0.012	0.012
Angular size at IR [μrad]	112	86	157
RMS beam size at IR [μm]	112	86	47
Luminosity [$10^{32} \text{ cm}^{-2} \text{ s}^{-1}$]	2.4	4.0	40.0

RHIC II : Beam-beam tune shift limited for 2 interaction regions

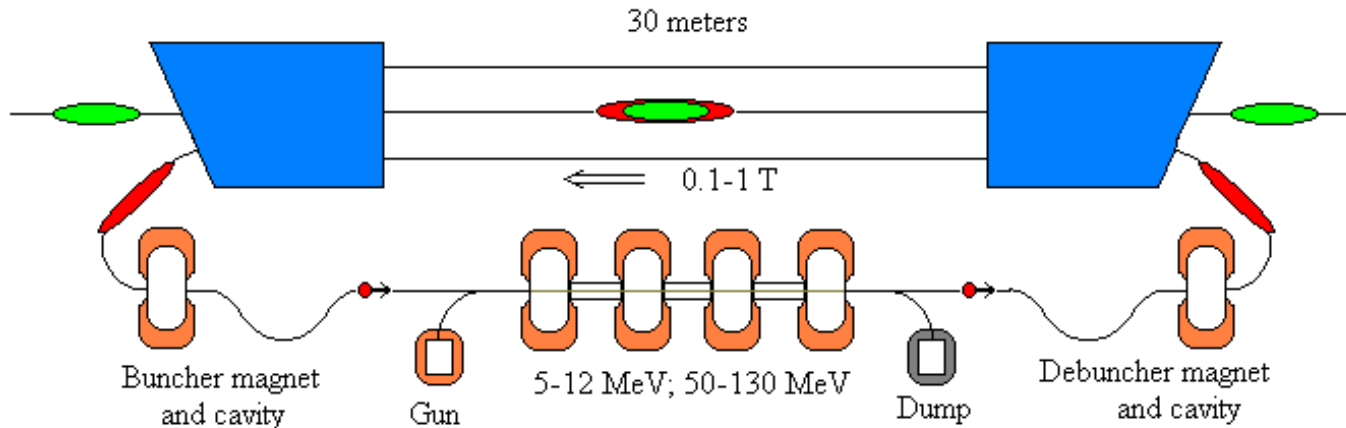
Future Upgrade: Mini-beta quads and more bunches

Will also require major detector upgrades

Electron Cooling at RHIC Storage Energy

- Electron beam cooling at full RHIC energy could eliminate this limitation and even reduce beam emittance further.
- Feasibility supported by study produced at BINP
- Bunched electron beam requirements for 100 GeV/u gold beams:
 $E = 54 \text{ MeV}$, $\langle I \rangle \leq 100 \text{ mA}$, electron beam power: $\leq 5 \text{ MW}$!
- Requires high brightness, high power, energy recovering superconducting linac, almost identical to IR FEL at TJNAF
- Has several applications at BNL: PERL, eRHIC (EIC)
- First linac based, bunched electron beam cooling system used at a collider
- First high p_t electron cooler to avoid recombination of e^- and Au^{79+}

The RHIC Electron Beam Cooler



R&D issues:

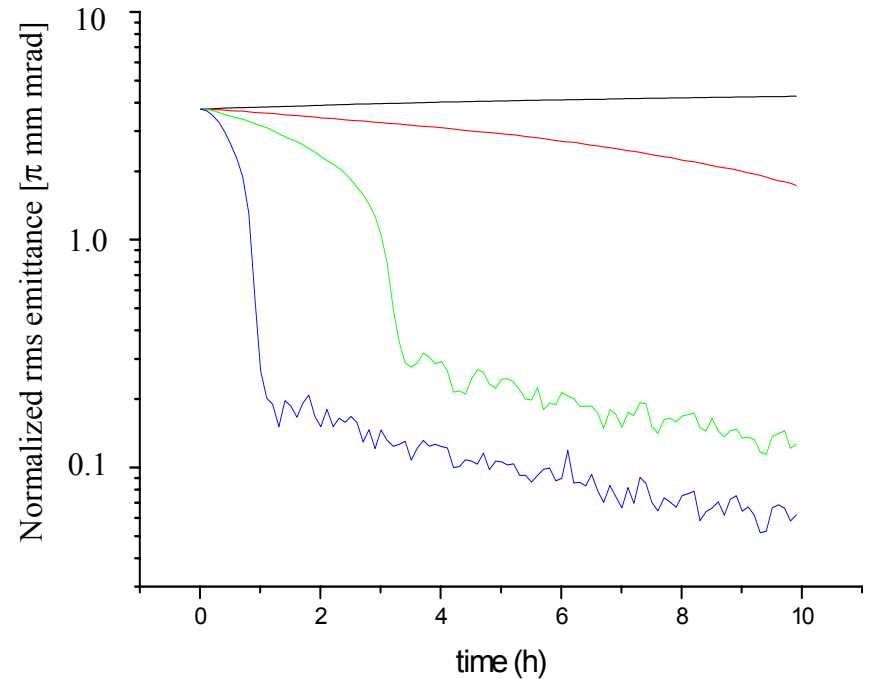
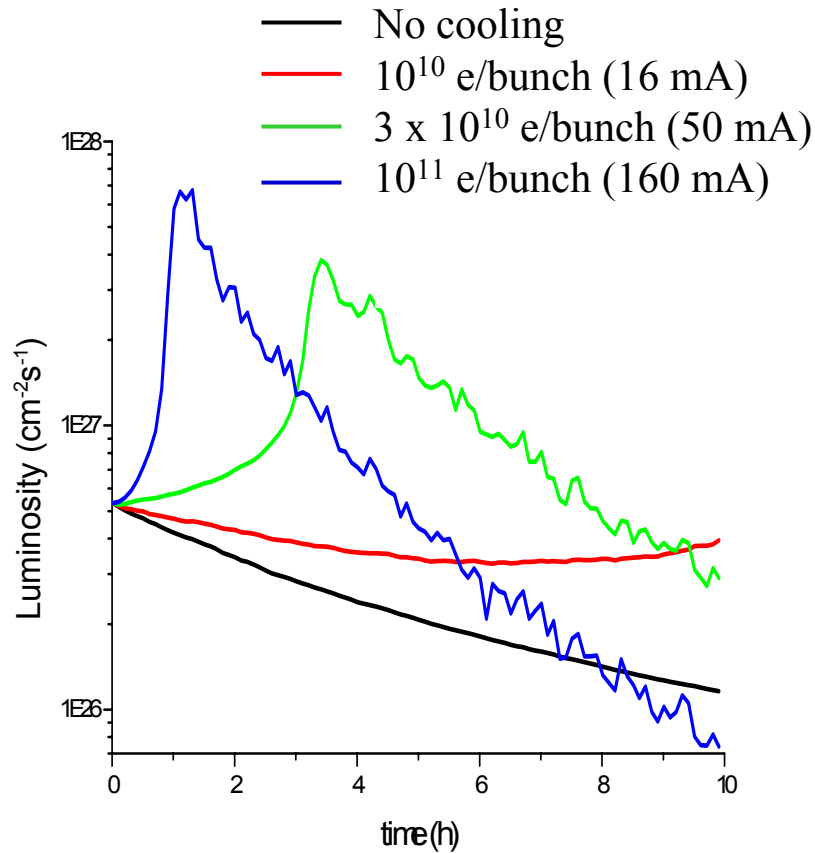
High intensity photocathode electron gun

High efficiency energy recovering sc linac with magnetized electron beam

Efficient electron beam transport and debunching/bunching

High precision (10 ppm) solenoid for 30 m cooling section.

RHIC Luminosity and Emittance with Cooling



Summary

- Highly successful operation of RHIC with gold beams and first operation with polarized proton beams
- RHIC luminosity upgrades (RHIC II):
 - with existing machine: $\times 4$
 - with full energy electron cooler: $\times 10$ possible
- RHIC e-cooling R&D program underway.

ELECTRON COOLING FOR RHIC

Review of the Principles of Electron Cooling for the Relativistic Heavy Ion Collider (RHIC)

Principal Investigators:

Vasily Parkhomchuk
parkhomchuk@inp.nsk.su
Budker Institute of Nuclear Physics,
Novosibirsk, 630090

Ilan Ben-Zvi
ilan@bnl.gov
Collider-Accelerator Department
And
National Synchrotron Light Source
Brookhaven National Laboratory
Upton NY 11973-5000

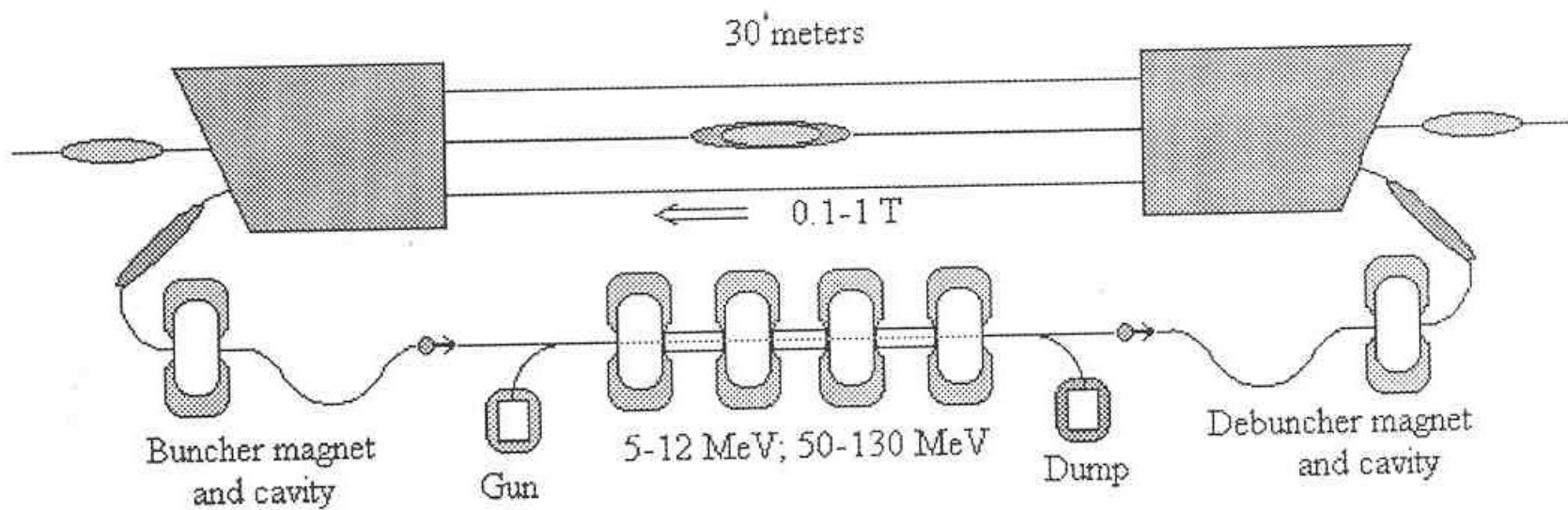
Table 1.1. GOLD nominal beam parameters at various stages

	Units	Injection	Store start	Store end
Nominal beam int. N_i	10^9	1.0	1.0	
Transverse emittance ϵ_{ni}	95% $\pi^* \mu\text{m}$, normalized	10	15	40
RMS bunch length σ_s	m	0.47	0.12	0.2
RMS momentum spread	0.001	0.27	0.53	0.9

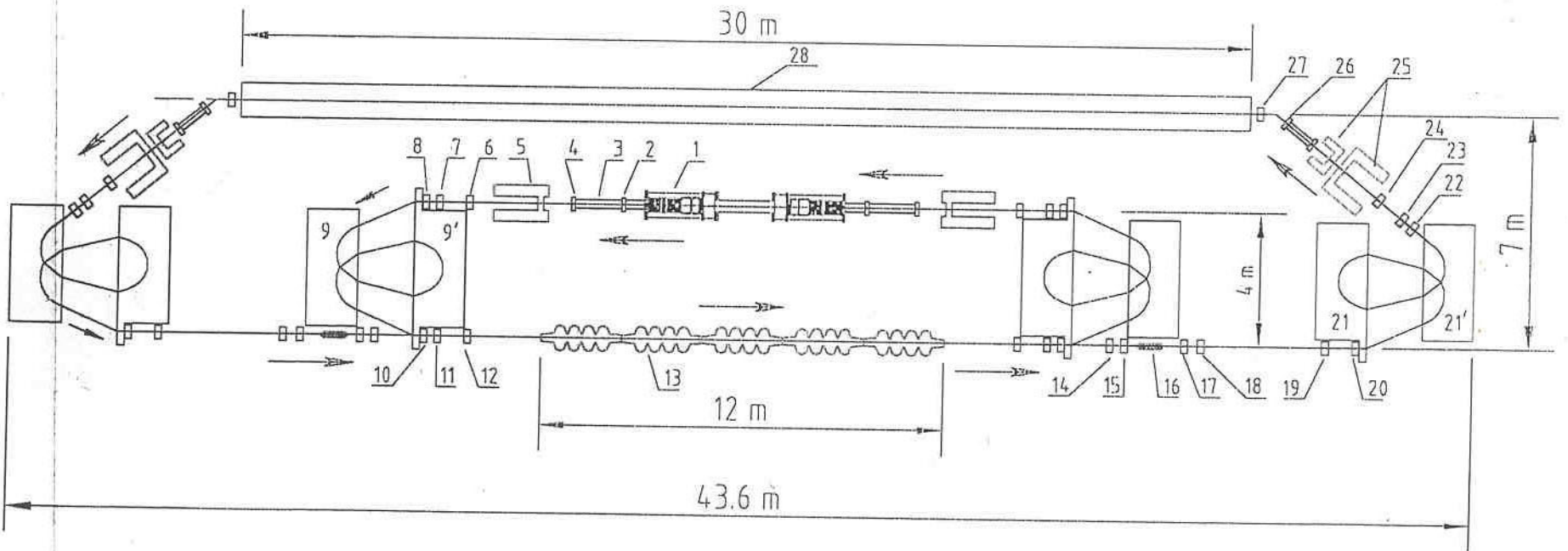
Table 1.2. List of basic parameters list used for the simulation of electron cooling in this section

Number of electron in a single cooling bunch		$N_e = 0 \text{---} 10^{11}$
Electron bunch length r.m.s.	[cm]	$\sigma_s = 20$
Frequency of repetition ion bunches	[MHz]	$f_b = 4.6$
Average electron current	[mA]	$I_{av} = 0 \text{---} 74$
Peak electron current	[A]	$I_{peak} = 0 \text{---} 9.6$
Magnet field at cooling section	[kG]	$B = 10$
Transverse electron temperature in beam's reference system	[eV]	$T_{\perp} = 1000$
Electron beam diameter	[mm]	$a = 2$

RHIC electron cooler layout



Electron Cooling System for RHIC collider (BNL)



3.7. Injection of the electron beam into the field of solenoid

Since we have a very strict limit on the transverse emittance of the electron beam inside the solenoid, a non-destructive method of injection of electrons into the field of the solenoid is very important. We will consider two possible methods of nondestructive injection of electrons into the field: (1) Injection of a flat electron beam using quadrupoles as the focusing elements [1-3]; (2) injection of the round electron beam generated by a magnetized cathode.

1. Injection of a flat electron beam using quadrupoles as the focusing elements.

For injecting a beam into the field of a solenoid we assume the optical system shown in Figure 3.7.1. The radius of the electron beam is $a_c=0.06$ cm in the magnetic field $B_{cool}=10$ kG of the cooling section. Let the magnetic field on the cathode of the electron gun be $B_{gun}=100$ G, then the radius of the electron beam is $a_{cgun}=0.6$ cm. After acceleration to an energy of $eU_0=2$ MeV, the electron bunch exits the magnet field and then is transformed from a round beam to a flat beam. Before entering the main solenoid, the beam is transformed back to a round beam by the inverse operation.

Let the wavelength of the Larmor spiral in the gun solenoid be λ . Then we choose the distance between skew-quadrupoles SKW1 and SKW2 to be $\pi\lambda$. The focal lengths of SKW1 and SKW2 are 2λ and -4λ , respectively. For the main solenoid we adopt a similar notation.

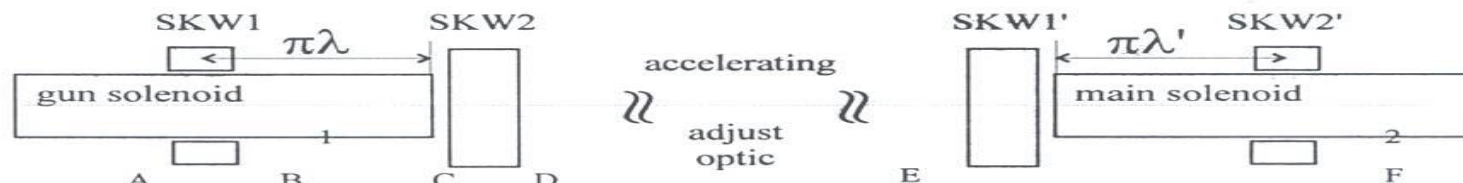


Figure 3.7.1. Schematic diagram of a matching transition of the electron beam between solenoids.

The value of the transverse momentum in the main solenoid can be evaluated from the invariance of the magnetic flux in the Larmor circle

$$r_{L1}^2 \cdot B_1 = r_{L2}^2 \cdot B_2 \quad (1)$$

Hence

$$\frac{\Delta p_2}{p_2} = \frac{\Delta p_1}{p_1} \frac{\gamma_1}{\gamma_2} \sqrt{\frac{B_2}{B_1}} \quad (2)$$

Thus, the initial spread of the transverse momentum in the injector should not exceed $\Delta p_1/p=1.3 \cdot 10^{-3}$ ($\gamma_2=100$, $\gamma_1=5$, $B_2=10^4$ G, $B_1=100$ G, $\Delta p_2/p \approx 6.4 \cdot 10^{-4}$) that is not so severe restriction.

The features of beam transport from one longitudinal magnetic field to another is as follows. If we consider the invariance of emittance as an invariance of the phase-space volume then the proper variables are $\{P_x = p_x + eA_x/c$, $Q_x = x$, $P_y = p_y + eA_y/c$, $Q_y = y\}$, where P is the generalized momentum and A the vector-potential of the magnetic field. As can be seen by the choice $A_x = -B \cdot y/2$, $A_y = B \cdot x/2$ for the gauge, there is a nonzero "magnetic emittance" for a beam generated in a longitudinal magnetic field. Note that this "magnetic emittance" isn't related to the spread of transverse momentum of the particles ($p_x=0$, $p_y=0$). After transition of beam from the zone with magnetic field to the zone without magnetic field, the "magnetic emittance" converts to a real emittance and a spread of the transverse momentum of the particles appears (Busch's theorem). However, with the special optics described below, it is possible to convert the "magnetic emittance" to the real emittance of just one component of particle motion, for example x . In this case, the correlation between x and y is eliminated and the beam can be transported with a standard optical system. The emittance of the y -component in the magnetic field free zone is defined by the thermal spread of transverse momentum in the magnetic field and the radius of the Larmor circle. Thus,

$$\epsilon_{yn} = \left[\frac{\epsilon'_n}{a_e} \right]^2 \frac{m_e c^2}{e B} \quad (3)$$

wavelength with a small resonator size. The length of the resonator and its wavelength are related by the equation:

$$\tan\left[\frac{\omega}{c}L_{cav}\right] = \frac{1}{Z_0\omega C}, \quad 1.(9)$$

where Z_0 is the impedance of the coaxial line, C is the value of the shunting capacitor, ω is the resonance frequency of the resonator and L_{cav} is its length.

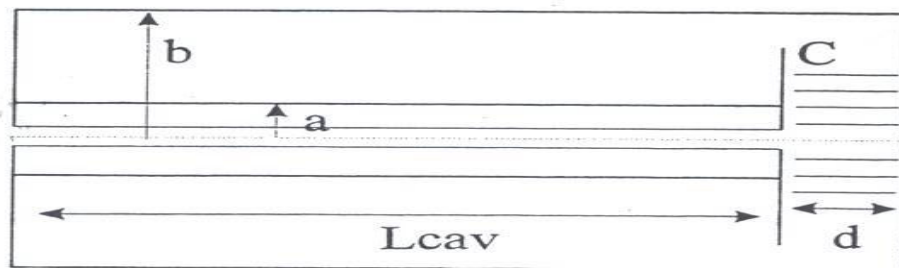


Figure 3.11. Schematic diagram of the energy-modulating RF cavity.

In order to linearize the functional dependence of the momentum increment on the longitudinal position it is necessary to use a harmonic combination of such resonators. The value of the final length of the bunch imposes constraints on the energy-modulating system of resonators. The non-linearity of the momentum increment cannot exceed $2 \cdot 10^{-3}$. This may be determined by observing the spread of electron longitudinal positions due to the non-linearity of the longitudinal momentum, which is approximately

$$\Delta s = 3\pi R \frac{\Delta p'}{p} \quad (10)$$

where Δs is the final length of the electron bunch and $\Delta p'$ is the nonlinear momentum increment. This requirement is easily achieved with two harmonics (the third harmonic has a relative amplitude of 0.05) for a phase interval of $\pm 50^\circ$. The suggested parameters of the RF-system are shown in the table below. For the fundamental we use two resonators, with a voltage of 360 kV each.

Table 3.4. Suggested parameters of the RF system.

a, cm	b, cm	D, cm	L_{cav} , cm	λ , cm	f, MHz	P, kW	U, kV
5	30	5	56	432	70	60	720/2
5	12	5	30	144	210	1	36

80
240

$\frac{4600}{0.24}$

the debunching system with the necessary modulation of energy for optimization of the bunch length and energy recovery at the main linac. The electron beam with a residual energy of 2 MeV is terminated in a beam dump.

An initial analysis of electron optics has been made using the thin-lens approximation. The betatron and dispersion function are shown in Figures 3.3 to 3.5. The detailed calculation of optic scheme for electron can be completed after a choice of parameters of electron transport system is made.

In the RF linac structure it is useful to use a special procedure for evaluation of betatron function. The motion of particle at acceleration can be written as

$$\frac{d^2x}{ds^2} + \frac{1}{\gamma(s)} \frac{d\gamma}{ds} \frac{dx}{ds} = 0 \quad (v/c \approx 1). \quad (1)$$

If we use the Ansatz:

$$x(s) = Aw_\gamma(s) \cos\left(\int_0^s \frac{ds'}{\gamma(s')w_\gamma^2(s')} + \varphi_0\right). \quad (2)$$

Then the differential equation becomes:

$$\frac{d^2w_\gamma}{ds^2} + \frac{1}{\gamma(s)} \frac{d\gamma}{ds} \frac{dw_\gamma}{ds} - \frac{1}{\gamma^2 w_\gamma^3} = 0, \quad (3)$$

which is similar to usual envelop equation. Thus one can calculate the dynamic variable w_γ for a given $\gamma(s)$ and then calculate $\beta(s)$ as:

$$\beta(s) = \gamma(s)w_\gamma(s)^2. \quad (4)$$

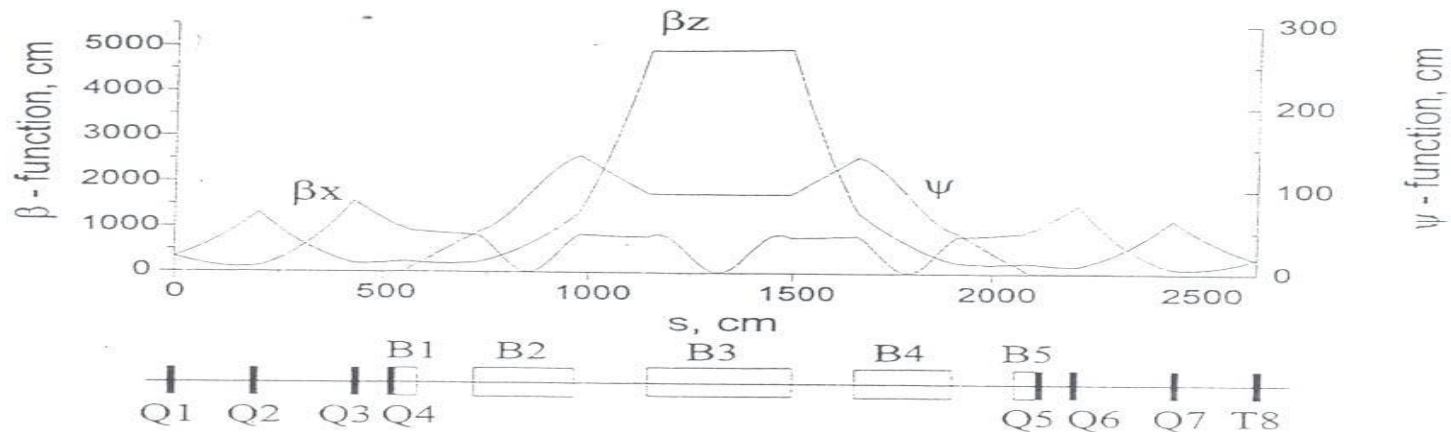


Figure 3.3. The sketch of betatron and dispersion functions from element 4 to

element 13.

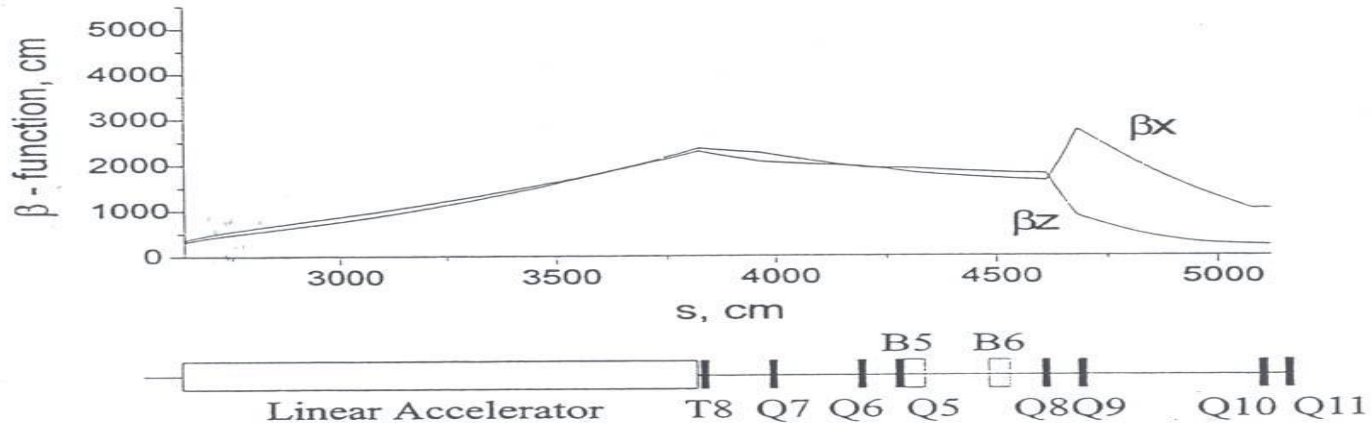


Figure 3.4. The sketch of betatron and dispersion functions from element 13 to element 21.

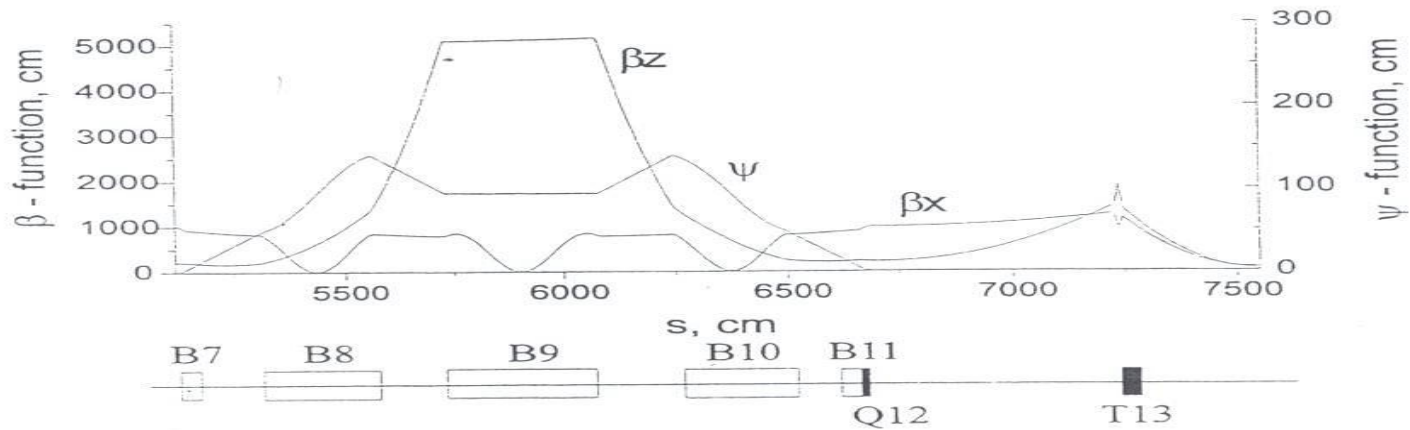
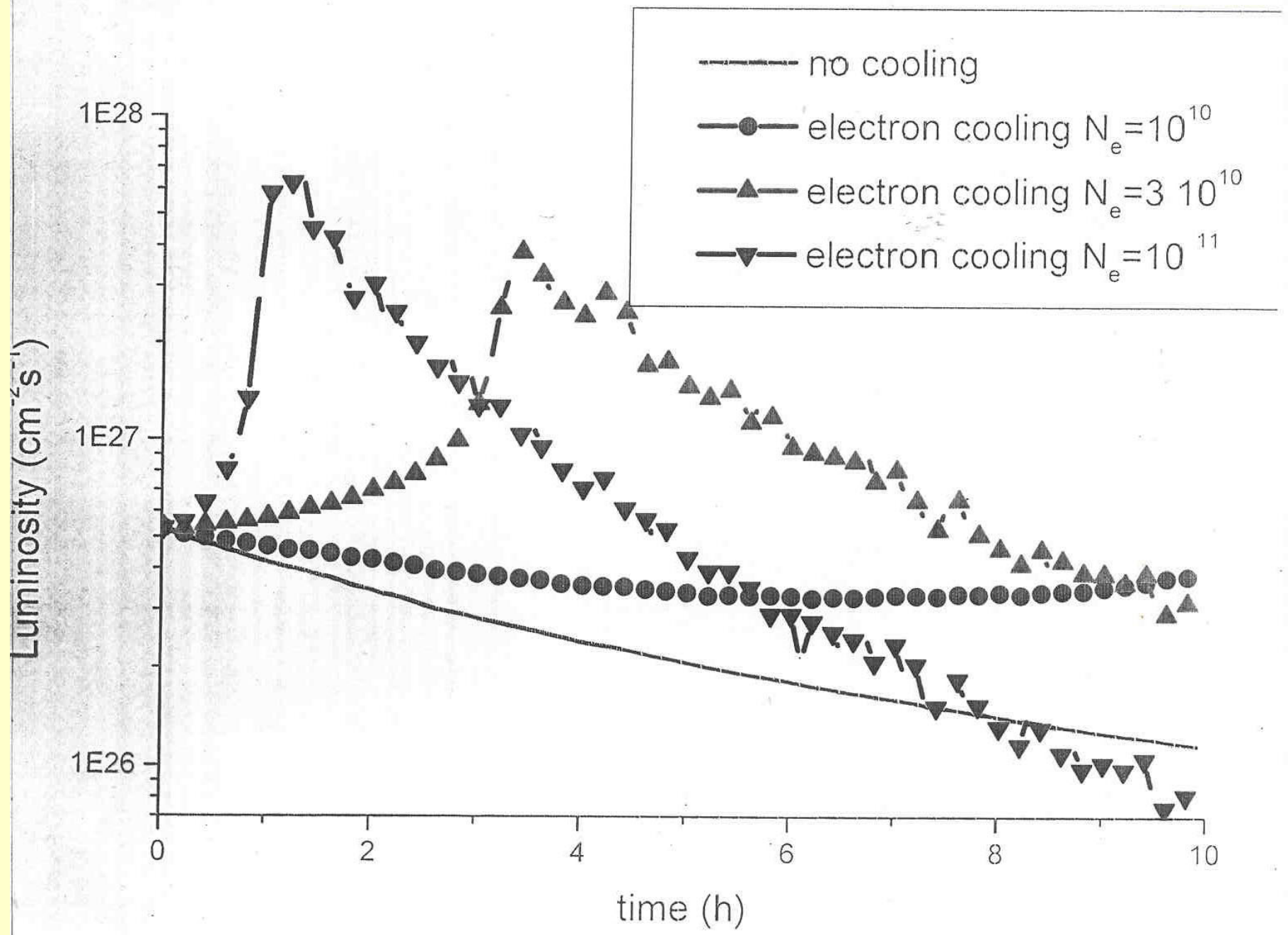
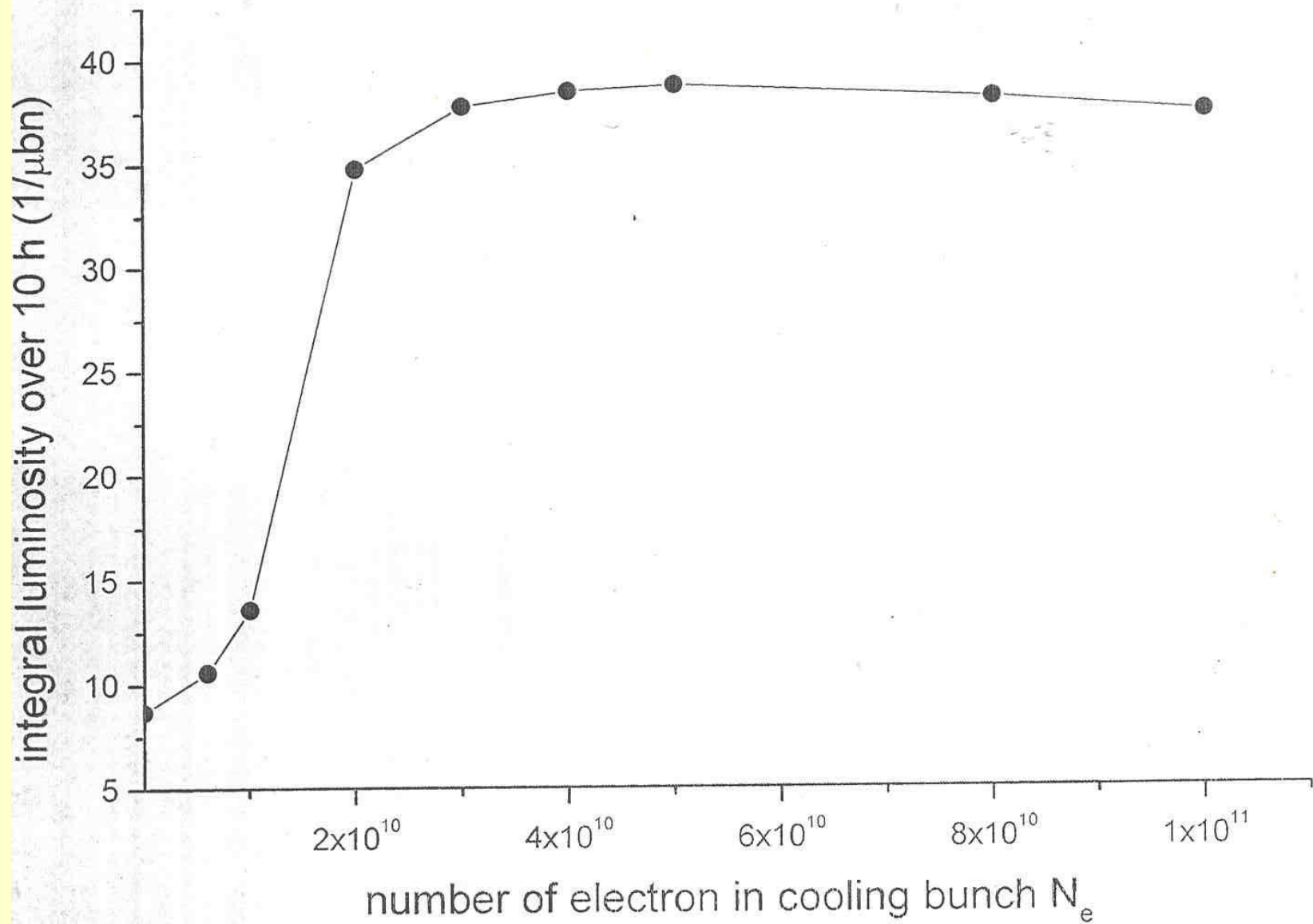


Figure 3.5. The sketch of betatron and dispersion functions from element 21 to element 21.





2. Luminosity under cooling

2.1 Beam Parameters at the Interaction Points

At RHIC, collisions take place at $n_{IP}=6$ Interaction Points. For simplifying the discussions below, we will assume equivalency of all the IPs, with parameters listed in the table 2.0:

Table 2.0

Parameter	Symbol	Value	Units
Beta function at IP	β_{IP}	2	m
Crossing angle		0	Radians
Number of ions per bunch	N_i	10^9	
Number of bunches in the ring	n_b	60	
Initial ion r.m.s. normalized emittance	ϵ_{ni}	3.7	mm·mrad
Initial r.m.s. bunch length	σ_s	22	cm
Initial momentum spread	σ_p	$1.46 \cdot 10^{-3}$	

2.2. Beam-beam interaction

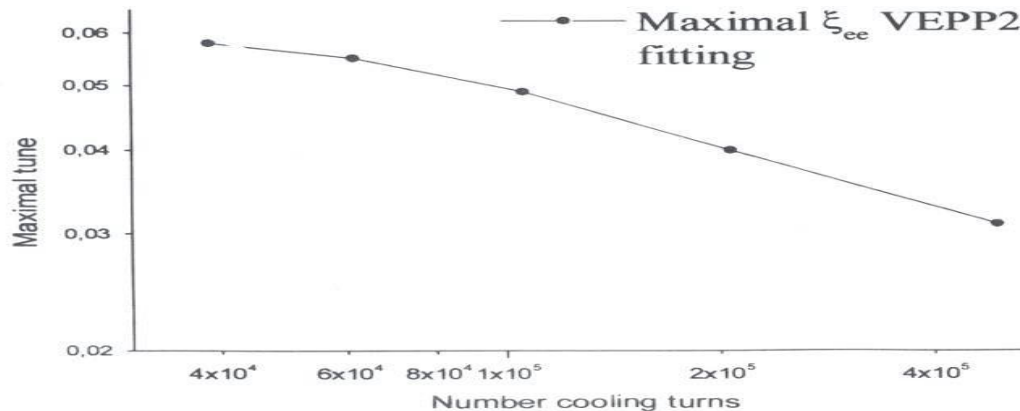
The main beam-beam parameter for the interaction is the linear tune shift at the IP:

$$\xi_{ii} = \frac{N_i r_i}{4\pi\epsilon n_i} \quad (1)$$

The beam-beam parameter for RHIC storage at top energy is $\xi_{ii}=3.8 \cdot 10^{-3}$. Nonlinear resonances also cause a diffusion of ions to large amplitude oscillations. The result of a simulation made at BINP shows that the power of this resonance for the proper ring lattice becomes significant if $\xi_{ii} > 0.05$. Any low-power cooling is useful for preventing the blowup of the beam during collisions of ion bunches for a small tune-shift. Experience with electron-positron colliders shows that increased cooling helps to reach a higher tune shift and luminosity. The Figure 2.1 shows measurement results of the maximal tune shift in the collider VEPP2M at an energy range 300-700 MeV [1] when the synchrotron radiation cooling changes significantly by changing the radiated power. The maximal beam-beam tune-shift as a function of the number of turns in one cooling time may be estimated by a simple power fitting approximation (Skrinsky formula):

$$\xi_{ii \max} = \frac{2}{N_{cooling}^{1/3}} \cdot (2)$$

The solid line in the figure shows calculation according this line.



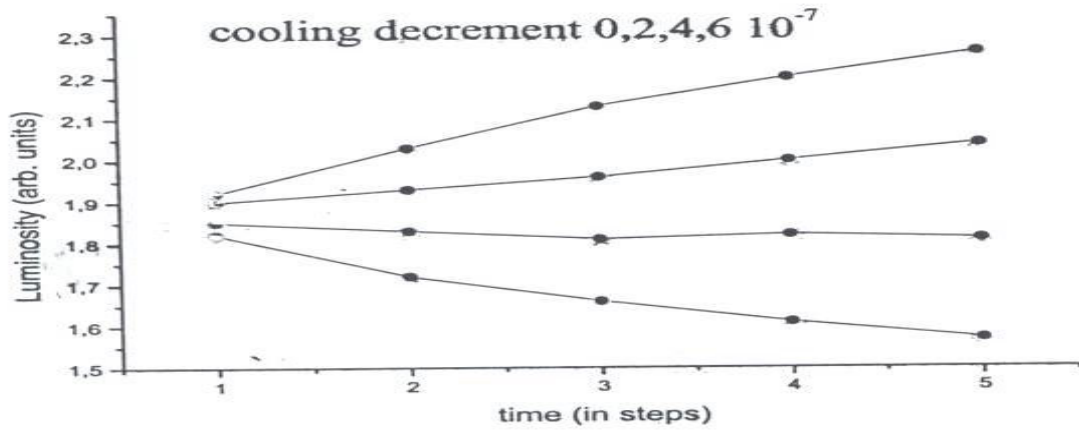


Figure 2.2. Luminosity vs. time for different cooling decrement.

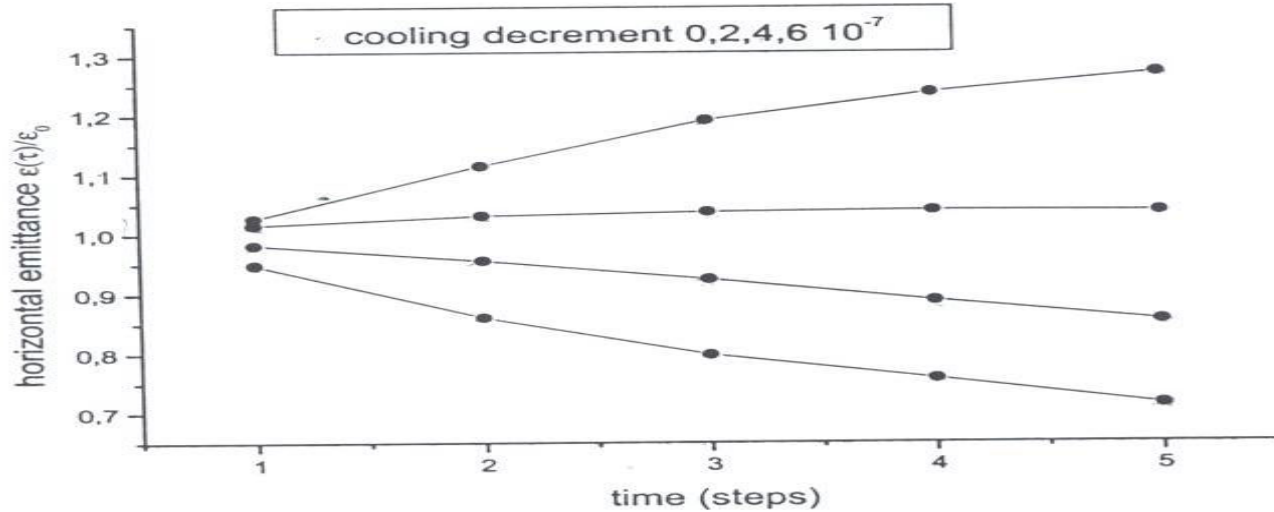


Figure 2.3. Horizontal emittance vs. time for different cooling decrement.

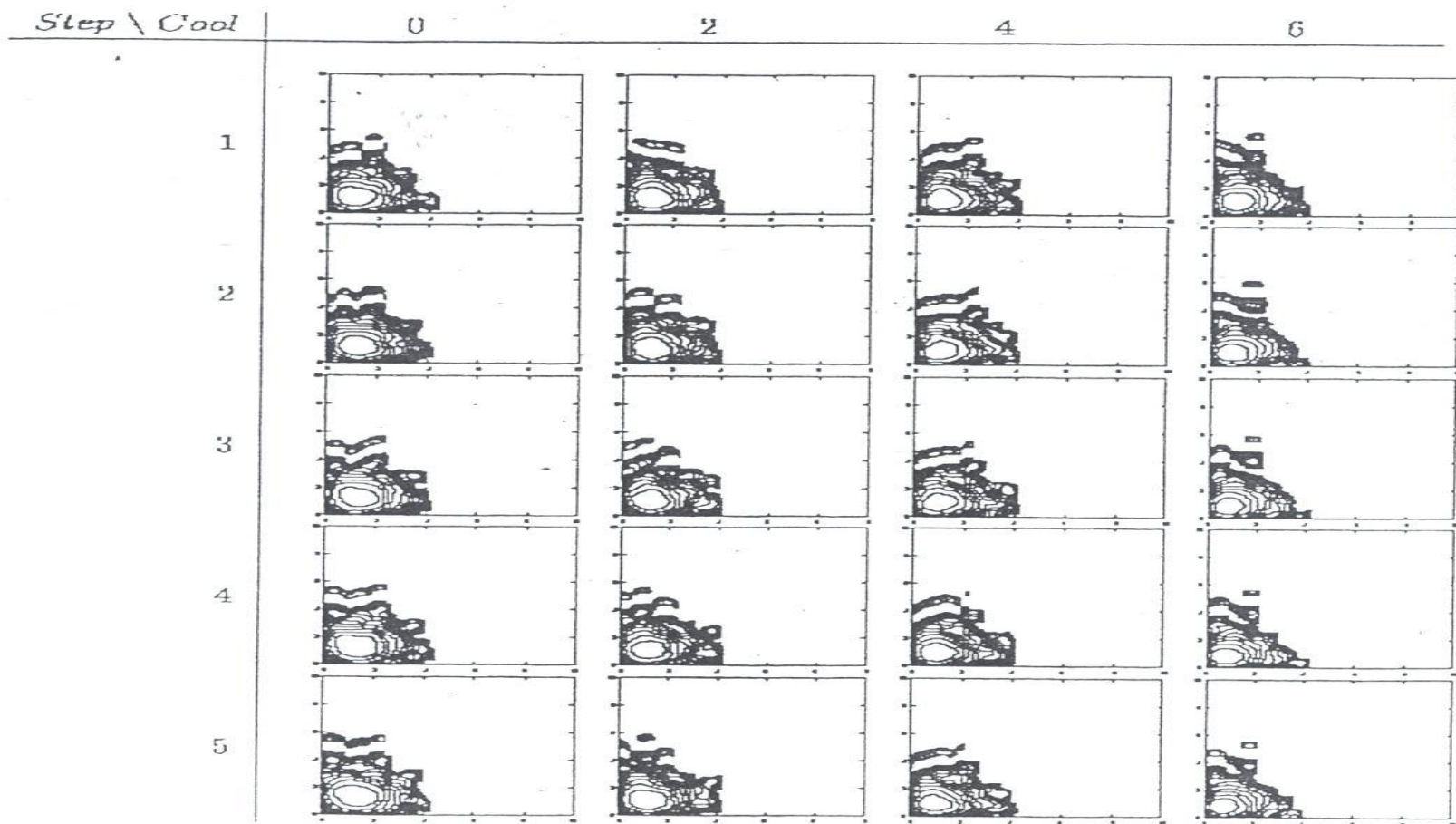
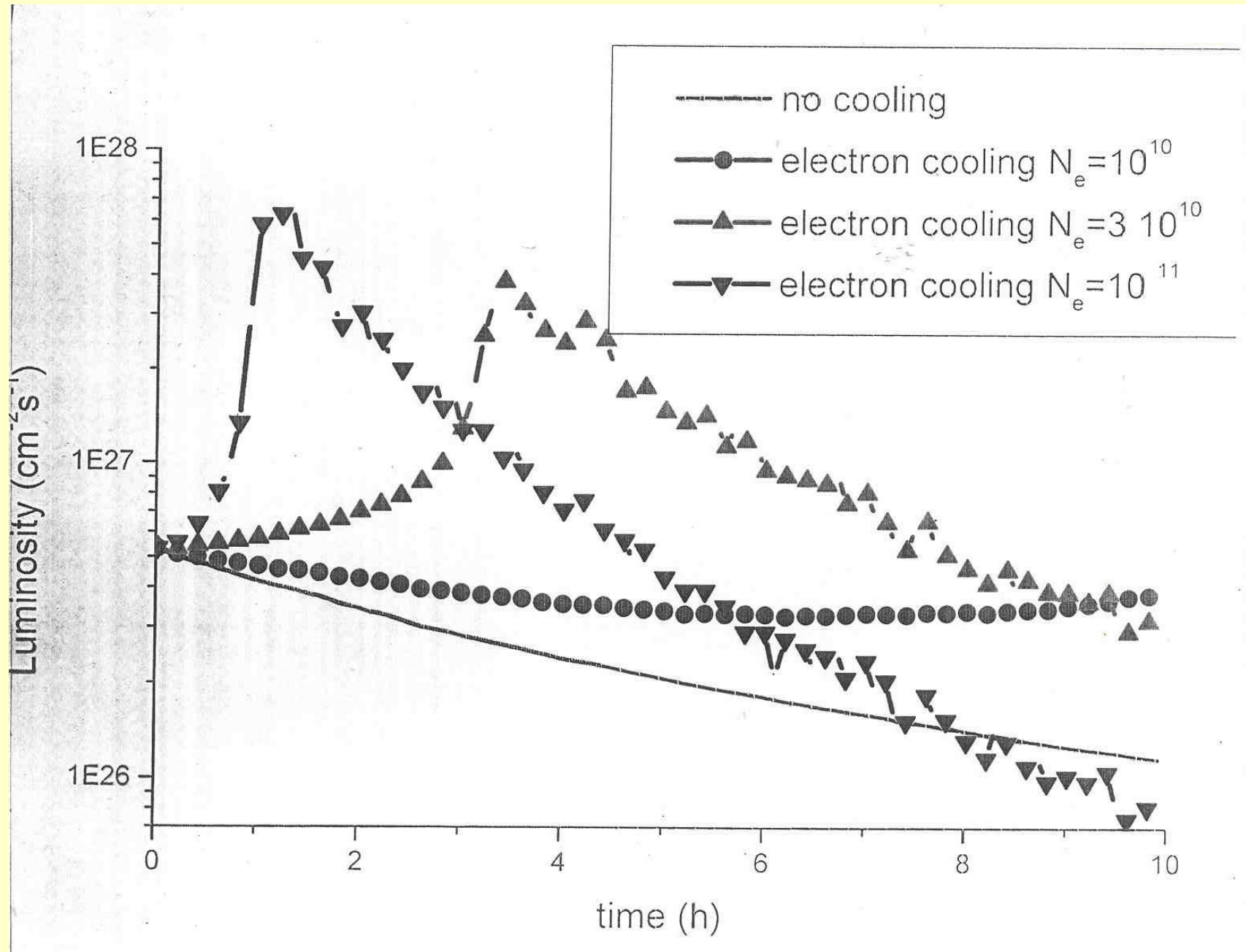


Figure 2.6. Contours of x-y distribution of ion beam for different cooling rates at different moment of time (step).



parameters: An r.m.s. bunch of length $\sigma=1.1$ m, a repetition frequency 4.6 MHz, average currents of 7.5 and 15 mA (all other parameters are to be found in rep4inj.mcd).

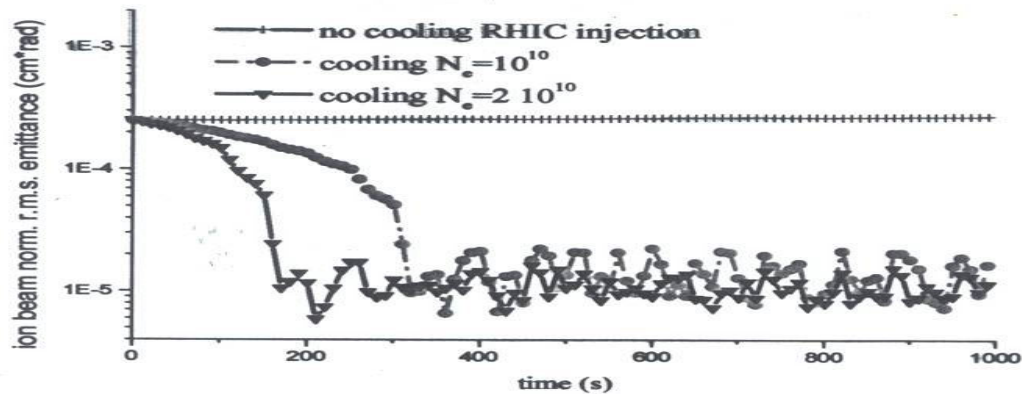


Figure 1.9. The transverse ion emittance (r.m.s. normalized) versus storage time at the injection energy.

Without cooling, the initial emittance increases from 2.5 mm*mrad to 2.7 mm*mrad and the bunch length from 1.1 m to 1.11 m. Cooling was made with redistribution of the cooling rate so that longitudinally the beam is not cooled, to reduce IBS. For cooling at injection energy, the electron beam temperature can be about 100 eV and the magnetic field of the cooling solenoid may be reduced down to 1 kG (instead of 10 kG required at the top energy.) As a result of the decreased field the losses on injection increase but for a cooling time of 1000 s the loss is not significant. Figure 1.10 shows the number of ions in the bunch versus time under this condition.

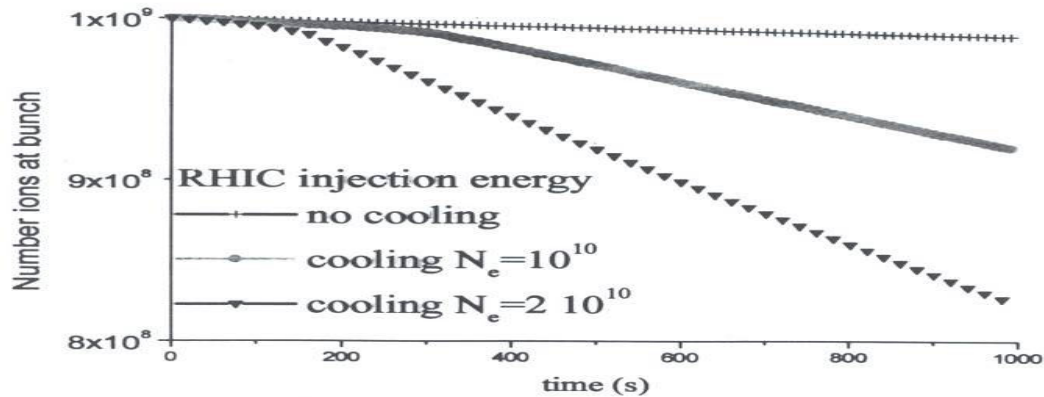


Figure 1.10. The number of ions in a bunch versus storage time at injection energy.

From figures 1.10 one can see that the ion losses over a period of 1000 s are nearly 20%. For injection, this loss is not very significant. The loss can further be suppressed by decreasing the electron current

3.5 Main linac

For electron cooling of RHIC we need an electron beam with an energy of 52 MeV, more than 10^{10} electrons in a single bunch, an energy spread of $\Delta\gamma/\gamma=10^{-4}$ or better and a transverse momentum spread of $\Delta p_{\perp}/p=4\cdot 10^{-4}$ or better. The main factors affecting the energy and momentum spread of the electron beam in a linear accelerator are the following:

1. Wake field produced by higher-order modes of the cavity on the energy spread of particles.
2. The time dependence of the accelerating RF voltage during the passage of a short electron bunch.
3. The influence of a space-charge field on the energy spread of particles.
4. The influence of inhomogeneity of the magnetic and transverse electric components on the particle's motion.

The bunch is placed at a phase of $\theta = -10^\circ$ in order to produce a linear correlation between the longitudinal momentum and position in the bunch (chirp). This chirp will later serve for debunching of the electrons.

1. The longitudinal wake fields for LEP (350 MHz) and CEBAF(1.5 GHz) accelerating structures were calculated.

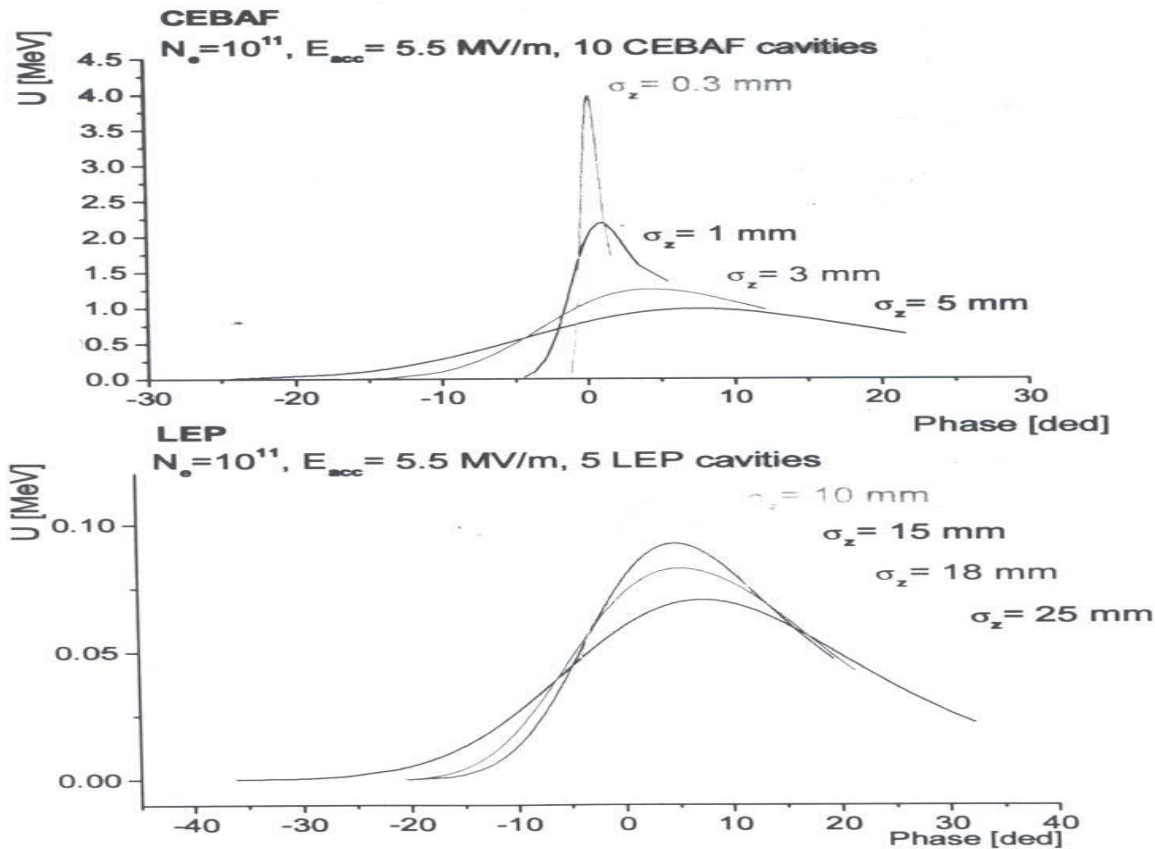


Figure 3.5.1. The longitudinal wake fields for LEP and CEBAF accelerating structures.

The LEP and CEBAF accelerating structures consist of 5 and 10 cells, respectively. The average accelerating gradient is $E=5.5$ MeV/m. The results of calculation are shown in Figure 3.5.1. The increment of particle energy spread as a

$$K2_x = \frac{4N_e r_e x^3}{\gamma(x+y)\Delta s \varepsilon_{xn}^2} = \langle \text{space charge term} \rangle / \langle \text{emittance term} \rangle$$

(13)

we calculate the values of the beam size and space-charge strength terms for a couple of bunch charges:

Table 3.5. Beam size and space-charge strength terms for two representative bunch charges.

Ne	E(MeV)	Δs (cm)	x	y	$K1_x$	$K2_x$
10^{11}	2	30	1.5	0.5	2.7	2.9
10^{10}	2	30	1.5	0.5	0.27	0.29
10^{10}	1	30	1.5	0.5	1.4	0.5

One can see that the electron beam dynamics is space-charge dominated, and for transporting a beam bunch with $N_e=10^{11}$ electrons we need a strong focusing system with beta-functions of about 50-100 cm. The r.m.s. beam parameters are shown in Figure 3.13. for various values of the number of electrons in a single bunch ($N_e=10^9, 10^{10}$ and 10^{11}).

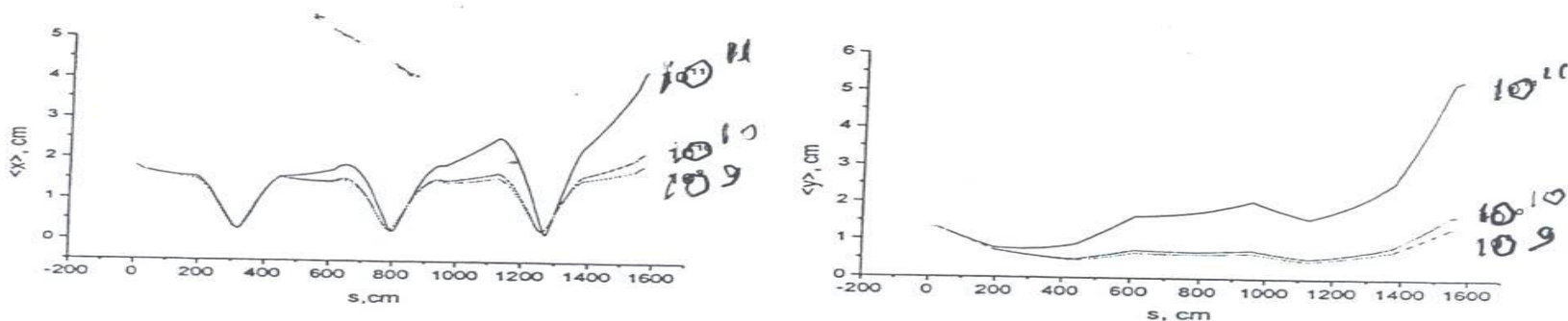


Figure 3.13. The r.m.s. parameters of the electron beam vs. the longitudinal coordinate.

We can see that the effect of the space-charge isn't significant for $N_e=10^{10}$, but it is crucial for $N_e=10^{11}$. For transporting $N_e=10^{11}$ in a single bunch, it is necessary to provide a stronger focusing system with β -function of about 50-100 cm or increase the injection energy.

It was shown in [1] that the emittance growth is related to the difference of the field energy of the bunch and an equivalent bunch with uniform density. For the case of a highly space-charge dominated beam, a special form is required for the charge distribution of the bunch in order to preserve the density distribution. For that reason, additional studies of the emittance growth in intense electron bunch are very desirable.

Study on Electron Cooling Facility for RHIC

EIC Workshop, February 26, 2002

Ilan Ben-Zvi, Jorg Kewisch, Dong Wang

Brookhaven National Laboratory

A lot of energy and ideas are from participants of weekly e-cooling meeting and others who helped in this study.

L. Ahrens, M. Brennan, M. Harrison, A. Hershcovitch,
M. Iarocci, D. Lowenstein, W. MacKay, S. Ozaki,
S. Peggs, T. Roser, T. Satogata, T. Srinivasan-Rao,
N. Towne, D. Trbojevic, X. Wang, J. Wei, J. Wu,
V. Yakimenko, Q. Zhao, etc.

Outline

- **Overview**
- **Electron Beam Parameters for RHIC e-cooling**
- **Goals of RHIC e-cooling Test Facility**
- **Layout and design considerations**
- **Simulations**
- **Summary**

Overview:

Electron Cooling for RHIC

- 1998~2000

Advanced optics concept for beam transport
(Y. Derbenev)
Demonstration of high current e- beam with
ERL(JLAB)



Initial studies for RHIC e-cooling

- April, 2001

Feasibility study for RHIC e-cooling
(BINP&BNL, C-A/AP/47, 2001)

- 2001 ~ now

A new round of study is underway at BNL
aiming at a design of practical e-cooling
facility for **RHIC lum. upgrade and EIC.**

Cooling evaluations

Electron beam facility designs

R&D of key technologies

- 2002 ~

Start 'Electron Cooling Test Facility' at
BLDG 939, BNL.

First, a s.c. RF-gun will be installed in May.
Other equipments will be added by stages.

Simulations of e-cooling in RHIC

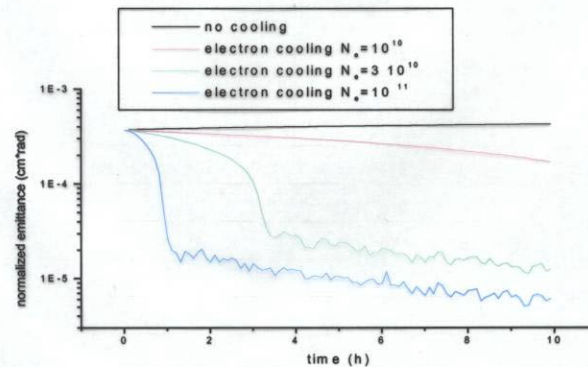
RHIC Parameters for e-cooling calculation

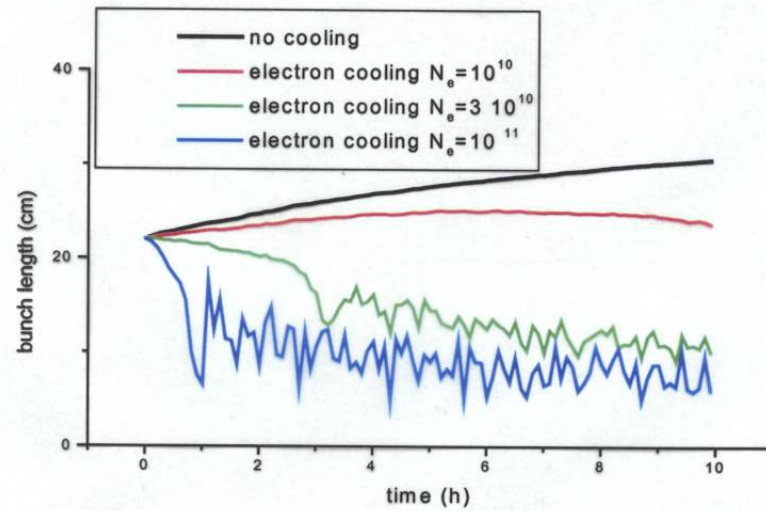
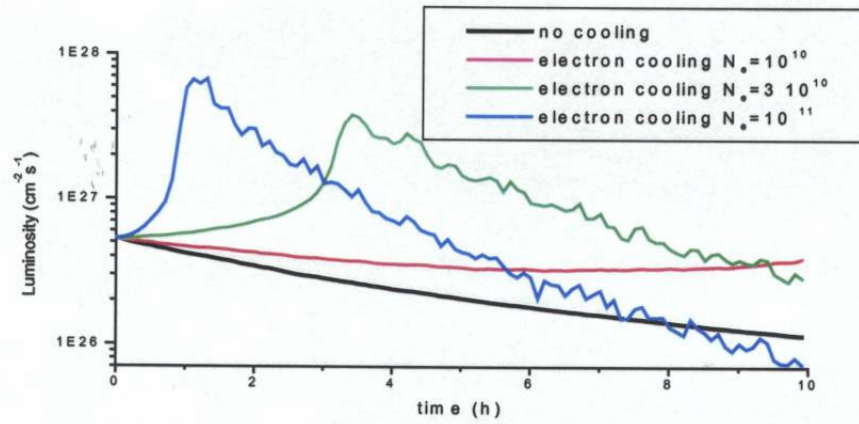
Beam energy	GeV/u	100
Bunches/ring		120(360)
Particles/bunch		10^9
Cooler solenoid length	m	30
Solenoid strength	Tesla	1.0
Transverse emittance(nor.)	pi.mm.mrad	15
Longitudinal emittance	eV.s	0.5
Beta functions at cooler	m	60
Bunch length	cm	~30

Starting point:

SIMCOOL(BINP), installed at BNL

- simplest models for e-cooling and IBS(Intra-beam scattering), good for fast estimations.
- used in Feasibility Study Report and still the basis of our e- beam facility design.





Crosscheck and more

BETACOOOL(JINR), installed at BNL

- **more options with several different models in cooling and IBS, etc.**

Problems:

Incomplete documentations.

IBS calculations don't work well.

Some discrepancies among simulation results with different electron cooling models/methods.

Example:

Cooling rate comparison with different model/options

	D-S model	Parkhomchuk model
Single particle	~4	1
Gaussian beam	~14	~4

Electron cooling force only, no other effects.
Same conditions of RHIC and e beams.

(What we are using is the most conservative one.)

Improvements:

Refined Betacool:

agreement with JINR group

new code, complete documentations

BNL experience in IBS, further developments here.

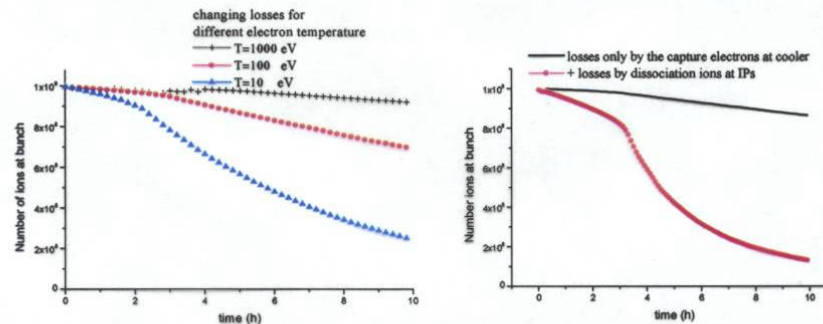
New code: novel solution, talk at BNL soon

Basic parameters of electron beams required for RHIC e-cooling

Electron beam energy	55MeV($\gamma = 107.6$)
Charge/bunch	5 nc
Repetition rate	9.4 MHz(120 b.)
Average electron current	47 mA
Bunch length at cooler	3~30 cm(TBD)
Beam radius at cooler	~ 0.8 mm
Transverse emittance(nom.)	10~50 mm.mrad
Energy spread at cooler	10^{-4}

Note: above parameters may change with

⇔ better understanding to physics,
e.g., **recombination** issue.



⇔ improvements or difficulties in technology aspects, e.g., photo-injector, solenoid.

BNL is planning to build the **E-cooling Test Facility for RHIC**

Goals:

To study the key physics and technology issues

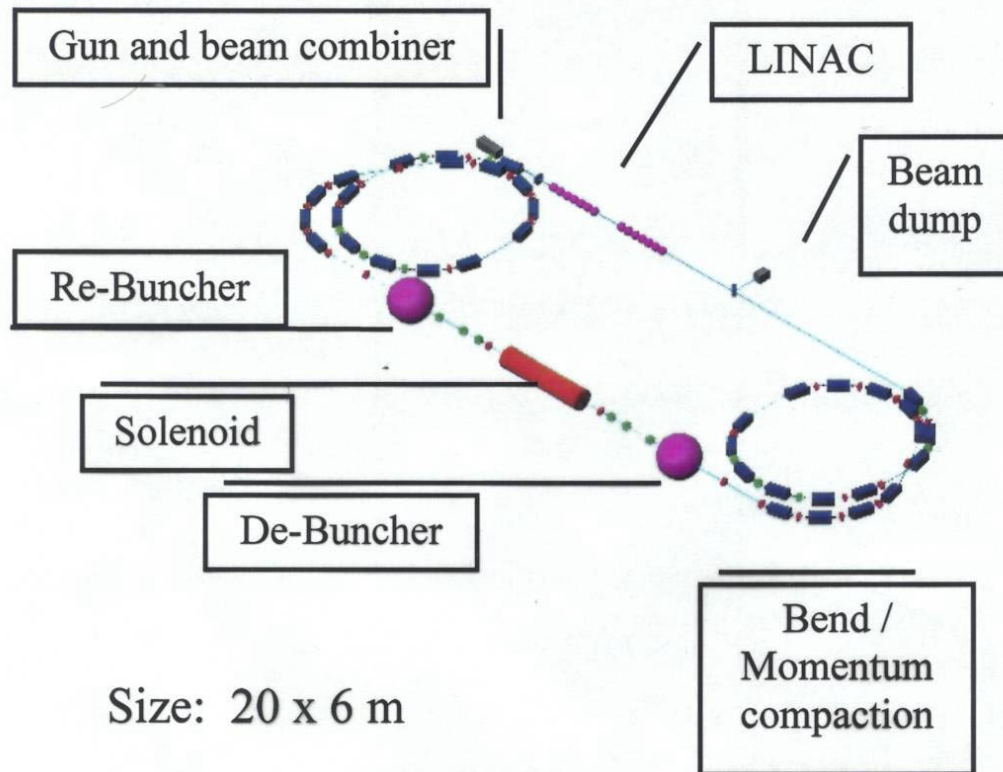
- **high performance e- source: photo-injector**
- **super-conducting RF technology with energy recovery at 55MeV×50mA**
- **transport of (magnetized) e- beam, (de)compressions, compensations to various effects, space charge, CSR, and so on**
- **high precision solenoid(one section)**
- **beam dump**
- **instrumentations**
etc.

Test facility will be a phased project.

Eventually, it will be ready to apply to the RHIC.

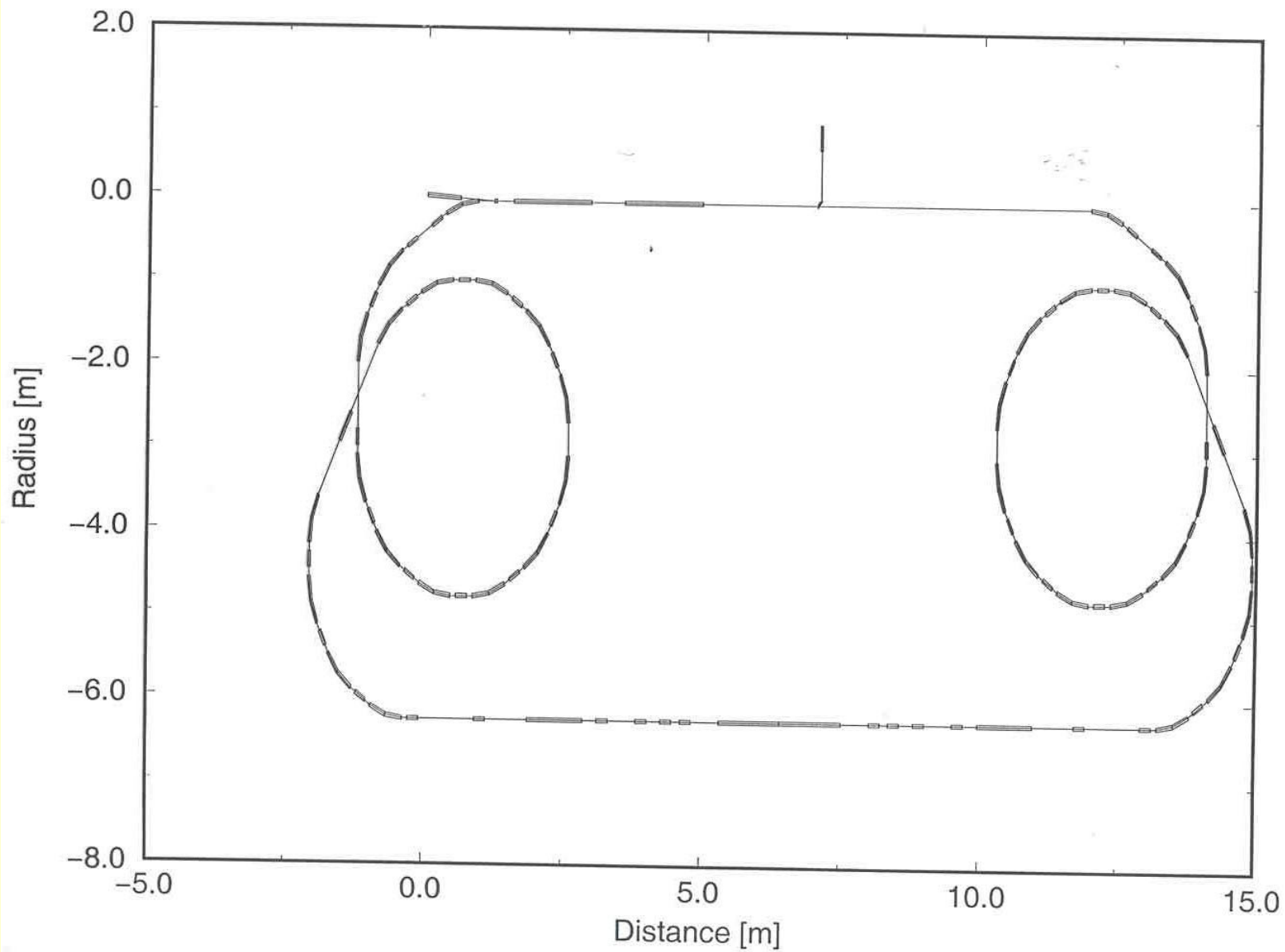
Layout of Test Facility

Location: Building 939 (for neutral beam test facility in the past), BNL



Sketch of electron beam facility for e-cooling

rc2



RHIC electron cooling test facility

Bunch rotation optics

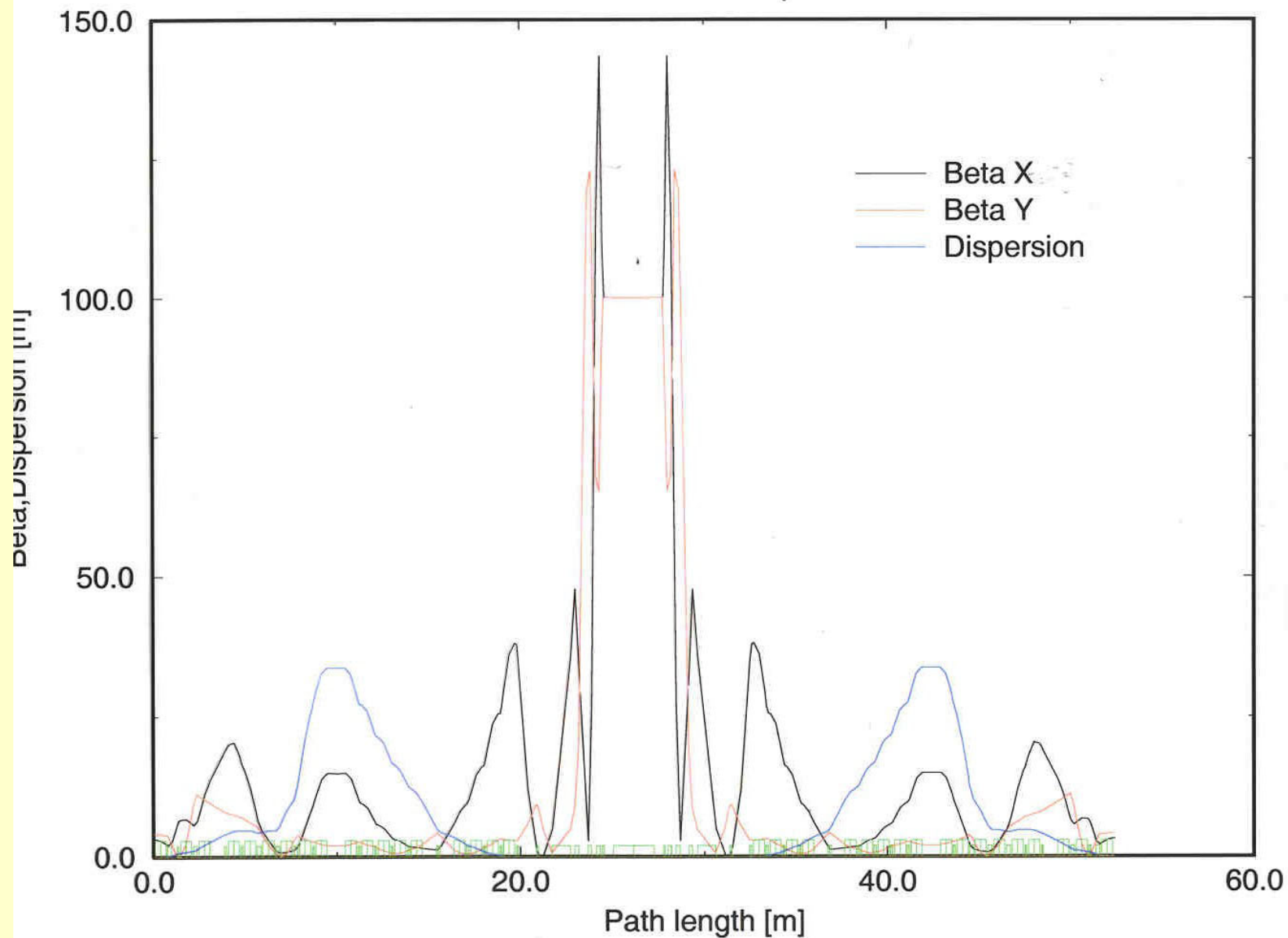


Photo-injector

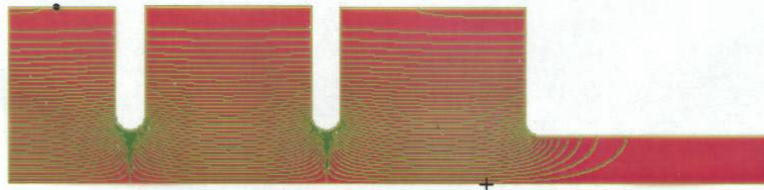
The e- source is crucial for getting high quality beams.

A 1.3 GHz 2½-cell RF-gun with a photocathode is chosen for

- its advantages in producing high charge and high quality electron beams.
- BNL has expertise in the field
- same frequency as linac

Gun design:

Cooperating with AES(Advanced Energy System).
Gun will be built there, then installed in Test Facility.



Cathode material and laser:

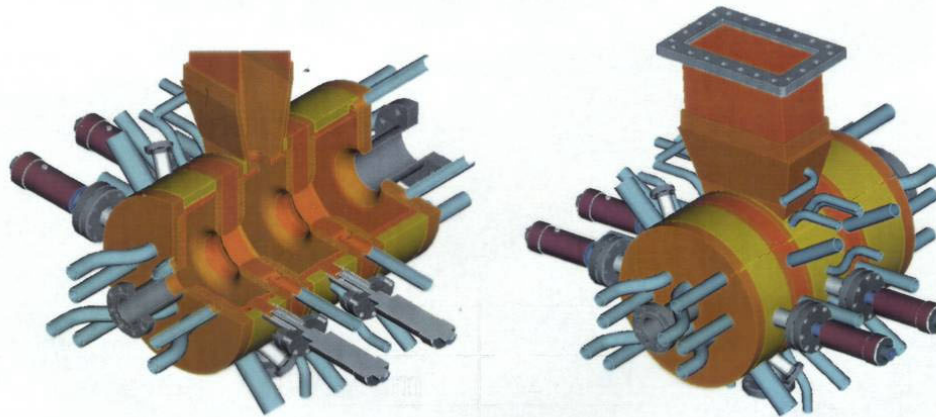
R&D is to be done to determine cathode material and corresponding laser system. (T. Srinivasan-Rao, Instrumentation Division)

Major issue for gun: **high dissipated power**

Field (MV/m)	15	20	25
Diss. power (kw)	773	1373	2140
Ave. power den. (w/cm^2)	293	520	810
Max. power den. (w/cm^2)	359	638	937

120°C operating temperature.

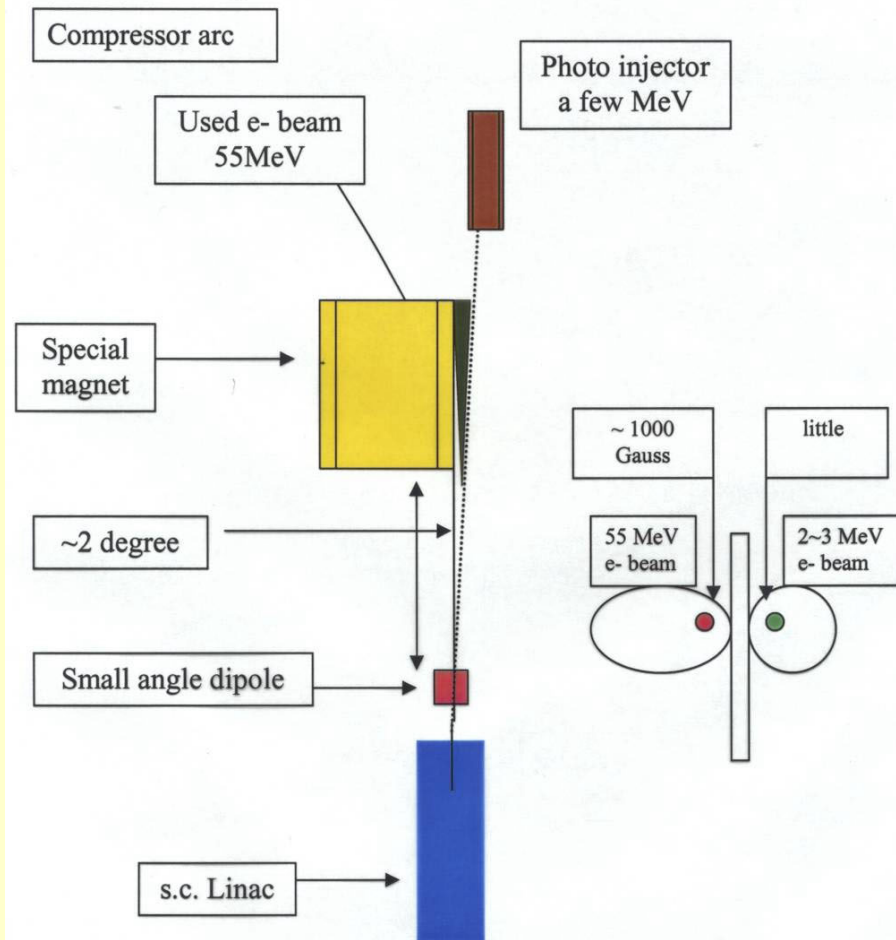
Thermal and mechanical designs are being performed in AES. It appears that it is workable at least with 15 MV/m field gradient.



Preliminary water cooling design(AES)

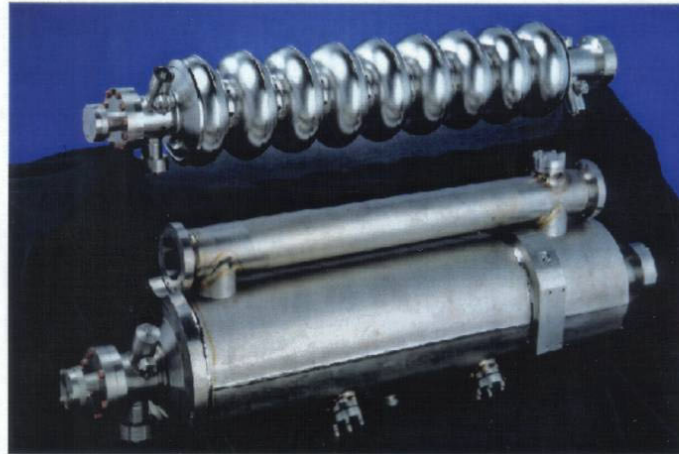
Gun to Linac: Beam Merger

Try to avoid any large bending angle chicane or like.



Linac

- 1.3GHz, 3 or 4 TESLA 9-cell cavities
- good performance
- agreement with DESY in production of cavities for BNL in ~ 2 years
- Gradient in test facility: ~ 20 MV/m
- Energy at exit: up to 55 MeV
- cw operation: no fundamental problems.



This workshop: a lot of things to learn from JLAB and others on high power cw operation with Energy Recovery.

Cryogenic issue: **Heat load(2K):**

TESLA Test 8-cavity cryostat module:

11 W (5 Hz), including HOM,

RHIC e-cooling 3-cavity cw-mode:

3 x 20W(14MeV/m) ~ 40W(20MeV/m)

= 60~120W + HOM

($Q=1 \times 10^{10}$ at up to 20 MeV/m, if higher, say, 1.5×10^{10} , it is better)

Cryogenic capability in BLDG 939 (M. Iarocci)

- set a limit.
- may have to operate in **pulsed mode** mainly and test in cw mode for short time.

Solenoid design

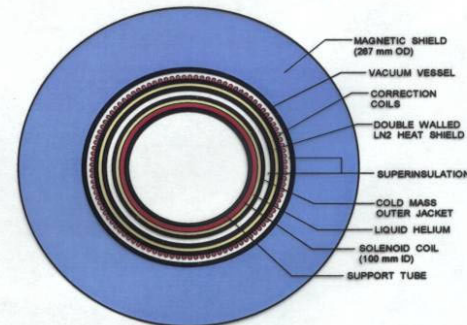
(M. Harrison, A. Jain,
Superconducting
Magnet Division)

~ 10^{-5} field quality
very challenging

Beam dump

(A. Hershcovitch)

~50 mA @ 2~3 MeV



Optimizations of beam performance of photo-injector

Gun working parameters at 5 nc

Frequency: 1.3GHz
Number of cells: 2 ½ cell
Cathode radius: ~ 0.9 cm
Laser pulse length: ~ 20 ps
Initial RF phase: ~ 15 degree
Magnetic field at cathode: 0~100 Gs
Gradient at cathode: 15 MV/m
Energy at exit: ~ 2.35 MeV
External field: 3 solenoid coils

Optimization with PARMELA: non-magnetized beam

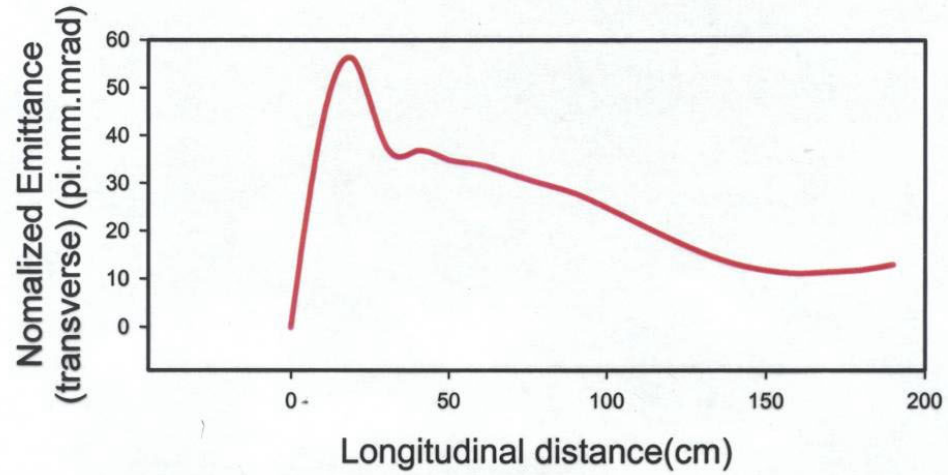
Major parameters	Unit	Exit of RF-gun	Entrance of linac
Beam energy	MeV	2.35	2.35
Trans. emittance	mm.mrad	35	15
Long. emittance	KeV.deg	32.3	72.1
Energy spread	%	2.2	4.3

Magnetized beam case(some arguments):

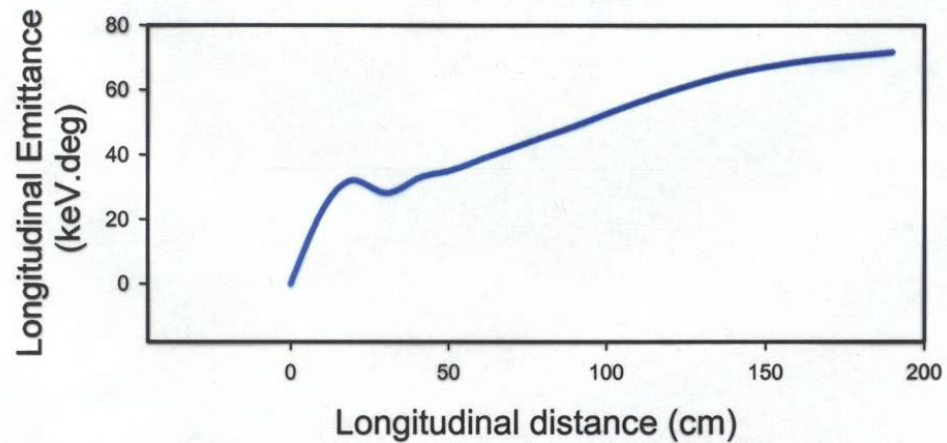
- **Transverse emittance: larger by a factor of 2~3.**
- **Beam size: no problem.**

L-band RF-gun for RHIC e-cooling

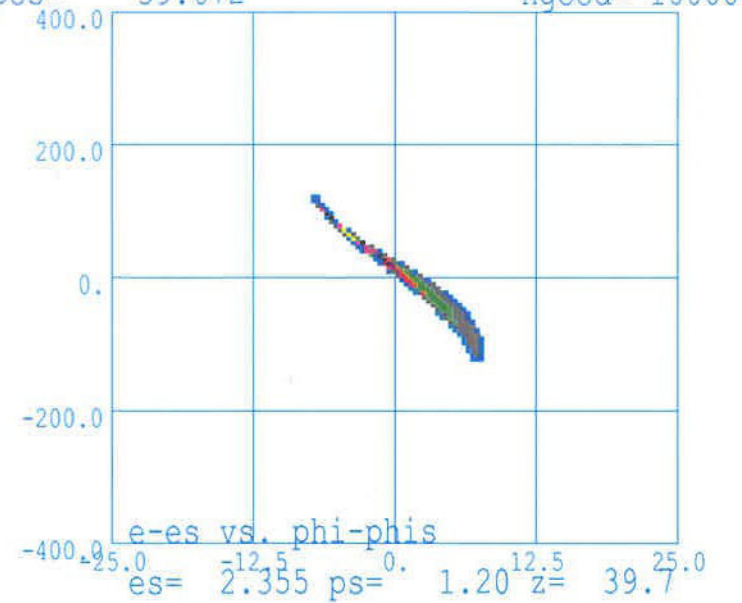
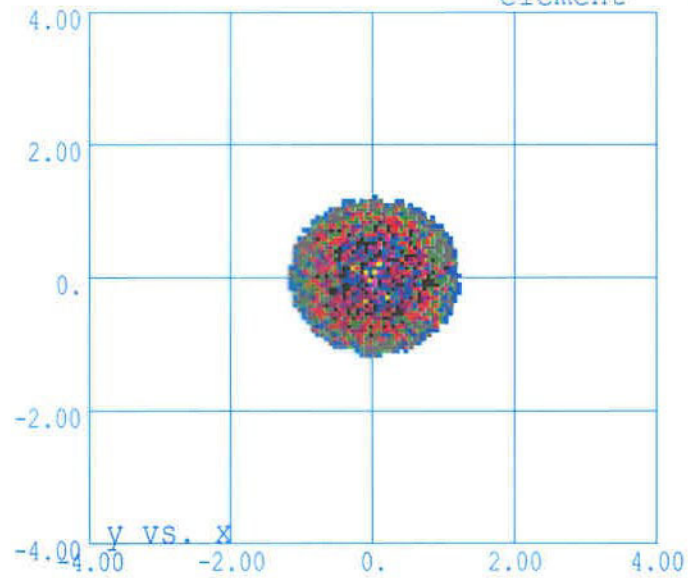
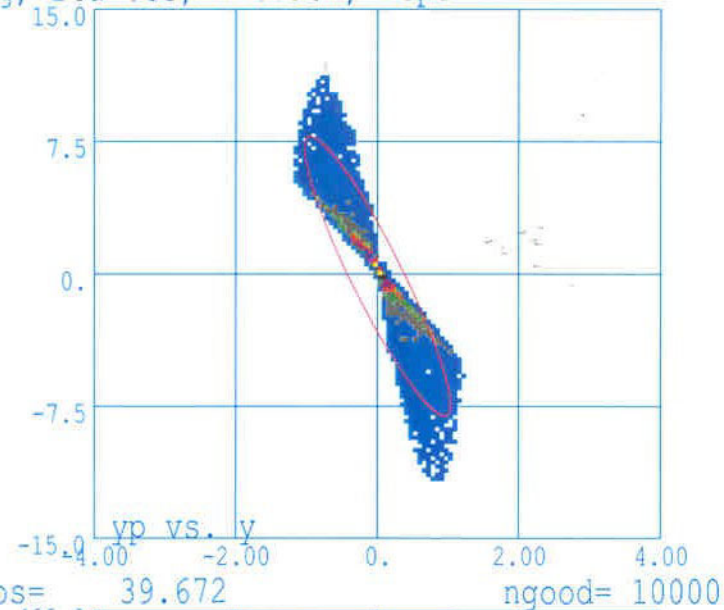
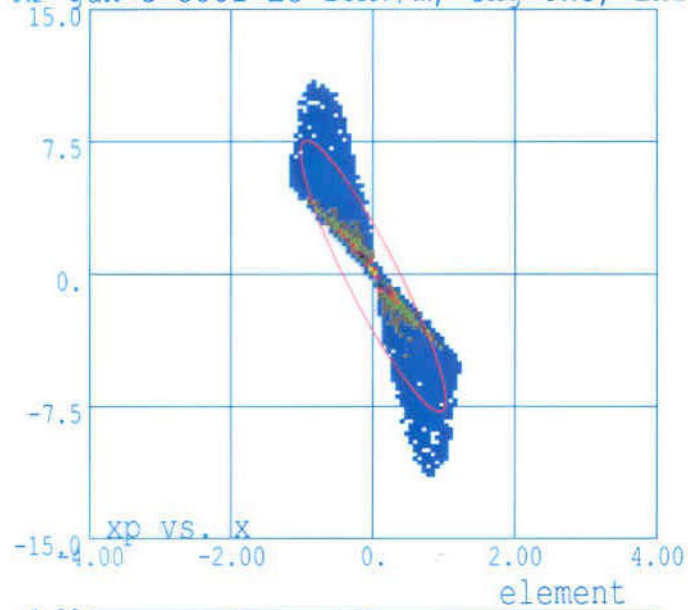
Transverse Emittance



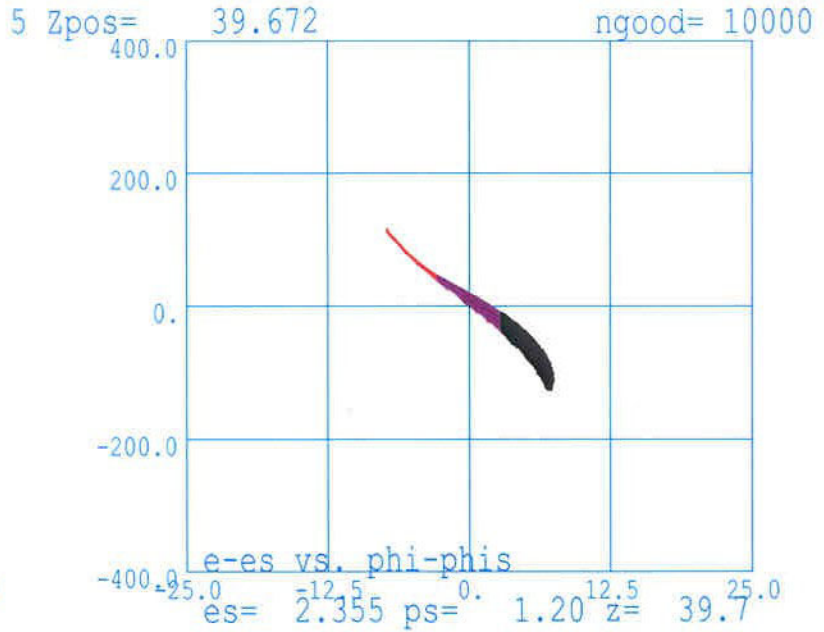
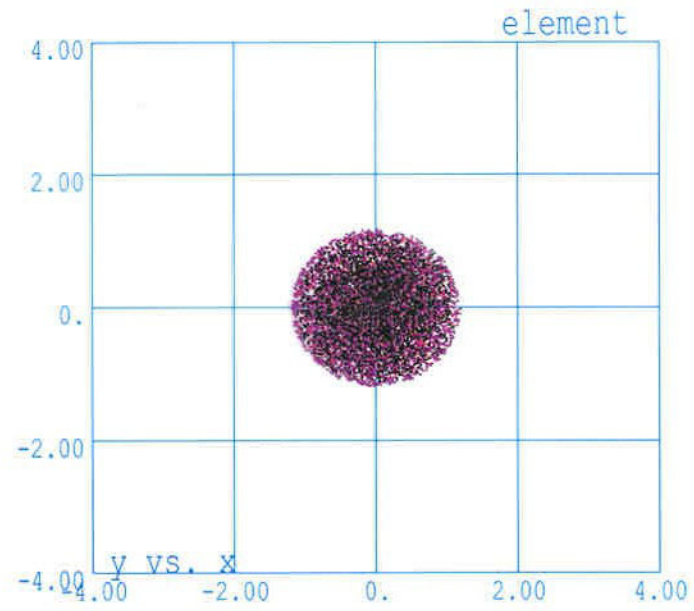
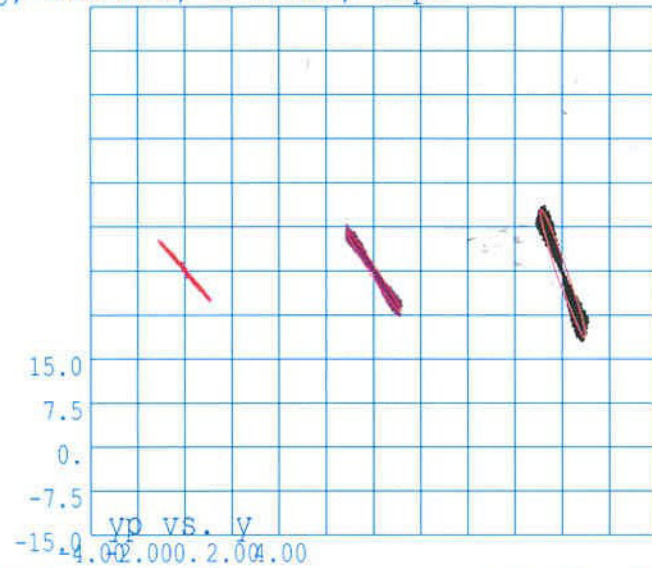
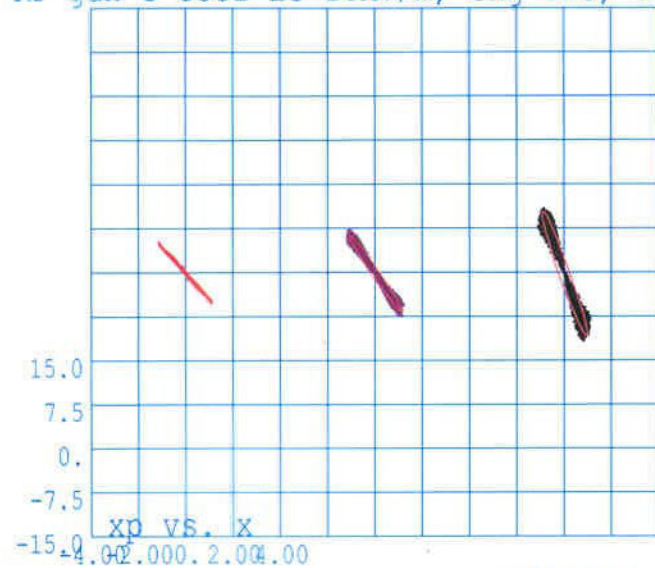
Longitudinal Emittance



RF-gun e-cool $E_c=15\text{MV/m}$, $chg=5\text{nc}$, $ini=15\text{deg}$, $Bca=0\text{Gs}$, $r=0.9\text{cm}$, 10ps



RF-gun e-cool $E_c=15\text{MV/m}$, $chg=5\text{nc}$, $ini=15\text{deg}$, $Bca=0\text{Gs}$, $r=0.9\text{cm}$, 10ps



Beam transport: start-to-end simulation

Crucial for the final electron beam quality at cooler.
Still underway.

- **Preserve/control emittance**
various effects, non-linearities, CSR, etc.
- **Preserve angular momentum**
Optics matching. (Derbenev, Burov)
(but how well we can do it with energy spread?)
- **Minimize the energy spread:**
decompression
+ RF cavity(28MHz, 200MHz, or higher, to be determined)
- **Back to linac:**
compression + RF cavity

Current lattice design stresses the **flexibilities**.

A lot of modifications are expected to address the issues found in particle tracking simulations.

Summary

- **Progress in all aspects of study on electron cooling for RHIC has been made in BNL recently. Results so far are encouraging.**
- **The concept of the E-cooling Test Facility for RHIC is defined. Design of layout and photo-injector are done. Start-to-end simulations and multi-bunch effects calculations are being performed.**
- **Hardware installation will start this May. More R&D are to be conducted.**
- **Still a lot of issues to be addressed. Your input is needed.**

Thank you.

Polarized Electron Sources for a Linac-Ring EIC

M. Farkhondeh

MIT-Bates Linear Accelerator Center

Middleton, MA 01949, USA

EIC Workshop

BNL, February 26, 2002

OUTLINE

- **Fundamentals of polarized electron sources**
- **Polarized source for a linac-ring EIC**
- **Options for the laser system and injector**
- **Issues for EIC polarized source**
- **Summary**

Fundamentals of PES

To date, photoemission from GaAs is the the only practical method of producing polarized electrons for accelerators.

Two fundamental principles:

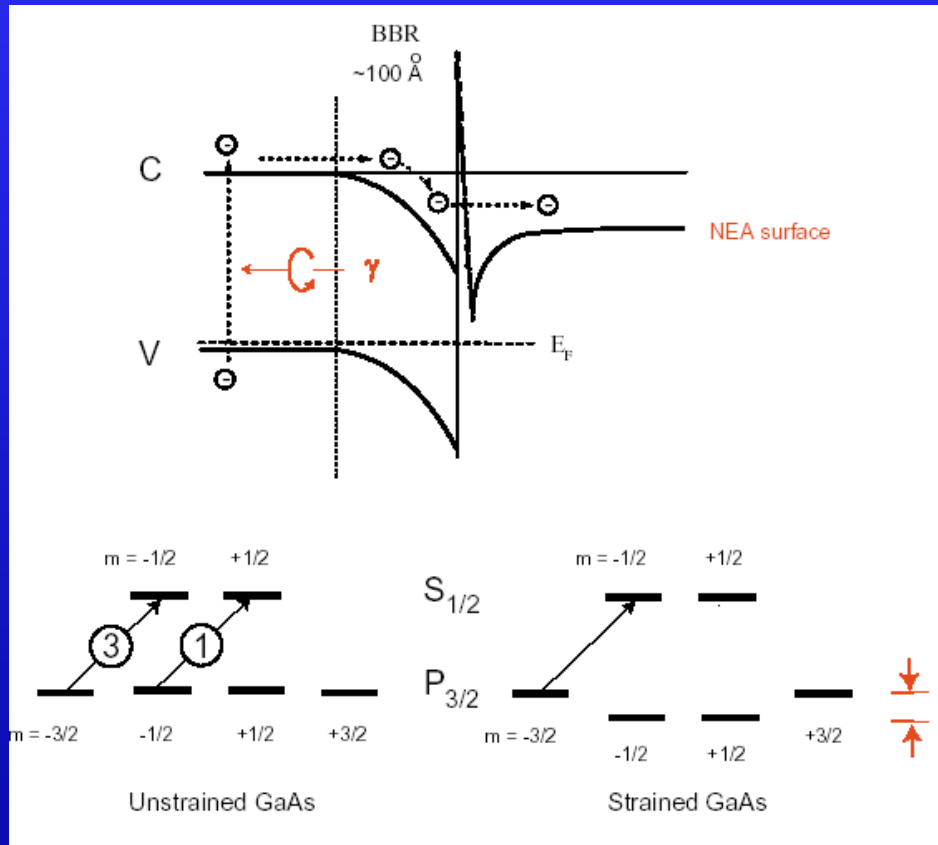
- **Conservation of Angular Momentum:**

 - excitation of the electrons in the valance band to the conduction band with circularly polarized photons**

- **Negative Electron Affinity (NEA):**

 - achieving NEA by lowering the work function to allow the conduction band electrons to escape**

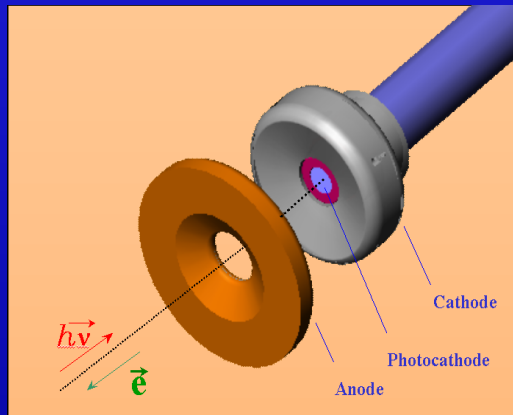
Polarized Photoemission



Courtesy T. Maruyama, SLAC

A Basic Polarized Electron Source

- A GaAs based photocathode in a gun structure
- Provisions in the gun chamber to achieve NEA (Cs and O₂, NF₃)
- A laser system to illuminate the surface of the photocathode with circularly polarized photons of correct wavelength
- An injector to transport and to accelerate the electrons



2002 EIC
workshop

2002 EIC
workshop

A Basic Polarized Source

- Electron beam current :

$$I(mA) = \lambda(nm) P_{laser}(W) QE(\%) / 124$$

- Quantum Efficiency (QE)

- Bulk GaAs: 2-10 % with ~40% polarization

- strained GaAsP: 0.1-0.5 % with >70% polarization

To produce 135 mA beam:

Sample	QE (%)	Polarization	λ (nm)	P_{laser} (W)
Bulk	5	40	780	~5
Strained	0.1	80	850	~200

PES Parameters for the Linac-Ring EIC

- average current: 135 mA in a 28 MHz bunch train
- electrons per bunch: 3×10^{10} (~ 5 nC per bunch)
- normalized beam emittance: < 60 mm-mrad

This average current is ~ 3 orders of magnitude more than what is produced by today's accelerator based polarized sources (J-Lab, Bate and Mainz). The FEL at J-lab runs at 5 mA average current using bulk GaAs photocathodes. At MIT-Bates peak currents of ~60 mA in the test beam line have been produced. The beam emittance requirement is modest.

Laser Systems (need > 200 W power)

- Lasers with RF structure.

Electrons are produced in bunches at the laser frequency; challenging at 28 MHz. Existing systems provide at best a few Watts of power at 500 MHz (M. Poelker) .

Do not exist for EIC currents and frequency. Laser farm

- High power CW diode lasers

CW e beams are produced and subsequently bunched with accelerator structure to the desired frequency; bunching may be difficult at 28 MHz. Today, fiber coupled diode array lasers have power ~ 100 Watts.

Issues: bunching and capture efficiencies at 28 MHz .

OPTION 1

(P. Hartman, C. Sinclair of Jefferson-Lab at previous EIC workshops)

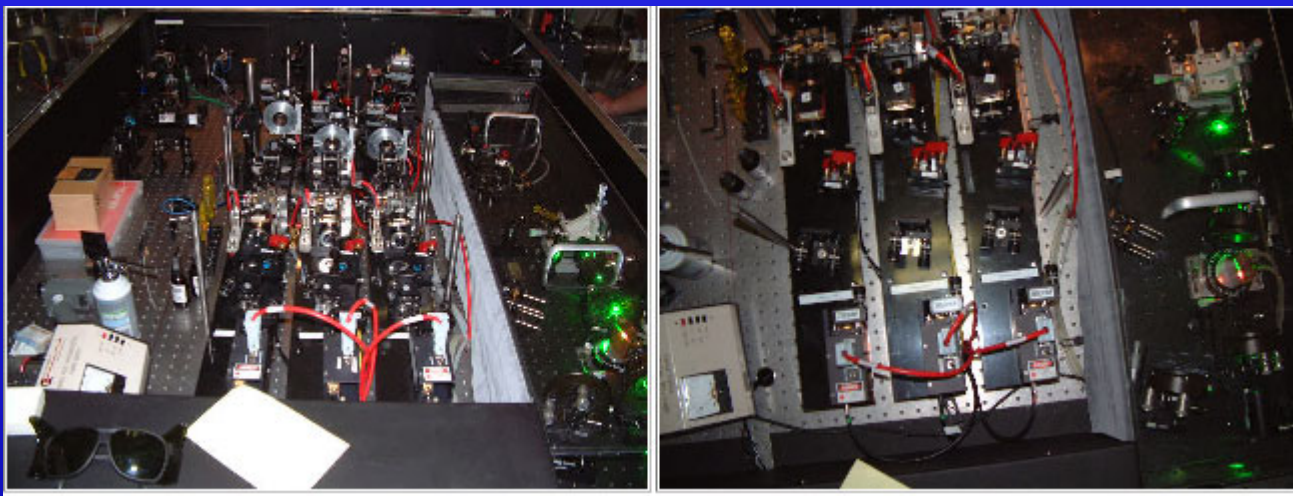
Laser with 28 MHz structure:

with a laser spot size $\sim 3 \text{ cm}^2$, $\text{QE} = 0.1\%$ for high P will need $\sim 200 \text{ W}$ laser for $1/e$ lifetime. Using the best cathode lifetimes at J-lab with $100\text{-}200 \mu\text{A}$ average currents and $\sim 0.2 \text{ mm}$ laser spot, and extrapolating to the EIC currents, he states that 1 week of continuous beam can be maintained.

“... This is a very considerable extrapolation, and must be demonstrated to be believed.” C. Sinclair.

M. Poelker is working on a laser system at lower frequency for a Hall-C experiment.

Jefferson Lab's New Laser/G-Zero Table



http://www.jlab.org/accel/inj_group/laser2001/laser2001.html

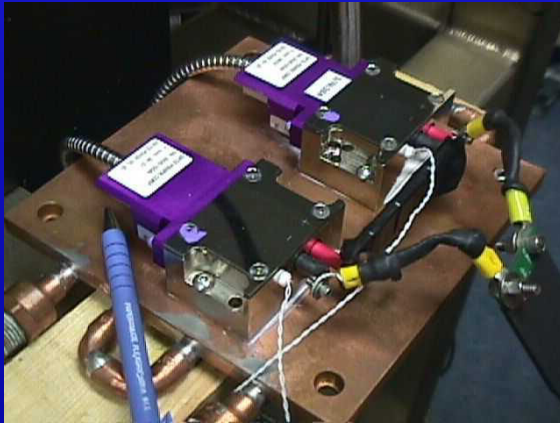
M. Poelker, et. al.

OPTION 2

High power CW fiber coupled diode array lasers with no RF structure

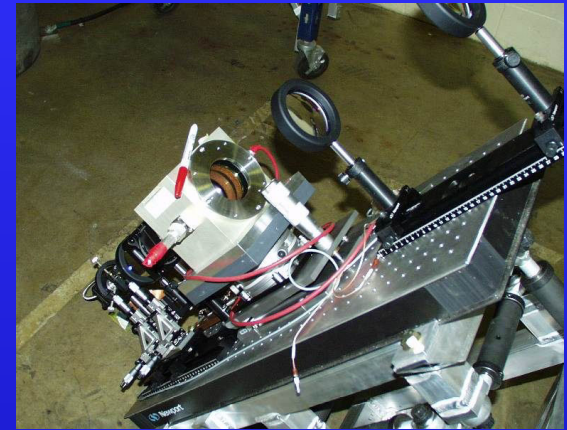
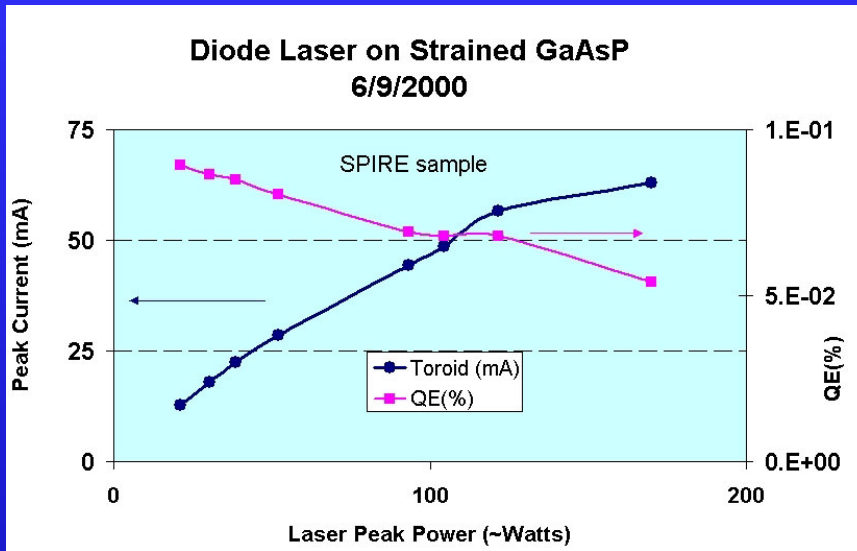
- These inexpensive lasers produce ~ 60 - 100 W power at fixed wavelength but have very large emittance (200 mm-mr). Can couple multiple bars into a single fiber for higher power.

Peak currents of ~ 60 mA at 1% duty cycle have been demonstrated. High average current needs to be demonstrated.

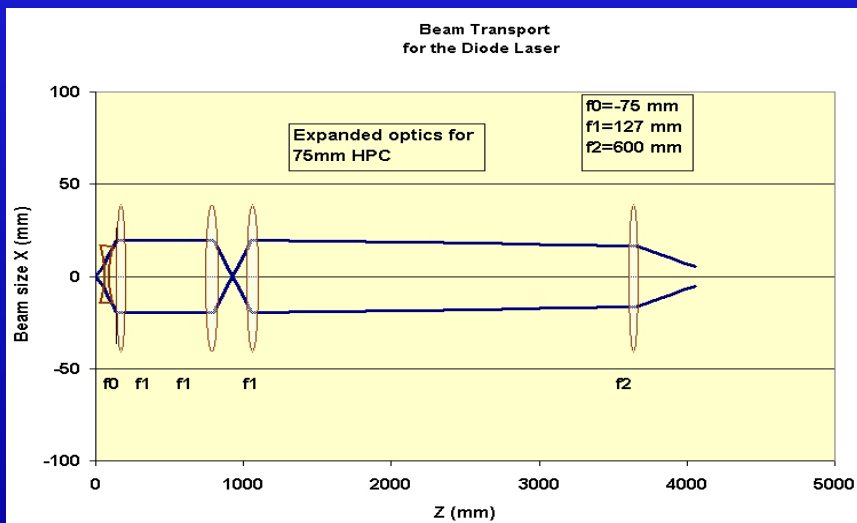


MIT-Bates laser
setup

Laser: OPTION 2 ...



Large aperture optics
can use waveplates
instead of Pockels cells



MIT optics and
results

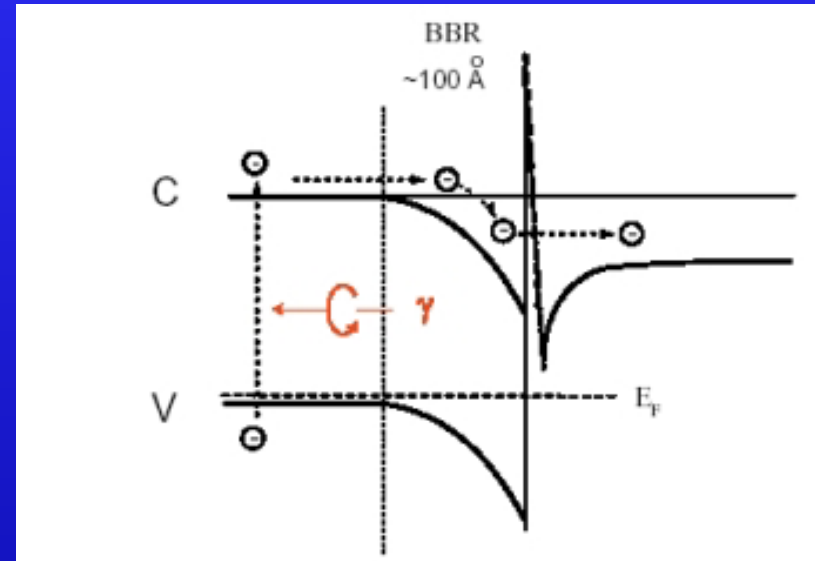
2002 EIC
workshop

Issues for Linac-Ring PES :

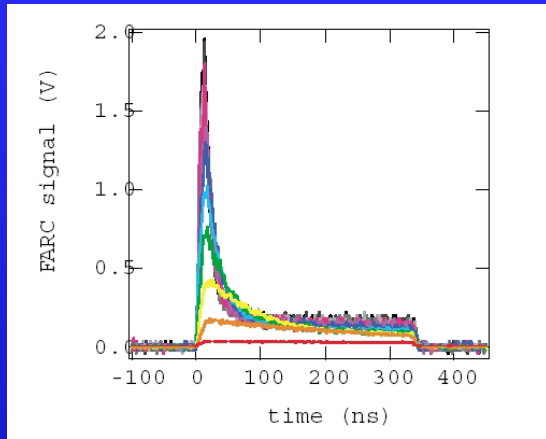
- **Surface charge limit**
- **Average currents**
- **Laser systems**

Surface Charge limit

- electrons are trapped on the surface before recombining with holes.
- beam current not proportional to laser intensity
- effect more severe in high P that have low QE's
- time scale of ~ 100 ns



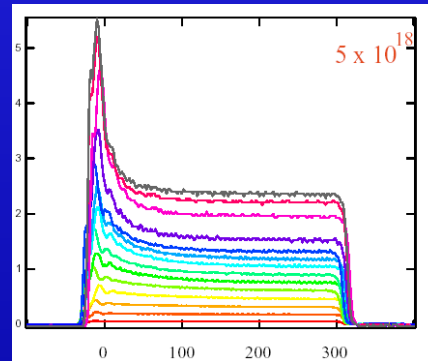
Surface Charge limit



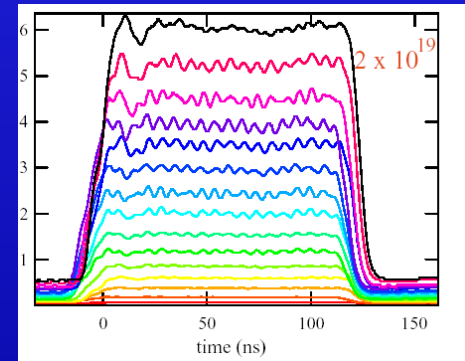
Data from SLAC

Increasing Charge limit:

- Increase doping concentration
- superlattice structure
- large band-gap material
- larger cathode area



5×10^{18}

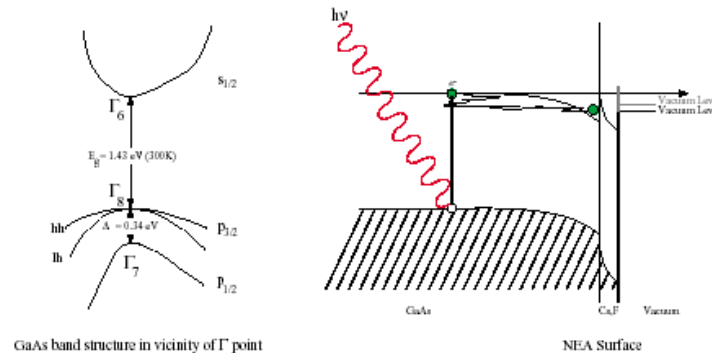


2×10^{19}

Surface Charge limit

Surface Charge Limit

Charge output is not proportional to light intensity



- Photon absorption excites electrons to conduction band
- Electrons can be trapped near the surface
- Electrostatic potential from trapped electrons raises affinity
- Increased affinity decreases emission probability
- Affinity recovers after electron recombination

T. Maruyama, SLAC

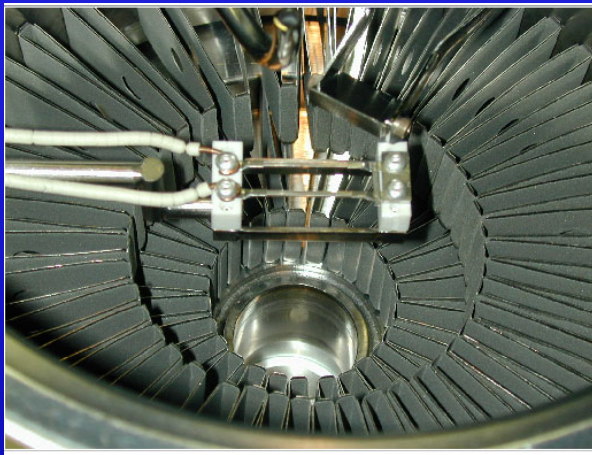
Average Current:

100-200 mA average current is three orders of magnitude over today's currents. Need serious R &D and tests to probe this new territory

- **Photocathode lifetime is a strong function of vacuum condition between anode and cathode and presently is limited by the ion back bombardment of the surface of photocathode**
- **Excellent UHV vacuum condition well into Extreme High Vacuum XHV is essential.**

Average Current:

Excellent vacuum conditions achieved at J-lab and MIT-Bates by adding large capacity NEG pumps near the anode-cathode region which lead into very long photocathode lifetimes.



J-Lab added massive
NEG pumps below the
anode plate



MIT added NEG pumps
on top

Laser Systems:

More than 200 W of laser power is needed to produce ~ 100 mA average current assuming no surface charge limit.

- Lasers with RF structure at these high power levels do not exist. CW diode array lasers approaching ~ 60 -100 Watts exist today but need to evaluate the feasibility and the efficiency of bunching the electron beam at 28 MHz and handling large emittance.

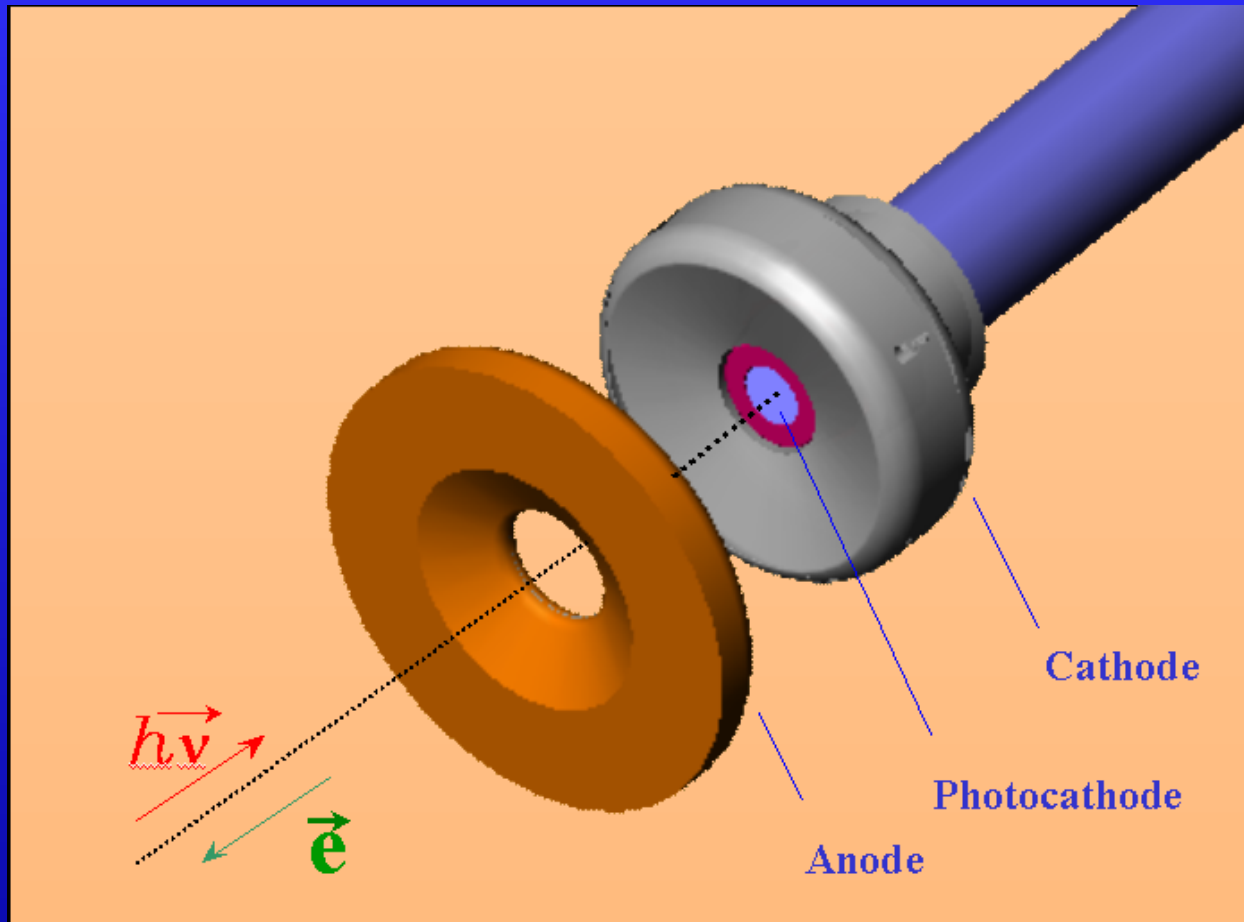
The MIT-Bates Test Setup and the laser system may be a suitable benchmark for R&D on the latter option.

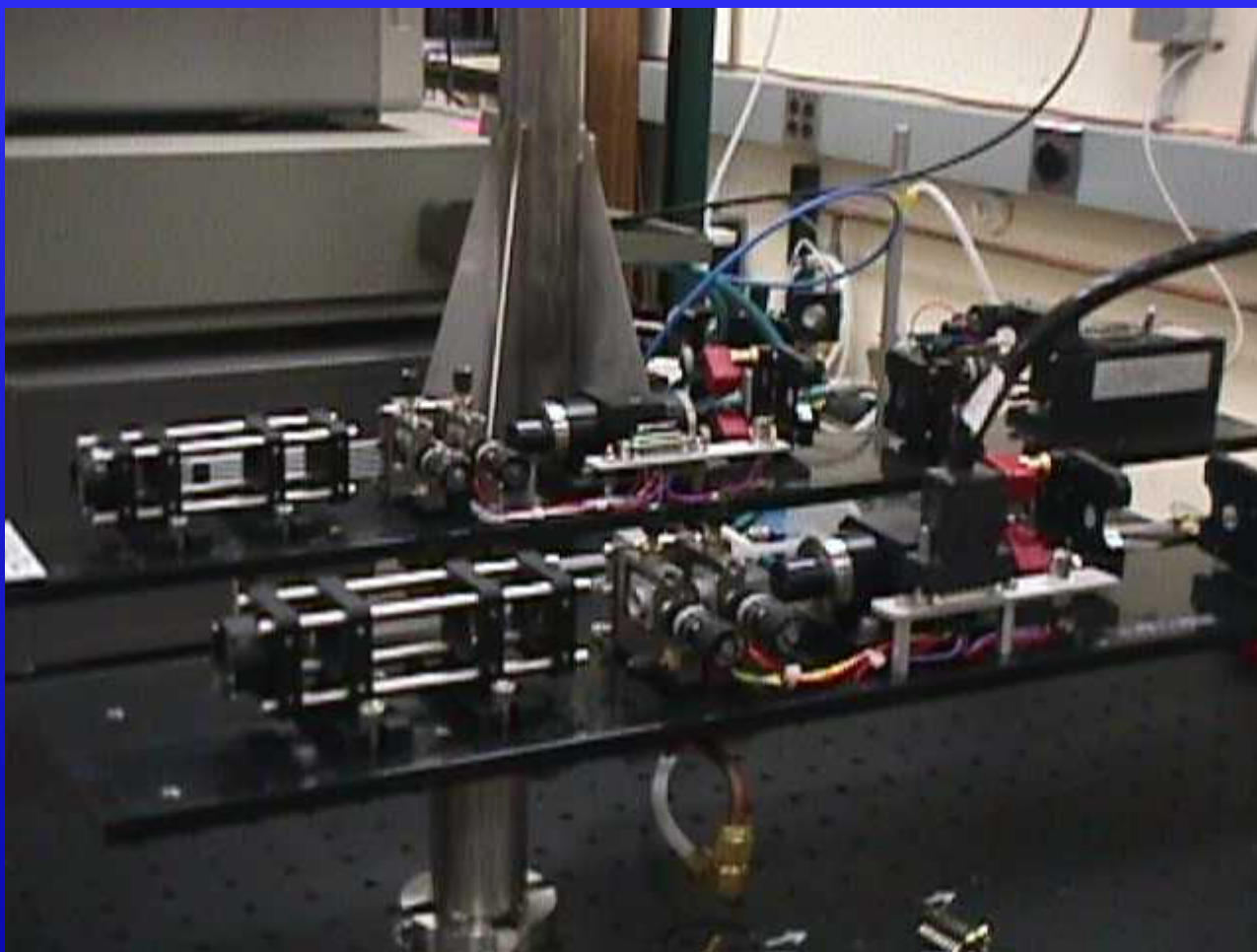


MIT 60 keV test beam setup

Summary

- **EIC average currents of 100-200 mA highly polarized electron beam is very challenging, but seems feasible by extrapolating the performance of the existing polarized sources.**
- **EIC frequencies of 28-56 MHz may be a difficult regime for both types of laser systems.**
- **Based on high peak current photoemission tests at MIT and at SLAC, surface charge limit may be overcome for EIC currents.**
- **Need serious R&D efforts to demonstrate the feasibility of achieving the EIC injection for a Linac-Ring EIC.**





**Jefferson Lab 500 MHz laser system
(M. Poelker)**

**2002 EIC
workshop**

PESP-2002

Polarized Electron Sources and Polarimeters, Satellite Workshop of SPIN-2002

TOPICS:

- *Physics of Polarized Electron Photocathodes*
- *Polarized Electron Sources*
- *Low Energy Polarimeters*
- *Application of polarized electron sources*
- *Polarized Sources and Parity-Violating experiments*

International Advisory Board:

- K. Aulenbacher (Munich)*
- T. Nishitani (Nagoya Univ.)*
- J. C. Kaldenbach (SLAC)*
- Yu. A. Izrael (SPTU)*
- Ol. Poedker (Jefferson Lab)*
- A. S. Tikhonov (Novosibirsk)*
- T. Maruyama (SLAC)*

Local Organizing Committee:

- Ol. Farkhondeh (Chair) MIT-Bates*
- B. Franklin MIT-Bates*
- E. Wolff MIT-Bates*
- C. Tschalutz MIT-Bates*
- E. Trinitadonikh MIT-Bates*
- T. Zverev MIT-Bates*
- A. Melnik MIT-Bates*
- G. Bullard (Conf. Secretary)*

Sponsored by:

- *International and Local Organizing Committees of the Spin Physics Symposium*
- *MIT-Bates Linear Accelerator Center*

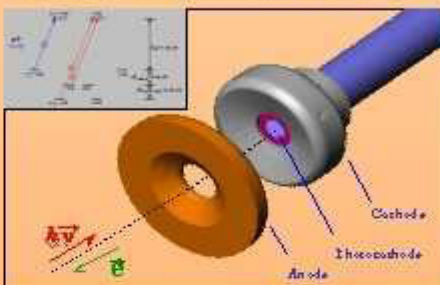
For More Information:

<http://mitbates.mit.edu/pesp2002>

pesp2002@batespop.mit.edu

September 4-6, 2002

MIT-Bates Linear Accelerator Center



PESP-2002

TOPICS:

- *Physics of Polarized Electron Photocathodes*
- *Polarized Electron Sources*
- *Low Energy Polarimeters*
- *Application of polarized electron sources*
- *Polarized Sources and Parity-Violating experiments*

International Advisory Board:

K. Aulenbacher (Mainz)
T. Nakanishi (Nagoya Univ.)
J. Clendenin (SLAC)
Yu. A. Mamaev (SPTU)
M. Poelker (Jefferson Lab.)

Local Organizing Committee:

T. Maruyama (SLAC)
M. Farkhondeh (Chair) MIT-Bates
W. Franklin MIT-Bates
E. Ihloff MIT-Bates
C. Tschalaer MIT-Bates
E. Tsentalovich MIT-Bates
T. Zwart MIT-Bates
A. McInnis MIT-Bates

Sponsored by:

- *International and Local Organizing Committees of the Spin Physics Symposium*
- *MIT-Bates Linear Accelerator Center*

For More Information:

<http://mitbates.mit.edu/pep2002>

pep2002@batespop.mit.edu



Polarized Electron Sources and Polarimeters, Satellite Workshop of SPIN-2002

September 4-6, 2002

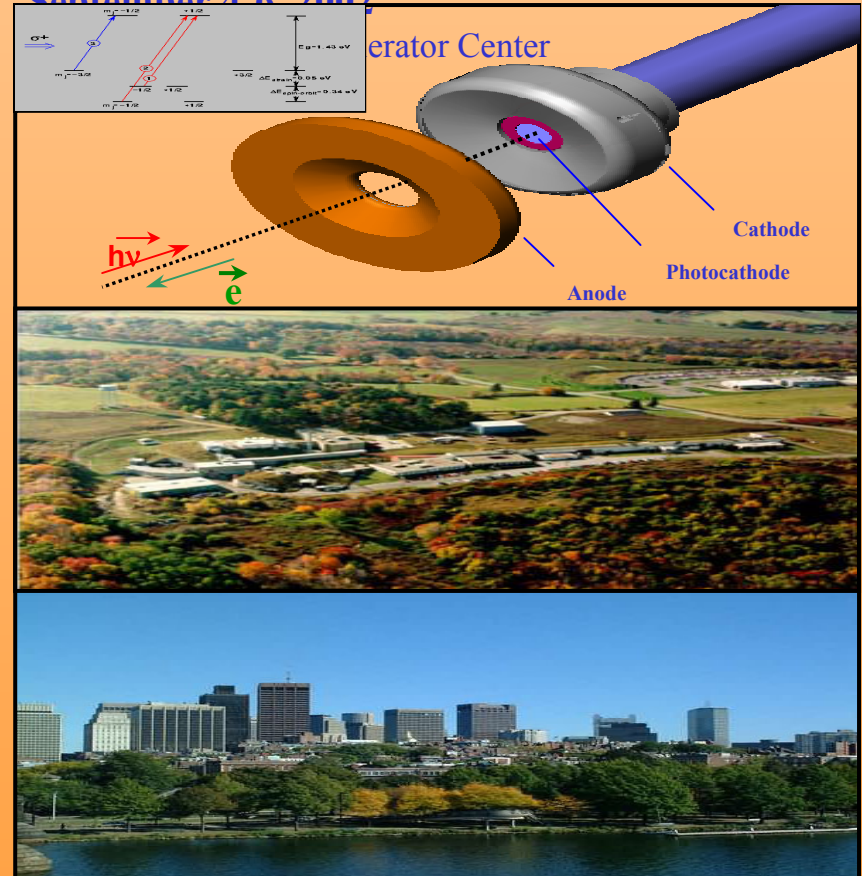


Photo:FreeFoto.com



EXTRA material

**Polarized Electron Sources for a Linac-Ring EIC
(PES-LIR-EIC)**

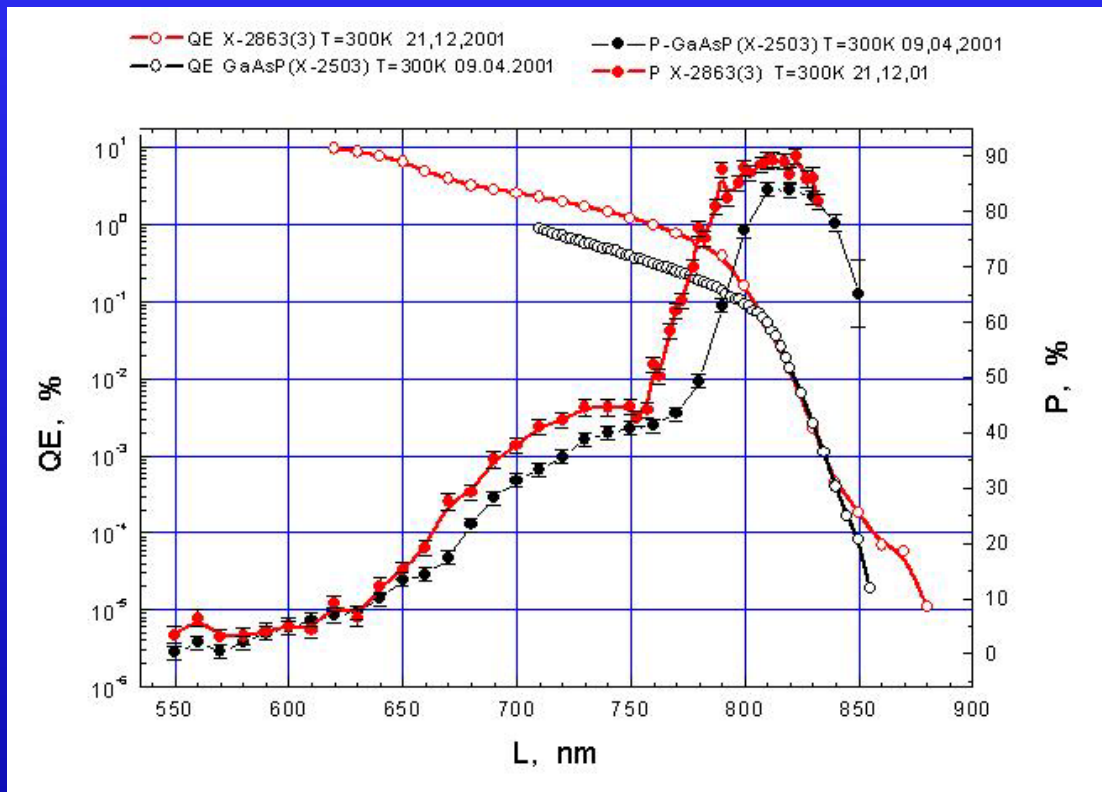
M. Farkhondeh

**MIT-Bates Linear Accelerator Center
Middleton, MA 01949, USA**

EIC Workshop

BNL, February 26, 2002

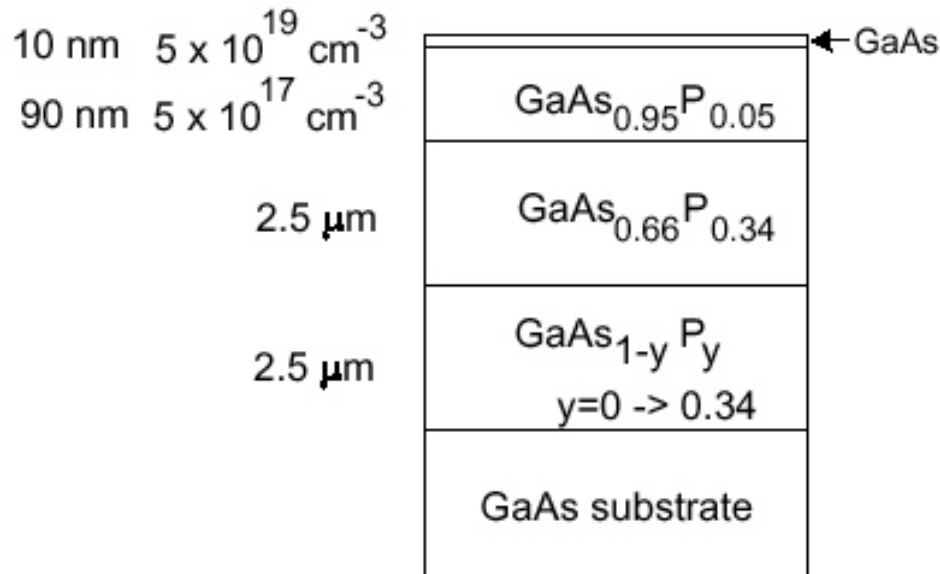
**2002 EIC
workshop**



St. Petersburg sample

NLC peak micro-bunch current = 9 A.

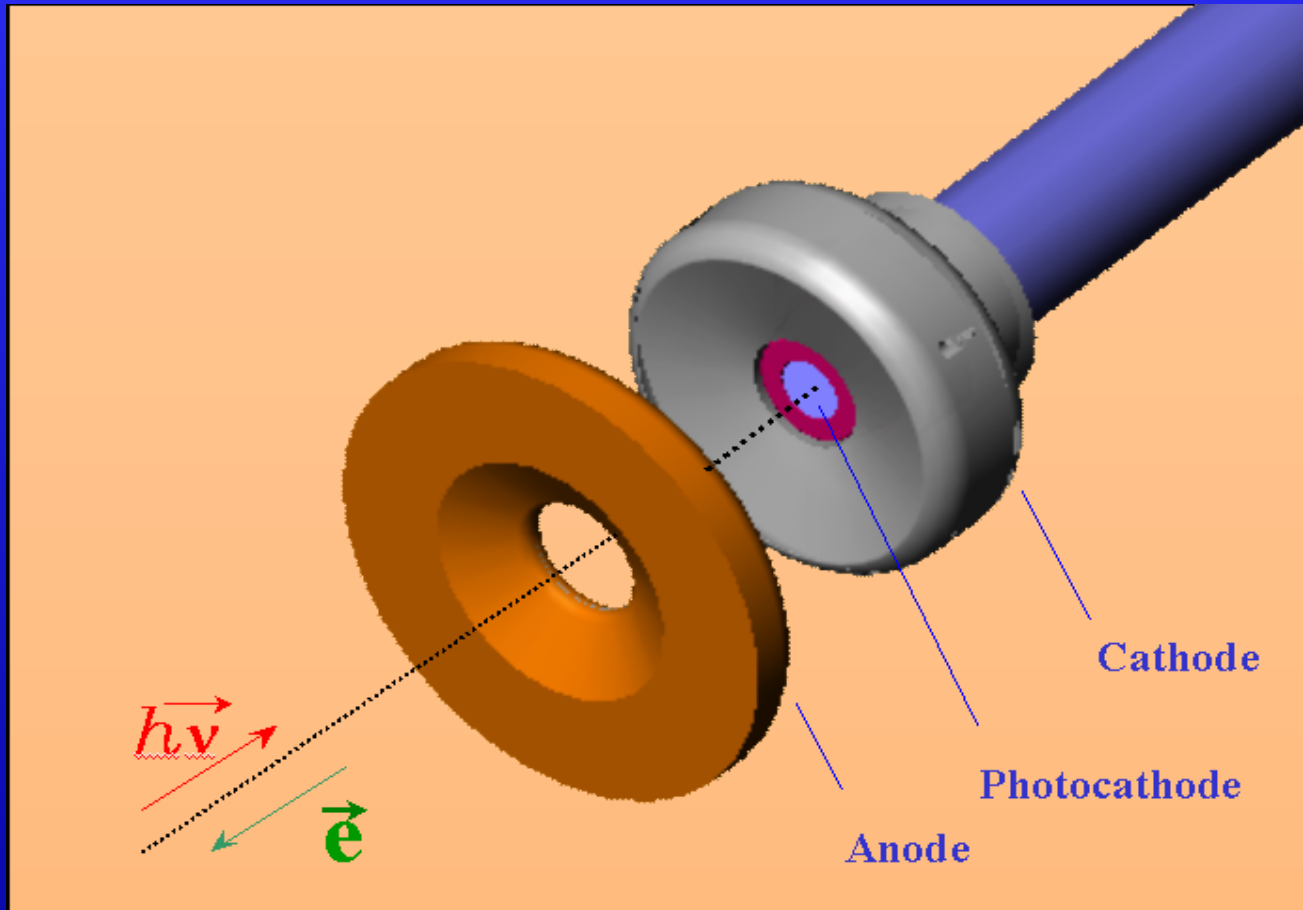
Used a modified version of SLC cathode MOCVD-grown by Bandwidth Semiconductor (formerly Spire):



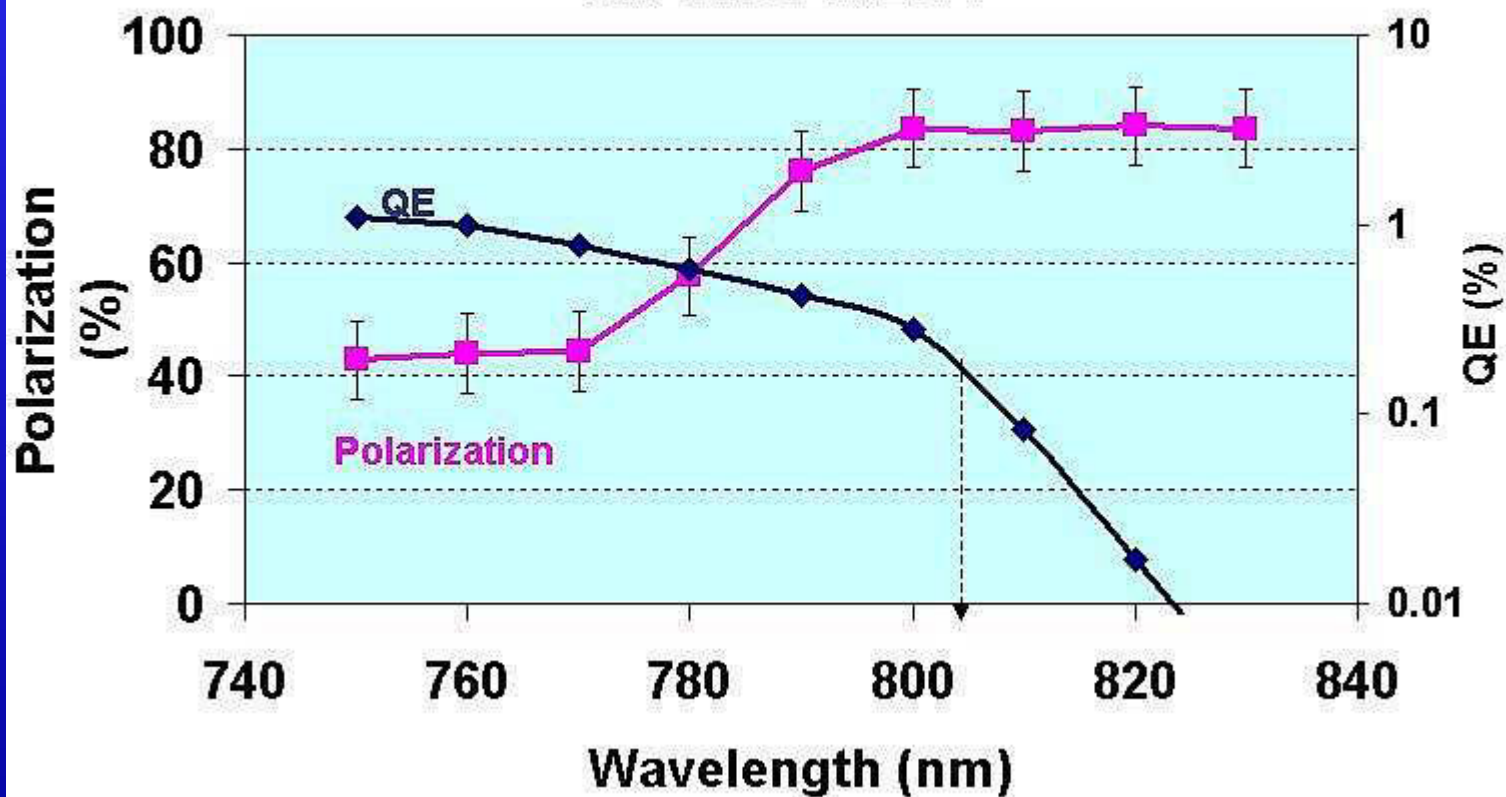
**SLAC sample grown by Bandwidth
semiconductor Inc.**

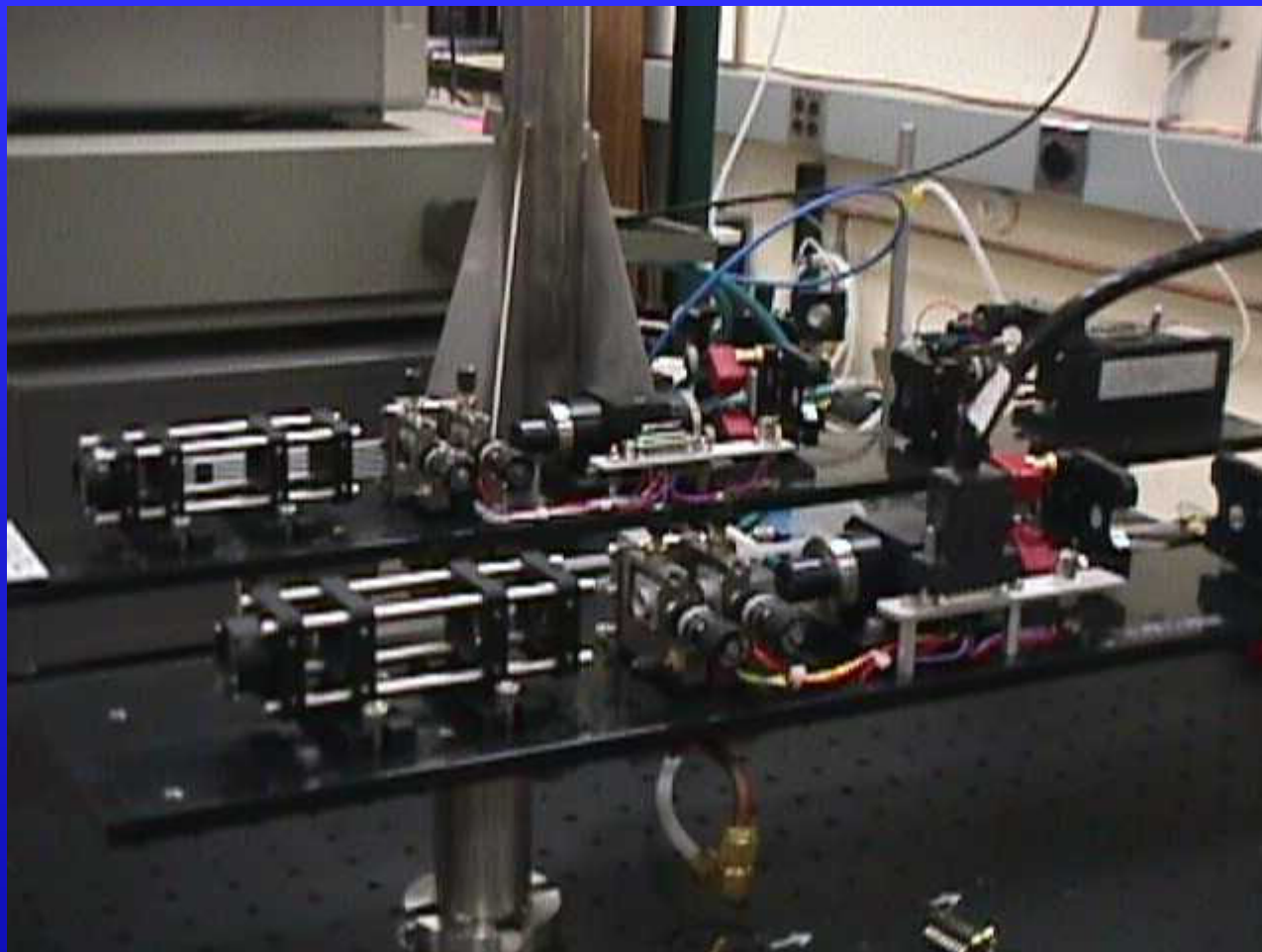
**2002 EIC
workshop**

A Basic PES



Strained GaAsP
MIT-Bates 12/2000



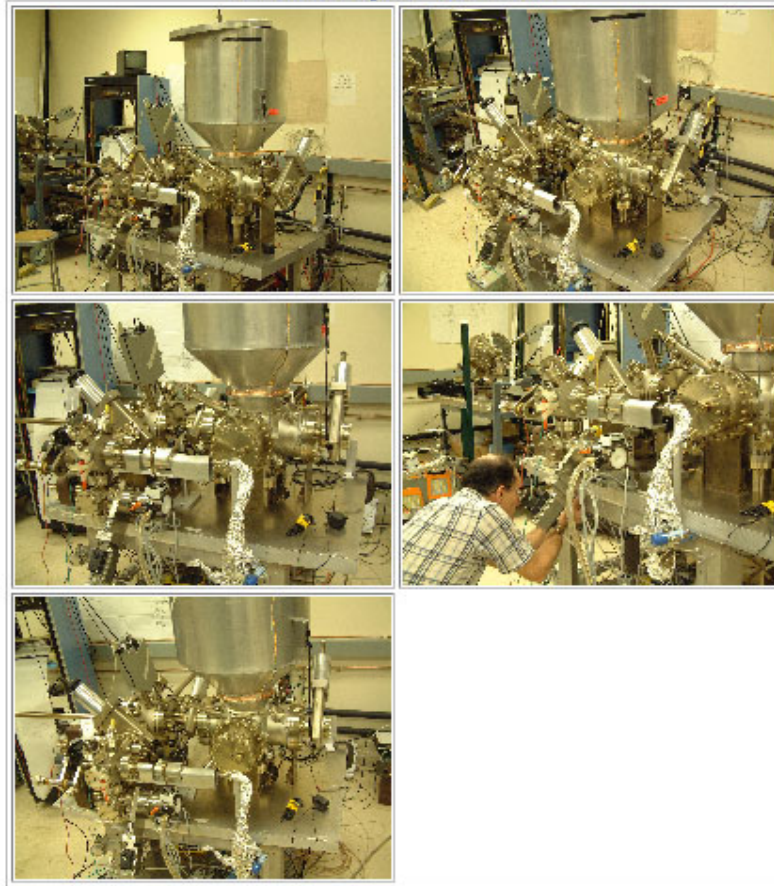


**Jefferson Lab 500 MHz laser system
(M. Poelker)**

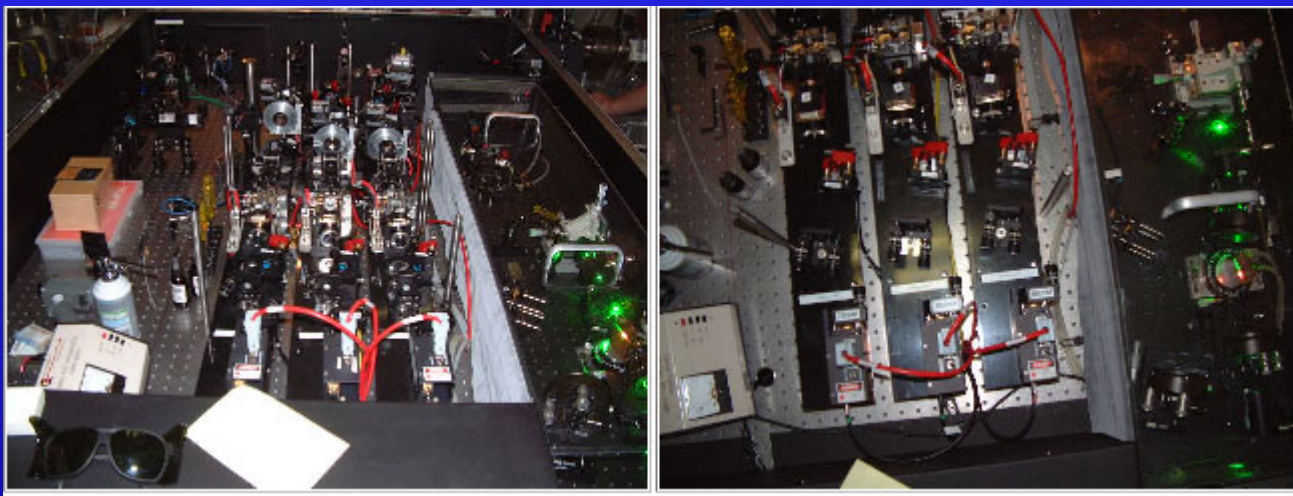
Jefferson
Lab Test
Load-Lock
Gun

Best Technology Load-lock Polarized Electron Gun

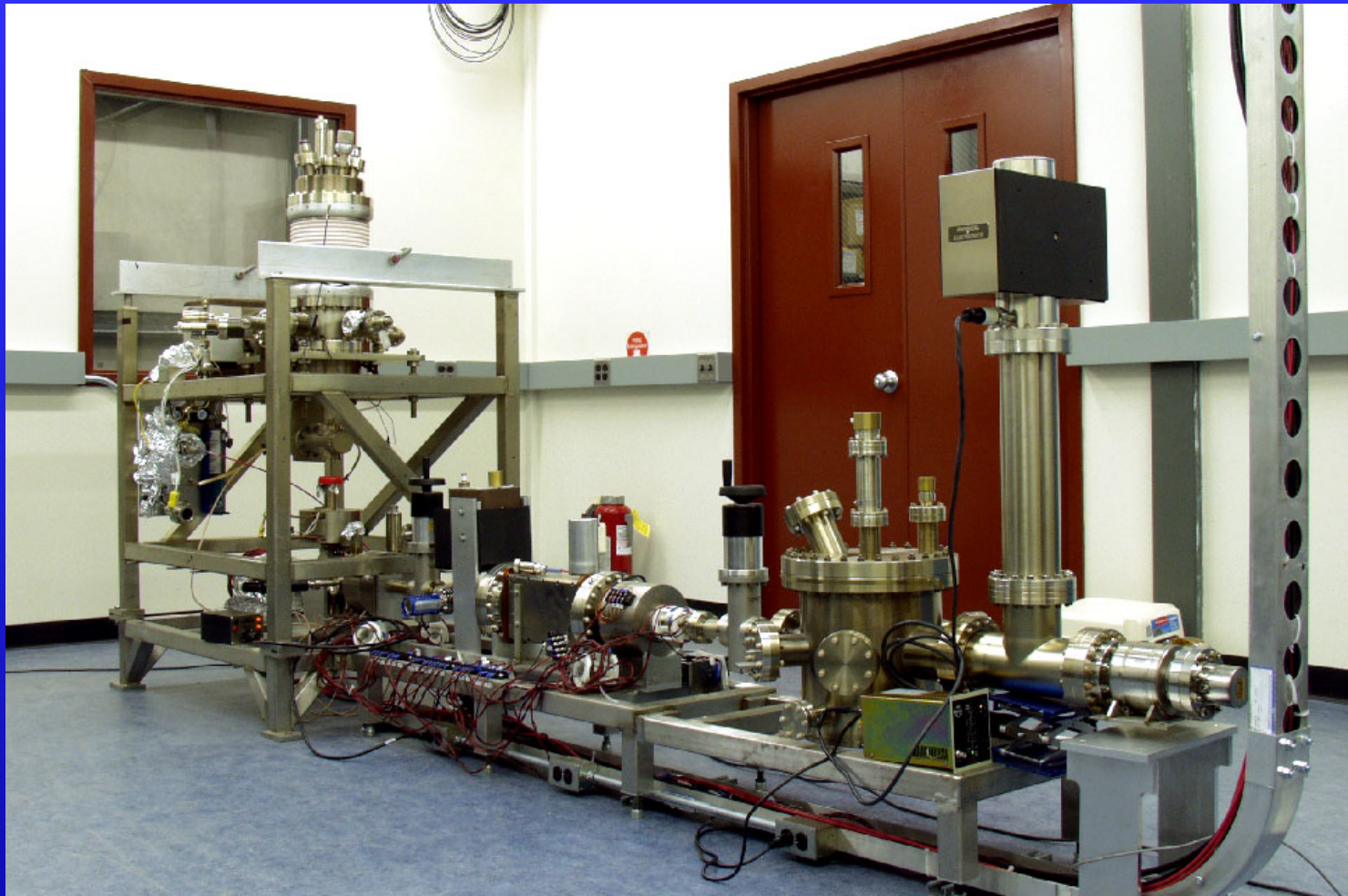
January 14, 2002



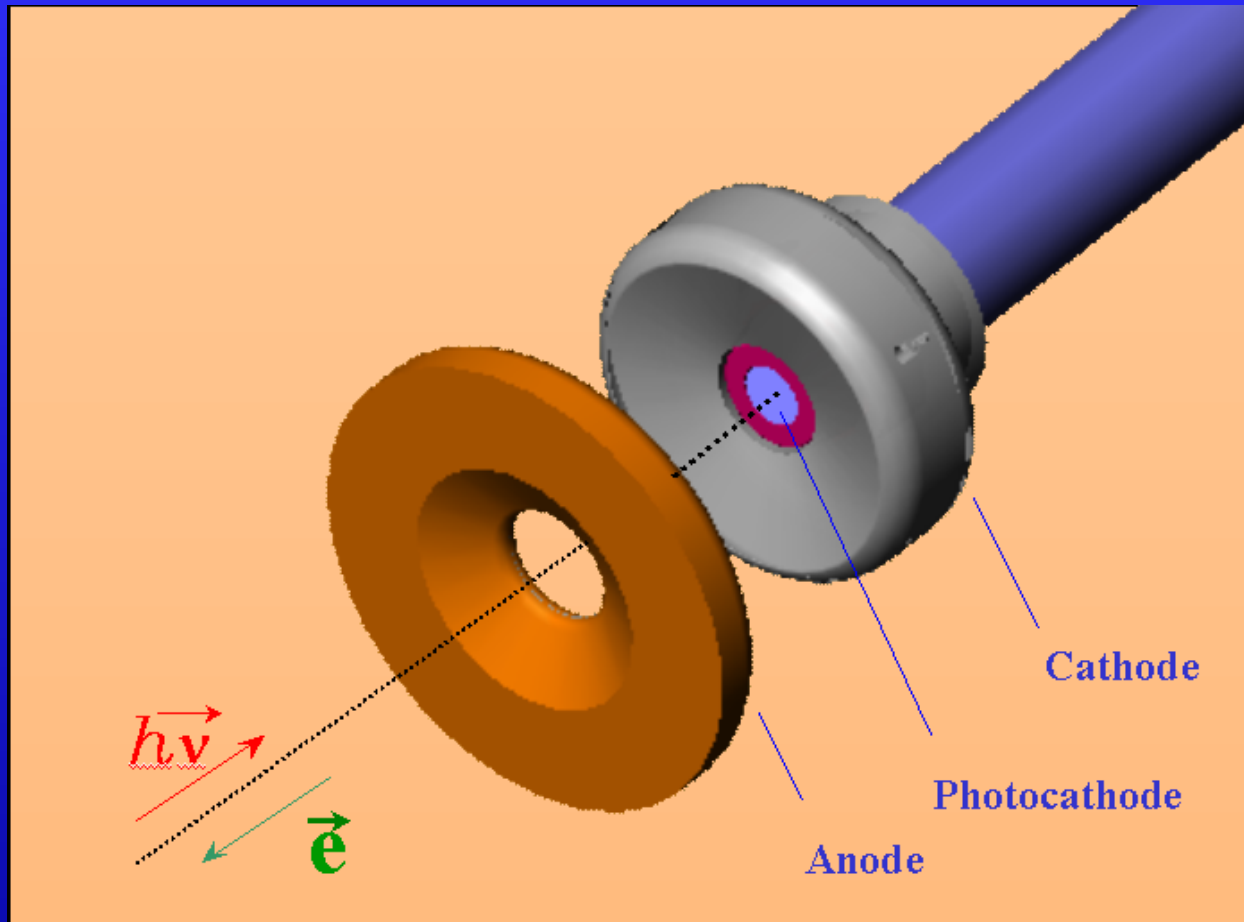
Jefferson Lab's New Laser/G-Zero Table



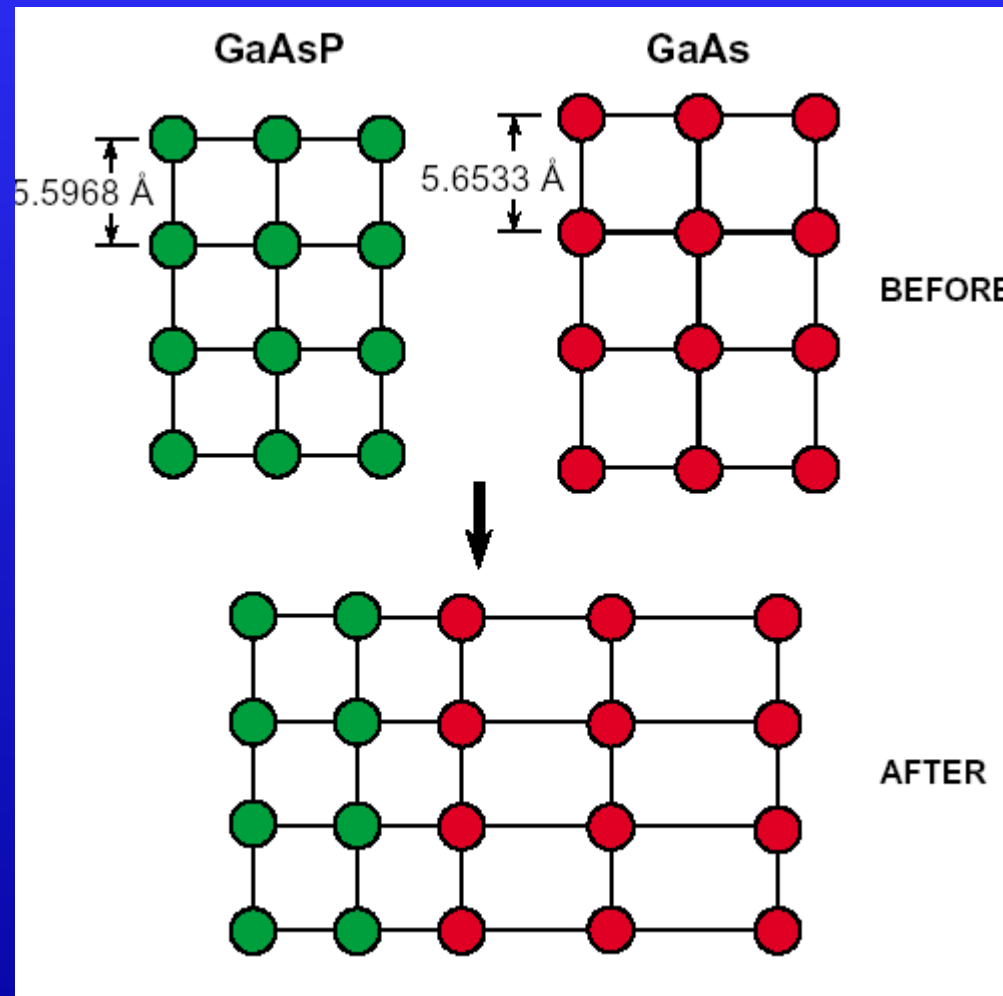
http://www.jlab.org/accel/inj_group/laser2001/laser2001.html



MIT 60 keV test beam setup



Strained layer GaAsP on GaAs substrate

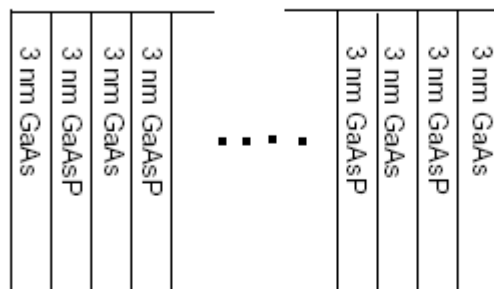


Courtesy T. Maruyama, SLAC

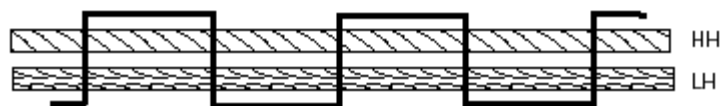
2002 EIC
workshop

Strained Superlattice

Strained Superlattice



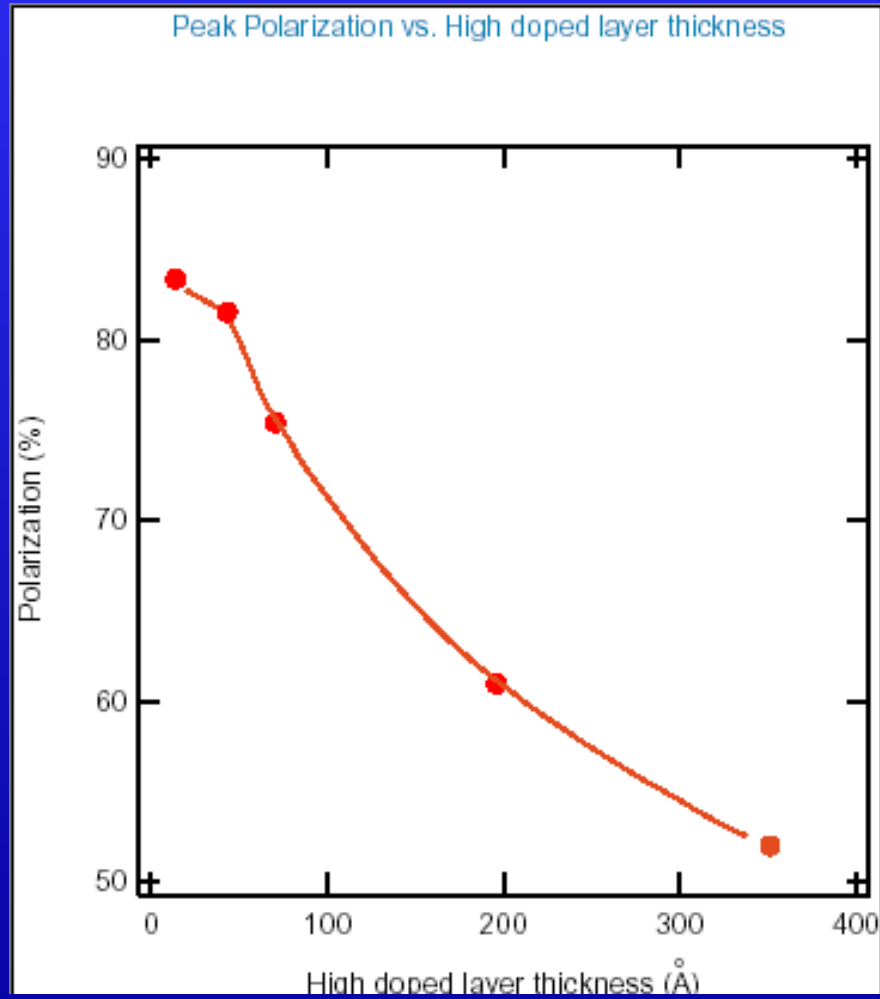
strained GaAs unstrained GaAsP strained GaAs unstrained GaAsP



Courtesy T. Maruyama, SLAC

2002 EIC
workshop

Effect of high doping on strained samples (SLAC data)



Courtesy T. Maruyama, SLAC

2002 EIC
workshop

Energy Recovering Linac Issues

L. Merminga

Jefferson Lab

EIC Accelerator Workshop
Brookhaven National Laboratory
February 26-27, 2002



Outline

- Energy Recovery
- RF Stability in Recirculating, Energy Recovering Linacs (ERLs)
- Instability Mechanism / Single-cavity Threshold
- RF Control and Beam Loading Instabilities
 - Theory
 - Experiment
- Transverse Beam Breakup (BBU)
 - Theory
 - Experiment
- Higher Order Mode Power Dissipation
 - Theory
 - Experiment
- Conclusions



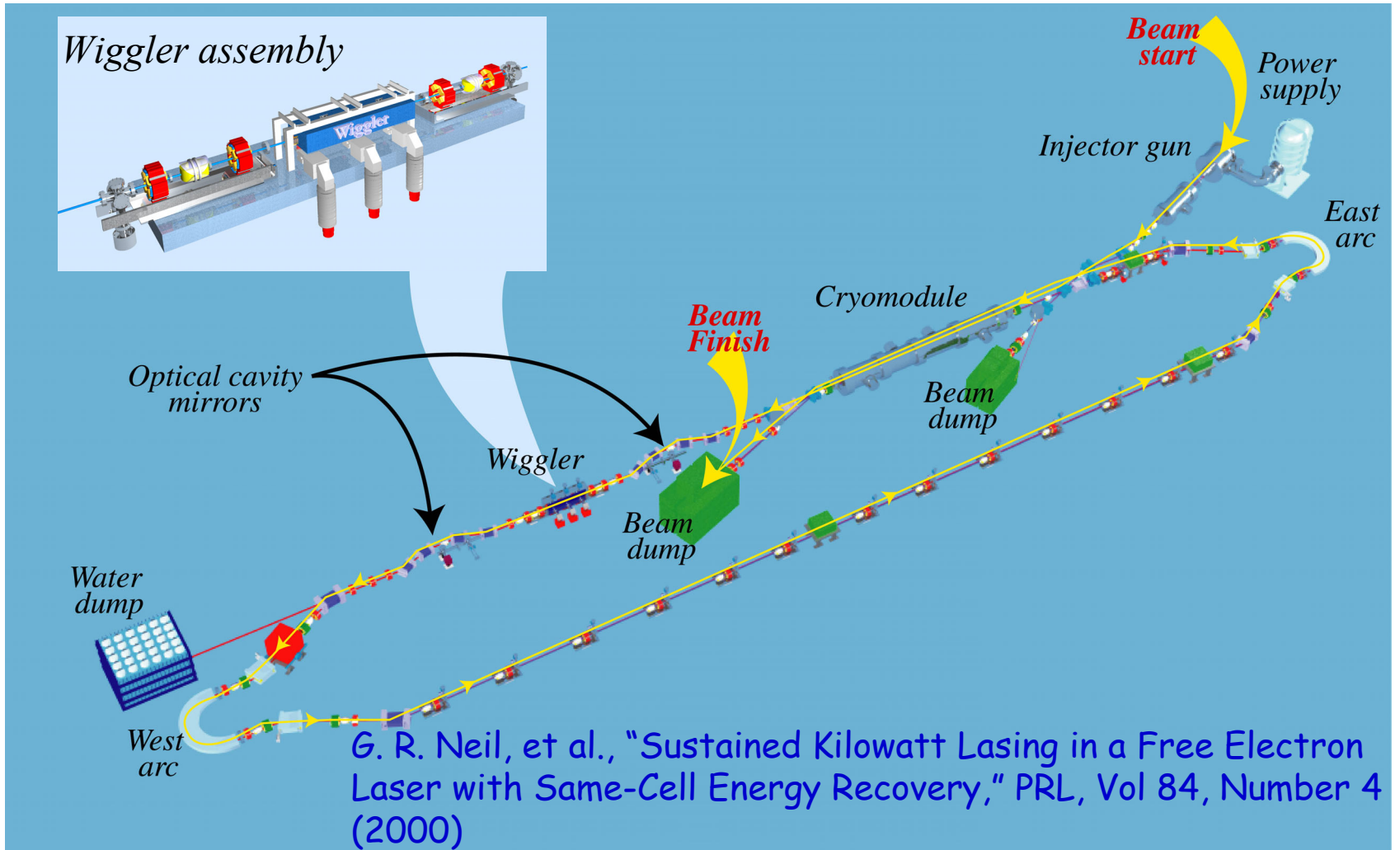
Energy Recovery

- Energy recovery is the process by which the energy invested in accelerating a beam is returned to the rf cavities by decelerating the same beam.
- There have been several energy recovery experiments to date, the first one at the **Stanford SCA/FEL***.
- Same-cell energy recovery with cw beam current up to 5 mA and energy up to 50 MeV has been demonstrated at the **Jefferson Lab IR FEL**. Energy recovery is used routinely for the operation of the FEL as a user facility.
- More ER experiments planned, most immediate at **JAERI FEL**.

* T.I. Smith, et al., "Development of the SCA/FEL for use in Biomedical and Materials Science Experiments," NIM A 259 (1987)

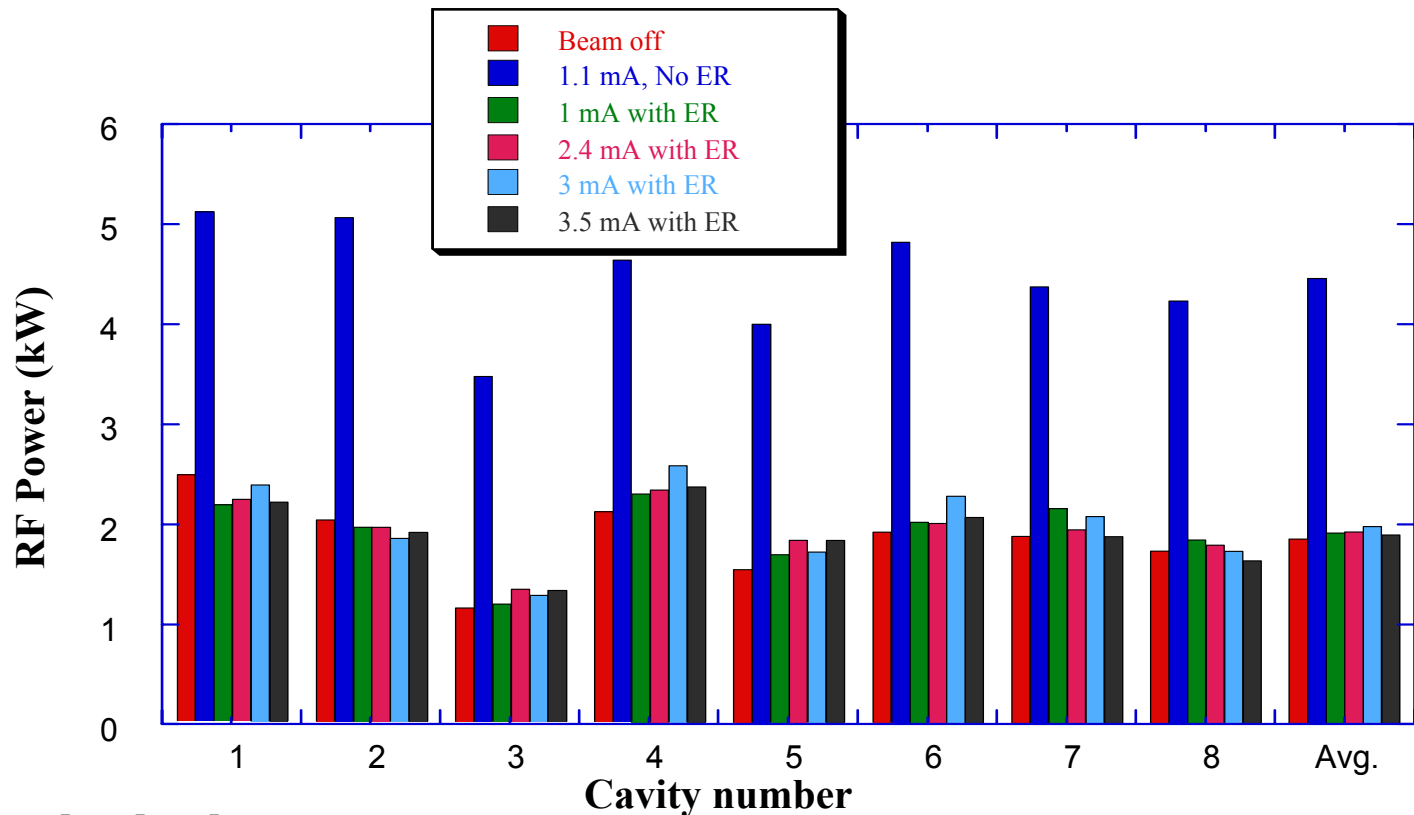


The JLab 2.13 kW IRFEL and Energy Recovery Demonstration

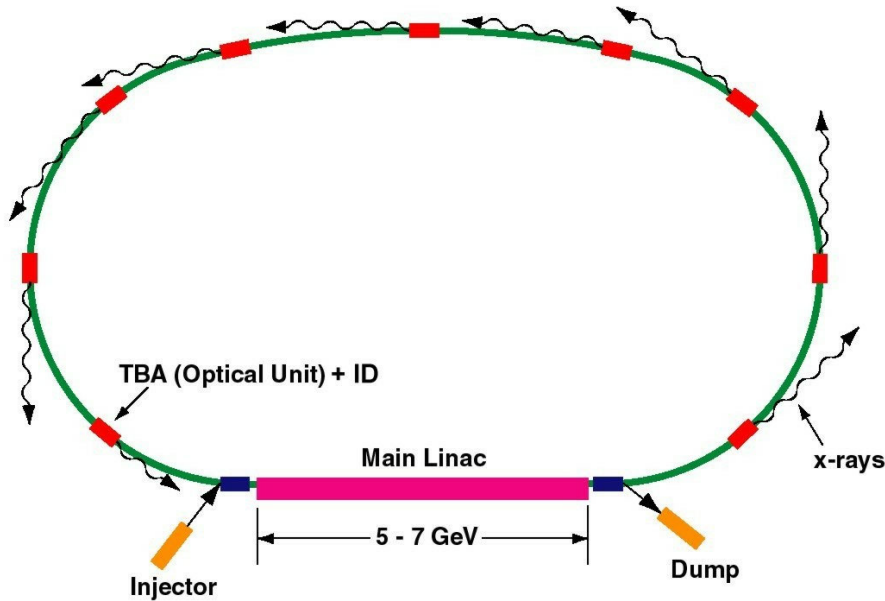


RF Power Requirements with Energy Recovery

With energy recovery the required linac rf power is ~ 16 kW, nearly independent of beam current. It rises to ~ 36 kW with no recovery at 1.1 mA.



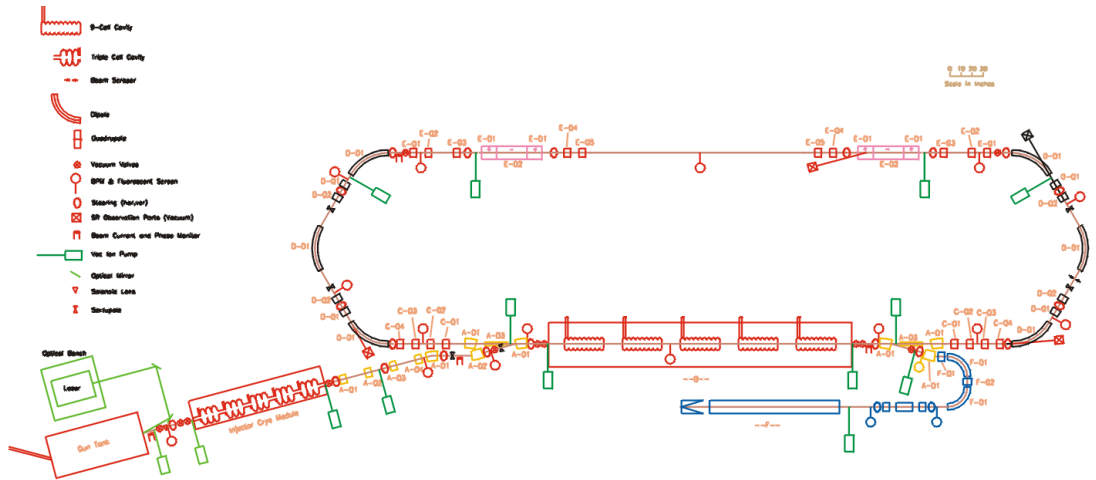
The Cornell ERL and ERL Prototype



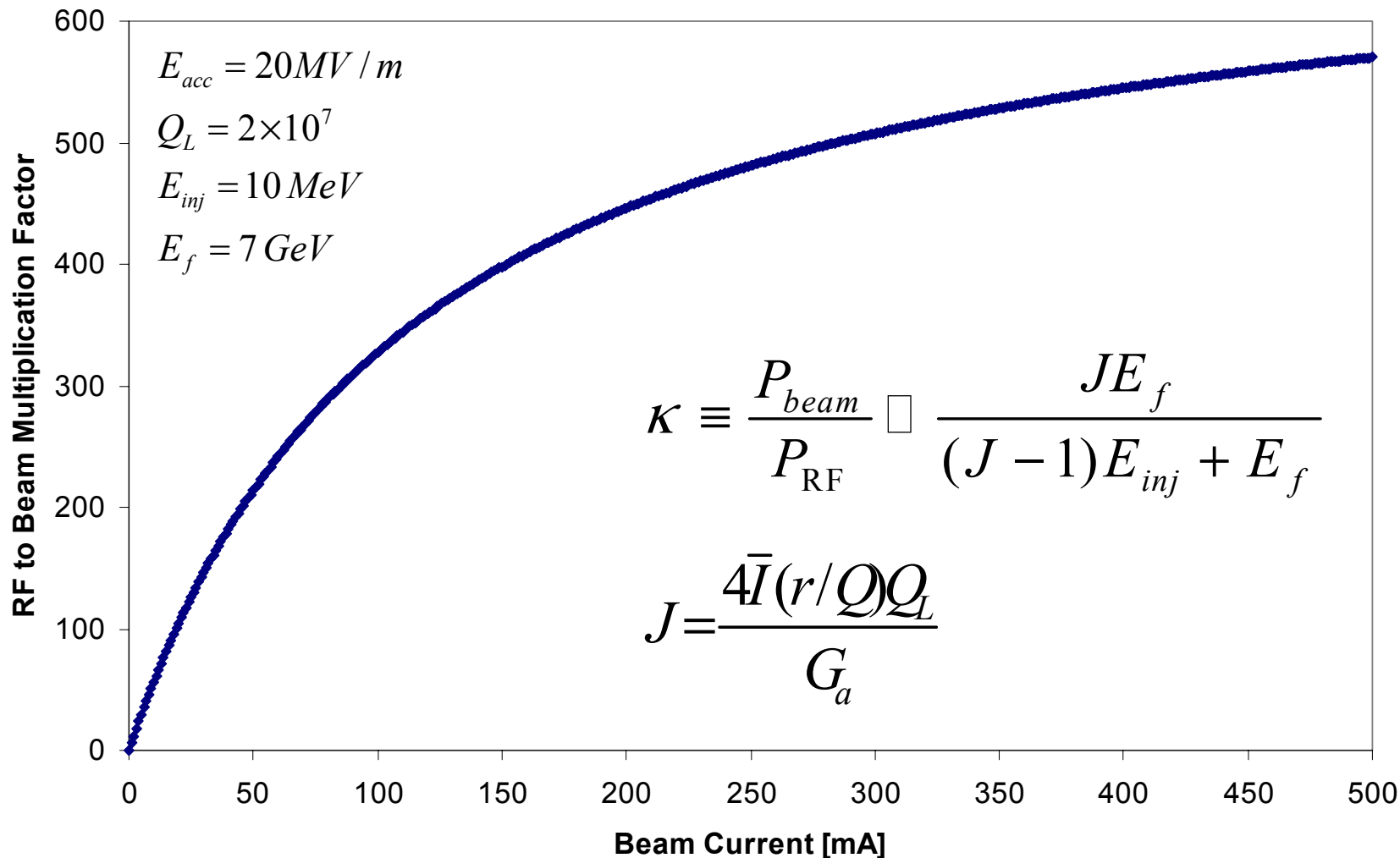
Beam Energy	5-7 GeV
Injection Energy	10 MeV
Beam current	100 mA

Beam Energy	100 MeV
Injection Energy	5 MeV
Beam current	100 mA

Courtesy: I. Bazarov



RF to Beam Multiplication Factor in an ideal ERL

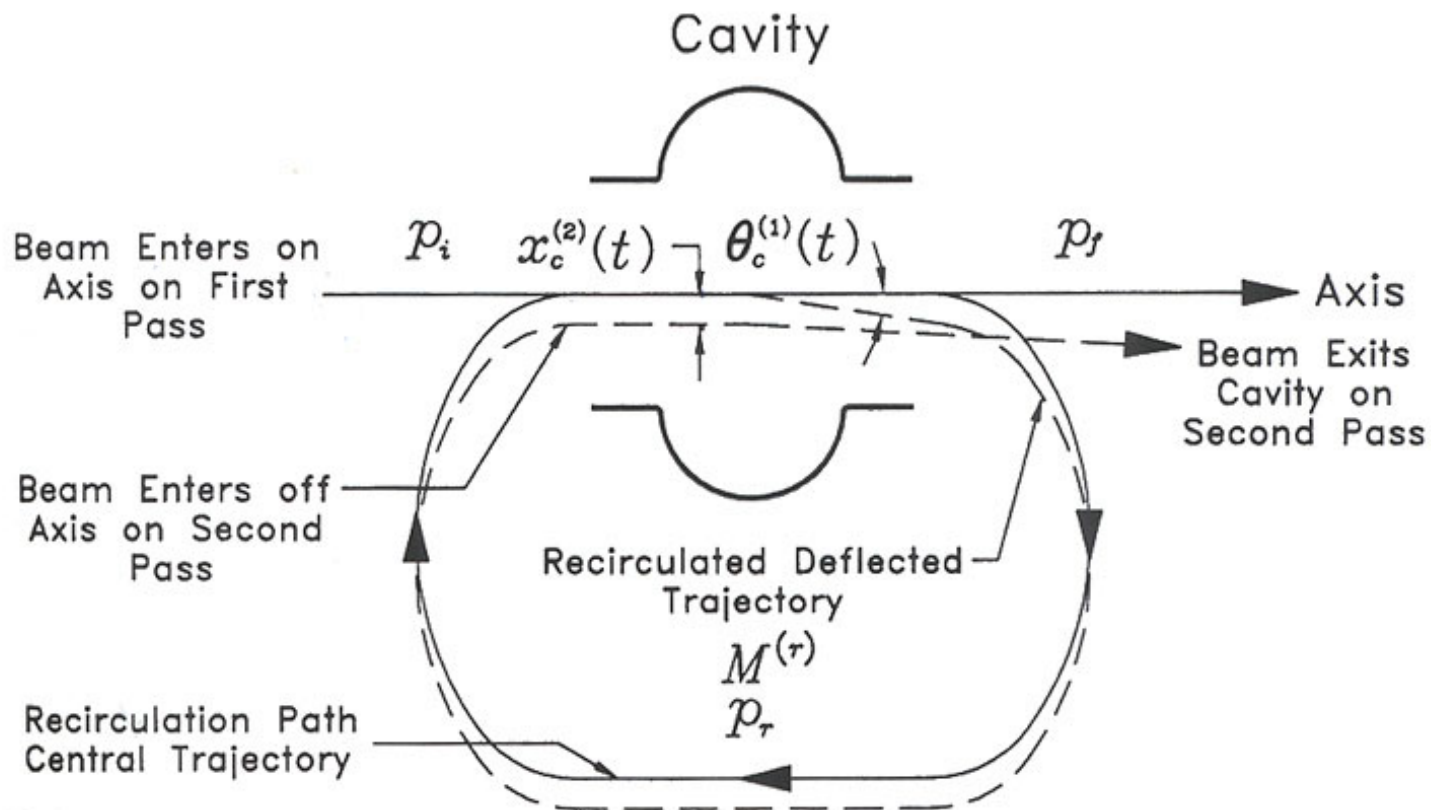


RF Stability in Energy Recovering Linacs

- Collective effects driven predominantly by high-Q superconducting cavities and can potentially limit average current
- In a recirculating linac, the feedback system formed between beam and cavities is closed and instabilities can result at sufficiently high currents
- Instabilities can result from the interaction of the beam with
 - fundamental accelerating mode -> beam loading instabilities
 - transverse HOMs -> transverse BBU
 - longitudinal HOMs -> longitudinal BBU
- The basic mechanism is the same:



Instability Mechanism



Courtesy: N. Sereno, Ph.D. Thesis (1994)



Instability Threshold

- There is a well-defined threshold current that occurs when the power fed into the mode equals the mode power dissipation
- An analytic expression that applies to all instabilities:

$$I_{th}^{(1)} = \frac{-2p_r c}{e(R/Q)_m Q_m k_m M_{ij} \sin(\omega_m t_r) e^{\omega_m t_r / 2Q_m}}$$

- For $i,j = 1,2$ or $3,4$ and $m \rightarrow \perp$ HOM \Rightarrow Transverse BBU
- For $i,j = 5,6$ and $m \rightarrow ||$ HOM \Rightarrow Longitudinal BBU
- For $i,j = 5,6$ and $m \rightarrow$ Fundamental mode \Rightarrow Beam-Loading Instabilities



Beam Loading Instabilities

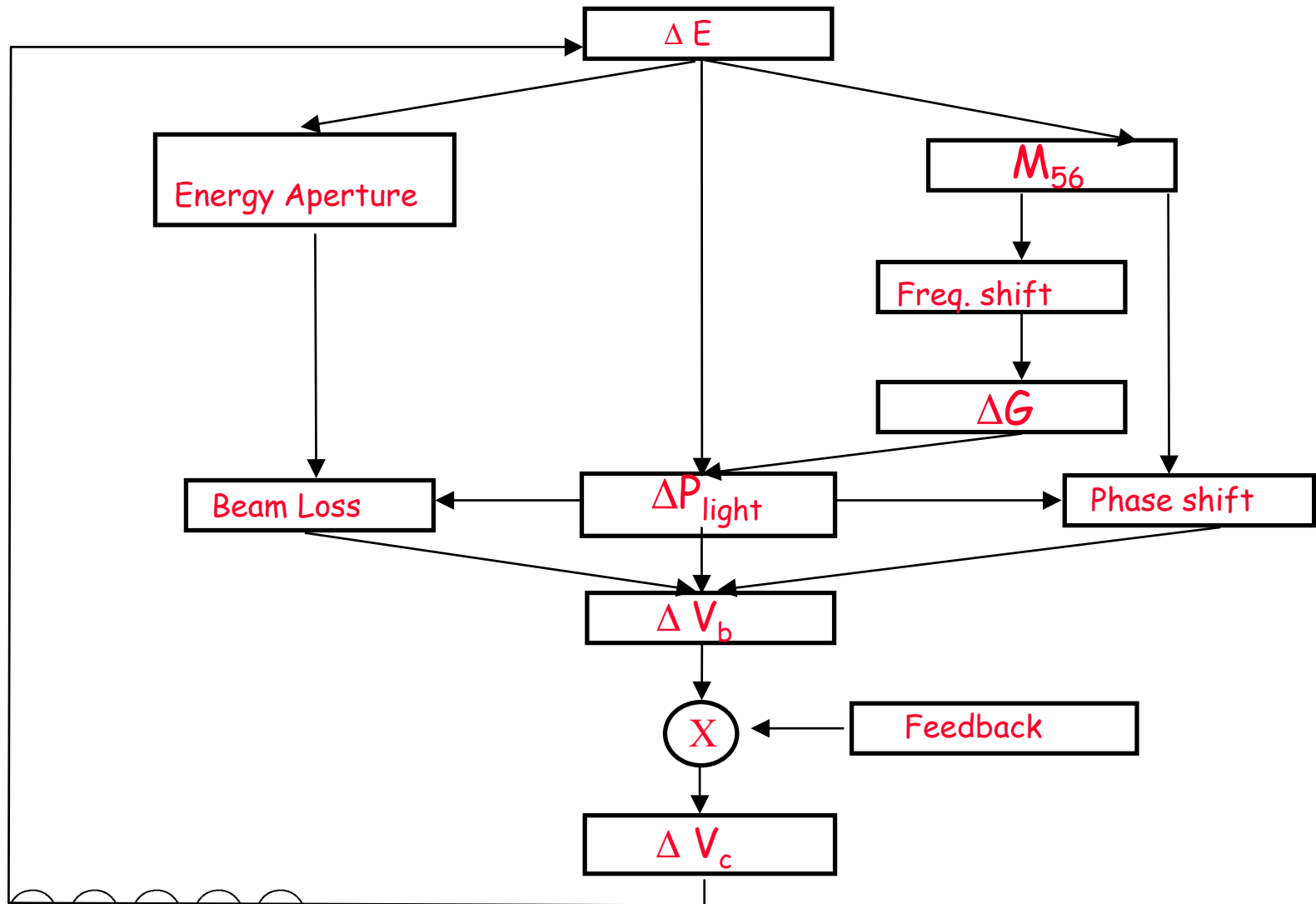
- Instabilities can arise from fluctuations of cavity fields.
- Two effects may trigger unstable behavior:
 - Beam loss which may originate from energy offset which shifts the beam centroid and leads to scraping on apertures
 - Phase shift which may originate from energy offset coupled to M_{56} in the arc
- Instabilities predicted and observed at LANL, a potential limitation on high power recirculating, energy recovering linacs.

M_{56} is the momentum compaction factor and is defined by:

$$\Delta l = M_{56} \frac{\Delta E}{E}$$



Beam Loading Instabilities Flow Chart



Beam Loading Instabilities: Theory

- Model of the system includes:
 - Beam-cavity interaction
 - Precise representation of low level rf feedback
 - FEL interaction
- Model was solved analytically and numerically
- Predicts instability exists in the IRFEL ($I_{th} \sim 27 \text{ mA}$) however is controlled by LLRF feedback ($I_{th} \sim 1 \text{ A}$)
- Experimental data from the IRFEL are quantitatively consistent with the model, with the FEL turned off. Model reproduces data qualitatively, with the FEL turned on*

*Presented at the 1999 FEL Conference, Hamburg



RF Control in ERLs

- Phases may not differ by precisely 180°
 - Typical expected path length control adjustment leads to $\sim 0.5^\circ$ deviation from 180°



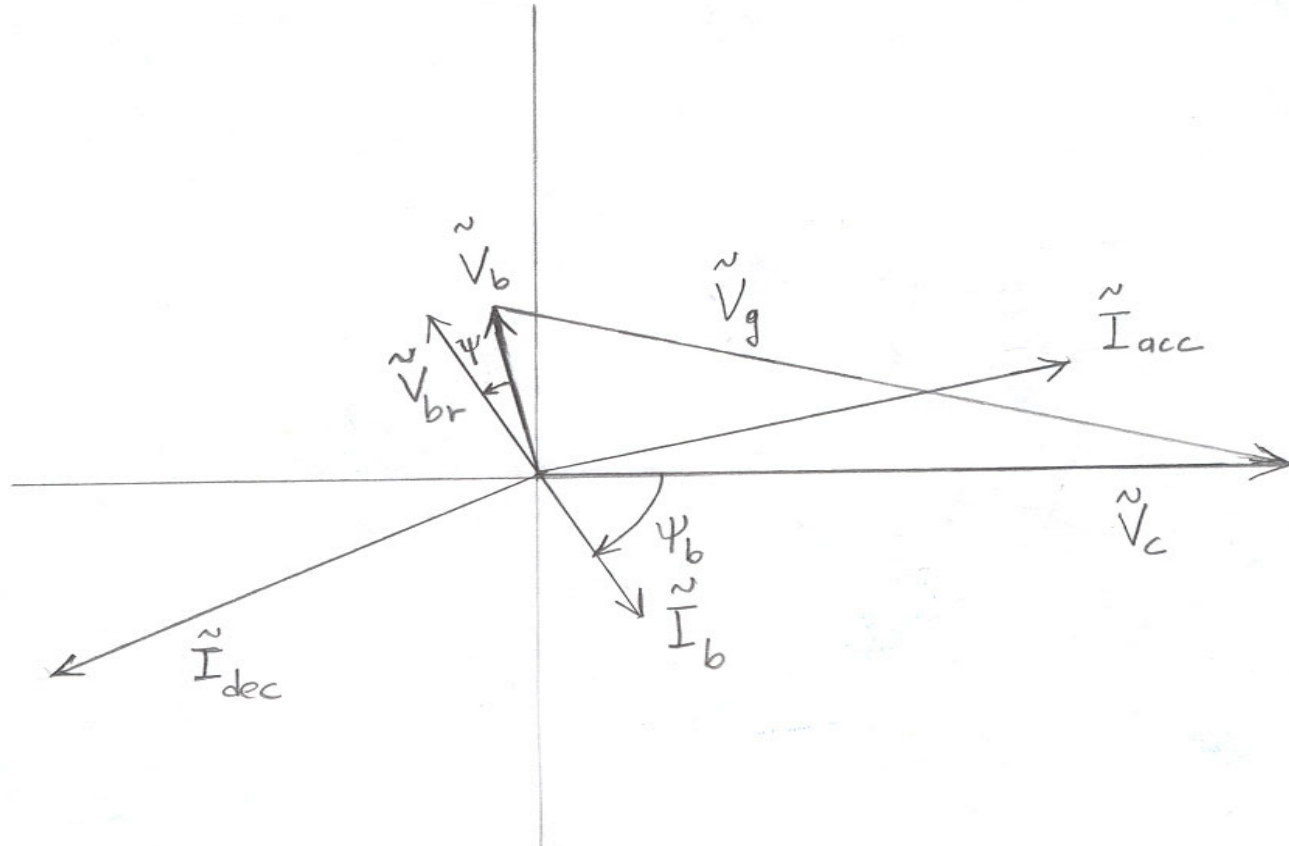
- Beam loss may occur, resulting in beam vectors of unequal magnitude

⇒ All of the above give rise to a net beam loading vector, typically of reactive nature in the case of phase errors

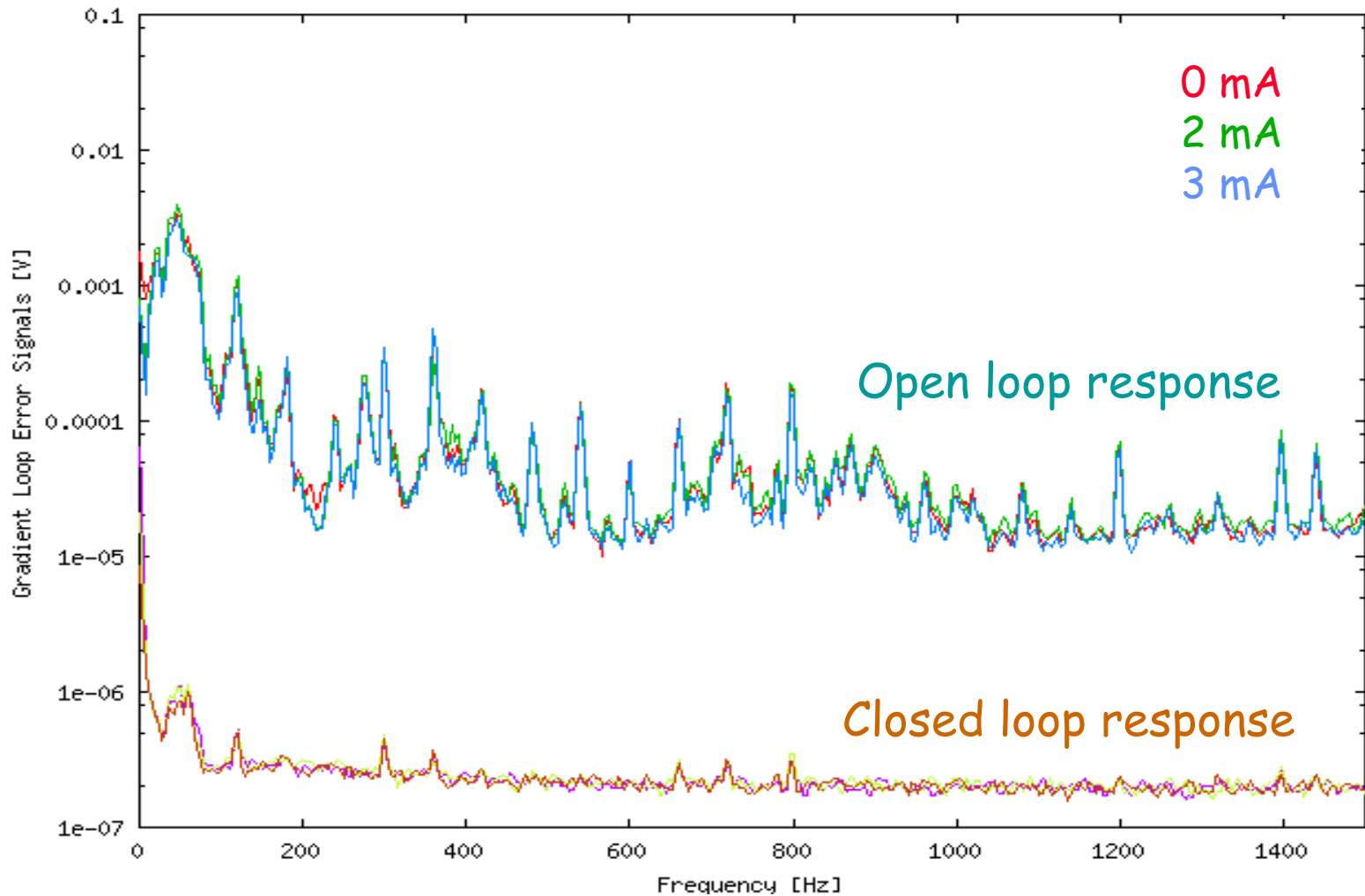
⇒ Increase of rf power requirements and reduction of κ



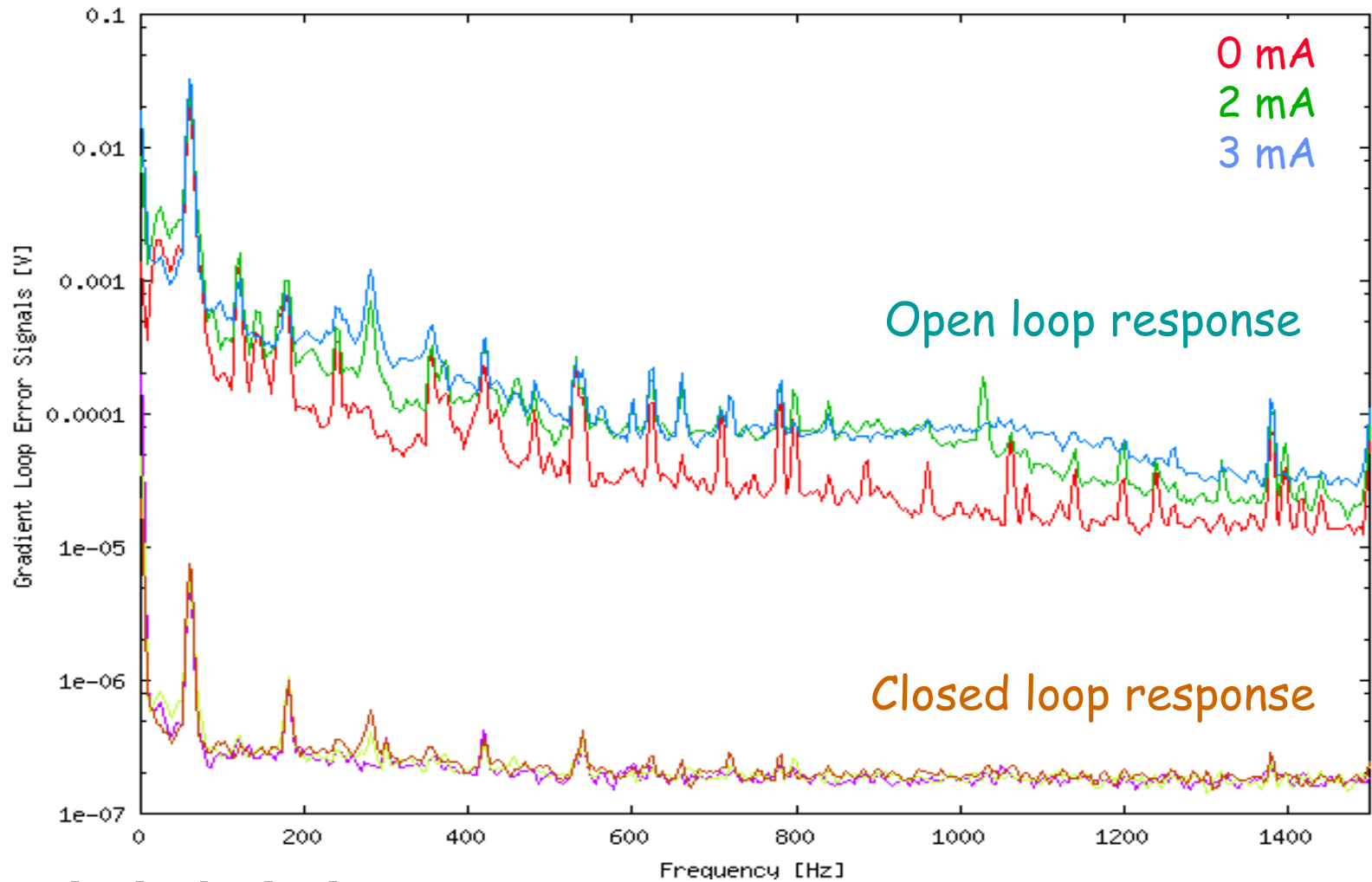
Energy Recovery Phasor Diagram



RF Control (Linac)



RF Control (Injector)

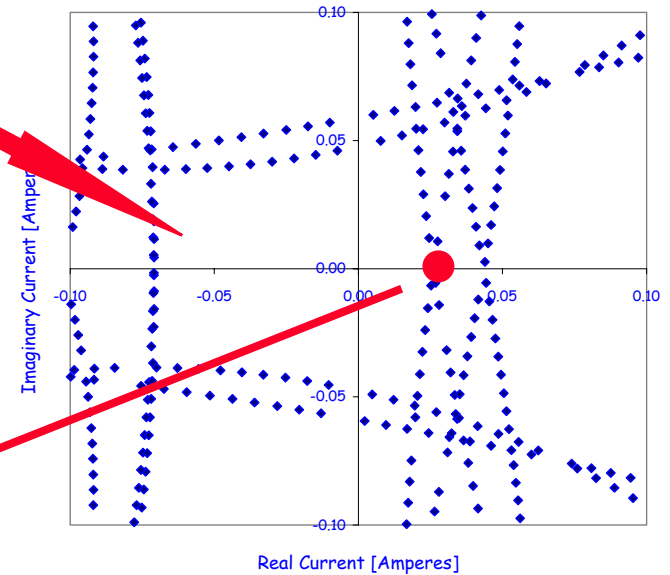
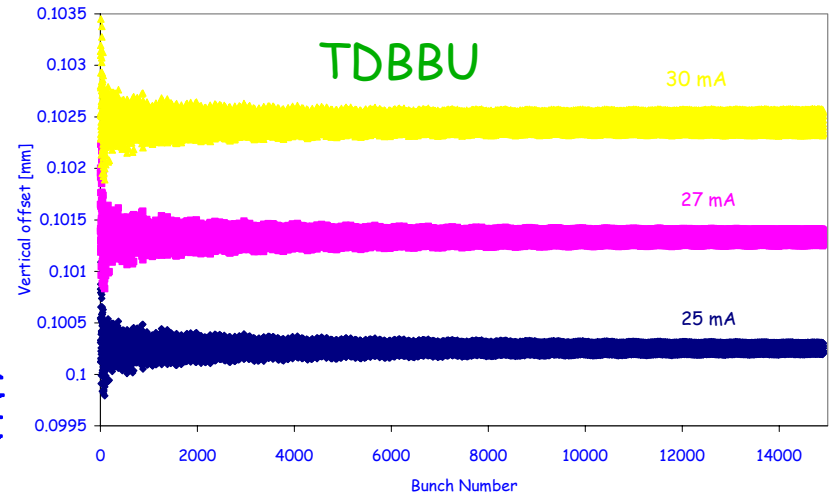
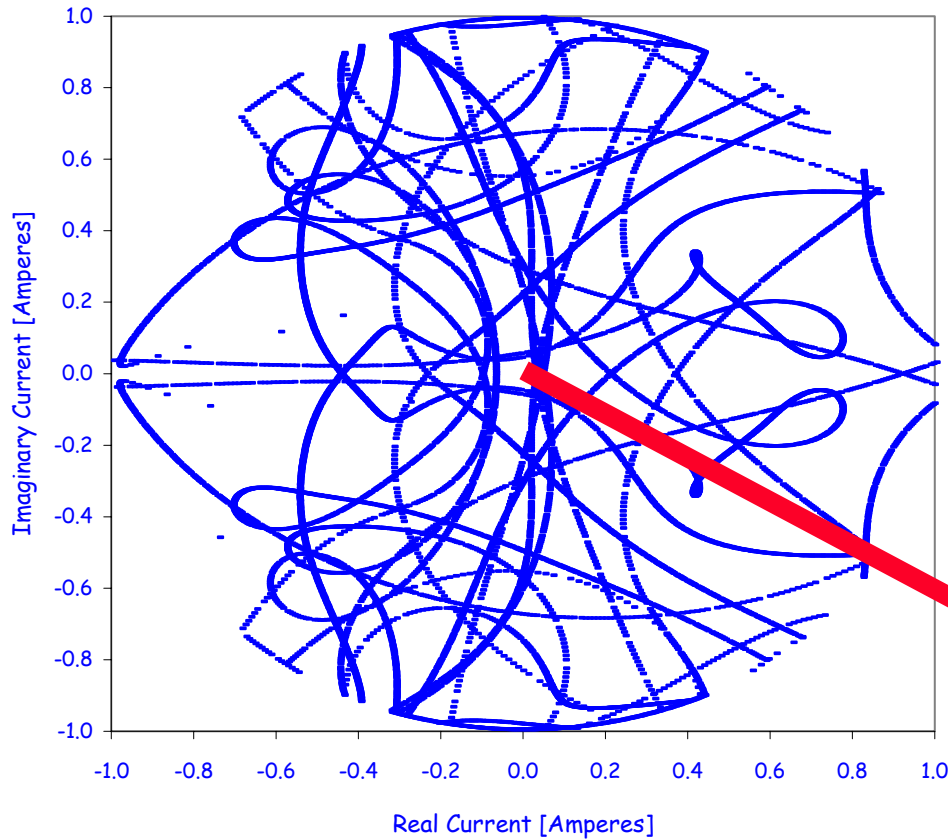


Transverse BBU: Theory

- Analytic models include:
 - Description of the effect for distribution of cavities along linac with several recirculations in impulse approximation (Bisognano, Gluckstern 1987)
 - Generalization to include subharmonic bunching (Yunn 1991)
- ⇒ For N-passes, M-cavities, solution reduces to finding M-eigenvalues of M-dimensional matrix, or $N \times M - 1$ for subharmonic bunching
- Numerical codes:
 - **TDBBU**: A 2D simulation code (Krafft, Bisognano, Yunn 1987)
 - **MATBBU**: A computational tool that solves the exact equations for a given configuration (Yunn, Merminga 2001)



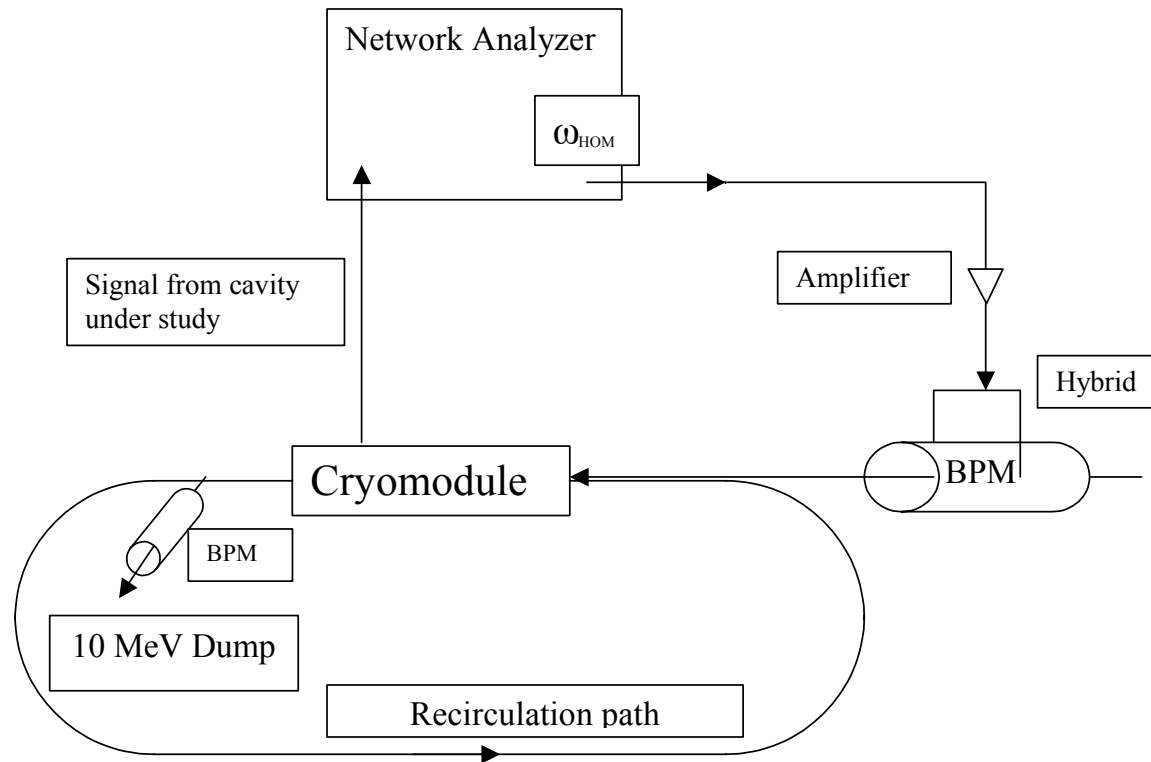
BBU Stability Plots for the JLab IR FEL



Threshold current = 26.3 mA



Transverse BBU: Experiment



Typical RF Cavity Response to Beam Excitation

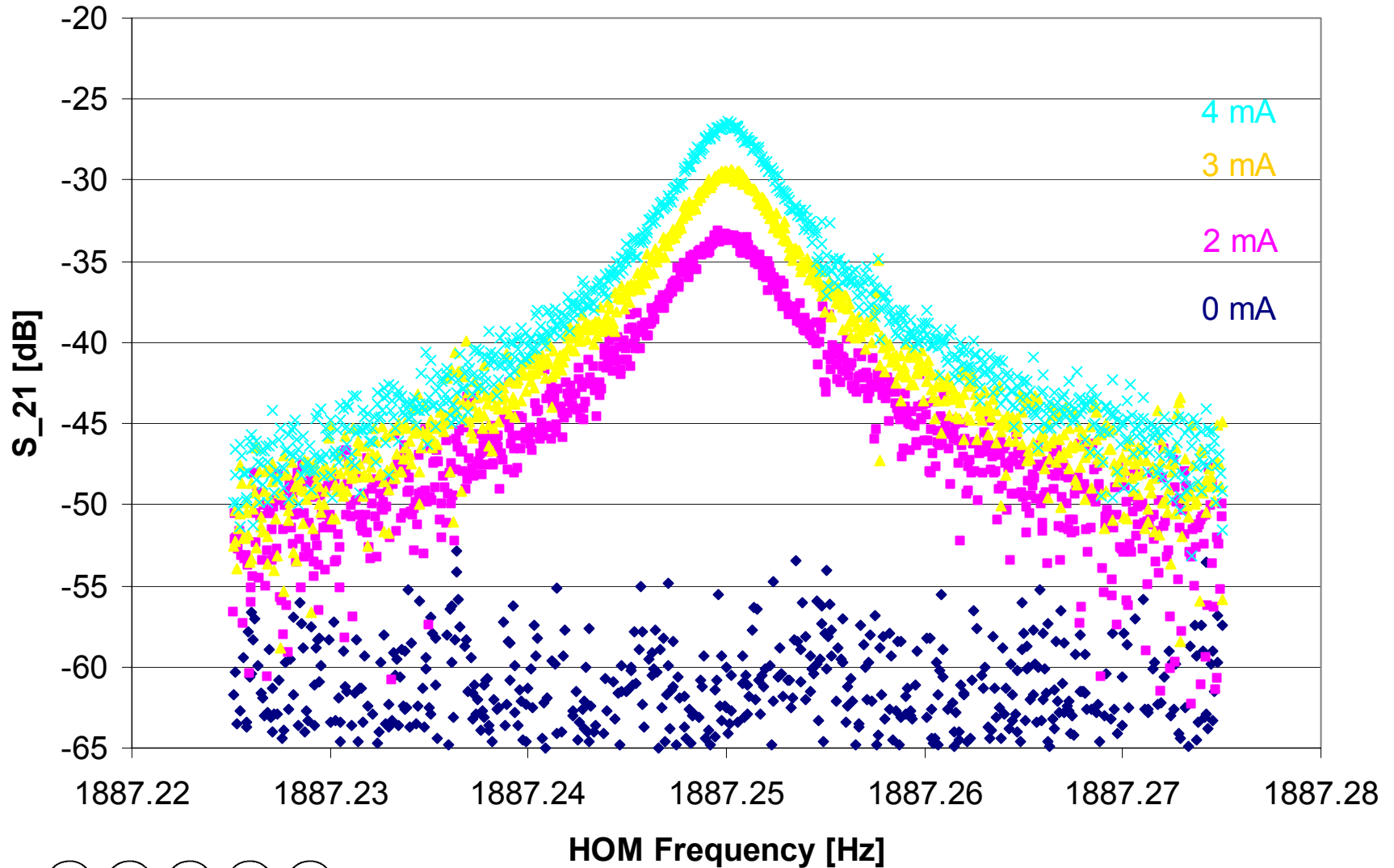
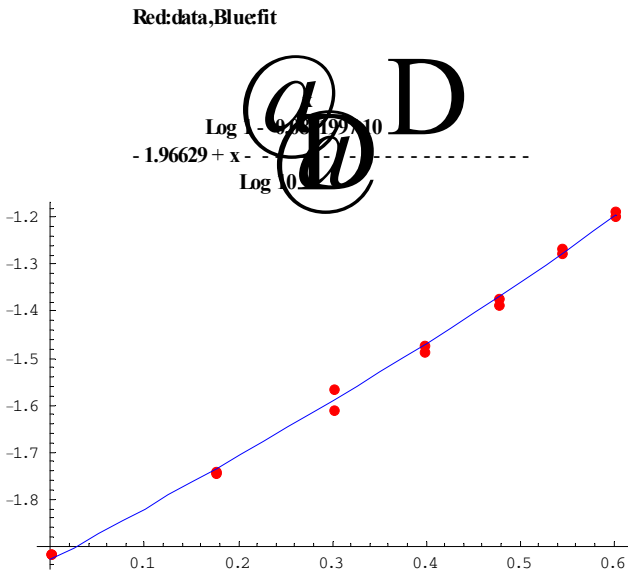


Table of BBU Data

Cavity	HOM Freq. (Measured)	R/Q (Meas.)	Q (Meas.)	Energy	Optics Setting	I _{th}
	[MHz]	[Ω]		MeV		mA
4	1730	0.08	3.8×10^7	48	Nominal	16
4	1730	0.08	3.8×10^7	37	1	18.4
4	1895	22.02	1.6×10^5	48	Nominal	21.4
4	1895	22.02	1.6×10^5	37	1	15.6
4	1895	22.02	1.6×10^5	37	Nominal	<0
5	1818	13.74	4.5×10^4	37	2	15.0
5	1818	13.74	4.5×10^4	37	3	6.9
5	1887	22.21	4.0×10^5	37	3	12.5
5	1887	22.21	4.0×10^5	37	4	11.3
5	1887	22.21	4.0×10^5	37	2	32.0
5	1887	22.21	4.0×10^5	37	3	16.4



BBU Data Analysis



$\log|S_{21}|$ vs. $\log(I_0)$

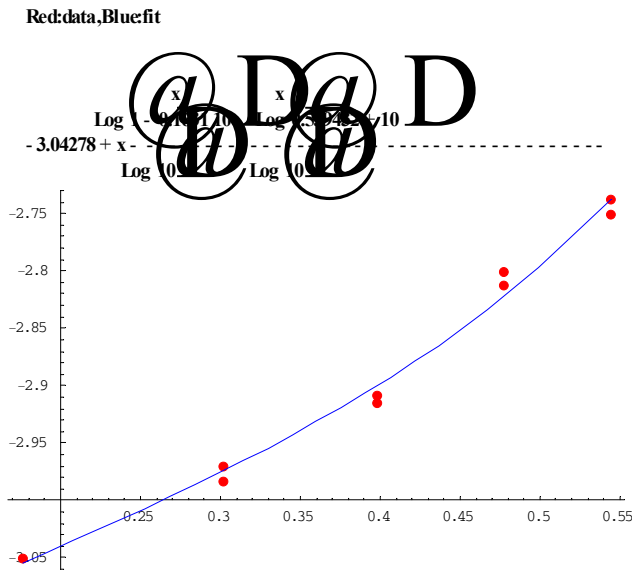
$$\log |S_{21}(\omega)| = a_0 + \log(I_0) - \log[(1 - a_1 I_0)(1 + a_2 I_0)]$$

$$\Rightarrow I_{th} = 1/a_1 = 6.9 \text{ mA}$$

Data were fitted to 1st and 2nd order models and thresholds were derived:

$$\log |S_{21}(\omega)| = a_0 + \log(I_0) - \log(1 - a_1 I_0)$$

$$\Rightarrow I_{th} = 1/a_1 = 12.5 \text{ mA}$$



$\log|S_{21}|$ vs. $\log(I_0)$



Conclusions from BBU Experiment

- Threshold current in the IR FEL recirculating linac varies between **7 mA** and **32 mA** for varying accelerator setup
- Under the nominal FEL configuration, threshold current is between **16 mA** and **21 mA**
- Theoretical prediction is **27 mA** \Rightarrow agreement within **~40%**
- Observed optics dependence has not been quantified yet
- More exact analysis tools are being developed



HOM Power

- High average current, short bunch length beams in srf cavities excite HOMs. Power in HOMs, primarily longitudinal:

$$P_{\text{HOM}} = 2k_{\parallel} Q^2 f_{\text{bunch}}$$

(factor of 2 for energy recovery)

- For $I_{\text{ave}} = 100 \text{ mA}$, $Q = 0.5 \text{ nC} \Rightarrow P_{\text{HOM}} \sim 1 \text{ kW per cavity}$ for $k_{\parallel} = 10.3 \text{ V/pC}$ at $\sigma_z \sim 0.7 \text{ mm}$
- In the IRFEL: $I_{\text{ave}} = 5 \text{ mA}$, $P_{\text{diss}} \sim 6 \text{ W}$
- Fraction of HOM power dissipated on cavity walls depends on the bunch length
- It can potentially limit I_{ave} and I_{peak} due to finite cryogenic capacity



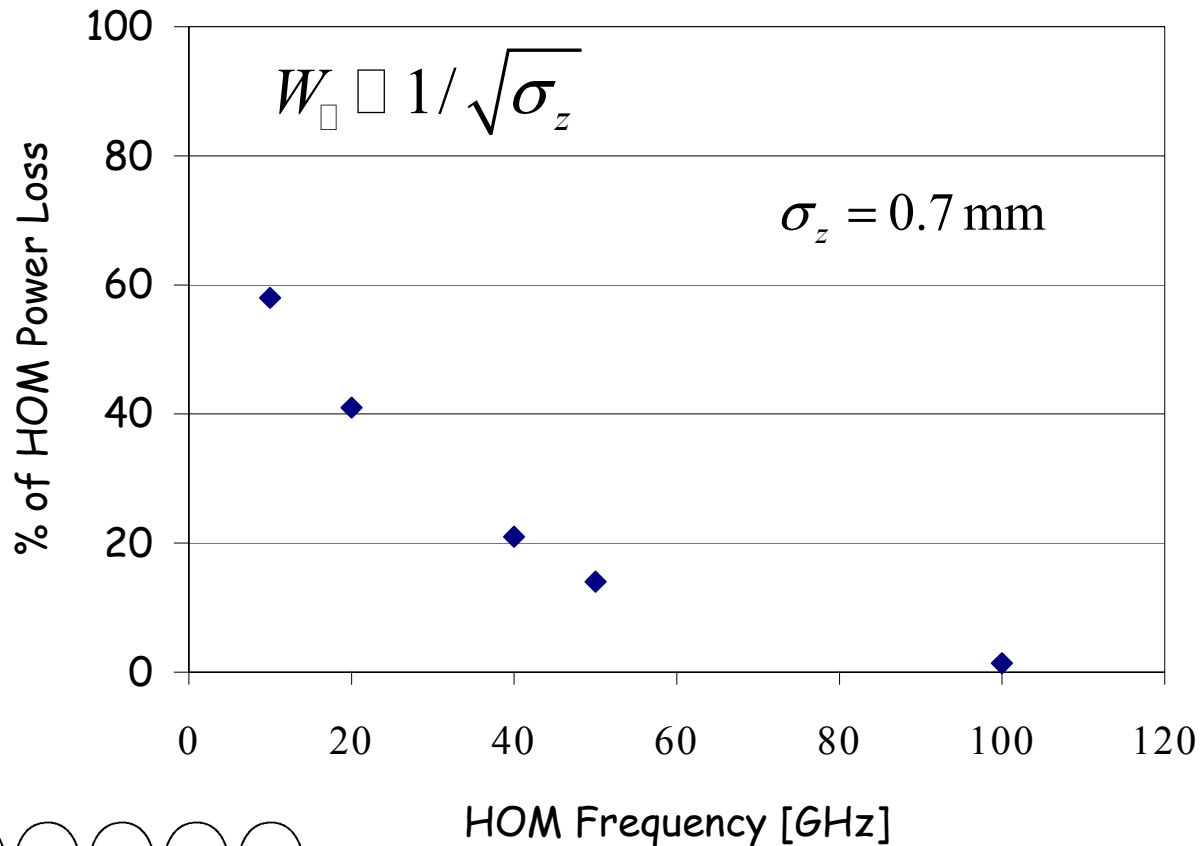
HOM Power Dissipation: Theory

- The fraction of HOM power dissipated on cavity walls increases with HOM frequency, due to $R_s \sim \omega^2$ degradation from BCS theory
- We developed a model that estimates fraction of power dissipated on the walls and specifies HOM-power extraction efficiency required
- We found:
 - Frequency distribution of HOM power: >90% of HOM power is in modes < 100 GHz
 - Fraction of power dissipated on the cavity superconducting walls is
 - a strong function of bunch length
 - much less than the fundamental mode load
 - High frequency fields propagate along the structure



Frequency Distribution of HOM Losses

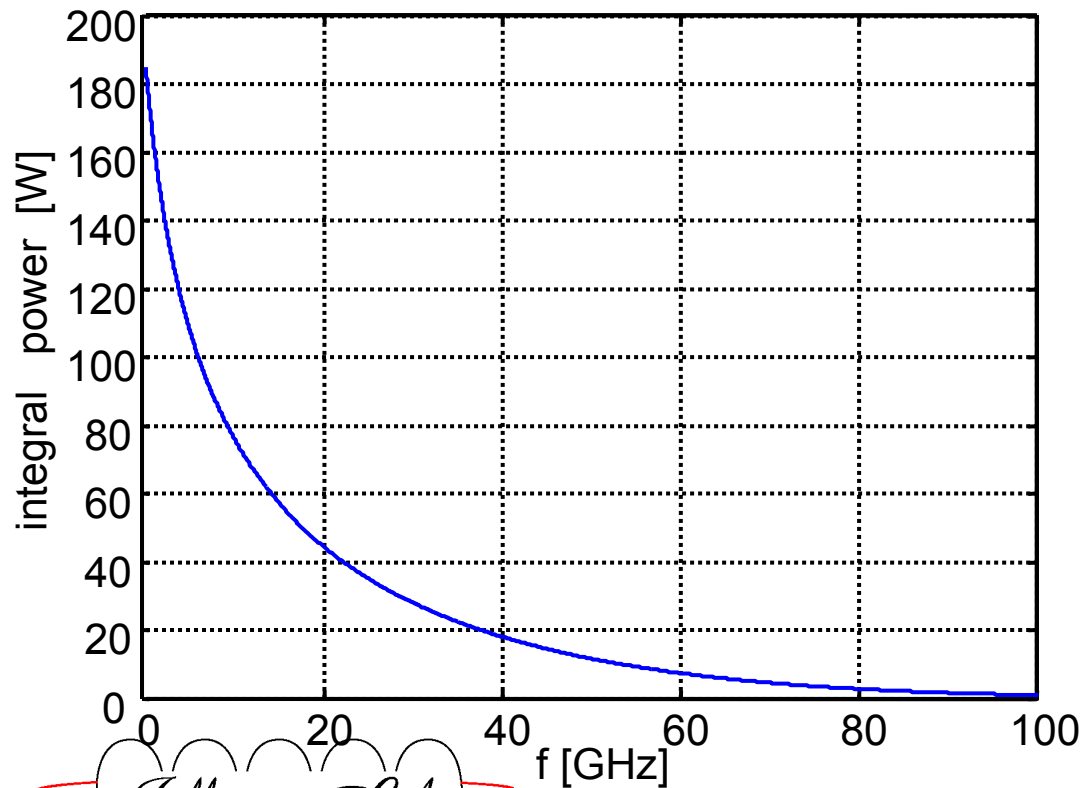
% of HOM power in frequencies above f_{HOM} , as function of f_{HOM}



Frequency Distribution of HOM Power

Monopole Mode Single Bunch Power Excitation per 9-Cell Cavity

$$\sigma_z = 0.7 \text{ mm} \quad Q_{\text{bunch}} = 77 \text{ pC}$$



P	= 185 W
P(f>5 GHz)	= 108 W
P(f>10 GHz)	= 76 W
P(f>20 GHz)	= 45 W
P(f>40 GHz)	= 18 W
P(f>80 GHz)	= 3 W



Frequency Distribution of HOM Losses

- ~40% of HOM losses occur at frequencies below ~4 GHz
 - ⇒ In TESLA cavities this power will be extracted by input couplers and HOM couplers and be absorbed in room temperature loads
- The remaining losses, at high frequencies ≥ 4 GHz, will propagate along the structure and be reflected at normal and superconducting surfaces
 - ⇒ on-line absorbers are required
- Effect of losses in frequency range beyond the threshold for Cooper pair breakup (750 GHz) in superconducting Nb has been investigated: the resulting Q_0 drop is negligible

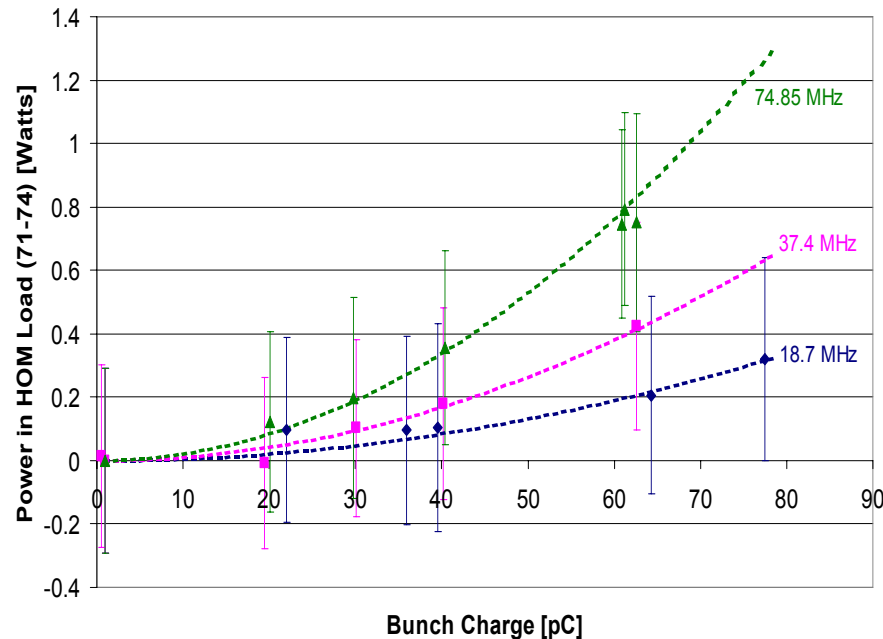


HOM Power: Experiment

- HOM power dissipation may impose design choices to improve cryogenic efficiency
- HOM power was measured with temperature diodes placed on the two HOM loads of the 5-cell CEBAF cavity
- Measurements were repeated at different values of the bunch charge and bunch repetition frequency



HOM Power vs. Bunch Charge



- Measured HOM power dissipated at the loads is 1.6 W at 60 pC, 5 mA, $\sigma_z = 2.5$ ps
 - Calculated total HOM losses at 60 pC, 5 mA is 4.2 W
 - Calculated fraction of HOM power in frequencies ≤ 15 GHz is $\sim 50\%$ or 2.1 W
- \Rightarrow Loss factor agrees within 25%



Extrapolation to Higher Currents

- **5 mA** energy recovering linac: **JLab IR FEL**
Transverse BBU threshold ~ 27 mA
RF instabilities threshold ~ 27 mA w/out fdb, ~1 A with fdb
HOM power ~ 6 W/cavity
- **10 mA** energy recovering linac: **JLab IR FEL Upgrade**
Transverse BBU threshold ~ 50 mA if $Q \sim 10^5$
RF instabilities threshold ~ 27 mA w/out fdb, ~1 A with fdb
HOM power ~ 40 W/cavity
- **100 mA** energy recovering linac: **Cornell ERL**
Transverse BBU threshold ~ 200 mA
RF instabilities threshold ~ 22 mA w/out fdb, ~1 A with fdb
HOM power ~ 160 W/cavity
- **Where is the limit?**



Where is the limit?

- At the present time, transverse BBU appears to be the limiting instability
 - However,
 - Better damping of HOMs in multi-cell cavities and
 - Bunch-by-bunch transverse feedback, similar to the B-Factory (4 nsec!), may be possible
- ⇒ $I_b \sim 0.5 - 1$ A conceivable?
- Something else?



Conclusions

- RF stability in recirculating, energy recovering linacs is theoretically well understood
- Experimental verification of simulation codes and models is being pursued at the JLab IR FEL. Quantitative agreement between simulation codes and experimental data has been demonstrated
- Greater capabilities for experimental verification of the models are offered with:
 - the 10 mA JLab FEL Upgrade
 - the 100 mA Cornell ERL Prototype
- Inspired by the success of JLab IR FEL, energy recovery is emerging as a powerful application of rf superconductivity. The question is "Where is the limit of energy recovery, in the multi-dimensional space of I_{ave} , E_b , Q_{bunch} , σ_z , ... ?"



RF Issues in Energy Recovery Linacs

Jean Delayen

Jefferson Lab
Newport News, VA

EIC Accelerator Workshop
BNL, 26-27 February 2002



Outline

- Energy Recovery Linacs (ERLs)
 - Examples
 - Basic features
- Efficiency of ERLs
 - Power Requirements
- RF Stability
- Higher-Order Modes Issues
- Conclusions



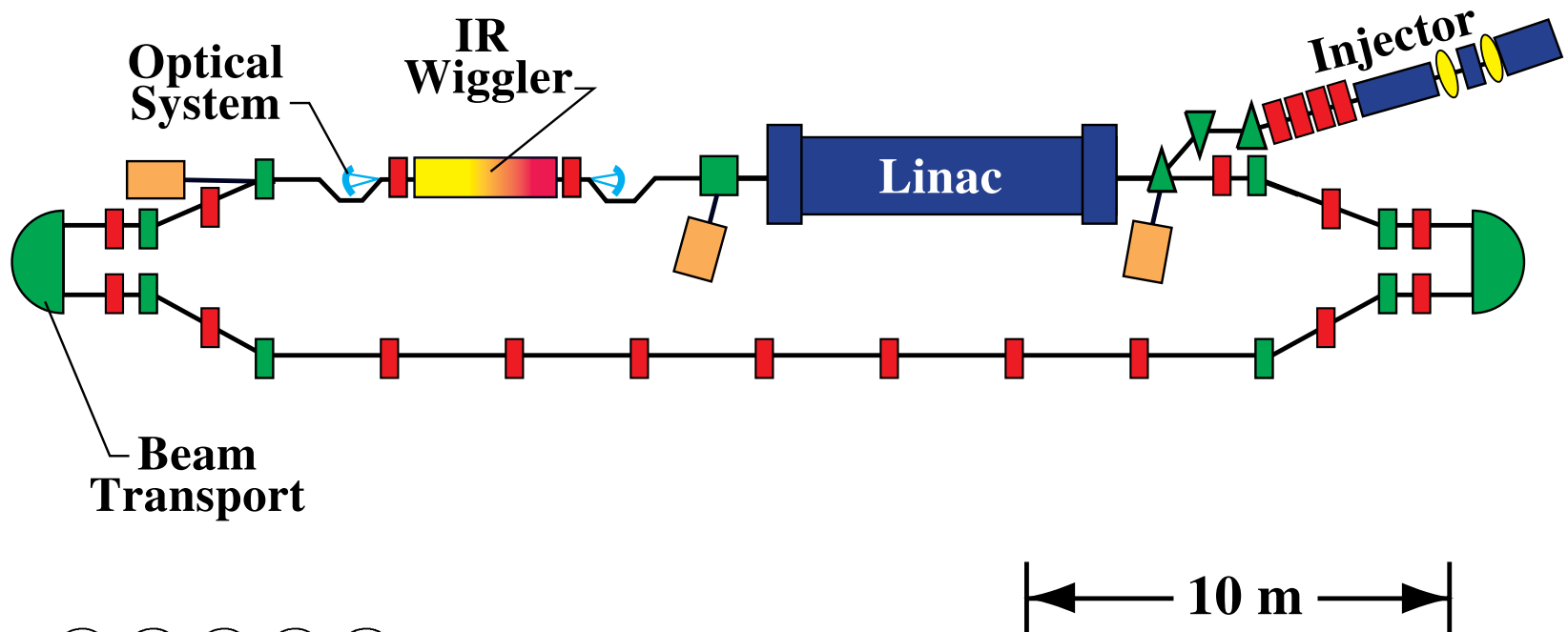
Energy Recovery Linacs

- Energy recovery is the process by which the energy invested in accelerating a beam is returned to the rf cavities by decelerating the same beam.
- There have been several energy recovery experiments to date
 - Stanford SCA/FEL
 - Los Alamos FEL
 - CEBAF front end
- Same-cell energy recovery with cw beam current up to 5 mA and energy up to 50 MeV has been demonstrated at the Jefferson Lab IR FEL. Energy recovery is used routinely for the operation of the FEL as a user facility.



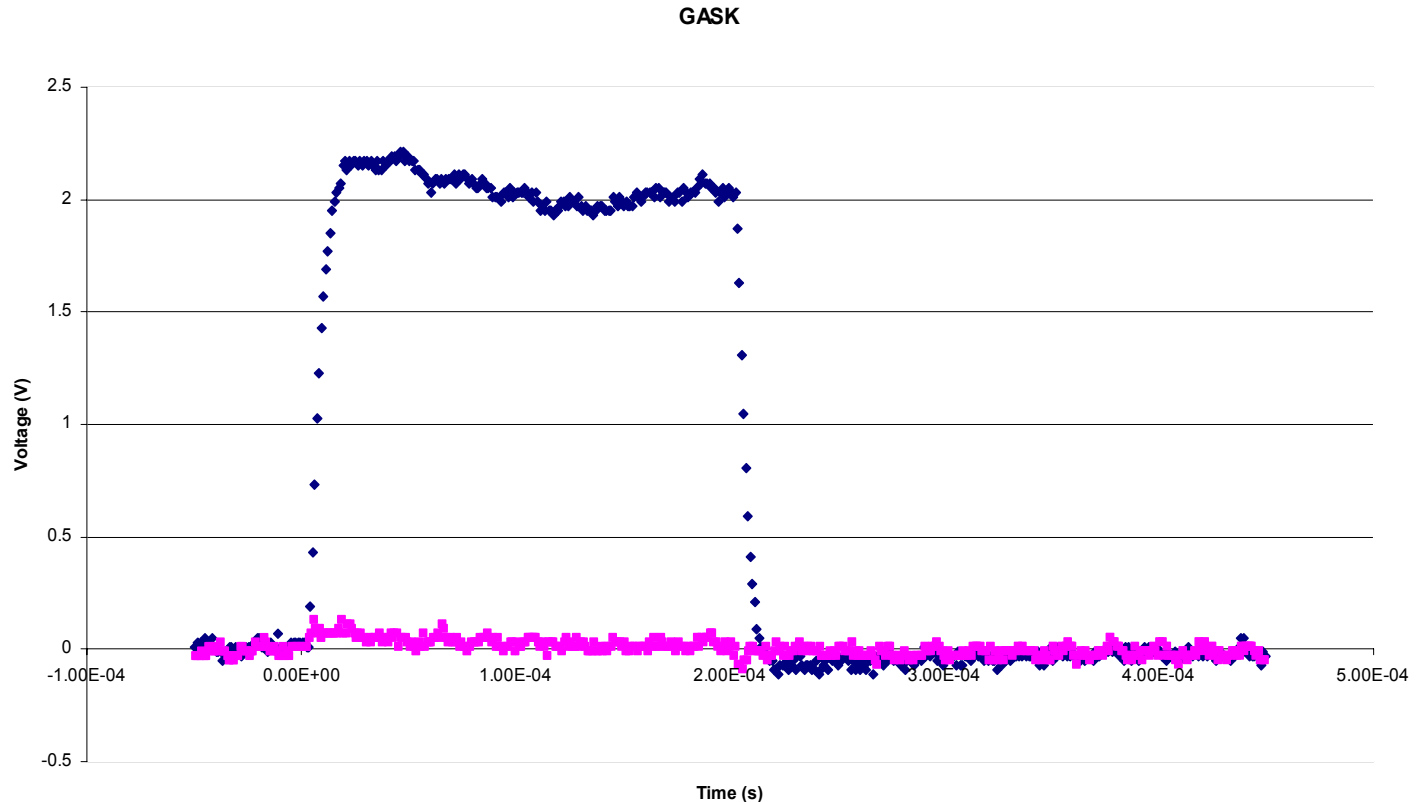
The JLab 1.7 kW IRFEL and Energy Recovery Demonstration

G. R. Neil, et al., "Sustained Kilowatt Lasing in a Free Electron Laser with Same-Cell Energy Recovery," *Physical Review Letters*, Volume 84, Number 4 (2000)



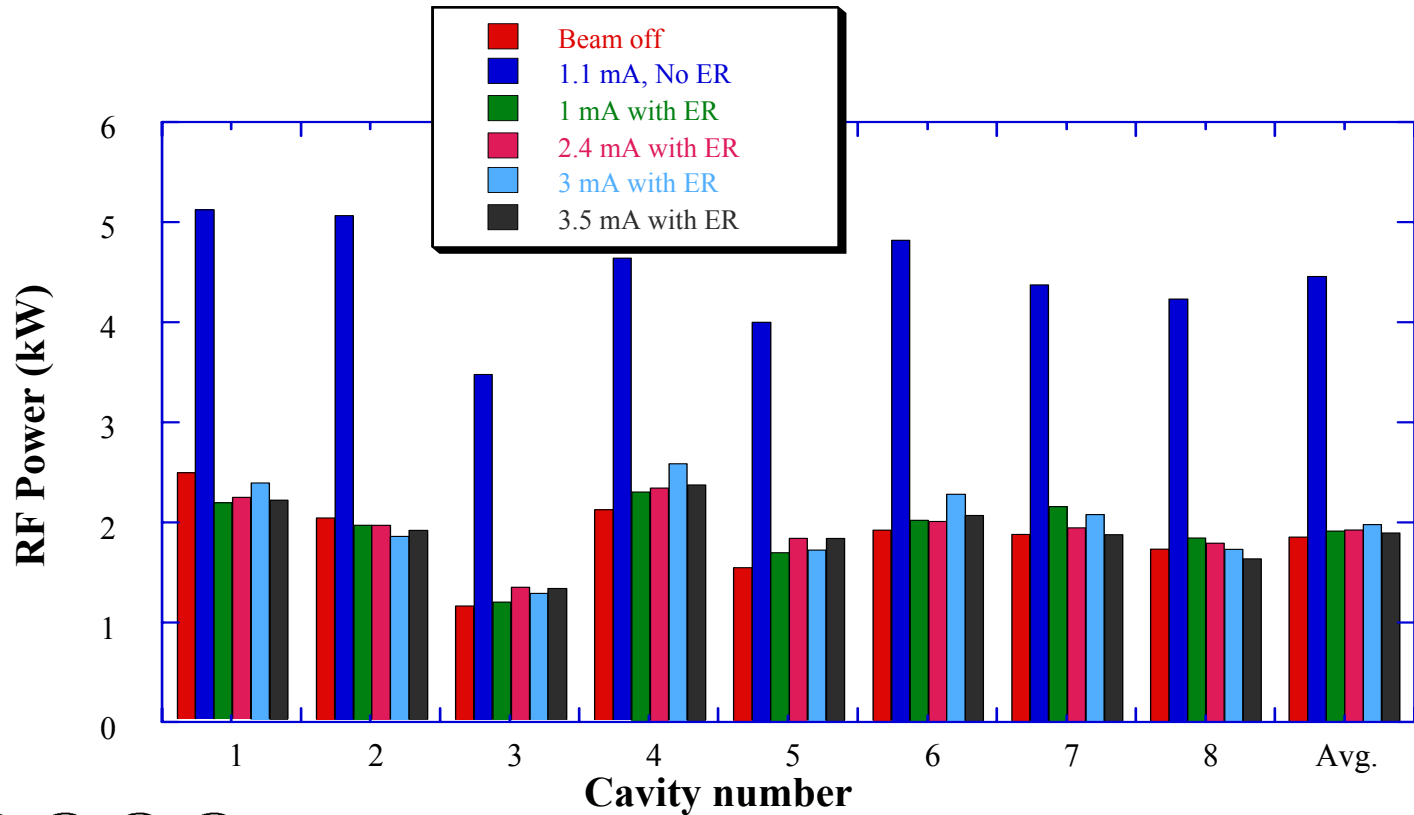
Demonstration of Energy Recovery

Gradient modulator drive signal in a linac cavity measured without energy recovery (signal level around 2 V) and with energy recovery (signal level around 0).

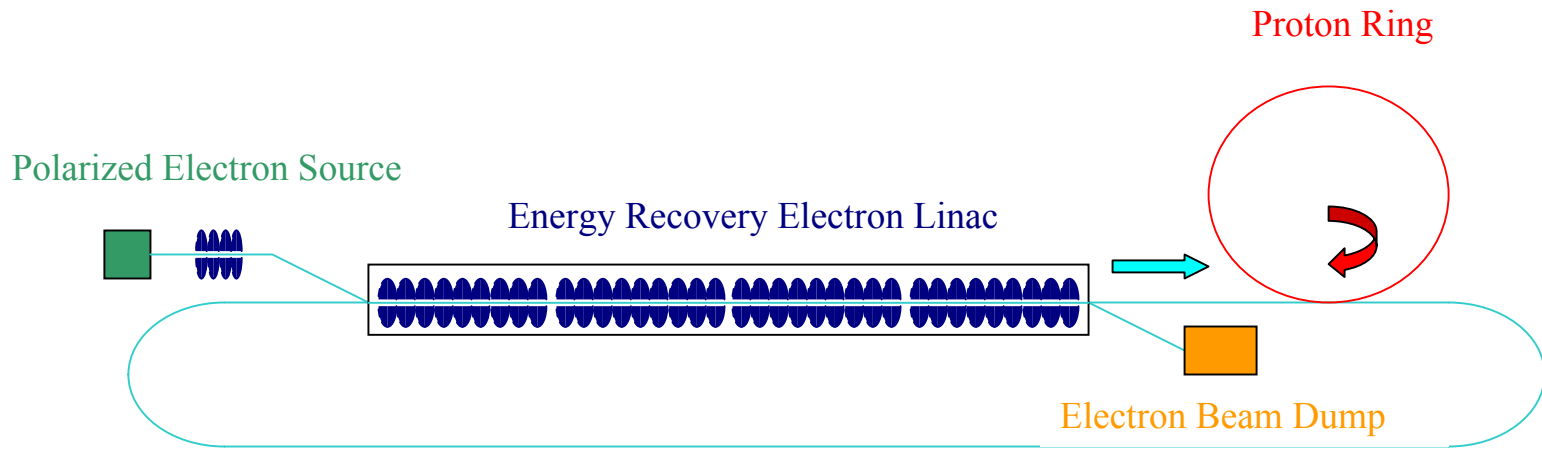


Demonstration of Energy Recovery

With energy recovery the required linac rf power is ~ 16 kW, nearly independent of beam current. It rises to ~ 36 kW with no recovery at 1.1 mA.



Linac-Ring Collider: Schematic Layout



Features of Energy Recovery

- With the exception of the injector, the required rf power is nearly independent of beam current.
 - Increased overall system efficiency.
- The electron beam power to be disposed of at beam dumps is reduced by ratio of E_{\max}/E_{inj} .
 - Thermal design of beam dumps is simplified
 - If the beam is dumped below the neutron production threshold, then the induced radioactivity (shielding problem) will be reduced.



RF to Beam Multiplication Factor for an ideal ERL

$$J = \frac{P_b}{P_g} = \frac{\text{Power absorbed by accelerated beam}}{\text{Generator power needed to create and control rf fields}}$$

$$J = \frac{VI}{\frac{V_c^2}{2\left(\frac{R}{Q}\right)Q_L}} = \frac{2I}{E} \left(\frac{R}{lQ} \right) Q_L$$

$$K = \frac{\text{Accelerated beam power}}{\text{Installed rf power}}$$

$$K = \frac{JE_f}{(J-1)E_{inj} + E_f}$$



RF to Beam Multiplication Factor for an ideal ERL

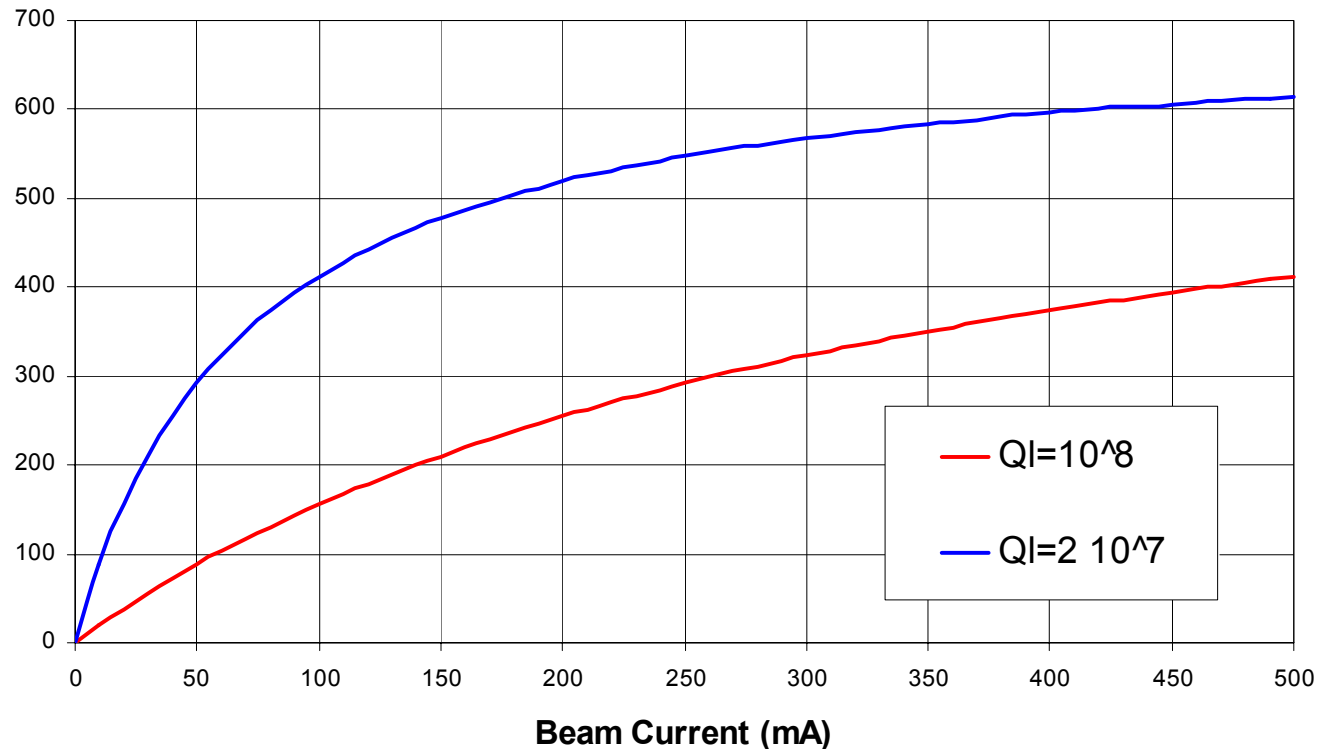
$$E_{acc} = 20 \text{ MV} / m$$

$$R / lQ = 1000 \Omega / m$$

$$E_{inj} = 10 \text{ MeV}$$

$$E_f = 7 \text{ GeV}$$

RF to Beam Multiplication Factor



RF to Beam Multiplication Factor for an ideal ERL

- The efficiency of an ERL (as measured by the rf to beam multiplication factor) increases with current
 - Asymptotic value is E_{\max}/E_{inj}
- The efficiency increases with the loaded Q of the energy-recovering cavities



Q_{ext} Optimization

- Condition for optimum coupling:

$$\beta_{\text{opt}} = \sqrt{(b+1)^2 + \left(2Q_0 \frac{\delta f_d}{f_0}\right)^2}$$

and

$$P_g^{\text{opt}} = \frac{V_c^2}{2(r/Q)Q_0} \left[|b+1| + \sqrt{(b+1)^2 + \left(2Q_0 \frac{\delta f_d}{f_0}\right)^2} \right]$$

- In the absence of beam ($b=0$):

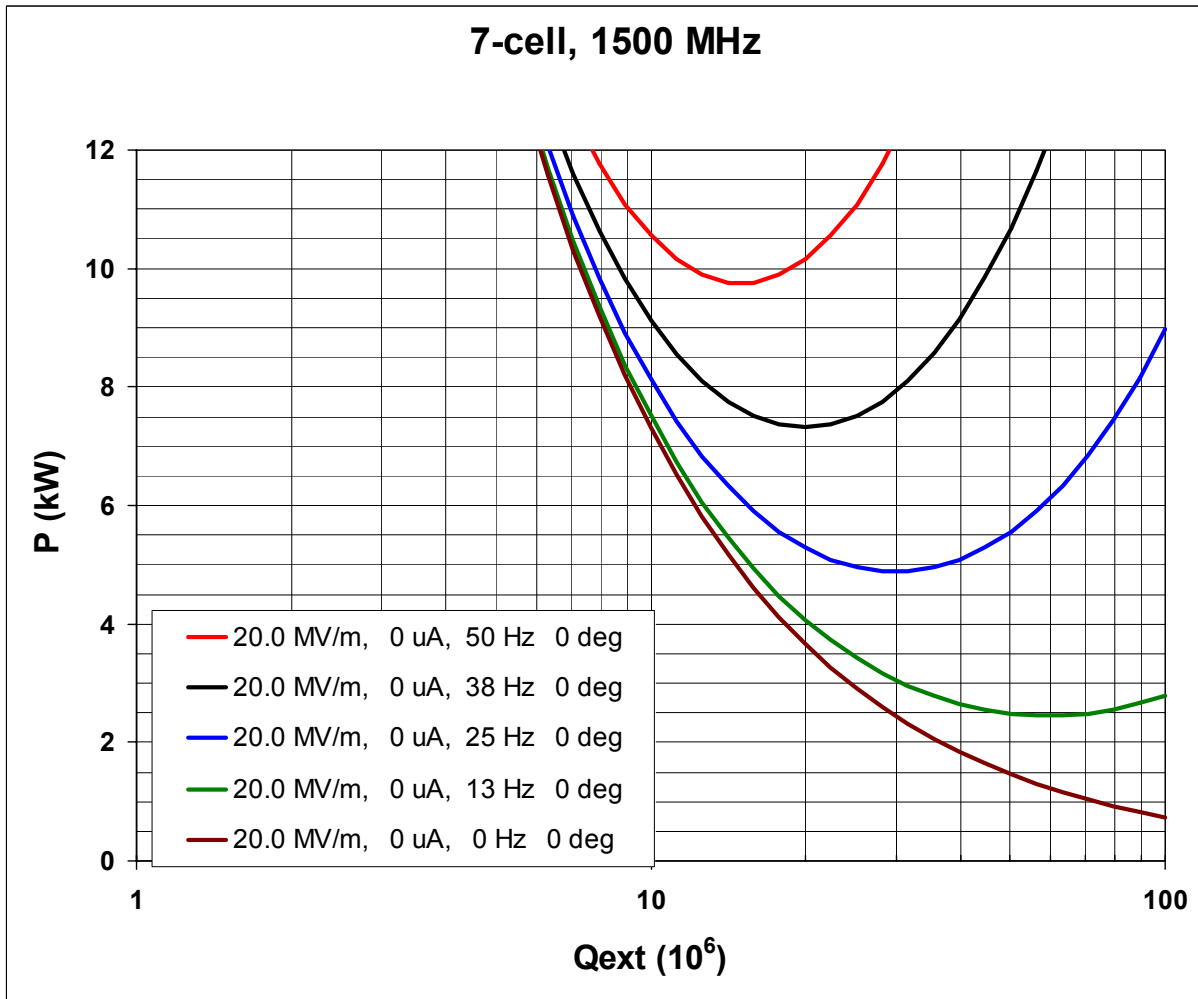
$$\beta_{\text{opt}} = \sqrt{1 + \left(2Q_0 \frac{\delta f_d}{f_0}\right)^2}$$

and

$$P_g^{\text{opt}} = \frac{V_c^2}{2(r/Q)Q_0} \left[1 + \sqrt{1 + \left(2Q_0 \frac{\delta f_d}{f_0}\right)^2} \right] \square 2\pi U \delta f_d$$



Generator Power vs. Loaded Q



Q_{ext} for ERL Injector and Linac Cavities

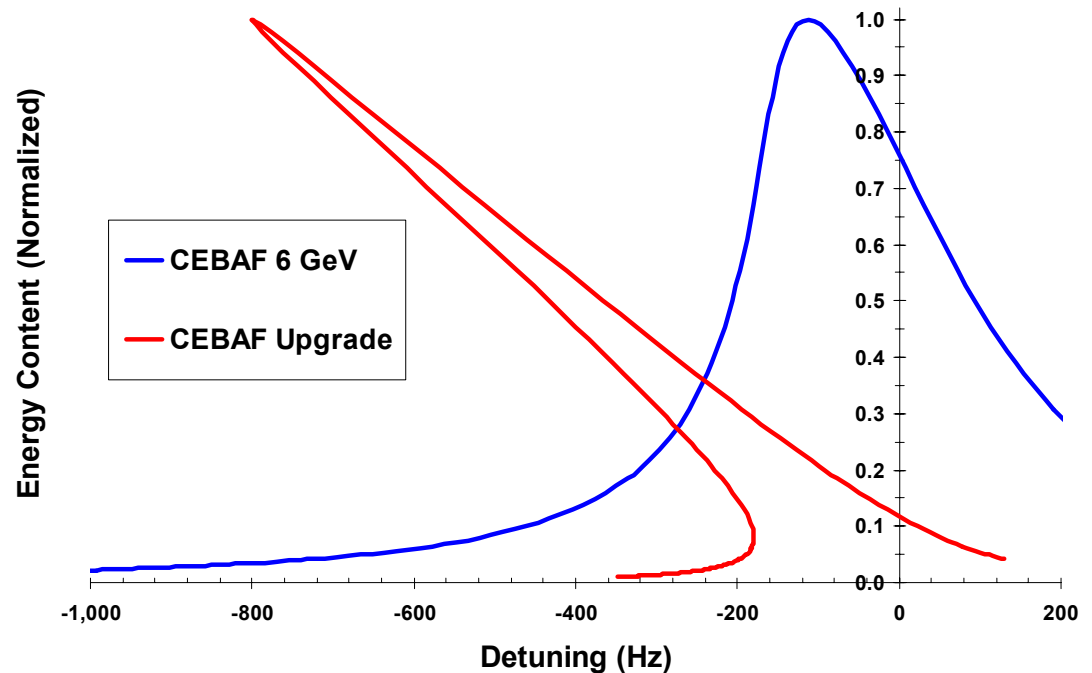
- ERL Injector (2-cell) cavities:
 - $f_0=1300$ MHz, $Q_0=5 \times 10^9$, $V_c=1$ MV per cavity, $L_{\text{cav}}=23$ cm
 - For $I_0=100$ mA \Rightarrow Optimum $Q_L=4.6 \times 10^4 \Rightarrow P_g=100$ kW per cavity
 - Note: $I_0 V_a = 100$ kW \Rightarrow optimization is entirely dominated by beam loading
- ERL linac (9-cell) cavities:
 - $f_0=1300$ MHz, $Q_0=1 \times 10^{10}$, $V_c=20$ MV/m, $L_{\text{cav}}=1.04$ m,
 - $R/Q=1036$ ohms, $\delta f_m=25$ Hz
 - Resultant beam current, $I_{\text{tot}}=0$ mA (energy recovery)
 - \Rightarrow Optimum $Q_L=2.6 \times 10^7 \Rightarrow P_g=8$ kW per cavity with $\delta f_m=25$ Hz
 - Note: optimization is entirely dominated by amplitude of microphonic noise



Increasing the Efficiency of ERLs

What is the maximum achievable loaded Q for energy-recovering cavities?

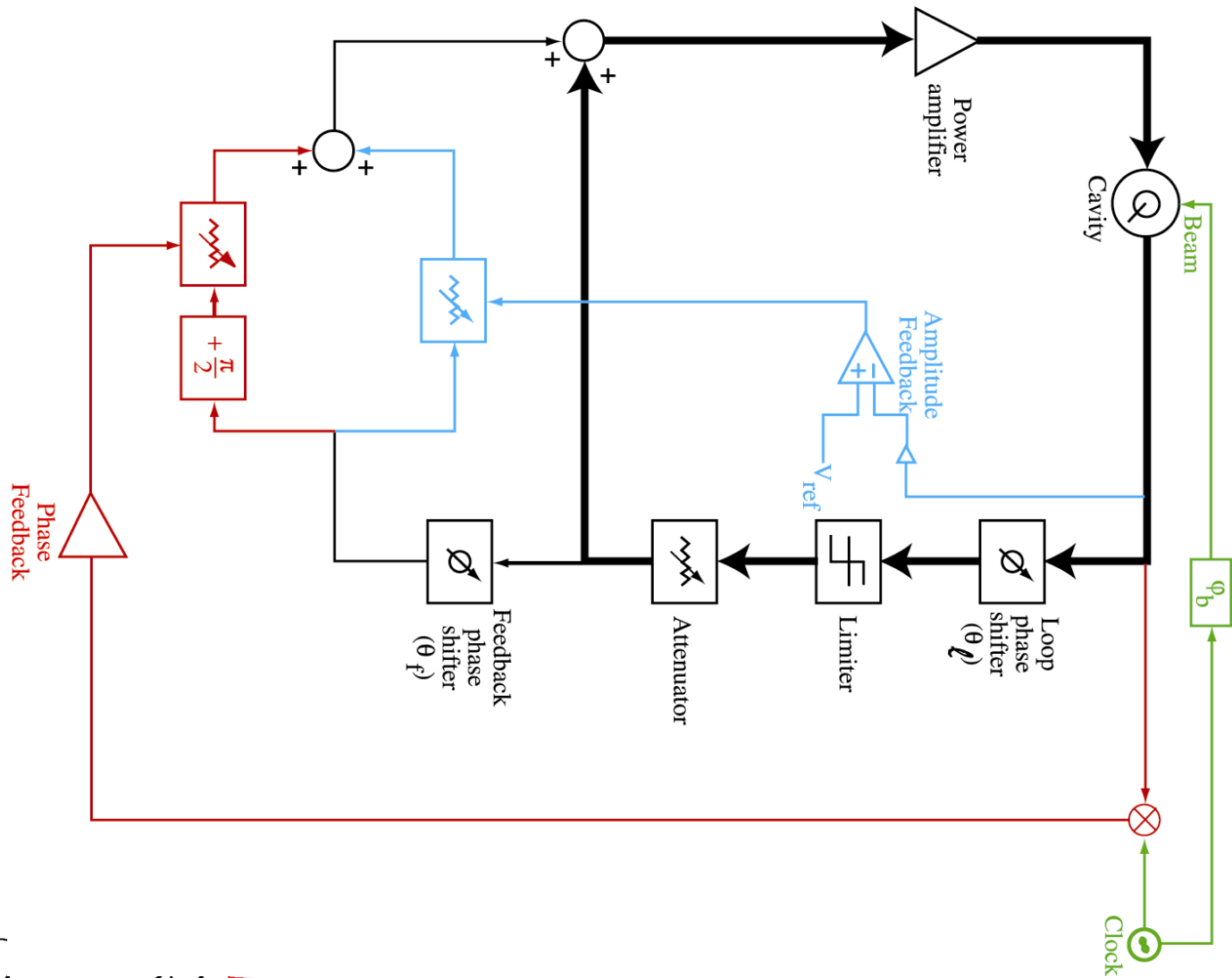
- Microphonics control
- Lorentz force detuning



- Non-ideal energy recovery



Self-Excited Loop – Block Diagram

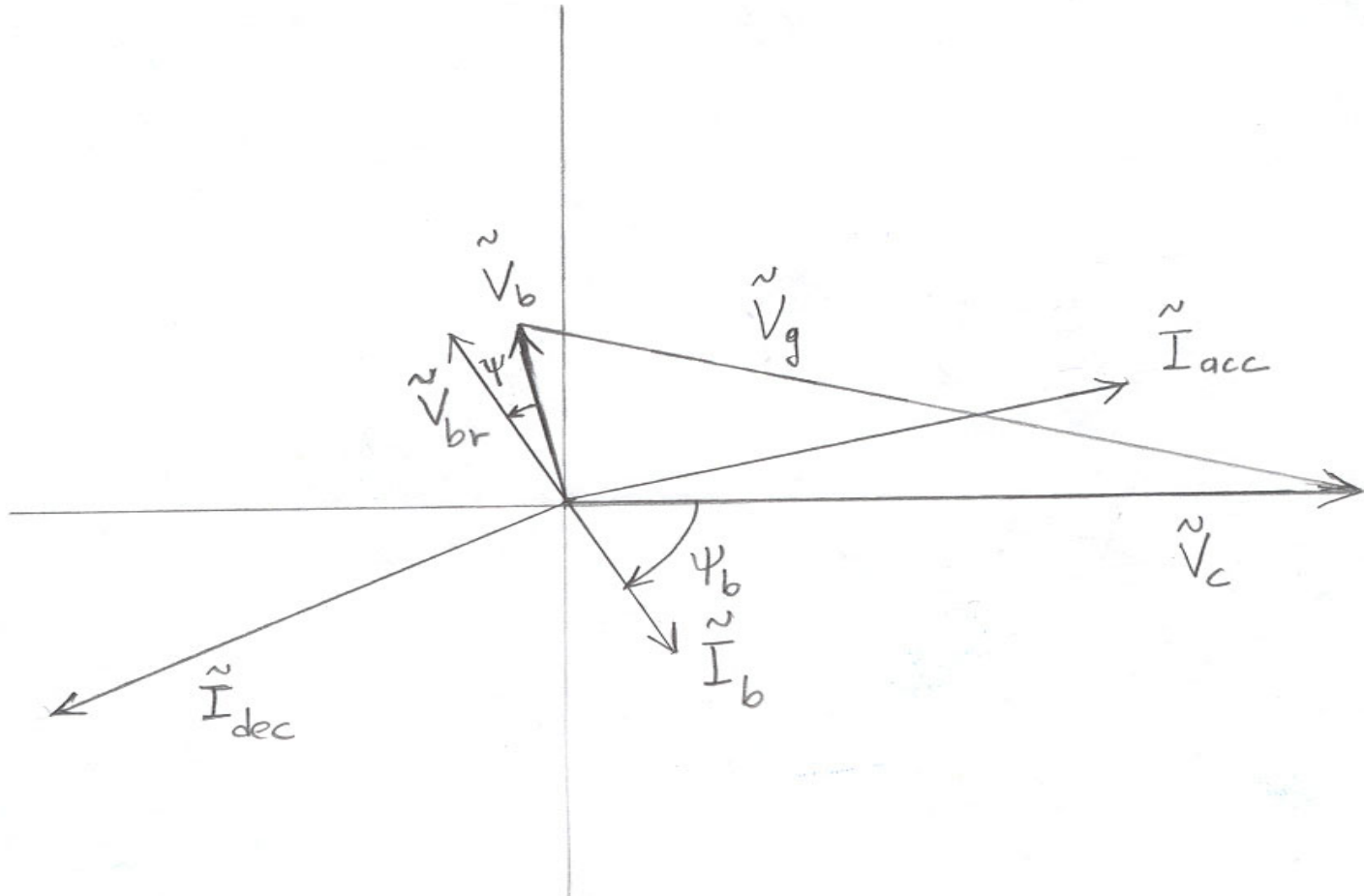


Non-Ideal Energy Recovery

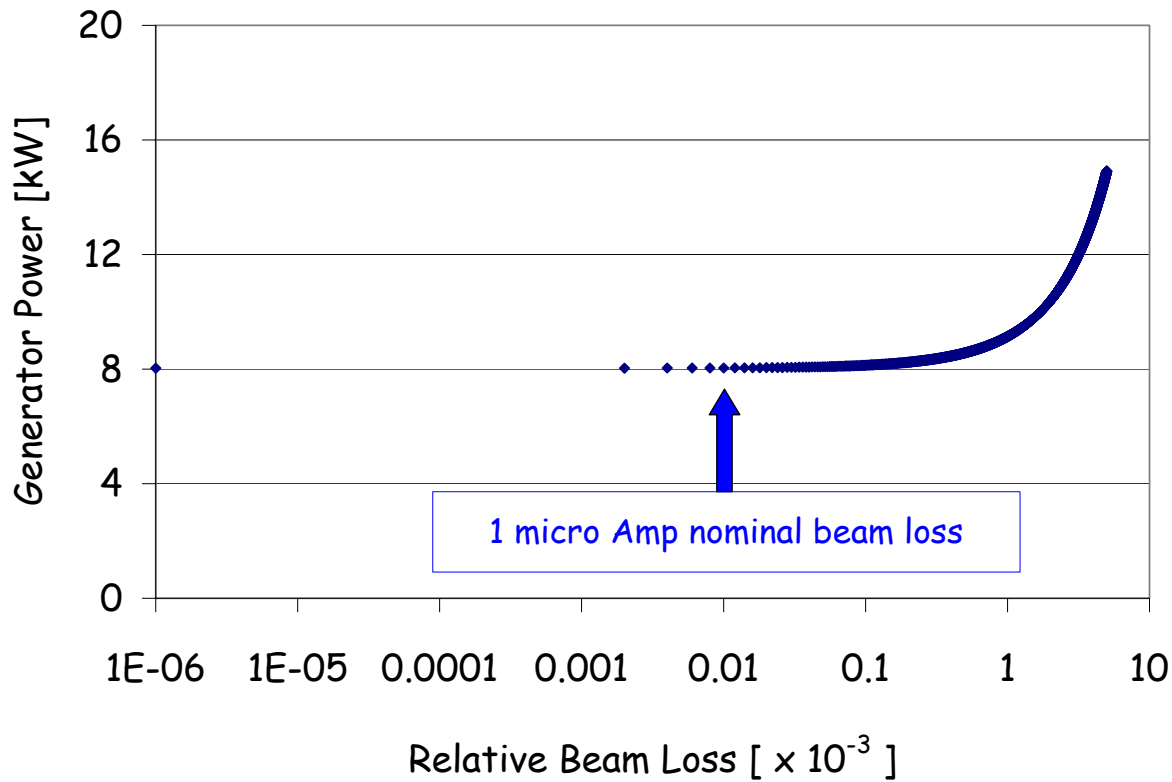
- Ideal energy recovery assumes perfect cancellation of 2 large and opposite vectors
 - Accelerated and decelerated beams are equal in magnitude and 180° out of phase at the fundamental frequency
 - In practice there will be a residual net current:
 - Phases may not differ by precisely 180°
 - Typical expected path length control adjustment leads to $\sim 0.5^\circ$ deviation from 180°
 - Beam loss may occur, resulting in beam vectors of unequal magnitude
 - High-frequency beam current fluctuations
- ⇒ All of the above give rise to a net beam loading vector, of random amplitude and phase, but that will typically be reactive
- ⇒ Increase of rf power requirements and reduction of κ



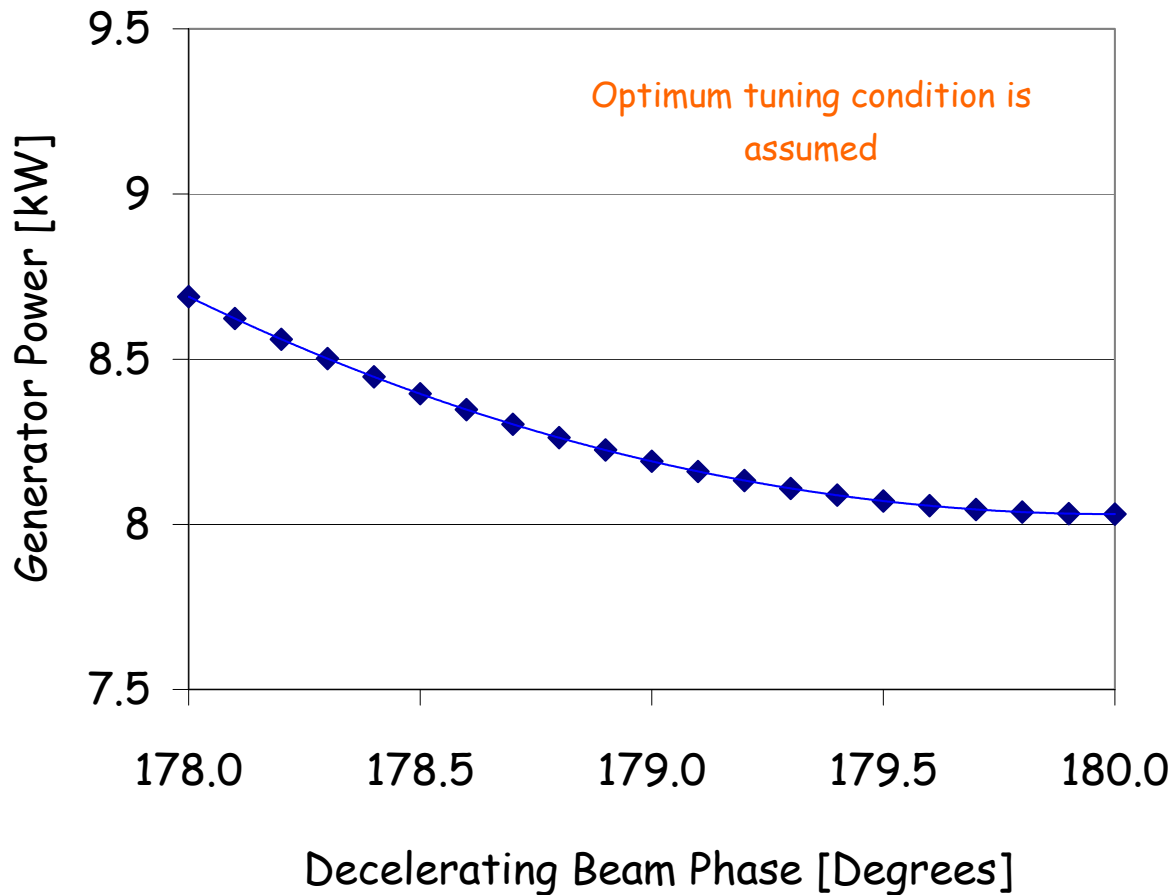
Energy Recovery Phasor Diagram



Sensitivity Analysis: Beam Loss



Sensitivity Analysis: Phase Errors



Amplitude and Phase Stability Requirements

- Specifications set by the users on energy spread and timing jitter will impose requirements on the phase and amplitude stability in the cavities
- These requirements will determine the characteristics of the LLRF control system, including gain and bandwidth of the feedback loops
- In ERLs, additional constraints on the LLRF system design may be imposed due to possible longitudinal instabilities



RF Instabilities

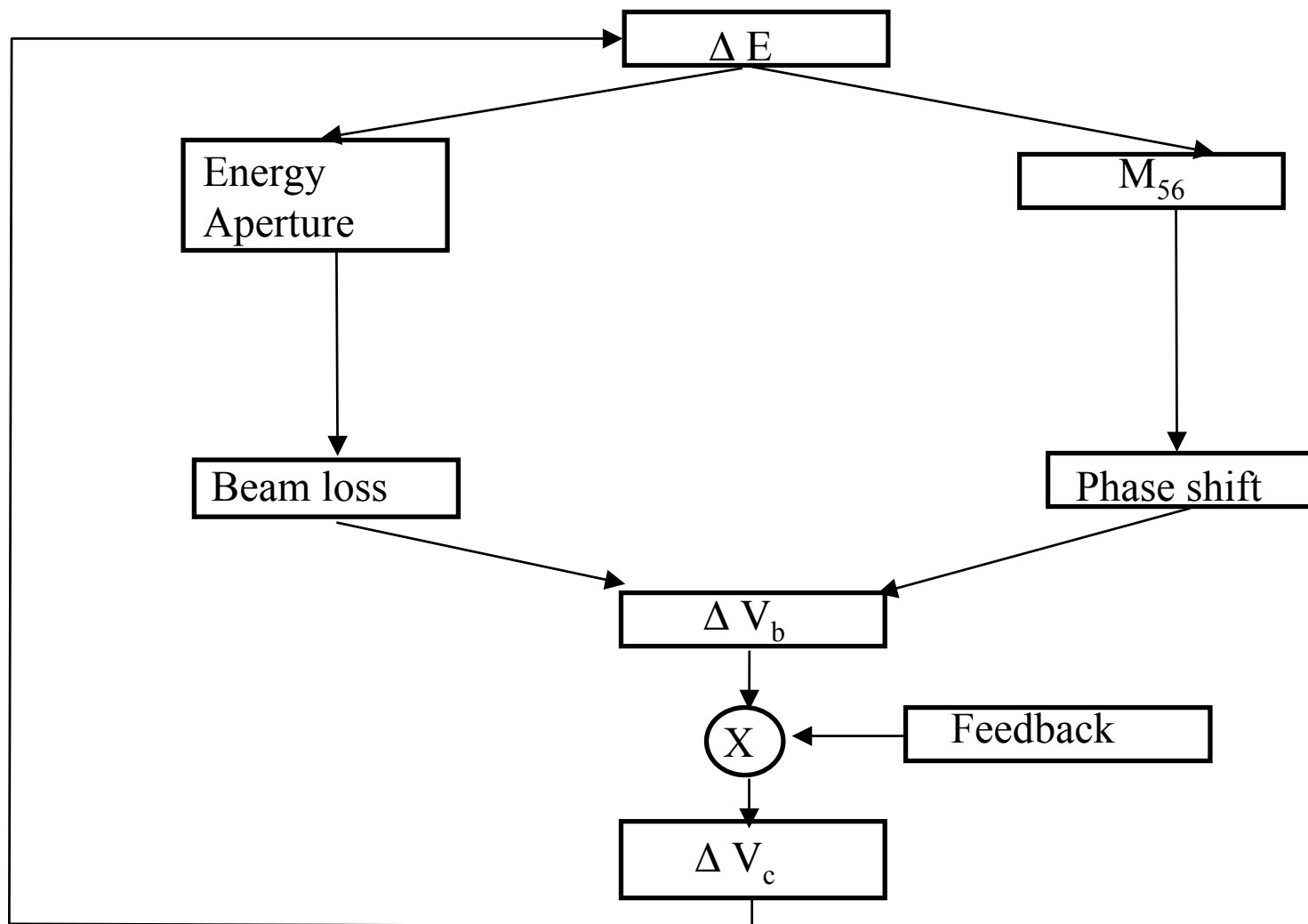
- Instabilities can arise from fluctuations of cavity fields.
- Two effects may trigger unstable behavior:
 - Beam loss which may originate from energy offset which shifts the beam centroid and leads to scraping on apertures.
 - Phase shift which may originate from energy offset coupled to M_{56} in the arc
- Instabilities predicted and observed at LANL, a potential limitation on high power recirculating, energy recovering linacs.

M_{56} is the momentum compaction factor and is defined by:

$$\Delta l = M_{56} \frac{\Delta E}{E}$$



RF Stability Flow Chart



RF Stability Studies

- Model has been developed (Lia Merminga) in support of the Jlab FEL program. It includes:
 - beam-cavity interaction,
 - low level rf feedback
 - FEL interaction
- Solved analytically and numerically
- Model predicts instabilities that agree with experimental measurements performed on JLab IRFEL
 - Agreement is quantitative with FEL off
 - Agreement is qualitative with FEL on
- Instabilities can be controlled by LLRF feedback
 - Further analysis and modeling is needed to understand the rf stability issues of ERLs with much higher current (Control of random reactive loading currents in superconducting cavities)



Higher Order Modes

- Even in the case of perfect energy recovery cancellation of accelerated and decelerated beam occurs only at the fundamental mode frequency
- Coupling to other monopole modes
 - HOM power dissipation
- Coupling to dipole modes
 - Beam breakup instabilities



HOM Power Dissipation

- Accelerated and decelerated beams will couple to the (non fundamental) monopole modes and will deposit energy in those modes
- Power dissipated depends on product of bunch charge and average current

$$P_{diss} = 2k_{\square} Q \langle I \rangle$$

- For typical TESLA-type cavities $k \sim 8.5$ V/pC for $\sigma_z \sim 1$ mm

$$\langle I \rangle \sim 250 \text{ mA}, \quad Q \sim 2 \text{ nC}$$

$$P_{diss} \sim 8 \text{ kW/cavity}$$

- Need a better understanding of where that power goes
Only a small fraction ends up on the cavity walls
- Need engineering development of HOM absorbers



Beam Breakup Instabilities

- Coupling of accelerated and decelerated beams to dipole modes
- Single bunch, single pass effects: limit the bunch charge
 - Energy spread induced by variation of longitudinal wake field across bunch
 - Emittance growth induced by single-bunch transverse BBU



(Multi-Bunch) Beam Breakup Instabilities

- Multi-pass, multi-bunch effects: limit the average current
- Recirculating beam through a cavity can lead to transverse instabilities
 - Transverse displacement on successive recirculations can excite HOMs that further deflect initial beam
 - Feedback loop between beam and cavities
 - Threshold current above which the system becomes unstable
 - Because of their high Q, superconducting systems can be more sensitive to this type of instability
- TDBBU: 2d beam breakup code used for simulation (Krafft, Bisognano, Yunn)
 - Being benchmarked at the JLab FEL
 - Predicts threshold current of ~ 250 mA, and rise time of ~ 2 msec.



Conclusions

- Energy recovery superconducting linacs are very efficient devices for certain applications
 - They can approach the efficiency of storage rings while preserving the beam properties of linacs
- Concept has been fully demonstrated and is used routinely in a user facility
- Studies have uncovered no fundamental show stoppers
- The ultimate limits of the energy-recovering concept have not been fully determined
 - Highest Q_1 for the cavities while maintaining phase and amplitude stability requirements
 - Highest current that can be accelerated/decelerated
 - Preservation of rf stability
 - Avoidance BBU instabilities
 - Extraction of HOM power
 - Control of beam loss



Analysis and Simulation of Beam-Beam Effects in a Linac-Ring Collider

R. Li, K. Beard, J. Boyce, G. Krafft, L. Merminga, B. C. Yunn

Jefferson Lab

V. Lebedev

Fermilab

J. J. Bisognano

SRC, Univ. Wisconsin-Madison



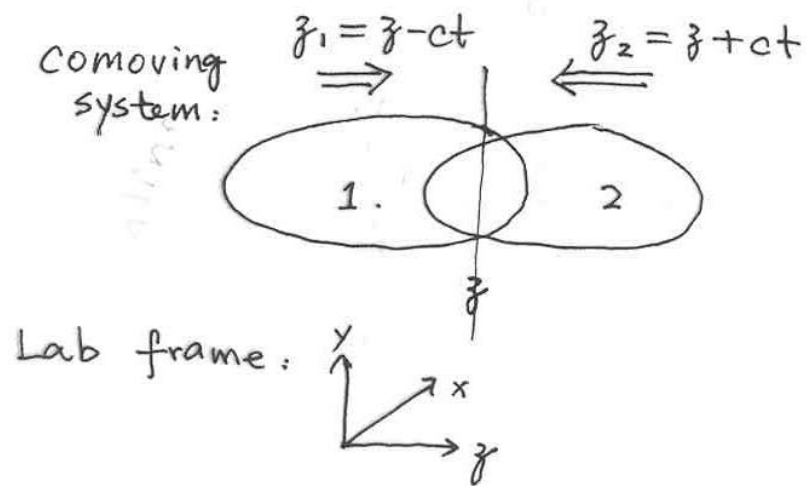
- Introduction
- Strong-Strong Beam-Beam Simulation
- Analysis of the Beam-Beam Kink Instability in the Linac-Ring B Factory
- Strong Head-Tail Instability in a Linac-Ring e-p Collider
- Summary



1. Introduction

Luminosity: reaction events produced by unit reaction
Cross section area

$$\mathcal{L} = zc f_c \int n_1(x, y, z-ct) n_2(x, y, z+ct) d^3\vec{r} dt$$



$$\mathcal{L} = \frac{N_+ N_- f_c}{2\pi \sqrt{\sigma_{x+}^2 + \sigma_{x-}^2} \sqrt{\sigma_{y+}^2 + \sigma_{y-}^2}}$$

(Gaussian bunches)

Desired Luminosity $> 10^{33} \text{ cm}^{-2} \text{ s}^{-1}$

Linear Beam-Beam Tune Shift (ring-ring)

For e^+e^- collider, focusing force on a particle in e^+ beam due to the interaction of opposing e^- beam is:

$$F_{y+} = e(1+\beta^2) \frac{\partial V(x,y)}{\partial y} \approx - \frac{2N \cdot e^2 y}{\sigma_{y-}(\sigma_{x-} + \sigma_{y-})} \quad (y \ll \sigma_y, \beta \rightarrow 1)$$

$$\left(\nabla^2 V = 4\pi \rho, \quad \rho(x,y) = \frac{N \cdot e}{2\pi \sigma_{x-} \sigma_{y-}} e^{-\frac{x^2}{2\sigma_{x-}^2} - \frac{y^2}{2\sigma_{y-}^2}} \right)$$

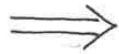
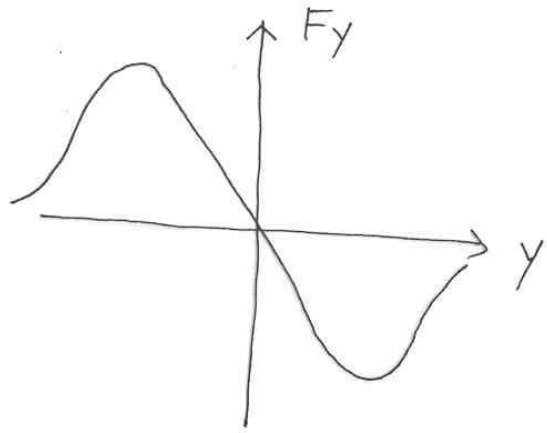
$$M = \begin{bmatrix} 1 & 0 \\ -\frac{1}{f_{y+}} & 1 \end{bmatrix} \begin{bmatrix} \cos 2\pi \nu_y & \beta_{y+}^* \sin 2\pi \nu_y \\ -\frac{1}{\beta_{y+}^*} \sin 2\pi \nu_y & \cos 2\pi \nu_y \end{bmatrix}, \quad \frac{1}{f_{y+}} = \frac{2N \cdot r_0}{\sigma_{y+} \sigma_{y-} (\sigma_{x-} + \sigma_{y-})}$$

$$\cos 2\pi(\nu_{y+} + \frac{1}{2}\xi_{y+}) = \frac{1}{2} \text{Tr} M$$

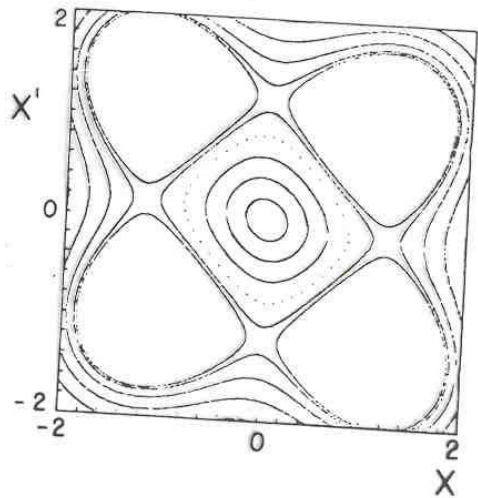
$$\xi_{y+} = \frac{r_0 N \cdot \beta_{y+}^*}{2\pi \sigma_{y+} \sigma_{y-} (\sigma_{x-} + \sigma_{y-})} \quad (y \leftrightarrow x, + \leftrightarrow -)$$

Beam-Beam Tune Shift Limit

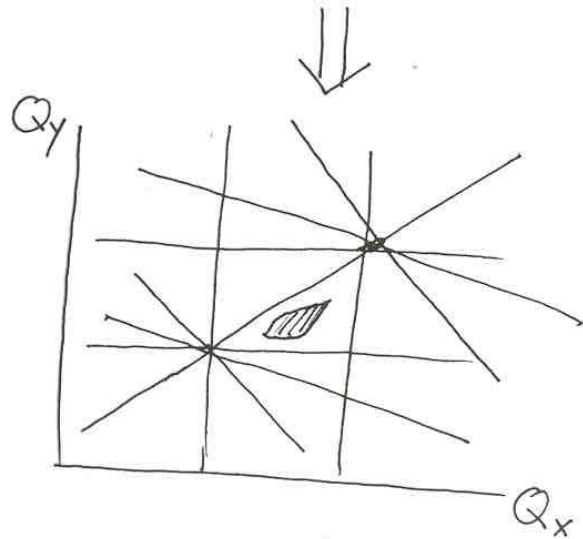
(nonlinear effect)



$\xi_y \propto \frac{F_y}{y}$ amplitude dependent



islands and separatrix



working area

Observed Limit (diffusion)

$$\xi < 0.05$$

(e^+e^- ring)

Motivation for Linac-Ring Colliders

[Grosse-Wiesmann]

e^-e^+ collider

<Advantages>

<disadvantages>

Ring-Ring

- economic

• E_{cm} limited by SR

• \mathcal{L} limited by $\sum_{x,y}$

Linear Collider

- No SR
- No $\sum_{x,y}$ limit

• e^+ production and damping

• beamstrahlung

Linac-Ring

- two machines relatively decoupled (?)
- accumulation of e^+

• lower $N_- \Rightarrow$ low σ_{xy}
lower γ_-
high $\frac{N_+}{\sigma_{xy}}$

\Downarrow
high disruption of e^-

Disruption

e^- being focused by the e^+ beam

$$D_{y-} = \frac{\sigma_{z+}}{f_{y-}} = \frac{2N_+ r_e \sigma_{y+}}{\gamma_- \sigma_{y+} (\sigma_{x+} + \sigma_{y+})}$$

$D_{y-} \gg 1 \Rightarrow$ electrons oscillate through the positron bunch

- Special Feature of Beam-Beam Interaction in a Linac-ring collider:
 - stored bunch collides with highly disrupted e^- bunch
 - need strong-strong simulation to study the evolution of the strong (e^+) beam in the process of interaction with the highly disrupted weak (e^-) beam.
 - e^- acts as active impedance
 - jitter in linac beam

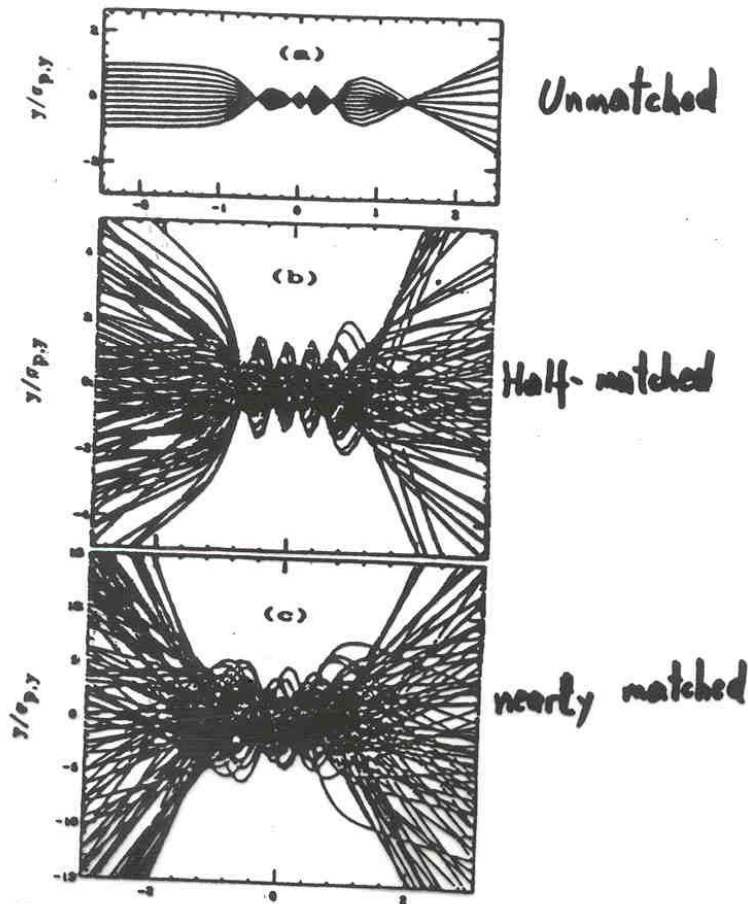


Figure 2. The trajectories of individual electrons traveling from left to right through a positron bunch are plotted with respect to the center of mass of the positron bunch. The positron bunch extends from -1 to +1 along the abscissa. (a) Individual electrons with parallel trajectories colliding with a strong positron bunch exhibit localized pinching or foci. (b) Colliding electrons with more realistic pre-collision trajectories also show the pinching effects, though not as strong. (c) Electron trajectories after bunch optics have been "matched" according to the procedure discussed in Ref. 5. The foci have been reduced significantly.

All o
offset wer
bunches v
calculation.

Figur
with no π
and negat
shows the
plotted in
bunch. Fi
each slice,
Figure 4b
It is clear
tend to di

Figur
Figure 5a
are for x
calculation
6 but mat

The a
any detect
a minimur
macroparti
these resul
further stu
before any

Finall
is shown is
the lumin
(For all of
 4×10^{24} c

2. Strong-Strong Beam-Beam Simulation

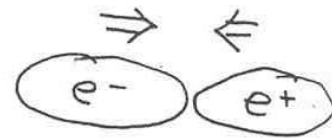
(1) about the code

(2) beam-beam in a ring-ring B factory

(3) beam-beam in a linac-ring B factory

(1) About the code

Beam-Beam Interaction



Interaction Region

bunch



slice



macroparticles



- Bunches are modeled by transverse slices populated with finite number of macroparticles with finite size

- Elliptical macroparticles are Gaussian in $x-y$ plane

$$R^{(\text{macro})} = \frac{\sigma_x^{(\text{macro})}}{\sigma_y^{(\text{macro})}} \approx R^{(\text{bunch})}$$

- During collision, only macroparticles in overlapping slices experience mutual forces

Force Calculation

$$\vec{F}(\vec{r}_i^{(+)}) = \sum_m \vec{f}(\vec{r}_i^{(+)} - \vec{r}_m^{(+)})$$

For Gaussian distribution,

$$\rho_m(x, y) = \frac{n_m e}{2\pi \sigma_{mx} \sigma_{my}} \exp\left(-\frac{x^2}{2\sigma_{mx}^2} - \frac{y^2}{2\sigma_{my}^2}\right) \quad \left\{ \begin{array}{l} \nabla^2 \phi = \rho_m / \epsilon_0 \\ \vec{E} = -\nabla \phi \end{array} \right.$$

- Field in terms of complex error function [Bassetti & Erskine]:

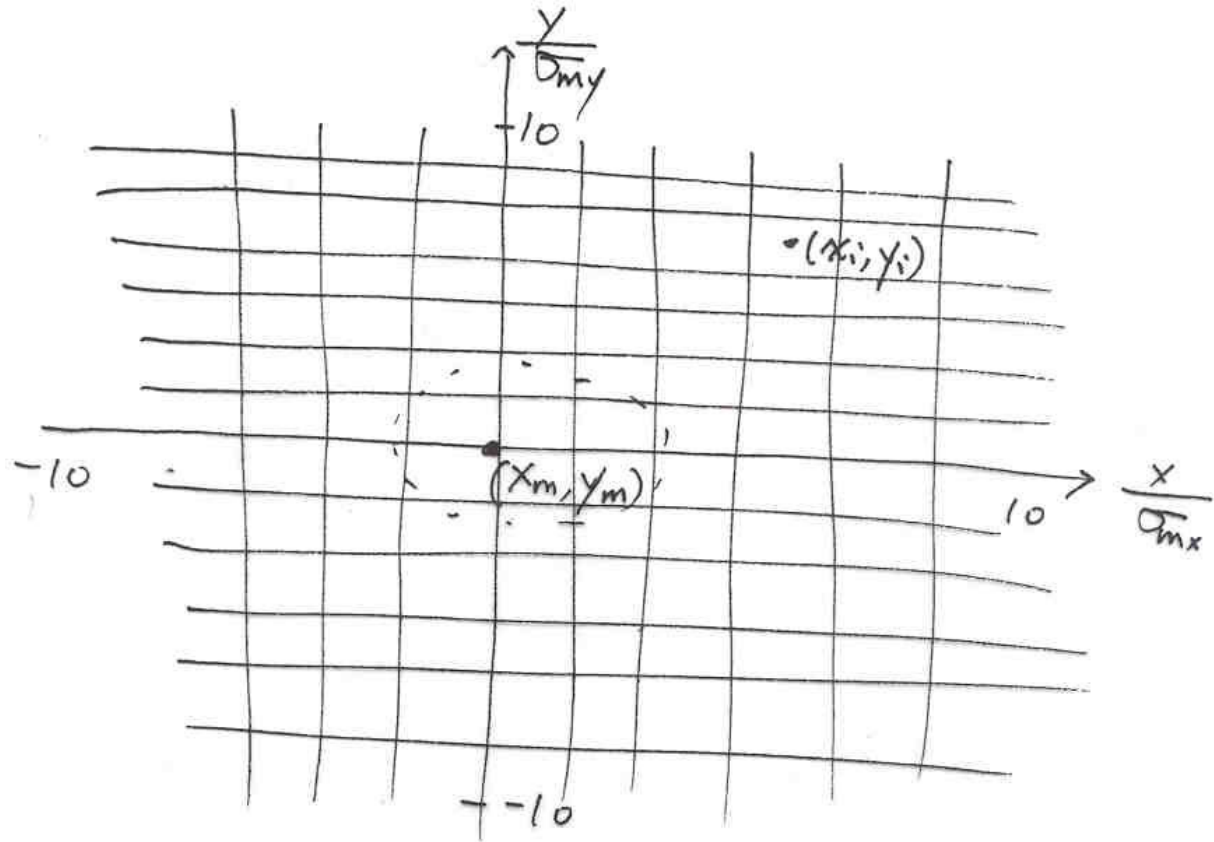
$$(E_x, E_y) = \frac{n_m e}{z \epsilon_0 \sqrt{2\pi(\sigma_{mx}^2 - \sigma_{my}^2)}} (\text{Im} \zeta, \text{Re} \zeta)$$

$$\text{with } \left\{ \begin{array}{l} \zeta = W\left(\frac{x+iy}{\sqrt{z(\sigma_{mx}^2 - \sigma_{my}^2)}}\right) - e^{-\frac{x^2}{2\sigma_{mx}^2} - \frac{y^2}{2\sigma_{my}^2}} W\left(\frac{x \frac{\sigma_{my}}{\sigma_{mx}} + iy \frac{\sigma_{mx}}{\sigma_{my}}}{\sqrt{z(\sigma_{mx}^2 - \sigma_{my}^2)}}\right) \\ W(z) = e^{-z^2} \text{erfc}(-iz) \end{array} \right.$$

- Use lookup table for $f_{x,y}\left(\frac{x_i - x_m}{\sigma_{mx}}, \frac{y_i - y_m}{\sigma_{my}}, R = \frac{\sigma_{mx}}{\sigma_{my}}\right)$

- Luminosity $L_{\text{total}} = \sum_{i,m} L^{(im)}$

- Lookup table for force calculation



given aspect ratio

choice of $\sigma_{m,x,y}$ and N_m

Noise Consideration

macroparticle model:

$$P(\vec{x}, t) = \int d\vec{x}' S(\vec{x} - \vec{x}') \rho_c(\vec{x}', t)$$

Fourier transform

$$\tilde{P}(\vec{k}, t) = \hat{S}(\vec{k}) \tilde{\rho}_c(\vec{k}, t)$$

Gaussian macroparticle

$$q_m e^{-\frac{k_x^2 \sigma_{mx}^2}{2} - \frac{k_y^2 \sigma_{my}^2}{2}}$$

Gaussian centroid distribution

$$N_m e^{-\frac{k_x^2 \sigma_{Bx}^2}{2} - \frac{k_y^2 \sigma_{By}^2}{2}}$$

Effective rms bunch size

$$\sigma_{Bx}^{\text{eff}} = \sqrt{\sigma_{Bx}^2 + \sigma_{mx}^2}, \quad \sigma_{By}^{\text{eff}} = \sqrt{\sigma_{By}^2 + \sigma_{my}^2}$$

\Rightarrow smooth and realistic representation requires

$$\left(\frac{\sigma_{m,x,y}}{\sigma_{Bx,y}} \right)^2 \ll 1 \quad (\text{realistic})$$

$$N_m \gg N_0 = \frac{\sigma_{Bx} \sigma_{By}}{\sigma_{mx} \sigma_{my}} \quad (\text{overlap})$$

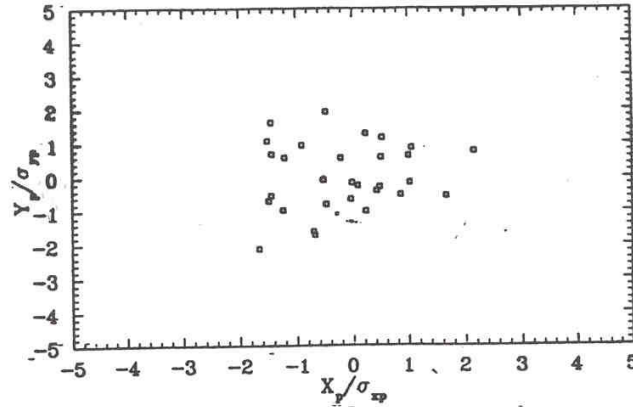
Example:

$$\frac{\sigma_{mx}}{\sigma_{Bx}} = \frac{1}{2},$$

$$\sigma_{Bx}^{\text{eff}} \approx 1.12 \sigma_{Bx}$$

Force calculated using macro-particle mode

$R = 3.93$



center of 30 macroparticles simulating a Gaussian slice
 Figure 1: Transverse distribution of 30 macro-particle in e+ bunch slice

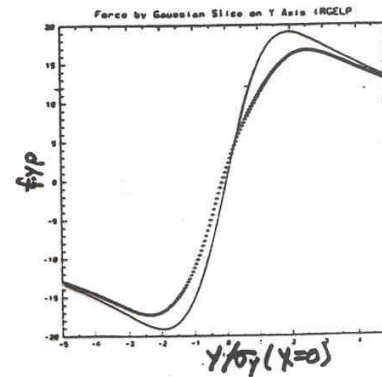
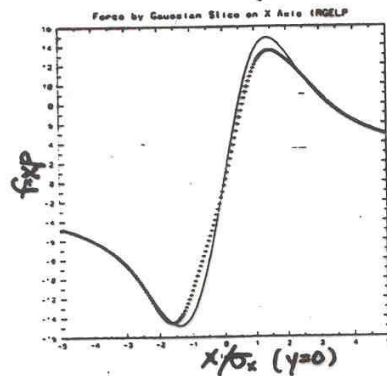


Figure 2: Force calculated by macro-particle model (dotted curves) compared to analytical results (solid curves)

$$\frac{\sigma_{mx,y}}{\sigma_{Bx,y}} = \frac{1}{2}$$

Comparison of Results obtained using different number of macro particles

$$N_m^- = 360, N_m^+ = 1000$$

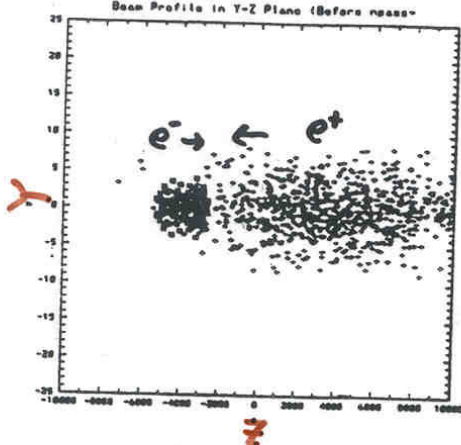


Figure 1: Beam profiles after 3000 collision ($N_e = 360, N_p = 1000$)

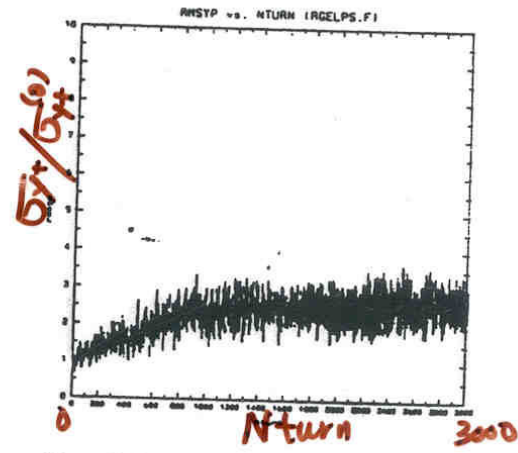


Figure 3: Positron beam blowup after 3000 collision ($N_e = 360, N_p = 1000$)

$$N_m^- = 1440, N_m^+ = 4000$$

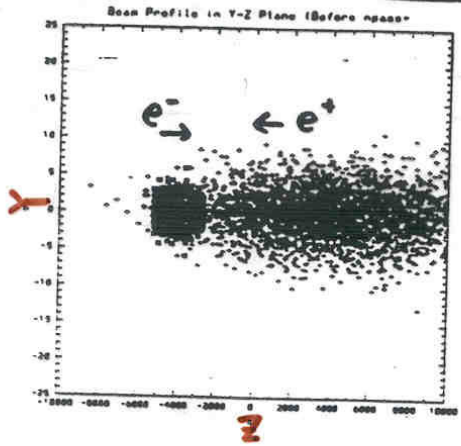


Figure 2: Beam profiles after 3000 collision ($N_e = 1440, N_p = 4000$)

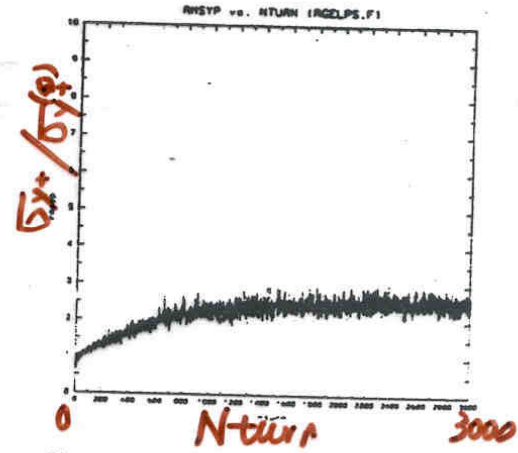
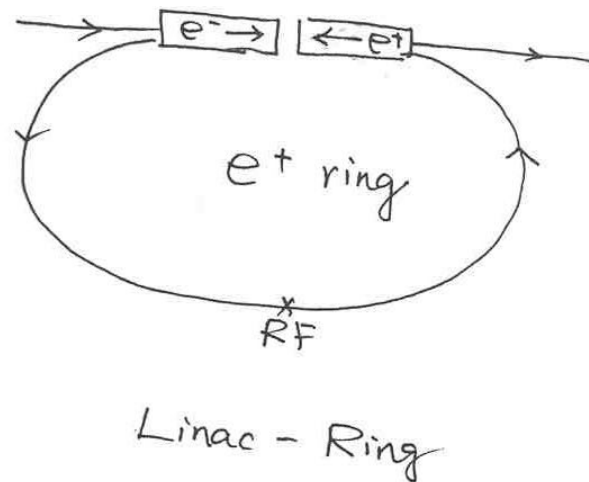
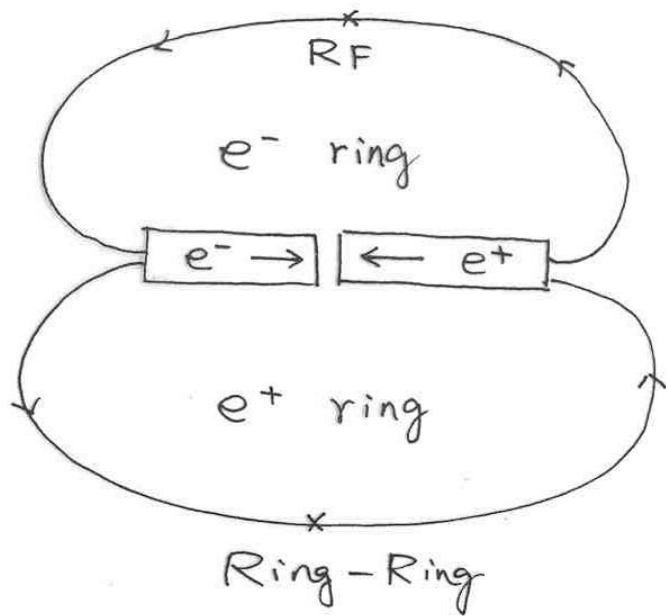


Figure 4: Positron beam blowup after 3000 collision ($N_e = 1440, N_p = 4000$)

Layout of the Program



Beam Dynamics Includes:

- Beam-Beam Interaction at IR
- Linear Matrix in the Ring
- Transverse: damping due to RF, and quantum excitation
- Longitudinal: synchrotron oscillation, radiation damping, quantum excitation

(2) Ring-Ring Beam-Beam Effects

Simulation

benchmark with existing beam-beam results in a ring-ring B factory

of macro-particles in each bunch = 300

slices in each bunch = 5

macroparticle size $\frac{\sigma_{mx,y}}{\sigma_{Bx,y}} = 0.5$

Aspect ratio $R = \frac{\sigma_{mx}}{\sigma_{my}} = \left(\frac{\sigma_{Bx}}{\sigma_{By}} \right)_{\text{nominal}} = 25$

— Parameter List (PEP II SLAC Proposal)

— Plots for one pass

— Long Term Behavior $\{\sigma_x, \sigma_y, \mathcal{L}, \xi_y\}$

— Beam-Beam Tune Shift Limit

— Flip-Flop Instability

(1) Parameter List (SLAC Proposal)

Table 4-23. Main B Factory parameters used in the beam-beam simulation studies.

	LER (e ⁺)	HER (e ⁻)
E [GeV]	3.1	9
s _B [m]	1.26	1.26
f _c [MHz]	238	238
V _{RF} [MV]	8.0	18.5
f _{RF} [MHz]	476.0	476.0
φ _s [deg]	170.6	168.7
α	1.15 × 10 ⁻³	2.41 × 10 ⁻³
v _s	0.0403	0.0520
σ _L [cm]	1	1
N _b	5.61 × 10 ¹⁰	3.88 × 10 ¹⁰
ε _{nx} [nm-rad]	92	46
ε _{ny} [nm-rad]	3.6	1.8
β _x [*] [cm]	37.5	75.0
β _y [*] [cm]	1.5	3.0
σ _{0x} [*] [μm]	186	186
σ _{0y} [*] [μm]	7.4	7.4
τ _x [turns]	4400	5014
τ _y [turns]	4400	5014

$$\rightarrow \mathcal{L}_0 = 3 \times 10^{33} \text{ cm}^{-2} \text{ s}^{-1}$$

$$\xi_{0x}^+ = \xi_{0y}^+ = \xi_{0x}^- = \xi_{0y}^- = 0.03$$

$$Q_x = 0.09, \quad Q_y = 0.06$$

(2) One pass

Equilibrium Beam Profile Before 1st Pass

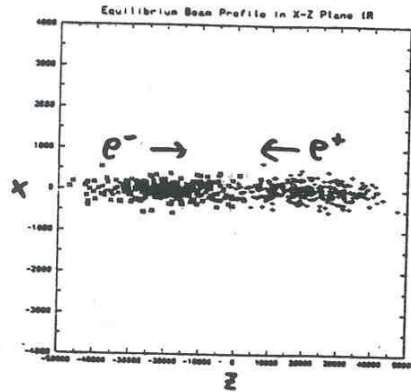


Figure 1: Initial beam profile in X-Z plane

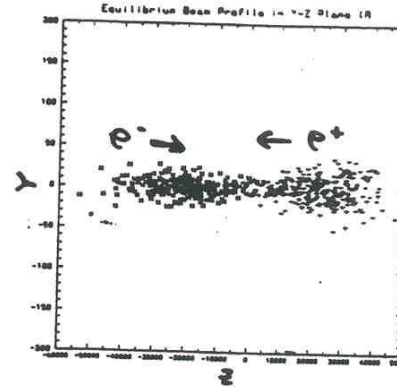


Figure 3: Initial beam profile in Y-Z plane

Longitudinal Charge Distribution

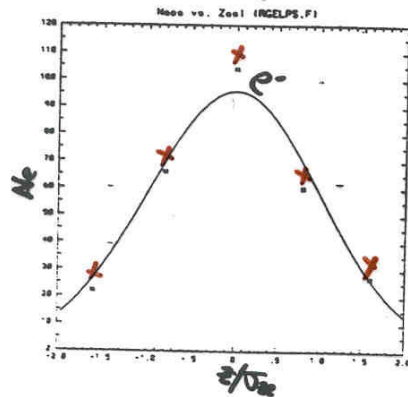


Figure 2: Longitudinal distribution of e- macro-particles

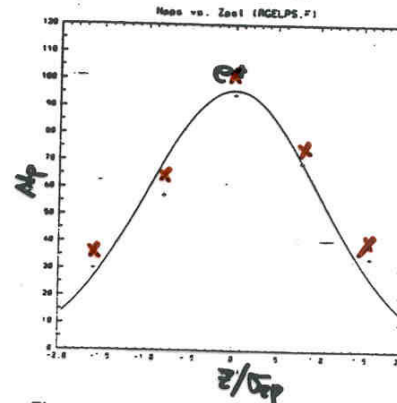


Figure 4: Longitudinal distribution of e+ macro-particles

$$L_{cal} = 2.78 \times 10^{33}$$

$$L_0 = 3.02 \times 10^{33}$$

(3) Long Term Behavior (3 damping times)

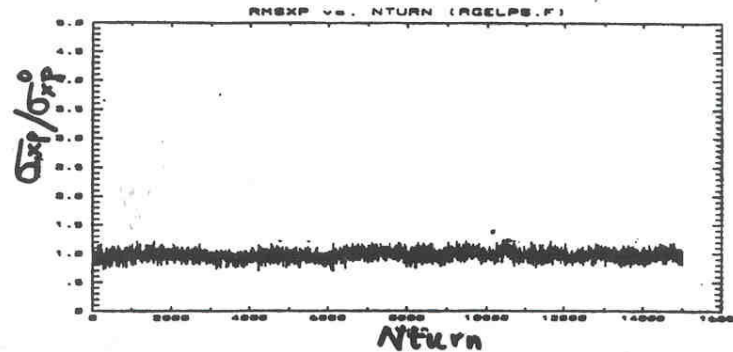


Figure 1: Horizontal blowup in three damping times

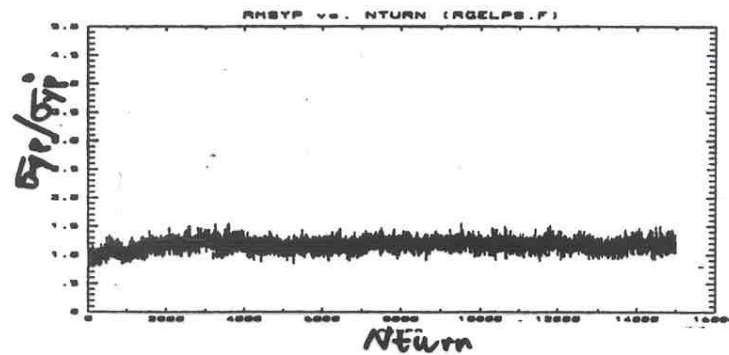


Figure 2: Vertical blowup in three damping times

For each given $\{N_e, N_p\}$, can obtain
a set of equilibrium $\{\sigma_{xo}, \sigma_{yo}, \sigma_{xp}, \sigma_{yp}, \mathcal{L}\}$

$$\{Q_x, Q_y\} = \{0.09, 0.06\}$$

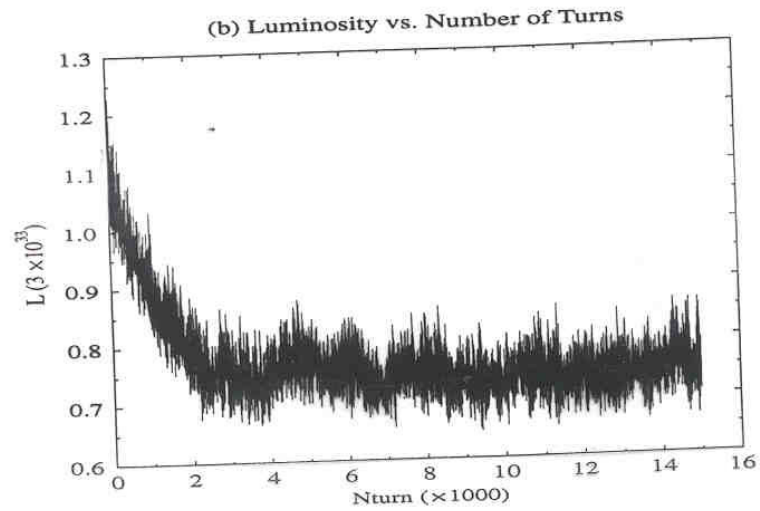
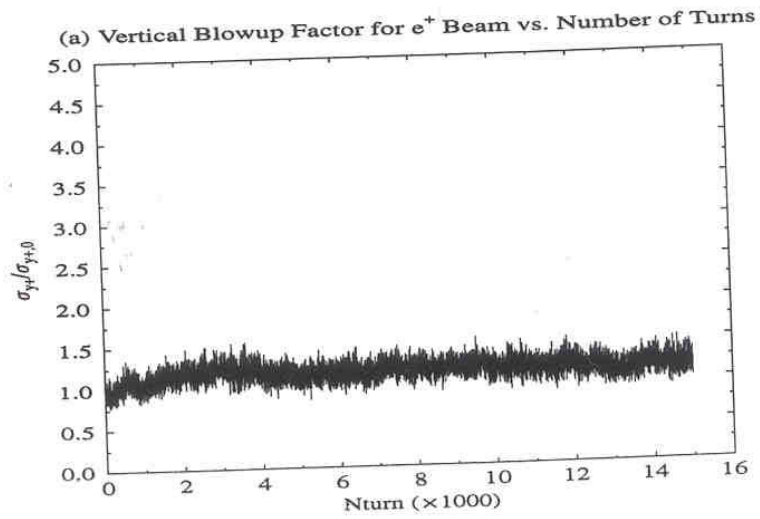
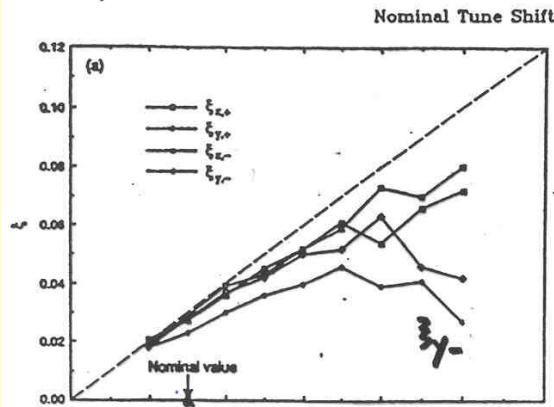
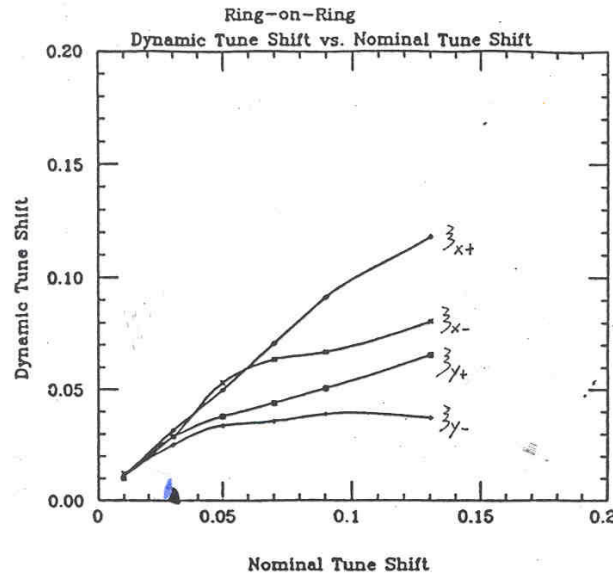
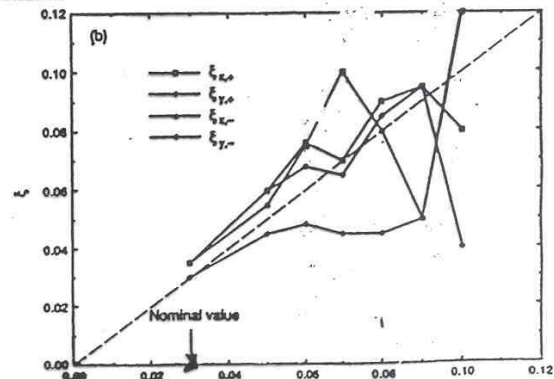


Figure 9: Beam blowup (a) and luminosity (b) for the positron beam during 15000 turns for parameters in Table 2.



Results from ←
Tennyson's code



(5)

Flip-Flop Effect in Storage Ring / Storage Ring



Coherent coupling
of transverse modes
in the two rings

This phenomenon was observed by R. Siemann and S. Krishnagopal using simulation which solves EM fields generated by round beams.

Our code allows general beam distribution \Rightarrow should be able to display the same effect.

Feature: at tunes just below quarter-integer, the beam distribution in the two rings oscillate in an anti-correlated manner between hollow and core with period 2.

(3) Linac-Ring Beam-Beam Effects

Simulation

$$\# \text{ of macroparticles in } \begin{cases} e^- \\ e^+ \end{cases} \text{ bunch} = \begin{cases} 360 \\ 1000 \end{cases}$$

$$\# \text{ of slices in } \begin{cases} e^- \\ e^+ \end{cases} \text{ bunch} = \begin{cases} 9 \\ 45 \end{cases}$$

$$\text{macrosize } \frac{\sigma_{m,x,y}}{\sigma_{B,x,y}} = 0.5$$

$$\text{aspect ratio } R = \frac{\sigma_{mx}}{\sigma_{my}} = \left(\frac{\sigma_{Bx}}{\sigma_{By}} \right)_{\text{design}} = 3.93$$

- Parameter List (Sam Heifets)
- Plots for one pass
- Kink Instability
- Long Term Behavior
- Beam-Beam Tune Shift Limit (w. and w/o matching)

(3) Linac-Ring Beam-Beam Effects

Simulation

$$\# \text{ of macroparticles in } \begin{cases} e^- \\ e^+ \end{cases} \text{ bunch} = \begin{cases} 360 \\ 1000 \end{cases}$$

$$\# \text{ of slices in } \begin{cases} e^- \\ e^+ \end{cases} \text{ bunch} = \begin{cases} 9 \\ 45 \end{cases}$$

$$\text{macrosize} \frac{\sigma_{mxy}}{\sigma_{Bxy}} = 0.5$$

$$\text{aspect ratio } R = \frac{\sigma_{mx}}{\sigma_{my}} = \left(\frac{\sigma_{Bx}}{\sigma_{By}} \right)_{\text{design}} = 3.93$$

- Parameter List (Sam Heifets)
- Plots for one pass
- Kink Instability
- Long Term Behavior
- Beam-Beam Tune Shift Limit (w. and w/o matching)

(3) Linac-Ring Beam-Beam Effects

Simulation

of macroparticles in $\begin{Bmatrix} e^- \\ e^+ \end{Bmatrix}$ bunch = $\begin{cases} 360 \\ 1000 \end{cases}$

of slices in $\begin{Bmatrix} e^- \\ e^+ \end{Bmatrix}$ bunch = $\begin{cases} 9 \\ 45 \end{cases}$

macrosize $\frac{\sigma_{m,x,y}}{\sigma_{B,x,y}} = 0.5$

aspect ratio $R = \frac{\sigma_{mx}}{\sigma_{my}} = \left(\frac{\sigma_{Bx}}{\sigma_{By}} \right)_{\text{design}} = 3.93$

- Parameter List (Sam Heifets)
- Plots for one pass
- Kink Instability
- Long Term Behavior
- Beam-Beam Tune Shift Limit (w. and w/o matching)

(1) Parameter List (Sam Heifets)

B-Factory Parameter List by Heifets, et.al.

Linac	Storage Ring	Collision
$E_c = 3.5 \text{ GeV}$	$E_p = 8.0 \text{ GeV}$	$L = 10^{34} \text{ cm}^{-2} \text{ sec}^{-1}$
$N_e = 0.544 \times 10^9$	$N_p = 6.1 \times 10^{11}$	$D_{ey} = 273.7, D_{ex} = 69.6$
$I_{av} = 1.6 \text{ mA}$	$I_{av} = 1.94 \text{ A}$	$\xi = 0.06$
$f_{RF} = 1.5 \text{ GHz}$	$n_B = 30$	$f_c = 20 \text{ MHz}$
$l_z^c = 2.2 \text{ psec}$	$s_B = 15 \text{ m}$	$\beta_{ey}^* = \beta_{px}^* = 3.33 \text{ mm}$
$\epsilon_{ez} = 5.75 \text{ nm}, \epsilon_{ey} = 0.37 \text{ nm}$	$\epsilon_{px} = 5.75 \text{ nm}, \epsilon_{py} = 0.057 \text{ nm}$	$\beta_{py}^* = 21.55 \text{ mm}$
$P = 5.65 \text{ MW}$	$P = 15.1 \text{ MW}$	$\sigma_{e,x}^D = \sigma_{p,x}^* = 4.37 \mu\text{m}$
Power Loss = 2.0W/cav	$E' = 2.5 \text{ MeV/cavity}$	$\sigma_{e,y}^D = \sigma_{p,y}^* = 1.11 \mu\text{m}$
$f_c = 20 \text{ MHz}$	$n_{cav} = 50$	
	$C = 450 \text{ m}$	
	$R_p = 10$	
	$\alpha = 2.0 \times 10^{-3}$	
	$\sigma_\delta = 2.45 \times 10^{-3}$	
	$\sigma_x^p = 3.33 \text{ mm}$	
	$\left(\frac{L}{n}\right)_{tot} = 0.5 \text{ ohm}$	
	$\rho_{bend} = 45 \text{ m}$	
	$\tau_x = 0.9 \text{ msec}, \tau_y = 2.4 \text{ msec}$	
	$\tau_\delta = 6.9 \text{ msec}$	
	$L_{cell} = 5 \text{ m}$	
	$\beta_x = 9.8 \text{ m}, \beta_y = 1.4 \text{ m}$	
	$D_x = 0.255 \text{ m}$	

$$Q_s = 0.07$$

$$\text{Choose } Q_x = 0.64, Q_y = 0.54$$

$$\frac{\tau_x}{T_0} = 600, \frac{\tau_y}{T_0} = 1600, \frac{\tau_E}{T_0} = 4600$$

(2) Plots for One Pass

Beam Profile Before 1st pass

After 1st pass

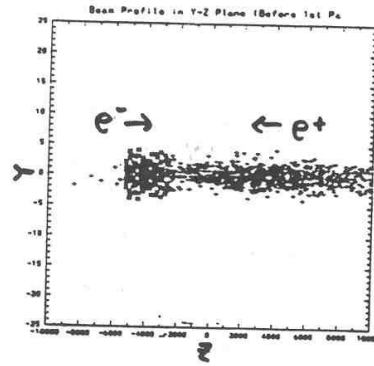


Figure 5: Initial beam profile in Y-Z plane

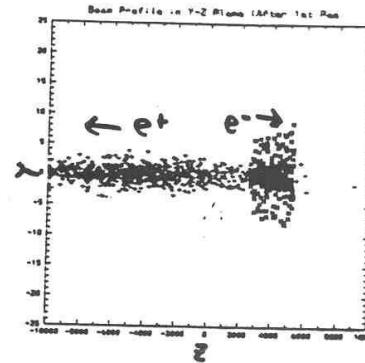


Figure 7: Beam profile in Y-Z plane after first collision

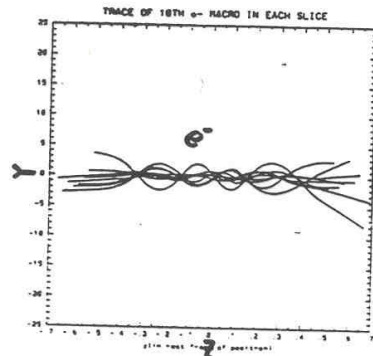


Figure 6: Trace of e^- particles in Y-Z plane in the rest frame of positron bunch

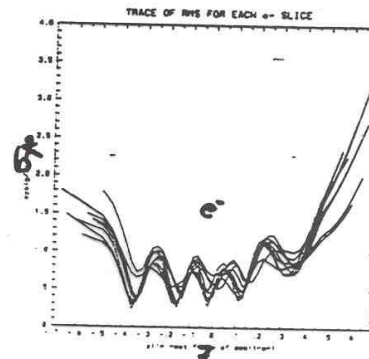


Figure 8: Trace of RMS for e^- slices in Y-Z plane in the rest frame of positron bunch

The deep modulation of e^- envelope could have strong impact on the stability of the positron bunch.

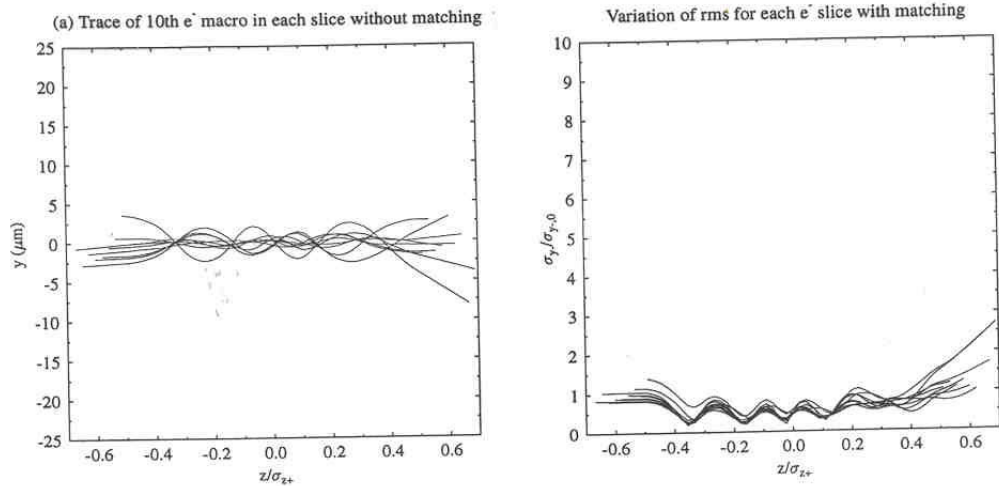


Figure 14: Trace of e⁻ macros (a) and variation of rms for e⁻ slices (b) in Y-Z plane in the rest frame of the e⁺ bunch *without* matching.

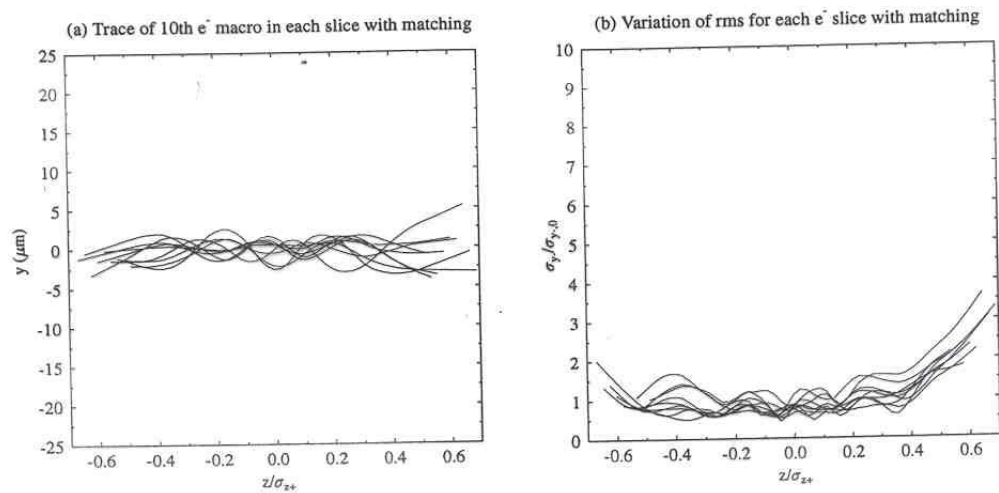
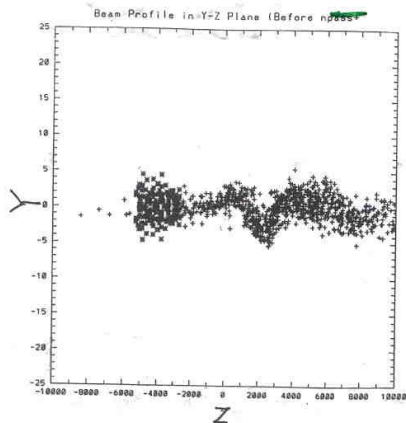


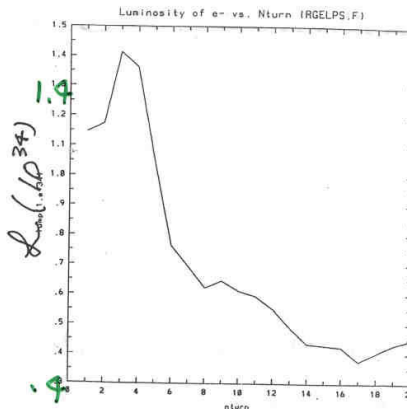
Figure 15: Trace of e⁻ macros (a) and variation of rms for e⁻ slices (b) in Y-Z plane in the rest frame of the e⁺ bunch *with* matching.

Kink Instability and Synchrotron Oscillation

Beam Profile after 20 turns

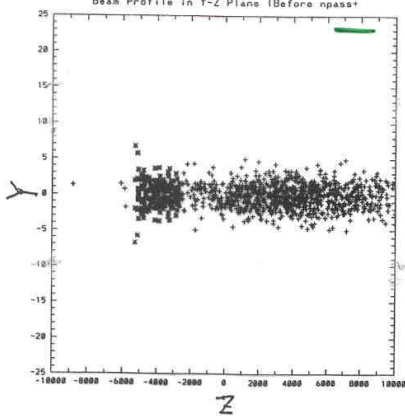


Luminosity vs. Nturn

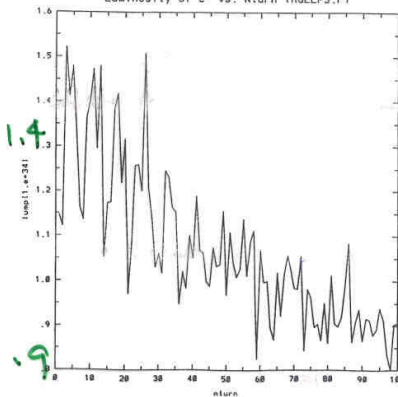


(a) beam-beam force + matrix. (random offset) 0 Nturn 20

Beam Profile after 100 turns



Luminosity v. N-turn.



(b) beam-beam force + matrix + syn. osci. (random offset). 0 100
($\gamma_s = 0.07$)

(3) Long Term Behavior

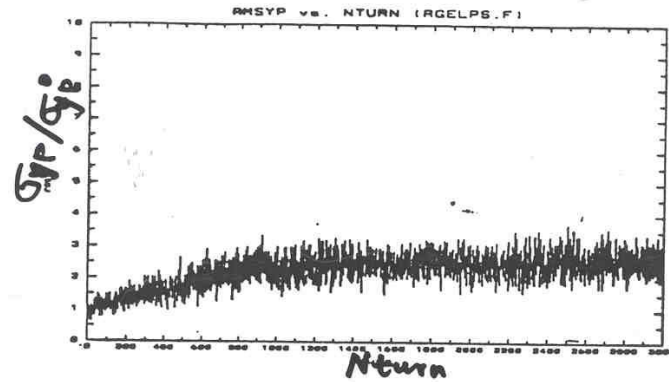


Figure 1: Positron beam blowup in 3000 turns

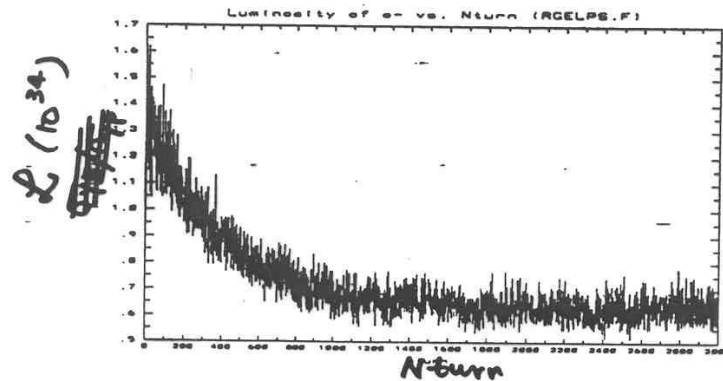
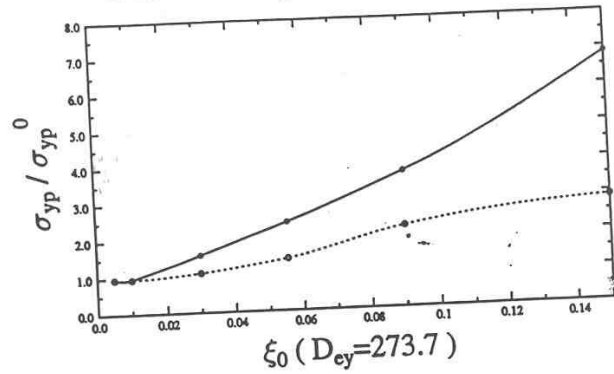


Figure 2: Luminosity in 3000 turns

Given (N_x, N_y) , can obtain an equilibrium set of $(\sigma_{x+}, \sigma_{y+}, L)$

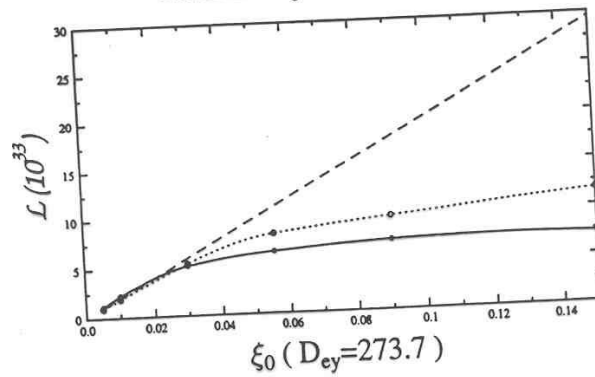
(4) Beam-Beam Tune Shift limit

Beam Blowup Factor vs. Tune Shift



— No matching
- - - With matching

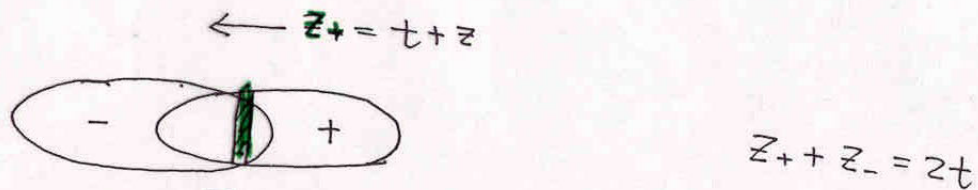
Luminosity vs. Tune Shift



$$(\nu_x, \nu_y) = (0.64, 0.54)$$

3. Analysis of Coherent Kink Instability

- Coherent growth of transverse displacement of e^+ beam
 - ribbon bunch model ($\sigma_x \gg \sigma_y$)
 - constant offset of the e^- beam for each collision
 - longitudinal uniform distribution



Coupled equations for vertical offsets of overlapping slices in e^-e^+ bunch

— Eq. of motion for \bar{y}_+ , \bar{y}_- ($c=1$)

$$\left\{ \begin{array}{l} \left(\frac{\partial}{\partial t} + \frac{\partial}{\partial z} \right)^2 \bar{y}_- = -k_-^2 [\bar{y}_- - \bar{y}_+] \\ \left(\frac{\partial}{\partial t} - \frac{\partial}{\partial z} \right)^2 \bar{y}_+ = -k_+^2 [\bar{y}_+ - \bar{y}_-] \end{array} \right. \quad \text{with} \quad \begin{array}{l} k_-^2 = a \frac{\lambda_+}{f_{y-}} \\ k_+^2 = a_+ \frac{\lambda_-}{f_{y+}} \end{array}$$

↑ using the linear part of beam-beam kick

Coupled Equation of Motion

(in comoving coordinates)

$$e^- \left\{ \begin{array}{l} \frac{d^2 \bar{y}_-(z_-, t)}{dt^2} + k_-^2 \bar{y}_-(z_-, t) = k_-^2 \bar{y}_+(z_+ = zt - z_-, t) \quad (c=1) \\ \frac{d^2 \bar{y}_-(z_-, t)}{dt^2} = 0 \end{array} \right.$$

$(0 < z_- < l_-)$ $\left(\frac{z_-}{2} \leq t \leq \frac{z_- + l_-}{2}\right)$

$\left(0 \leq t \leq \frac{z_-}{2} \text{ or } \frac{l_+ + z_-}{2} \leq t \leq \frac{l_+ + l_-}{2}\right)$

$$e^+ \left\{ \begin{array}{l} \frac{d^2 \bar{y}_+(z_+, t)}{dt^2} + k_+^2 \bar{y}_+(z_+, t) = k_+^2 \bar{y}_-(z_- = zt - z_+, t) \\ \frac{d^2 \bar{y}_+(z_+, t)}{dt^2} = 0 \end{array} \right.$$

$(0 < z_+ < l_+)$ $\left(\frac{z_+}{2} \leq t \leq \frac{z_+ + l_-}{2}\right)$

$\left(0 \leq t \leq \frac{z_+}{2} \text{ or } \frac{l_- + z_+}{2} \leq t \leq \frac{l_+ + l_-}{2}\right)$

Using Laplace transform



For $\tau_- = t - \frac{z_-}{2}$:

$$\begin{aligned} \bar{Y}_-(z_-, t = \tau_- + \frac{z_-}{2}) &= \bar{Y}_-(z_-, t = \frac{z_-}{2}) \overset{= y_0}{\cos k_- \tau_-} + \bar{Y}'_-(z_-, t = \frac{z_-}{2}) \overset{= 0}{\frac{\sin k_- \tau_-}{k_-}} \\ &+ k_- \int_0^{\tau_-} d\tau'_- \sin k_- (\tau_- - \tau'_-) \bar{Y}_+(z_+ = 2\tau'_-, t = \frac{z_-}{2} + \tau'_-) \end{aligned}$$

($0 \leq z_- \leq l_-$, $0 \leq \tau_- \leq \frac{l_-}{2}$)

For $\tau_+ = t - \frac{z_+}{2}$:

$$\begin{aligned} \bar{Y}_+(z_+, t = \tau_+ + \frac{z_+}{2}) &= \bar{Y}_+(z_+, t = \frac{z_+}{2}) \cos k_+ \tau_+ + \bar{Y}'_+(z_+, t = \frac{z_+}{2}) \frac{\sin k_+ \tau_+}{k_+} \\ &+ k_+ \int_0^{\tau_+} d\tau'_+ \sin k_+ (\tau_+ - \tau'_+) \bar{Y}_-(z_- = 2\tau'_+, t = \tau'_+ + \frac{z_+}{2}) \end{aligned}$$

($0 \leq z_+ \leq l_+$, $0 \leq \tau_+ \leq \frac{l_+}{2}$)

integral of kicks from e' slices

Integral Equation ($0 \leq z_+ \leq l_+$, $0 \leq \tau_+ \leq \frac{l_-}{z}$)

$$\bar{Y}_+(z_+, t = \tau_+ + \frac{z_+}{z}) = \bar{Y}_+^{(0)}(z_+, t = \tau_+ + \frac{z_+}{z}) + \int_0^{\tau_+} k_+ d\tau'_+ \sin k_+(\tau_+ - \tau'_+) \underbrace{\int_0^{z_+} \frac{k_-}{z} dz'_+ \sin \frac{k_-(z_+ - z'_+)}{z}}_{\sim \Lambda \bar{y}_+()} \bar{Y}_+(z'_+, t = \tau'_+ + \frac{z'_+}{z})$$

with initial conditions:

$$\bar{Y}_+^{(0)}(z_+, t = \tau_+ + \frac{z_+}{z}) = \bar{Y}_+(z_+, t = \frac{z_+}{z}) \cos k_+ \tau_+ + \bar{Y}'_+(z_+, t = \frac{z_+}{z}) \frac{\sin k_+ \tau_+}{k_+} + y_0 \cos \frac{k_- \tau_+}{z} (1 - \cos k_+ \tau_+)$$

- For $\Lambda = \left(\frac{k_+ l_-}{z}\right)^2 \frac{k_- l_+}{z} \ll 1$ (example: $\frac{k_+ l_-}{z} \approx 0.1$, $\frac{k_- l_+}{z} = 17$,)
 $\Lambda = 0.17$

\Rightarrow First order iteration

Multipass

$$X_N \approx \frac{\lambda N}{(1-\eta)(\eta-1)} M_2 (M^{(B)})^{N-2} [O(M^{(B)}A) \dots]$$

$$X_{n+1} = M^{(R)} [M^{(B)} X_n + A + \lambda O(X_n) + \lambda P(A)]$$

$$M^{(R)} = \begin{pmatrix} \cos 2\pi \nu_\beta & \beta^* \sin 2\pi \nu_\beta \\ -\frac{1}{\beta^*} \sin 2\pi \nu_\beta & \cos 2\pi \nu_\beta \end{pmatrix}$$

In the regime of initial linear growth,
for $X_0=0$, $M^{(R)}=I$.

$$\overline{Y}_+ (z_+, t_N) = -y_0 N \left(\frac{k+l_-}{4} \right) \left(\frac{k_+ z_+}{4} \right) \sin \frac{k+l_-}{2} \left(N - \frac{3}{2} \right) \sin \frac{k_+ z_+}{2}$$

— sinusoidal oscillation in both space and time

$$|\overline{Y}_+| \propto N \cdot z_+$$

Previous Observation in Simulation of Linac-Ring B factory

e^-	e^+	Collision
$E_e = 2 \text{ GeV}$	$E_p = 10 \text{ GeV}$	$L_0 = 5.42 \times 10^{34} \text{ cm}^{-2} \text{ sec}^{-1}$
$N_e = 0.5 \times 10^9$	$N_p = 10^{12}$	$D_{ey} = 90, D_{py} = 0.01$
$l_e = 500 \mu\text{m}$	$l_p = 500 \mu\text{m}$	$y_0 = y_{\text{offset}} = 0.1 \mu\text{m}$
$\sigma_{ey} = 0.3 \mu\text{m}$	$\sigma_{py} = 0.3 \mu\text{m}$	
$\sigma_{ex} = 3 \mu\text{m}$	$\sigma_{px} = 3 \mu\text{m}$	

Table 1: Parameter List in Simulation

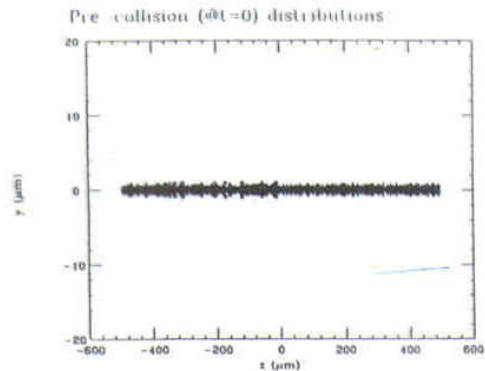


Figure 3: Pre-collision distribution in the simulation for the first collision, with $z < 0$ for the electron bunch and $z > 0$ for the positron bunch, modeled by 2000 macro-particles in 50 slices for each bunch. The offset is $y_0 = 0.1 \mu\text{m}$.

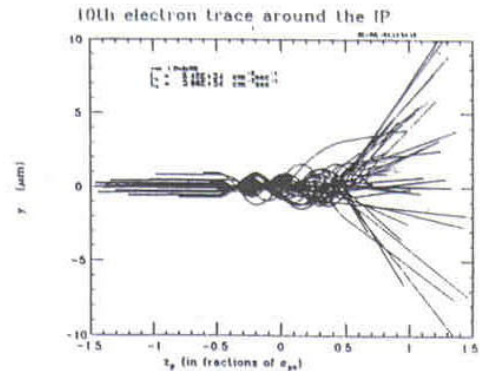


Figure 4: Trace of 10th macro-particle in each slice of the electron bunch, plotted in the rest frame of the positron bunch

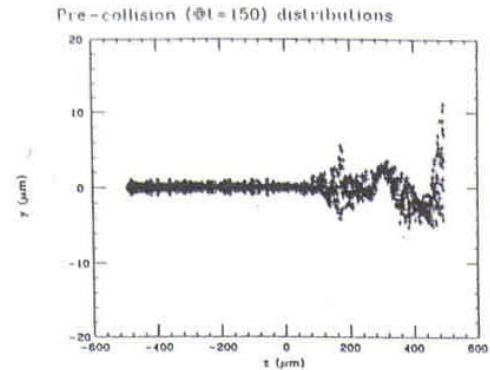


Figure 5: Pre-collision distribution in the simulation for 150th collision, with $z < 0$ for the electron bunch and $z > 0$ for the positron bunch. The offset is $y_0 = 0.1 \mu\text{m}$ for every collision.



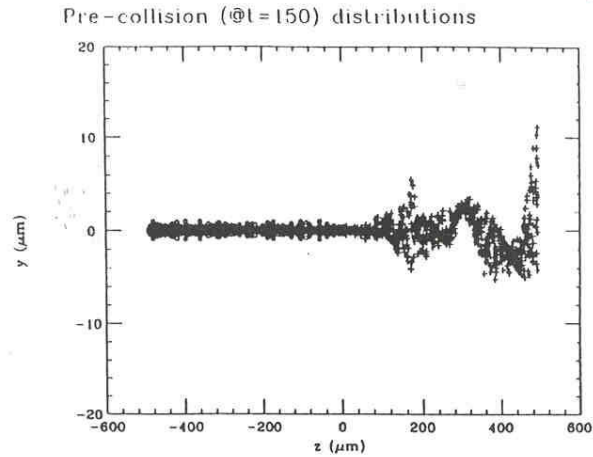


Figure 5: Pre-collision distribution in the simulation for 150th collision, with $z < 0$ for the electron bunch and $z > 0$ for the positron bunch. The offset is $y_0 = 0.1\mu\text{m}$ for every collision.

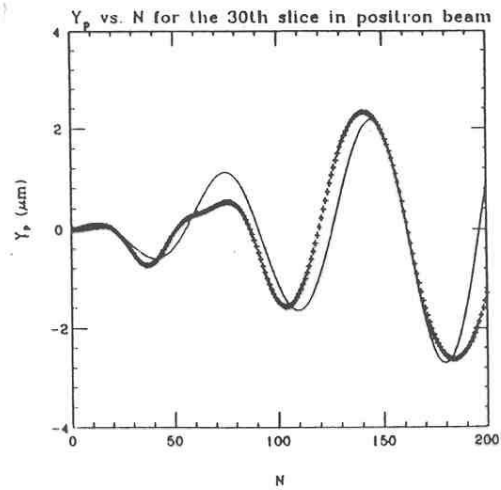


Figure 6: Comparison of analytical results (solid curve) with numerical results (dotted curve) for Y_p vs. collision number N with $z_p/l_p = 0.6$.

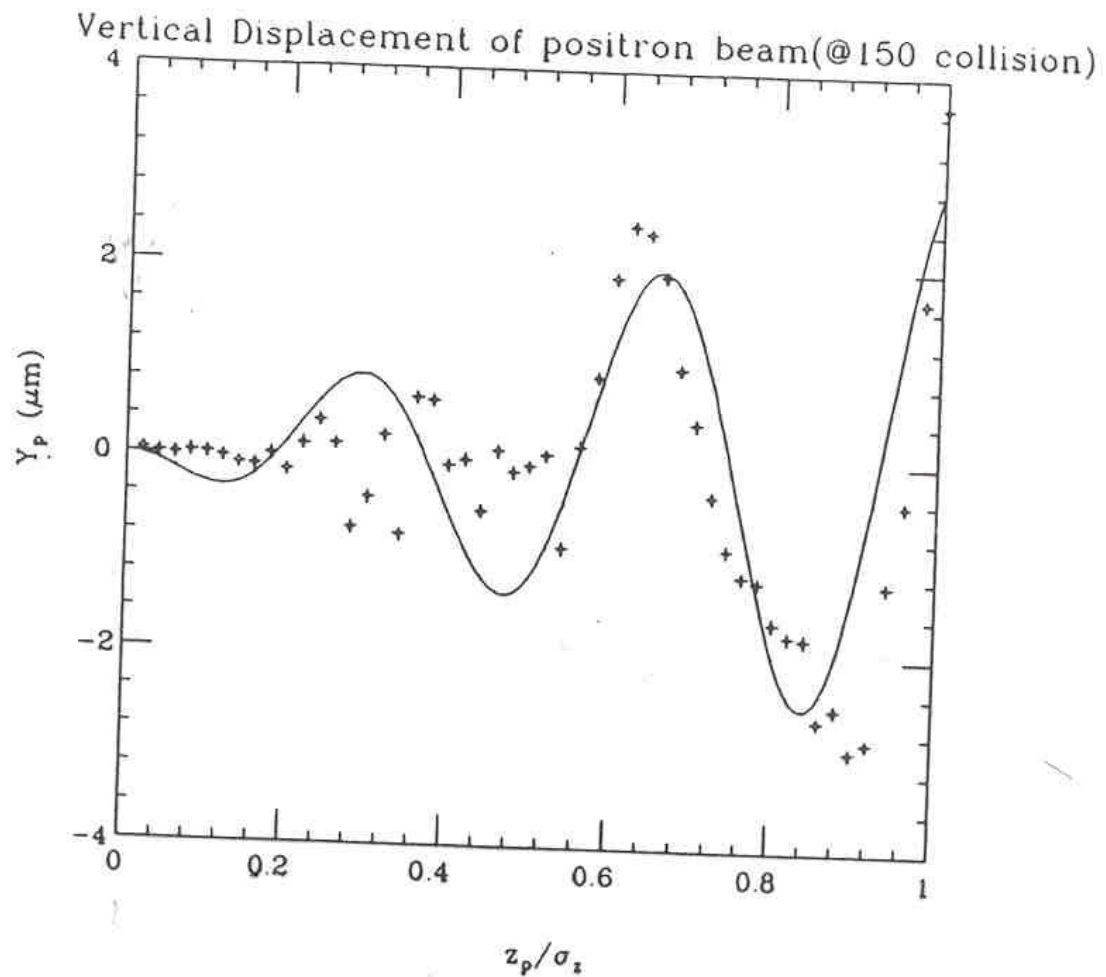


Figure 7: Comparison of analytical results (solid curve) with numerical results (dotted curve) for Y_p vs. the longitudinal distance z_p at the pre-collision state for $N = 150$.

Recent Design of Linac-Ring Electron-Ion Collider

AN ENERGY RECOVERY ELECTRON LINAC-ON-PROTON RING COLLIDER

L. Merminga, G. A. Krafft, Jefferson Lab, Newport News, VA 23606, USA
 V. A. Lebedev, FNAL, Batavia, IL 60510, USA



Figure 1. Schematic layout of the electron linac – proton ring collider.

Table 1: Parameter table for linac-ring scenarios

Parameter	Units	Design 1	Design 2
E_e	GeV	5	5
E_p	GeV	50	50
N_e	ppb	1.1×10^1 ₀	1.1×10^{10}
N_p	ppb	1.0×10^1 ₁	1.0×10^{11}
f_c	MHz	150	150
σ_e^*	μm	25	25
σ_p^*	μm	60	25
ϵ_e	nm	6	6
ϵ_p	nm	36	6.25
β_e^*	cm	10	10
β_p^*	cm	10	10
σ_z^p	cm	10	10
σ_z^e	mm	1	1
ξ_p	–	.004	.004
Δv_L	–	.004	.024
D_e	–	.78	4.6
I_e	A	.264	.264
I_p	A	2.4	2.4
L	$\text{cm}^2 \text{sec}^{-1}$	6.2×10^{32} ₂	2.1×10^{33}



4. Strong Head-Tail Instability in a Linac-Ring e-p Collider

Assumptions: Linear beam-beam force
very short e bunch

(betatron phase variation in IR is not yet included: $l_+ \ll \beta_{y+}^*$)

- Two Particle (or Slice) Model
- Vlasov Analysis



Two - Macroparticle Model

- Particle "1" of the proton beam with offset y_1 will kick the electron bunch centroid

$$\Delta y'_- = \frac{y_1}{4f_-}$$

$$\left(f_-^{-1} = \frac{2N_+ r_e}{\gamma_- \sigma_{y+} (\sigma_{x+} + \sigma_{y+})} \right)$$

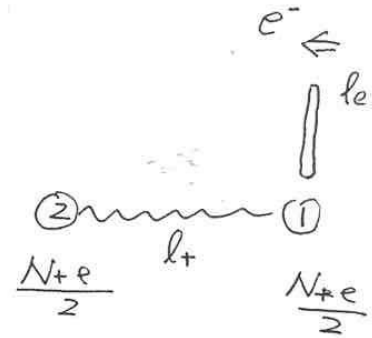
- Particle "2" at l_+ behind "1" sees e^- bunch offset

$$\Delta y_- = \Delta y'_- \cdot l_+$$

- The e^- bunch then kick "2" by

$$\Delta y'_2 = \frac{\Delta y_- - y_2}{2f_+}$$

$$\left(f_+^{-1} = \frac{2N_- r_e}{\gamma_+ \sigma_{y-} (\sigma_{x-} + \sigma_{y-})} \right)$$



For $k_+^2 = \frac{1}{2f+c} \ll k_\beta^2$, $\alpha^2 = \frac{l_+}{8f+f-c} \propto D_{-3+}$

$$\begin{cases} Y_1'' + k_\beta^2 Y_1 = 0 \\ Y_2'' + k_\beta^2 Y_2 = \alpha^2 Y_1 \end{cases}$$

Let $\tilde{Y}_{1,2} = Y_{1,2} + i \frac{1}{k_\beta} Y'_{1,2}$, $\Gamma = \frac{\pi \alpha^2}{2k_\beta k_s}$

$$\begin{bmatrix} \tilde{Y}_1 \\ \tilde{Y}_2 \end{bmatrix}_{s=\frac{c}{2}} = e^{-i \frac{k_\beta c_s}{2}} \begin{bmatrix} 1 & 0 \\ i\Gamma & 0 \end{bmatrix} \begin{bmatrix} \tilde{Y}_1 \\ \tilde{Y}_2 \end{bmatrix}_{s=0}$$

After $s = \frac{c_s}{2}$, "1" and "2" switch role,

$$\begin{bmatrix} \tilde{Y}_1 \\ \tilde{Y}_2 \end{bmatrix}_{s=c_s} = \underbrace{e^{-\frac{i k_\beta c_s}{2}} \begin{bmatrix} 1 & i\Gamma \\ 0 & 1 \end{bmatrix} e^{-\frac{i k_\beta c_s}{2}} \begin{bmatrix} 1 & 0 \\ i\Gamma & 1 \end{bmatrix}}_M \begin{bmatrix} \tilde{Y}_1 \\ \tilde{Y}_2 \end{bmatrix}$$

Stability Criteria:

$$|M - \lambda I| = 0, \quad |\lambda| \leq 1$$

$$\Rightarrow \Gamma \leq 2, \quad \text{or} \quad \frac{D \cdot \zeta_+}{\nu_s} \leq \frac{16}{\pi} \left(\frac{\sigma_{z+}}{l_+} \right)$$

(choice of l_+ is somewhat arbitrary).

• Example:

$$\zeta_+ = 0.004, \quad \nu_s = 3 \times 10^{-4}, \quad D = 0.78, \quad \frac{\zeta_+ D}{\nu_s} = 10$$

$$D = 4.6, \quad \frac{\zeta_+ D}{\nu_s} = 61$$

Two Particle Model vs. Vlasov Analysis

Two Particle Model:

- Gives clear picture of the interaction mechanism and cause of instability
- Overlooked the behavior of beam-beam kick from electron slice on the ion bunch along the ion bunch length
- Simplified the localized beam-beam kick as distributed interaction

Vlasov Analysis:

- Consider dynamics of vertical dipole moments of a ribbon ion bunch in a storage ring colliding with a ribbon electron bunch from linac
- Hourglass effect on synchrotron coupling is not included $l_+ \ll \beta_{y+}^*$
- Electron bunch is described by delta-like slice $l_- \ll l_+$
- Uniform longitudinal charge distribution $\lambda_{z+} = 1/l_+$



Dynamics of the Stored Ion Beam

- Equation of motion for an ion particle: ($k_\beta = \omega_\beta / c, k_s = \omega_s / c, C$: circumference of the ring)

$$\left\{ \begin{array}{l} \frac{dy}{ds} = u_y \\ \frac{du_y}{ds} + k_\beta^2 y = - \underbrace{\frac{y - \bar{y}_-}{f_+} \sum_{n=0}^{\infty} \delta(s - z/2 + nC)}_{\frac{F_y(z,s)}{E}} \end{array} \right. \quad \left\{ \begin{array}{l} \frac{dz}{ds} = -\eta \delta \\ \frac{d\delta}{ds} = k_s^2 z / \eta \end{array} \right.$$

- Vlasov equation for the distribution function $g(y, u_y, z, \delta, s)$

$$\frac{\partial g}{\partial s} + u_y \frac{\partial g}{\partial y} + \frac{F_y(z,s)}{E} \frac{\partial g}{\partial u_y} + (-\eta \delta) \frac{\partial g}{\partial z} + \frac{k_s^2 z}{\eta} \frac{\partial g}{\partial \delta} = 0$$

- Using action-angle transformation, we have for $f(q, \theta, r, \varphi, s)$

$$\left\{ \begin{array}{l} y = q \cos \theta \\ u_y = -k_\beta q \sin \theta \end{array} \right. \quad \left\{ \begin{array}{l} z = r \cos \varphi \\ \frac{\eta \delta}{k_s} = r \sin \varphi \end{array} \right.$$

$$\frac{\partial f}{\partial s} + k_\beta \frac{\partial f}{\partial \theta} + k_s \frac{\partial f}{\partial \varphi} + \frac{F_y(z,s)}{E} \frac{\partial f}{\partial u_y} = 0$$



Analysis of Dipole Motion Using Linearized Vlasov Equation

- Linear beam-beam interaction force
- Neglecting hourglass effect

- Using action-angle transformation, we have for $f(q, \theta, r, \varphi, s) = f_0(q)g_0(r) + f_1(q, \theta, r, \varphi, s)$

$$\begin{cases} y = q \cos \theta \\ u_y = -k_\beta q \sin \theta \end{cases} \quad \begin{cases} z = r \cos \varphi \\ \frac{\eta \delta}{k_s} = r \sin \varphi \end{cases} \quad \begin{aligned} f_1(q, \theta, r, \varphi, s) &= -\frac{\partial f_0}{\partial q} [e^{i\theta} g_+(r, \varphi, s) + e^{-i\theta} g_-(r, \varphi, s)] \\ g_\pm(r, \varphi, s) &= \sum_{l=-\infty}^{\infty} R_l^\pm(r, s) e^{il\varphi} \end{aligned}$$

$$\frac{\partial f_1}{\partial s} + k_\beta \frac{\partial f_1}{\partial \theta} + k_s \frac{\partial f_1}{\partial \varphi} + \frac{F_y(z, s)}{E} g_0(r) \frac{\partial f_0}{\partial u_y} = 0$$

- Analogy to the **broad band transverse wake function and impedance**

$$\frac{F_y(z, s)}{E} = -\sum_{n=0}^{\infty} \delta(s - \frac{z}{2} - nC) \frac{y_+ - \bar{y}_-(z, s)}{f_+}, \quad \bar{y}_-(z, s = \frac{z}{2} + nC) = \frac{k_-}{2} \int_{-\infty}^{\infty} dz' W^\perp(z - z') \bar{y}_+(z', s' = nC),$$

$$W^\perp(z) = \sin \frac{k_- z}{2} H(z), \quad \begin{cases} \text{Re} Z^\perp = \frac{\pi}{2} \left[\delta(\omega - \frac{k_- c}{2}) - \delta(\omega + \frac{k_- c}{2}) \right] \\ \text{Im} Z^\perp = \frac{k_- c}{4\omega} \left[\frac{1}{\omega - \frac{k_- c}{2}} + \frac{1}{\omega + \frac{k_- c}{2}} \right] \end{cases}$$



Equation for Single Collision

- Expansion in terms of modes for a **uniform bunch distribution**

$$R_l^\pm(r, s) = W_0(r) \sum_{M=0}^{\infty} a_{lm}^\pm(s) h_m^{|l|}(r)$$

$$h_m^{|l|}(r) = \sqrt{4\pi \frac{(|l|+2m+1/2)m!\Gamma(|l|+m+1/2)}{(|l|+k)!\Gamma(m+1/2)}} \left(\frac{r}{\hat{z}}\right)^{|l|} P_m^{(|l|, -1/2)}\left(1 - \frac{r^2}{2\hat{z}^2}\right)$$

- Equation for a_{lm}^\pm before and after a single collision:

$$\begin{cases} a_{lm}^{(+)} - a_{lm0}^{(+)} = \sum_{l', m'} M_{lm, l'm'} a_{lm}^{(+)} - a_{lm0}^{(+)} \\ a_{lm}^{(-)} - a_{lm0}^{(-)} = -\sum_{l', m'} M_{lm, l'm'} a_{lm}^{(+)} - a_{lm0}^{(+)} \end{cases}$$

- Coupling matrix

$$M_{lm, l'm'} = \underbrace{i^{l-l'} [\text{sign}(l)]^l [\text{sign}(l')]^{l'}}_{c_{l,l'}} \int_{-\infty}^{\infty} dk [Z^\perp(k)c] g_{|l|m}(k) g_{|l'|m'}(k),$$

$$g_{|l|m}(k) = \sqrt{\frac{(|l|+2m+1)\Gamma(m+1/2)\Gamma(|l|+m+1/2)}{2\pi m!(|l|+m)!}} \frac{J_{|l|+2m+1/2}(k\hat{z})}{\sqrt{k\hat{z}}}$$



Stability Analysis

- Equation for a beam-beam interaction and ring transport

$$\begin{pmatrix} a_{lm}^{(+)} \\ \vdots \\ a_{lm}^{(-)} \\ \vdots \end{pmatrix}_{n+1} = \underbrace{\begin{pmatrix} e^{-i\mu\beta} & & & \\ & \ddots & 0 & \\ & & 0 & e^{i\mu\beta} \\ & & & \ddots \end{pmatrix} \begin{pmatrix} e^{i\mu_s} & & & \\ & \ddots & 0 & \\ & & 0 & e^{i\mu_s} \\ & & & \ddots \end{pmatrix} \begin{pmatrix} I+M & M \\ -M & I-M \end{pmatrix}}_{\Xi} \begin{pmatrix} a_{lm}^{(+)} \\ \vdots \\ a_{lm}^{(-)} \\ \vdots \end{pmatrix}_n$$

- Expression for coupling matrix M

$$M_{lm,l'm'} = c_{l,l'} \pi \xi_+ \chi \left[c_{\text{odd}} J_\mu(\chi) J_{\mu'}(\chi) + i c_{\text{even}} \left(\frac{(-)^{(\mu-\mu')/2}}{\sin \frac{(\mu+\mu')\pi}{2}} J_{\max(\mu,\mu')}(\chi) J_{-\min(\mu,\mu')}(\chi) - \frac{4}{\pi^2} \frac{\sin \frac{(\mu-\mu')\pi}{2}}{\mu^2 - \mu'^2} \right) \right]$$

with $\mu = |l| + 2m + 1/2, \mu' = |l'| + 2m' + 1/2,$

$$c_{\text{odd}} = (1 + (-)^{|l|+|l'|+1})/2, \quad c_{\text{even}} = (1 + (-)^{|l|+|l'|})/2$$

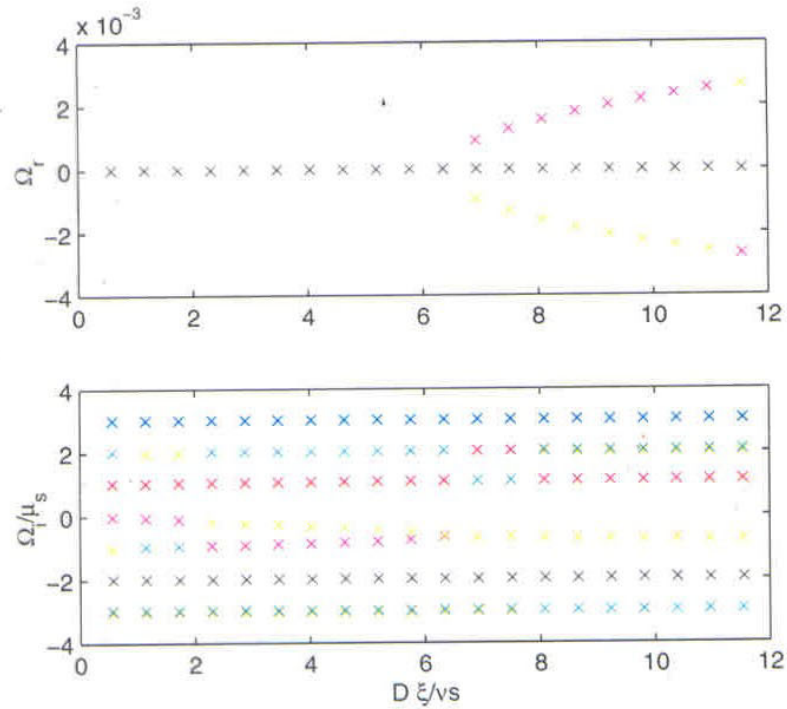
- Stability requires:

$$|\Xi - \lambda I| = 0, \quad \lambda = e^{\Omega_r + i\Omega_i}, \quad \Omega_r \leq 0$$

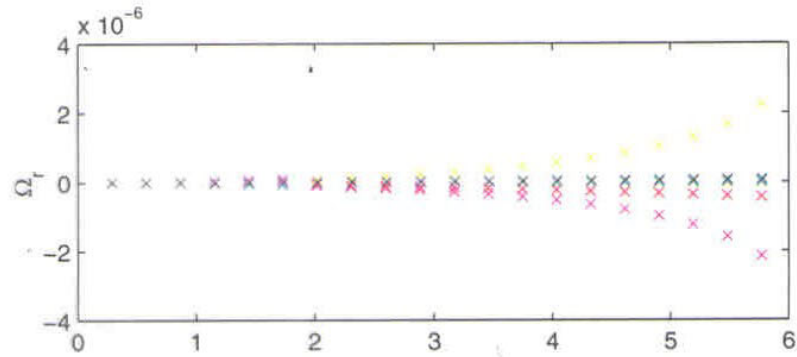


Transverse Mode Coupling

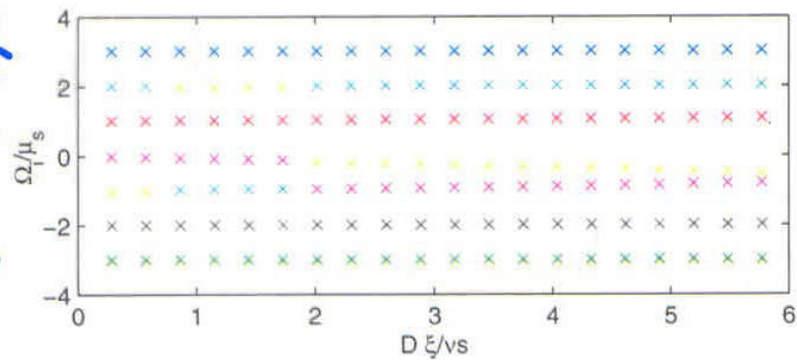
Ω_r and Ω_i/μ_s vs. $D_- \xi_+/\nu_s$ by varying ξ_+ for $\bar{D}_- = 4$ and $\nu_s = 0.001$



Small Growth Rate in the “Stable” Region

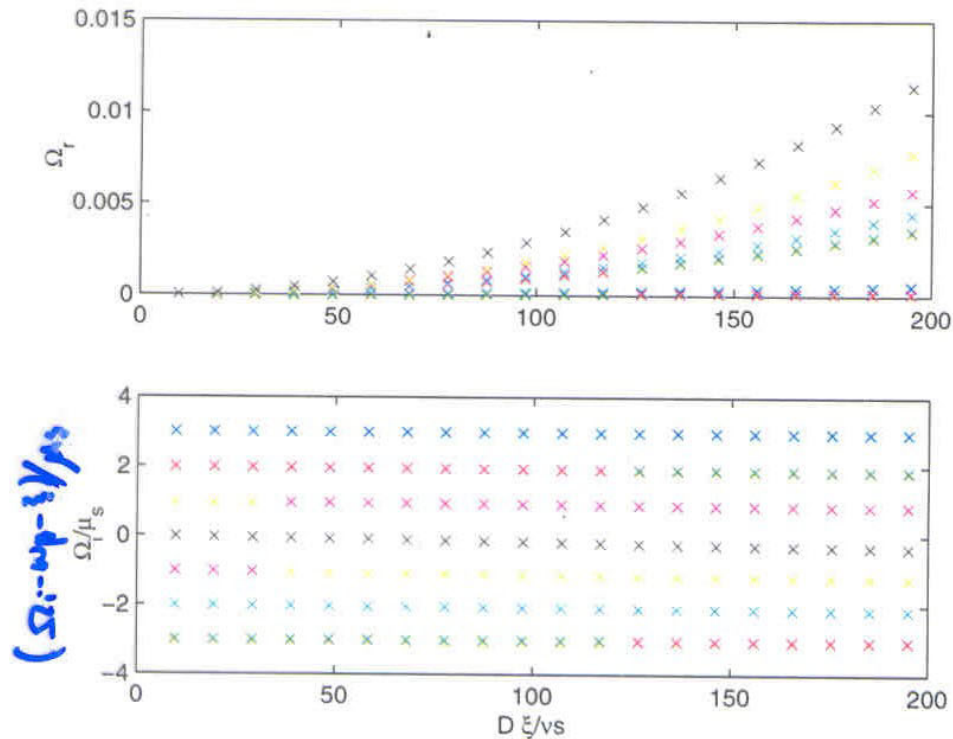


$(\Omega_r - \omega_p) / \mu_s$



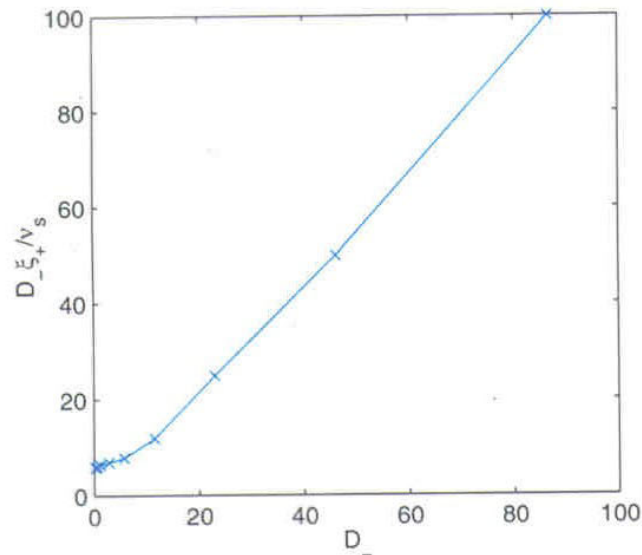
Growth Rate for Highly Disruption Case

Mode growth for ξ_+ from 0 to 0.05 while fixing $D_- = 273$ and $\nu_s = 0.07$, which are parameters used in our earlier study of linac - ring B factory



Threshold vs. Disruption

- For higher disruption, the electron-oscillate through the ion bunch, the kink instability threshold depends weaker on the disruption parameter.



Conclusion

- A Strong-strong beam-beam simulation was earlier developed to study beam-beam effects in a linac-ring B factory, and is recently modified to study beam-beam effects in a linac-ring EIC.
- Both simulation and analysis showed kink instability with bunch length effect for a linac-ring collider. Analysis was based on linear beam-beam force approximation.
- Head-tail effect due to betatron phase change in the IR for linac-ring beam-beam was studied by Perevedentsev [PRST 4, 024403 (2001)] and later by Yunn [Jlab-TN-01-017], which is not yet included in the present Vlasov analysis.
- For the head-tail and strong head-tail instability analysis, we need to include effects of full nonlinearity of beam-beam interaction, and compare with simulation.



Electrons are not protons:
electron polarisation in rings, decoherence and spin matching

•
D.P. Barber

•
Deutsches Elektronen-Synchrotron (DESY)

Hamburg Germany

26 February 2002

Abstract

Although depolarisation in proton and electron beams in storage rings and ring accelerators is rooted in the spin-orbit coupling embodied in the Thomas-BMT equation, the details of the depolarisation mechanisms are very different. In particular the polarisation of a high energy proton beam depends on its history whereas the polarisation of a high energy electron beam can depend strongly on the depolarising effects of synchrotron radiation. In both cases the spin distributions are most efficiently described in terms of the invariant spin field. The invariant spin field also provides the best framework for quantifying the differences. A good example of the differences is provided by the use of a Siberian Snake in an electron storage ring.

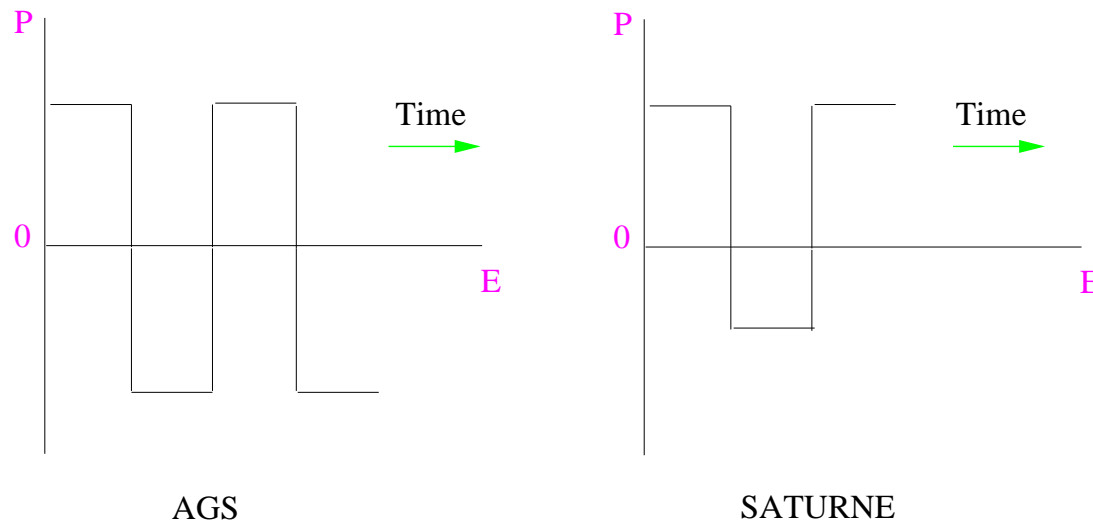
Snakes are essential for preserving proton spin polarisation during acceleration to high energy and can help to stabilize spin motion at the top energy. But snakes can be inappropriate for stored high energy electron beams which are self-polarised via the Sokolov-Ternov effect or prepolarised before injection at the full energy. For example, snakes can, in effect, “switch off” the Sokolov-Ternov effect and at high energy a single snake, installed to constrain the equilibrium polarisation direction (\vec{n}_0) to the machine plane can lead to a prohibitive increase in radiative depolarisation. The latter point will be demonstrated with a simple, exactly solvable model of spin decoherence and the result will be compared with that from the standard Derbenev-Kondratenko-Mane (DKM) calculation based on an exact expression for the invariant spin field. The model is a useful pedagogical tool for demonstrating the meaning and limitations of the DKM approach and for demonstrating the danger of horizontal \vec{n}_0 .

Depolarisation of electrons by synchrotron radiation increases strongly with energy and can be especially strong if the ring is misaligned or has spin rotators to provide longitudinal polarisation at interaction points. But the depolarisation can be reduced by “linear spin matching”, i.e. by a careful choice of the optics in sections of the ring. Spin matching is conveniently carried out in terms of the 8×8 spin-orbit transfer matrices of the SLIM formalism. This approach emphasizes the locality of the required “spin transparency”, is convenient for diagnosis and allows computer algebra to be used.

The central differences:

- Proton depolarisation during acceleration by resonance crossing: memory, deterministic, “reversible”.

Proton spin INFORMATION preservation during resonance crossing.



The final polarisation depends on the history.

- Electron depolarisation by synchrotron radiation “noise”, irreversible, short memory, independence of history.

Stationary spin-orbit states in rings

- We don't discuss particle dynamics by sitting on the closed orbit.
- We also shouldn't discuss spin dynamics by sitting on the closed orbit — we must get out into phase space.

And understand STATIONARY SPIN-ORBIT STATES:

====> “Invariant spin field”.

- Essential for understanding/calculating high order e^\pm depolarisation.

And indispensable for understanding proton spin dynamics at very high energy (e.g. HERA at 800 GeV).

Can then compare the two phenomenologies very easily.

- ====> Maximum attainable polarisation
- ====> Starting point for perturbation theory — if needed, e.g. noise, non-linear fields, beam-beam....

Invariant fields: phase space Protons

- Canonical particle coordinates: $\vec{u} \equiv (x, p_x, y, p_y, z, p_z)$ Indep. var. = azimuth, s

- For electrons at high energy: $\vec{u} \equiv (x, p_x, y, p_y, \sigma, \eta = \delta E/E_0)$

- Phase space density, $\rho(\vec{u}; s)$: Liouville: ρ constant along particle orbits =====>

$$\frac{\partial \rho}{\partial s} = \{H_{orb}, \rho\}$$

- Stationarity: $\rho(\vec{u}; s) = \rho(\vec{u}; s + C)$
i.e. 1-turn periodicity of the (statistical) **scalar FIELD** $\rho(\vec{u}; s)$

although individual particles MOVE AROUND IN PHASE SPACE.

Spin motion in electric and magnetic fields:

The T-BMT spin precession equation:

$$\frac{d\vec{S}}{ds} = \vec{\Omega} \times \vec{S}$$

\vec{S} : spin expectation value

$\vec{\Omega}$: depends on $\vec{B}, \vec{E}, \vec{\beta}, \gamma$

In transverse magnetic fields:

$$\Omega \propto (a + 1/\gamma) \cdot B$$

$a = (g - 2)/2$ where g is the relevant g factor.

$a = 1.793\dots$ for protons.

$a = -0.143$ for deuterons.

($a = 0.00115\dots$ for electrons.)

Invariant fields: spin

How can a proton beam be fully polarised but the polarimeter gives ZERO?

Invariant fields: spin Protons

- Local spin polarisation $\vec{P}(\vec{u}; s)$: T-BMT. \implies PARTIAL differential equation:

$$\frac{\partial \vec{P}}{\partial s} = \{H_{orb}, \vec{P}\} + \vec{\Omega}(\vec{u}; s) \times \vec{P}$$

- Stationarity: $\vec{P}(\vec{u}; s) = \vec{P}(\vec{u}; s + C)$
i.e. 1-turn periodicity of the (statistical) **vector FIELD** $\vec{P}(\vec{u}; s)$
although individual particles MOVE AROUND IN PHASE SPACE AND THEIR SPINS MOVE TOO.

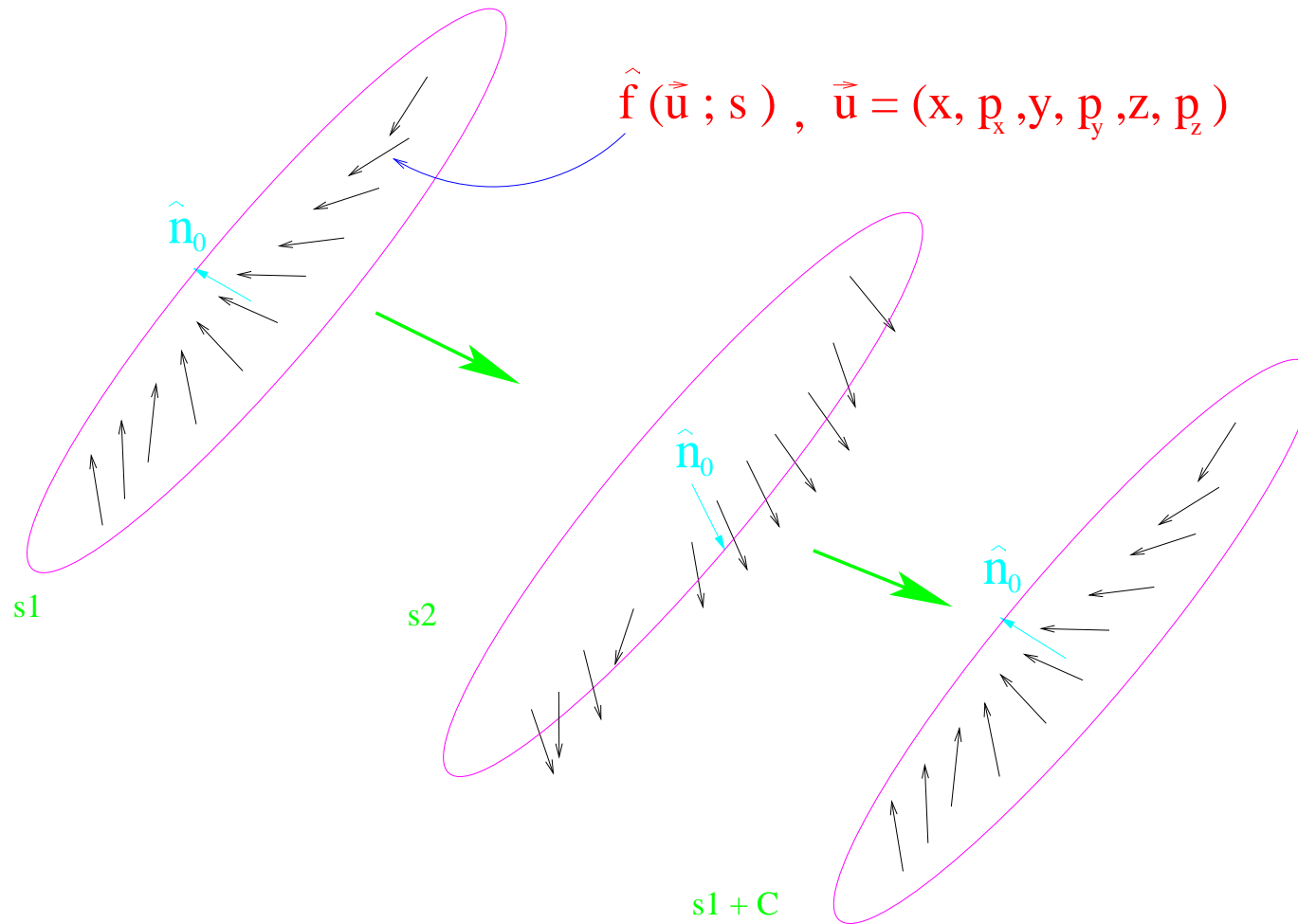
- $|\vec{P}|$ is constant along orbits: $\implies \hat{n}(\vec{u}; s) = \vec{P}/|\vec{P}|$

$$\frac{\partial \hat{n}}{\partial s} = \{H_{orb}, \hat{n}\} + \vec{\Omega}(\vec{u}; s) \times \hat{n}$$

- Stationarity: $\hat{n}(\vec{u}; s) = \hat{n}(\vec{u}; s + C) \implies \hat{n}$ is called the **INVARIANT SPIN FIELD**.
- Non-trivial** T-BMT solution satisfying CONSTRAINTS.
- Solutions obeying these constraints are unstable (illdefined) at spin-orbit resonances.

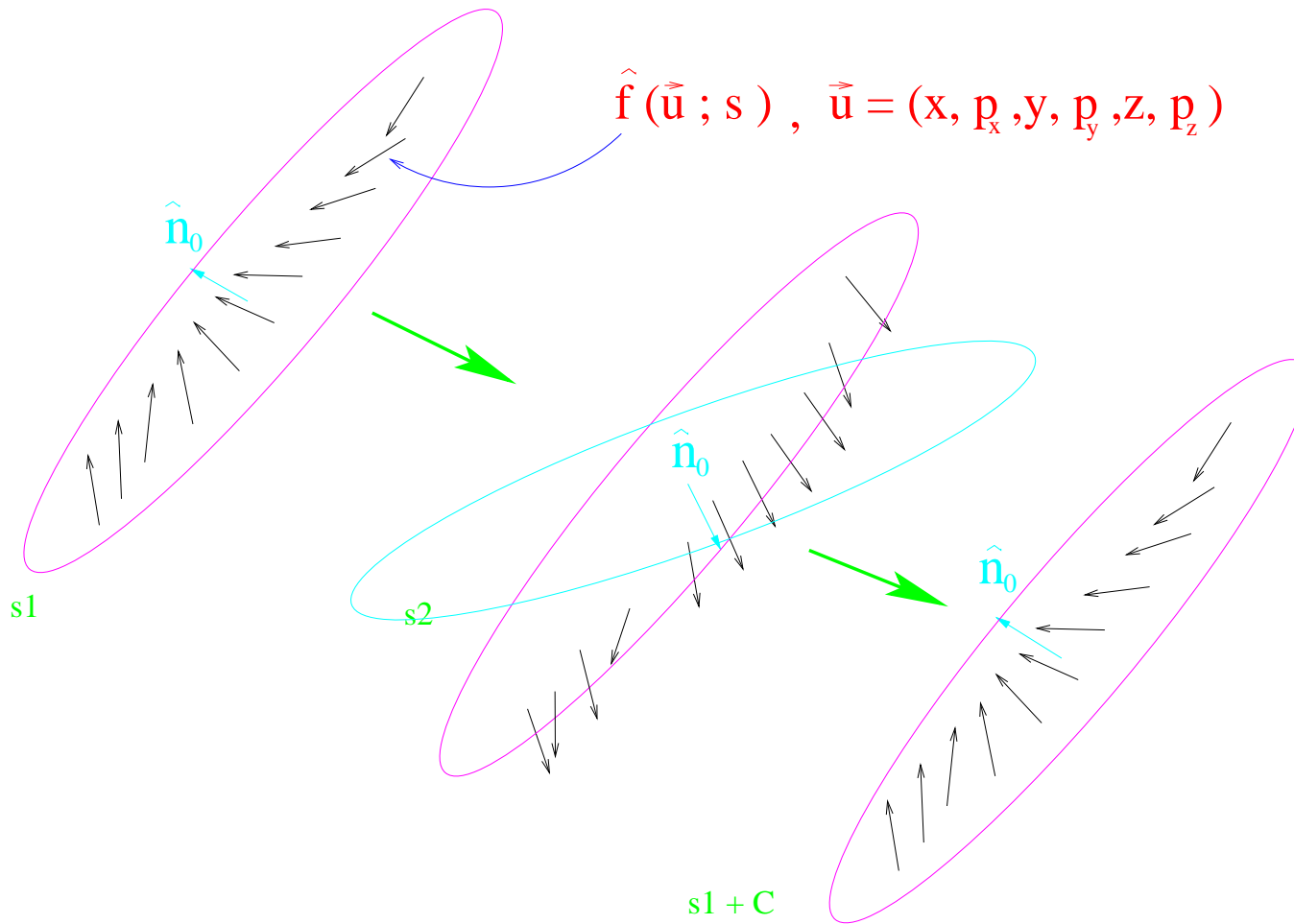
The invariant spin field (n-axis, Derbenev–Kondratenko vector)

A pre-established s-periodic unit vector field at each phase space point



The invariant spin field (n-axis, Derbenev-Kondratenko vector)

A pre-established s-periodic unit vector field at each phase space point



The Invariant Spin Field, \hat{n}

- $\vec{n}(M(\vec{u}; s); s) = R_{3 \times 3}(\vec{u}; s) \vec{n}(\vec{u}; s)$

This is NOT the eigenproblem $\vec{N}(\vec{u}; s) = R_{3 \times 3}(\vec{u}; s) \vec{N}(\vec{u}; s)$

\hat{n} is NOT a “closed spin solution”!!!

Instead, the field seen **AS A WHOLE** is invariant.

- On the closed orbit $\hat{n}(\vec{u}; s) \longrightarrow \hat{n}(\vec{0}; s) \equiv \hat{n}_0(s)$.
- $\implies \hat{n}$ and $\hat{n}_0(s)$ should not be confused!!!
- The invariant spin field for 1 plane of orbit motion is a smooth closed vector curve.
- For 3 planes of orbit motion \hat{n} is on a smooth surface but is not closed.

The invariant spin field (ISF):

defines one axis of a local orthonormal coordinate system
at each point in phase space and azimuth for describing spin motion

— **Pre-established** at each s, \vec{u}, γ_0 independently of the presence of particles or spins.

**For protons: the invariant spin field
defines the maximum attainable equilibrium polarisation.**

$$\vec{P}_{eq}(\vec{J}, \vec{\phi}; s) = P(\vec{J}) \hat{n}(\vec{J}, \vec{\phi}; s)$$

$$|\vec{P}_{meas}(s)| = |\langle P(\vec{J}) \hat{n}(\vec{J}, \vec{\phi}; s) \rangle_s| \leq |\langle \hat{n}(\vec{J}, \vec{\phi}; s) \rangle_s|$$

Over one turn, the particles of an equilibrium phase space distribution replace each other, and spins set parallel to the local \hat{n} 's replace each other too.

Even if the spin field is very complicated: once in equilibrium, stay in equilibrium — but small \vec{P}_{meas} .

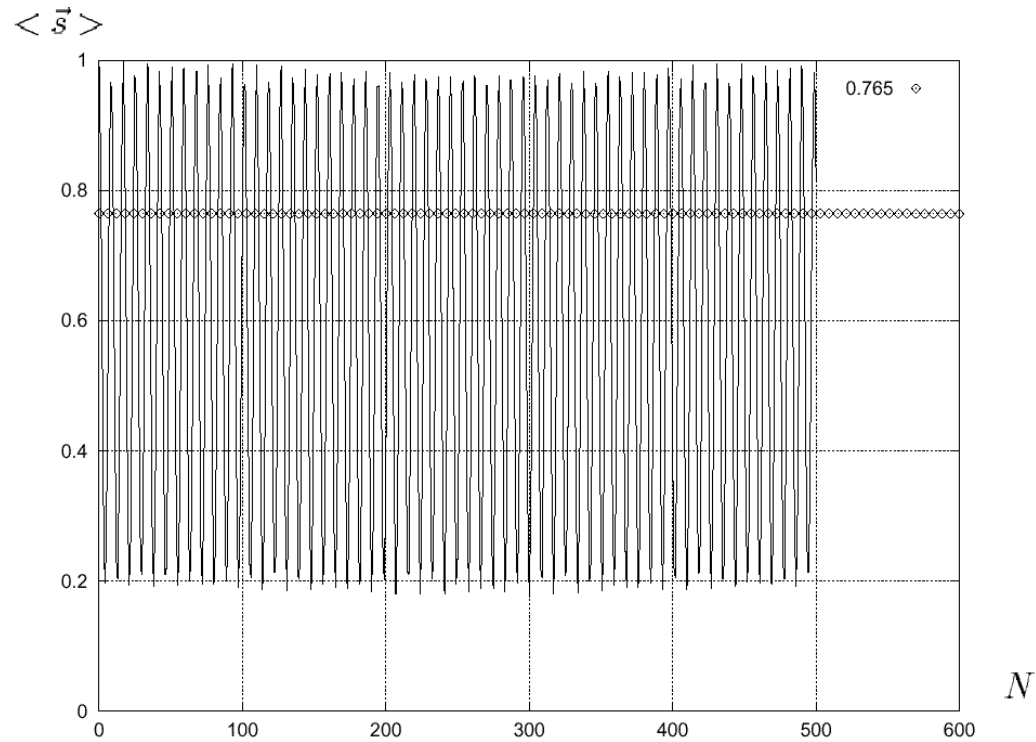


Figure 1: HERA protons at about 800 GeV: propagation of a beam that is initially completely polarised parallel to \vec{n}_0 leads to a fluctuating average polarisation. For another beam in which the spins are initially parallel to their local \vec{n} the average polarisation stays constant, in this case equal to 0.765.

The stable spin direction?

- The ISF gives the stable POLARISATION directionSSSSSSSSSSSS.
- \hat{n}_0 gives the stable spin direction on the closed orbit.
BUT THERE ARE NO PARTICLES ON THE CLOSED ORBIT!
- At very high energy
 $\langle \hat{n}(\vec{J}, \vec{\phi}; s) \rangle_s$ and $\langle P(\vec{J}) \hat{n}(\vec{J}, \vec{\phi}; s) \rangle_s$ need not be parallel to $\hat{n}_0(s)$

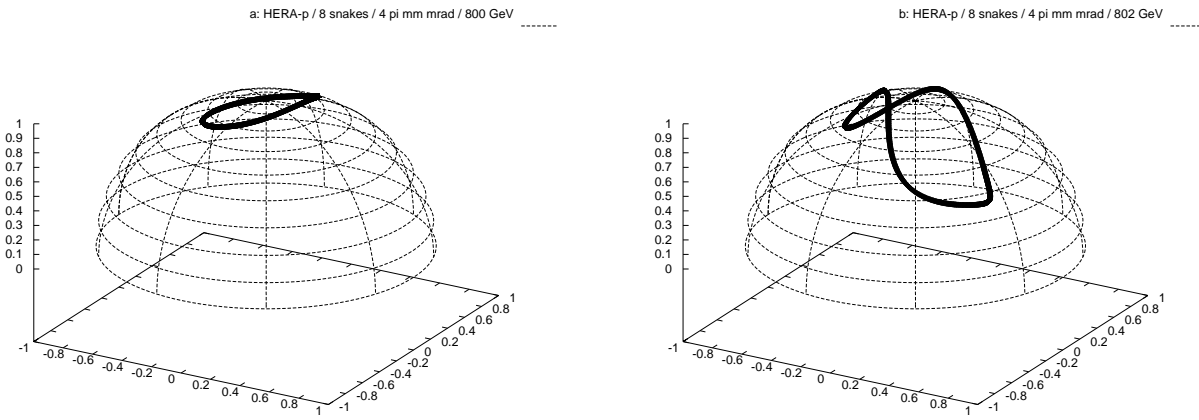


Figure 2: The \hat{n} -vector for the 4π mm mrad ellipse at 800 *GeV* (left) and 802 *GeV* (right).

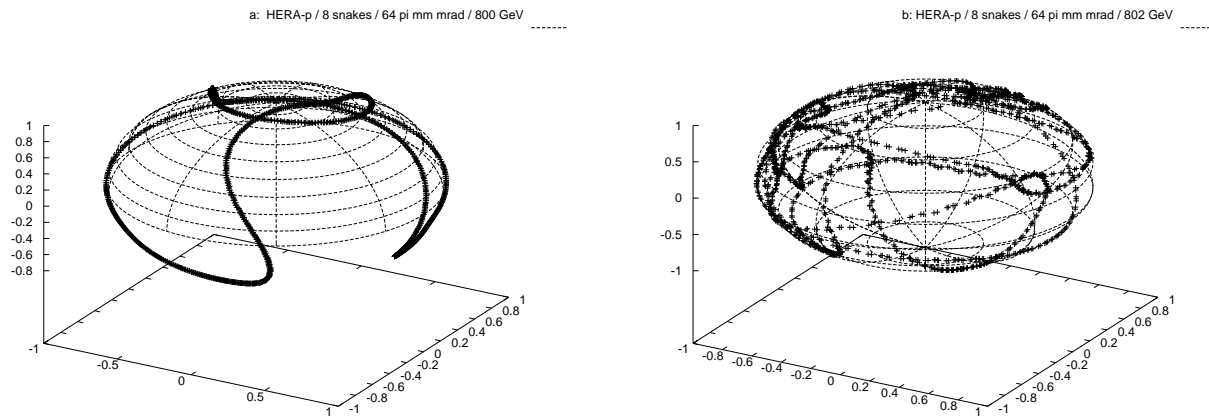


Figure 3: The \hat{n} -vector for the 64π mm mrad ellipse at 800 *GeV* (left) and 802 *GeV* (right).

The spin tune:

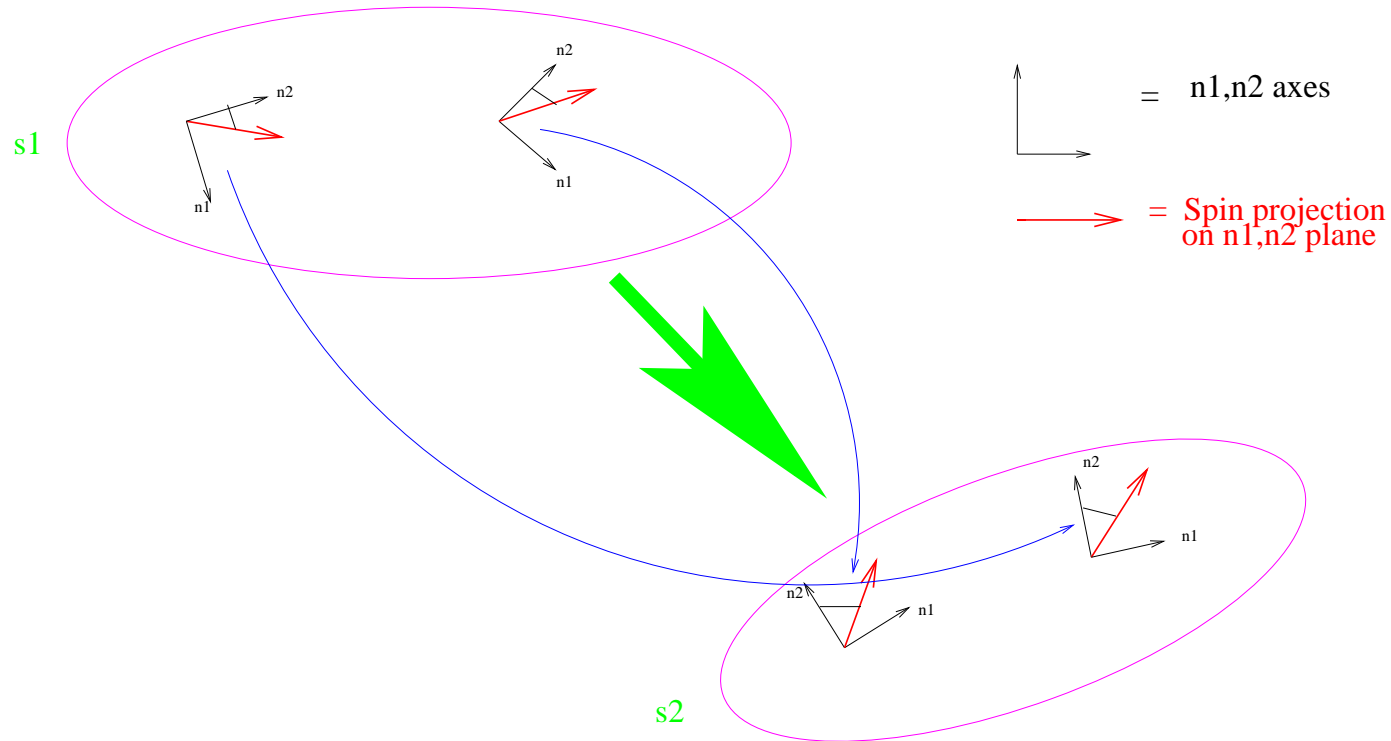
In transverse magnetic fields:

$$\delta\theta_{spin} = a\gamma \cdot \delta\theta_{orbit}$$

- $a\gamma$ is called the “naive spin tune”:
- It is a natural spin frequency of the system.
- At 27.5 GeV for electrons $a\gamma = 62.5$
- At 920 GeV for protons $a\gamma = 1759$ –BIG!!
- \implies 1 mrad of orbit deviation causes $> \pi/2$ of spin precession!!!!
High fields \implies extreme sensitivity.

The real spin tune: measures rate of precession around \hat{n}

Attaching coordinate axes to each phase space point



Spin precession rate w.r.t. n_1, n_2 is the same at all phase space points with same J_x, J_y, J_z .

→ Amplitude dependent spin tune! $\nu_{\text{spin}}(\mathbf{J})$

The real spin tune:

Not a single number, but an **equivalence class**

with elements related by “gauge transformations” of the **local** coordinate systems.

Even without snakes, the real spin tune $\nu(\vec{J})$ does NOT oscillate with synchrotron motion: although $a\gamma$ does.

Spin-orbit resonance.

- Interleaved vertical and horizontal (quad and imperfection) fields.
- Rotations around different axes don't commute.
- If the spin and (linear) orbit motion are in resonance:

$$\nu_{spin}(\vec{J}) = m + m_x \cdot Q_x + m_z \cdot Q_z + m_s \cdot Q_s$$

====> **CRAZY** spin field:

- High order resonances even for perfectly linear spin motion. (non-commutation).
- Two main groups of resonances:
 - Integer resonances due to motion along the **distorted** periodic orbit ==> strong tilt of \hat{n}_0 from ideal.
 - Synchro-beta ('intrinsic') resonances due to **synchro-beta oscillations** AROUND the distorted periodic orbit.

$$====> |\hat{n}(\vec{u}; s) - \hat{n}_0(s)| \quad \text{LARGE.}$$

$$====> |\langle \hat{n}(\vec{J}, \vec{\phi}; s) \rangle_s| \quad \text{SMALL — geometry.}$$

$$\text{e.g. } \approx 60^\circ \quad \text{====> } P_{meas} \approx 0.5 \quad \text{!!!!}$$

SPIN98 + M. Vogt thesis 2000.

With no snakes, spin tune rises with energy and resonances are crossed.

With snakes REAL spin tune ($\neq 1/2$) and can still hit resonances even with perfect alignment!!!!

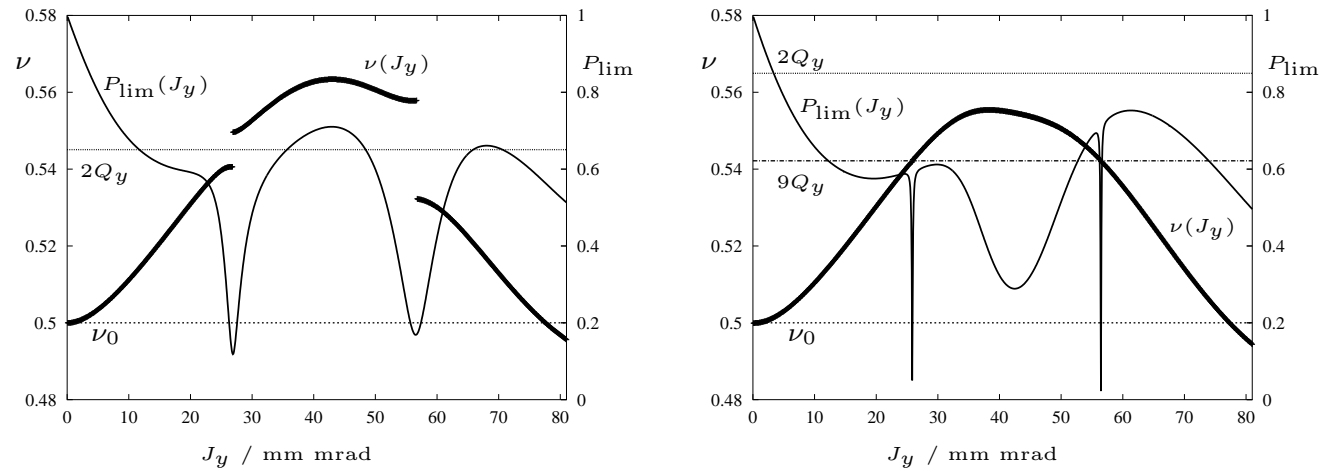
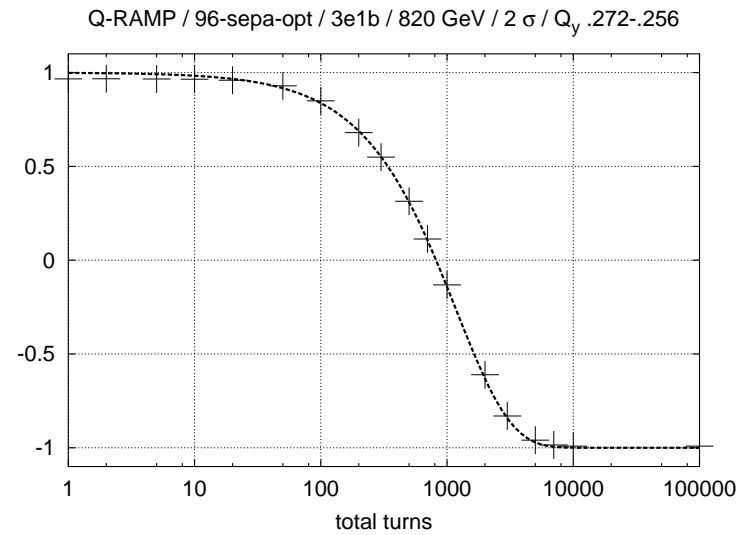
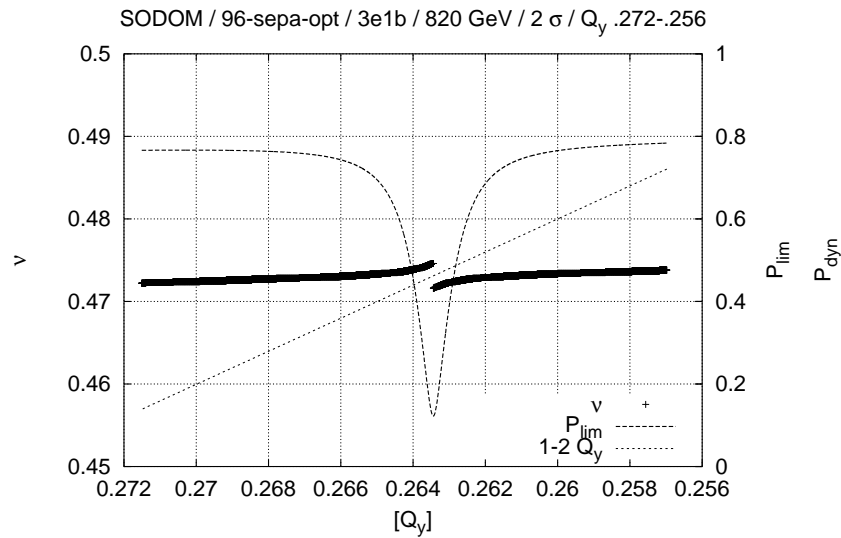
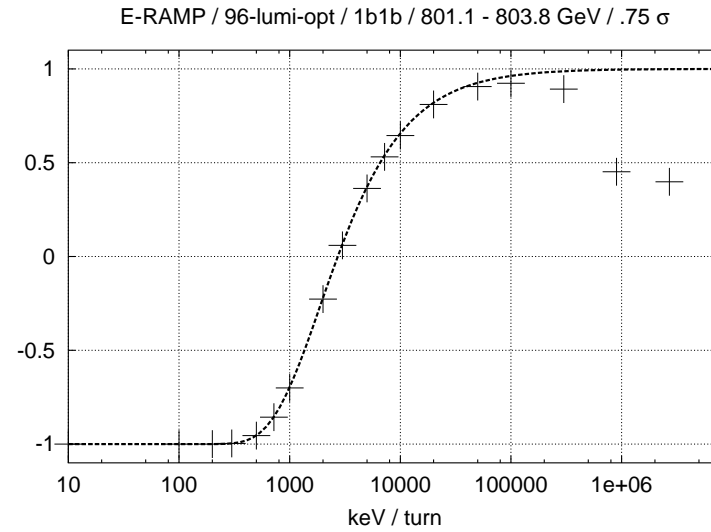
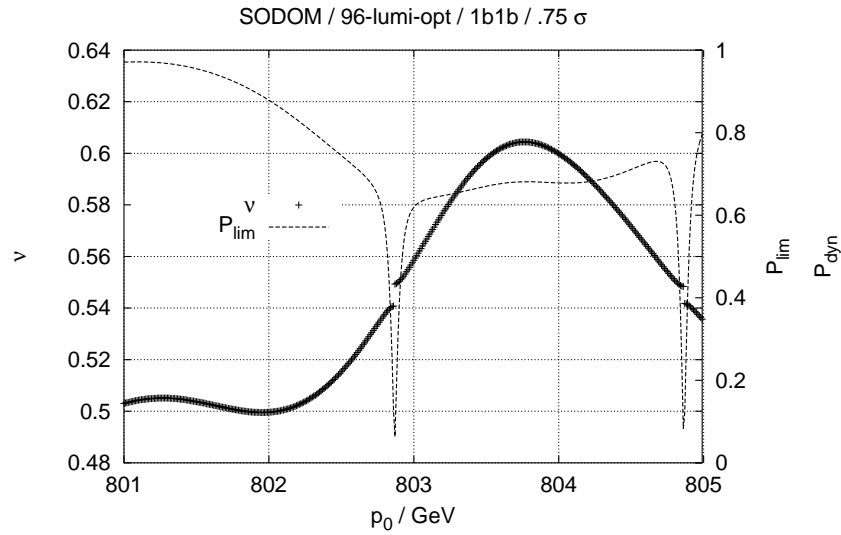


Figure 4: The amplitude dependent spin tune ν and the static polarisation limit P_{lim} vs. vertical orbital action J_y as calculated with SPRINT for the HERA- p . Left: vertical tune $Q_y = 32.2725$, right: $Q_y = 32.2825$.

SPIN2000 + M. Vogt thesis 2000.



- Top left:
Energy scan of P_{lim} and ν for HERA- p with flatteners and a 4 snake scheme (rad., 45° , rad., 45°) with purely vertical motion at 0.75σ .
- Top right:
The dependence of the final P_{dyn} after ramping through the resonance at approximately 802.7 GeV on the energy gain per turn.
- Bottom left:
Tune scan of P_{lim} and ν for HERA- p with flatteners and a 4 snake scheme (long., -45° , rad., 45°) with purely vertical motion at 2σ .
- Bottom right:
The dependence of the final P_{dyn} after ramping through the resonance at $[Q_y] \approx 0.2635$ on the total number of turns.

Acceleration: evolution through stationary states?

At fixed γ_0 :

$$\frac{d \vec{S} \cdot \hat{n}}{ds} = 0$$

along an orbit (angle between 2 T-BMT solutions is constant).

During acceleration (using pre-established) $\hat{n}(\vec{u}; s, \gamma_0)$: $\frac{d \vec{S} \cdot \hat{n}(\vec{u}; s, \gamma_0)}{ds} \neq 0$

If

$$\frac{d\gamma_0}{ds} \quad \text{and} \quad \frac{\partial \hat{n}(\vec{u}; s, \gamma_0)}{\partial \gamma_0}$$

are small enough $\vec{S} \cdot \hat{n}$ is an adiabatic invariant and a stationary spin distribution transforms to a new stationary spin distribution with the same $P(\vec{J})!!!$ Spin can follow $\hat{n} !!!$

If a \vec{J} dependent resonance is crossed, $P(\vec{J})$ can change but $\vec{P}(\vec{J}, \vec{\phi}; s)$ is still parallel to $\hat{n}(\vec{J}, \vec{\phi}; s)$

$$|\vec{P}_{meas}(s)| = |\langle P(\vec{J}) \hat{n}(\vec{J}, \vec{\phi}; s) \rangle_s| \leq |\langle \hat{n}(\vec{J}, \vec{\phi}; s) \rangle_s|$$

$$|P(\vec{J})| \leq 1$$

HISTORY!

The Froissart–Stora formula for crossing resonances

$$\frac{P_{\text{final}}}{P_{\text{initial}}} = 2 e^{-\frac{\pi|\epsilon|^2}{2\alpha}} - 1$$

- ϵ is the “resonance strength”, a measure of the dominant spin perturbation at resonance (Fourier component),
- α expresses the rate of resonance crossing.

Very fast resonance crossing: Large $\frac{|\epsilon|^2}{2\alpha}$: polarisation preserved.

Very slow resonance crossing: Small $\frac{|\epsilon|^2}{2\alpha}$: adiabatic invariance \implies full spin flip.

Electrons

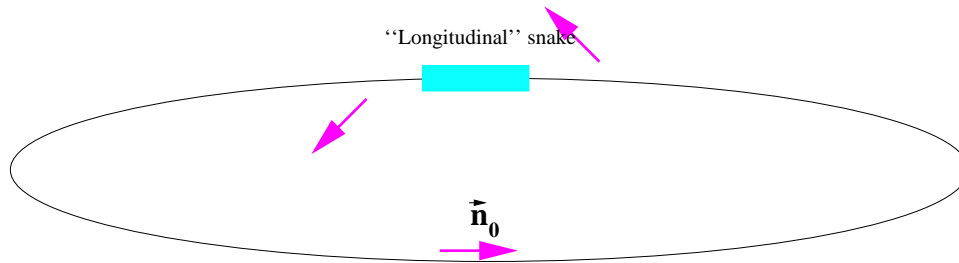
- Synchrotron radiation: \implies polarisation build up by the Sokolov–Ternov effect!!!
- Synchrotron radiation: \implies noise and damping.
- \implies Stochastic orbital motion in the magnetic fields
- \implies Spin diffusion \implies depolarisation!!!!
- The resulting polarisation comes from a balance of polarisation and depolarisation.
- How to calculate???

For an overview of polarised electron phenomenology see:

“Electron polarisation in rings”, D.P. Barber, Snowmass 2001, Working Group M5

at <http://snowmassserver.snowmass2001.org/>

A simple model example: a single Siberian Snake in a perfect flat smooth ring.



Ideal snake: no syncho-beta dependence $\longrightarrow \vec{n}_0$ horizontal everywhere

Synchrotron phase space (σ, η) , smooth dispersion and quads.

$$\hat{n}_0(s) \equiv \cos(g_6(s))\hat{e}_1 + \sin(g_6(s))\hat{e}_2,$$

$$\hat{n} \equiv \cos(f)\hat{e}_1 + \sin(f)\hat{e}_2$$

$$f(\sigma, \eta; s) = g_6(s) + \sigma g_{19}(s) + \eta g_{20}(s) \implies (\text{T} - \text{BMT solution along orbit } \sigma(s), \eta(s))$$

At HERA, 27.5 GeV, $|\hat{n}(\sigma, \eta; s) - \hat{n}_0(s)| \iff 200 \text{ mrad} \implies |\langle \hat{n} \rangle| \approx 1$

Simple model continued:

The corresponding stochastic differential equation for the spin-orbit motion

$$\begin{pmatrix} \sigma'(s) \\ \eta'(s) \\ \psi'(s) \end{pmatrix} = \begin{pmatrix} 0 & -\kappa & 0 \\ \Omega_s^2/\kappa & -2\alpha_s/C & 0 \\ 0 & \pm 2\pi\nu_0/C & 0 \end{pmatrix} \cdot \begin{pmatrix} \sigma(s) \\ \eta(s) \\ \psi(s) \end{pmatrix} + \sqrt{\omega} \cdot \begin{pmatrix} 0 \\ \zeta(s) \\ 0 \end{pmatrix}$$

For notation:

K. Heinemann, DESY Report 97-166 (1997) and Los Alamos archive: physics/9709025.

D.P. Barber, M. Böge, K. Heinemann, H. Mais, G. Ripken, Proc. 11th Int. Symp. High Energy Spin Physics, Bloomington, Indiana (1994). AIP Proceedings 343.

K. Heinemann, D.P. Barber 1996

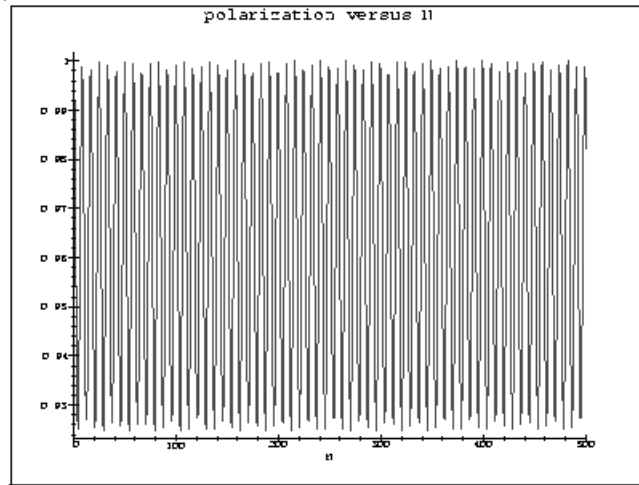


Figure 5: No radiation, spins initially set parallel to \hat{n}_0 , 27.5 GeV HERA: initial state not in equilibrium \implies oscillating polarisation.

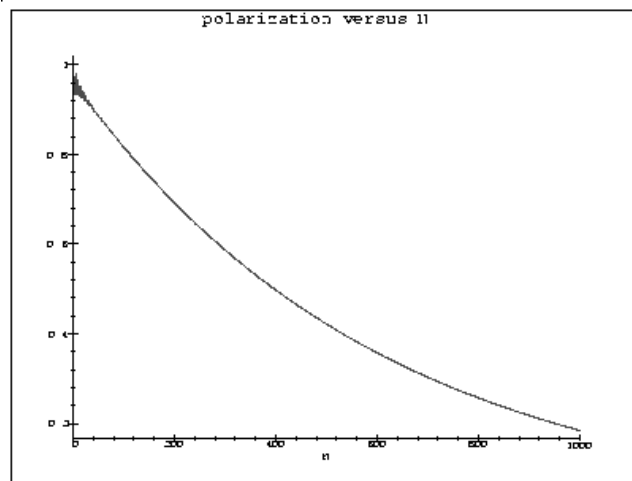
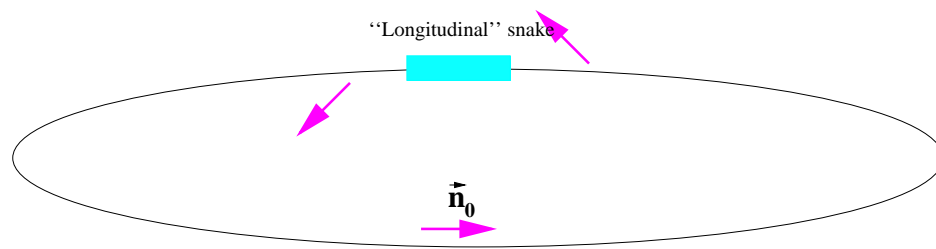


Figure 6: With radiation, spins initially set parallel to \hat{n}_0 , 27.5 GeV HERA: after transients $\vec{P}(\sigma, \eta; s)$ parallel to $\hat{n}(\sigma, \eta; s)$ with the (σ, η) independent $|P|$ falling exponentially.

A single Siberian Snake in a perfect flat ring.



\vec{n}_0 horizontal everywhere:	HERA	$\tau_{\text{dep}} = 260$	millisecs at 27.5 GeV
	eRHIC	τ_{dep}	tens of seconds at 10 GeV
	MIT-Bates	τ_{dep}	hours at few hundred MeV

No Sokolov-Ternov \longrightarrow very exciting possibility to observe
 “kinetic polarization” at MIT-Bates ring.

Full 3-D spin motion

Particle transport in the presence of damping and diffusion.

Fokker-Planck equation:

$$\frac{\partial \rho}{\partial s} = \mathcal{L}_{\text{FP,orb}} \rho$$

where with synchrotron photon emission modelled as additive noise the orbital Fokker-Planck operator can be decomposed into the form:

$$\mathcal{L}_{\text{FP,orb}} = \underbrace{\mathcal{L}_{\text{ham}}}_{\mathcal{L}_{\text{ham}} \rightarrow \text{Liouville}} + \underbrace{\mathcal{L}_0 + \mathcal{L}_1 + \mathcal{L}_2}_{\text{damping and noise}} .$$

Without the S–T terms, the corresponding form for the
Polarisation Density $\vec{\mathcal{P}}$:

$$\frac{\partial \vec{\mathcal{P}}}{\partial s} = \mathcal{L}_{\text{FP,orb}} \vec{\mathcal{P}} + \vec{\Omega}(\vec{u}; s) \times \vec{\mathcal{P}}$$

Barber + Heinemann 1990's

$$\vec{P}(s) = \int d^6u \vec{\mathcal{P}}(\vec{u}; s).$$

This equation:

- can be derived in a classical picture,
- is homogeneous in $\vec{\mathcal{P}}$ i.e. it's “universal”,
- is valid far from spin–orbit equilibrium,
- contains the whole of depolarisation!

After including the S–T terms, this becomes (Derbenev + Kondratenko, Barber + Heinemann):

$$\underbrace{\frac{\partial \vec{\mathcal{P}}}{\partial s} = \mathcal{L}_{\text{ham}} \vec{\mathcal{P}} + \vec{\Omega}(\vec{u}; s) \times \vec{\mathcal{P}} + \mathcal{L}_0 \vec{\mathcal{P}} + \mathcal{L}_1 \vec{\mathcal{P}} + \mathcal{L}_2 \vec{\mathcal{P}}}_{\equiv \text{Damping and noise free part}} + \underbrace{\frac{1}{\tau_0(\vec{u})} \left[\vec{\mathcal{P}} - \frac{2}{9} \hat{v}(\vec{\mathcal{P}} \cdot \hat{v}) + \frac{8\hat{b}(\vec{u})}{5\sqrt{3}} \rho \right]}_{\text{ST in BKS form}} + \underbrace{\text{X-terms}}_{\text{Kinetic pol.}}$$

SMALL

↓

≡ T-BMT equation (BIG)

↓

Stationary state

↓

\hat{n} -axis (Invariant spin field) → DETERMINES DIRECTION

↓

Rate of polarisation loss \propto Functional of $\hat{n}, \partial_{\vec{u}} \hat{n}, \partial_{\vec{u}}^2 \hat{n} \dots$ (e.g. DK formula).

⇒ large near spin orbit resonances — since \hat{n} is then very sensitive to \vec{u} .

The Derbenev–Kondratenko–Mane Formula: full 3–D.

$$P_{\text{eq,DK}} = -\frac{8}{5\sqrt{3}} \frac{\oint ds \langle |K|^3 \hat{b} \cdot \left[\hat{n} - \frac{\partial \hat{n}}{\partial \eta} \right] \rangle_s}{\oint ds \langle |K|^3 \left\{ 1 - \frac{2}{9} (\hat{n} \cdot \hat{v})^2 + \frac{11}{18} \left| \frac{\partial \hat{n}}{\partial \eta} \right|^2 \right\} \rangle_s}$$

$$\tau_{\text{dep}}^{-1} = \frac{5\sqrt{3} r_e \gamma^5 \hbar}{8 m_e C} \oint ds \left\langle |K|^3 \frac{11}{18} \left(\frac{\partial \hat{n}}{\partial \eta} \right)^2 \right\rangle_s$$

\hat{b} field direction, K curvature

$\langle \rangle_s$: ensemble average.

$$\vec{P}_{\text{meas}}(s) = P_{\text{eq,DK}} \langle \hat{n} \rangle_s \approx P_{\text{eq,DK}} \hat{n}_0 \quad \text{since } |\hat{n}(\vec{u}; s) - \hat{n}_0(s)| \quad \text{SMALL.}$$

Check the DKM formula for the Barber – Heinemann model:

Exact result of model:

$$\tau_{spin}^{-1} = \frac{d^2}{\lambda_0^2} \cdot \frac{\omega}{2 c \lambda L} \cdot \frac{1}{\{\cosh(cL/2) + \cos(\lambda L)\}} \cdot \left(2\lambda \sinh(cL/2) - c \sin(\lambda L) \right)$$

DKM version using the expression for $\hat{n}(\sigma, \eta : s)$:

$$(c_0 \tau_{dep})^{-1} = \frac{d^2}{\lambda_0^2} \cdot \frac{\omega}{2 \lambda_0 L} \cdot \frac{1}{\{1 + \cos(\lambda_0 L)\}} \cdot \left(\lambda_0 L - \sin(\lambda_0 L) \right).$$

- Resonance denominators
- BIG effect even way off resonance
- ==> Avoid \hat{n}_0 in horizontal plane!!!
 ==> Avoid that spin couples to dispersion (sync. phase space is BIG).

For electrons with radiation:

- The VALUE of the polarisation $P_{\text{eq,DK}}$ is the same at all phase space points and azimuth s .
- The DIRECTION of the polarisation is parallel to \hat{n}
- At practical energies $|\hat{n}(\vec{u}; s) - \hat{n}_0(s)|$ SMALL e.g. ≤ 100 mrad away from resonances.
- The rate of depolarisation depends on the DERIVATIVE $\partial\hat{n}/\partial\eta$
- An estimate for pure synchrotron motion: $\sigma_\eta \approx 10^{-3}$, $|\hat{n}(\vec{u}; s) - \hat{n}_0(s)| \approx 1$ mrad
 $\implies |\partial\hat{n}/\partial\eta| \approx 1 \implies P_{\text{eq,DK}} \approx 0.60!!!$
- Very close to resonances $\hat{n}(\vec{u}; s)$ is a very sensitive function of \vec{u} so that $\partial\hat{n}/\partial\eta$ can be large and the equilibrium $P_{\text{eq,DK}}$ can be small.
- For electrons, even without Sokolov–Ternov build up, the equilibrium of the spin DIRECTIONS (along the spin field \hat{n}) is established by noise and damping.
- For protons, the equilibrium of the spin DIRECTIONS is established during acceleration.

Full calculation of $\hat{n}(\vec{u}; s)$ is HARD and needs big computing power

High order perturbation theory: Unitarity problems near resonances.

SMILE (S.R. Mane),

SpinLie (Yu. Eidelmann and V. Yakimenko).

Nonperturbative:

SODOM (K. Yokoya),

SPRINT (K. Heinemann, G. H. Hoffstaetter, M. Vogt).

====> linearize

SLIM/SLICK (A.W. Chao (D.P. Barber)) , SITF (J. Kewisch),

ASPIRIN (V. Ptitsin)

Linearization ignores most non-commutation ====> only first order resonances. Unitarity problems.

SLIM/SLICK/SITF I.

$$\vec{\Omega} = \vec{\Omega}^{\text{co}} + \vec{\omega}^{\text{sb}}$$

$\vec{\omega}^{\text{sb}}$ is small (?)

In practical electron rings $\hat{n}(\vec{u}; s)$ is close to $\hat{n}_0(s)$ so use:

$$\hat{n}(\vec{u}; s) = \hat{n}_0(s) + \alpha(\vec{u}; s)\hat{m}(s) + \beta(\vec{u}; s)\hat{l}(s)$$

where $\sqrt{\alpha^2 + \beta^2} \ll 1$

We write the components $\omega_s^{\text{sb}}, \omega_x^{\text{sb}}, \omega_y^{\text{sb}}$ in the form

$$\begin{pmatrix} \omega_s^{\text{sb}} \\ \omega_x^{\text{sb}} \\ \omega_y^{\text{sb}} \end{pmatrix} = \mathbf{F}_{3 \times 6} \begin{pmatrix} x \\ p_x \\ y \\ p_y \\ \sigma \\ \eta \end{pmatrix}$$

SLIM/SLICK/SITF II.

In linear approximation the combined orbit and spin motion is described by 8×8 transport matrices of the form

$$\hat{\mathbf{M}} = \begin{pmatrix} \mathbf{M}_{6 \times 6} & \mathbf{0}_{6 \times 2} \\ \mathbf{G}_{2 \times 6} & \mathbf{D}_{2 \times 2} \end{pmatrix}$$

acting on the vector (\vec{u}, α, β) ,

SLIM/SLICK/SITF III.

The eigenvectors for one turn defined by $\hat{\mathbf{M}}(s_0 + C, s_0) \cdot \vec{q}_\mu = \hat{\lambda}_\mu \cdot \vec{q}_\mu$ are written in the form

$$\vec{q}_k(s_0) = \begin{pmatrix} \vec{v}_k(s_0) \\ \vec{w}_k(s_0) \end{pmatrix}, \quad \vec{q}_{-k}(s_0) = [\vec{q}_k(s_0)]^*$$

for $k = I, II, III$;

Then with respect to the $(\hat{n}_0, \hat{m}, \hat{l})$ frame,

$$\begin{aligned} \frac{\partial \hat{n}}{\partial \eta} &\equiv i \sum_{k=I,II,III} \{v_{k5}^* \vec{w}_k - v_{k5} \vec{w}_k^*\} \\ &= -2 \operatorname{Im} \sum_{k=I,II,III} v_{k5}^* \vec{w}_k \end{aligned}$$

Note that this is independent of the phase space vector and emittances!

The v_{k5}^* describe the coupling of the orbit to radiation.

$$\frac{\partial \hat{n}}{\partial \delta} \equiv \sum_{3modes} \text{coupling of spin to orbit} \times \text{coupling of orbit to radiation}$$

Spin matching I.

To minimize depolarisation, minimise the coupling of the spin to the orbit at dipoles where the coupling of orbit to radiation does not vanish.

$$\vec{w}_k(s_0) = - \left[\mathbf{D}(s_0 + C, s_0) - \hat{\lambda}_k \right]^{-1} \mathbf{G}(s_0 + C, s_0) \vec{v}_k(s_0)$$

for $k = I, II, III$;

Minimize the appropriate parts of the 1-turn SPIN-ORBIT coupling matrix $\mathbf{G}(s_0 + C, s_0) \implies$

Minimize the appropriate parts of the SPIN-ORBIT coupling matrix $\mathbf{G}(s + \Delta, s)$ for strings of elements: **SPIN TRANSPARENCY**

Spin matching II.

The matrix approach to linear spin matching: minimize $\mathbf{G}_{2 \times 6}$

Advantages:

- Direct connection to quantities appearing in SLIM (SLICK).
- Necessary for coupled systems (skew quads, solenoids).
- For a big ring:
Evaluation (numerical) of integrals in a thick lens optimization program is too slow \implies analytic integration? \implies integrals already contained in $\mathbf{G}_{2 \times 6}$.
- “Locality”: once $\mathbf{G}_{2 \times 6}$ is zero for a section of the ring it remains zero no matter what changes are made to the optics outside.
- Provides a systematic basis for investigation of the algebraic properties using e.g. REDUCE, MATHEMATICA, MAPLE.
- The interpretation is usually transparent, e.g. arbitrary string of quads and drifts.

Spin matching III.

The basic rules of self polarisation and spin matching.

- Keep \hat{n}_0 aligned to the field in as many of the ring dipoles as possible to drive S–T effect at full rate. E.g. minimize the regions around IPs where \hat{n}_0 is horizontal and there is radiation in dipoles.
- Minimize $G_{2 \times 6}$ across the regions around IPs where \hat{n}_0 is horizontal.
- Get a grip on the remaining effects of $G_{2 \times 6}$.
- Then do very good orbit correction to avoid the \hat{n}_0 tilts (resulting from misalignments) that couple spin to horizontal synchro–betatron motion and nullify the effect of good spin transparency.

Spin matching IV.

See the article by D.P. Barber and G. Ripken in the Handbook of Accelerator Physics and Engineering, Eds. A.W. Chao and M. Tigner, 2nd edition, World Scientific, 2002.

Higher order resonances. e.g. sync. side bands

Beam-beam forces!!!

February 27, 2002
EIC Accelerator Workshop, Ring-Ring Group
BNL

Self-Polarization Tests at Bates

J. Van der Laan and F. Wang

MIT Bates Linear Accelerator Center
21 Manning Road, P.O. Box 846, Middleton, MA, USA

- 1. The Kinetic polarization mechanism and the EIC project.**
- 2. Kinetic polarization at Bates South Hall Ring.**
- 3. The test plan**

1. The Kinetic polarization mechanism:

Why should we verify it experimentally for EIC ?

*Self-polarization of the e-ring is the key technical advantage of the EIC ring-ring option over others. At 10GeV, it is not totally trivial to achieve high P in short time.

*Kinetic Polarizing term in the DK formula has never been well verified experimentally.

*Calculations show significant reduction of the equilibrium polarization level caused by horizontal dipoles between the spin rotators on both sides of the IT region.

*If the reduction is true, then using higher fields in the arc dipoles or installing special polarizing wigglers are options to reduce the polarization losses. But what should we decide to do for the design?

We should not keep holding and guessing what to do about it if we can test this KP mechanism now with minimal efforts.

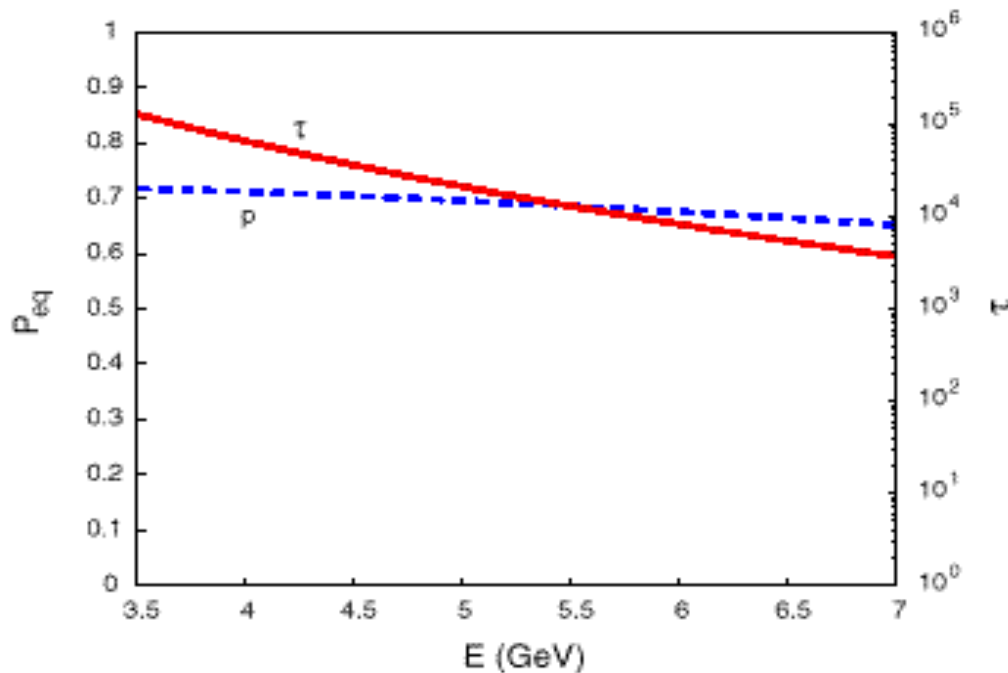


Figure1. The P_{eq} and the spin relaxation time vs. energy for the 3.5-7 GeV “EPIC” Electron Ring

“Concept for a Polarised Electron-Proton Collider with 15-30 GeV c.m. Energy and 10^{33} $\text{cm}^{-2}\text{s}^{-1}$ Luminosity” I.A. Koop et. Al. Pac200

The DK Formula:

$$P_{eq} = -\frac{8}{5\sqrt{3}} \frac{\alpha_-}{\alpha_+}; \quad \tau^{-1} = \frac{5\sqrt{3}}{8} \frac{e^2 \hbar \gamma^5}{m^2 c^2} \alpha_+ = \frac{5\sqrt{3}}{8} c \tilde{\chi}_c r_e \gamma^5 \alpha_+$$

$$\alpha_- = \left\langle \frac{\hat{b}}{|\rho|^3} (\hat{n} - \vec{d}) \right\rangle; \quad \alpha_+ = \left\langle \frac{1}{|\rho|^3} \left[1 - \frac{2}{9} (\hat{n}\hat{v})^2 + \frac{11}{18} |\vec{d}|^2 \right] \right\rangle$$

$$\vec{d} = \gamma \frac{d\vec{n}}{d\gamma}$$

is the spin orbit coupling vector.

$$\alpha_- = \frac{\int \left(\frac{\hat{b}}{|\rho|^3} (\hat{n} - \vec{d}) + \frac{\hat{b}_w}{|\rho_w|^3} (\hat{n}_w - \vec{d}_w) \right) ds}{(2\pi\rho + L_w)};$$

Two observations:

a) In general, if $\frac{\rho^2}{\rho_w^2} \gg 1$ Here: $\frac{L_w}{\rho_w^3} \bigg/ \frac{2\pi}{\rho^2} \gg 1$

Wiggler effect is dominant in self polarization.

At SHR: $\rho=9.14\text{m}$, $\rho_w=0.3-0.5\text{ m}$

A relative small high field wiggler can make difference.

b) Since α_- is **d** direction sensitive, while α_+ is only **d** amplitude dependent, therefore proper location and field direction of wigglers are essential for kinetic polarization.

2. Kinetic polarization at Bates South Hall Ring.

Bates South Hall Ring:

$C=190.204$ m

Energy: up to 1.5 GeV with existing RF system capacity.

One Siberian snake: Spin direction in horizontal plane. Spin tune=0.5

Measurement means: laser back-scattering Compton polarimeter, spin flipper.

This is a unique situation:

- **Spin in the horizontal plane.**
- **The SK self polarization mechanism does not work.**
- **The spin-orbit coupling vector can be aligned with guiding field or with transverse wiggler fields.**

The KP is dominant in self polarization.

Also at SHR energy range 0.3-1.5 GeV , $a\gamma$ changes from 1 to 3:

There are three “magic” energies which is convenient for experiment observations.

Previous KP research

*AmPS:

“Siberian snakes for electron storage rings”

V.Ptitsin and Yu. Shatunov

1997

Proposals for exploring KP mechanism at Bates:

*Proposal to S. Peter Rosen(Associate dir. Office of H Energy & Nuclear Physics DOE US)

Desmond. P. Barber

2000

* “Radiation Polarization in the BATES South Hall Ring”

M.Korostelev and Yu. M. Shatunov

2000

2.1 Descriptions of spin –orbit coupling vector, and the kinetic polarization.

The equation of spin motion , can be expressed in general as:

$$\frac{d\vec{S}}{ds} = (\vec{\Omega} + \vec{\omega}) \times \vec{S}$$

$\vec{\Omega}(s)$ is the angular frequency vector of spin precession, and is periodic, i.e. $\vec{\Omega}(s+C) = \vec{\Omega}(s)$ with C being the circumference of the ring.

Aperiodic parts such as betatron oscillations are contained in $\vec{\omega}(s)$.

The effects of closed orbit distortions are assumed to be included in the unperturbed part $\vec{\Omega}(s)$.

The base vectors for such a solution is expressed as $\hat{n}(s), \hat{m}(s)$ and $\hat{l}(s)$. They form a right-handed orthonormal base (SLIM notation).

Vector $\hat{n}(s)$ is periodical. And $\hat{m}(s), \hat{l}(s)$ satisfy

$$\begin{pmatrix} \hat{n}(s+C) \\ \hat{m}(s+C) \\ \hat{l}(s+C) \end{pmatrix} = \begin{pmatrix} 1 & 0 & 0 \\ 0 & \cos \mu & -\sin \mu \\ 0 & \sin \mu & \cos \mu \end{pmatrix} \begin{pmatrix} \hat{n}(s) \\ \hat{m}(s) \\ \hat{l}(s) \end{pmatrix}$$

$$\mu = 2\pi\nu_0 \quad \nu_0 = a\gamma$$

For the unperturbed part :

$$\begin{aligned} \frac{d\vec{S}}{ds} &= \vec{\Omega} \times \vec{S} \\ &= \vec{\Omega}_0 \vec{S} = \begin{pmatrix} 0 & -\Omega_y & \Omega_x \\ \Omega_y & 0 & -\Omega_z \\ -\Omega_x & \Omega_z & 0 \end{pmatrix} \vec{S} \end{aligned}$$

And can be solved in the form of $\vec{S}(s) = R(s, s_0) \vec{S}(s_0)$

Where R is the transfer matrix from s_0 to s.

As $R_{3 \times 3}$ is periodical and $\text{Det}[R]=1$, for this one turn matrix, there are three eigenvalues and three eigenvectors:

$$R(s_0 + C, s_0) \hat{E}_k = \lambda_k \hat{E}_k$$

$$\lambda_{1,2,3} = 1, \quad e^{\pm i2\pi\nu}$$

$$\hat{E}_1 = \hat{\eta}_1 = \hat{n}_0$$

$$\hat{E}_2 = \hat{\eta} = \hat{m}_0 + i\hat{l}_0$$

$$\hat{E}_3 = \hat{\eta}^* = \hat{m}_0 - i\hat{l}_0$$

At the first order approximation, the spin orbit coupling vector:

$$\vec{d} = \gamma \frac{\partial \hat{n}}{\partial \gamma} \approx \text{Re}(iD\hat{\eta}^*) \quad \text{is orthogonal to } \hat{n}.$$

In general: $D = D_\gamma + D_\beta$

For a practical case like at SHR:

Snake location dispersion free.

No x,y coupling outside the snake.

The D expression outside the snake: (E.A.Perevedentsev, V.Ptitsin & Yu. Shatunov)

$$D_\gamma = -\frac{\pi}{2} \sin(\pi\nu_0) + i\nu_0 \left(\pi - \int \frac{B_\perp}{\langle B_\perp \rangle} d\theta \right)$$

$$D_\beta = \frac{-\pi\nu_0}{4 \cos(\pi\nu_x)} [\cos(\pi\nu_0) \text{Im}(e^{i\pi\nu_x} J(\theta) G_{Ix}^*) + i \text{Im}(e^{i\pi\nu_x} J(\theta) G_{Iz}^*)]$$

$$G_{Ix,z} = f'_{Ix,z(out)} - f'_{Ix,z(in)}$$

$$J(\theta) = f'_{Ix} \psi'_x - f'_{Ix} \psi_x$$

f_i : first mode Floquet function, ψ dispersion.

For spin-matched snake: $G_{Ix,z}=0$, $D_\beta \rightarrow 0$.

$$\vec{d}_\gamma(\text{Vertical}) \Rightarrow -\frac{\pi}{2} \sin(\pi\nu_0)$$

$$\vec{d}_\gamma(\text{Horizontal}) \Rightarrow \nu_0 \left(\pi - \int \frac{B_\perp}{\langle B_\perp \rangle} d\theta \right)$$

The $|\vec{d}_\gamma|_H \equiv 0$ at internal target, and $=\nu_0\pi$ at snake straight.

2.2 The d and KP plots from SLICK and ASPIRIN:

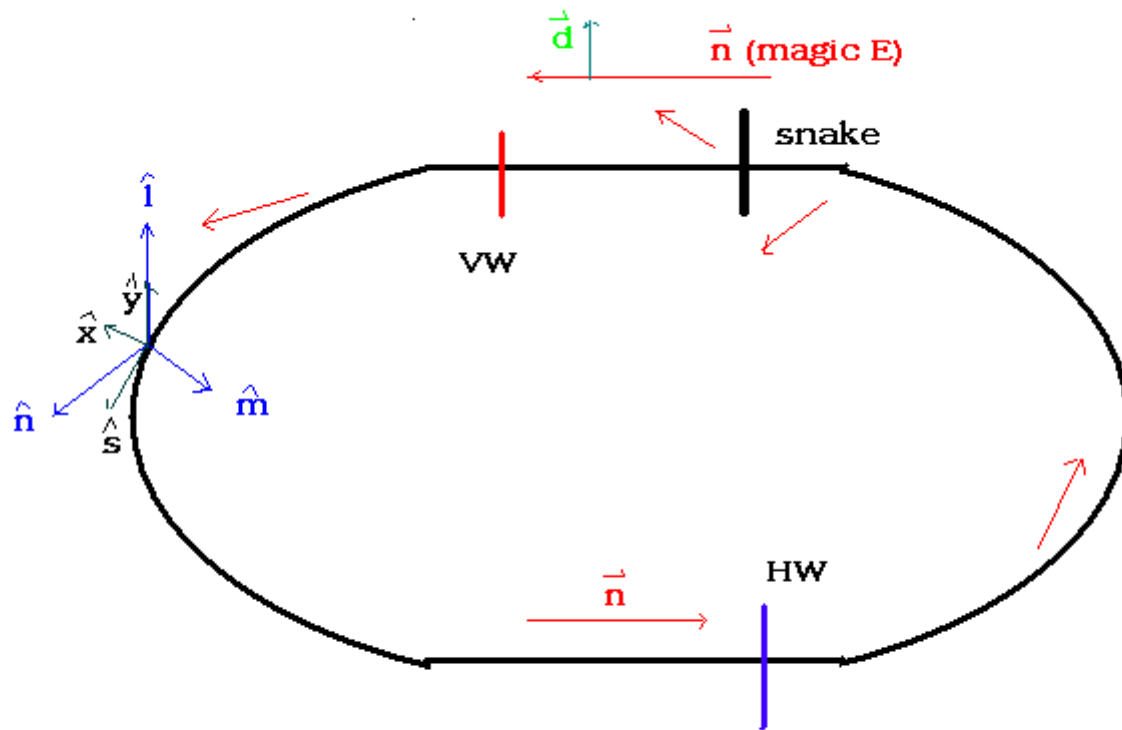


Figure 2. The spin directions and base vectors at SHR

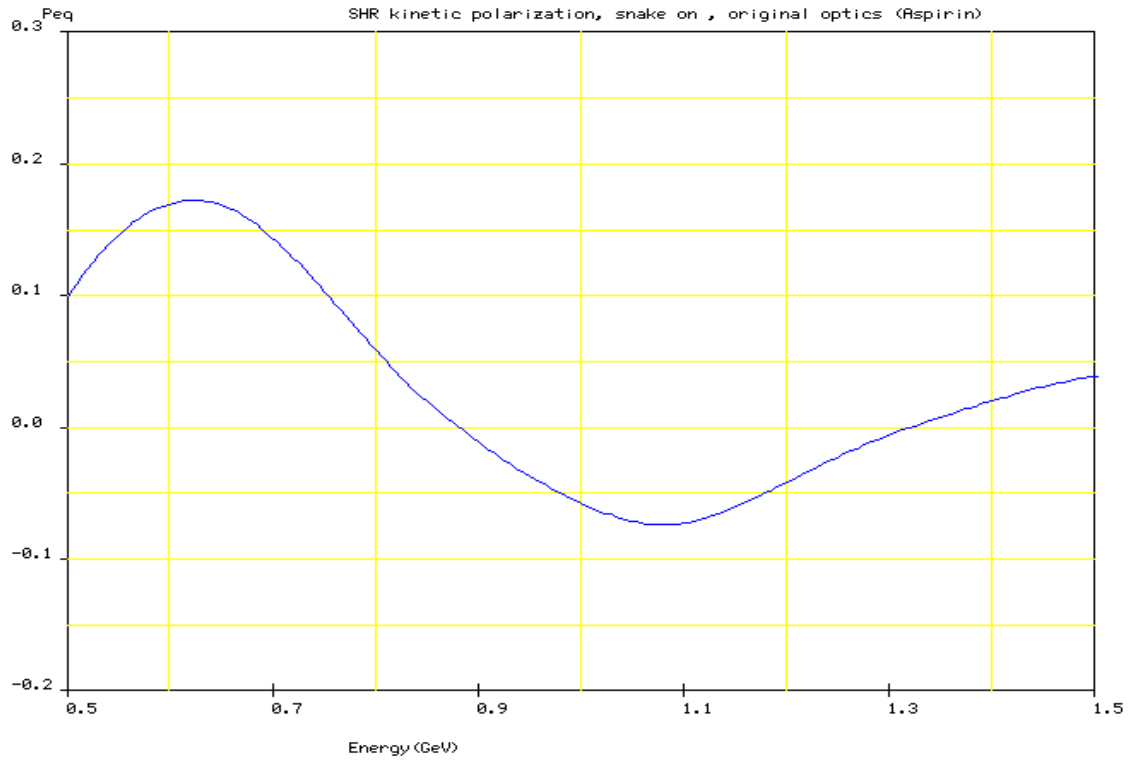
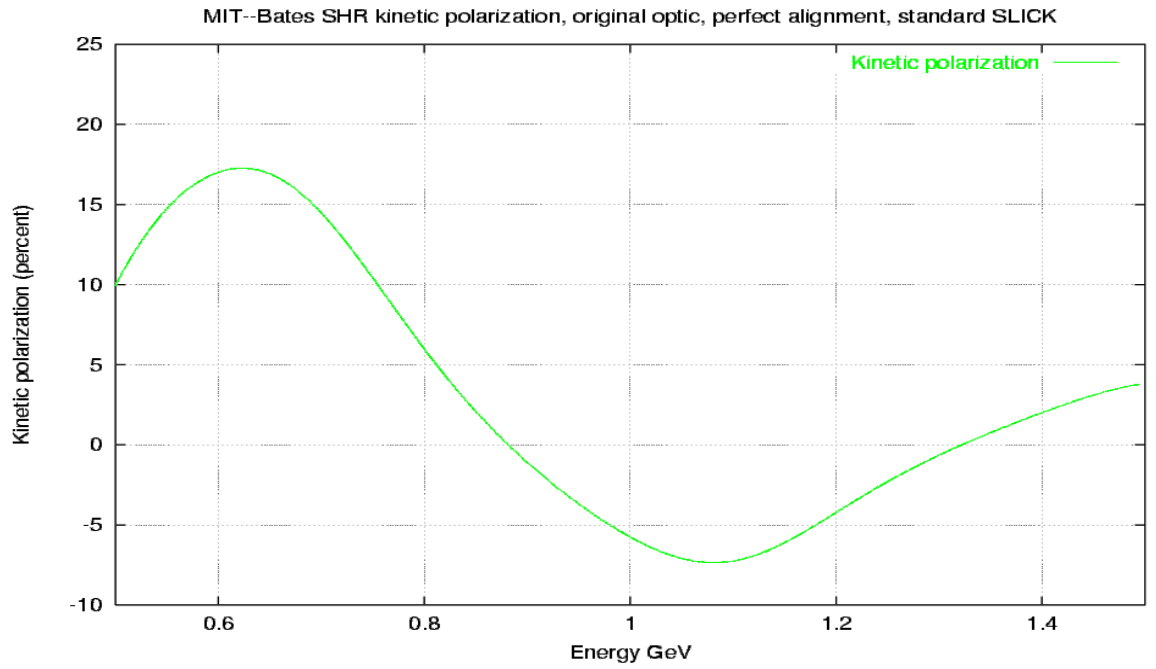


Figure 3. Total kinetic polarization with snake on

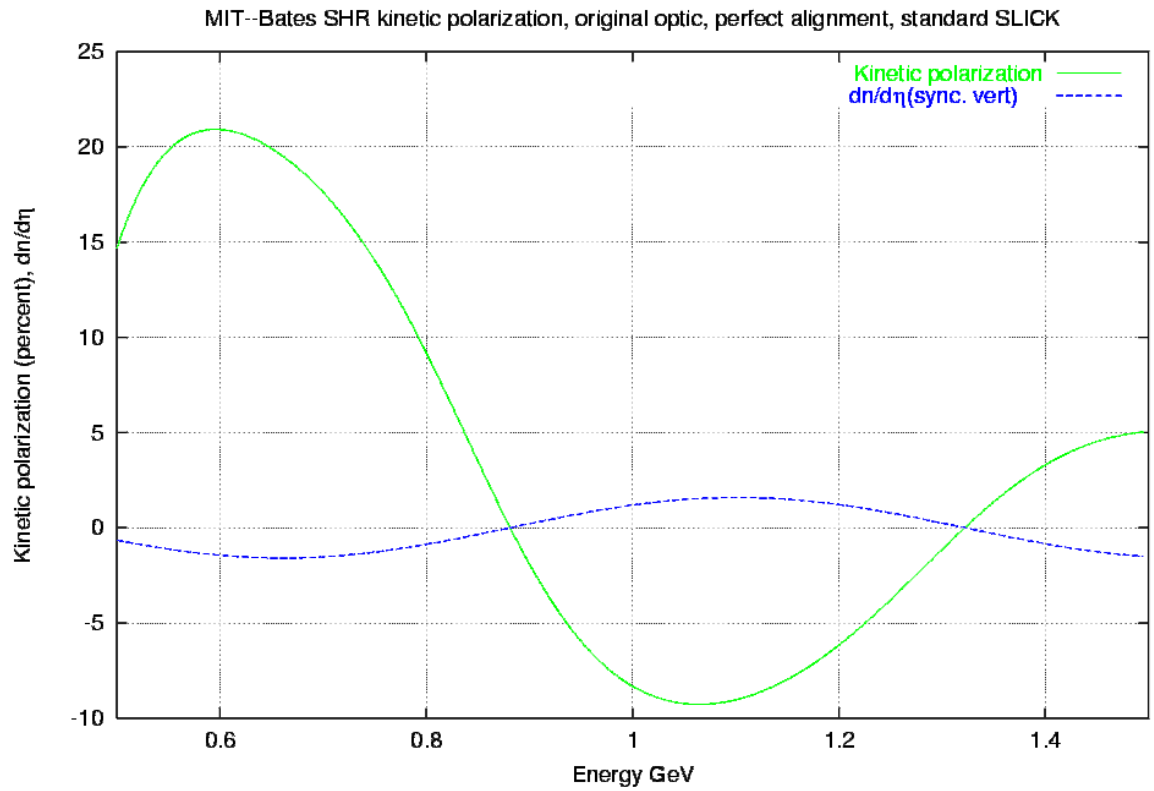


Figure 4. The Vertical part of synchrotron mode of the \mathbf{d}

The Vertical part of synchrotron mode of the \mathbf{d} is almost azimuthally independent.

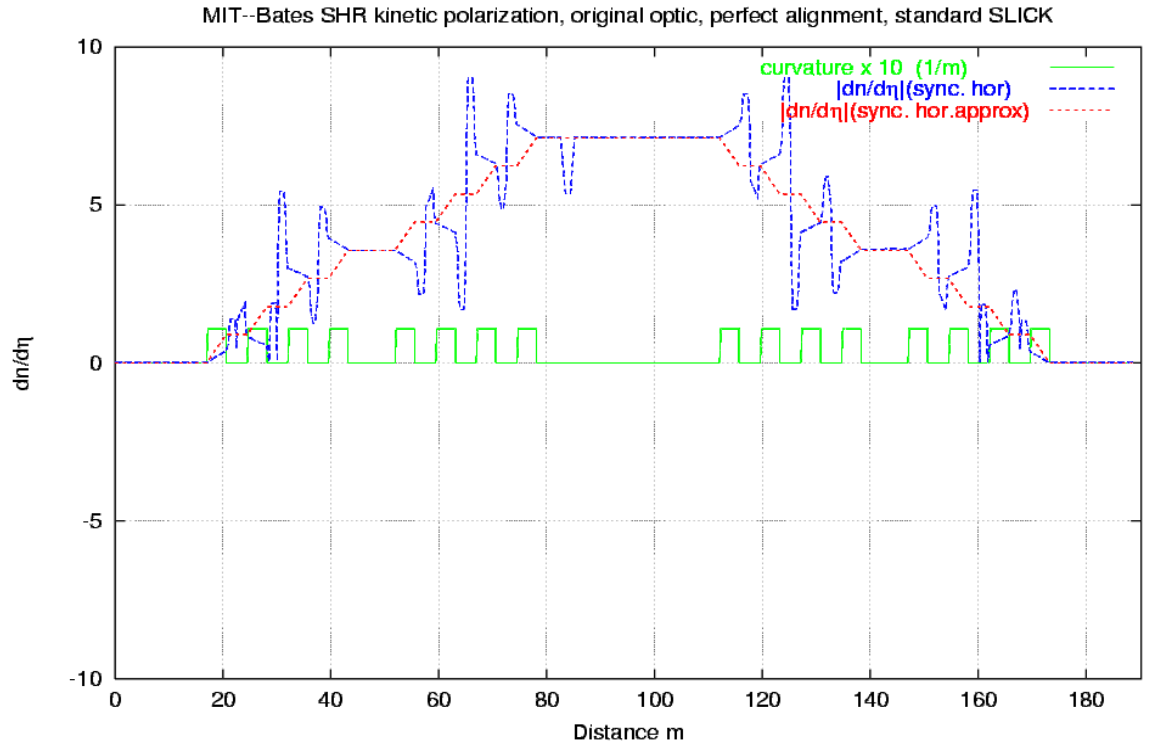
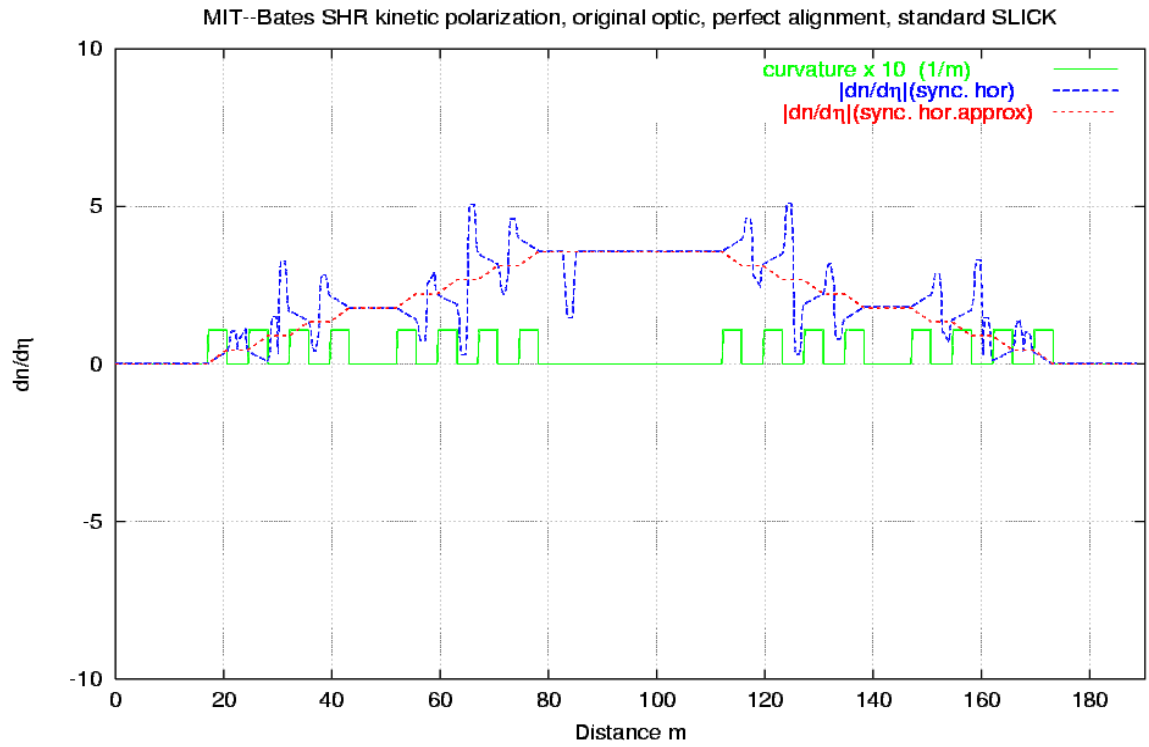


Figure 5. The horizontal part of the synchrotron mode of the d

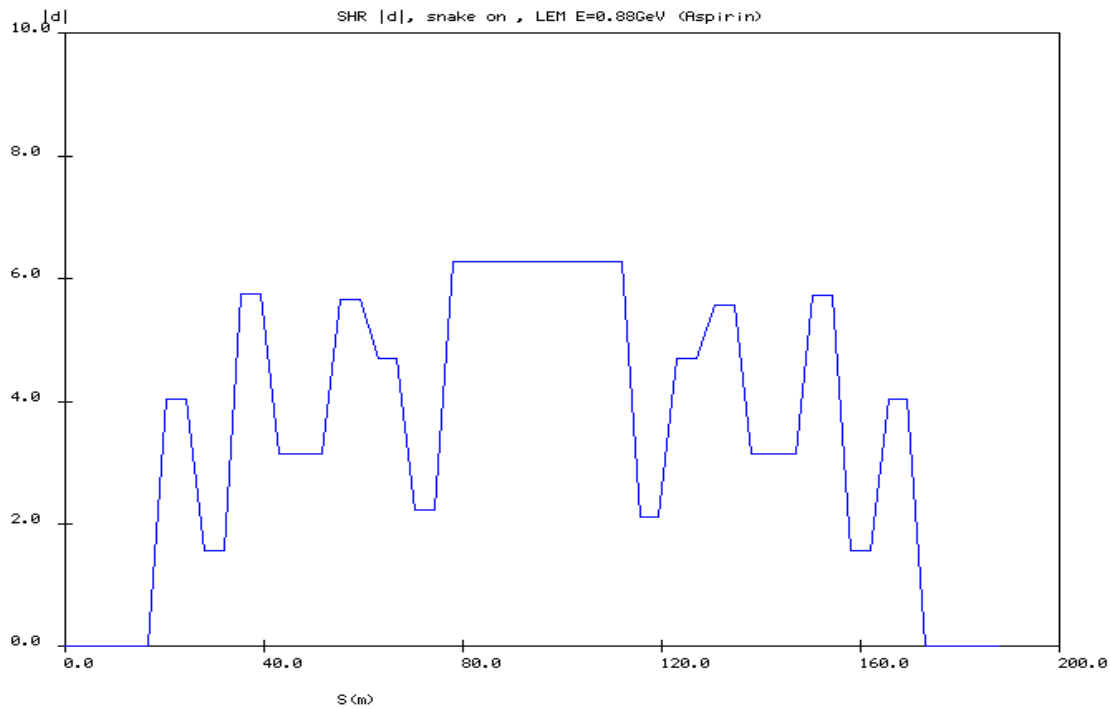
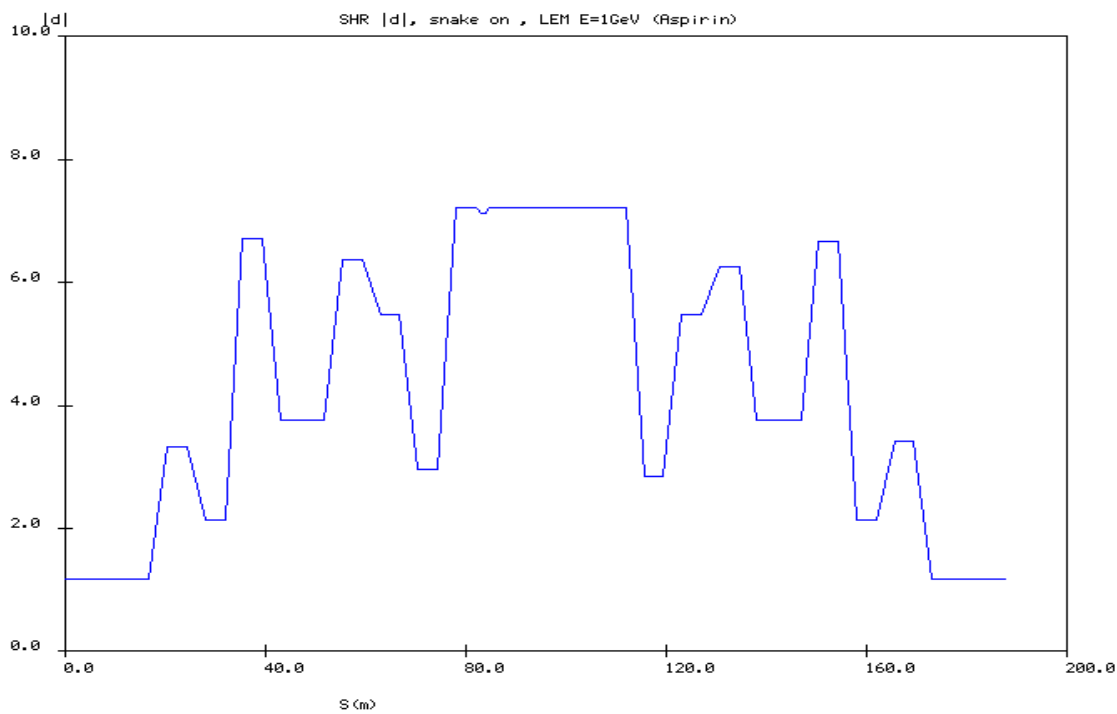


Figure 6. Total $|d|$ at magic energy



2.3 Wiggler connecting to Vertical component of the d vector

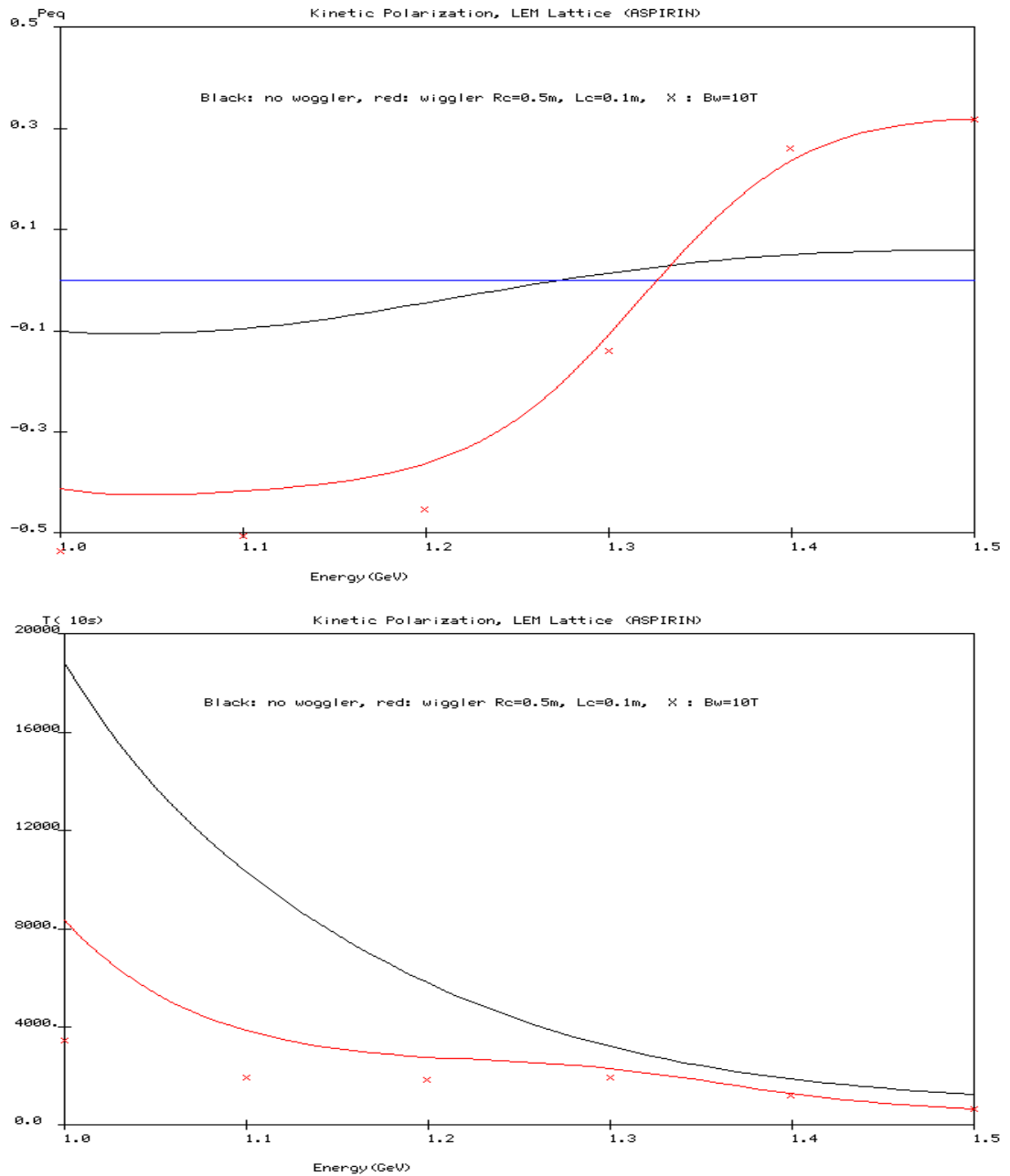


Figure 7. KP and polarization time vs. energy with horizontal wiggler at west straight

2.3 Wiggler connecting to the horizontal component of the \mathbf{d} vector

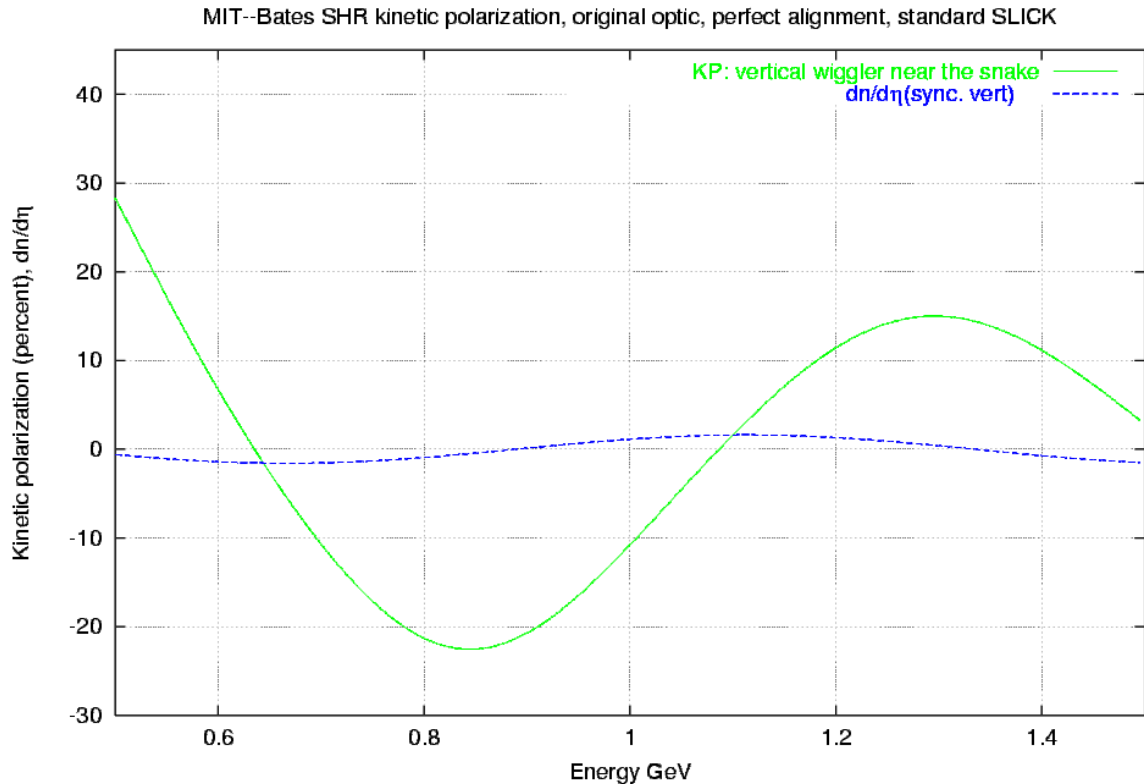


Figure 8.1 KP vs. energy with vertical wiggler at east straight.

- ◆ At “magic” energy, the horizontal \mathbf{d} is aligned with the vertical wiggler field. KP is maximized.
- ◆ While the vertical component of \mathbf{d} is zero at magic energies, so does the KP level achieved with H-wigglers.
- ◆ Due to large $|\mathbf{d}|$ values, at V-wiggler, the wiggler will well dominate the KP process. As a result **the P_{eq} level almost independent of wiggler field changes (still $B_w \gg B_b$)**.

Figure 8.2: Manual calculation of P_{eq} with double wiggler strength (C. Tschalar).

- ◆ The polarization time however will strongly depend on the wiggler field.

3. The Test plan

About the proposal by M.Korostelev and Yu. M. Shatunov (2000).

3.1 The test plan

Step1 :A

Purpose: Verification of KP from d (horizontal)

0.88 GeV, LEM Lattice

Vertical wiggler in the east straight (snake straight)

Expected $P_{eq} = 21\%$, longitudinal at internal target.

Polarization time ≈ 1700 sec

Measurement: Compton polarimeter.

Check: Spin flipper.

Hardware Requirement: One V-wiggler + necessary focussing q etc.

Step1 :B

Purpose: KP from d (Vertical)

1.1 GeV, LEM lattice.

Horizontal Wiggler in the west straight (internal target)

Location: W-straight, between Q10-Q11.

Two (or multi) 2856 RF cavities.

Expected $P_{eq} = 50.8\%$

Polarization time ≈ 1900 sec

Measurement: Compton polarimeter.

Check: Spin flipper.

Hardware Requirement:

1. One H-wiggler + necessary focussing q etc.

2. Full usage of the existing RF capacity with multi-cavities.

Step 2 :

Purpose: Complete Mapping of KP :

1.1-1.5 GeV LEM lattice.

Injection ~ 1.1 GeV.

Energy ramp required.

Add one more snake or use a single high field (10T) snake.

H-wiggler. Mapping: Vertical d

1.1, 1.5 GeV

V-Wiggler. Mapping: Horizontal d

1.32 GeV

Hardware Requirement:

1. A second snake or upgrade existing snake to 10T.

2. Ring energy ramping: dipole PS, sextupole coils etc.

3.2 Hardware requirement and discussions

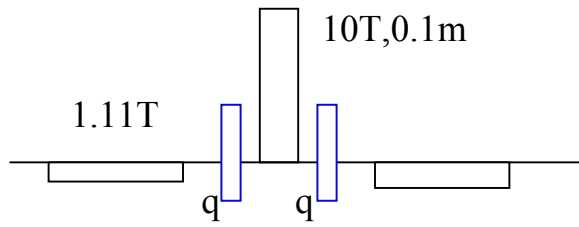
3.2.1 The “asymmetry” wiggler: ($B_c/B_s > 6$)

The centerpiece will be dominant.

0.1m Center dipole, Max. $B_c=10T$,

Compensation dipole, Max. $B_s=1/9 B_c$.

Additional focussing quadrupoles.



wiggler from the BINP proposal(2000)

- What happens if such an “original ”(no extra q’s and optics matching) wiggler is inserted?

For H-wiggler. v_x not changed, v_y increases (e.g. for LEM lattice from 0.1 to 0.128).

Distortion of Twiss parameters at snake is very small. D_β effect?

For V-wiggler. v_x increases (from 0.58 to 0.64), v_y no changes.

Distortion of β_x at snake location is obvious. D_β effect?

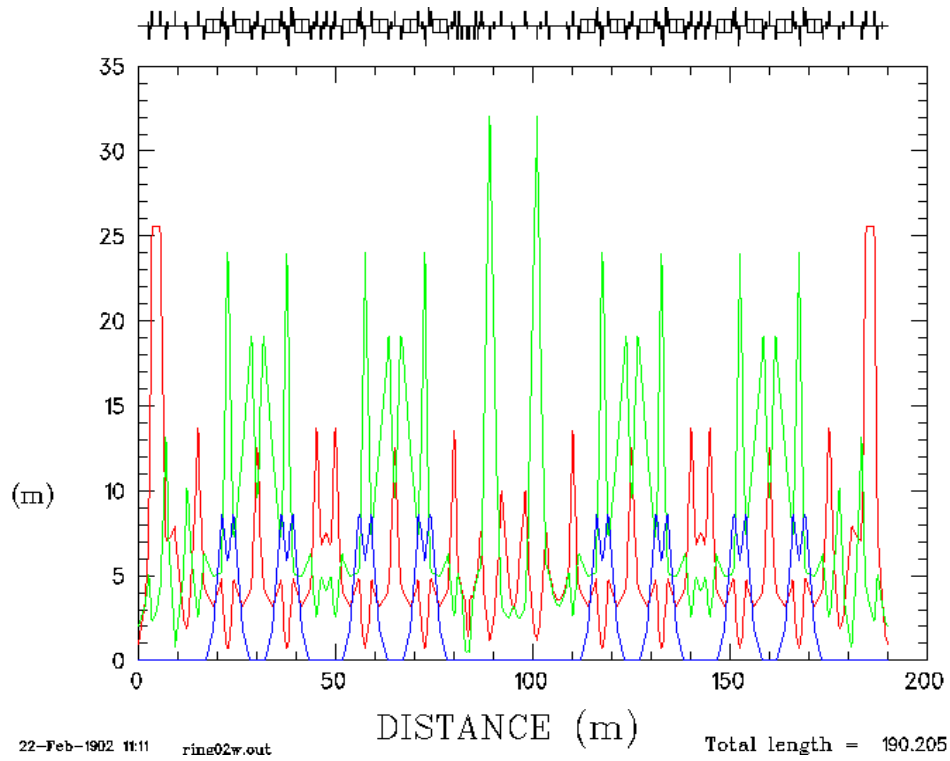


Figure 9.1 The unperturbed LEM lattice. Green- β_y , red- β_x .

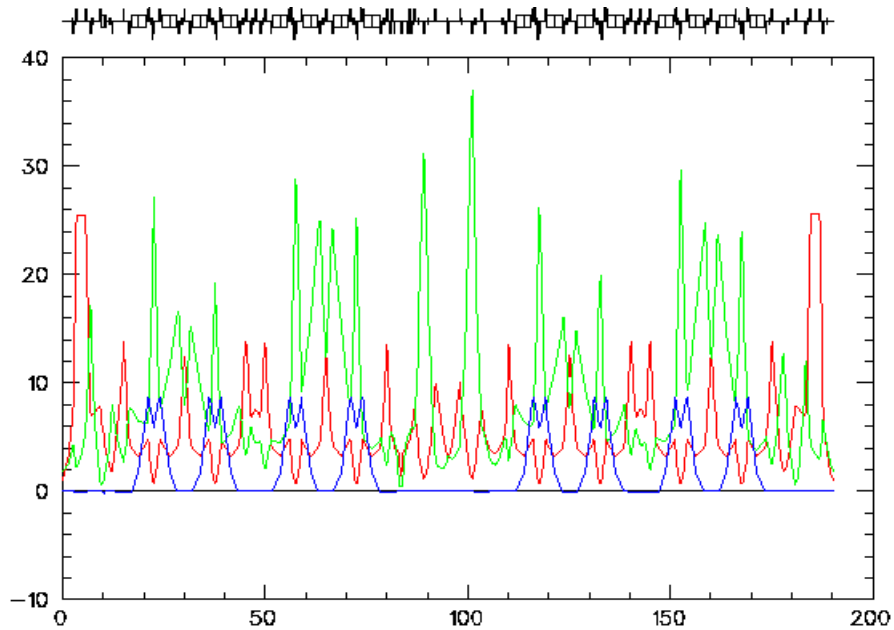


Figure 9.2 The perturbed lattice with an “original” horizontal wiggler.

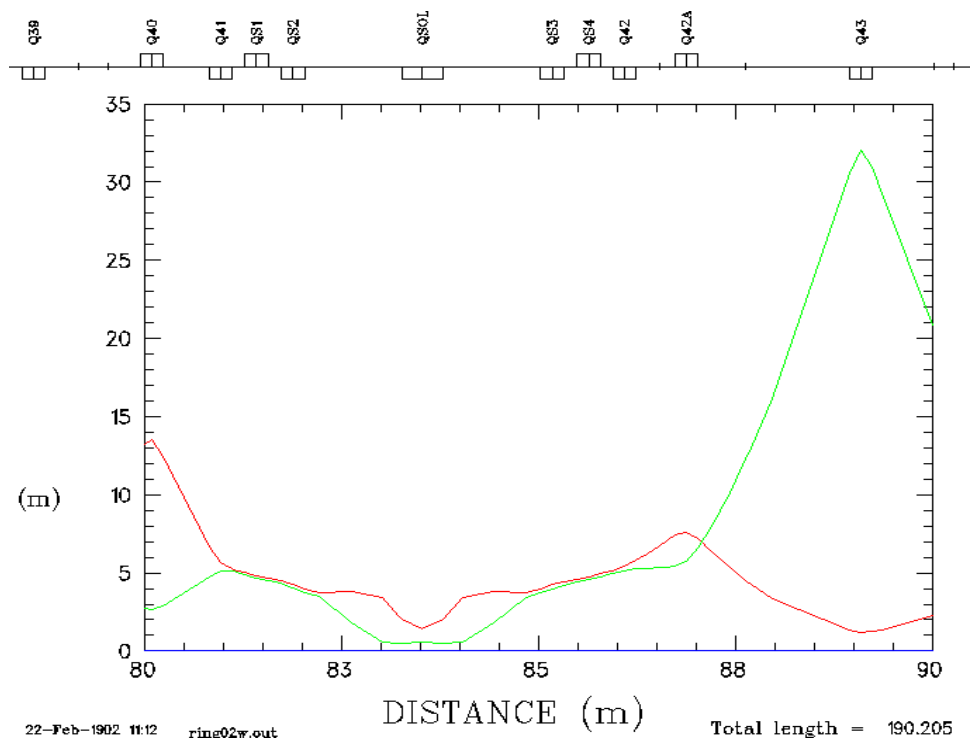


Figure 10.1 The unperturbed LEM lattice at snake location

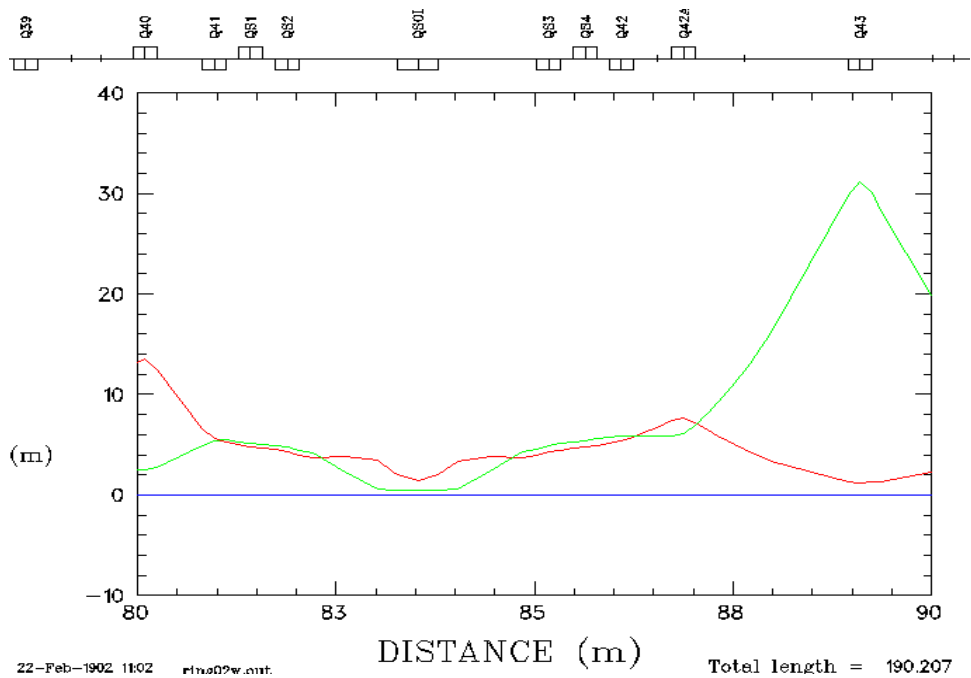


Figure 10.2 The perturbed lattice (snake location) with an “original” horizontal wiggler at west straight.

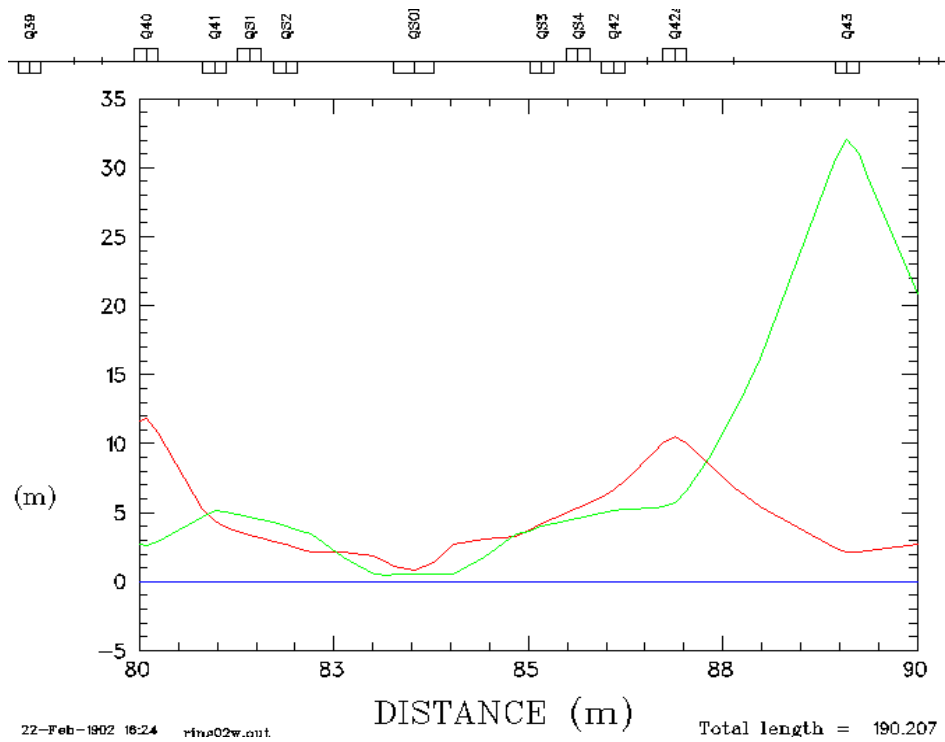


Figure 10.3 The perturbed lattice (snake location) with an “original” vertical wiggler at east-straight.

3.2.2 RF requirements
Synchrotron radiation loss

Wiggler: center piece: $\rho=0.5\text{m}$, $L=0.1\text{m}$

Compensations: $\rho=4.5\text{ m}$, $L=0.45\text{m}$

Wiggler*: $B(\text{center})=10\text{T}$, $B(\text{compensate})=1.11\text{T}$

E(GeV)	Loss Per turn(KeV)				Q life (sec), LEM Lattice		
	Dipoles	Wiggler	Wiggler *	Total	130kv	260kv	400kv
0.88	5.8		10.9	16.7	>10 hour		
1	9.7	6.3	14	23.7	1000		
1.1	14.2	9.1		23.2	1420		
1.1	14.2	9.1	17	31.2	28		
1.2	20.1	13	20	40.1	/	>10 hour	
1.35	32.1	20.45	25.6	57.7	/	290	
1.4	37.2	24	27.5	64.7	/	56	>10 hour
1.5	49	32		81	/	/	4000

RF System Parameters for SHR at 1.5 GeV

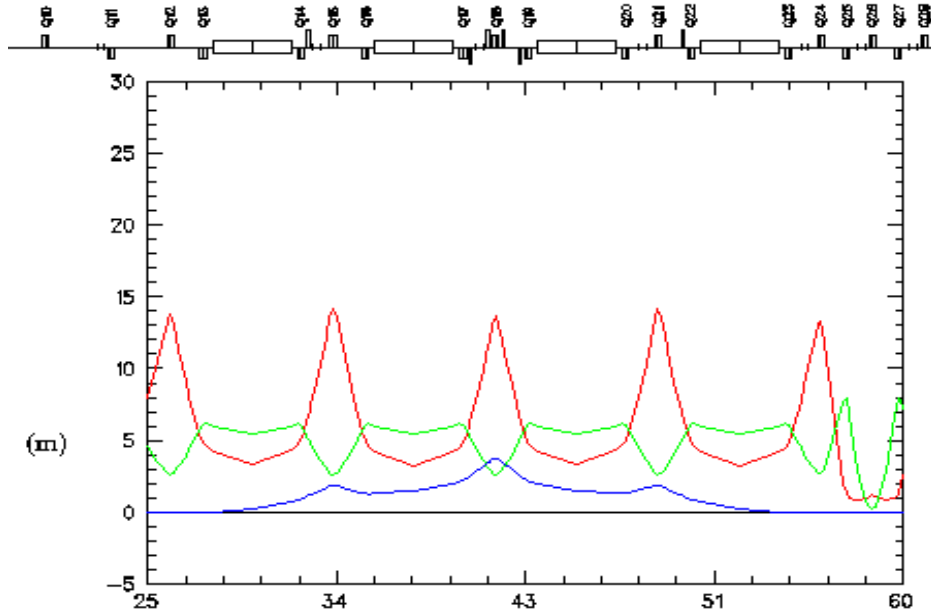
(Abbi Zolfaghari and Defa Wang)

RF frequency, f_{rf} [MHz]	2856
Harmonic number, h	1812
RF Voltage, V[kV]	448
Beam Current, I(mA)	100
Energy Loss/turn [keV]	49
Wiggler Loss /turn [keV]	32
Klystron Power, P[kW]	50
Number of cavities	4
Gap voltage/ Cavity, *Rs [M Ω]	0.9
Number of Klystron	1

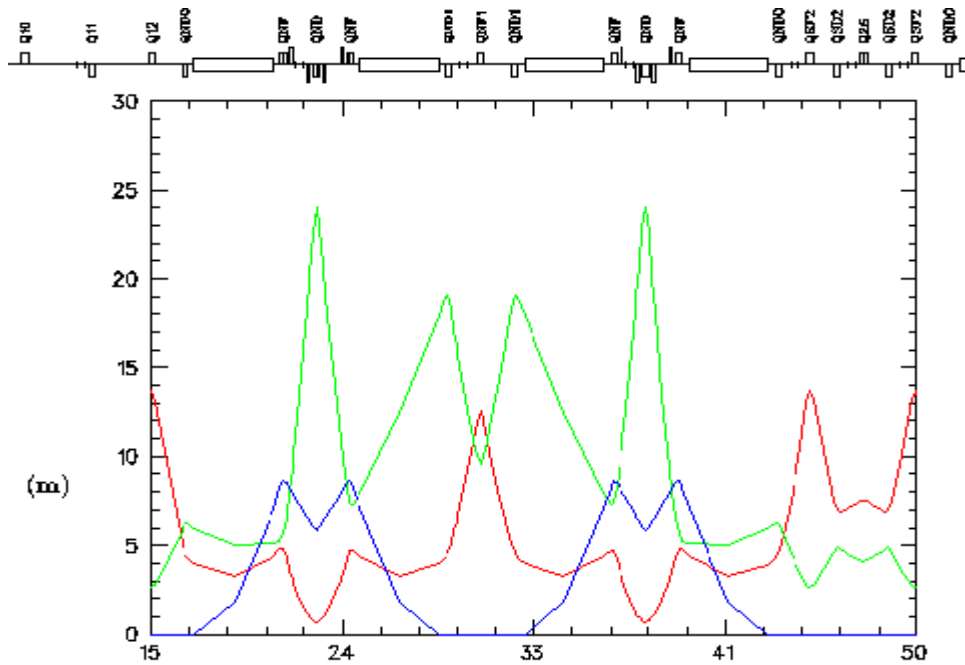
$$*R_s = V^2 / 2p$$

3.3 Bates planned tasks:

3.3.1 Ring Lattice up-grade



The original Lattice, Half of the 180° Bending section



The Low Emittance Lattice.

3.3.2 Polarimeter & spin flipper

(W.Franklin, T.Zward)

(a)Improvement of polarimeter performance.

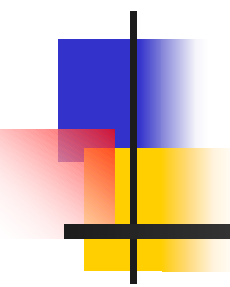
Steady high rate operation, systematic error reduction

(b)New Spin flipper

3.4 Schedule for KP test

Tasks	Status	Time (in month)			
		Design & Spec.	Manufacture	Installation	Test (Beam time)
Ring Lattice	Planned*				
Polarimeter	Planned				
Flipper	Planned				
V-wiggler		2	10	1	
H-wiggler		2	10	1	
RF cavities		2	10	1	
Dipole PS		2	10	1	
1 snake		2	10	1	
Sextupole coils		2	6	1	
KP test					3-4

* Planned tasks will be accomplished within next year.



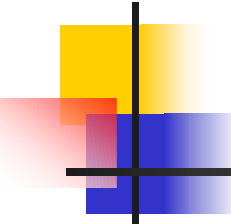
The HERA ep Interaction Regions

EIC AC Workshop

Brookhaven Nat Lab

26.02.2002

Uwe Schneekloth (DESY)

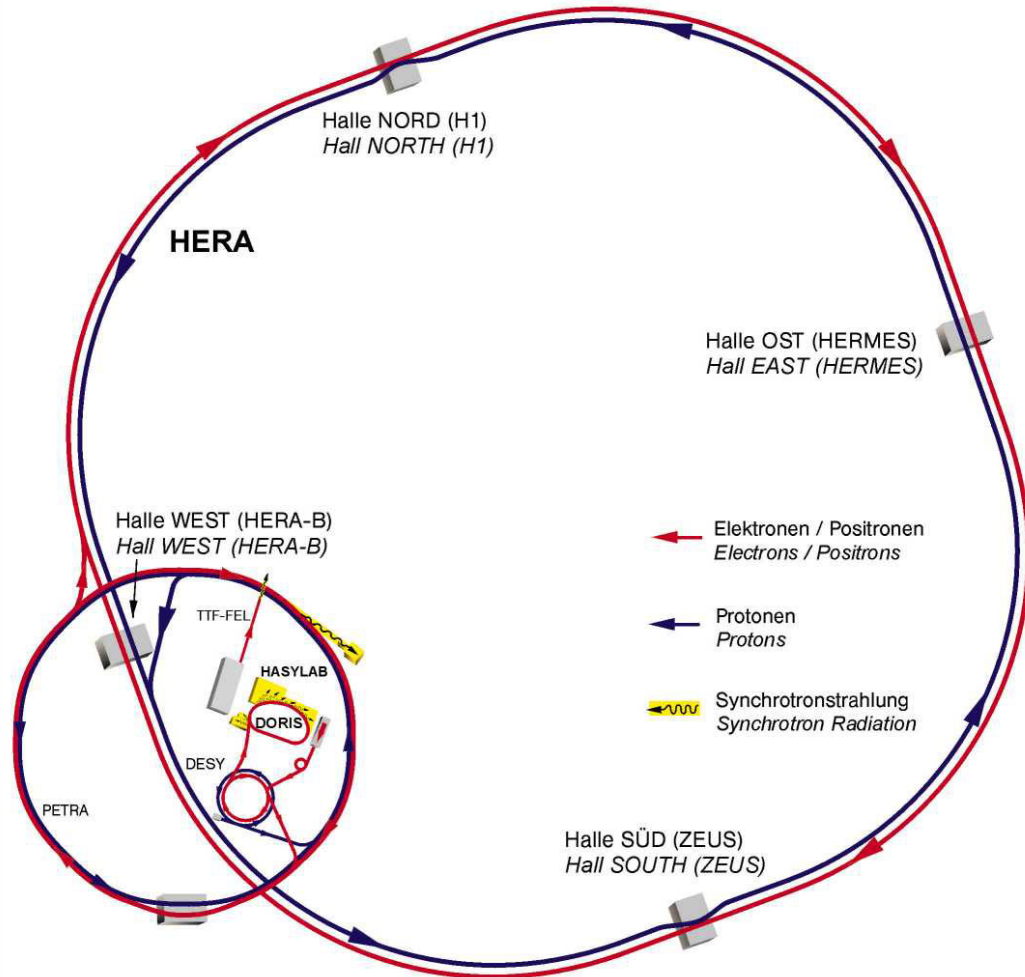


Outline

Design of original HERA interaction region and luminosity upgrade (HERA II) IR

- Design considerations
- Optics
- Layout of Interaction Points
- HERA Parameters
- Special Magnets
- Synchrotron Radiation
- Conclusions - Present Status

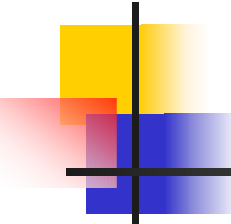
HERA Overview



Electron (positron) -
Proton Collider

Beam energies
protons 920 GeV
electrons 27.5 GeV

180 bunches
96 ns bunch spacing



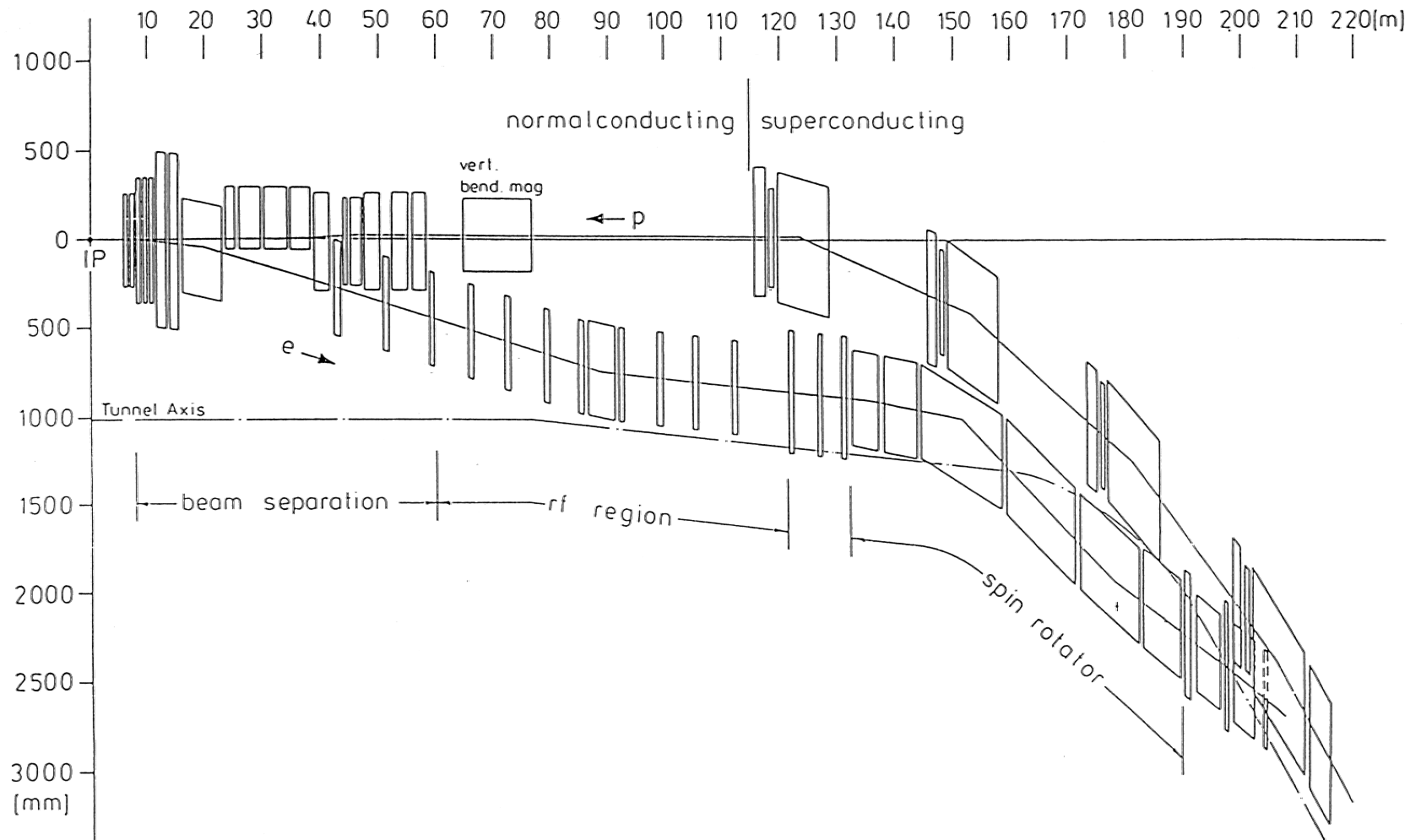
Design Considerations

- Very asymmetric beam energies
- High luminosity \Rightarrow low beta quads close to IP, high gradients (different focusing magnets for p and e beam)
- Early beam separation, use off-axis quad magnets (combined focussing and beam separation)
- Sufficient beam aperture

- Acceptable background conditions:
 - synchrotron radiation and
 - particle background
- Good detector acceptance
- Detector coverage down to small angles
- Little “dead” material in front detector components

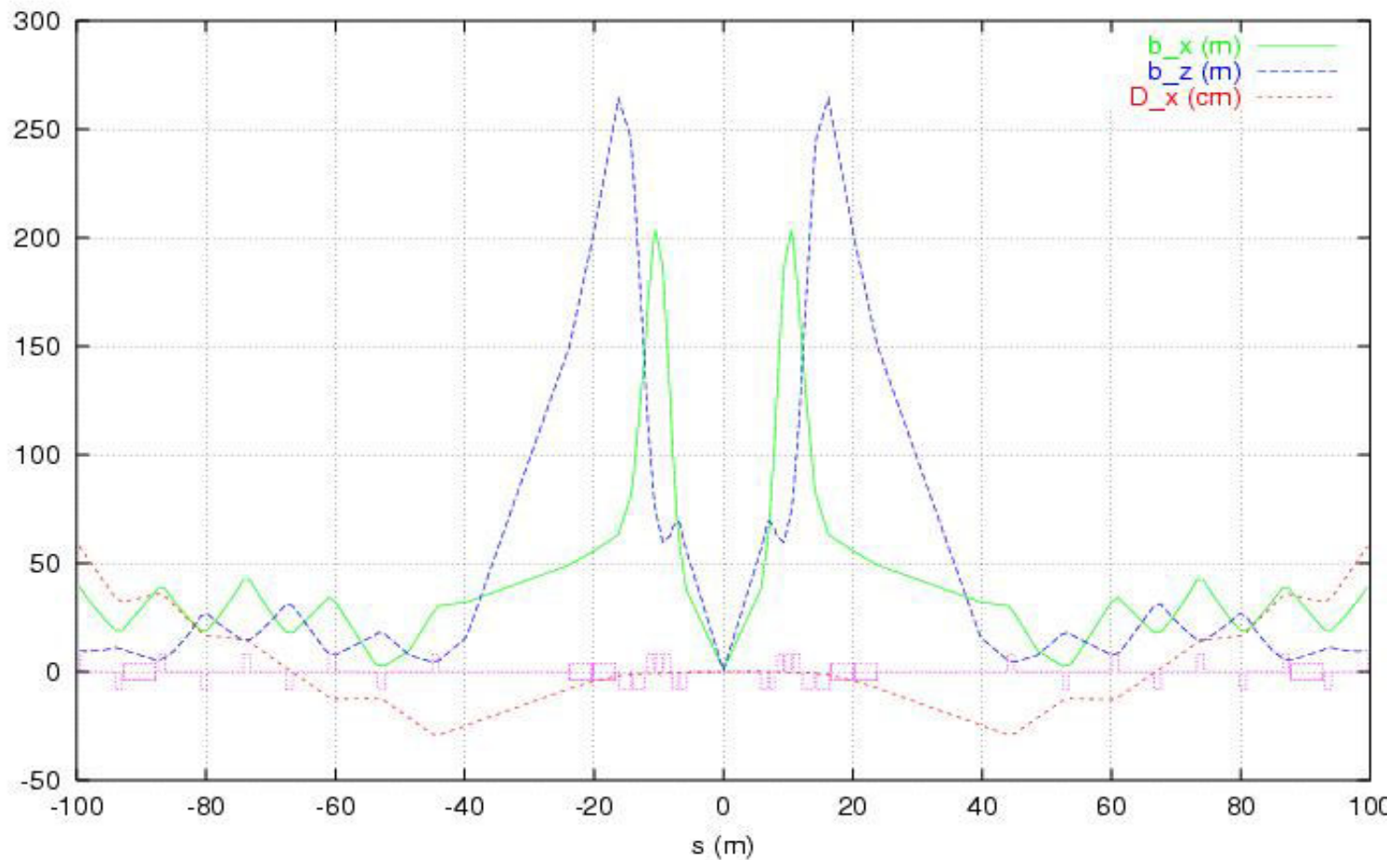
Layout of HERA I Straight Section

Top view of straight section (right side)



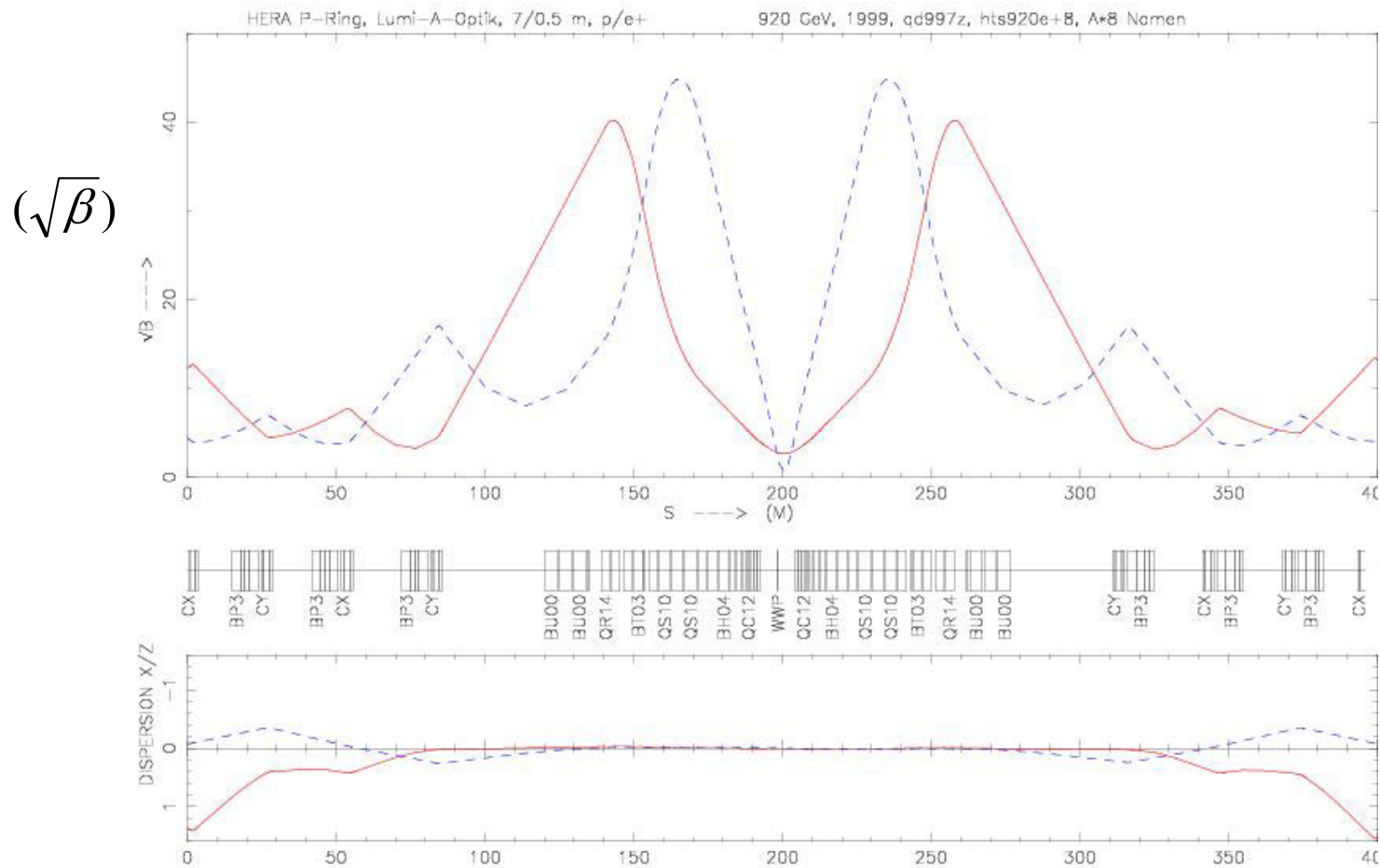
Optics of HERA I IP

β -function electron beam



Optics of HERA I IP

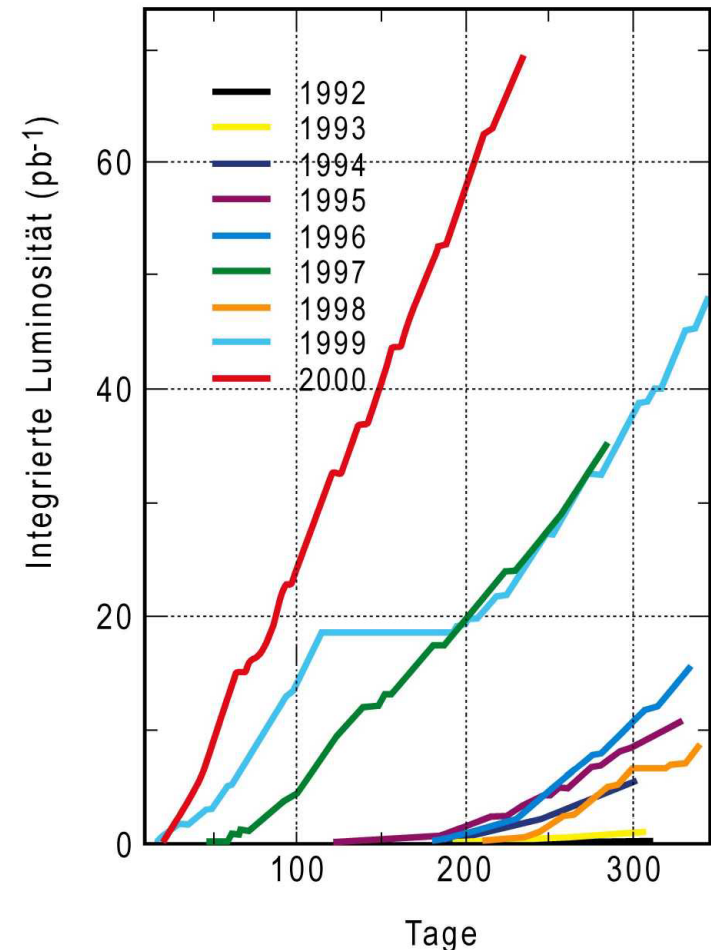
β -function and dispersion of proton beam



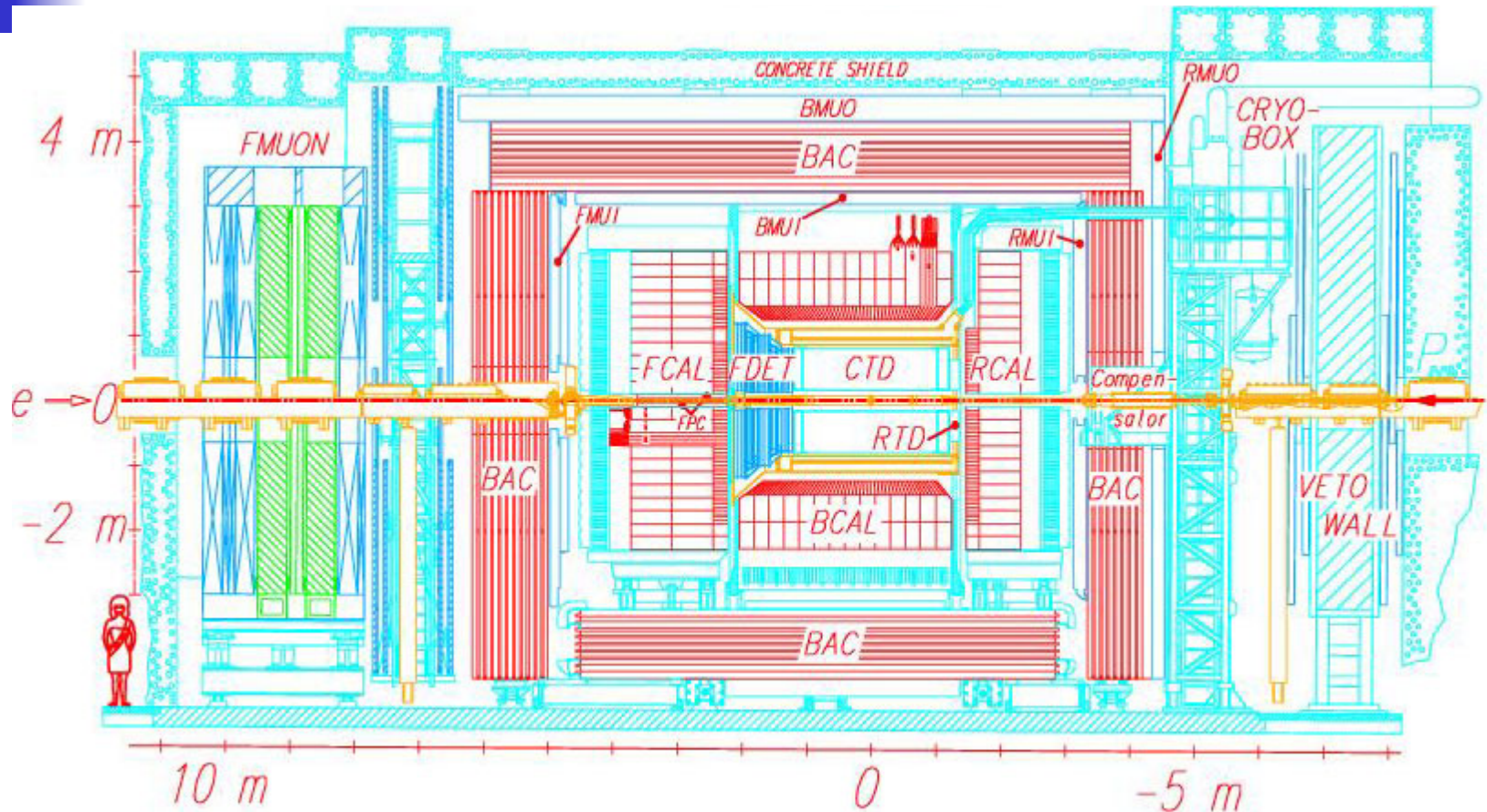
HERA I Parameters

		Design	2000
Beam energy (GeV)	p	820	920
	e	30	27.5
Beam emittance (nm)	p-hor/vert	5.72/5.72	4.1/4.1
	e-hor/vert	50/5	42/4
β^* function (m)	p-hor/vert	10/1	7/0.5
	e-hor/vert	2/1	1.0/0.6
Beam size (μm)	hor/vert	240/76	170/45
Aperture limit (sigma)	p-hor/vert	14/14	12/10
	e-hor/vert	>30	>15
Protons/bunch	(10^{11})	1	0.8
E beam current (mA)		58	50
Beam-beam tunes/shift	p-hor	.0016/.00035	.0019/.0003
	e-hor	0.02	0.0161
Luminosity ($10^{31} \text{ cm}^{-2} \text{ s}^{-1}$)		1.4	2.0

HERA-Luminosität 1992-2000



ZEUS Detector - HERA I IP

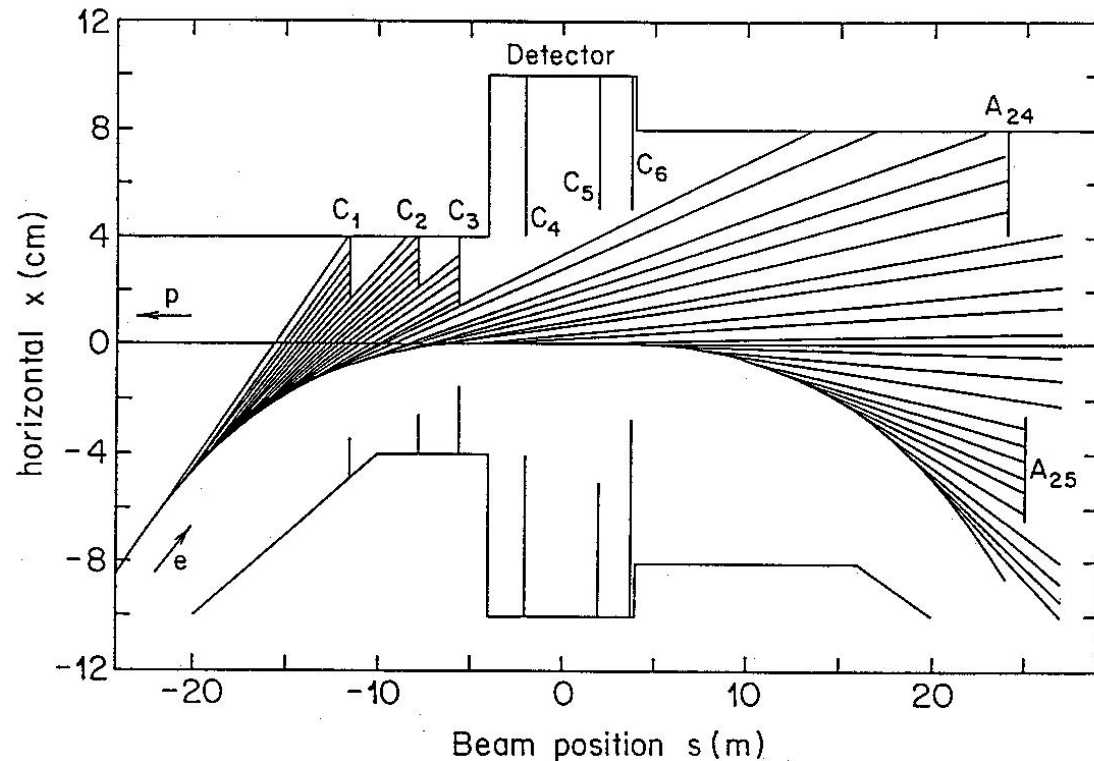


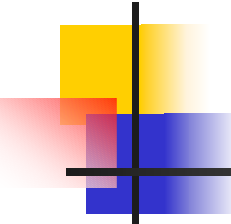
First HERA magnets (off-axis quads) at ± 5.8 m from IP
Calorimeter covers $>99.8\%$ of full solid angle
forward hole in calorimeter 6.3 cm diameter

Synchrotron Radiation - HERA I

Total power 6 kW (original design 18.6 kW at 35 GeV)
Critical energy 34 keV (original design 70 keV at 35 GeV)

- Detector shielded by 3 movable upstream collimators.
- Two fixed collimators near IP against back-scattering.
- Background conditions very low.





Luminosity Upgrade - HERA II

Increase luminosity by reducing beam size at IP

- Reduce beta functions of proton and electron beams at IP
- Reduce emittance of electron beam
(max. beam-beam tune-shift $\Delta\nu_y^e = 0.04$)

beta function

- Low beta quadrupole magnets as close as possible to IP
- Early beam separation
 - First magnet 1.7 m from IP (separation and focusing)
 - First proton quadrupole now at 11 m instead of 27 m from IP

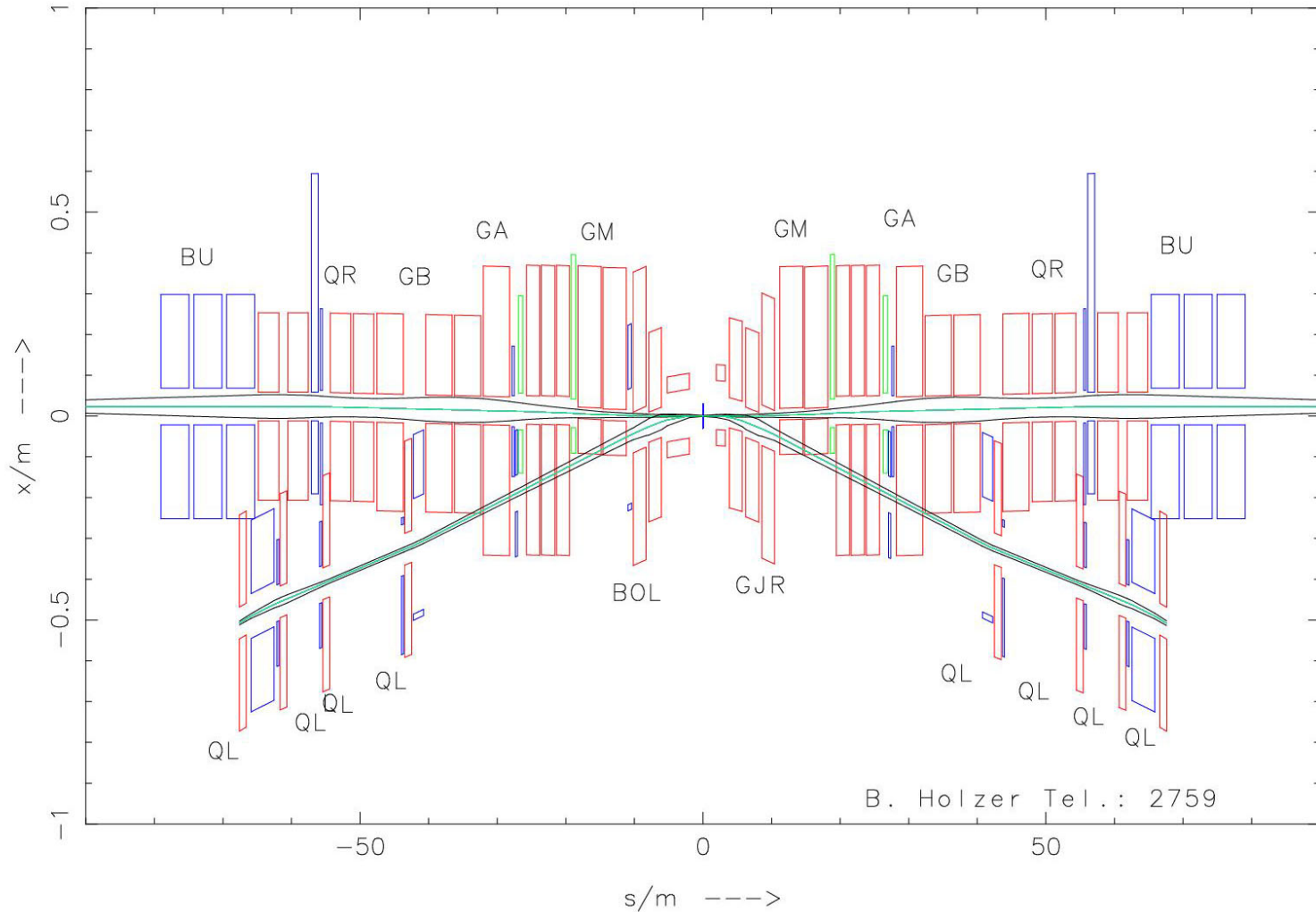
Electron beam emittance

- Electron machine lattice stronger focusing
- Phase advance per cell increased from 60° to 72° .

Constraints

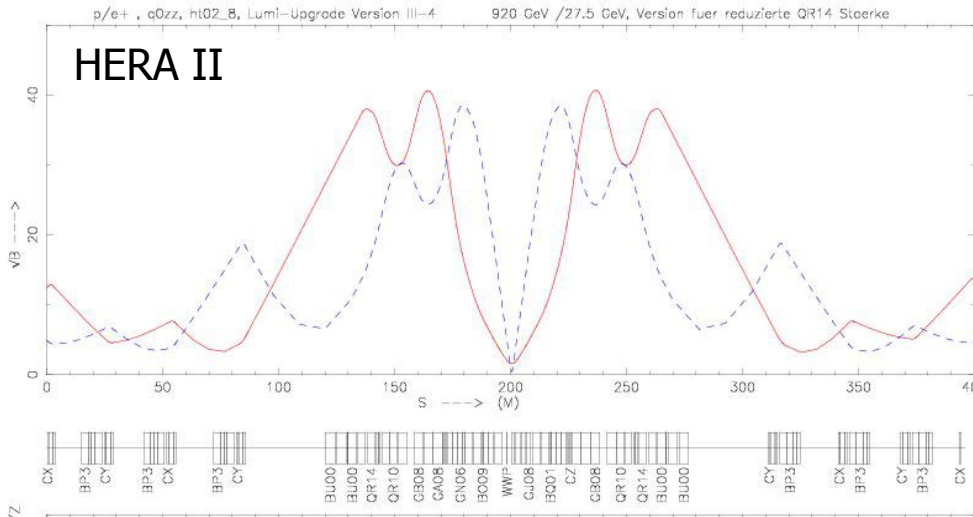
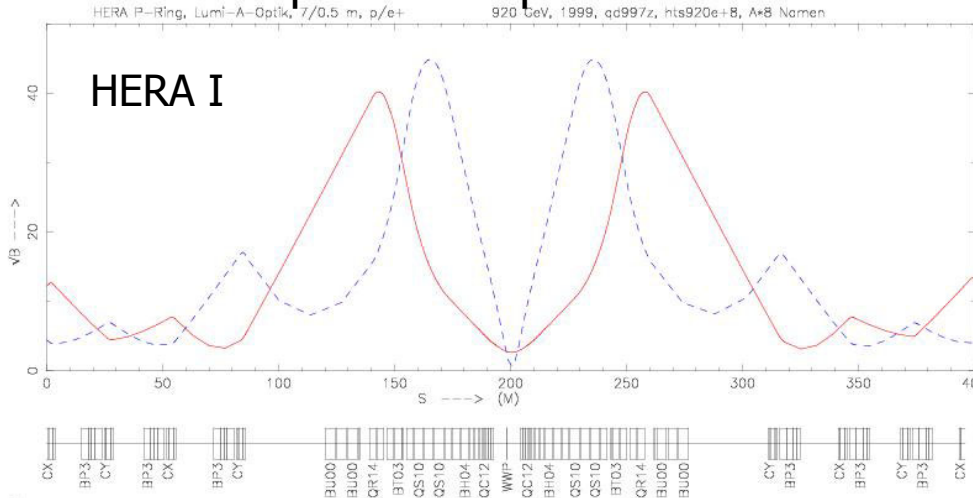
- Try to keep good forward and backward coverage of calorimeters
- No upstream synchrotron radiation collimators anymore
- Have to remove compensating solenoids

Layout of HERA II IR



Optics of HERA I and II IRs

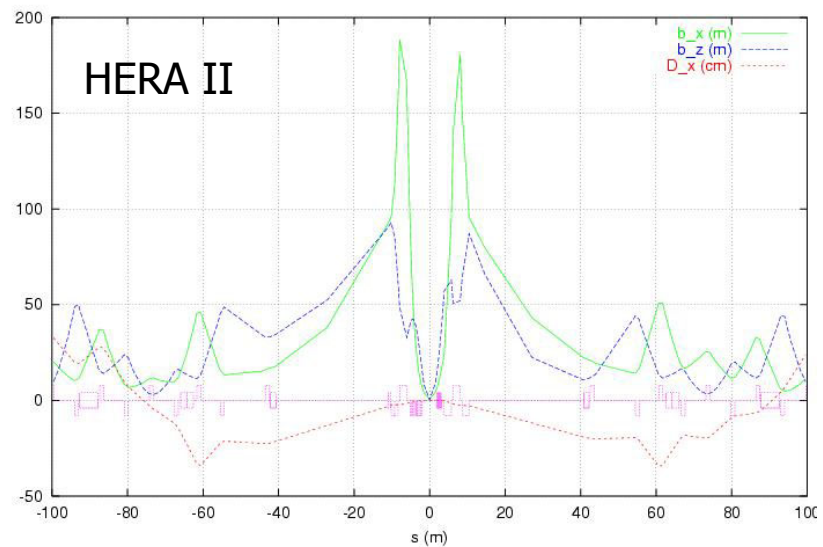
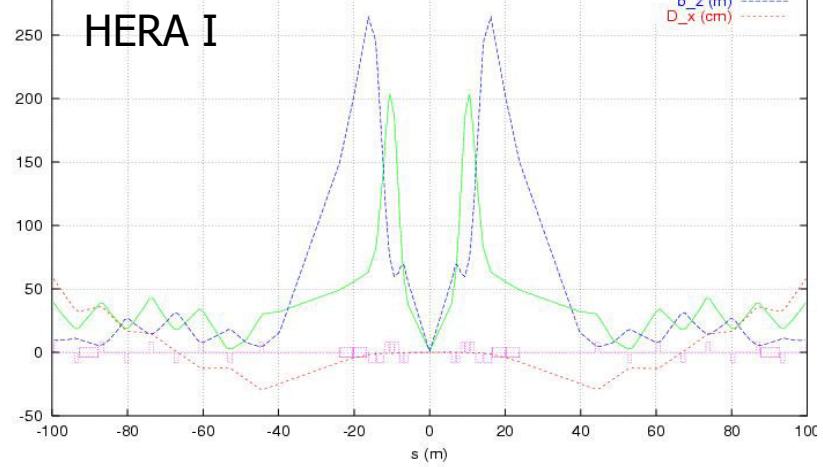
β -function proton beam



26.02.2002

HERA IR Design

β -function electron beam

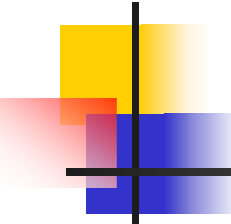


U. Schneekloth

13

Comparison HERA I and HERA II

		HERA I		HERA II	
		Design	2000	Design	exp. 2002
Beam energy (GeV)	p	820	920	920	920
	e	30	27.5	30	27.5
Beam emittance (nm)	p-hor/vert	5.72/5.72	4.1/4.1	5.1/5.1	4.1/4.1
	e-hor/vert	50/5	42/4	22/3.5	21/3.5
β^* function (m)	p-hor/vert	10/1	7/0.5	2.45/0.18	2.45/0.18
	e-hor/vert	2/1	1.0/0.6	0.60/0.26	0.60/0.26
Beam size (μm)	hor/vert	240/76	170/45	112/30	100/27
Aperture limit (sigma)	p-hor/vert	14/14	12/10	12/12	12/12
	e-hor/vert	>30	>15	20	20
Protons/bunch	(10^{11})	1	0.8	1	0.7
E beam current	(mA)	58	50	58	50
Beam-beam tuneshift	p-hor	.0016/.00035	.0019/.0003	.0033/.0005	.003/.0004
	e-hor	0.02	0.0161	0.0291	0.0278
Luminosity	($10^{31} \text{ cm}^{-2} \text{ s}^{-1}$)	1.4	2.0	7.3	5.1



Special Magnets for new IR

Super-conducting magnets

- 1.7m from IP
- Increased beam aperture
- Higher gradients possible
- Combined function magnet: several coils inside magnet
- Good field quality
- Very limited space
- More compact than normal conducting magnets
- Inside detector fields

Final design and manufacturing BNL

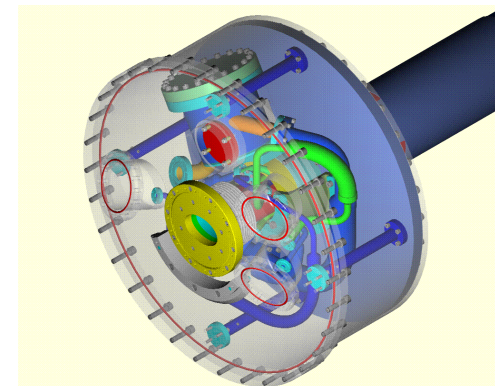
Normal conducting magnets

- 6 types of magnets
- New type of septum magnet: half quad/mirror plate with triangular cutout
- High gradients (30 T/m)
- Good field quality $\Delta B/B$ 10^{-4}
- Relatively large power

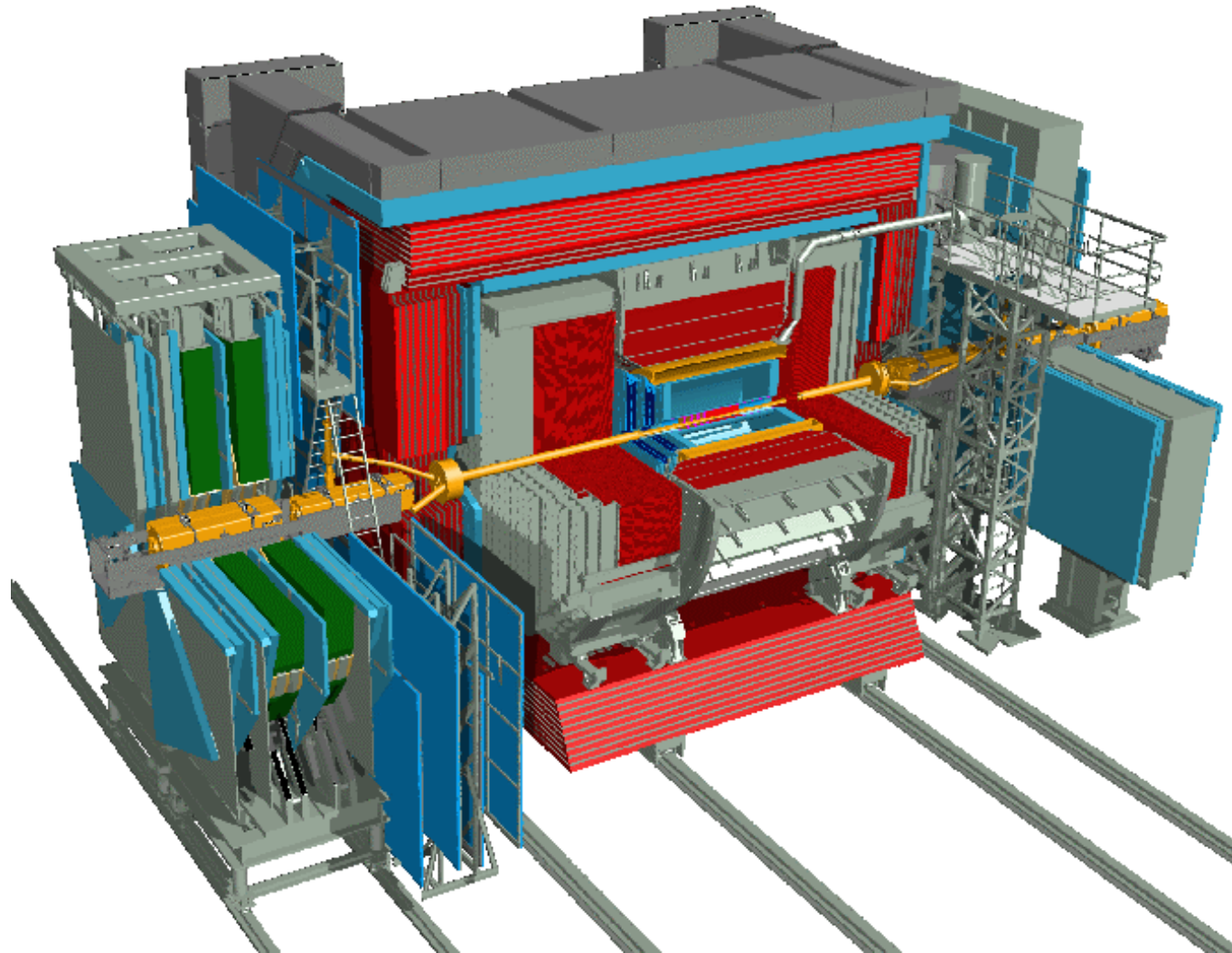
Final design and manufacturing
Efremov Institute, St.Petersburg

Superconducting Magnets (BNL)

		GO	GG
Quadrupole	Gradient	<i>13 T/m</i>	<i>3.5 T/m</i>
	Current	<i>500 A</i>	<i>500 A</i>
	Layers	<i>3</i>	<i>1</i>
Dipole	Field	<i>.168 T</i>	<i>.3 T</i>
	Current	<i>500 A</i>	<i>300 A</i>
	Layers	<i>1</i>	<i>2</i>
Skew Quad	Gradient	<i>1.24 T/m</i>	<i>.54 T/m</i>
	Current	<i>150 A</i>	<i>37 A</i>
	Layers	<i>Half length</i>	<i>1</i>
Skew Dipole	Field	<i>.0876 T</i>	<i>.04 T</i>
	Current	<i>150 A</i>	<i>37 A</i>
	Layers	<i>Half length</i>	<i>1</i>
Sextupole	Field	<i>4 T/m²</i>	<i>3 T/m²</i>
	Current	<i>20 A</i>	<i>20 A</i>
	Layers	<i>1</i>	<i>1</i>



ZEUS Detector - HERA II IP



GO Magnet installed in ZEUS



Normal Conducting Magnet (Efremov)

Special septum magnet (half-quadrupole)

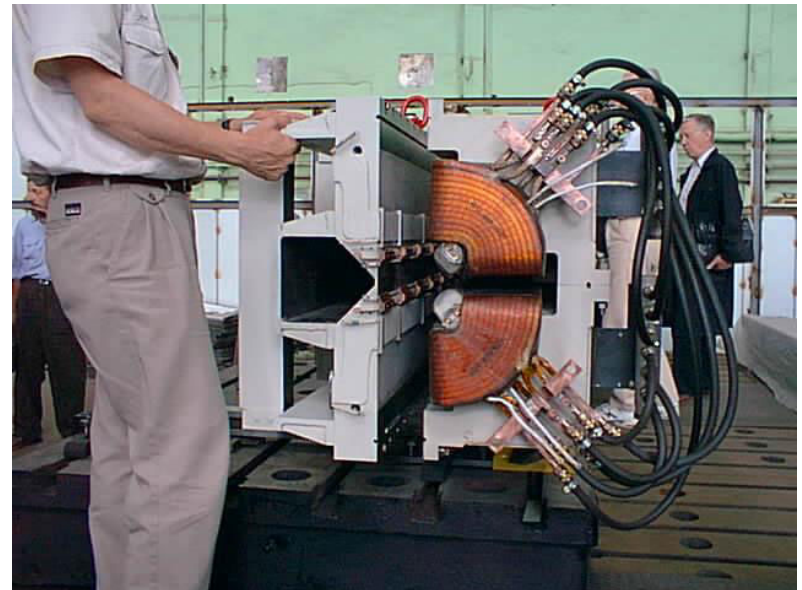
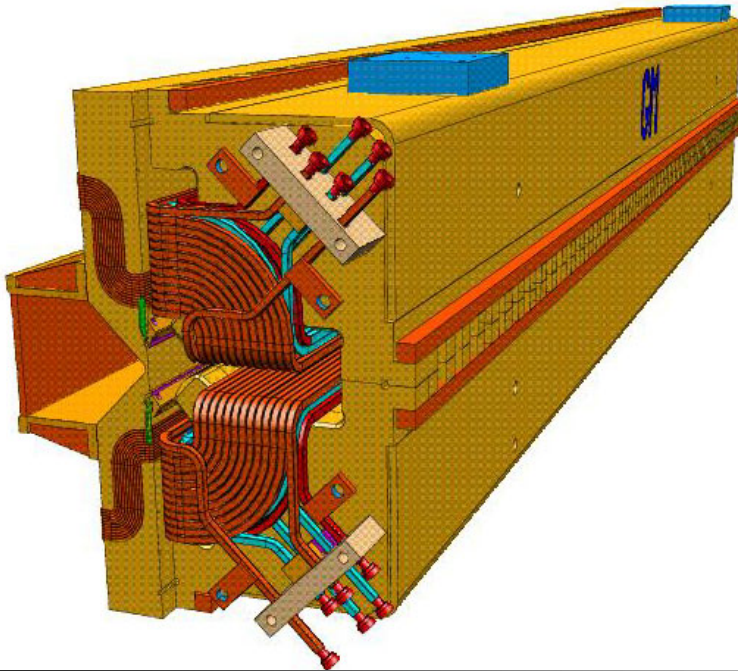
Function: focussing of proton beam, gradient 25 T/m

Mirror plate with triangular cutout for electron beam pipe

Beam separation 60 mm

Stray field (e-beam) < 10 G, field quality $< 3 \cdot 10^{-4}$ at 25mm

Two correction coils



Synchrotron Radiation - HERA II

Total power 18kW (26kW at 30GeV)

Critical energy up to 115 keV (150 at 30 GeV)

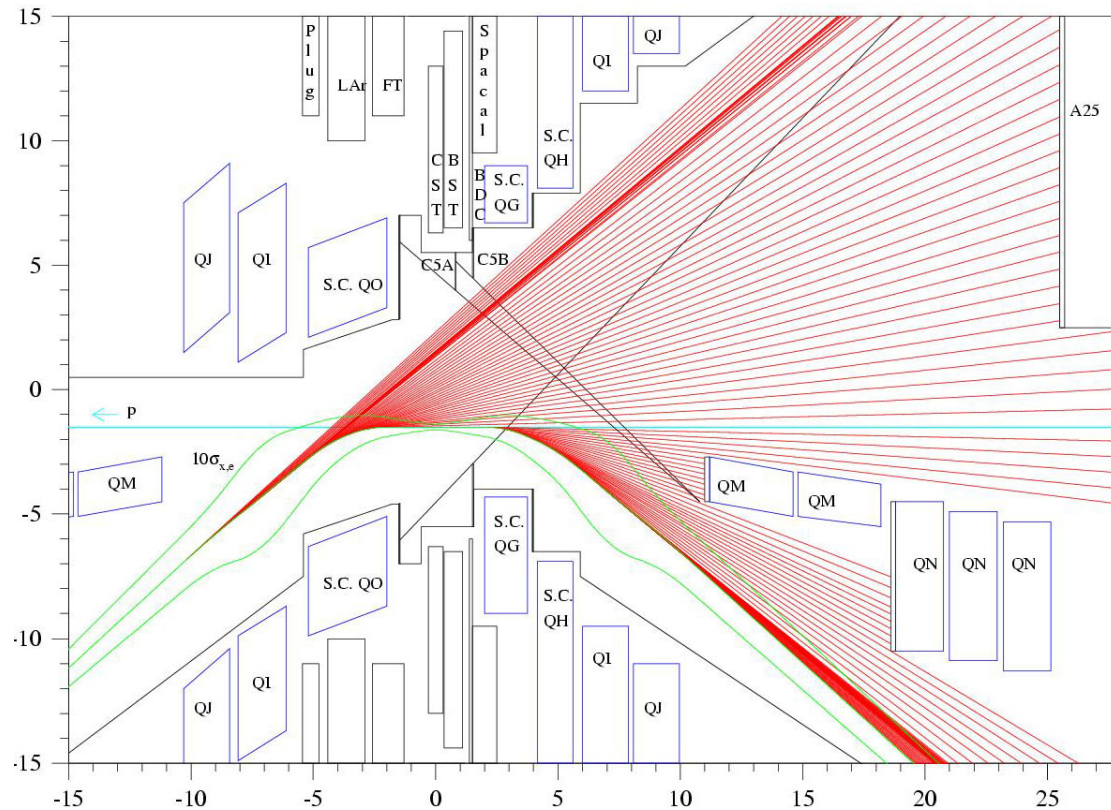
“No” upstream collimators

Radiation fan must pass through IR

Main background source: back-scattering from absorbers 11 to 27 m right of IP

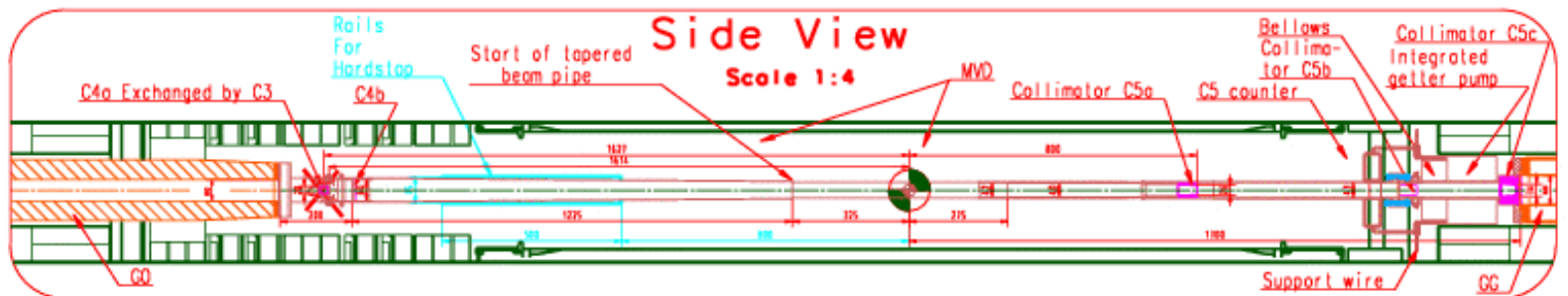
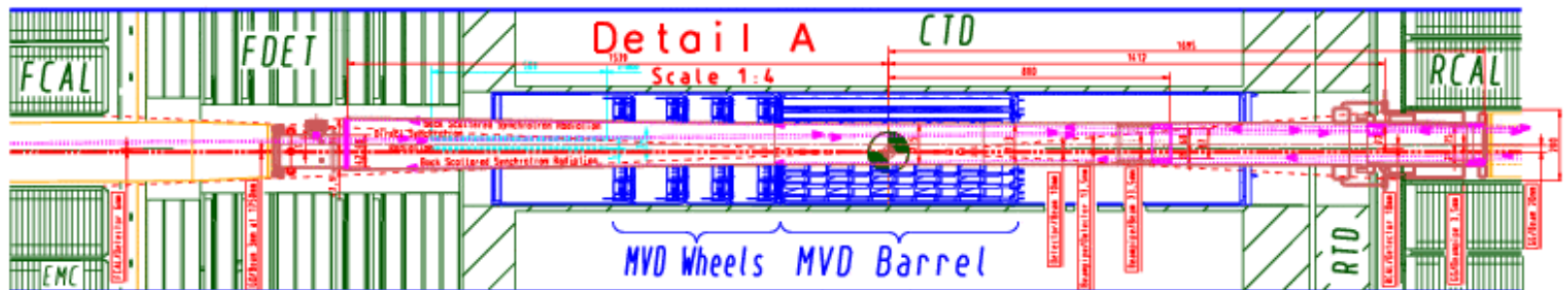
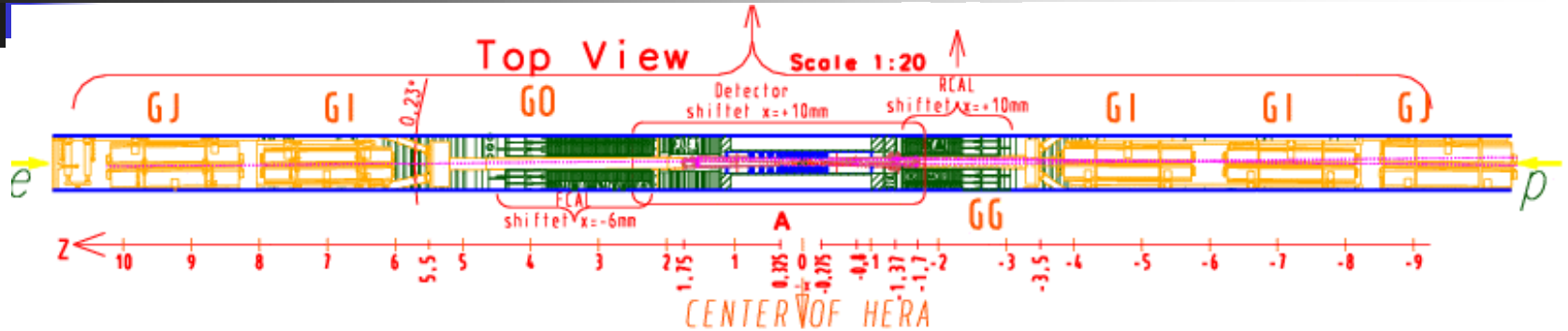
Small central beam pipe

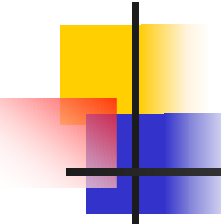
Top view of interaction region



Details: talk by D.Pitzl

Layout of Interaction Region





Conclusions - Present Status

HERA I IR: First magnets at 5.8 m from IP

HERA II IR:

- Magnets as close as possible to IP (1.7 m)
- No dipole magnet for beam separation
 - different electron and positron orbits
- Special magnets: super-conducting magnets, septum magnet, normal conducting magnets with high gradients
- No free space between magnets
- Big effort: 10 month shutdown for installation

Status

- Installation completed July 2001
- HERA re-commissioning started in August 2001
- Achieved design specific luminosity (with low currents)
- Synchrotron radiation background too high to turn on central drift chambers
- Need additional collimators, installation February/March

The PEP-II Interaction Region



BABARTM



U. Wienands, SLAC-PEP II

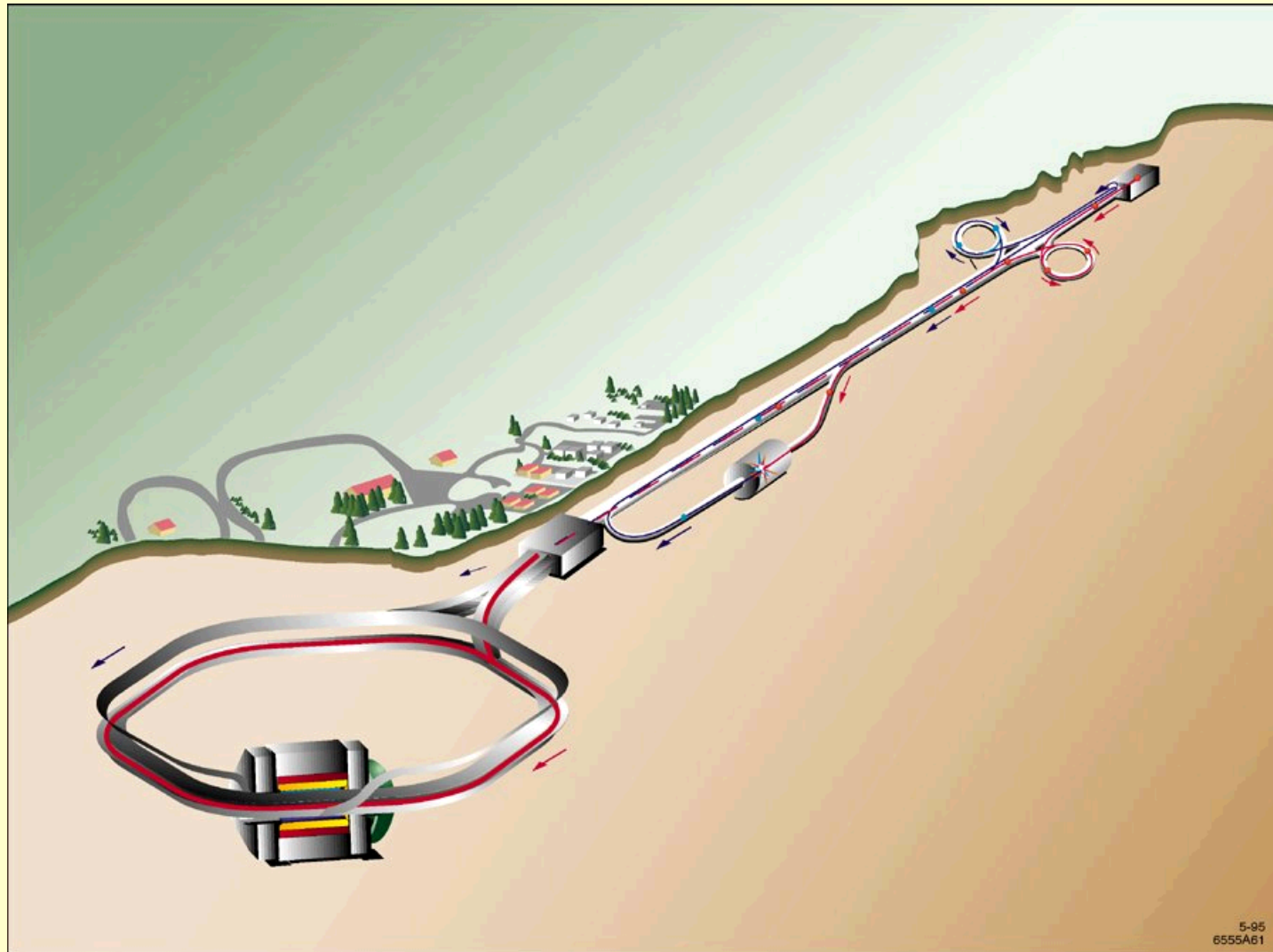
Outline of Talk

- PEP Overview
- IR Design Parameters & Lattices
- IR layout & components
- Some Performance Issues
- Summary

Acknowledgments

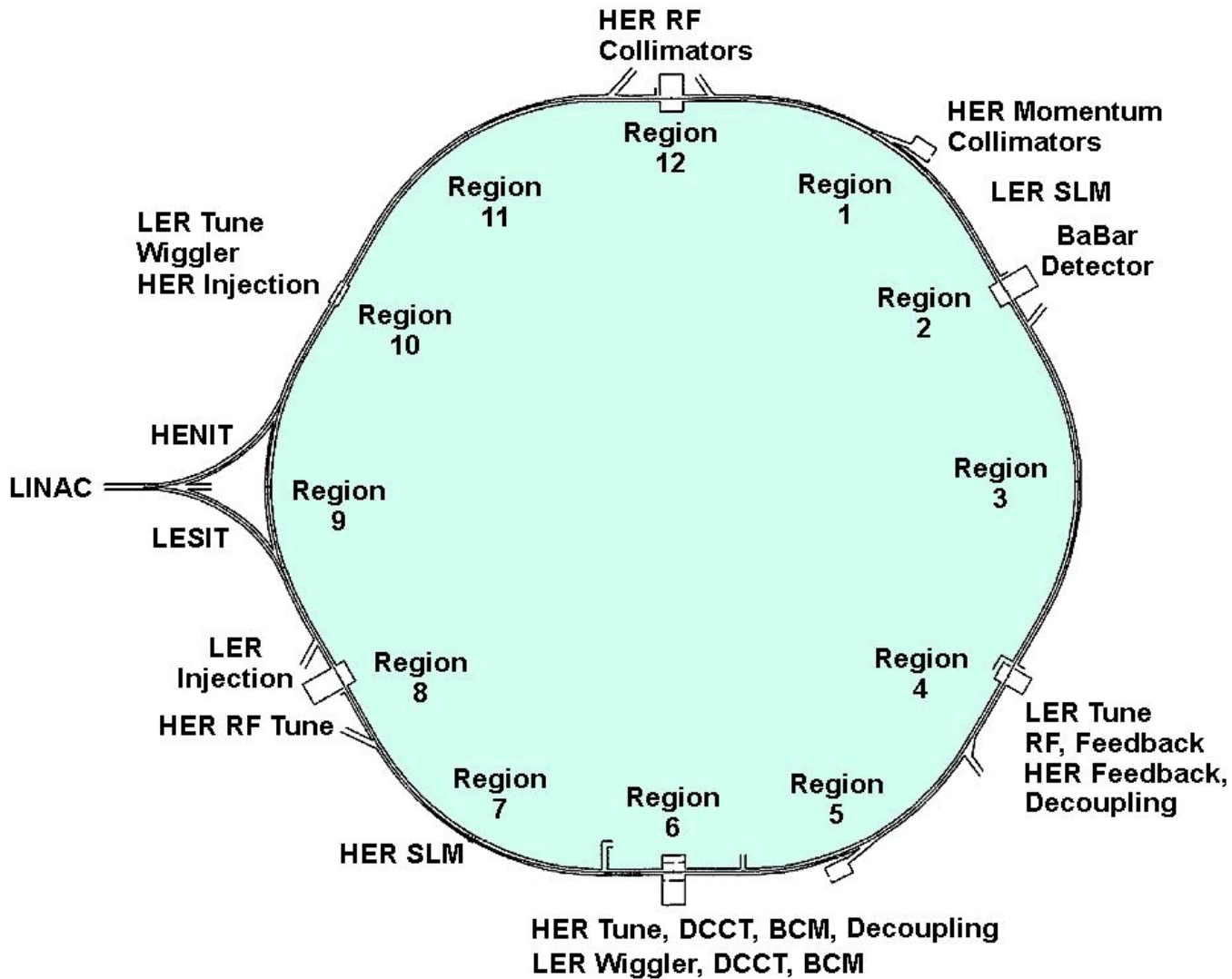
- Mike Sullivan, Stan Ecklund and Witold Kozanecki, who gave me numerous slides.
- Stan Ecklund, Mike Sullivan and Hobey DeStaebler were the leaders of the team that designed the fundamentals of the IR and guided the detailed hardware designs.

SLAC LINAC and PEP-II Ring



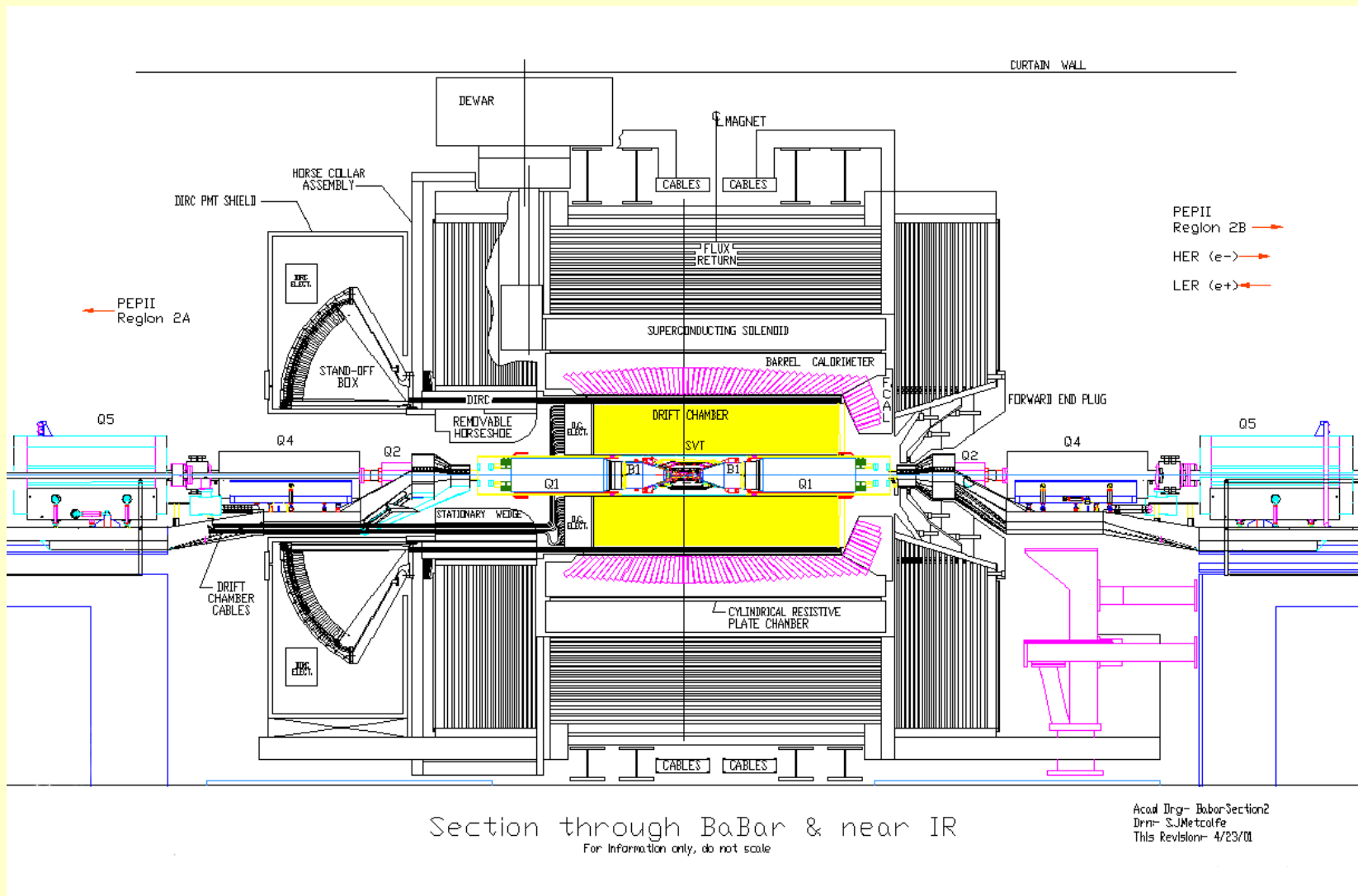
*U. Wienands, SLAC-PEP-II
EICAW IR talk ppt, 26-Feb-02*

PEP-II Ring



*U. Wienands, SLAC-PEP-II
EICAW IR talk ppt, 26-Feb-02*

The BABAR Detector



*U. Wienands, SLAC-PEP-II
EICAW IR talk ppt, 26-Feb-02*

PEP-II Parameters

	Design		Achieved (delivery)	
Energies e⁻ / e⁺ (GeV)	8.973	3.119		
Currents e⁻ / e⁺ (A)	0.75	2.14	0.98	1.68
Single beam currents (A)			0.95	2.10
Number of bunches		1658		762
Bunch currents e⁻ / e⁺ (mA)	0.45	1.29	1.24	2.09
Bunch spacing (m)		1.26		2.52
IP spot size σ_x^* / σ_y^* (μm)	155	4.7	147	5
Luminosity ($\times 10^{33}/\text{cm}^2/\text{sec}$)		3.0		4.51
Tune shift horiz. e⁻ / e⁺	0.03	0.03	0.059	0.069
Tune shift vert. e⁻ / e⁺	0.03	0.03	0.027	0.055
Integrated lumi. / 3 shifts (pb^{-1})		135		308
Integrated lumi. / week (pb^{-1})		785		1836
Integrated lumi. / 7 days (pb^{-1})		785		1865
Integrated lumi. / month (fb^{-1})		3.3		6.35
Beam crossing angle		0 (head-on)		0 (head-on)

*U. Wienands, SLAC-PEP-II
EICAW IR talk ppt, 26-Feb-02*

IR Design Parameters

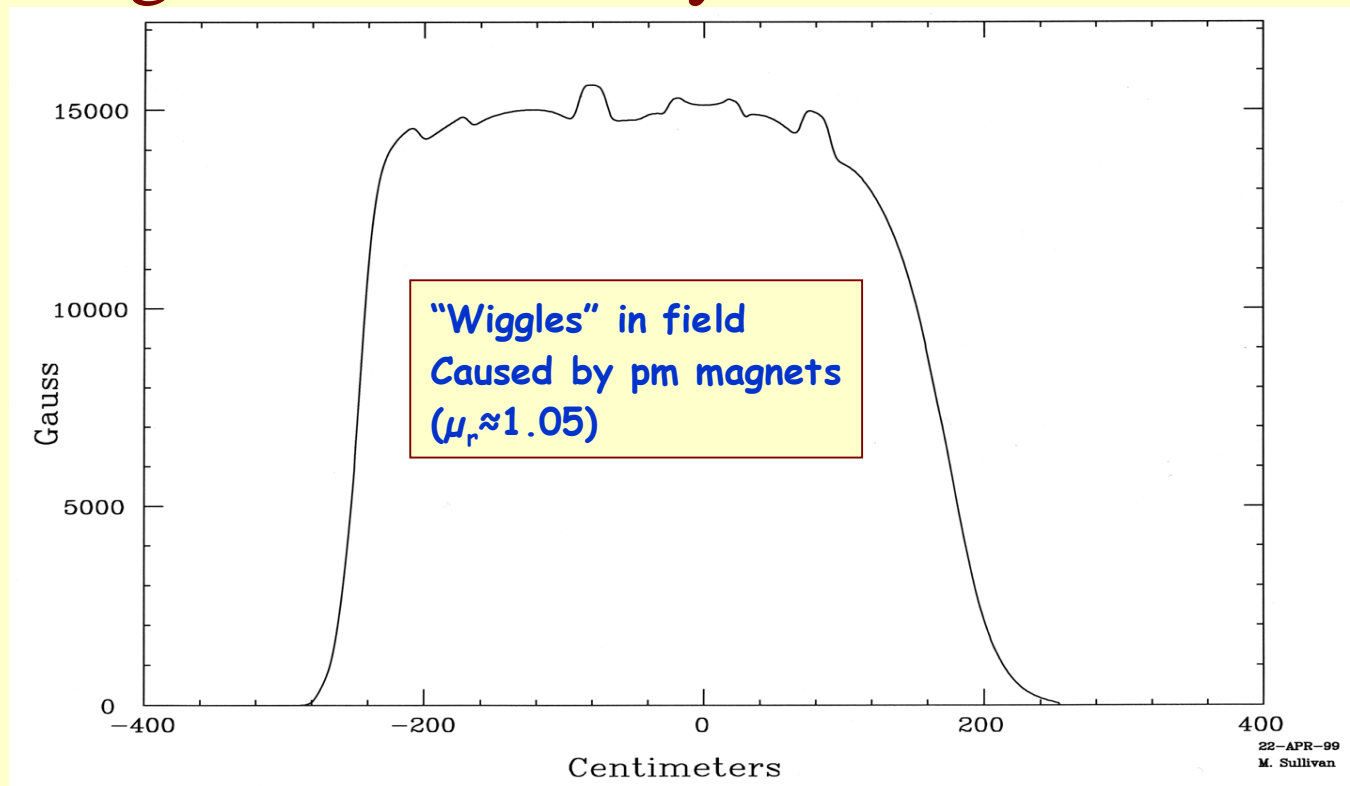
- Head-on collisions
- $\beta^*_{x/y} = 50/1.5$ cm
with room to lower to 33/1.0 cm
- Min. bunch spacing 1.25 m
- 1:3 ratio of beam energies
- Min. unobstructed forward angle 350 mr

IR Design Parameters (cont'd)

- Energy ratio \Rightarrow Use magnetic separation (B1)
- Bunch spacing \Rightarrow separating dipoles within detector field (avoid parasitic x-ings)
- Low β^* \Rightarrow 1st D-quad within detector field, common to both beams
- Separation \Rightarrow next (F)-quad *not* common (LER only)

The BABAR Solenoid

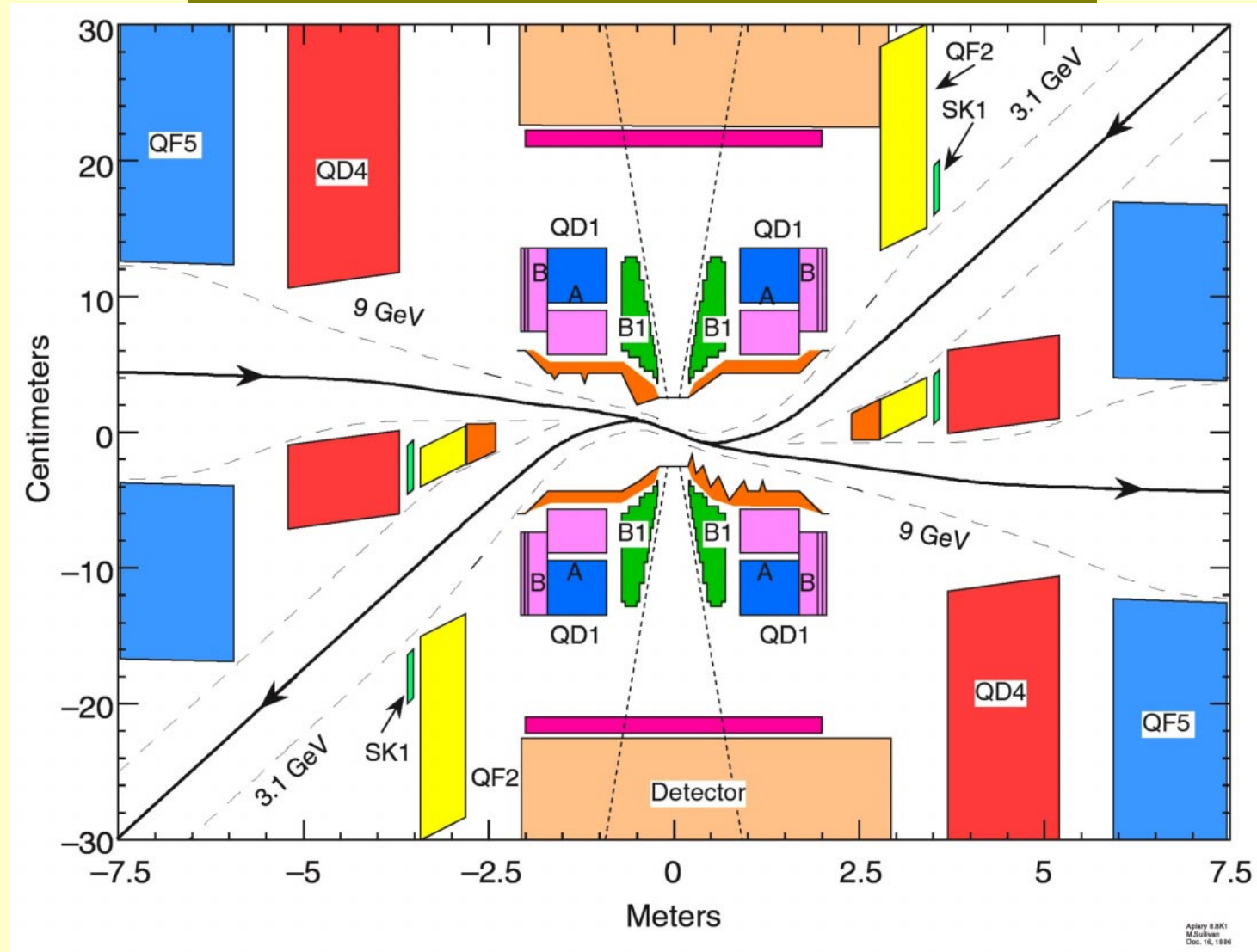
- About 5 Tm of B -field
- End fields clamped by shielding plugs
- Yawed against IR orbit by 16.8 mr



*U. Wienands, SLAC-PEP-II
EICAW IR talk ppt, 26-Feb-02*

PEP-II IR Schematic

M. Sullivan

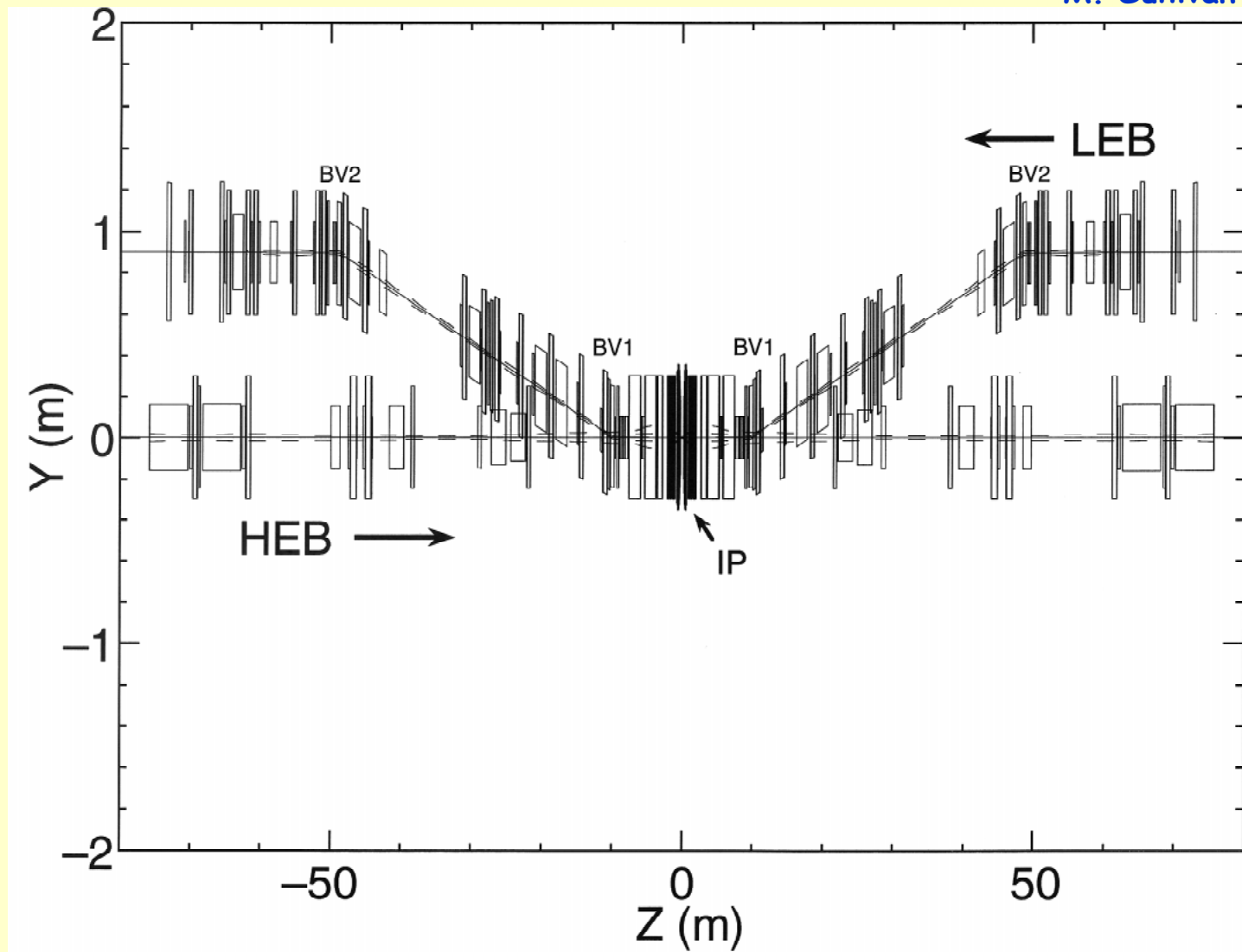


Aslery 8 BK1
M.Sullivan
Dec. 16, 1996

U. Wienands, SLAC-PEP-II
EICAW IR talk ppt, 26-Feb-02

Interaction Straight Side-View

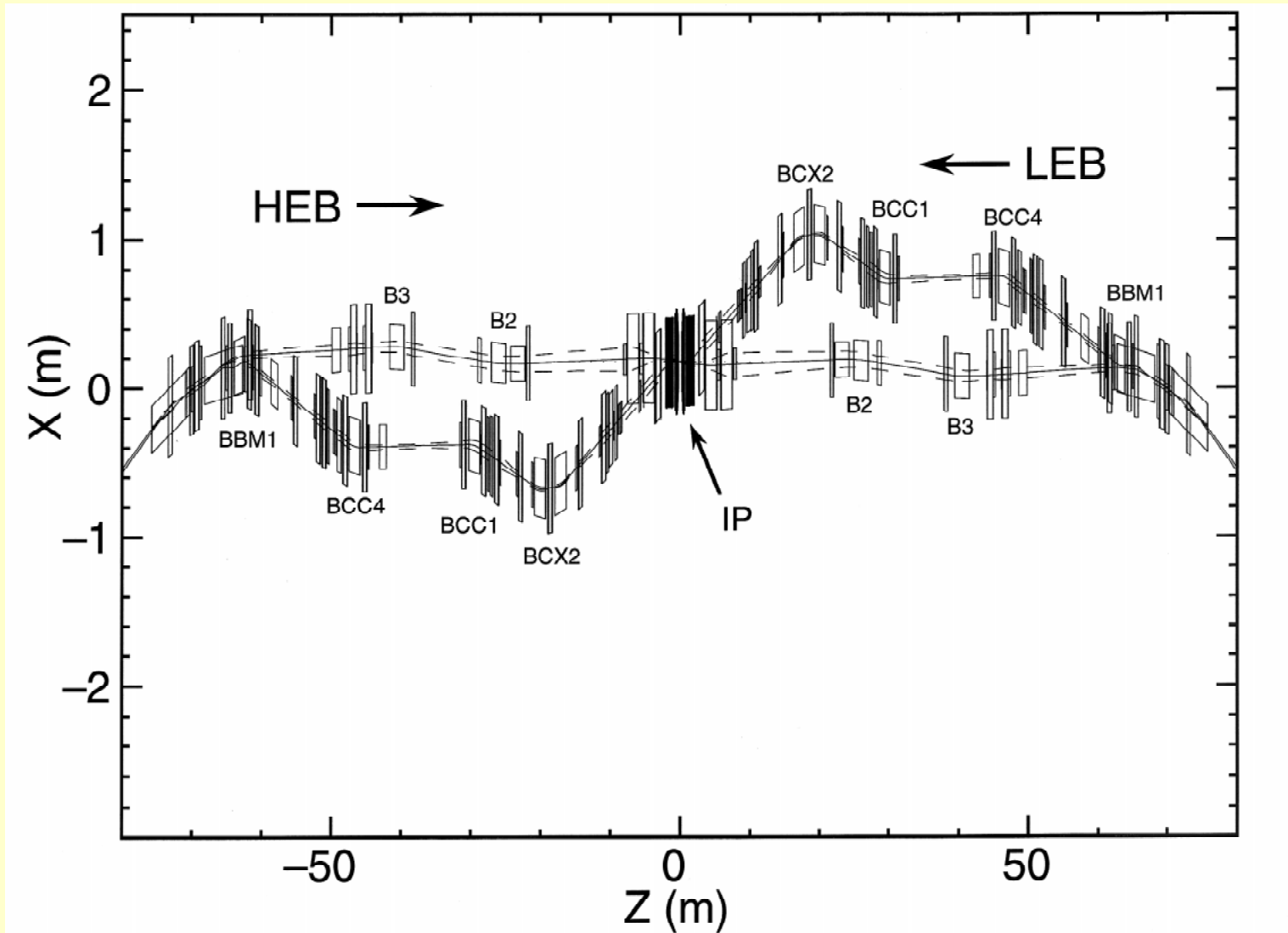
M. Sullivan



*U. Wienands, SLAC-PEP-II
EICAW IR talk ppt, 26-Feb-02*

Interaction Straight Top-View

M. Sullivan

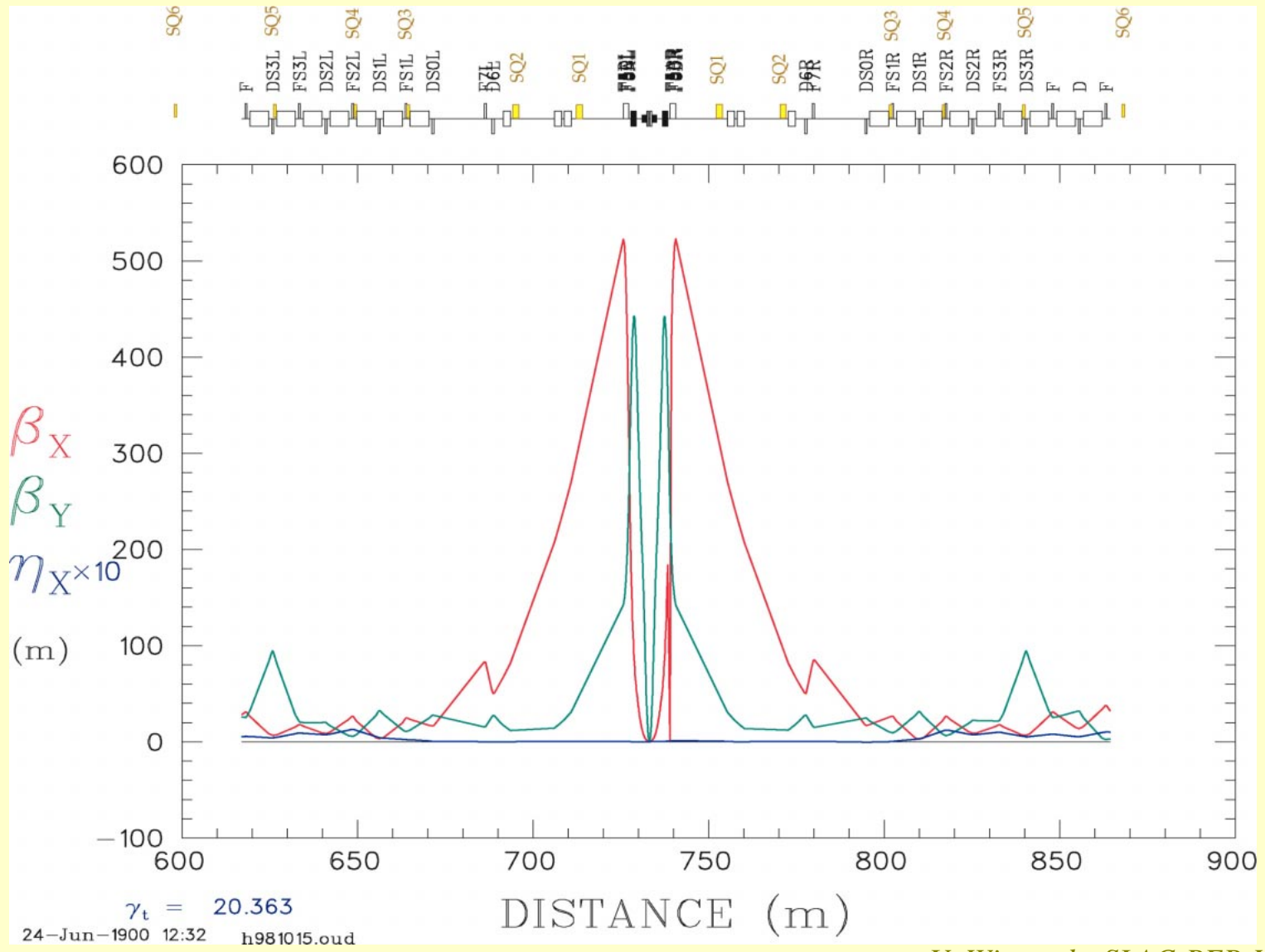


*U. Wienands, SLAC-PEP-II
EICAW IR talk ppt, 26-Feb-02*

HER IR Lattice

- Relatively “standard” doublet-focusing IR.
- $\hat{\beta} \approx 500$ m in insertion quadrupoles.
- Low-field dipoles match dispersion, stop s.r. fans from arc, sweep out some lost particles.

PEP-II HER IR Lattice

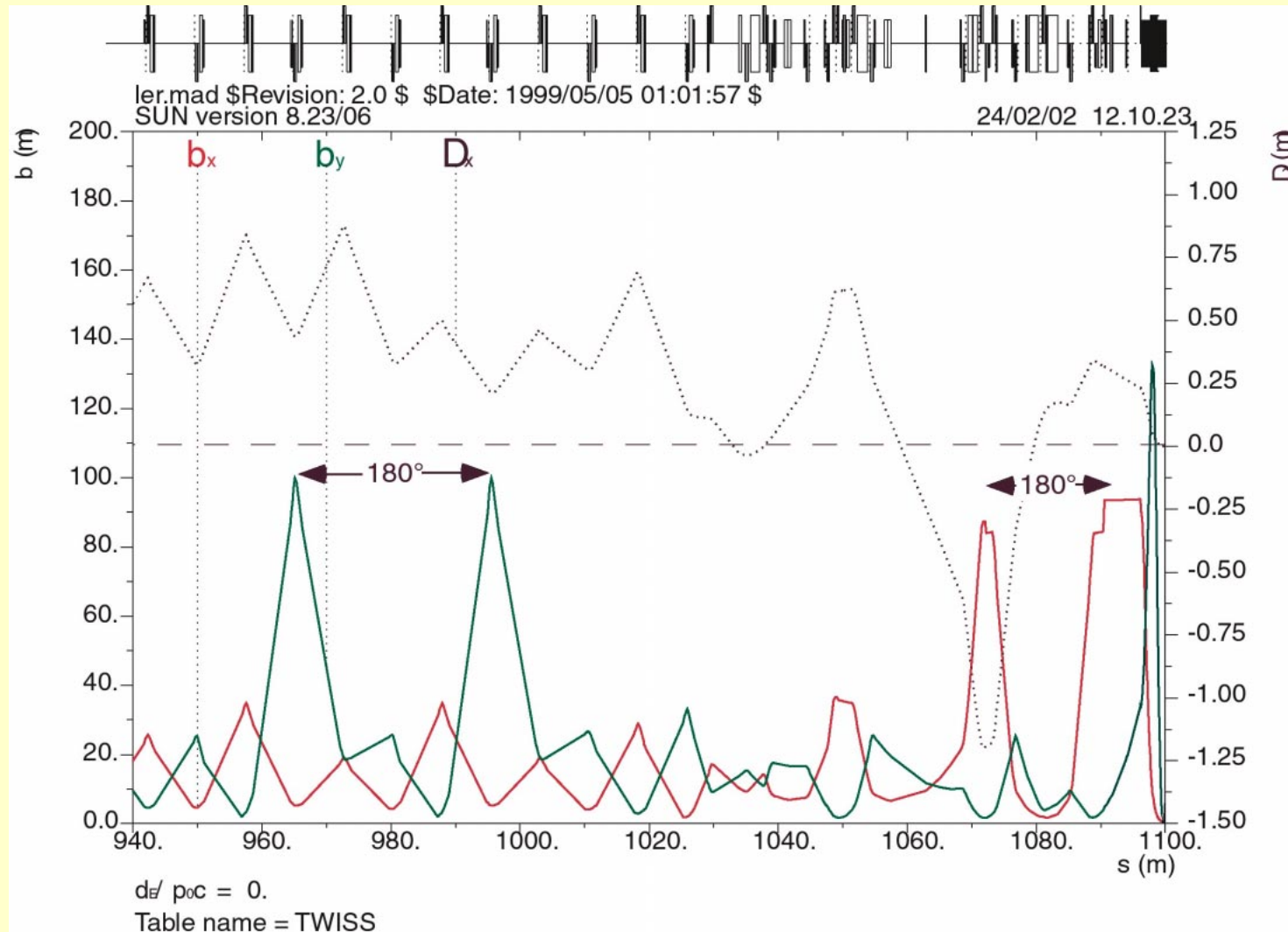


*U. Wienands, SLAC-PEP-II
 EICAW IR talk ppt, 26-Feb-02*

LER IR Lattice

- Local chromaticity compensation.
Use dispersion from B1 to achieve this,
plus 2 sextupoles (7.7T/m) 180° apart.
- $\beta \approx 100$ m in insertion quads & at sexts.
- 3-d geometry to meet HER beam.
- Skew quad component at QF2
part of solenoid compensation
=> use permanent-magnet ring.

PEP-II LER IR Lattice



*U. Wienands, SLAC-PEP-II
EICAW IR talk ppt, 26-Feb-02*

Beam-Stay-Clear

- Do not want to scrape close to detector
- BSC formula around the ring

$$\text{BSC} = 12\sigma + \text{c.o.d.}, \quad \text{or}$$

$$\text{BSC} = 12 \sqrt{\sigma^2 + (\eta\delta)^2} + \text{c.o.d.}$$

- BSC formula within IR 2:

$$\text{BSC} = 15\sigma + \text{c.o.d.}, \quad \text{or}$$

$$\text{BSC} = 15 \sqrt{\sigma^2 + (\eta\delta)^2} + \text{c.o.d.}$$

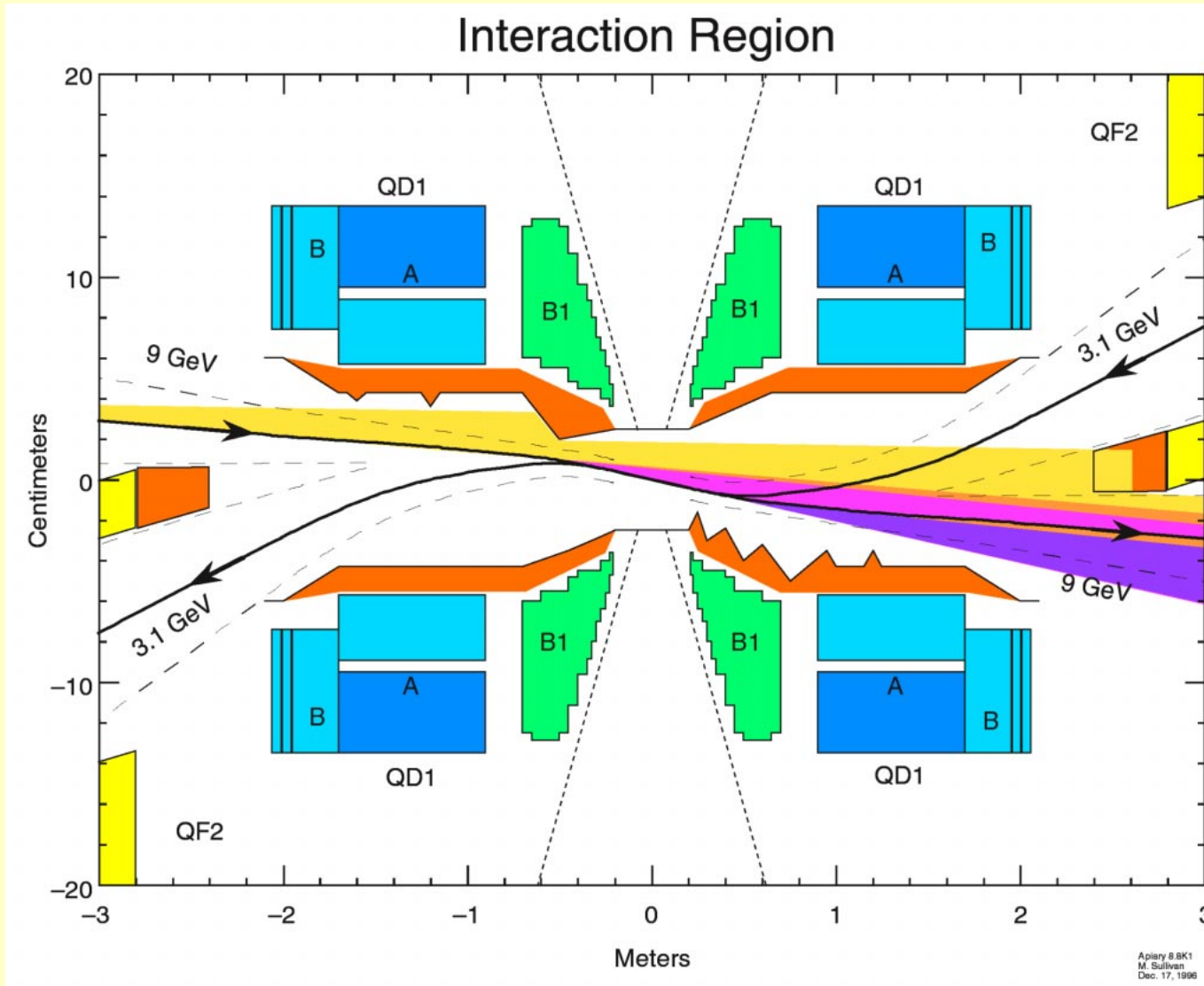
- (Although the c.o.d. in IR 2 is smaller than elsewhere)

S.R. Fans in the IR

- B1, the beam-separator, is the strongest dipole in the ring, $B_{\max} = 8.37$ kG.
- HEB fan generated is 56 kW, LEB fan, 20 kW from B1 and offset Q1 magnets (at 1 on 2.14 A). $\epsilon_c = 45$ keV (HEB), 5.3 keV (LEB)
- Most sr goes through the IP without interference, the remainder is absorbed by masks designed to protect detector acceptance from direct s.r. and scattered s.r.

PEP-II IR with HEB SR Fans

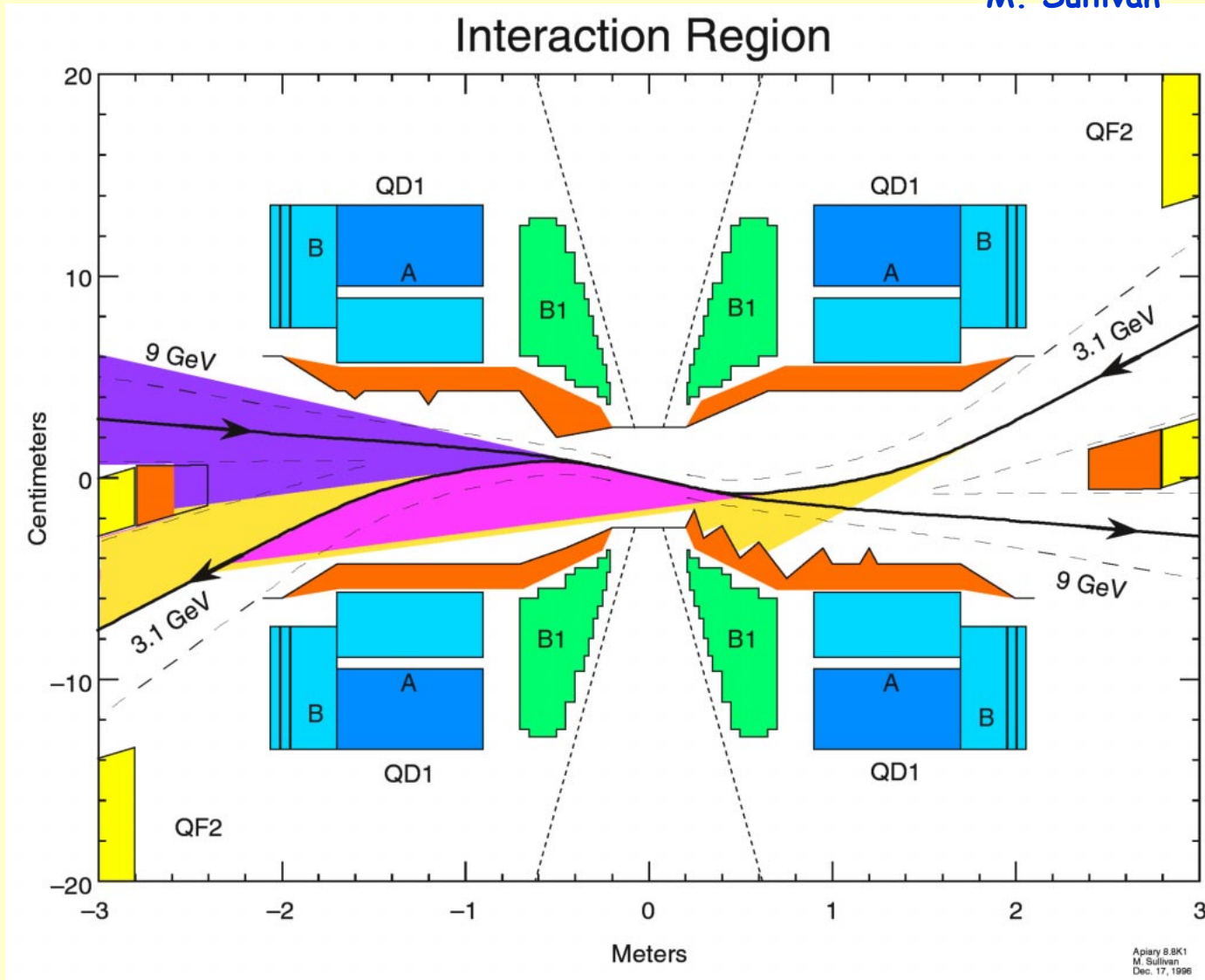
M. Sullivan



*U. Wienands, SLAC-PEP-II
EICAW IR talk ppt, 26-Feb-02*

PEP-II IR with LEB SR Fans

M. Sullivan



*U. Wienands, SLAC-PEP-II
EICAW IR talk ppt, 26-Feb-02*

Insertion Magnets

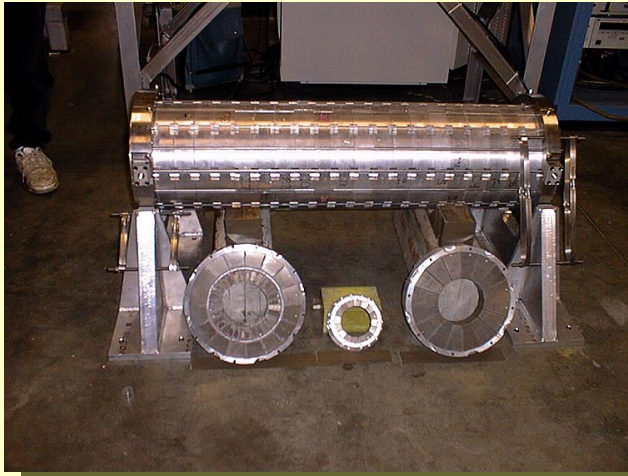
- PEP chose permanent magnets over s/c magnets because of time constraints.
- Due to high β , harmonics at 10^{-4} level.
- QD1a is combined quadrupole/dipole magnet.
- Rotatable magnet slice provides for skew-component adjustment.
- Significant detector field @ 1st Fe-Cu magnet
=> shaped mirror plate to counteract induced skew octupole

IR Magnet Details

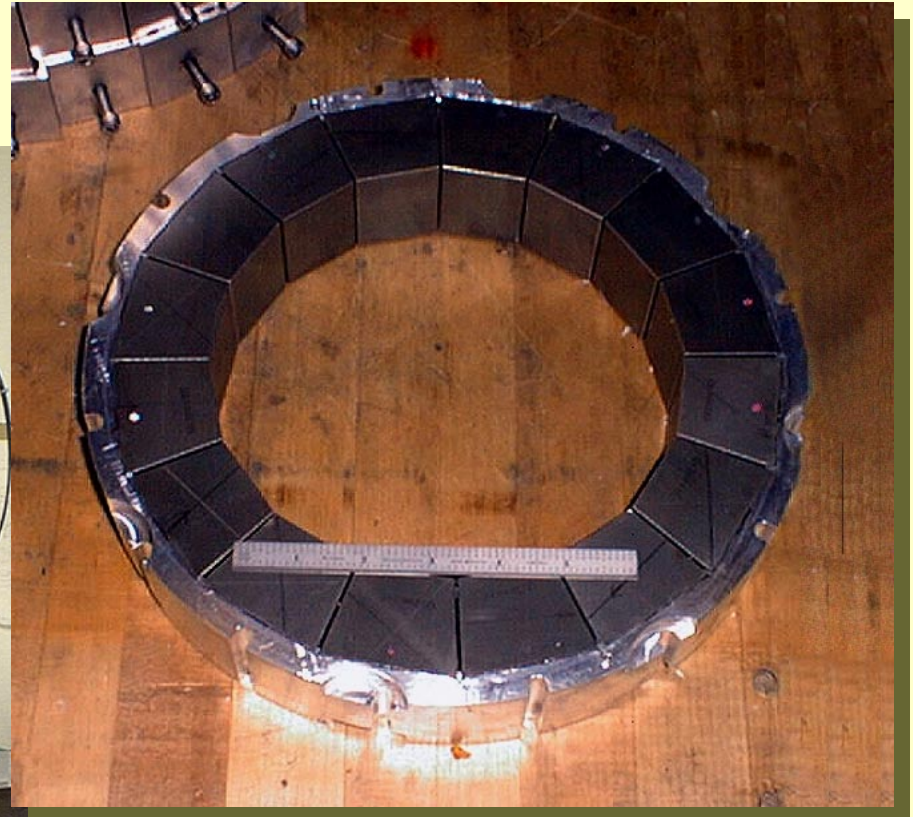
Magnet	From...To	Field	Aperture
	(cm)		(\emptyset ,cm)
B1	21.5...69.5	0.27...0.84 Tm	3.6...6
QD1	90...206	12.2...10.64 T/m + 0.35 T B_x	6...9
QF2	280...342	7.26 T/m (LER only)	9.56
QD4	350...520	7.57 T/m (HER only)	12
QF5	594...746	6.17 T/m (HER only)	16

IR SM₂Co₁₇ Magnets

Q1 magnet & rings



Q1a ring

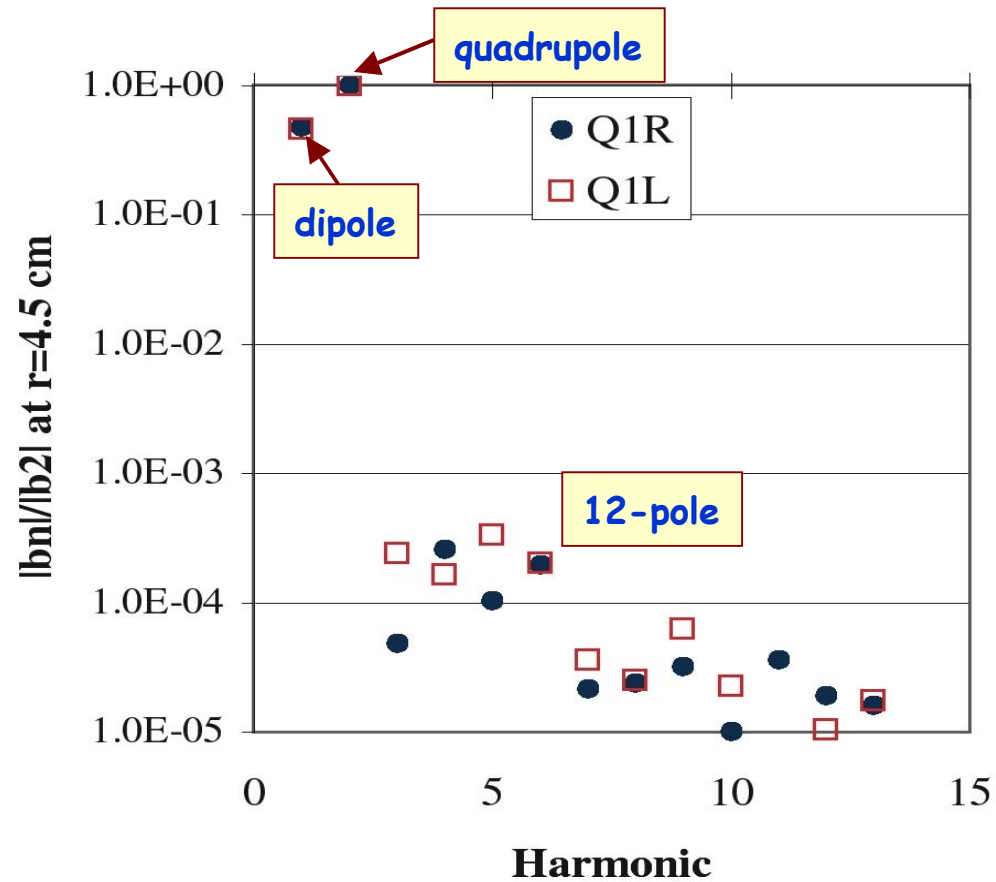


B1 magnet in measurement

*U. Wienands, SLAC-PEP-II
EICAW IR talk ppt, 26-Feb-02*

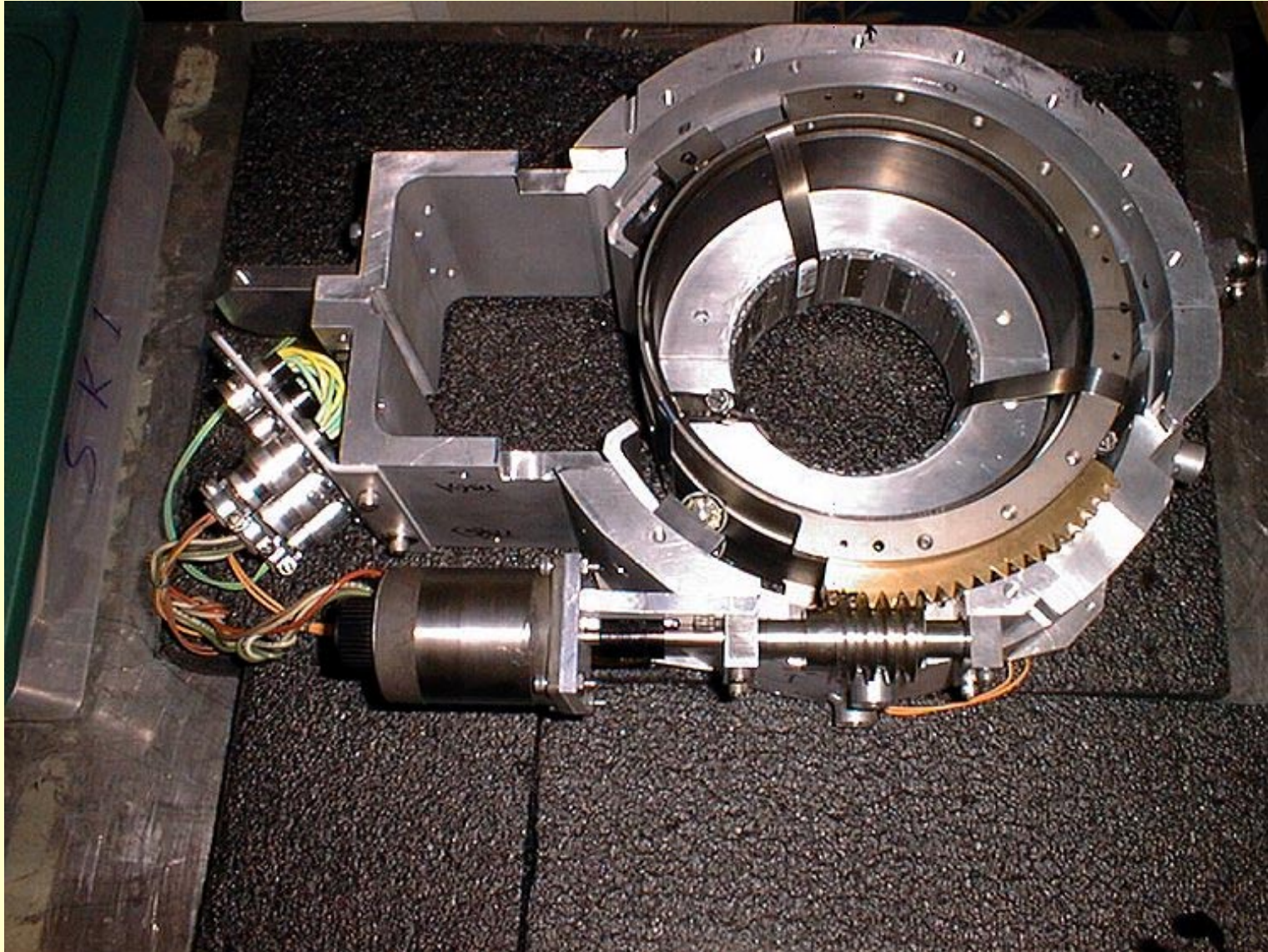
Q1a Magnetic Field Harmonics

S. Ecklund



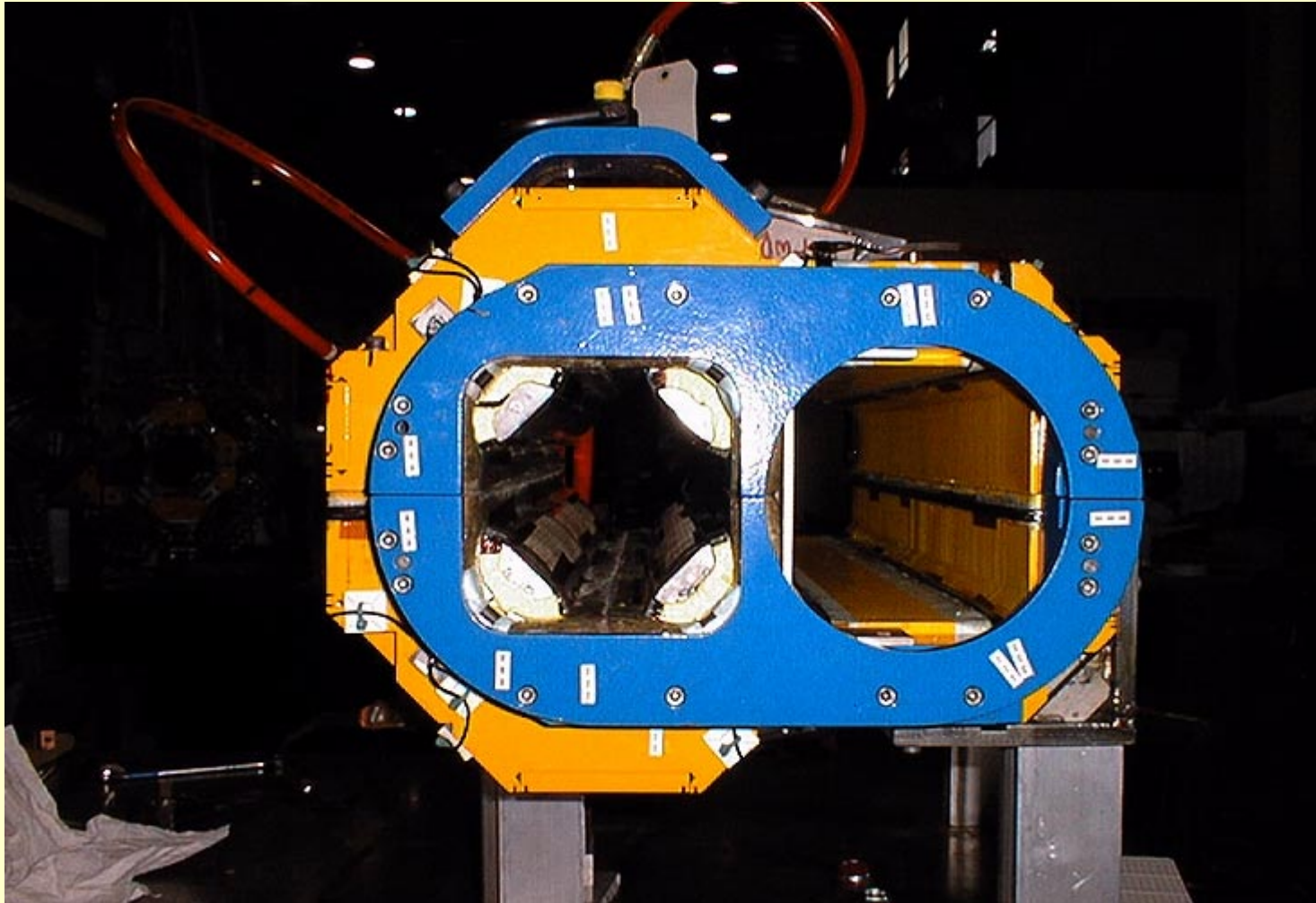
U. Wienands, SLAC-PEP-II
EICAW IR talk ppt, 26-Feb-02

SK1 Rotatable Quadrupole



*U. Wienands, SLAC-PEP-II
EICAW IR talk ppt, 26-Feb-02*

QF2 magnet with Mirror Plate

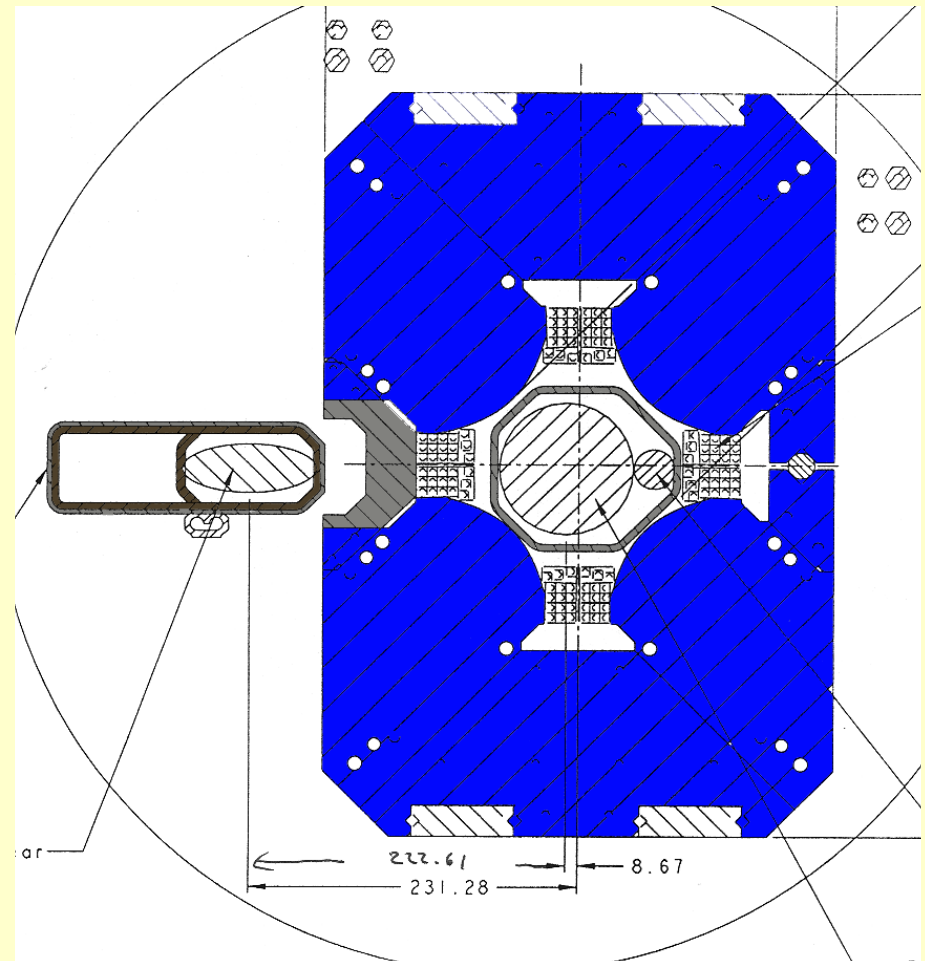
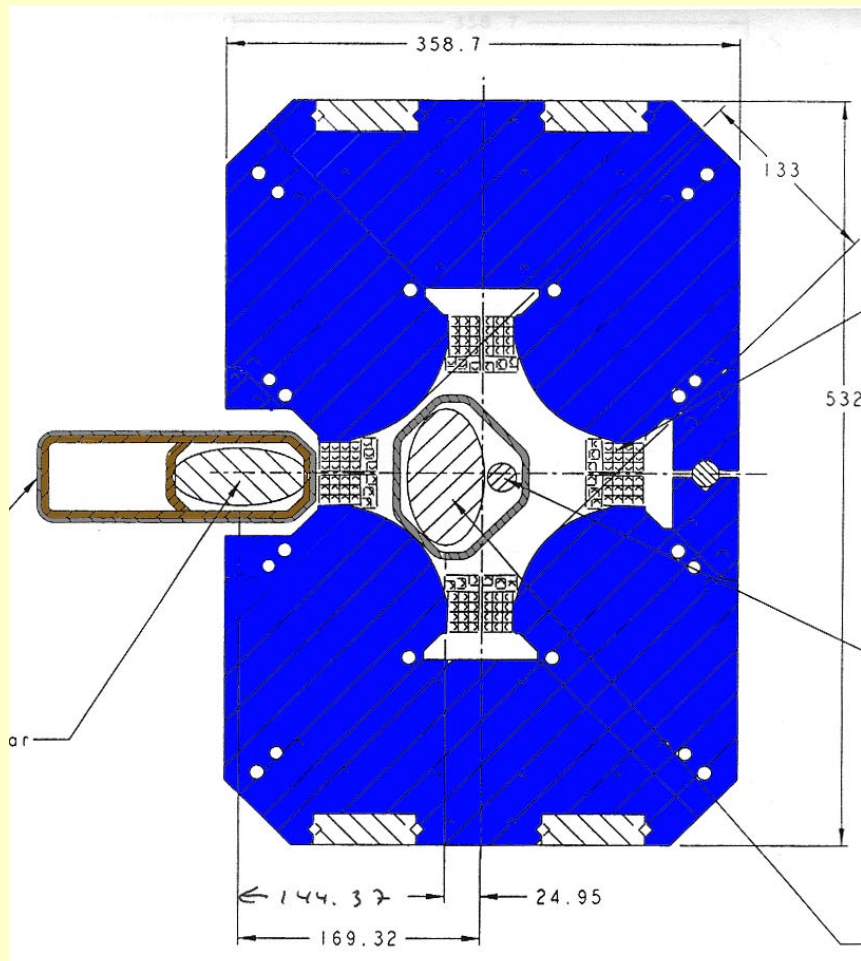


*U. Wienands, SLAC-PEP-II
EICAW IR talk ppt, 26-Feb-02*

HER IR Quad with Slot for LER

Front (IP) side

Back side

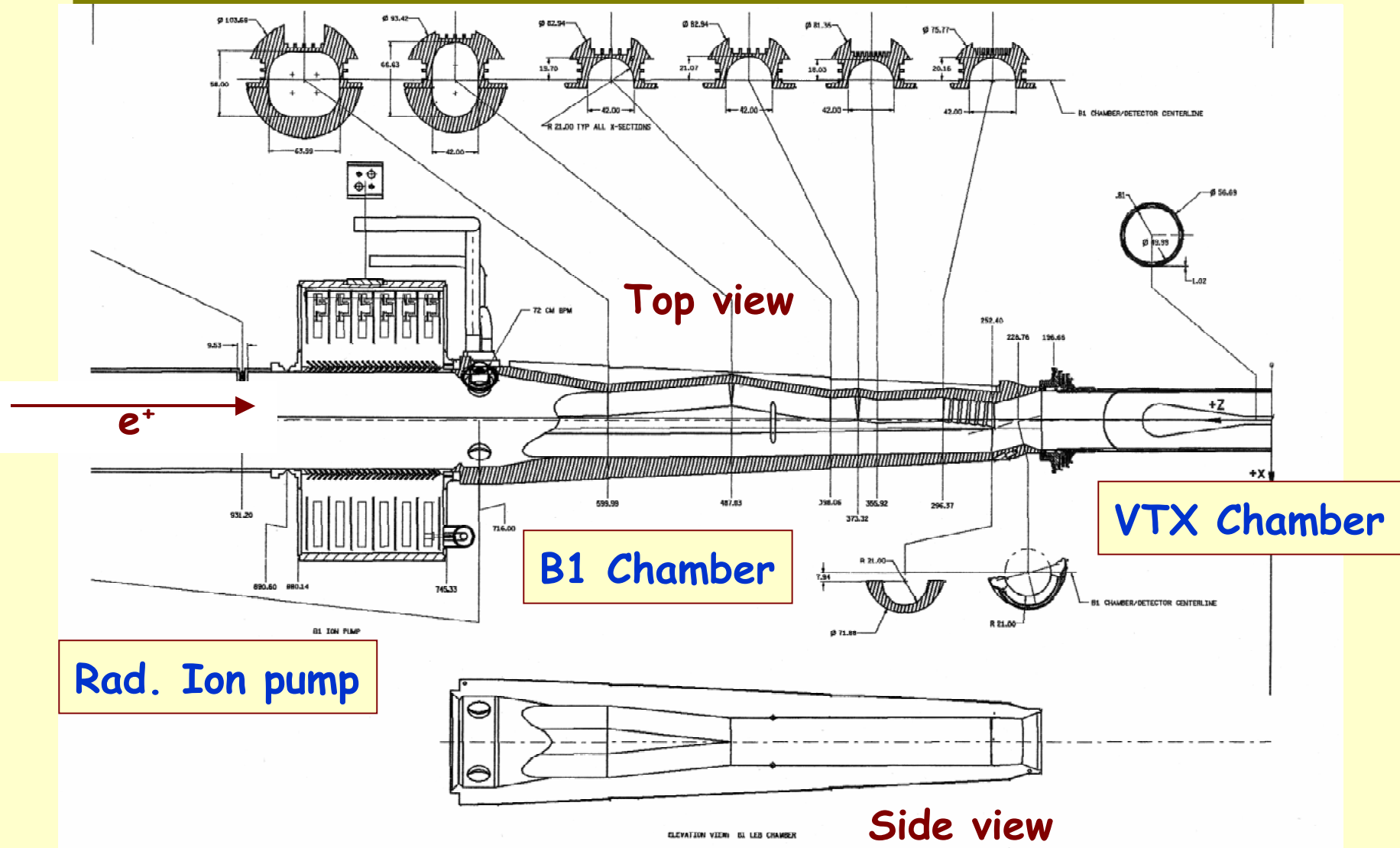


*U. Wienands, SLAC-PEP-II
EICAW IR talk ppt, 26-Feb-02*

IR Vacuum System

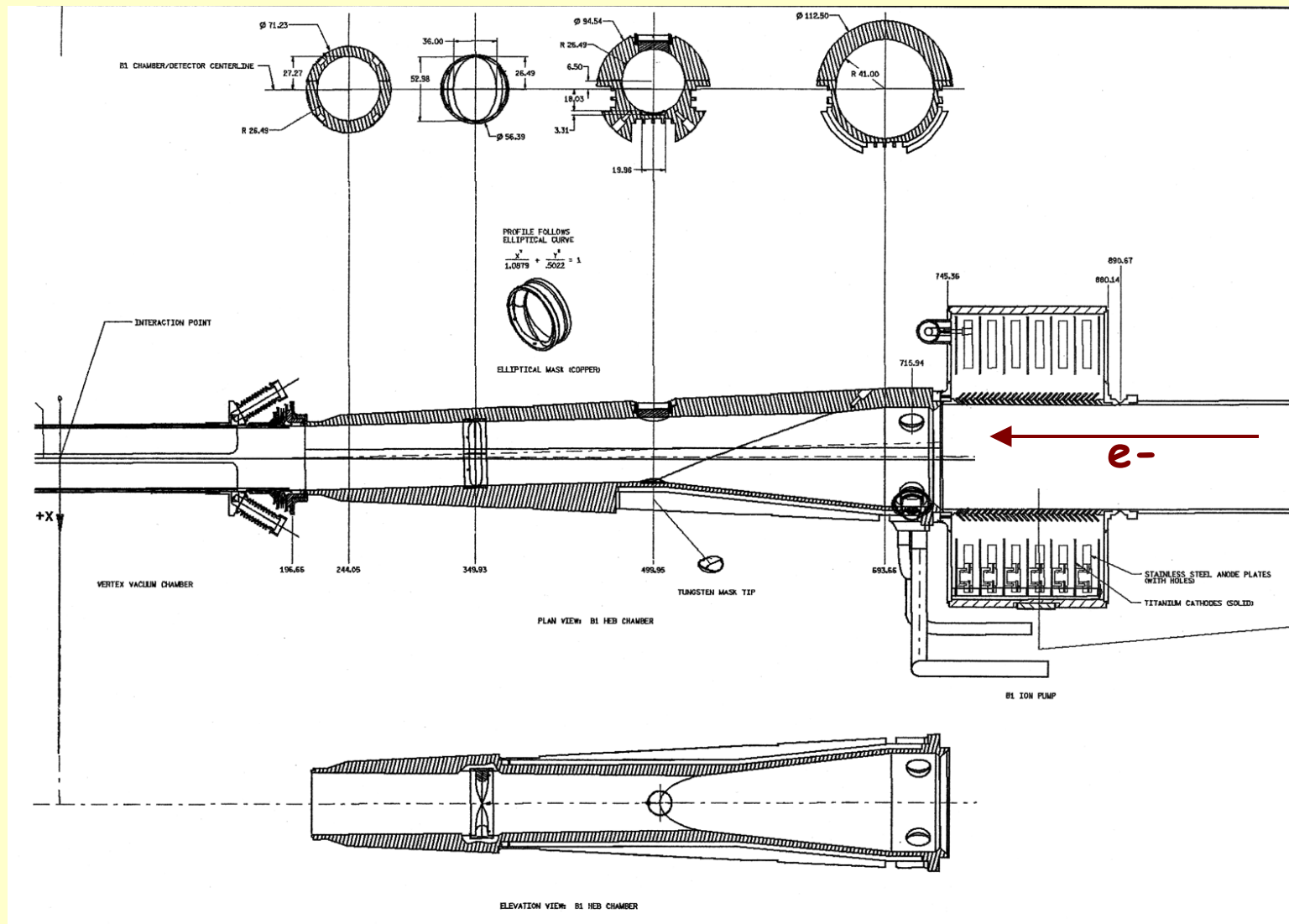
- $\leq 10^{-9}$ torr pressure (except in vtx chamber).
- 50 mm ID Be vertex chamber, ≈ 3.5 mm wall; LCW cooled, He cooling possible.
- Largest possible aperture in insertion quads.
- 2 radial ion pumps, ≈ 400 l/s each.
- NEG pumping in Q4&Q5 insertion magnets.
- Cu and GlidCop used extensively.
- S.R. masking in all chambers except vtx.
- HOM absorber @ bellows near “crotches”

Inner IR Forward Side Vacuum



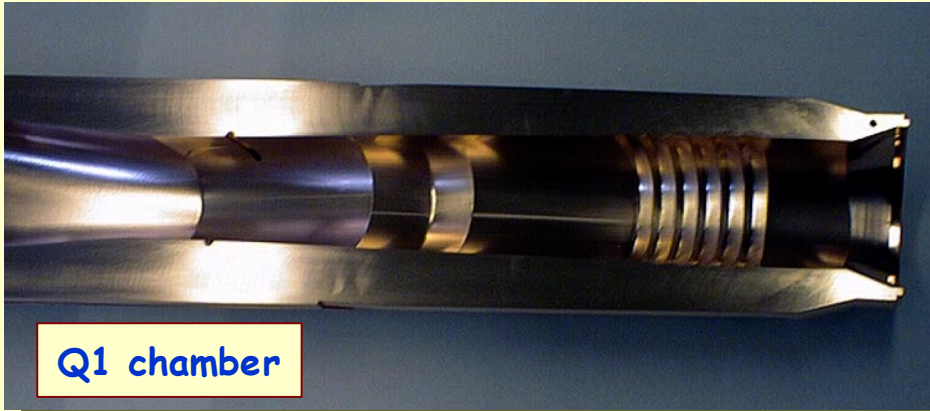
U. Wienands, SLAC-PEP-II
EICAW IR talk ppt, 26-Feb-02

Inner IR Backward Side Vacuum



*U. Wienands, SLAC-PEP-II
EICAW IR talk ppt, 26-Feb-02*

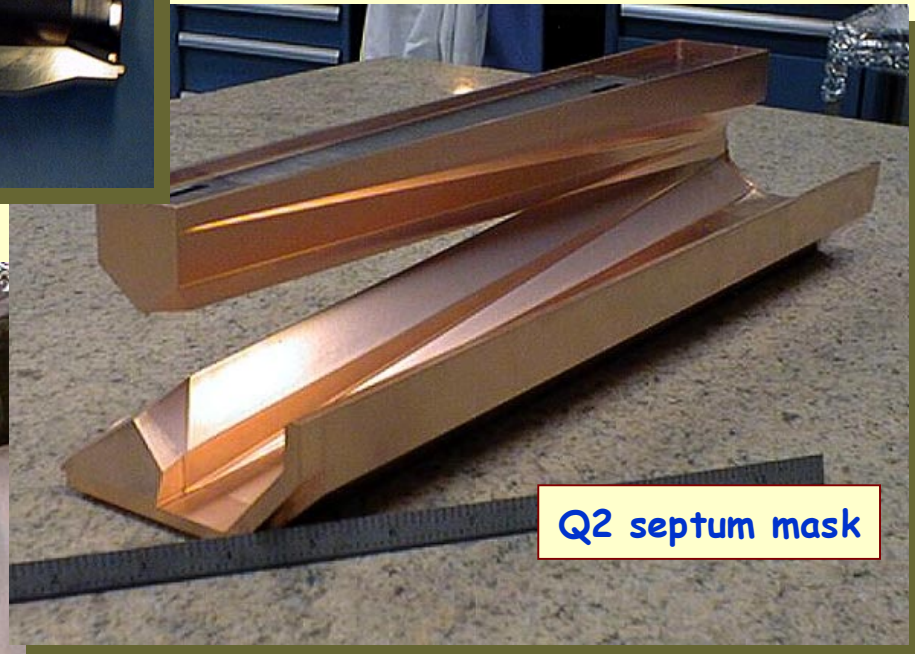
IR Vacuum Chambers



Q1 chamber



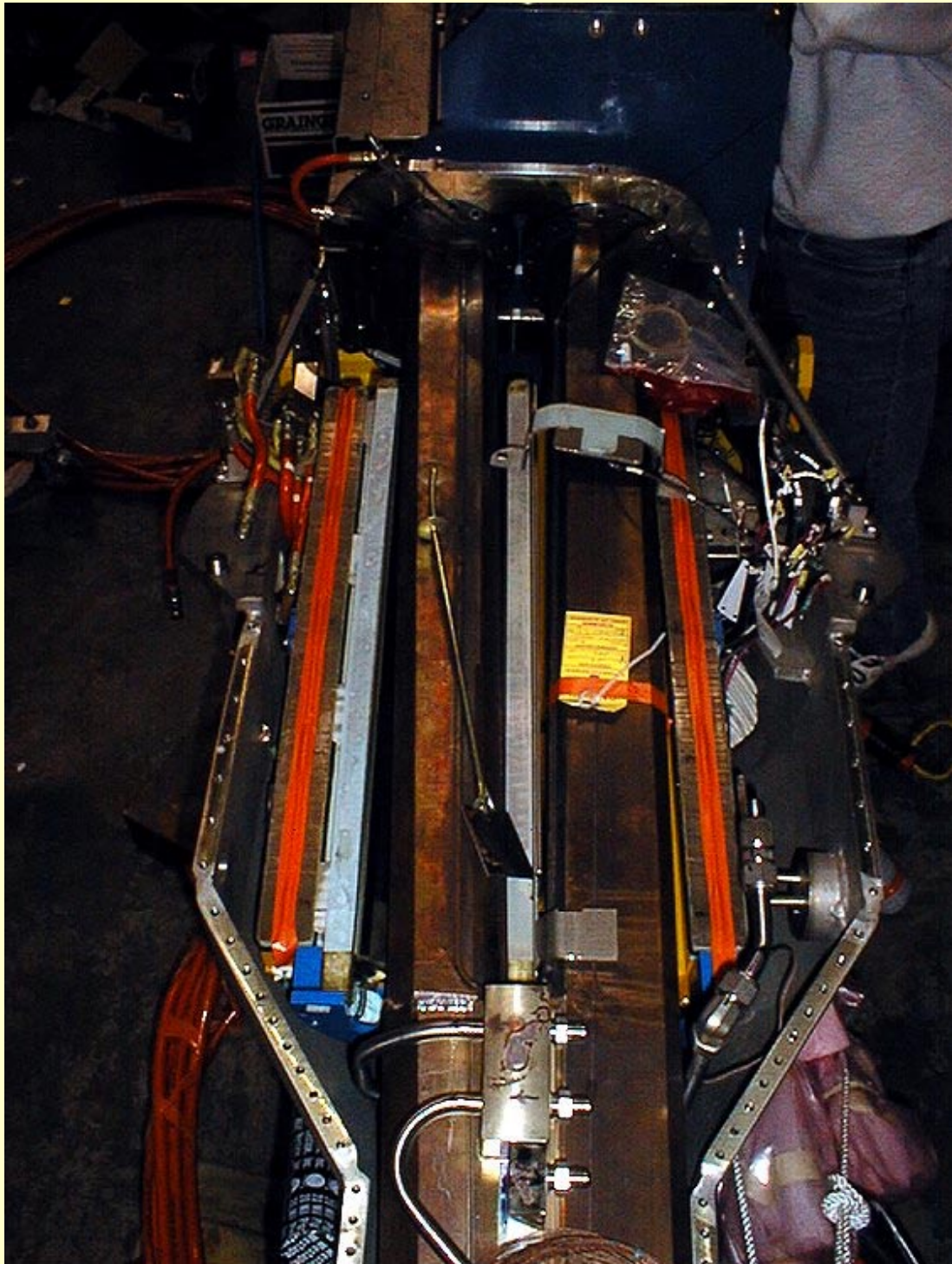
Be vertex chamber



Q2 septum mask

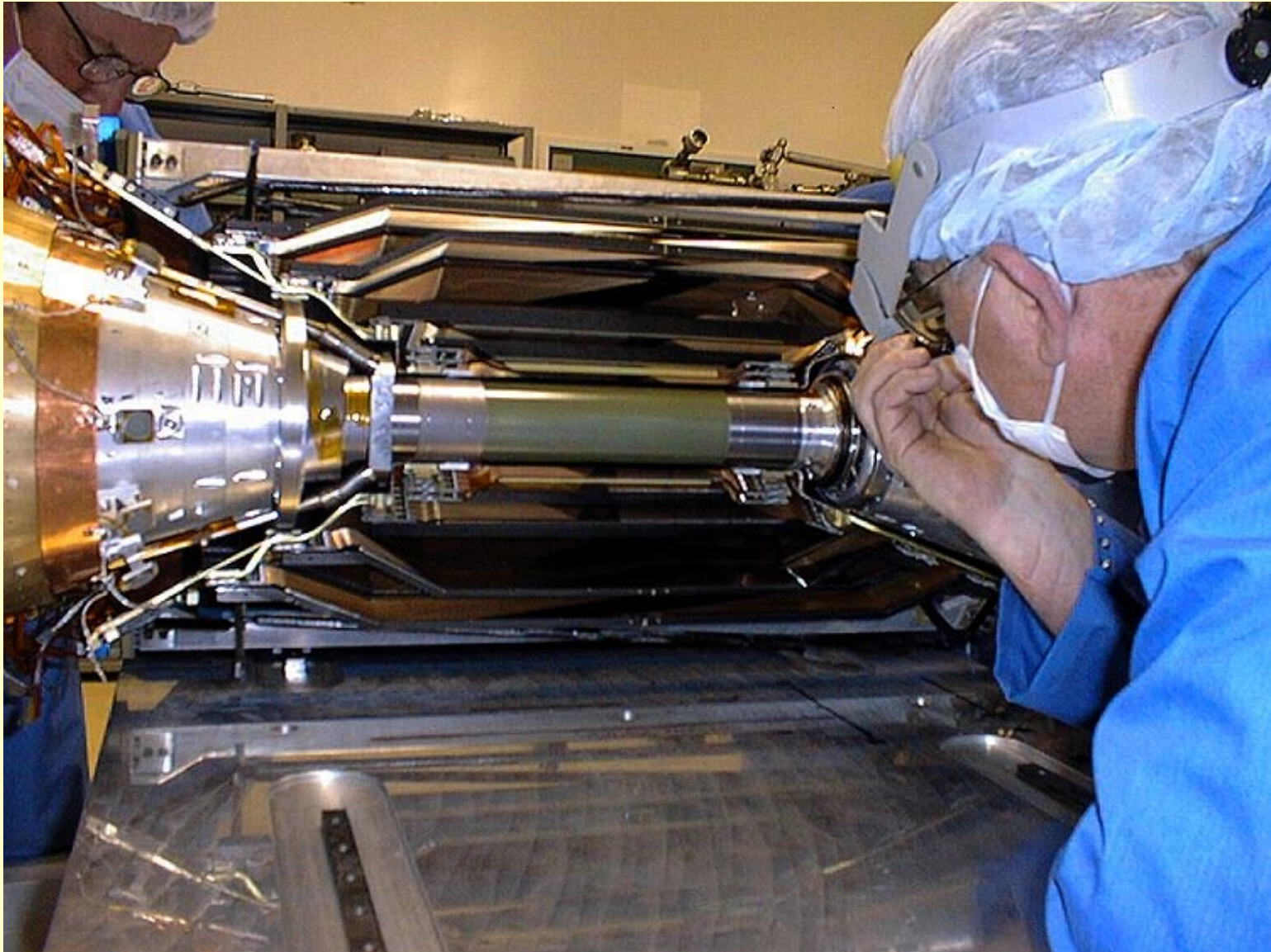
*U. Wienands, SLAC-PEP-II
EICAW IR talk ppt, 26-Feb-02*

Backward QF2 with Vacuum Chamber



*U. Wienands, SLAC-PEP-II
EICAW Talk ppt, 26-Feb-02*

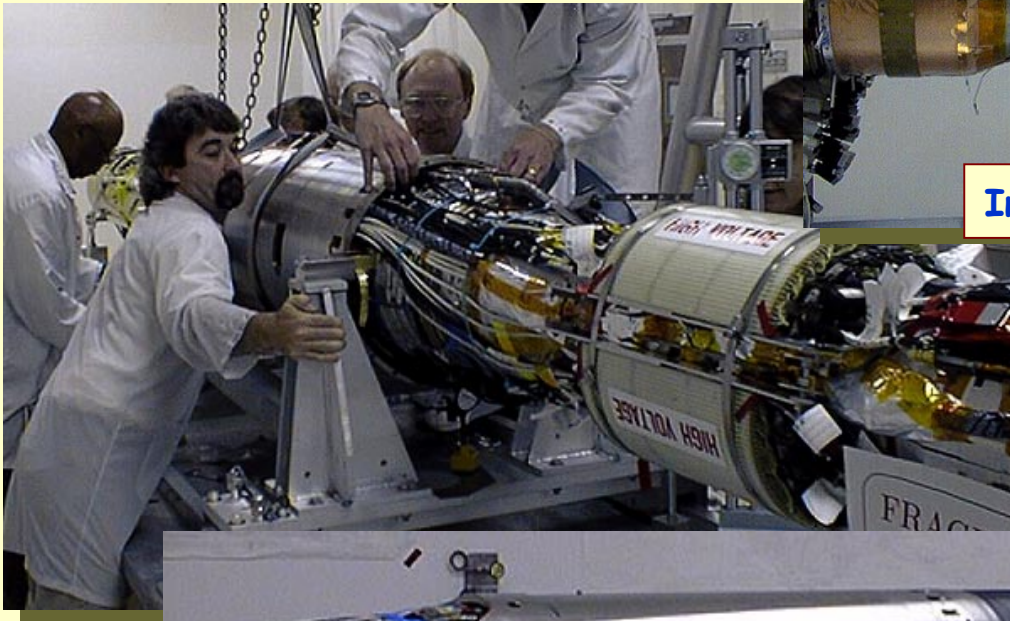
VTX Chamber with SVT



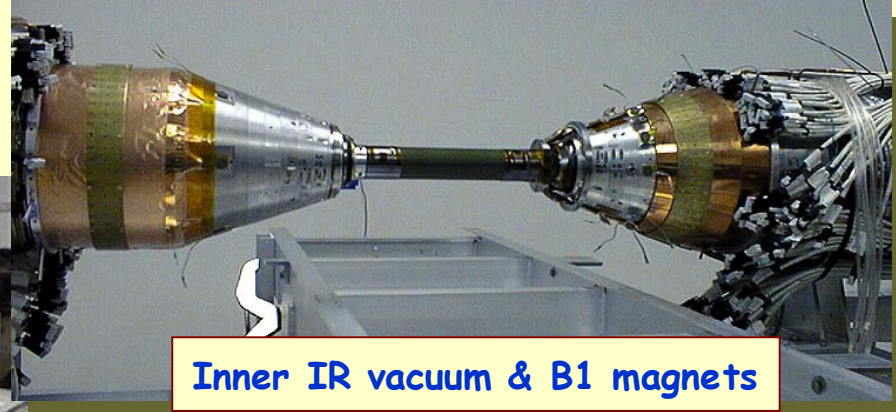
*U. Wienands, SLAC-PEP-II
EICAW IR talk ppt, 26-Feb-02*

IR support Tube Assy

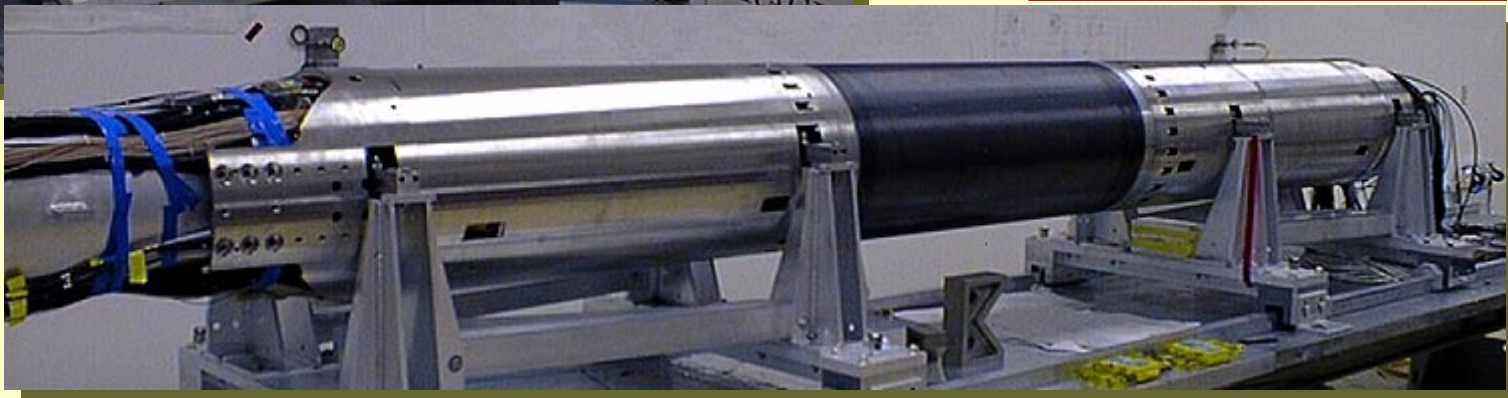
Support tube assembly



Inner IR vacuum & B1 magnets

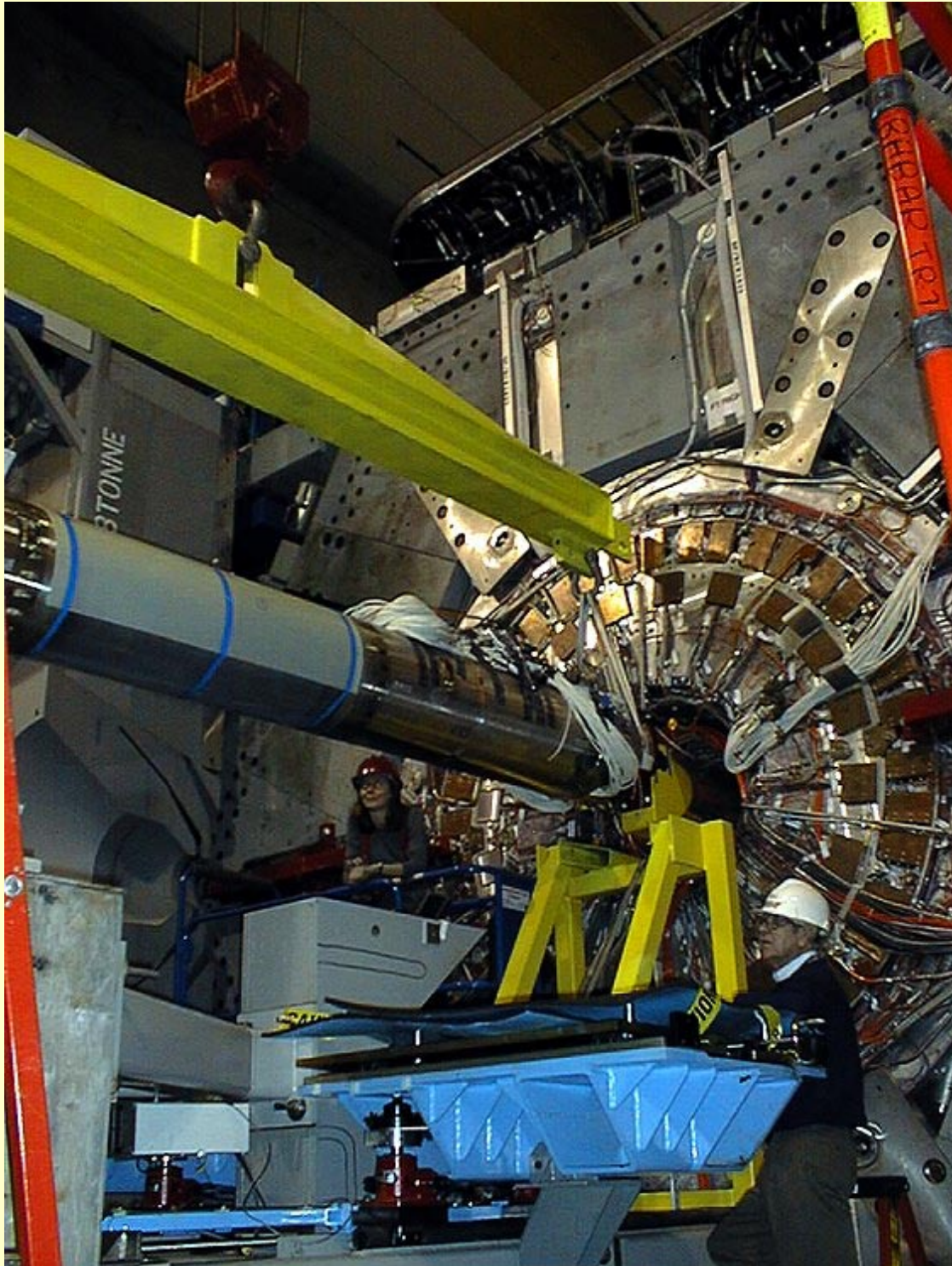


Support tube assembled



*U. Wienands, SLAC-PEP-II
EICAW IR talk ppt, 26-Feb-02*

Support Tube Installation



*U. Wienands, SLAC-PEP-II
EICAW Talk ppt, 26-Feb-02*

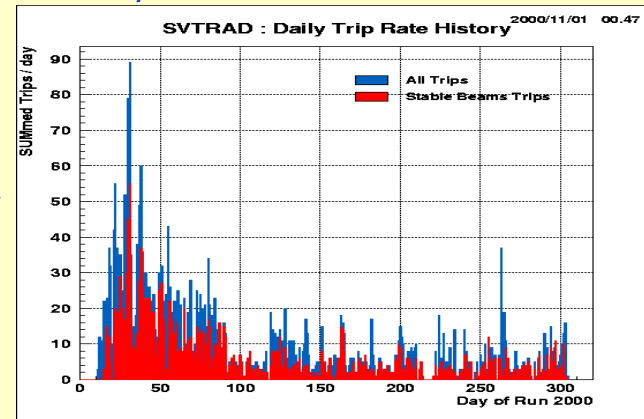
Background Issues

- Two background sources: lost particles and synchrotron radiation (x-rays)
- The former is aggravated by the separator dipole's sweeping debris into detector.
- The latter is aggravated by high s.r. power with significant x-ray contribution.

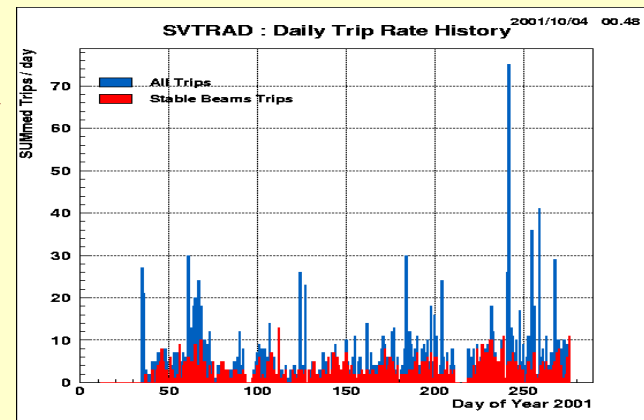
Backgrounds, spikes

- Compare Y2k with

T. Meyer/BaBar



- Y2k+1 trip rates

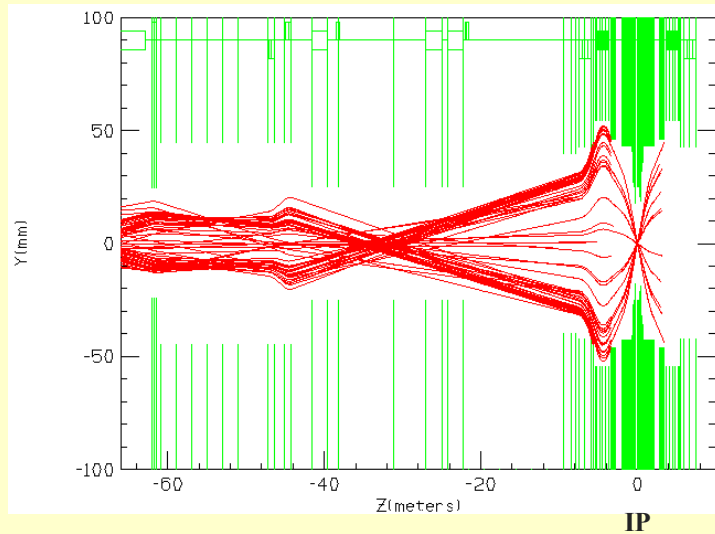


- “Dust trapping”
much reduced from
early Y2k rates

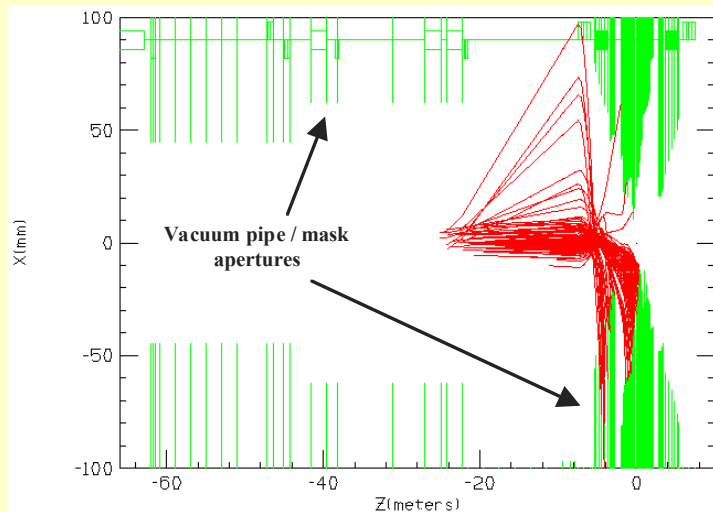
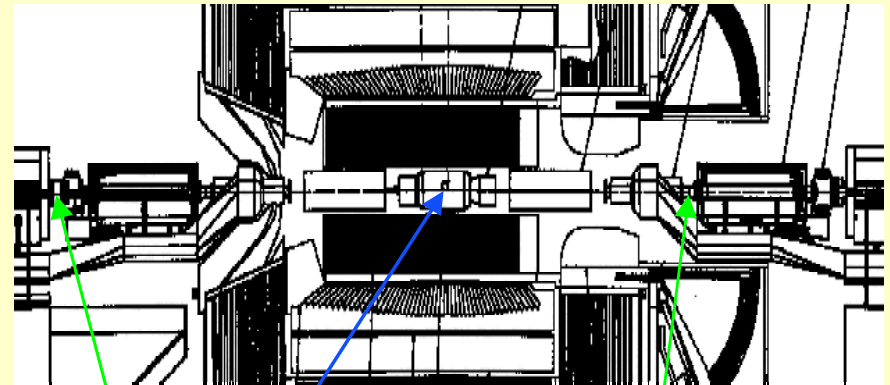
*U. Wienands, SLAC-PEP-II
EICAW IR talk ppt, 26-Feb-02*

Lost-Particle Backgrounds

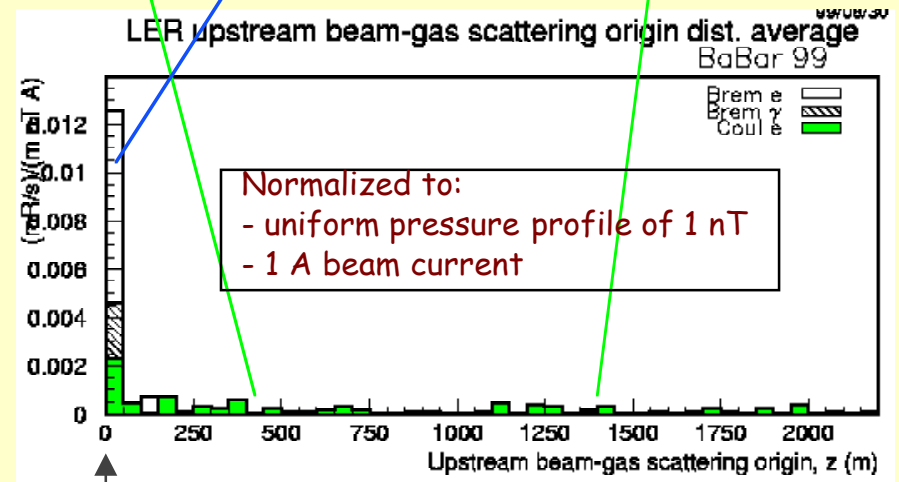
W. Kozanecki



**Coulomb scattering
in Arcs
(distant)**



**e⁻ Bremsstrahlung
in last 26 m
(near IR,
x-plane)**



IP

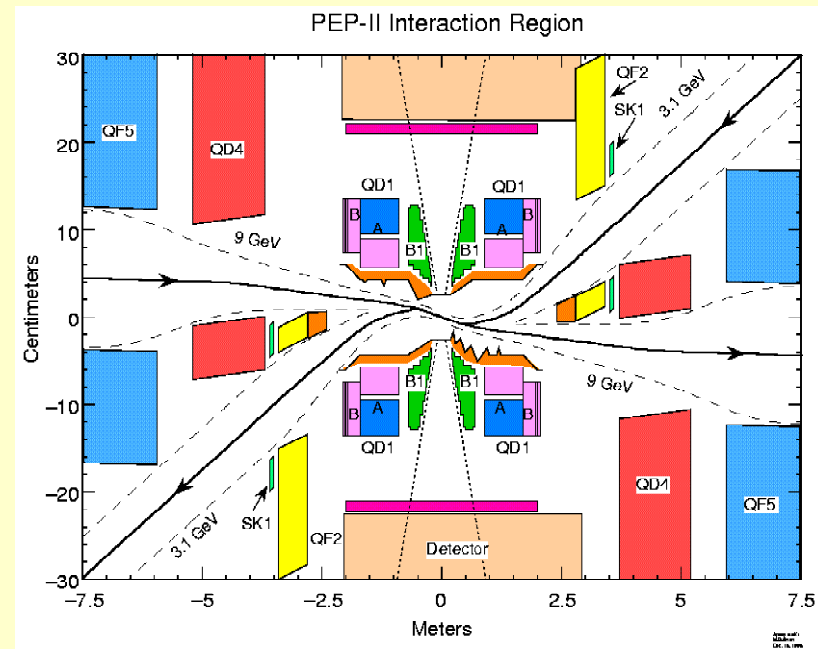
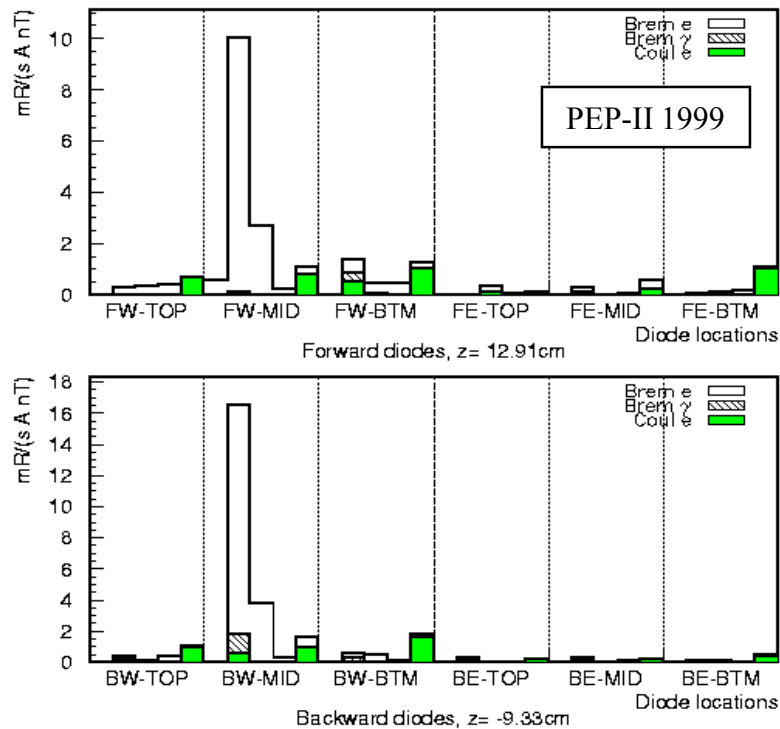
U. Wienands, SLAC-PEP-II
EICAW IR talk ppt, 26-Feb-02

Beam-gas backgrounds: X-ing angle

W. Kozanecki

Diode sensitivities to five HER zones

99/08/30 19.58



Guesses:

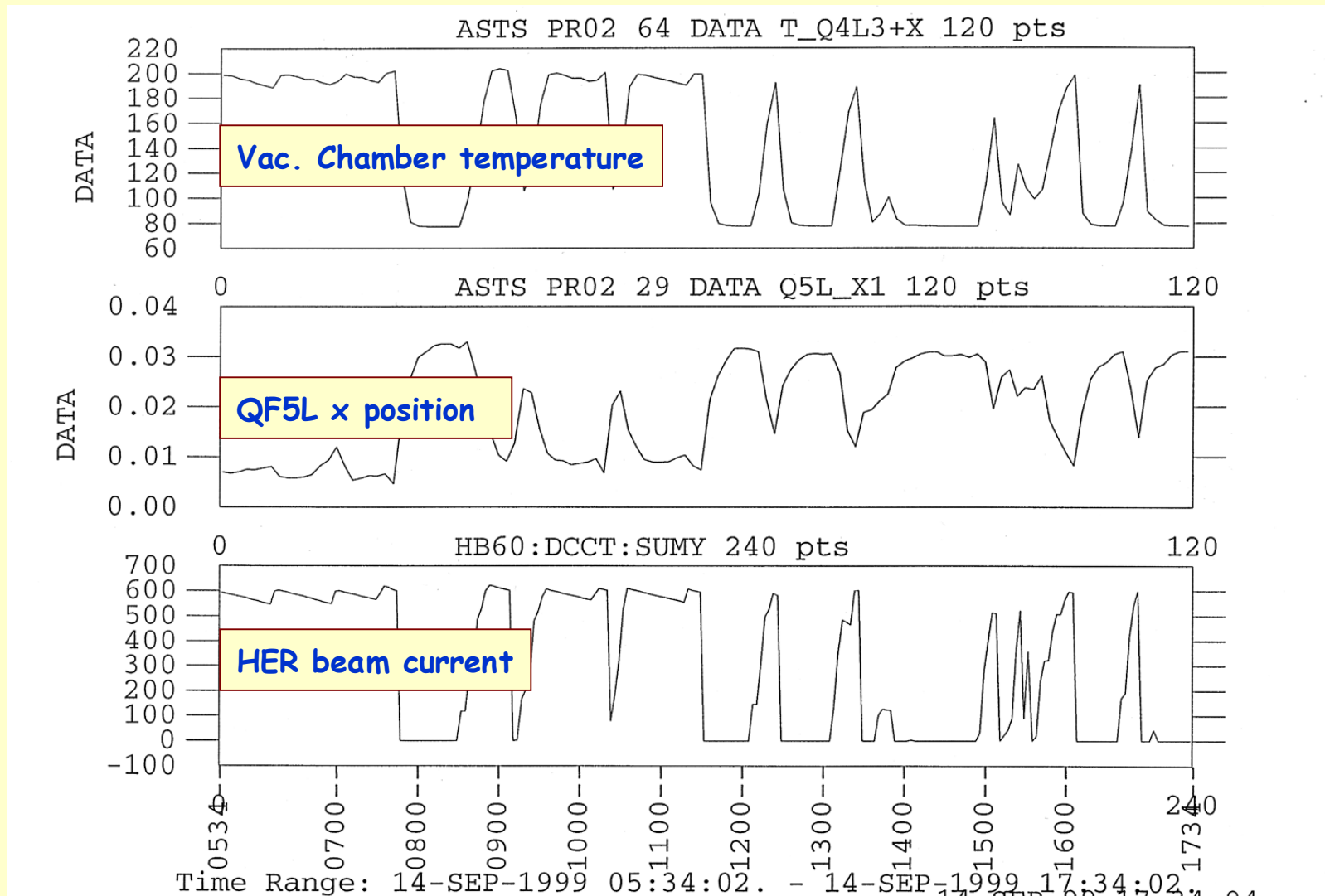
- The magnetic separation (B1, Q5) is largely responsible for the spikes in the horizontal plane.
- X-ing angle has the potential of reducing sensitivity in horizontal plane by ~ 1 order of magnitude for the SVT
- The relative gain will be smaller for other detectors (e.g. DCH)

*U. Wienands, SLAC-PEP-II
EICAW IR talk ppt, 26-Feb-02*

Some issues we encountered

- Vacuum and magnets move with beam current.
 - Thermal expansion quite significant
- A few s.r. masks hit by B1 fans and by B3 fans from the HER failed due to improper execution and design issues.
 - These have been replaced
- Be vertex chamber getting hot at forward end.
 - Septum chamber may be culprit
 - Replace with backward-end type chamber

Magnet shift with beam current

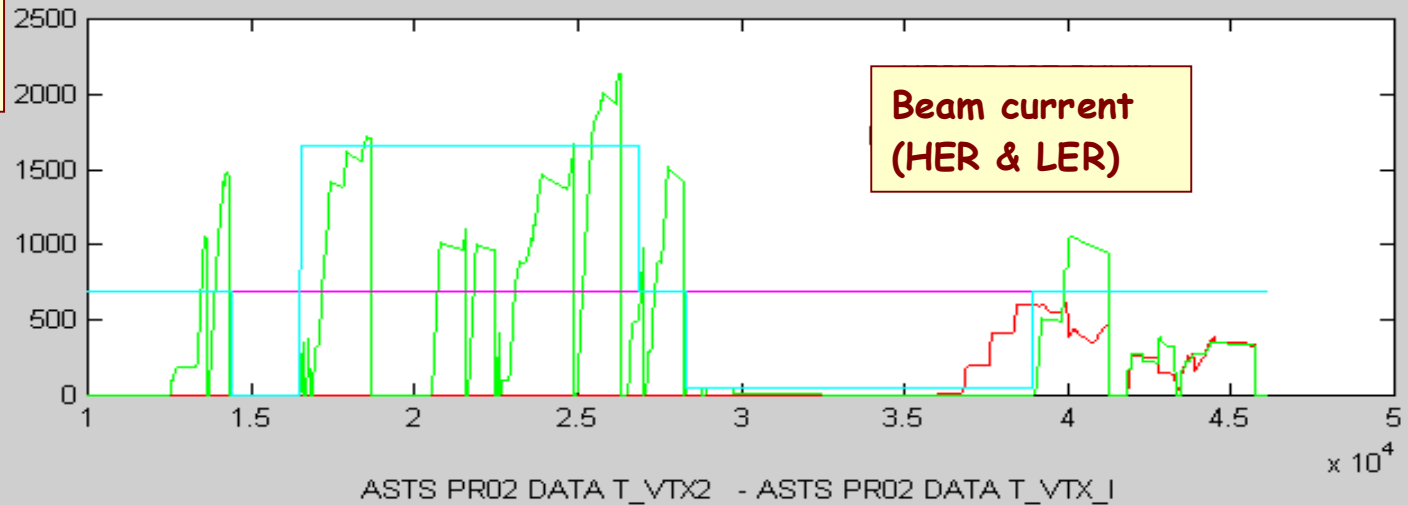


*U. Wienands, SLAC-PEP-II
EICAW IR talk ppt, 26-Feb-02*

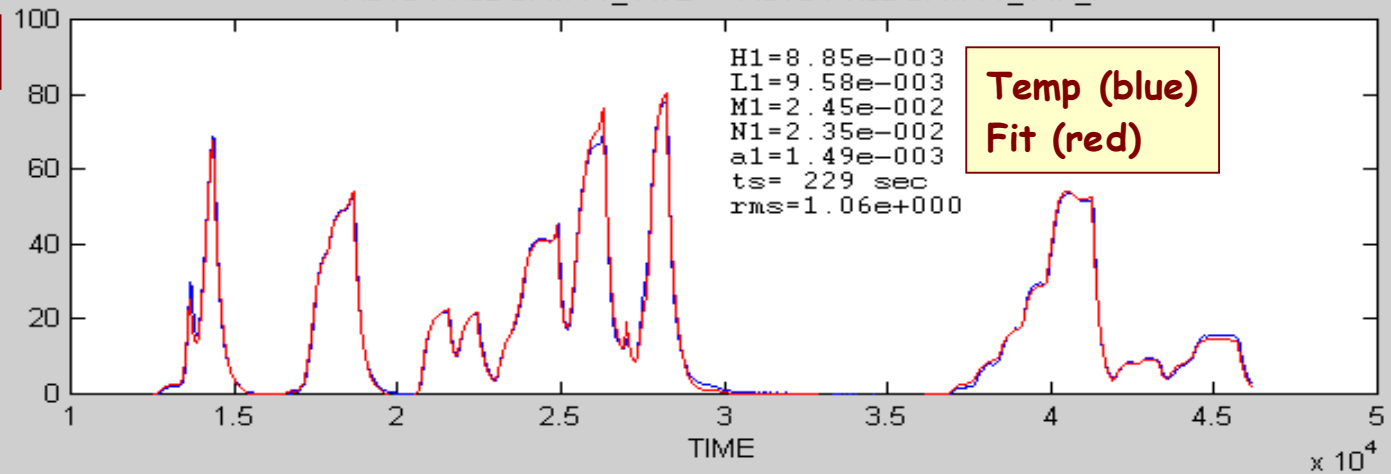
VTX pipe Temperature

VTX beam pipe thermocouple compared to model (S. Ecklund)

Beam current
(mA)



Δt ($^{\circ}\text{F}$)



*U. Wienands, SLAC-PEP-II
EICAW IR talk ppt, 26-Feb-02*

Be beam pipe at the center of BABAR

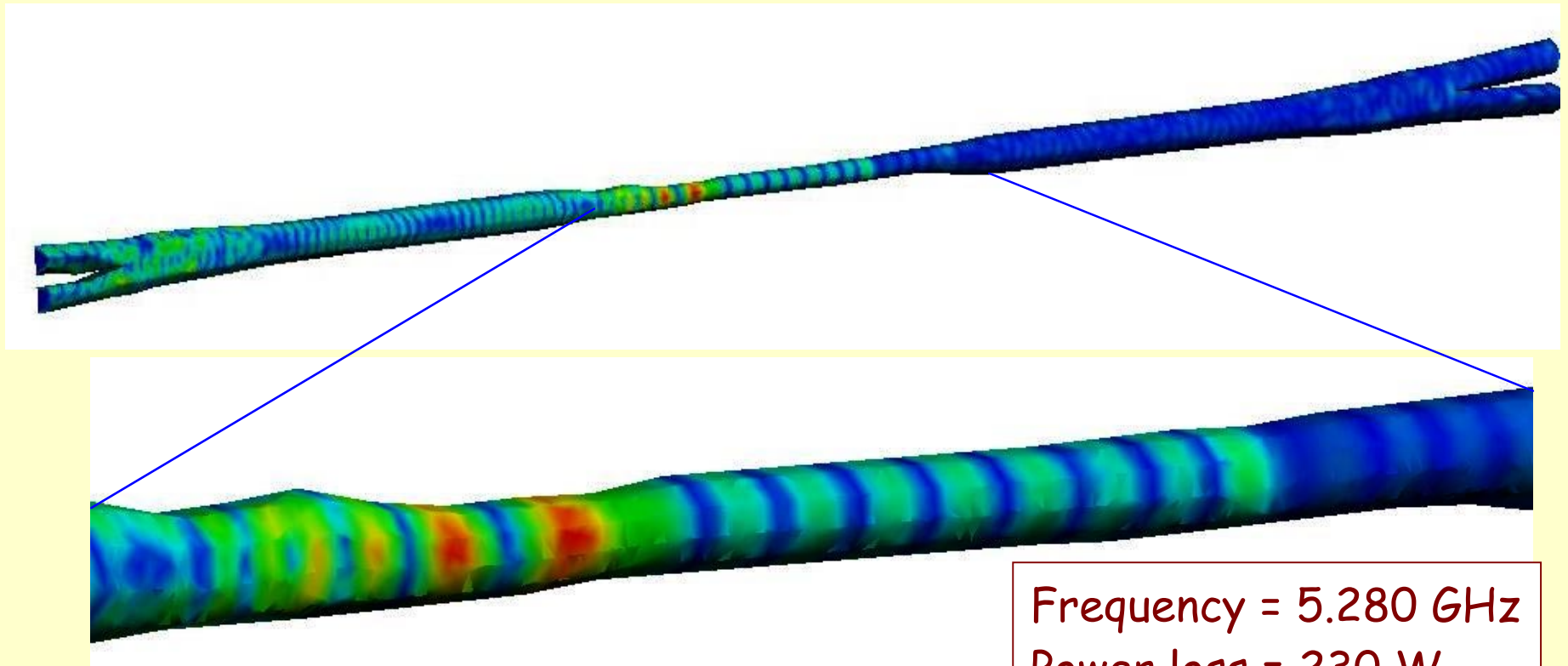


Bellows that is heating up

*U. Wienands, SLAC-PEP-II
EICAW IR talk ppt, 26-Feb-02*

Mode at Forward Mask

N. Folwell, C. Ng



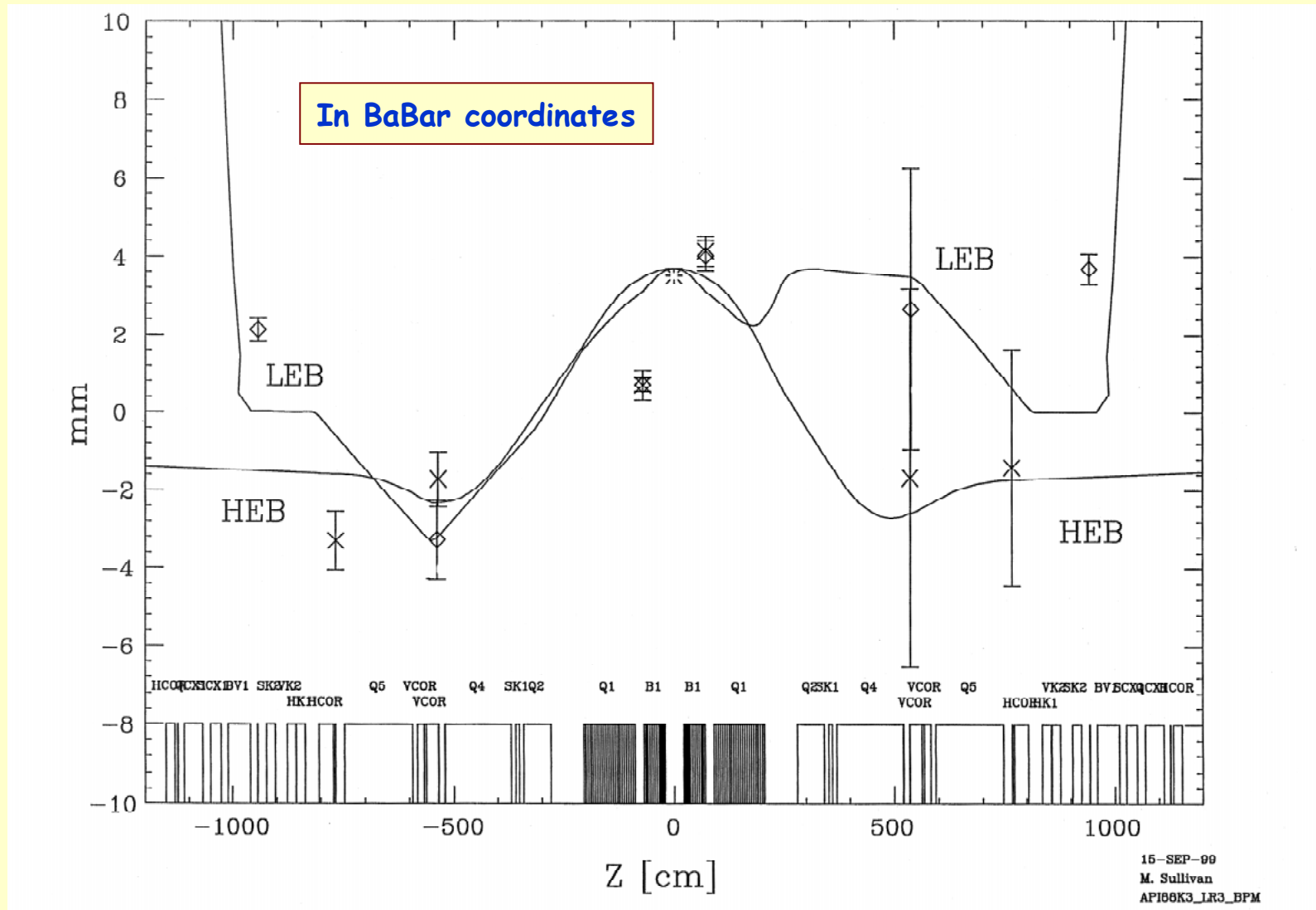
Frequency = 5.280 GHz
Power loss = 230 W

*U. Wienands, SLAC-PEP-II
EICAW IR talk ppt, 26-Feb-02*

More Issues...

- Solenoid coupling compensation operationally very difficult
 - Design correct, but no good diagnostic capability due to strong local coupling
 - Orbit deviations in local sextupoles change coupling
- Backgrounds have been higher than originally anticipated
 - But vacuum cleaned up considerably and detectors more rad. tolerant => “under control”

Vertical Orbit through IR

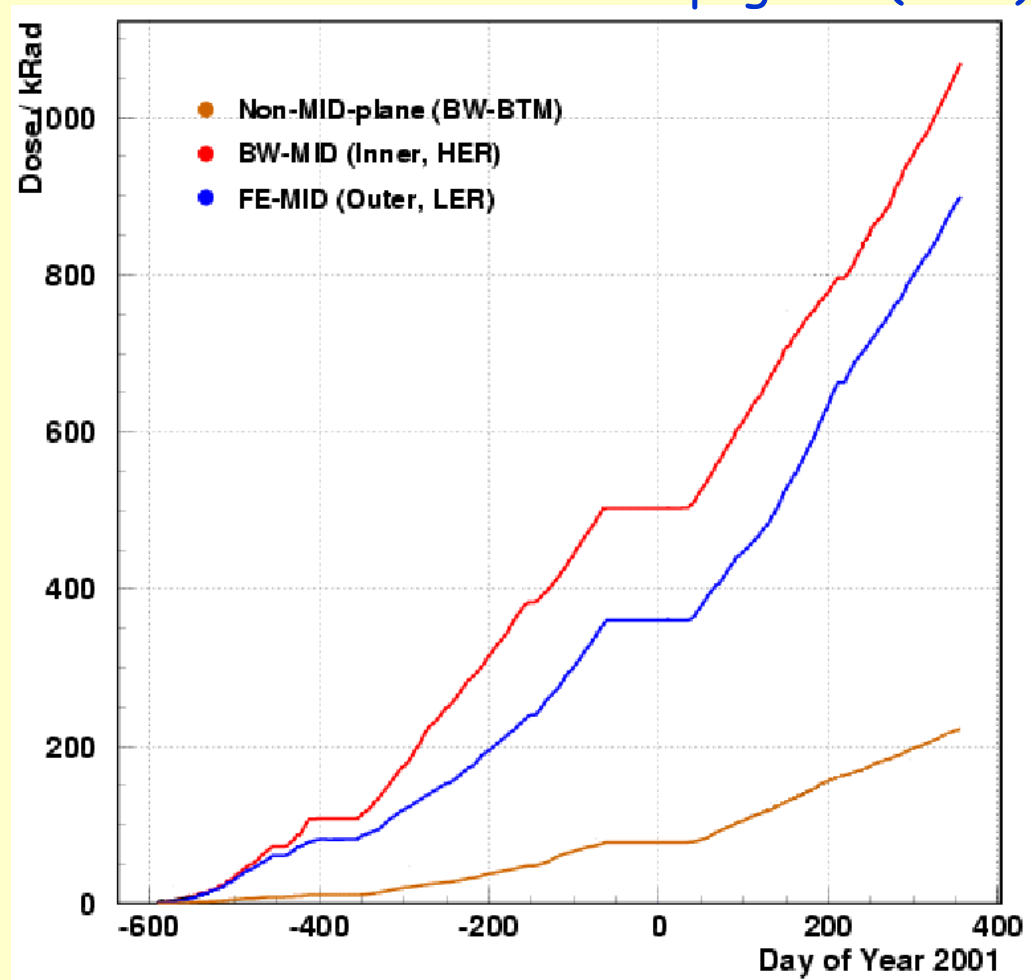


*U. Wienands, SLAC-PEP-II
EICAW IR talk ppt, 26-Feb-02*

SVT Radiation Monitoring

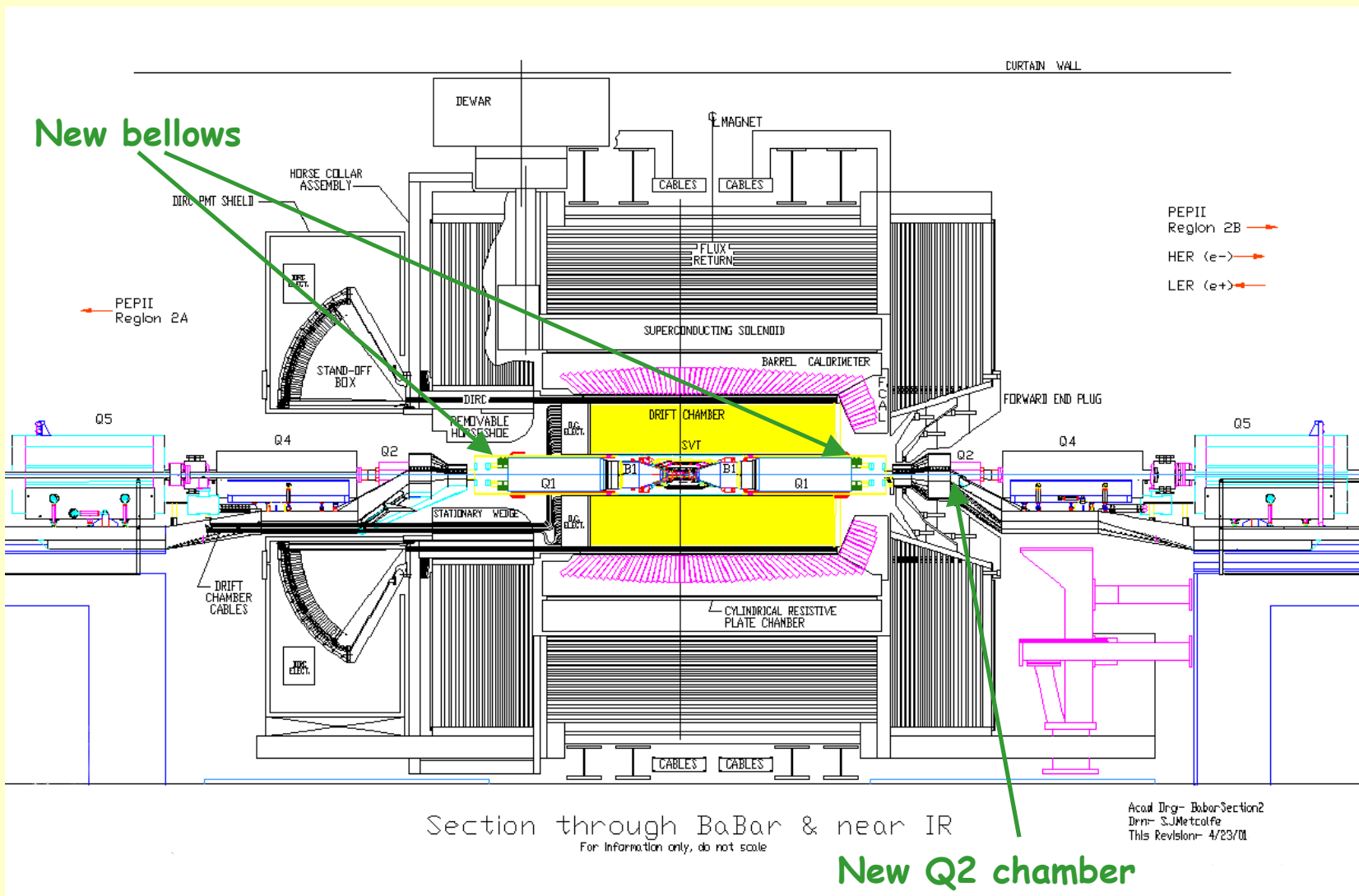
C. Campagnari (SVT)

- About 1 MR until end of Y2001 run.
- $\approx 13 \text{ kr/fb}^{-1}$
- Dominated by HER backgnd.



*U. Wienands, SLAC-PEP-II
EICAW IR talk ppt, 26-Feb-02*

Side view of the BABAR Detector



*U. Wienands, SLAC-PEP-II
 EICAW IR talk ppt, 26-Feb-02*

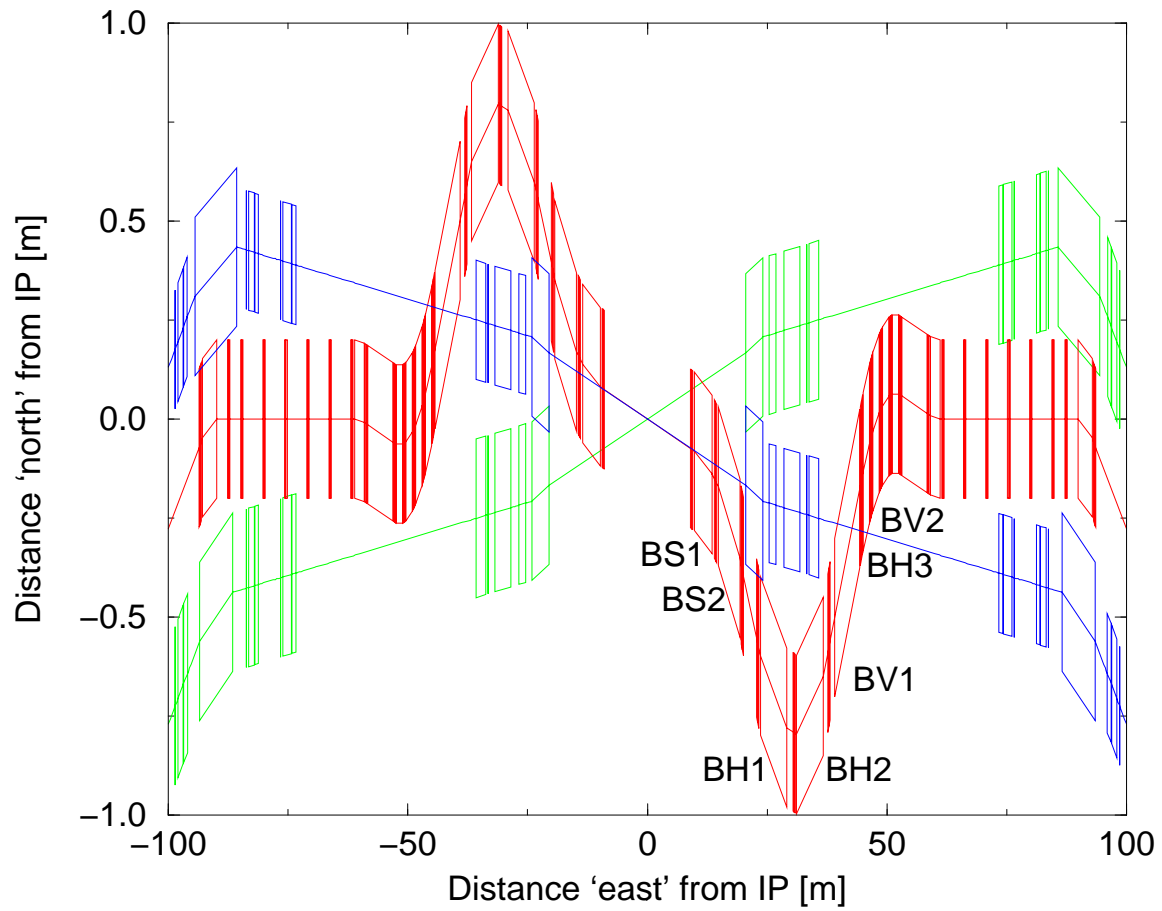
Summary

- The PEP-II IR is challenging due to
 - high beam currents, close bunch spacing;
 - zero crossing angle and forward angle clearance
- The requirements were met by
 - pm magnets within the detector, some common;
 - elaborate s.r. masking and shadowing of s.r.;
 - use of high-strength materials like GlidCop.
- The operational experience has been positive overall.

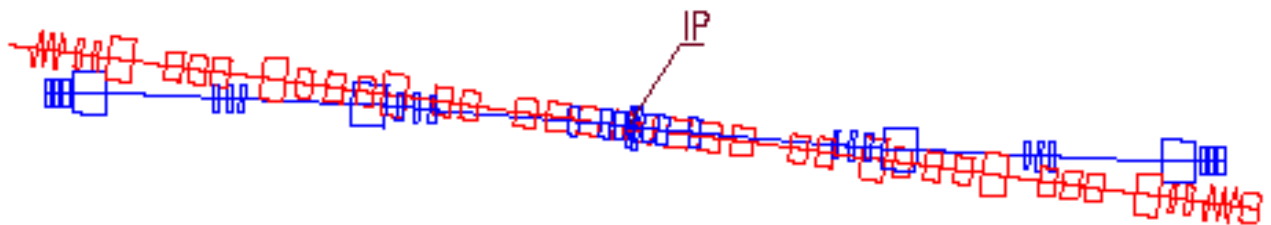
Luminosity scaling with IR parameters

S. Peggs, BNL

- **The “NIM” ring-ring IR optics ...**
 - with 3 beams
 - electron ring in the RHIC tunnel
 - geometrically constrained spin rotators
- **... works**, but is inferior to “green field” solutions such as that of **MIT-Bates**
- **BUT eRHIC now foresees**
 - **collisions only at IP12**
 - **electron ring outside the RHIC tunnel**
- **A merged IR optics design is possible**

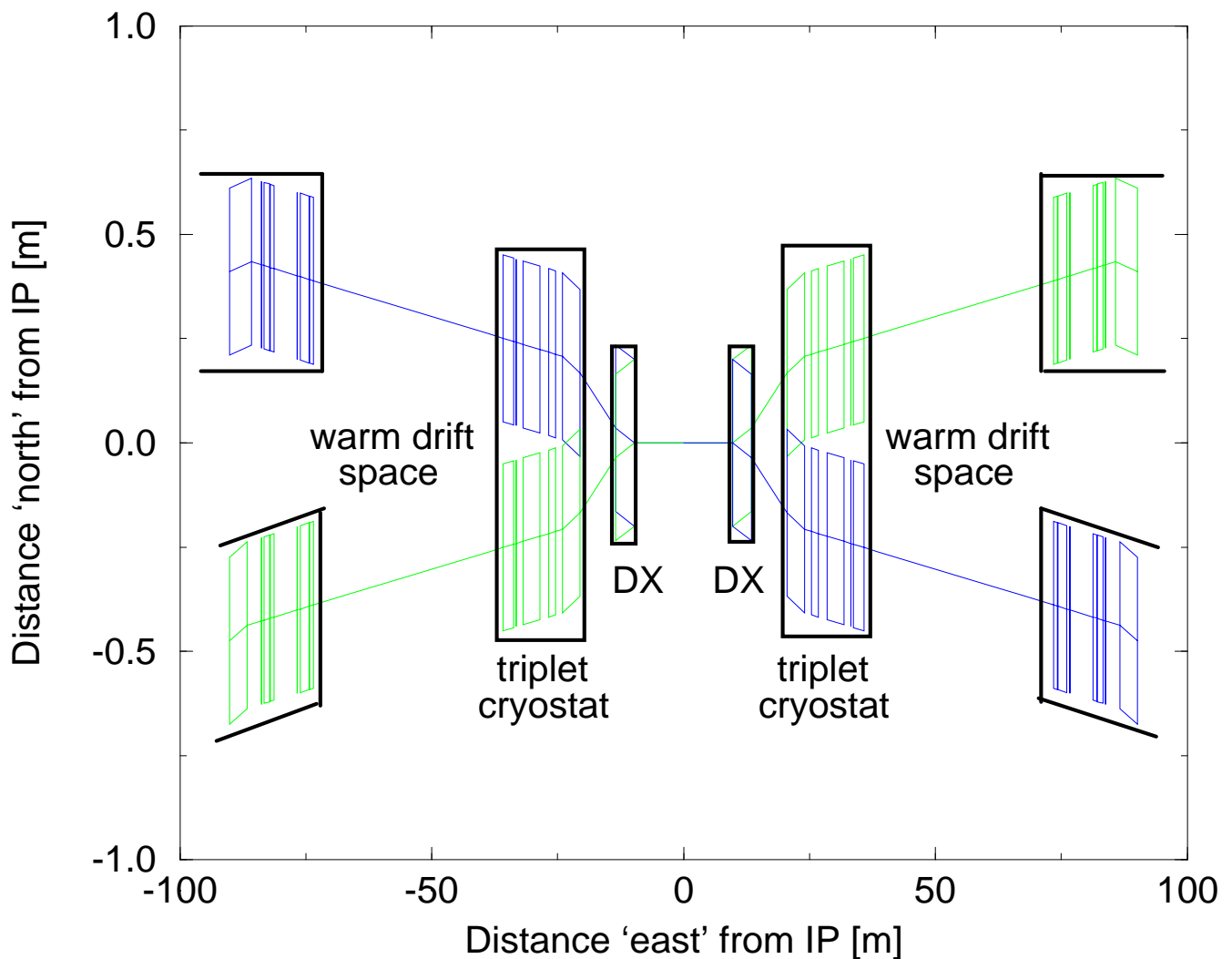


eRHIC “NIM” ring-ring solution



MIT-BATES green field solution

The existing RHIC geometric constraints are FULLY negotiable for collisions at IP12 with either ring-ring or linac-ring schemes.



How to use this freedom to get high luminosity from a merged IR optics design?

LUMINOSITY

Beam-beam parameters (round beams):

$$\xi_e = \frac{N_i}{\epsilon_e} \left(\frac{r_e Z}{4\pi \gamma_e} \right) \quad (1)$$

$$\xi_i = \frac{N_e}{\epsilon_i} \left(\frac{r_i (v/c)_i}{4\pi Z} \right) \quad (2)$$

Luminosity can be written

$$L = F_c \xi_e \xi_i \sigma_e'^* \sigma_i'^* \left(\frac{4\pi \gamma_e \gamma_i}{r_e r_i} \right) \quad (3)$$

Assuming operation at the beam-beam limit (ξ_e and ξ_i are fixed) ...

... then **how can the angular apertures $\sigma_e'^*$ and $\sigma_i'^*$ be maximized?**

RMS beam sizes at the IP:

$$\sigma_i^* = \sqrt{\frac{\beta_i^* \epsilon_i}{(\beta\gamma)_i}} \quad (4)$$

$$\sigma_e^* = \sqrt{\beta_e^* \epsilon_e} \quad (5)$$

ϵ_i is the *normalized* RMS ion emittance

ϵ_e is the *unnormalized* electron emittance

Similarly, the **angular beam sizes** are:

$$\sigma_i'^* = \sqrt{\frac{\epsilon_i}{\beta_i^* (\beta\gamma)_i}} \quad (6)$$

$$\sigma_e'^* = \sqrt{\frac{\epsilon_e}{\beta_e^*}} \quad (7)$$

This is why we make β^* small!

HOW SMALL?

- A number of beam sigmas n (≈ 6 for ions, ≈ 12 for electrons) must fit in a , the aperture of the interaction region (IR) quads, where β is largest
- Beta max is related to β^* by the (almost) constant “effective IR aperture distance” d

$$d = \sqrt{\beta\beta^*} \quad (8)$$

- So the limit on angular beam size (and hence luminosity) is

$$\sigma'^* \leq \frac{1}{n} \frac{a}{d} \quad (9)$$

Therefore

1. **Decrease d** – move the “center of gravity” of the IR quads in **as close as possible**, in part by having **as high gradient as possible**
2. **Increase a** – make the IR quads **as large bore as possible**

More complicated than it appears ...

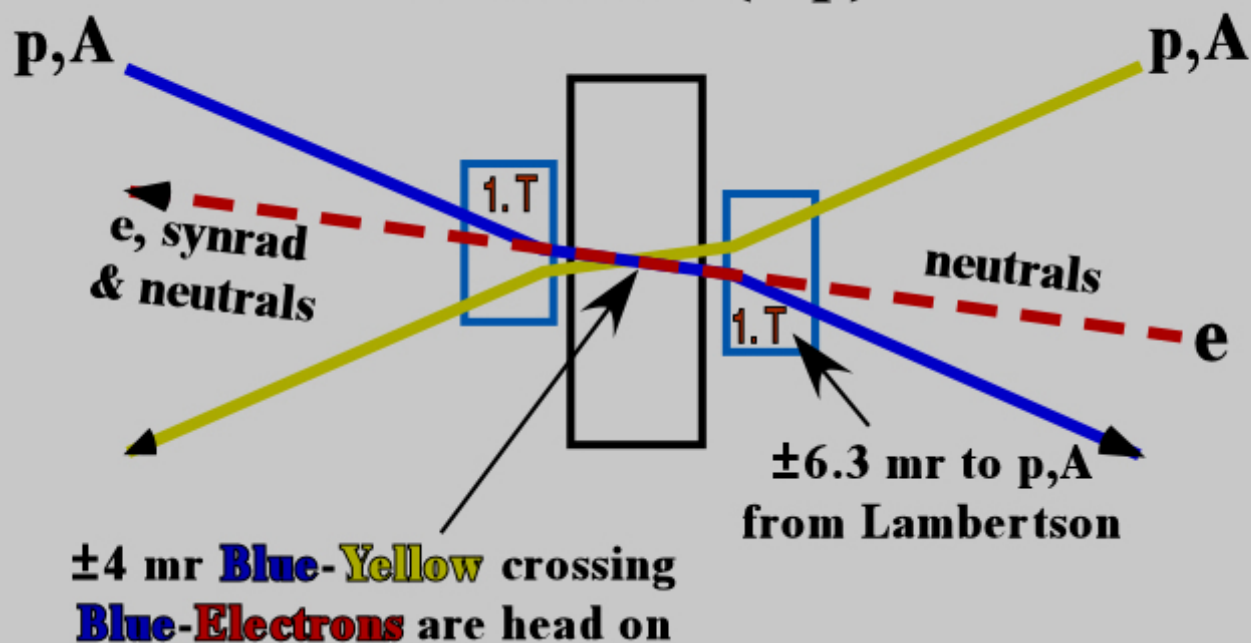
Want to shrink the IR with a photocopier, but cannot ...

- The focal length of an IR quad wants to decrease with its distance from the IP: $f \sim d$
- SO the quad length wants to get longer:
 $L_Q \sim 1/f \sim 1/d$
- OR the field gradient wants to increase:
 $dB/dx \sim 1/f \sim 1/d$
- IF L_Q increases, so also does d : **BAD**
- IF dB/dx increases, bore a must decrease: **BAD**

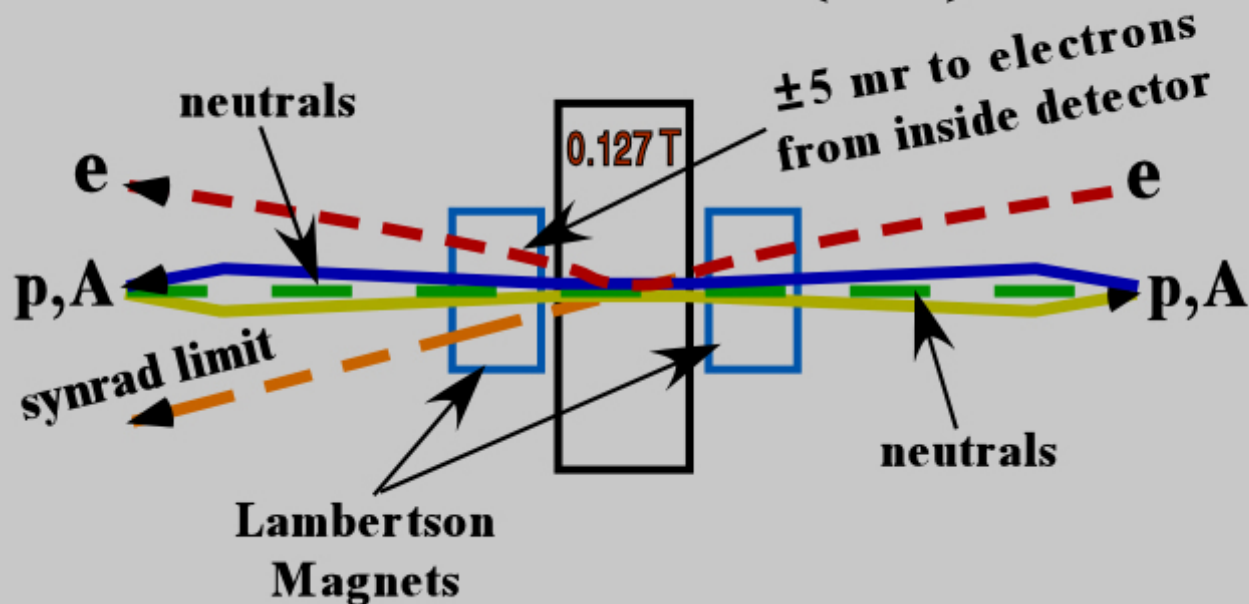
This is a nonlinear problem ...

... made more complicated by the need to worry about synchrotron radiation from the electrons

Plan View (top)



Elevation View (side)



	THERA	EPIC 2	eRHIC	eRHIC	HER
Scenario	linac-ring	linac-ring	linac-ring	ring-ring	(SLAC)
Ion specie	protons	protons	protons/gold	protons/gold	–
Luminosity , [$10^{32}\text{cm}^{-2}\text{s}^{-1}$]	.041	21	4.6/.036	3.5/.086	–
Dipole bend radius, [m]	608	~ 50	243	243	165
RMS beam size, σ^* [μm]	10	25	21/60	40/50	157
Bunch spacing, [ns]	211	6.7	35.5	35.5	4.2
IONS					
Ion energy, [GeV/u]	1,000	50	100/250	250/100	–
Ion rms emittance, [μm]	1.0	2.0	0.8/1.0	0.8/1.0	–
Ion average current, [A]	.071	2.4	.14/.68	.42/.42	–
Ion IP beta, β_e^* [m]	.10	.10	.15/.39	.53/.27	–
Ion b-b parameter, ξ_i	.0023	.004	.0046/.0015	.004/.004	–
Laslett SC tune shift	.0003	.024	.001/.003	.003/.003	–
ELECTRONS					
Electron energy, [GeV]	250	5	10	10	9
Electron emittance, [nm]	.2	6	3	18	49
Electron beam current, [A]	.000084	.264	.135/.135	.12/.37	1.5
Electron beam power, [GW]	.023	1.32	1.35/1.35	1.2/3.7	13.5
Synch. rad. power, [MW]	–	\sim .29	.49/.49	.43/1.3	7.2
Electron IP beta, β_e^* [m]	.50	.10	.15/1.2	.089/.139	.05/.50
Electron b-b parameter, ξ_e	.23	.35	.11/.57	.06/.06	.055

SUMMARY

1. **eRHIC now foresees**
 - **collisions only at IP12**
 - **electron ring outside the RHIC tunnel**
2. **A merged IR design has great prima facie flexibility**
3. Operation at the beam-beam limit, with a fixed number of bunches, **luminosity is optimized by maximizing a/d , the angular aperture at the IP**
4. **B-factory and HERA lessons** with different rigidity beams, and synchrotron radiation, **are directly relevant**

Spin Rotators with the Energy Range from 2 GeV to 10 GeV for eRHIC

J. Kewisch, BNL

Basics: The motion of spins is given by the BMT equation:

$$\frac{d\vec{s}}{dt} = \vec{\Omega} \times \vec{s}$$

with

$$\vec{\Omega} = \frac{e}{m\gamma} \left[(1 + a\gamma)\vec{B} - \frac{a\gamma^2}{\gamma+1}(\vec{v} \cdot \vec{B})\frac{\vec{v}}{c^2} - \left(a\gamma + \frac{\gamma}{\gamma-1} \right) \vec{v} \times \frac{\vec{E}}{c^2} \right]$$

Electrons: $a = 0.00115965$, Protons : $a = 1.79285$. For $\gamma \gg 1$ we get:

Transverse fields:

$$\vec{\Omega}_{\perp} = \frac{ea}{m} \vec{B}_{\perp}$$

$$\phi_s = (a+1)\gamma \cdot \alpha \approx a\gamma \cdot \alpha$$

$$L \cdot \vec{B}_{\perp}(\phi_s = 90^\circ) = 23\text{kG} \cdot \text{m}$$

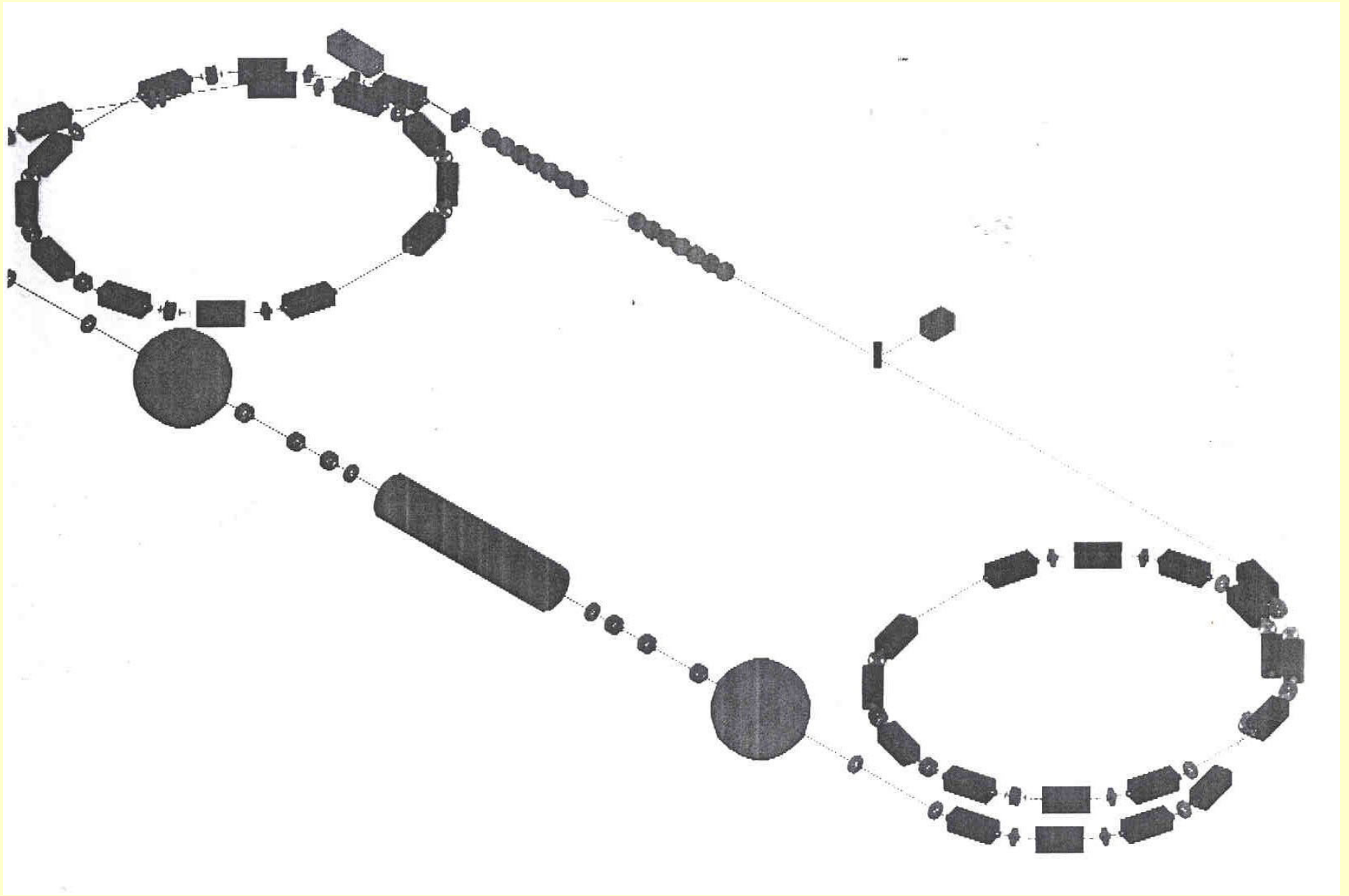
$$\alpha(\phi_s = 90^\circ, E = 2\text{GeV}) = 0.35\text{rad} = 20\text{deg}$$

Longitudinal fields:

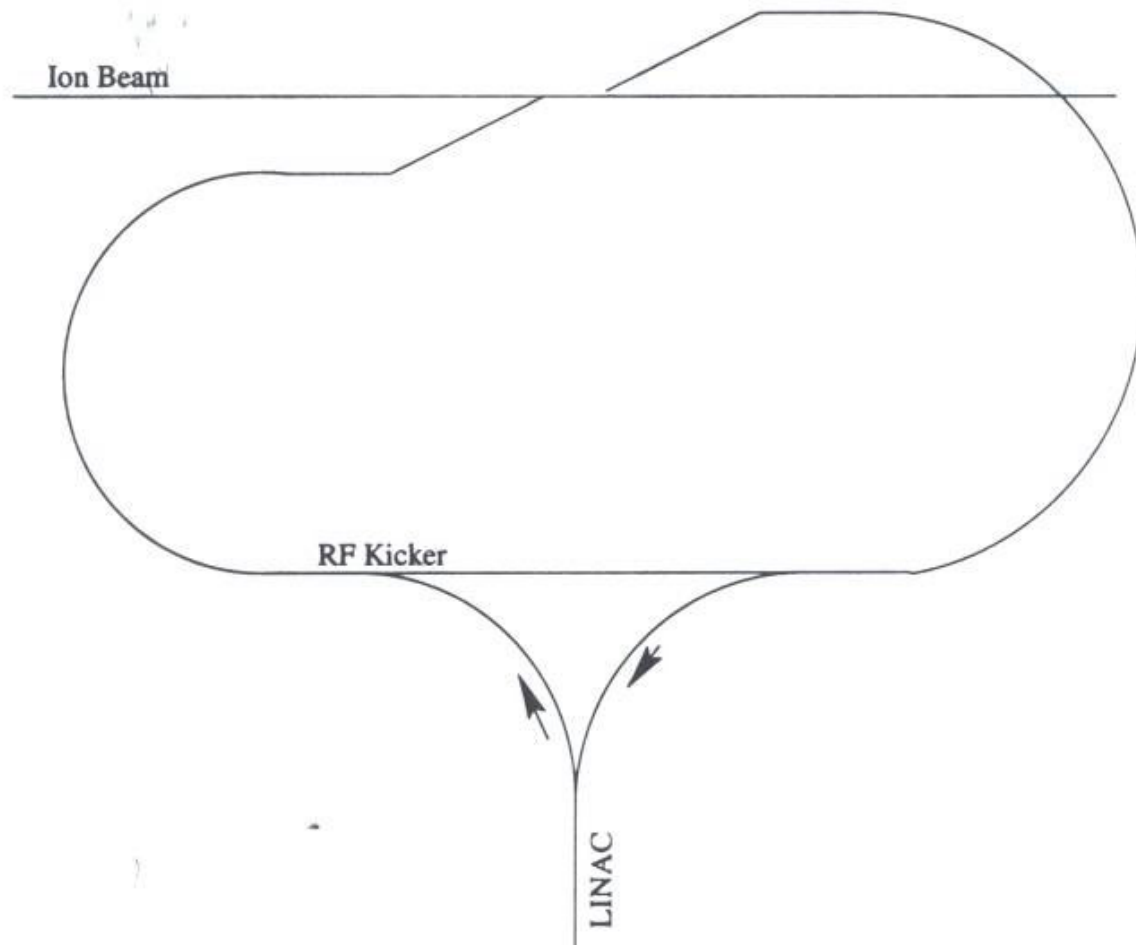
$$\vec{\Omega}_{\parallel} = \frac{e}{m\gamma}(1+a)\vec{B}_{\parallel}$$

$$\phi_s = \alpha$$

$$L \cdot \vec{B}_{\parallel}(\phi_s = 90^\circ, E = 10\text{GeV}) = 522\text{kG} \cdot \text{m}$$



Linac Ring Hybrid



Parameters for eRHIC at full energy

Scenario Species		Linac-Ring		Ring-Ring	
		P	Au	P	Au
Luminosity	x10**31	100.0	1.0	25.0	0.7
sigma*	microns	32.0	32.0	40.0	50.0
Ion parameters					
# / bunch	1.00E+09	200.0	1.2	94.0	1.2
Emittance	microns	0.9	0.5	0.8	1.0
Laslett	x0.001	6.0	5.3	3.0	3.0
Beam-beam	x0.001	4.0	4.0	4.0	4.0
beta*	cm	31.0	21.0	53.0	27.0
Electron parameters					
# / bunch	1.00E+10	2.9	4.8	2.6	8.1
Emittance	nm	6.0	6.0	18.0	18.0
Beam-beam	x0.001	382.0	180.0	60.0	60.0
beta*	cm	17.0	19.0	8.9	13.9

Ilan Ben-Zvi
HERA Future Workshop
Durham, December 6-7, 2001


BROOKHAVEN
NATIONAL LABORATORY

Linac-Ring hybrid (super conducting Linac with energy recovery)

Idea by Y. Derbenev

- The electron beam stays in the ring for 1000 turns and is then decelerated in the Linac for energy recovery
- The Linac current is reduced by a factor of 1000.
- There is no beam-beam collisions in the Linac.
- With a beam-beam parameter of 1000 the emittance growth due to beam-beam interaction is less than 1%.
- A low emittance lattice is required since 1000 turns is approximately one damping time. Combined function magnets can be used.
- Spin rotators or snakes are necessary.

Booster ring

$$\frac{P \cdot \tau_{pol}}{N_e} \approx \frac{R}{E}$$

Example: 10 GeV, 1 bunch $I=0.001$ A, $P_{den} = 6$ kW/m, $R=4.9$ m, $C= 50$ m, $\tau_{pol} = 0.2$ sec, $B = 67$ kG...Ooops

Example: 10 GeV, 1 bunch $I=0.001$ A, $B = 15$ kG, $R = 22$ m, $P_{den} = 0.3$ kW/m, $C = 200$ m, $\tau_{pol} = 15$ sec. $\tau_{pol}(360 \text{ Bunches}) = 1.5$ hours (required lifetime in main electron ring).

With 20 Bunches $P_{den} = 6$ kW/m and $\tau_{pol}(360 \text{ Bunches}) = 4.5$ Min.

At 2 GeV polarization time increases by a factor of 3125. Using "Super Magnets" Reduces polarization time by a factor 125. Resulting refill time is 2 hours.

Linac with polarized source (normal conducting)

This is a question to the engineers: what is less expensive?

Linac with polarized source (super conducting with energy recovery)

- Spin direction is determined at low energy using electric/magnetic fields.
- No spin rotators necessary.
- Helicity can be alternated.
- Beam power (1.4 GW) must be recovered.

Self-polarizing ring

$$\tau_{pol} = 98 \frac{R^3[m]}{E^5[GeV]} \cdot \frac{\langle R \rangle}{\langle R \rangle}$$

$$P[kW] = \frac{88.5 E^4[GeV]}{R[m]} \cdot I[Amp]$$

For $E = 10$ GeV and a radiation power density of 6 kW/m at $I_{beam} = 0.37$ A we get $R = 93.2$, $C = 1171.2$, $B = 3.5$ kG, $\tau_{pol} =$
26.4 min . Marginal

At 2 GeV this ring has a polarization time of 1375 hours. Possible to use variable length dipoles (with two coils). To keep the 26.4 min polarization time the magnets must be shortened by a factor of 56 (5.6 m -> 10 cm) which requires a field of 196 T.

Ridiculous

Options:

- Self-polarizing ring (small radius)
- Ring with injection of polarized beam (large radius)
 - Booster ring
 - Linac with polarized source (normal conducting)
- Linac with polarized source (super conducting with energy recovery)
- Linac-Ring hybrid (super conducting Linac with energy recovery)

Polarization time and equilibrium polarization

$$\frac{1}{\tau_{pol}} = \frac{5\sqrt{3}e^2\gamma^5\hbar}{8m^2c^2C} \oint \frac{1 - \frac{2}{9}(\vec{n} \cdot \vec{s})^2 + \frac{11}{18}\left(\frac{\partial\vec{n}}{\partial\delta}\right)^2}{|\rho(s)|^3} ds$$

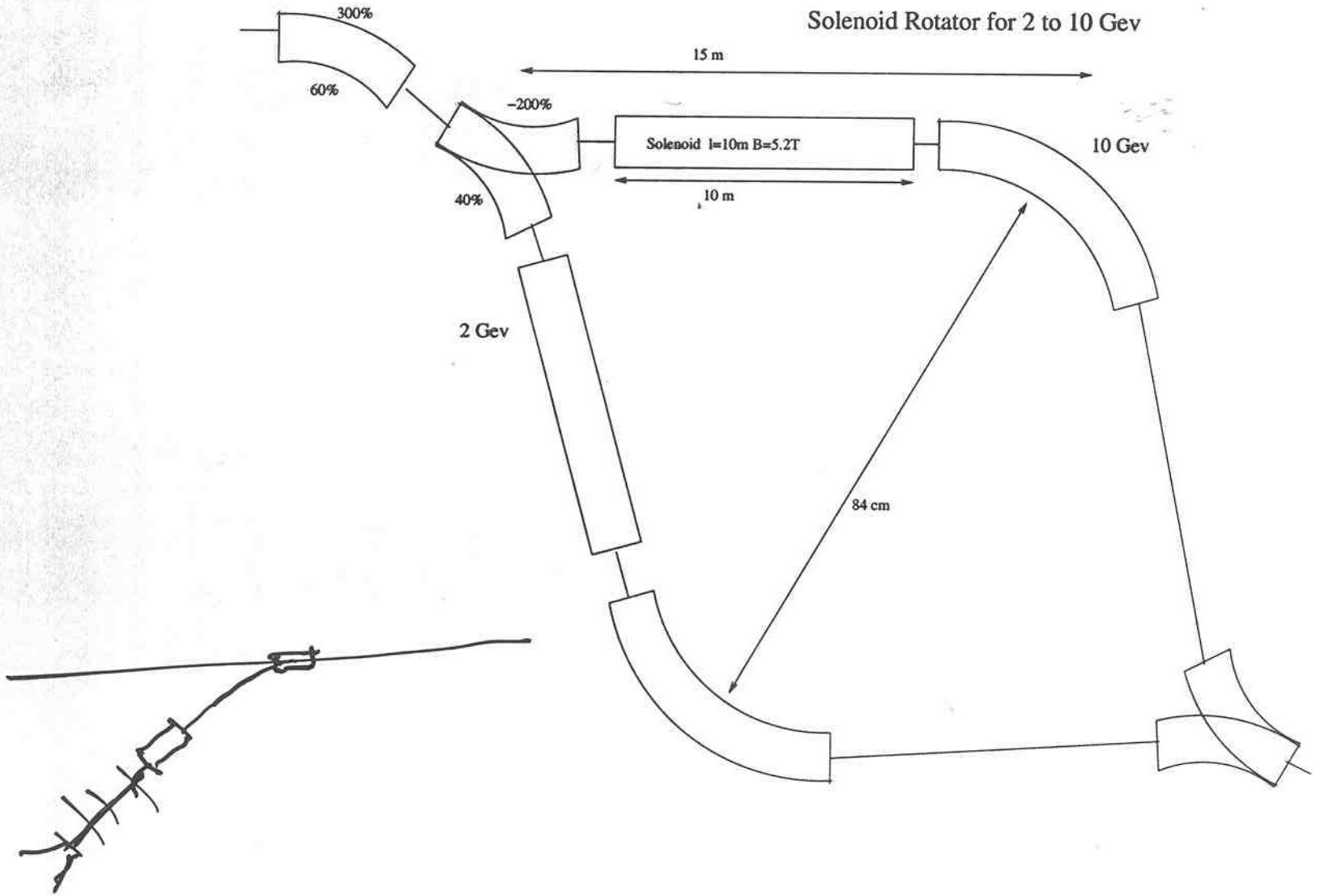
$$P_\infty = \frac{8}{5\sqrt{3}} \cdot \frac{\oint \frac{\vec{b} \cdot (\vec{n} - \frac{\partial\vec{n}}{\partial\delta})}{|\rho(s)|^3} ds}{\oint \frac{1 - \frac{2}{9}(\vec{n} \cdot \vec{s})^2 + \frac{11}{18}\left(\frac{\partial\vec{n}}{\partial\delta}\right)^2}{|\rho(s)|^3} ds}$$

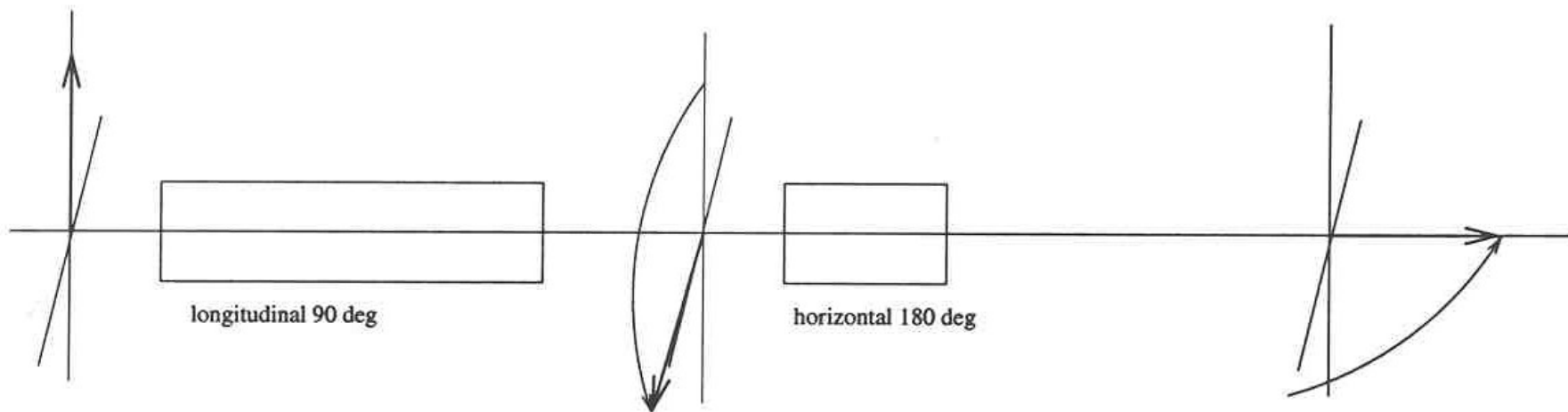
Spin matching

- Method to make the spin motion across a spin rotator independent of the electrons initial coordinates $(x, x', y, y', \Delta l, \frac{\Delta P}{P})$
- In the arcs the spin motion depends only on the vertical motion. The beam height is small.
- A spin rotator pair is spin matched if:
 - there are no quadrupoles inside the rotators.
 - the interaction region is anti-symmetric
 - the transverse matrices between the rotators are unit matrices.

For different conditions spin matching can be achieved through the use of spin matching computer codes.

Solenoid Rotator for 2 to 10 GeV





Spin rotations, spin tune shift and Sokolov-Ternov polarization for rotator E3

spin tune	V3	H3	V2	H2	V1	H1 + HTRA + HSEP	beam deflec- tion H4- [deg]	$\Delta\nu$ /pair of rotator	polarization [%]
67.6000671	47.85525	- 42.60509	- 88.62115	104.60579	40.76588	30.65434	.360133	.048510	84.239
61.0	37.22352	- 78.54513	- 68.93268	94.39271	31.70915	40.72333	.803376	.039480	79.073
61.5	39.06361	- 71.12339	- 72.34028	95.16642	33.27665	38.42985	.714949	.046639	80.780
62.5	41.43223	- 62.66395	- 76.72661	96.71384	35.29437	35.92247	.611210	.052414	82.289
64.5	44.58185	- 52.56476	- 82.55927	99.80868	37.97741	33.12917	.484674	.054330	83.512
66.5	46.83683	- 45.70158	- 86.73517	102.90352	39.89833	31.38996	.398559	.051297	84.058
68.5	48.60151	- 40.30989	- 90.00311	105.99836	41.40159	30.13006	.331957	.045819	84.383
70.5	50.03552	- 35.76712	- 92.65869	109.09321	42.62316	29.14668	.277254	.038845	84.621
72.5	51.22221	- 31.77677	- 94.85628	112.18805	43.63405	28.34324	.230706	.030864	84.823
74.5	52.21292	- 28.17173	- 96.69094	115.28289	44.47800	27.66531	.190144	.022171	85.012
76.5	53.04188	- 24.84892	- 98.22604	118.37774	45.18415	27.07930	.154191	.012967	85.196
78.5	53.73331	- 21.73904	- 99.50647	121.47257	45.77315	26.56265	.121899	.003395	85.380
80.5	54.30502	- 18.79497	- 100.56520	124.56742	46.26017	26.10001	.092601	- .006436	85.567
82.5	54.77049	- 15.98145	- 101.42719	127.66227	46.65668	25.67989	.065790	- .016439	85.755
84.5	55.14010	- 13.27257	- 102.11165	130.75710	46.97154	25.29385	.041083	- .026544	85.945
86.5	55.42187	- 10.64712	- 102.63344	133.85195	47.21156	24.93499	.018169	- .036689	86.137

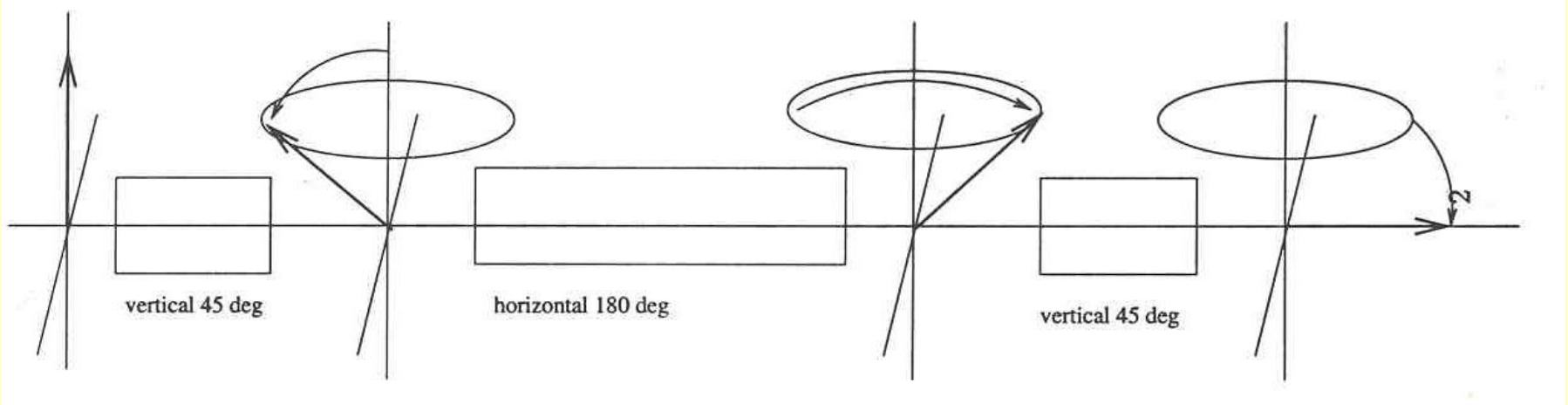
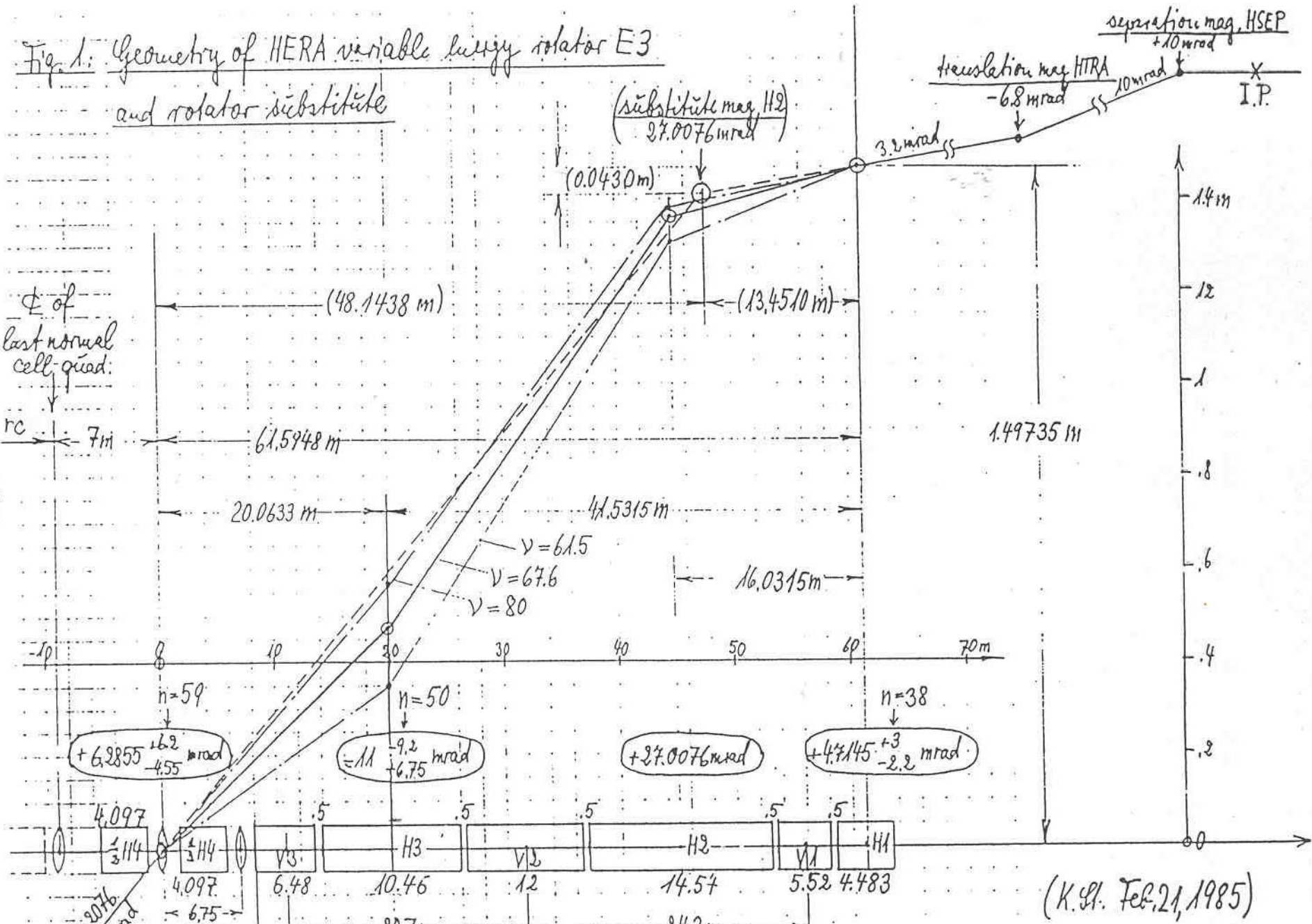
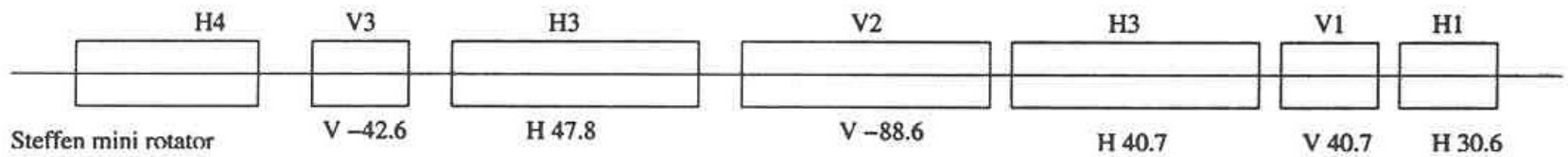
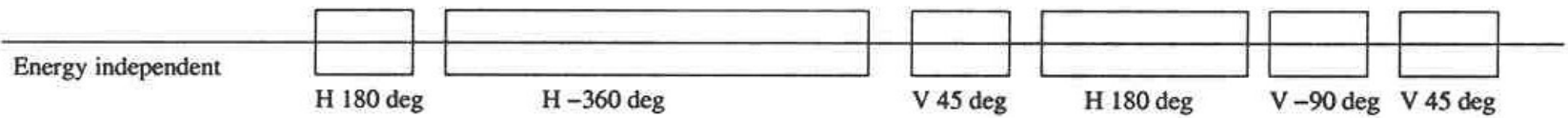
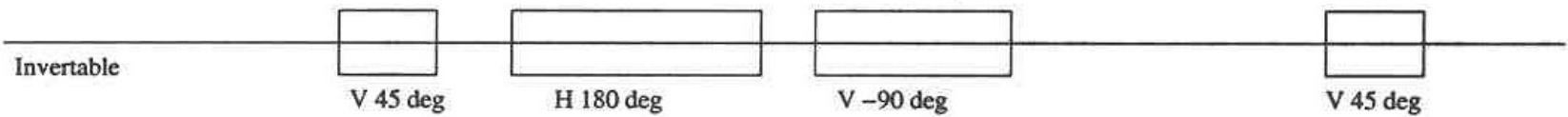
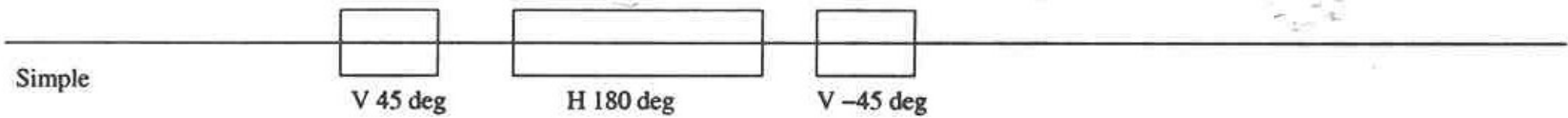


Fig. 1: Geometry of HERA variable lumpy rotator E3
and rotator substitute



(K.G. Feb. 21, 1985)



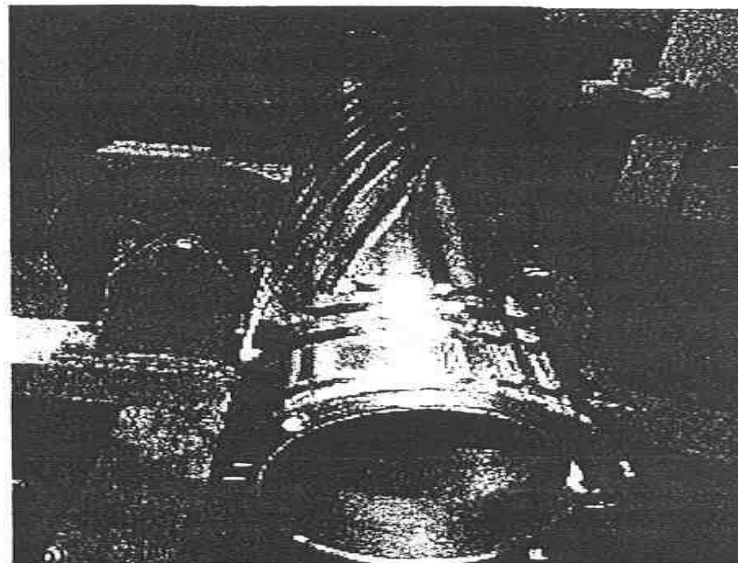
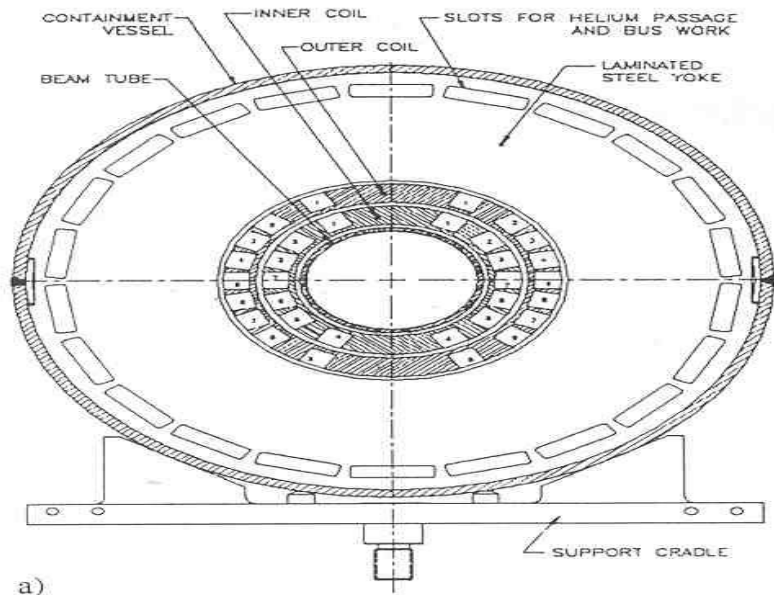


Figure 2: a) Cross section of a helical dipole. There are two layers of helical windings: 7 blocks in inner and 9 blocks in outer. b) A machined aluminum tube showing helical slots for the coil windings.

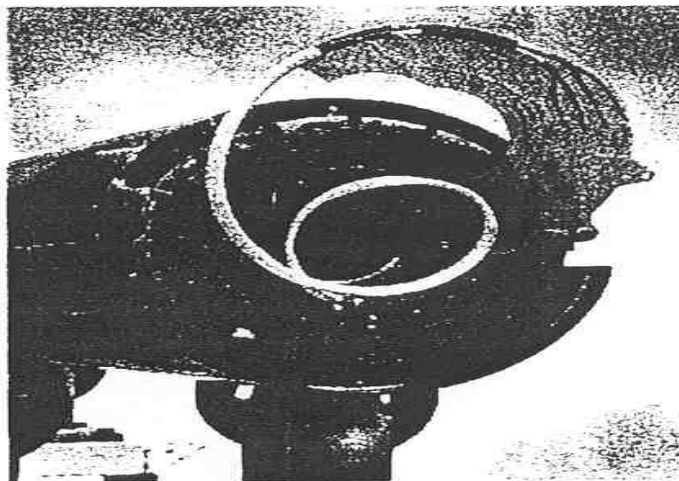
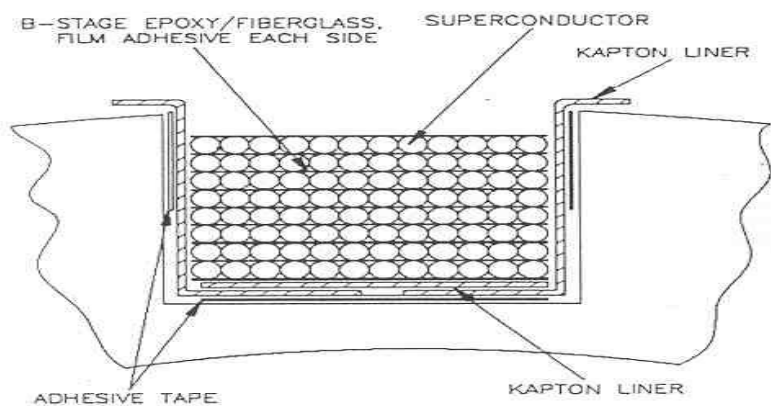


Figure 3: Left (a): Detailed cross section of one block of windings. Right (b): The lead end of a completed magnet showing the quench resistors and compact wiring harness. Since the separation between magnets is about 10 cm, the leads are attached to a pivoting plate for ease in wiring.

Building the Detector – Accelerator Interface

presented by,

Brett Parker, BNL/SMD

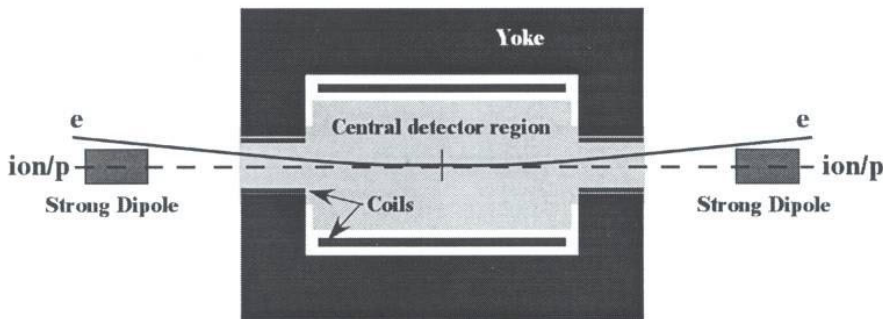


**My charge from
IR group leader:**

A) Integration of accelerator and detector components, dual role magnets.

B) Beam separation scheme(s), discussed in the context of the IP design flexibility to accommodate variable beam momenta, variable beam momentum ratio and variable collision schemes: ep, eA, pp and pA.

Design Principles, Tips and Tricks: Short list of EIC IR design suggestions.



- Weak dipole bend in the central region (e-beam synrad).
- Strong bend outside for protons/ions (e-beam shielded).
- Put quadrupole focusing in outer flux return yoke (β^*).
- Try to incorporate an antisolenoid close in (polarization).

Design Principles, Tips and Tricks: How to get the most from an EIC.



On television Norm Abram always has the correct tool to ensure that parts from his projects fit together smoothly. He makes home construction and renovation look simple.

Today I do not claim to have an IR design worked out which is ready to be built; however, I do plan to:

- Identify some of the tools which are needed.
- Give examples to illustrate a few useful tricks.
- And outline principles which should lead to a satisfactory IR design.



Norm Abram from the PBS series, "The New Yankee Workshop"

Main Theme:

IR space is precious and this fact forces experimentalists and accelerator designers to cooperate closely if they hope to achieve their goals. A powerful way to do this is to make the IR magnets serve dual purposes.

IR Leader: Please compare/contrast IR layouts with large & small momentum ratios.

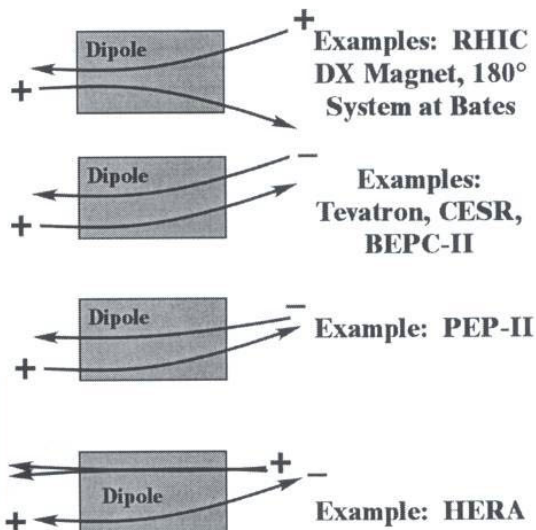


Ah...but what are the relative charges?

Dipole field separates like sign charges going in opposite directions. To separate opposite sign particles requires a momentum difference.

However for large momentum ratio a dipole field separates both polarities.

HERA: Protons @ 920 GeV and Electrons/Positrons @ 27.5 GeV for 33½:1 momentum ratio, so proton orbit is hardly changed by flipping dipole polarity.

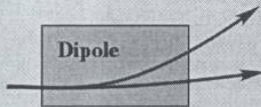


The dipole field appropriate to bend HERA electrons hardly effects the proton beam.

Synrad backgrounds and heating implicitly limit dipole fields used for beam separation.



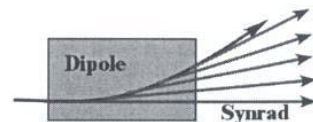
For EIC we are (probably) stuck with oppositely charged beams and have to use either a momentum ratio or a non-zero crossing angle to separate the beams.



All things being equal, one would like to use strong dipole fields to separate beams (spectrometer principle).

Note: Such a dipole may also be desired by experiments to momentum analyze secondary particles and separate out neutral particles.

- For HERA upgrade synrad backscatter background was major concern for experiments.
- Synrad heating of beampipe absorbers significant eRHIC design constraint at 2000 Yale workshop (e.g. use PEP-II heating limit). But using only soft bending gives up spectrometer functionality.*

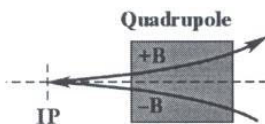
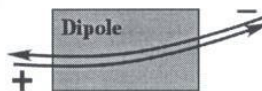


*See eRHIC note, Sebastion White, December 5, 1999.

A non-zero crossing angle permits even equal rigidity beams to be separated.



Examples: Tevatron, CESR, or BEPC-II beams in a dipole.



B-field reverses sign across a quadrupole centerline. So with a small seed displacement quadrupole defocusing can help to separate BEPC-II e^+ and e^- beams.

A similar trick could be used for EIC even without a crossing angle, if we start beam separation early enough. Then the first quadrupole could be used to help. We would have to adjust the quadrupole magnetic center so that the e-beam only sees small B-fields (large B-field is ok for p/ion beam).

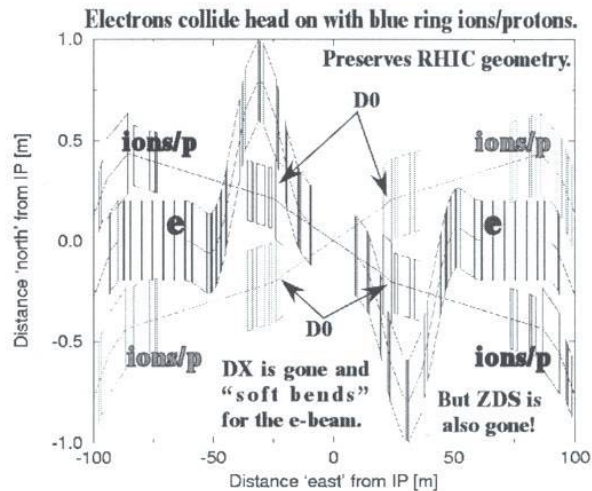
Accelerator Beam Line Layout and Experimental Physics Facts of Life.



The eRHIC layout presented by J. Kewish at the Yale 2000 Workshop, preserves RHIC geometry by crossing the ion/p beams from one D0 to diagonally opposite D0. Instead of 4.3 T DX dipole, electrons are deflected by 0.134 T BS1 dipole magnet for tolerable synchrotron radiation (synrad) production.

Experimental Concern:

S. White and others pointed out that this arrangement does not separate small angle particles and neutrals sufficiently from the circulating beams to do physics.

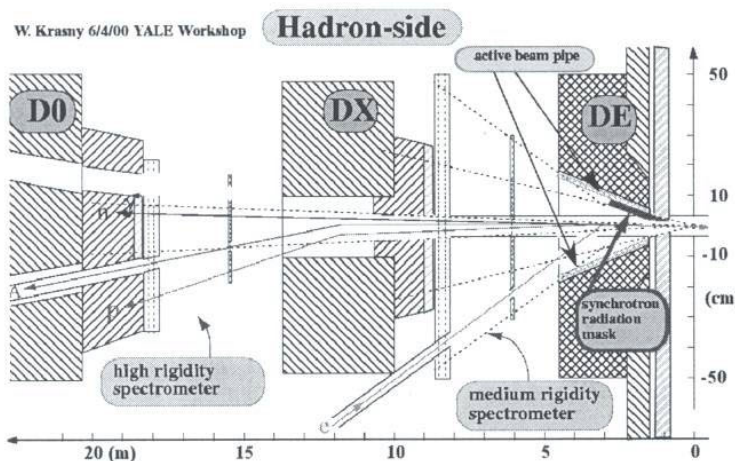


How can we recapture the "spectrometer functionality" provided by RHIC DX magnet?

Experimental Physics Layout and Some Magnet Design Facts of Life.



W. Krasny 6/4/00 YALE Workshop



DE dipole, integrated with experimental detector, gives weak bend to get past superconducting DX magnet. DX then provides strong bend for high rigidity spectrometer.

Design Dilemma:

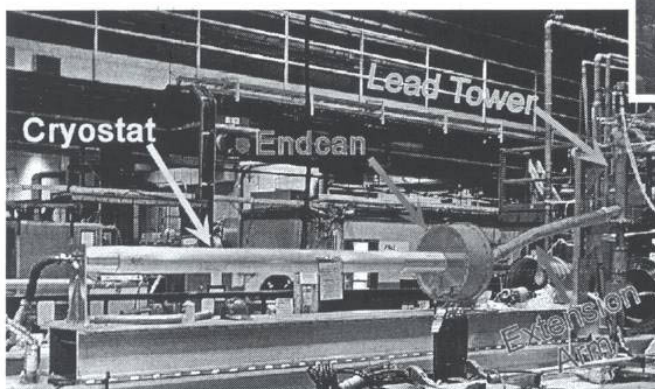
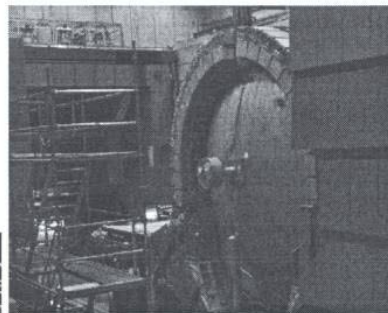
DE dipole field needed to clear DX is too high (synrad). Smaller field sends e-beam through DX yoke (leakage fields there are also too high).

How can we improve upon this layout while keeping the advantages of a weak – strong bend geometry?

HERA Example: Trading space between experimental detector and accelerator.

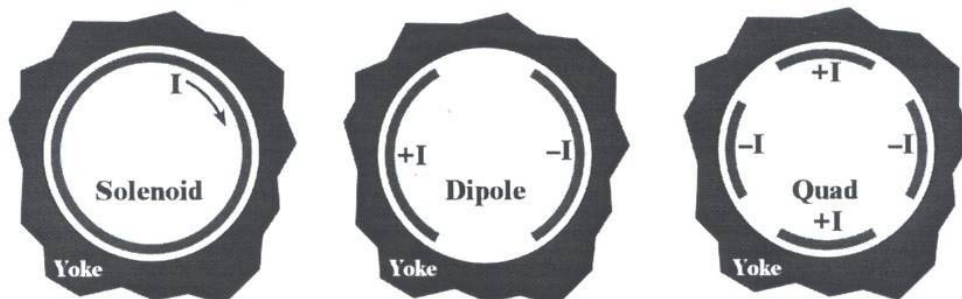


- Temptation for accelerator physicist is to put small diameter coils close to IP to start beam focusing and separation as early as possible.
- Then forced to choose between losing inner or outer aperture (some dead space is unavoidable).



Superconducting G0 magnet shown at left on test stand at BNL and installed into experiment H1 at DESY (above). G0 has a mini-cryostat to provide sufficient inner space for synrad and beams but not to take up too much radial space in detector.

Observation: A cylindrical yoke is compatible with many different coil types.

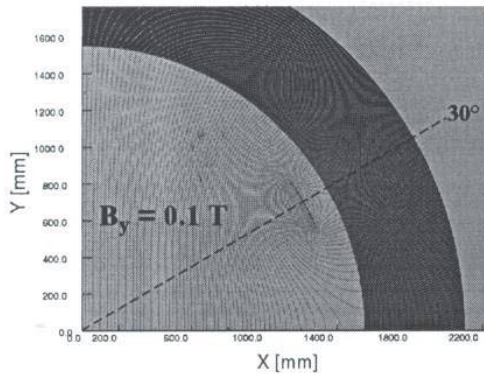


- Solenoidal and dipole coils both fill space with flux efficiently (uniform field).
- For quadrupole, peak field goes \propto Gradient $\times R_{\text{coil}}$ so a quadrupole coil is only practical for small coil radius (e.g. return yoke but not main body).

A cylindrical yoke is compatible with a low field strength dipole plus regular solenoid.



Dipole (1/4 Model + Boundary Conditions)



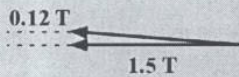
- ◆ Dipole with 0.1 T does not require excessive superconductor (even with $R_{coil} = 1.4$ m).
- ◆ Wind on top detector solenoid coil.
 - Avoid radiation length at small R.
 - Avoid issues with coil torques.
 - Even the partial coil shown at left, gives good field quality for beams.

Design shown has 10^{-5} field uniformity at $R = 80$ mm.

Tips and Tricks: Add a small transverse component to field in detector solenoid.



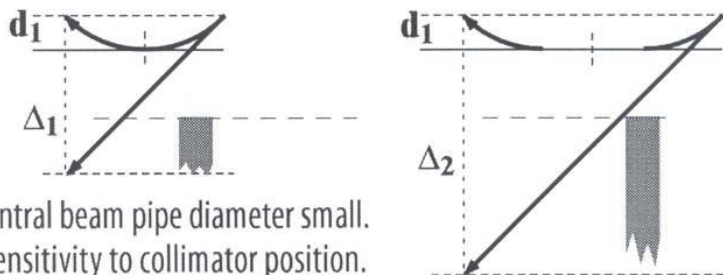
Consider the following: Add $0.12\text{ T} \perp$ inside a 1.5 T detector solenoid.



Magnitude changes $\approx \frac{1}{2}(0.12/1.5)^2 \times 100 = 0.3\%$
 Direction changes by $\approx (0.12/1.5) \times 1000 = 80\text{ mr}$

Effect is similar to tipping solenoid with respect to beam.

By keeping the bend center close to IP it is possible to pass synrad cleanly through both the experiment and the accelerator magnets.



- Keep central beam pipe diameter small.
- Avoid sensitivity to collimator position.

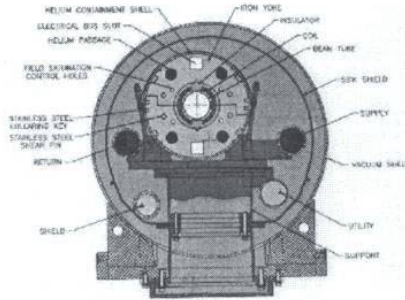
Beamline Layout and Magnet Design Facts of Life.



It is hard to get past a superconducting magnet while using only soft bends.*

* If your IR section length is too limited.

- Complicated to make through hole in cold mass and cryostat.
- And even then have to watch out for large fringe or leakage fields.



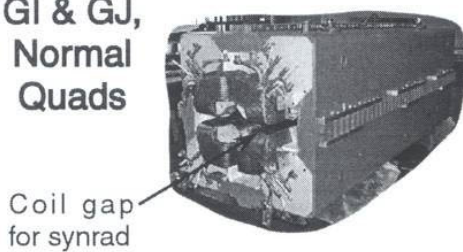
Yale 2000 eRHIC design avoids trouble by making D0 first superconducting magnet. But then there is no Zero Degree Spectrometer.

For $B_{pole} \approx 1$ T soft iron useful for field shaping and copper coils work fine for apertures that are not too large.

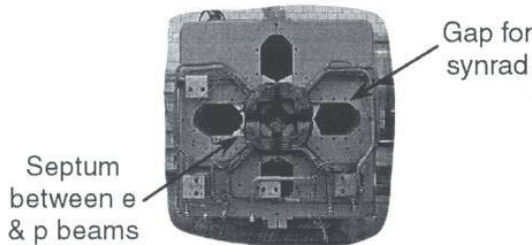
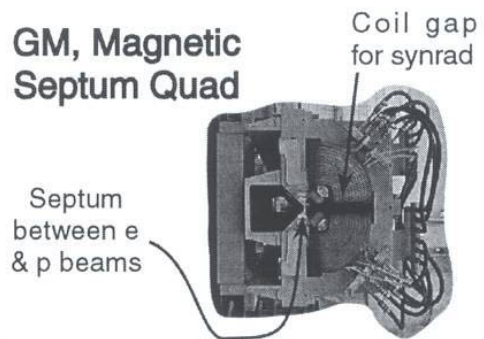
Some of the special magnets created for the HERA Luminosity Upgrade.



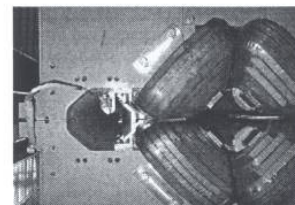
GI & GJ, Normal Quads



GM, Magnetic Septum Quad

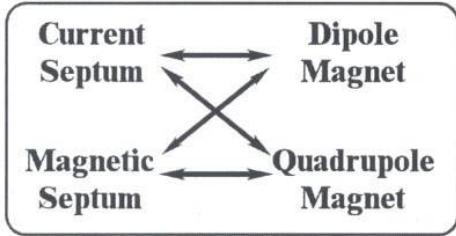


GN, Current Septum Quad



GA & GB, Normal Quads

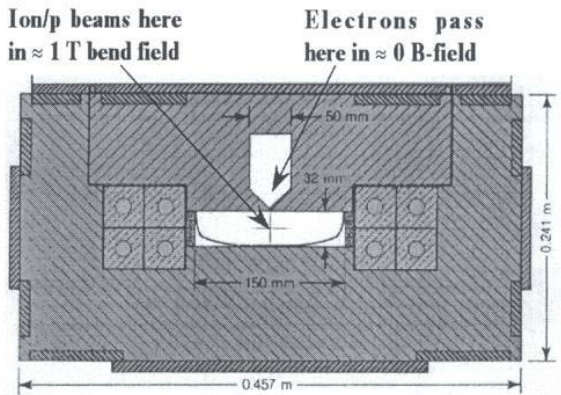
Design Principles: Septum magnets provide a variety of fields for beams.



Proposal: Investigate using a septum dipole outside EIC detector to provide spectrometer functionality.

- Provide apertures for many beams.
- Instrument to integrate with detector.
- Easier to get close to a warm magnet.
 - ▲ Maintaining lever arm offsets lower field.
 - ▲ Get magnet close in for large solid angle.

- Many septum magnet configurations are commonly used.
- Lambertson dipole, shown below, is typical for separating injected or extracted beams.

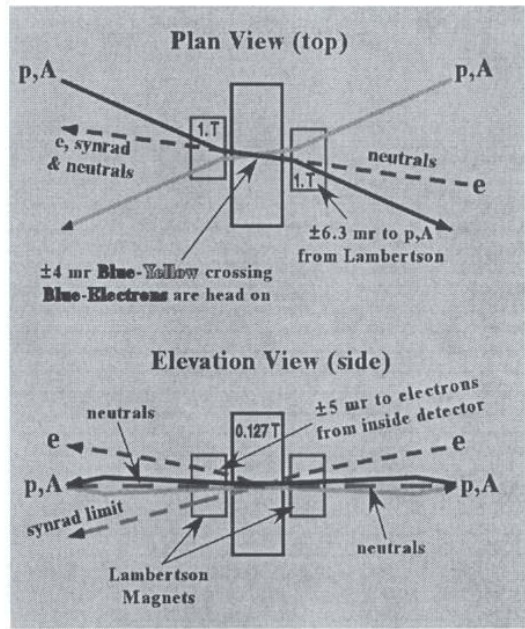


SSC Collider Ring Abort Lambertson Magnet

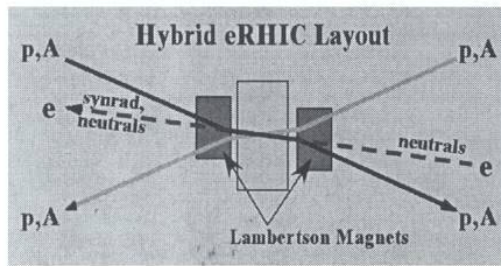
Proposal for hybrid eRHIC layout that is compatible with weak – strong bends.



- E-beam strikes head on with Blue at IP.
- A small vertical deflection inside detector separates electrons from circulating beams.
- Ions/p bent by 1 T field inside a Lambertson dipole (electrons in reduced B-field region).
- Long drift downstream of Lambertson gives spectrometer lever arm.
- Keep Lambertson short to pass synrad etc. via small Blue/Yellow crossing angle (but with reduced neutral separation).
- Small vertical kicks to Blue/Yellow beams compensated before triplets – proton spin should be ok.



Optimization and some features of the proposed hybrid eRHIC layout.



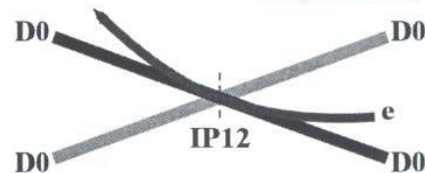
- For hybrid scheme to work well, will have to integrate Lambertson magnets with detector (instrument warm magnet).
- Ion/p crossing angle is critical parameter for optimization. Zero crossing angle possible, but then downstream gets filled in with magnets.

- ◆ If it really is deemed desirable to also have option for (p,A) and (A,A) then need to determine largest allowable crossing angle.
- ◆ Having a symmetric vertical bend for e-beam does not preclude using antisymmetric horizontal bends further from the detector.
- ◆ Moving Lambertson close to detector increases acceptance for all beams but also increases solid angle covered by septum.
- ◆ Separating beams via Lambertson magnets not limited to eRHIC.

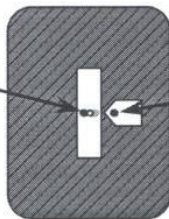
Design Options: Two weak – strong bend layouts (not recommended for eRHIC).



- Make the weak electron bend in the horizontal plane.
- Then with Lambertson magnet can have strong bends in the vertical plane (compatible with 8.3 mr crossing angle eRHIC scheme).



Ions/protons and neutrals
Deflection is in the vertical plane



Electrons

Adjust until the yellow and blue path lengths are same.



Option A: Elevation View



Option B: Elevation View

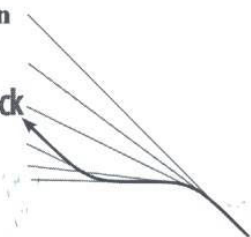
Both options put strong vertical bends in RHIC yellow and blue rings. But this is not really advisable (likely impact to RHIC proton spin program).

Design Principles, Tips and Tricks: Use of symmetric and antisymmetric bends.



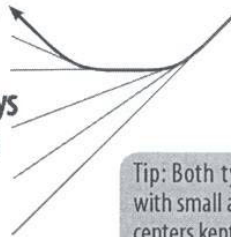
Antisymmetric Bend Geometry Synrad Fan

Fan folds back on itself



Symmetric Bend Geometry Synrad Fan

Fan always stays on same side



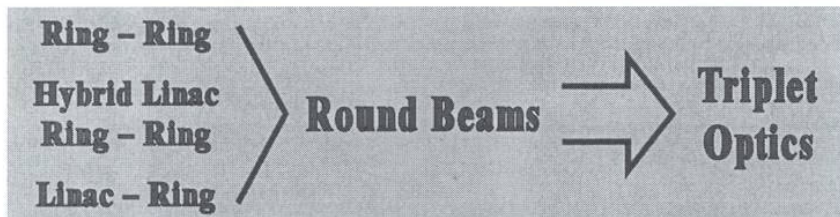
Tip: Both types work best with small angles and bend centers kept close together.

- Antisymmetric helps to keep far downstream apertures smaller.
- Antisymmetric provides opportunity for some optics cancellations.

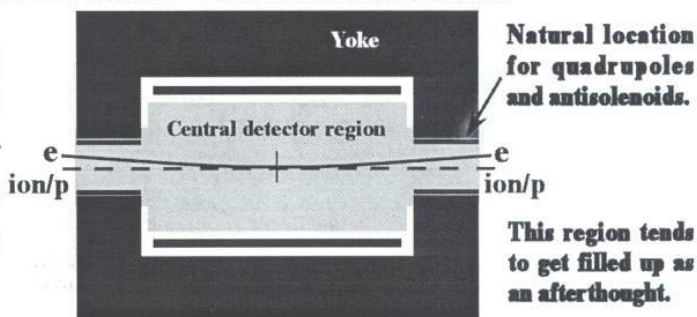
Trick: Keep weak – strong bend scheme by using Lambertson septum to leverage effect of a small vertical kick close to IP.

Note that we can mix the two geometries shown above. Overall geometry with hard bends from spin rotator can be antisymmetric but with small symmetric bump near IP to use Lambertson magnet.

Design Principle: For $\beta^* \approx 0.1 - 0.4$ m, try to put first quadrupole about 1 m from IP.

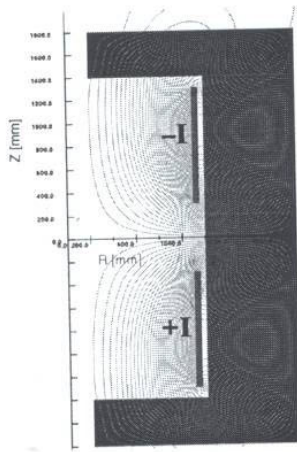


- Consider from the beginning integrating large aperture quadrupoles in return yoke.
- Offset magnet center and/or add dipole field so e-beam sees reduced B-field.

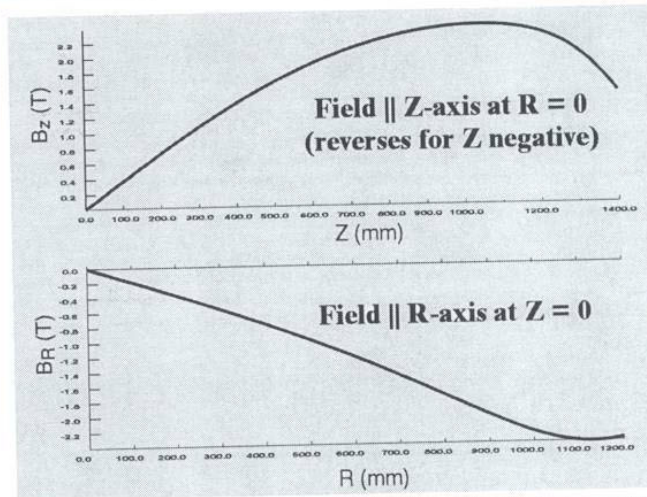


Also skew quadrupole pairs may be needed in region outside detector.

Provocative Question: Can we combine solenoid and antisolenoid in one magnet?



Double Solenoid Model



So far the best that has been proposed is to put small diameter, high field superconducting antisolenoid coils inside the detector. But such magnets limit experimental acceptance, perturb the detector field and are hard to support. Is a double solenoid configuration, as outlined above, useful for doing physics?

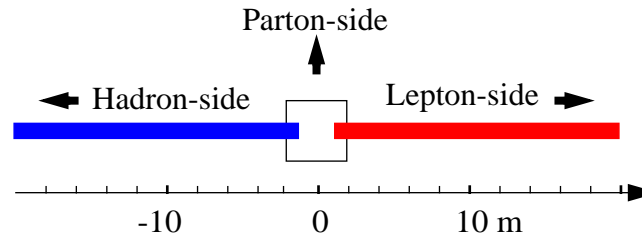
The detector – accelerator interface and getting the most from EIC (summary).



- For basic design can build upon existing experience (HERA, B-factories).
- Some technological choices are more accommodating of experimental requirements (e.g. linac – ring: energy variability, no spin rotators) but cost considerations will force groups to set priorities.
- Investigate new ideas:
 - ◆ Integrate weak dipole field into the detector solenoid.
 - ◆ Integrate detector components into accelerator magnets.
 - ◆ Try using Lambertson style magnets for beam separation.
 - ◆ Integrate large aperture quadrupoles in solenoid return yoke.
 - ◆ Investigate utility of double solenoid scheme for detector.
- None of the above are magic fixes; however, in order to really push the limits on luminosity, particle acceptance, kinematic range etc. many elements will have to serve dual purposes.

The traditional split (fight) for accelerator/experimental real estate might not yield the best result. Figure out how to cooperate from the beginning.

Toy Model of a Detector for EIC



PLAN:

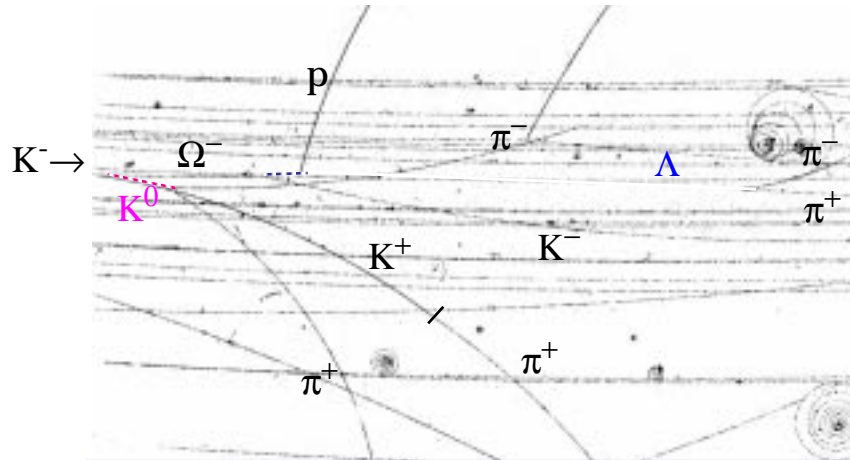
Revisit our toy model (cf. Whitepaper March 2001) in the context of interaction regions design.

“Strong interaction between detector and accelerator will be needed”

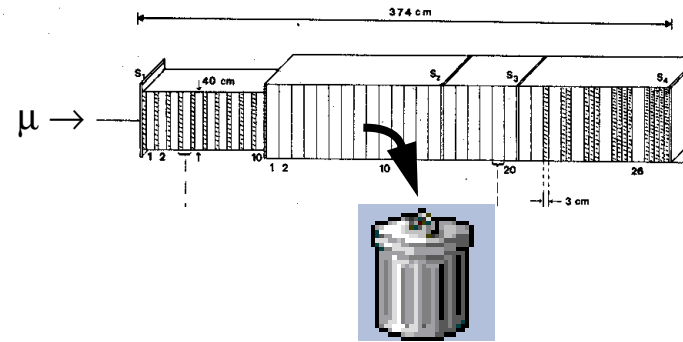
G. Hoffstaetter (Snowmass 2001)

TRANSPARENT versus OPAQUE TARGET

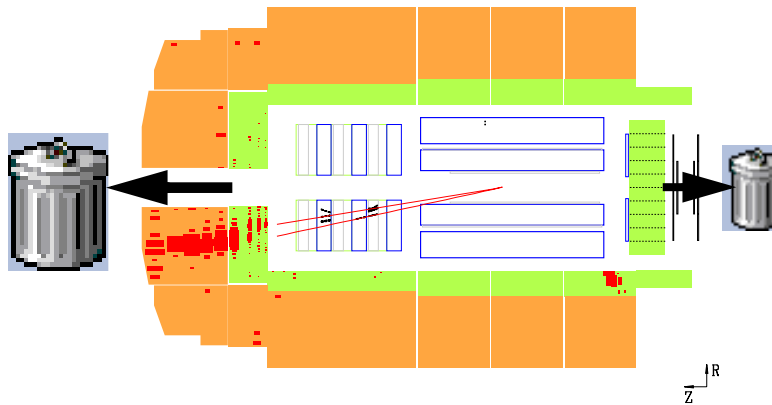
2 m HBC 1968



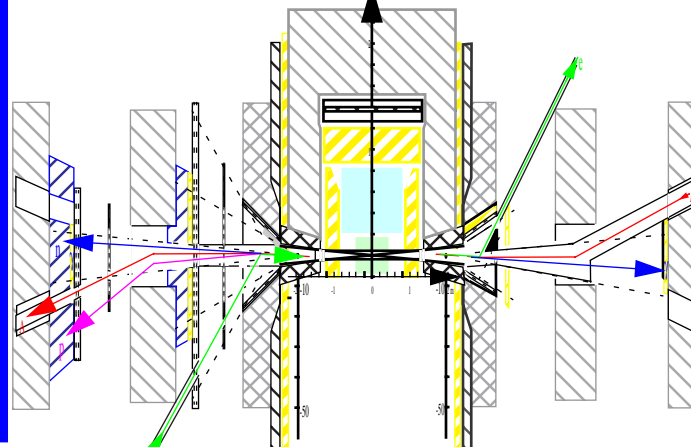
EMC 1980



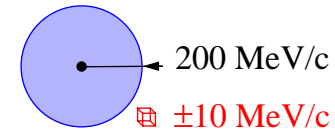
HERA1 1992



e-RHIC 200x



General



Toy model goals:

- 4π acceptance for a complete final state identification
- “spectroscopic resolution” resolution for target remnants and jets

Machine requirements:

- beam divergence and crossing angle
- reasonable luminosity and backgrounds
- “active beam pipes”, “active collimators” and “skew vacuum chambers”

Near beam detector requirements:

- rates, background rejection, resolution (spacal, SiO₂-fibers,...)
- special designs? (active beam pipes)

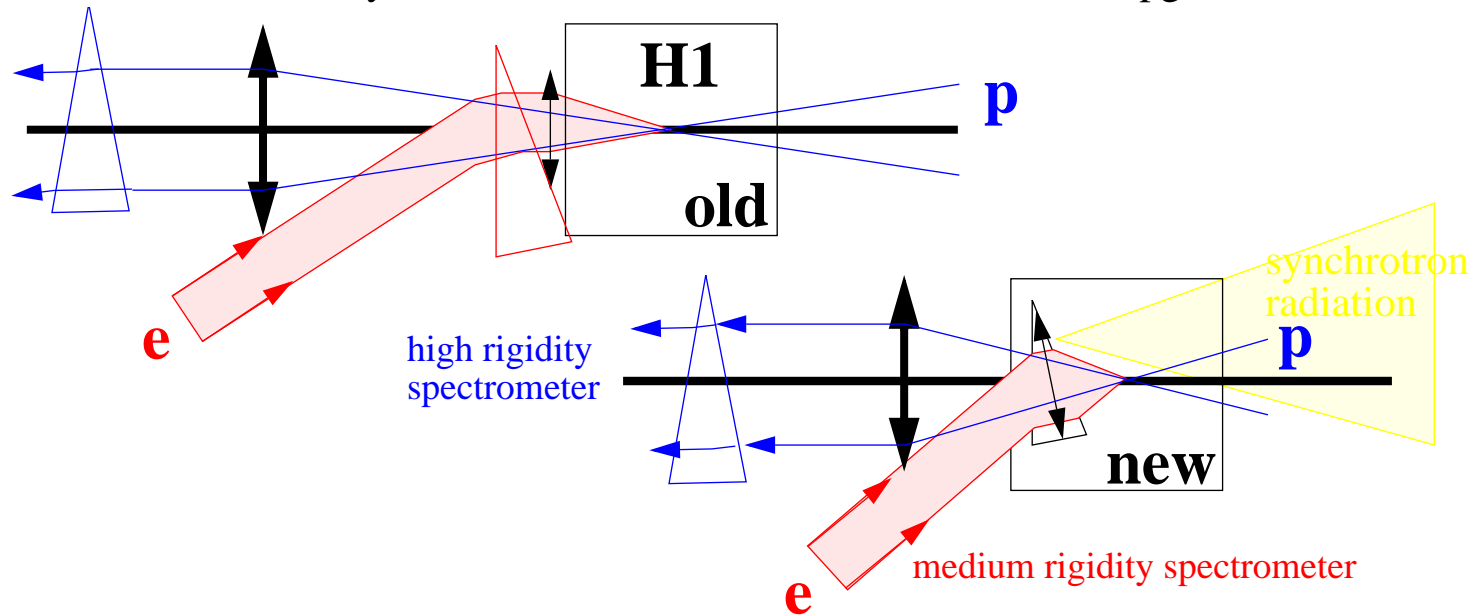
Compatibility of near beam detectors with other goals:

- p-A, A-A, polarization, high luminosity...

Machine Requirements

In-beam spectrometers

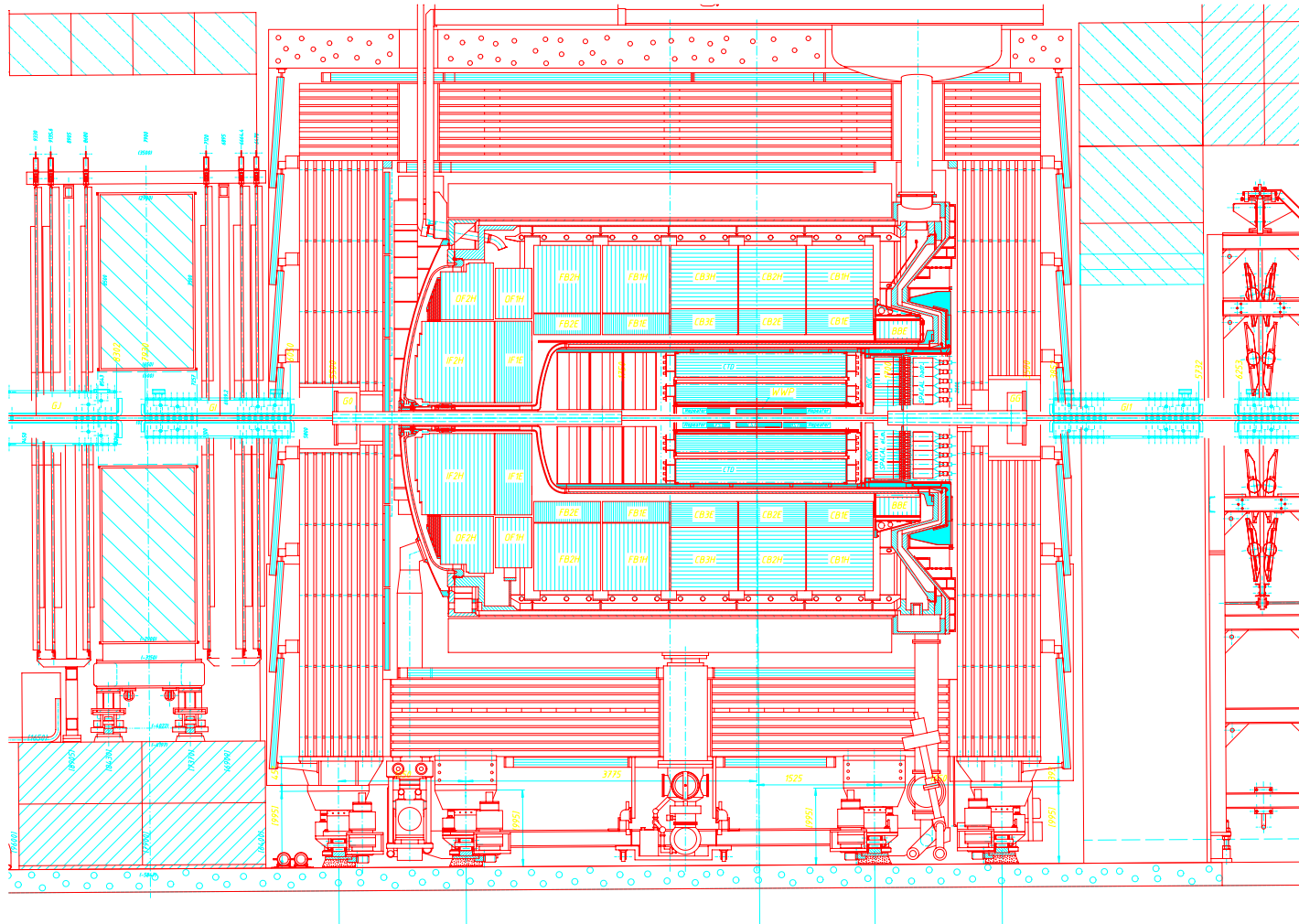
Novel feature of the toy model? It comes from the HERA hi-lumi upgrade¹:



(“magnets inside detector - detector inside magnets” G.H. ibid.)

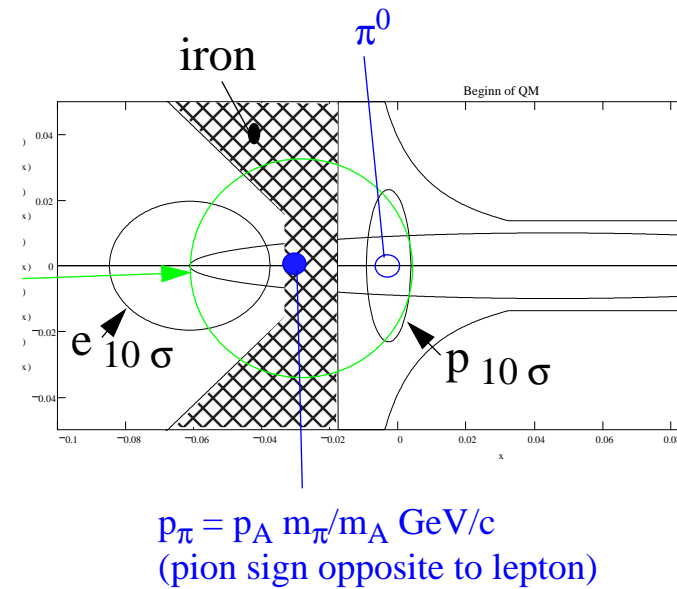
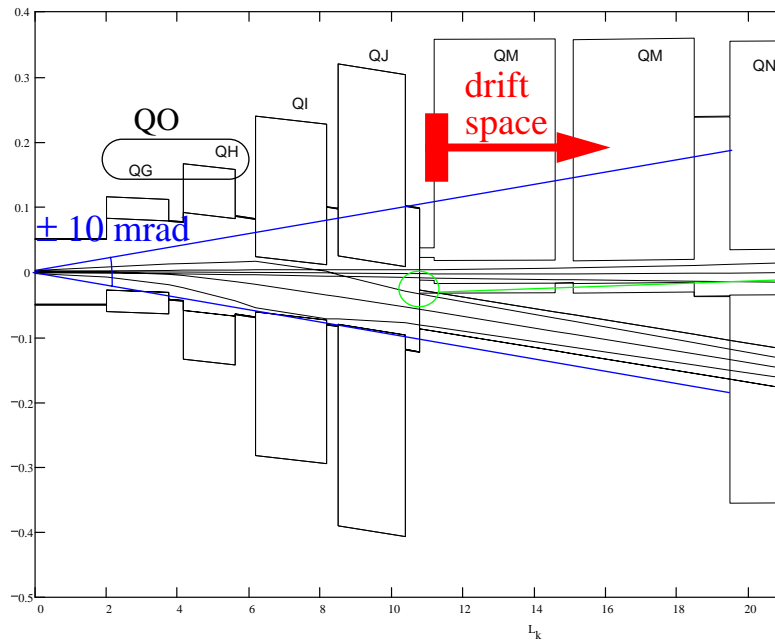
1. cf. “Evolution of HERA detectors towards e A physics”, E.B., Physics with HERA as eA collider workshop, DESY 25/05/99

Magnets inside detector ...



Spectrometer design parameters:

- aperture of medium and of high rigidity spectrometers
- length of drift space between spectrometers
- $\int B dl$ (fixed by beam optics)
- beam divergence (as low as possible)



Detector Requirements

Hadron-side

-main functions (left to right):

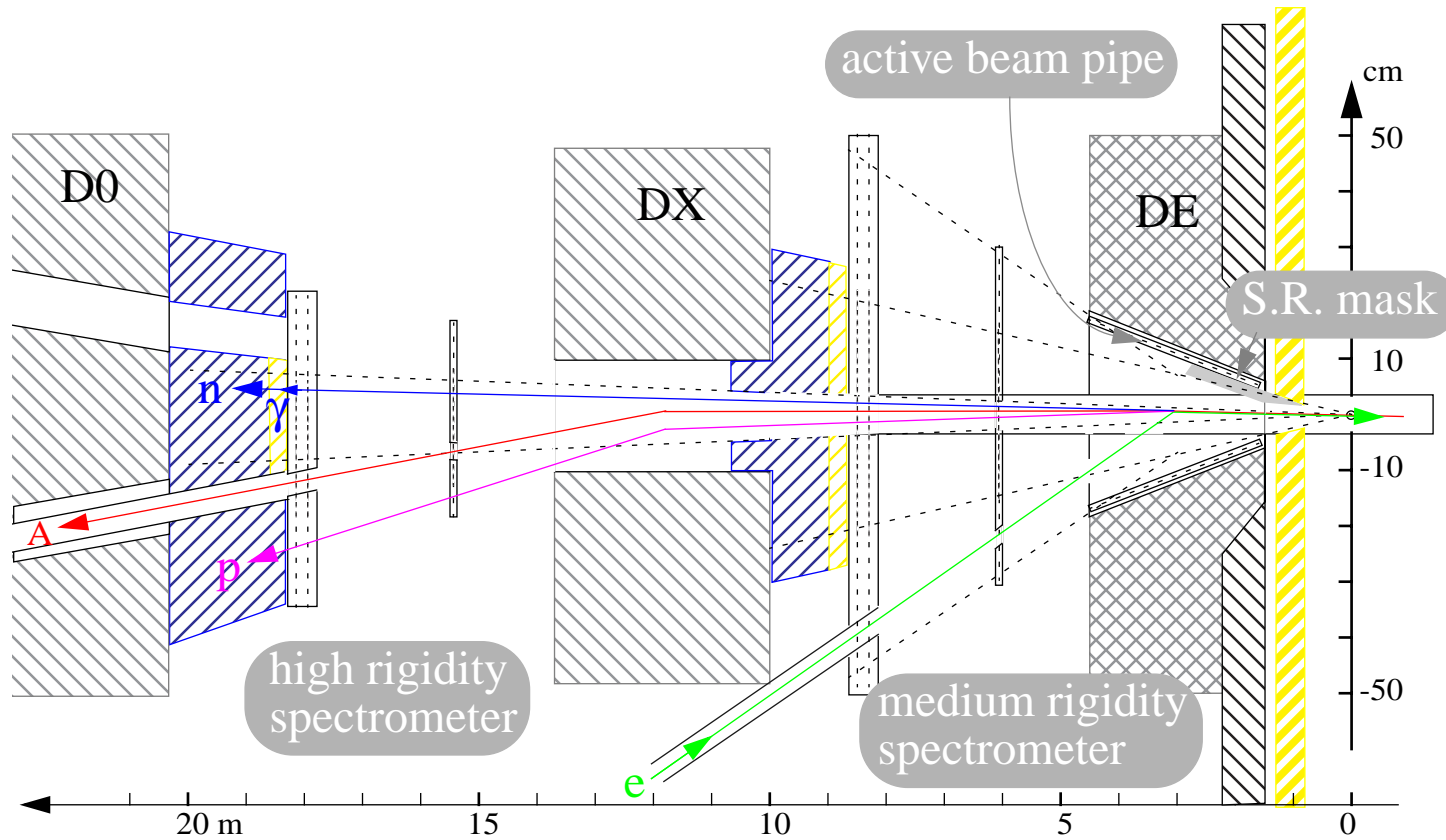
Roman pots (not on plan): diffractive scattering on beam (or same rigidity ion)

High rigidity spectrometer: EM calo for nuclear $\gamma(\pi^0)$; hadron calo for measuring evaporation neutrons and identifying p^+ & ions; tracking for measuring evaporation p^+ & ions

Medium rigidity spectrometer: EM calo for π^0 s; hadron calo for measuring wounded neutrons and identifying ions & wounded p ; tracking for measuring nuclear π^\pm , wounded p^+ and ions

Rapidity gap π -tagger: close the acceptance for charged particles emitted in the DIS process and tags diffractive events

Toy model ~hadron-side~:



- both spectrometer trackers using MWPC and drift chambers (or μ strips) at center.
- scintillating fiber calo for medium and high rigidity calorimeters (plastic or SiO_2 ?)
- scintillating fiber tracker (“active beam pipe”) for rapidity gap π -tagger

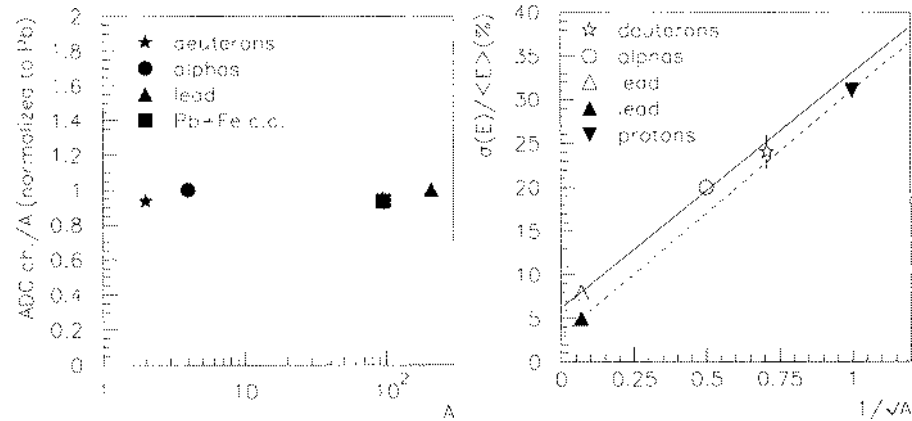
Detector details

High Rigidity Spectrometer question: plastic or SiO₂ fibers?

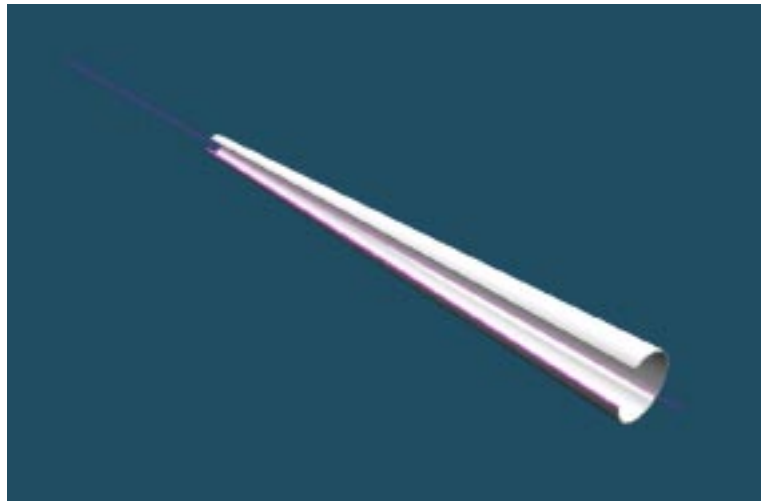
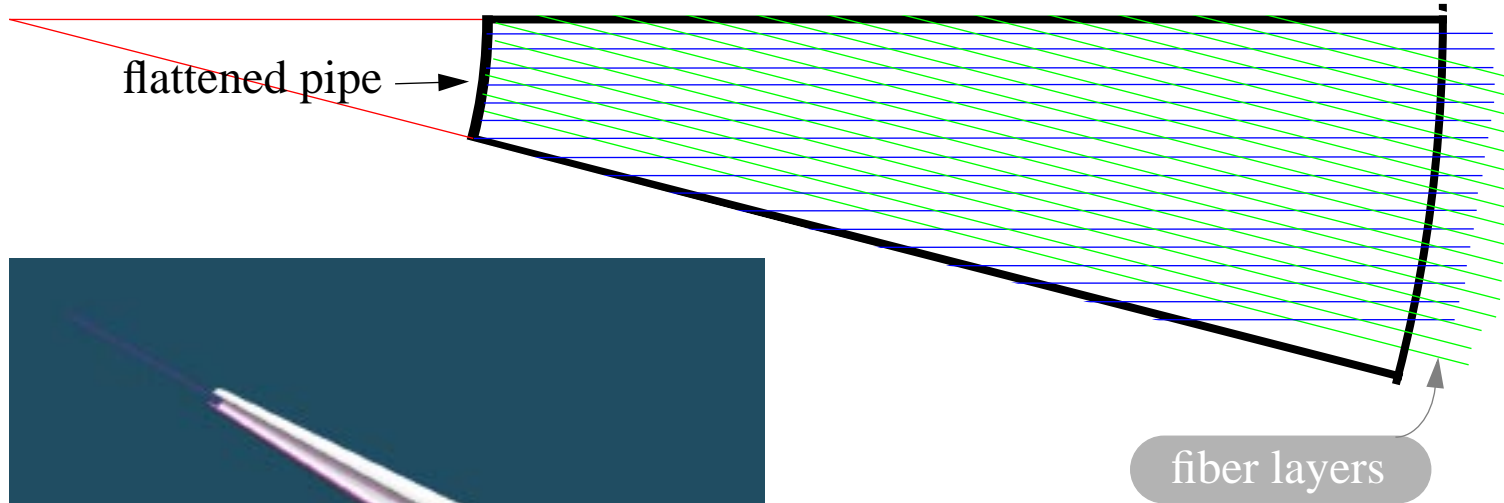
- Plastic has better energy resolution, is cheaper and easier to build. Spacial type hadronic resolution (30%/√E) is needed for spectator-neutron identification (D beam), but with a more radiation resistant design than former H1 FNC.
- SiO₂ is radiation hard and gives highest spatial resolution. Needed for heavy ions (backed by dE/dx measurement?).

SiO₂ fiber in NA50

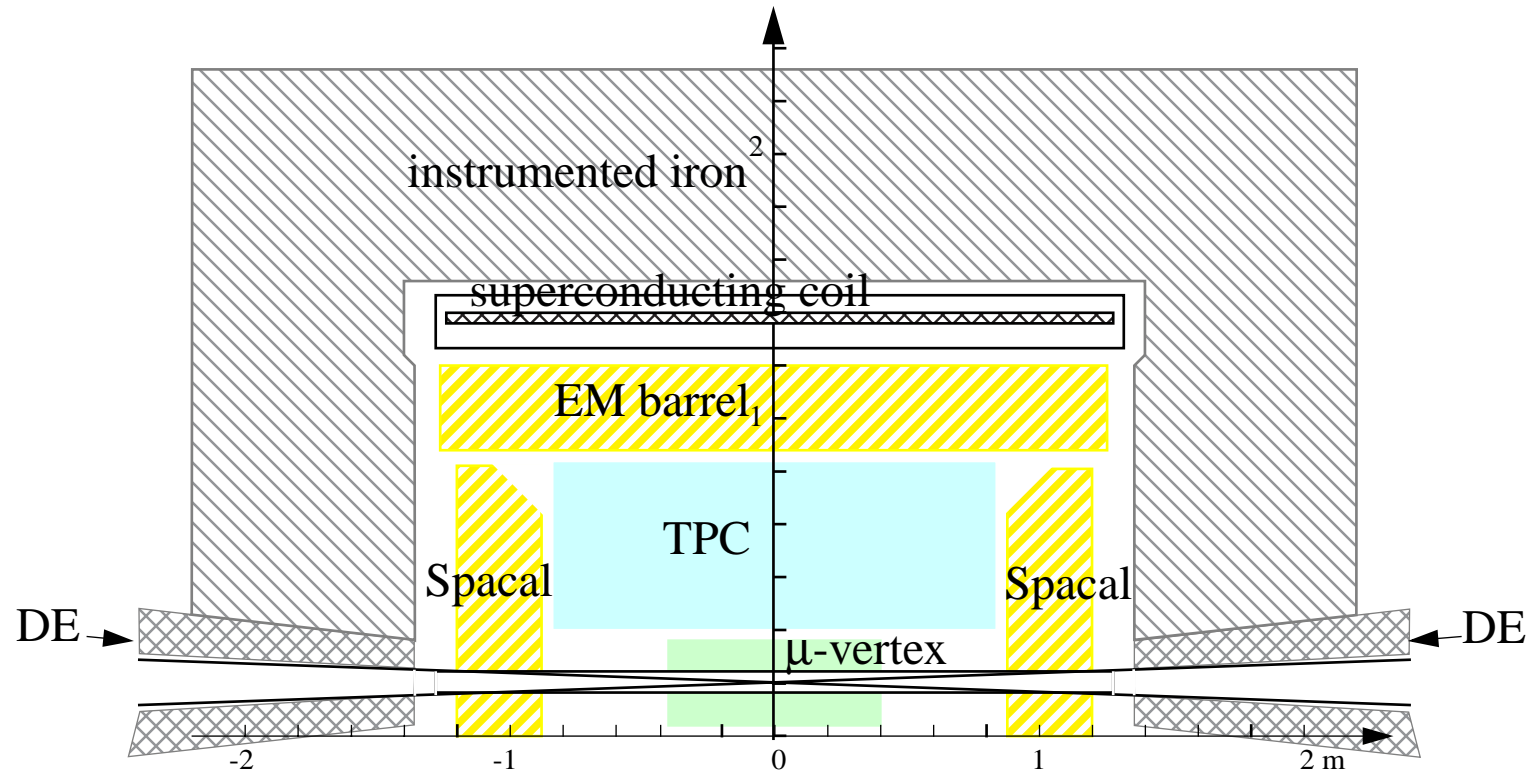
Arnaldi et al NIM A411 (1998) 1



active beam pipe:

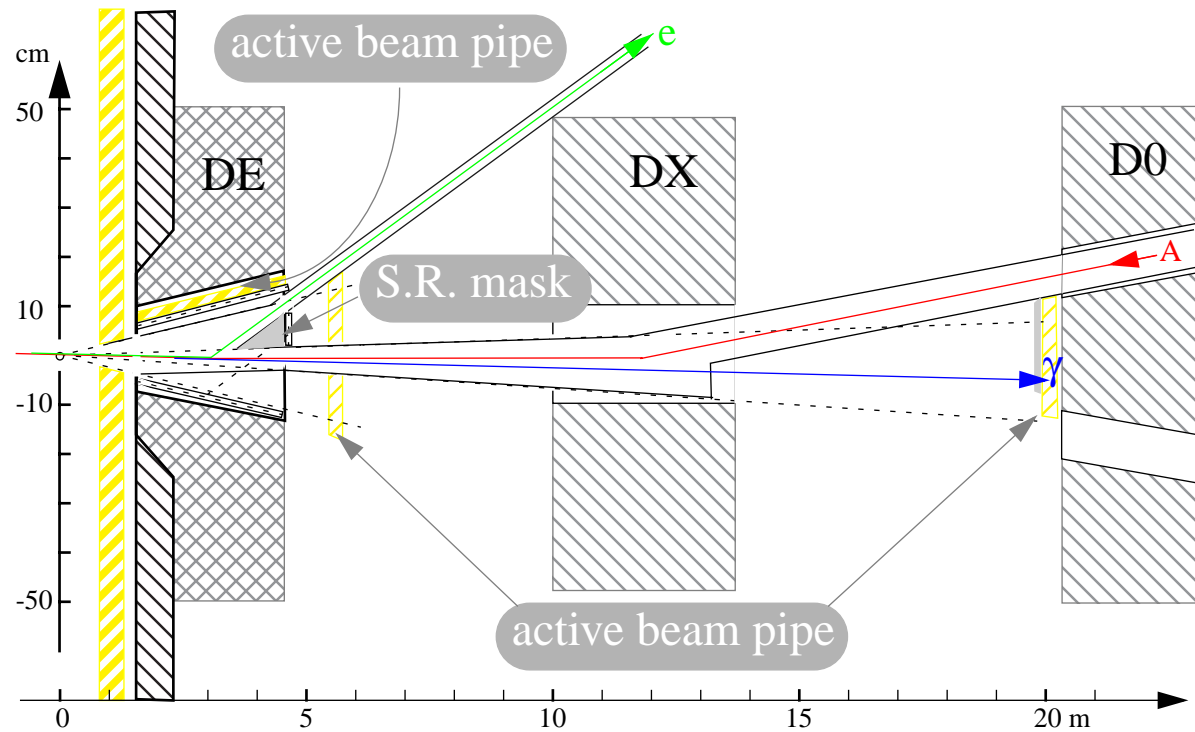


Toy model ~parton-side~ (good jet analysis, but not very high luminosities):



- Barrel is TPC backed by gas EM calorimeter inside magnet ($= \aleph/2^3$)
- Both endcaps are Spacal (=H1)
- μ -vertex provides small angle tracking

Toy model ~lepton-side~ (left to right):

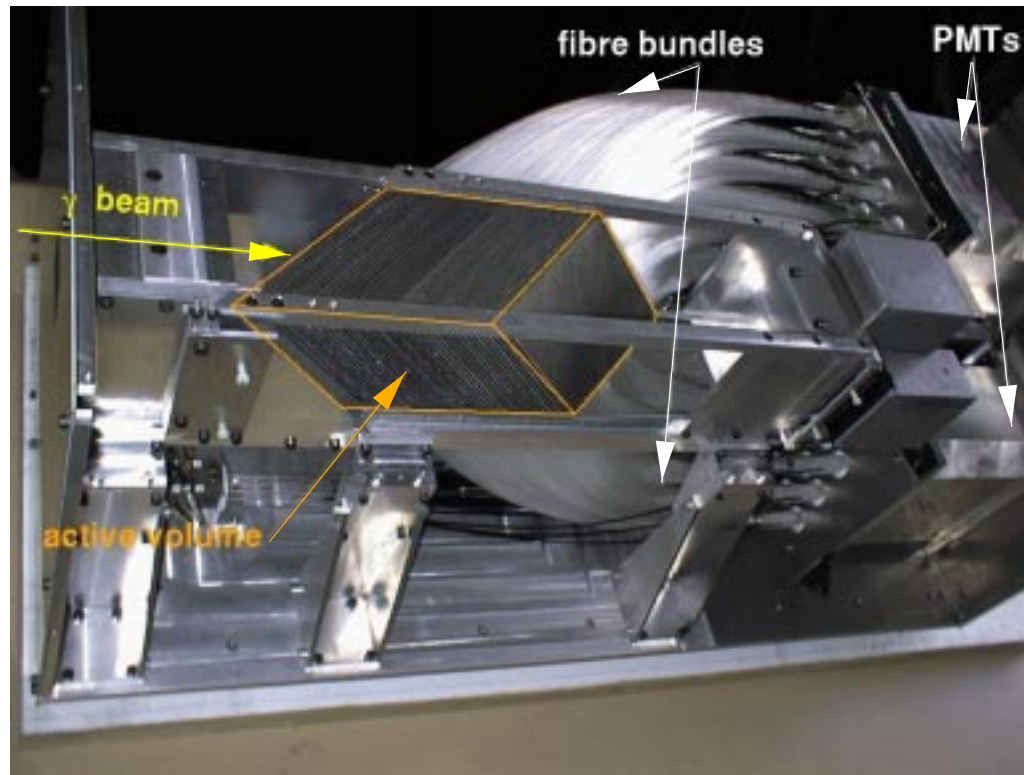


electron tagger: tracker measure e^- up to 10 GeV (photoproduction or DIS tagging) and closes acceptance for π 's; backing EM calo confirms e^- tagging.

γ tagger: measure Bethe-Heitler spectrum and tags initial bremsstrahlung; receives copious synchrotron radiation.

Toy Model:

- active beam pipe for electron tagger backed by Spacal on electron side
- quartz fiber calorimeter for γ tagger (takes up to a few γ per bunch cross)



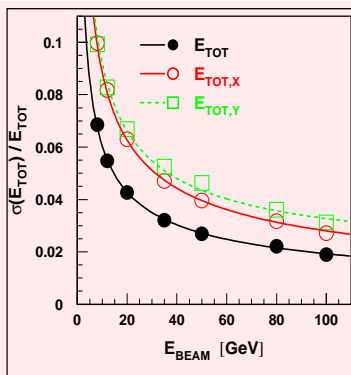
Arnd E. SPECKA, Ecole Polytechnique, France

specka@poly.in2p3.fr

Properties of new H1 SiO₂ fiber luminometer (thanks to A.Specka for the plots!).

ENERGY RESPONSE

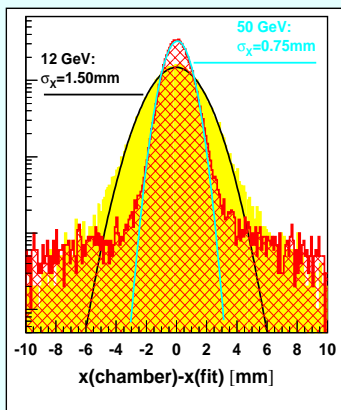
Resolution: (electrons)
 - constant term compatible with 0
 - stochastic term $19\%/\sqrt{E[\text{GeV}]}$
 sampling fluctuations: $16\%/\sqrt{E[\text{GeV}]}$
 photostatistics: $9\%/\sqrt{E[\text{GeV}]}$
 Linearity: better than 1%



For earlier work on this type of detector see P.Gorodetzky et al NIM A361 (1995) 161-179

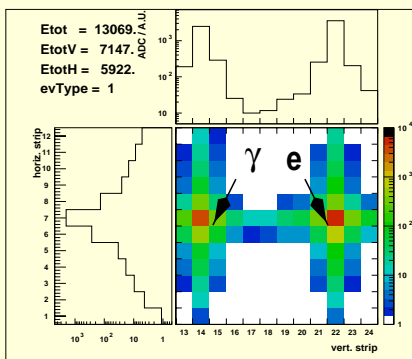
POSITION RECONSTRUCTION

Granularity: 10 mm
 Resolution: $5 \text{ mm}/\sqrt{E[\text{GeV}]}$



BREMSSTRAHLUNG EVENTS: SEPARATION OF e AND gamma

Run 30179 Event 1084 (pos 484)



Summary of Toy Model Parameters

detectors	type	$\delta\alpha\delta\beta$	precision	char.	granularity
central tracker	TPC	$10^{-3}\times 10^{-3}$	$\sigma/p=0.5\%p$? X0	
μ _vertex	Si	$10^{-3}\times 10^{-3}$.02 X0	15x15 μ m
Barrel EM	Gas	$10^{-2}\times 10^{-2}$	$\sigma/E=18\%/ \sqrt{E}$	X0=1.7cm	3.5x3.5cm
endcap EM	Spacal 2÷1	$3.10^{-3}\times 3.10^{-3}$	$\sigma/E=7\%/ \sqrt{E}$	X0=.84cm	4x4cm
had calo	Inst.iron		$\sigma/E=90\%/ \sqrt{E}$	4.5 λ	20x20cm
spectro track1	DC	$10^{-3}\times 10^{-3}$	$\sigma/p=.02\%p$	0.2 X0	5x5mm
spectro track2	MWPC(1mm)	$10^{-3}\times 10^{-3}$	$\sigma/p=.05\%p$	0.2 X0	1x1mm
spectro calo _{EM}	Spacal 4÷1	$2.10^{-4}\times 2.10^{-4}$ ^a	$\sigma/E=9.5\%/ \sqrt{E}$	X0=.7cm	3x3cm
spectro calo _{had}	Spacal 4÷1	$4.10^{-4}\times 4.10^{-4}$	$\sigma/E=30\%/ \sqrt{E}$	7 λ	3x3cm
e& π -taggers	sci.fiber	$2.10^{-2}\times 10^{-1}$	$\sigma/E=1\&5\%$.3 X0	0.5x2cm
e-tag calo	Spacal 2÷1		$\sigma/E=7\%/ \sqrt{E}$	X0=.84cm	2x300cm
γ -tagger	W/SiO ₂ fiber	$10^{-4}\times 10^{-4}$	$\sigma/E=20\%/ \sqrt{E}$	X0=.5cm	2x2 cm

a. overestimated for high rigidity spectro

Background Rates

H1 background rates applied to the Toy model:

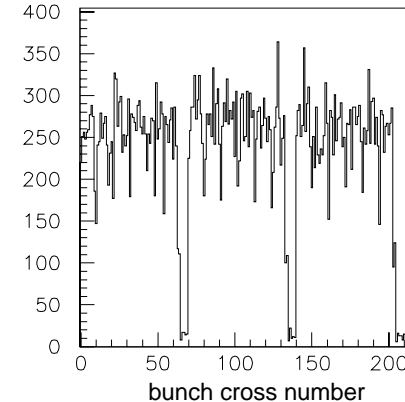
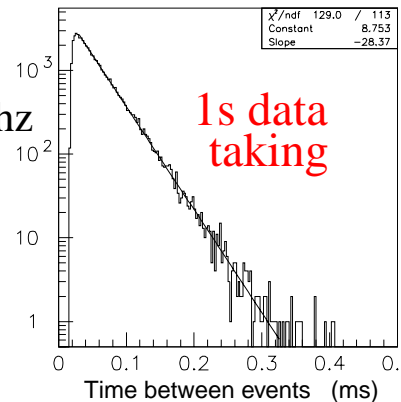
- proton induced background around 3×10^{-3} for a 5×10^{10} p/bunch for all detectors, $< 1.5 \times 10^{-3}$ for a single detector
- e^+ induced background 10^{-3} for $2.5 \times 5 \times 10^{10}$ e/bunch (not predictive for e_RHIC)

H1 1997

OR of 4 near-beam calorimeters: 28kHz

luminosity around $5 \times 10^{30} \text{ cm}^{-2} \text{ s}^{-1}$

(from E.B. et al, LPNHE 2001-10)



Performances of Spacal timing calorimeter¹:

- timing accuracy: $0.1 \text{ ns}/\sqrt{E}$, timing resolution: 30 ns
- consequences for the toy model ---> clean pileup rejection with $< 1\%$ loss

1- The electronics of the H1 lead/scintillating-fibre calorimeters, NIM A 426 (1999) 518-537

Shielding against synchrotron radiation at HERA

Daniel Pitzl
DESY

EIC Workshop
27.2.2002

- Synchrotron radiation
- Rate limits
- Shielding strategy
- Electron tracking
- Absorbers and backscattering
- Monitoring
- Summary

Synchrotron radiation

Power:

$$P = \frac{2}{3} \frac{I e}{4\pi\epsilon_0} \frac{\Delta\phi}{\rho} \left(\frac{E_e}{m_e c^2} \right)^4$$

or

$$P [\text{W}] = 14 I [\text{A}] \frac{\Delta\phi [\text{mrad}]}{\rho [\text{m}]} (E_e [\text{GeV}])^4$$

at HERA-II:

Beam current $I = 58 \text{ mA}$

Bending angle $\Delta\phi = 10 \text{ mrad}$

Bending radius $\rho = 400 \text{ m}$ (1280 m at HERA-I)

Beam energy $E_e = 27.6 \text{ GeV}$

$\Rightarrow P = 12 \text{ kW}$ on each side of the IP

Quadrupole radiation adds 15%.

Synchrotron spectrum

Universal spectrum, characterized by the critical energy:

$$E_c = \frac{3}{2} \frac{\hbar c}{R} \left(\frac{E_e}{m_e c^2} \right)^3$$

or

$$E_c [\text{keV}] = 2.22 \frac{(E_e [\text{GeV}])^3}{\rho [\text{m}]}$$

at HERA-II: $E_c = 120 \text{ keV}$

Photon spectrum:

$$\frac{dN_\gamma}{dE_\gamma} = \frac{P}{E_c^2} \frac{S(\xi)}{\xi}$$

with $\xi = E_\gamma/E_c$, and the spectral function:

$$S(\xi) = \frac{9\sqrt{3}}{8\pi} \xi \int_\xi^\infty K_{5/3}(x) dx$$

where $K_{5/3}$ is a modified Bessel function.

At low E_γ : $dN_\gamma/dE_\gamma \sim \xi^{-2/3}$

At high E_γ : $dN_\gamma/dE_\gamma \sim e^{-\xi}/\sqrt{\xi}$

Half the power is carried by photons above E_c

Photon rate and limits

Integrate spectrum:

$$N_\gamma = \frac{15\sqrt{3}}{8} \frac{P}{E_c} \sim E_e$$

at HERA-II: $N_\gamma = 2 \cdot 10^{18}/s$ on each side of the IP.

Limits:

- Drift chamber pattern recognition:
< 10 hits per bunch crossing = $10^8/s$ at HERA
- Drift chamber ageing:
Accumulated charge < 0.1 C/cm = $3 \cdot 10^8$ hits/s for
10 years
- Silicon radiation damage:
Dose < 100 Gy per year = $4 \cdot 10^8$ hits/s

Reduction factor of 10^{10} needed!

Shielding strategy

System of upstream collimators and downstream absorbers.

- Direct radiation must not hit anything close to the central detector.
- Central detector must be shielded against backscattering from primary absorbers.
- Only doubly-scattered radiation may reach the central detector.

Tracking code for direct radiation

- Electron tracking through magnet lattice in cm steps.
- Up to 10^6 'superelectrons' tracked to cover tails.
- Photons radiated tangentially to local orbit.
Radiation cone $\Delta\Theta \approx m_e/E_e = 18 \mu\text{rad}$ at HERA
neglected compared to beam divergence.
- Also 'analytic' calculation done using beam profiles.
- Need large horizontal aperture
 \Rightarrow elliptic excentric beam pipe.
- Special photon beam pipe extension downstream.
- Recent HERA problem: tight vertical tolerance
(9.2 mm opening at 3.7 m from IP).
Alignment tolerance for upstream magnets
(0.25 mrad) not reached
 \Rightarrow large backscattering into experiments.
Modifying absorbers this week.

Photon Interactions

- Rayleigh (coherent) scattering:

Few % of total cross section

$$d\sigma/d\Omega = \text{Thomson} \cdot \text{atomic form factor (tabulated)}$$

Forward peak, no photon energy loss

- Compton scattering:

Dominates above 120 keV in Cu, above 450 keV in W

$$d\sigma/d\Omega = \text{Klein-Nishina} \cdot \text{atomic structure function}$$

Forward and backward maxima (for $E_\gamma < m_e$)

- Photoeffect:

Dominates at low E_γ

Cross section vs E_γ tabulated

Contribution of K, L, M shells tabulated

Probability for Auger effect vs fluorescence tabulated

Line intensities (K_α, K_β) tabulated

EGS4 or GEANT4 can be used down to 1 keV

Backscattering

Albedo = fraction of backscattered photons

Universal curves for synchrotron radiation spectra with E_c from 10 to 500 keV calculated.

Absorber coating:

- Use high-Z material (W) as core for good absorption.
- Coat with medium-Z material (Ag) to absorb W fluorescence lines.
- Coat with lower-Z material (Cu) to absorb Ag lines, no too thick to create Compton backscattering.
- Optimal coating for HERA: 0.4 mm Ag and 0.2 mm Cu.
- Used for secondary collimators
- Primary absorbers are pure Cu for best thermal conductivity. Water cooled.

Synchrotron radiation monitoring

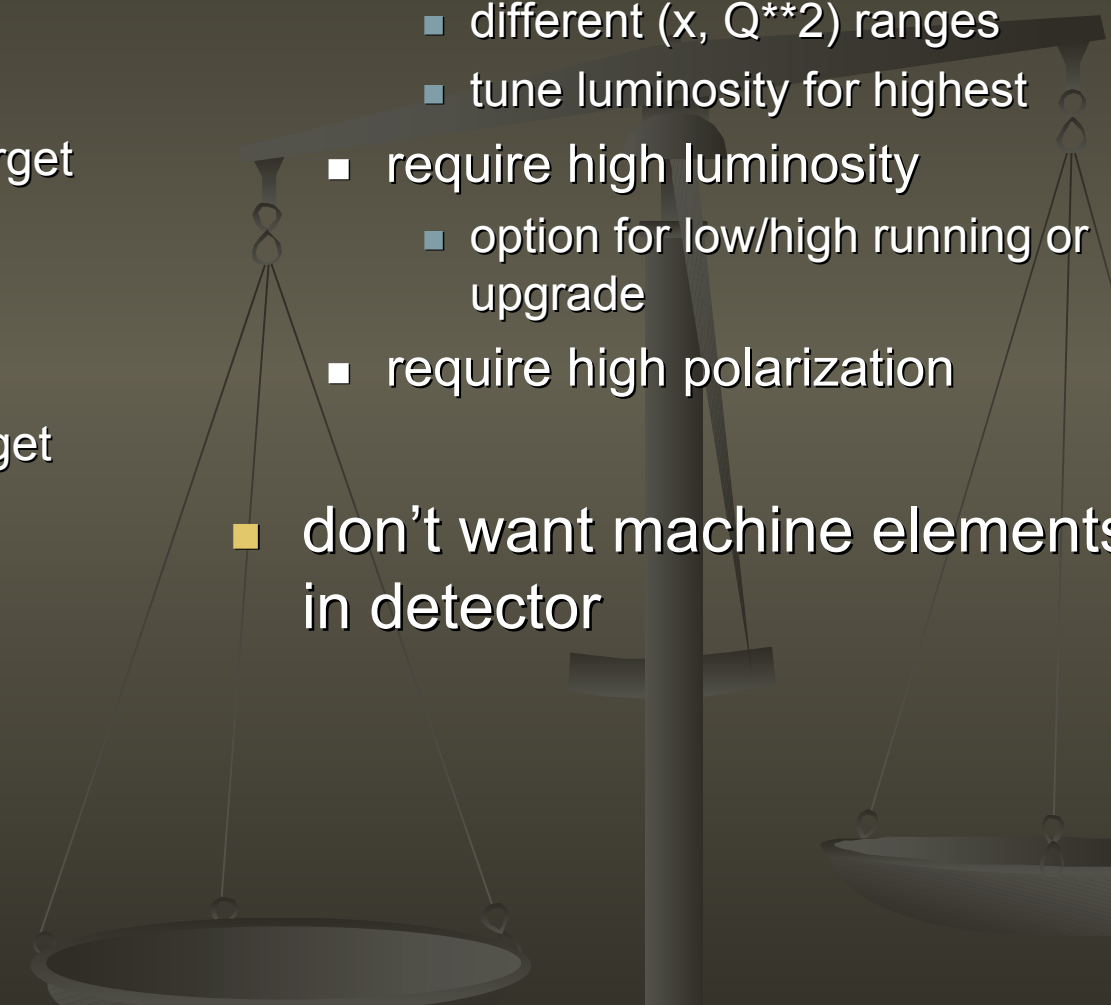
- Temperature monitoring at absorbers.
Problem: sensitivity at low currents.
- Photodetectors inside absorbers: measure photocurrent.
Problems: temperature correction and radiation damage.
- Silicon radiation monitors in central detectors.
Measure leakage current or hits above threshold.
Online display, warning levels and dump signal.
Problem: Si becomes transparent above 30 keV.
- TLD dosimeters for total dose.
Problem: no continuous readout

Summary

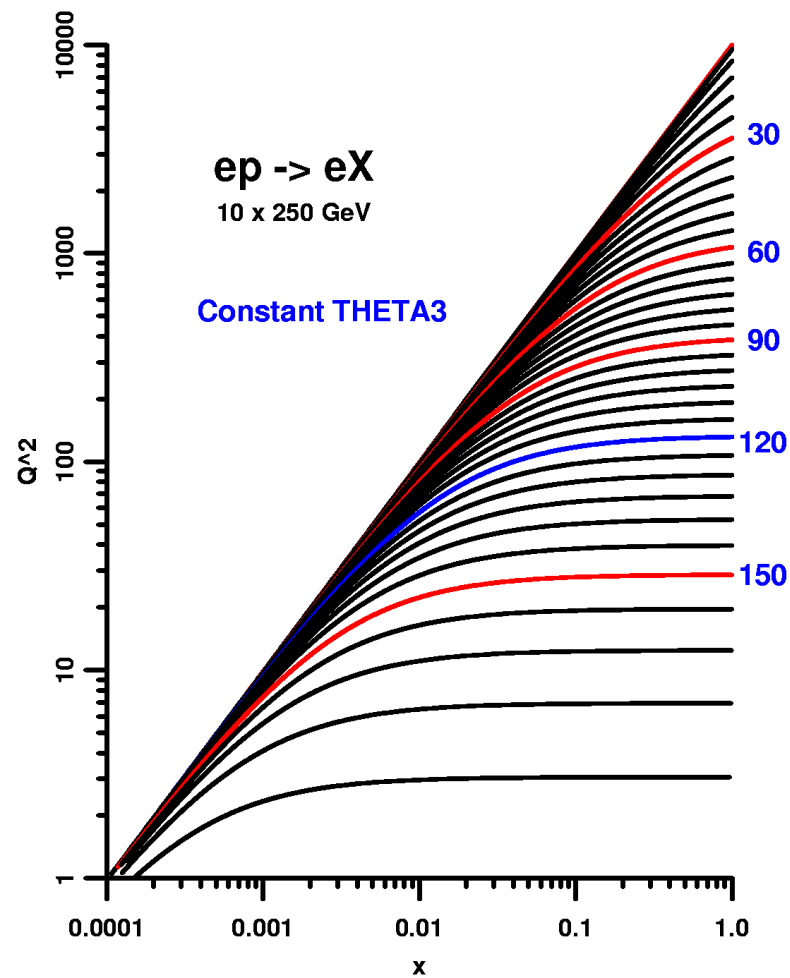
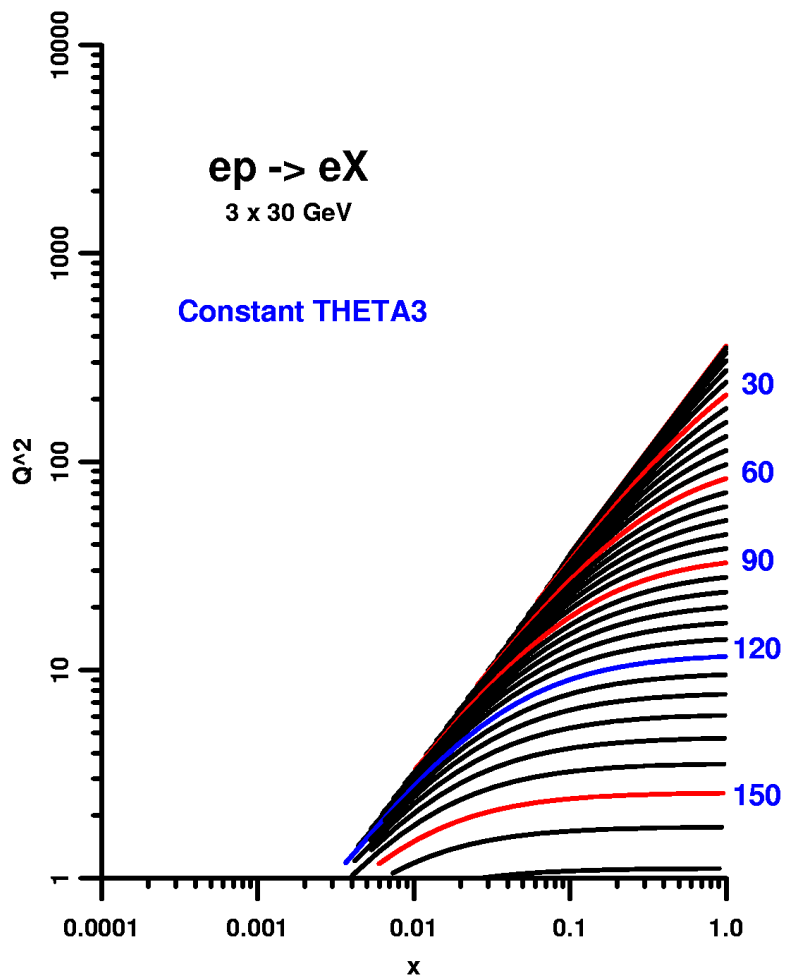
- Synchrotron radiation shielding determines the central beam pipe geometry.
- Required free path for direct radiation has consequences for downstream mini-beta magnets.
- Photon aperture limitations determine alignment tolerance for upstream magnets.

Luminosity Study

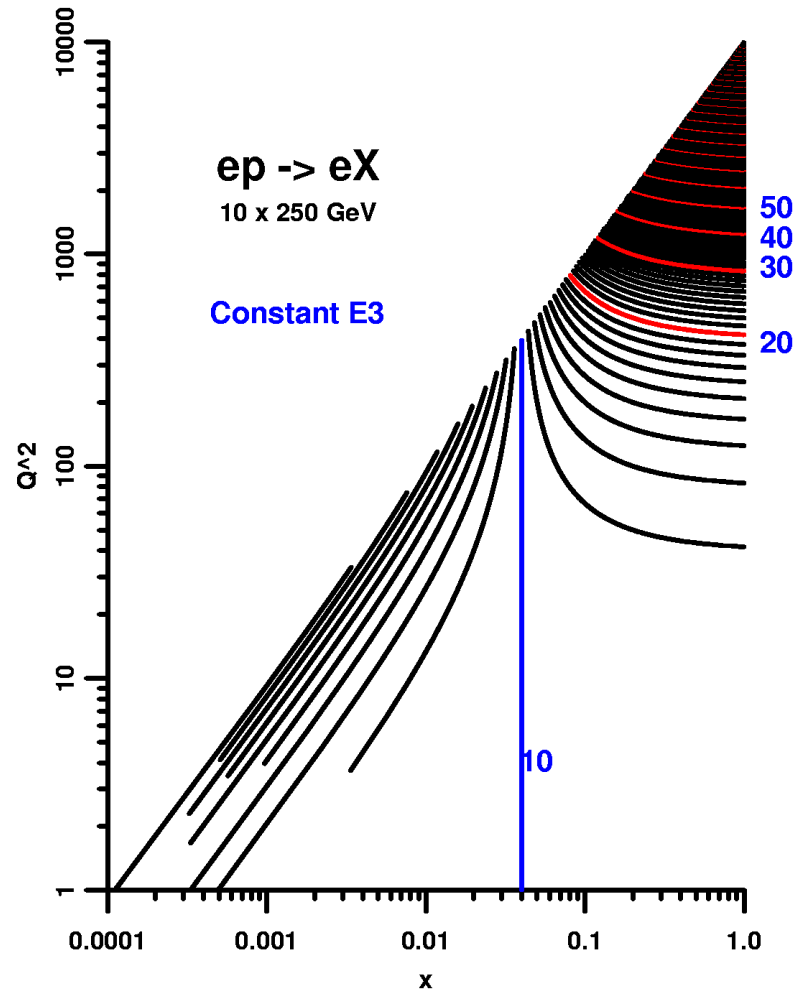
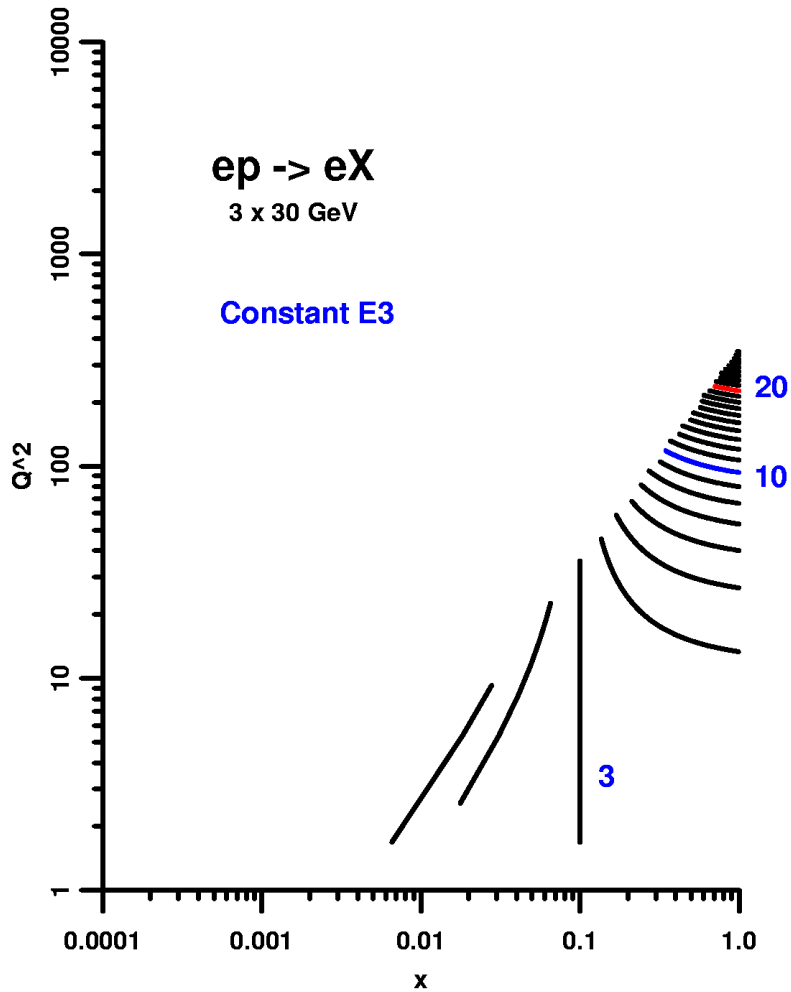
- 2 scenarios
 - 3 x 30 GeV
 - $s = 360 = q^{**2}$ max
 - $\sqrt{s} = 19 = W$ max
 - equiv. 192 GeV fixed target
 - 10 x 250 GeV
 - $s = 10000 = q^{**2}$ max
 - $\sqrt{s} = 100 = W$ max
 - equiv. 5.3 TeV fixed target
 - inclusive and exclusive
 - DIS
 - DVCS
 - polarization
 - detector options
- want to show
 - variable CM energies useful
 - different (x, Q^{**2}) ranges
 - tune luminosity for highest
 - require high luminosity
 - option for low/high running or upgrade
 - require high polarization
 - don't want machine elements in detector



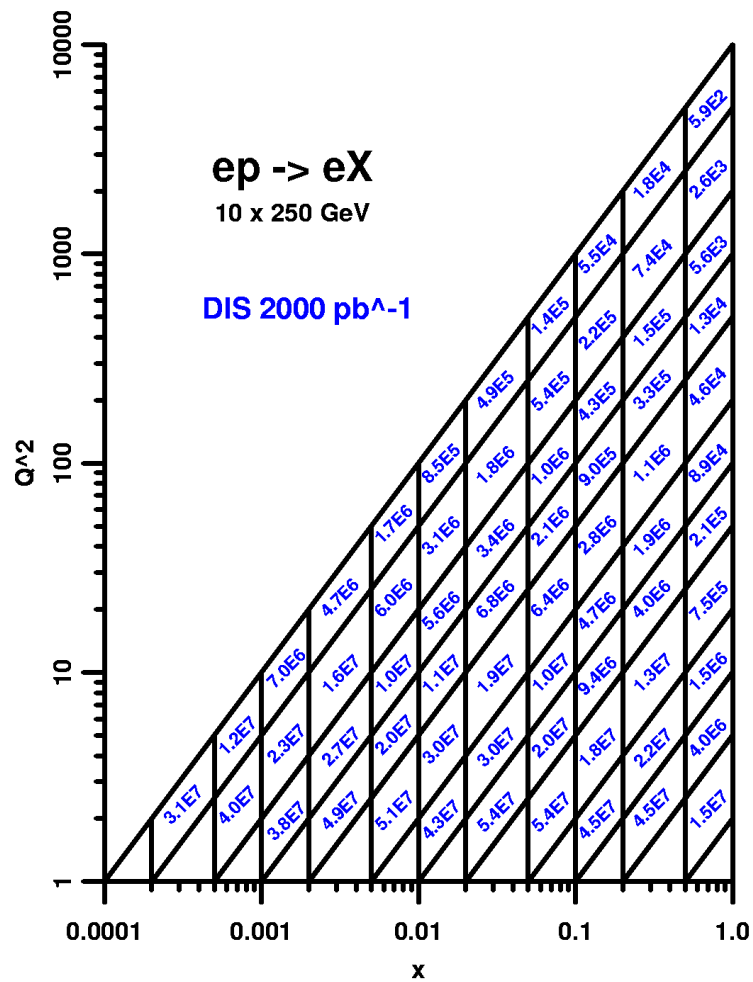
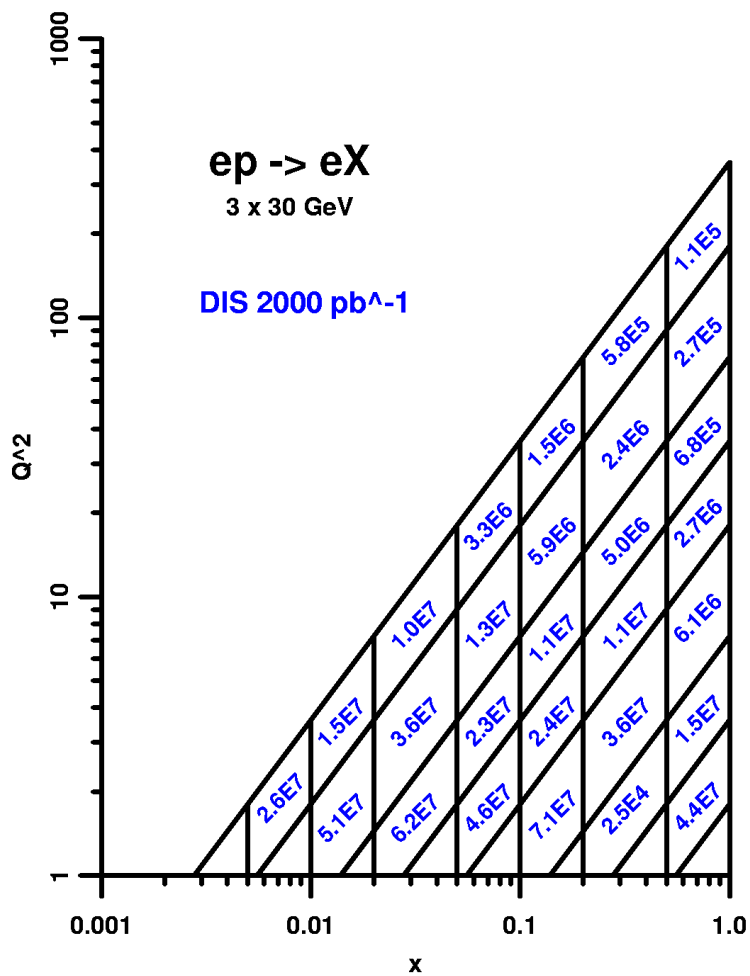
Electron Scattering Angle



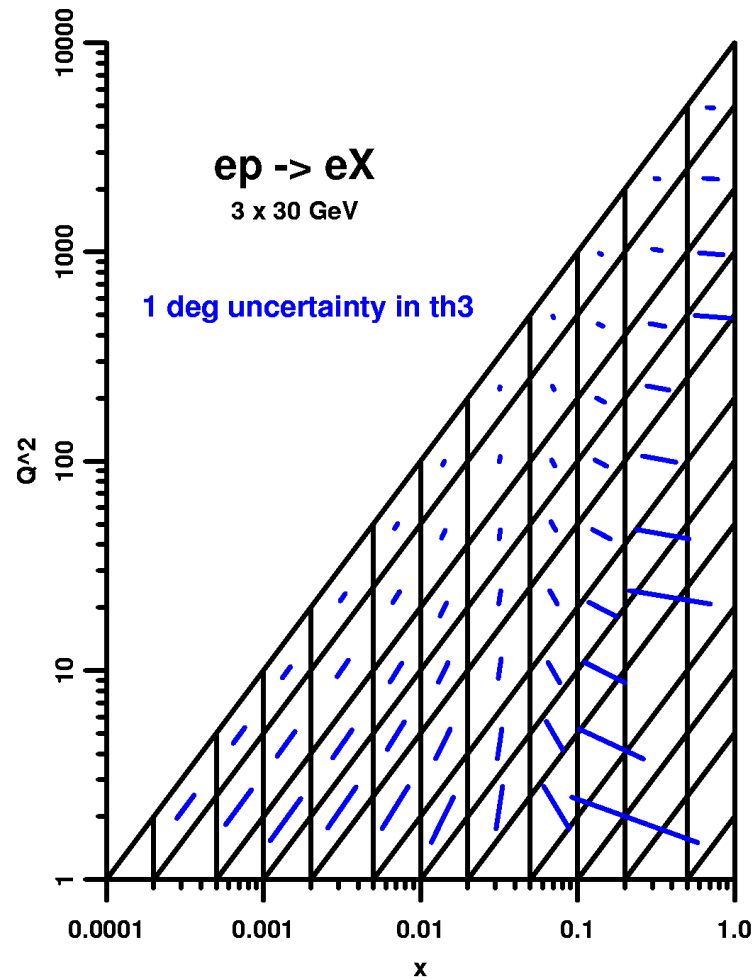
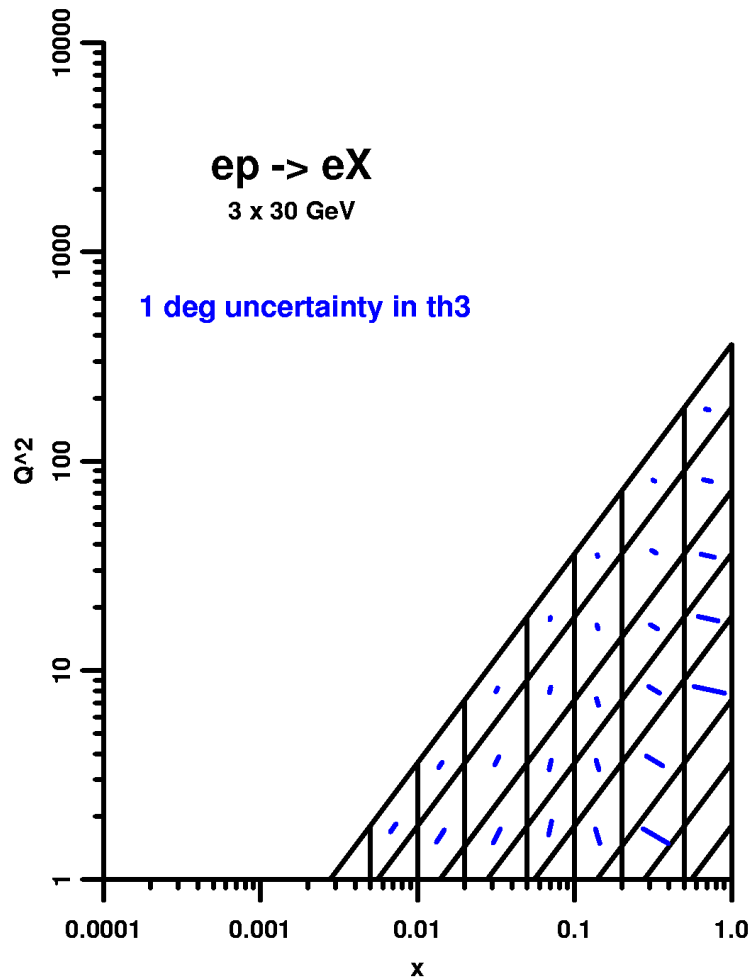
Electron Energy



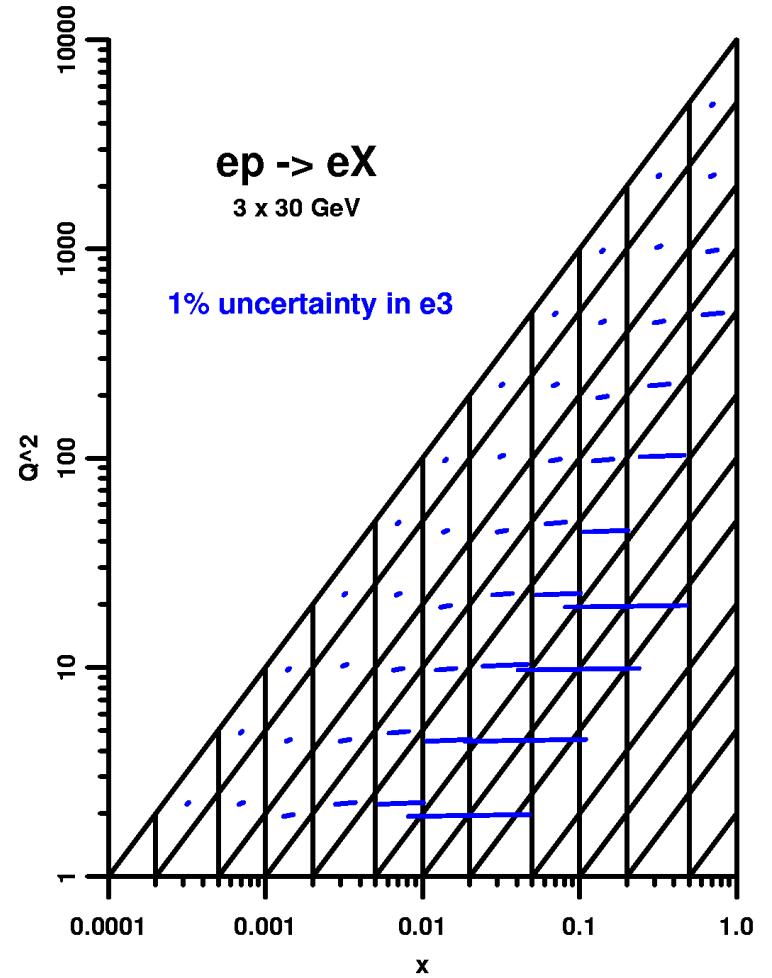
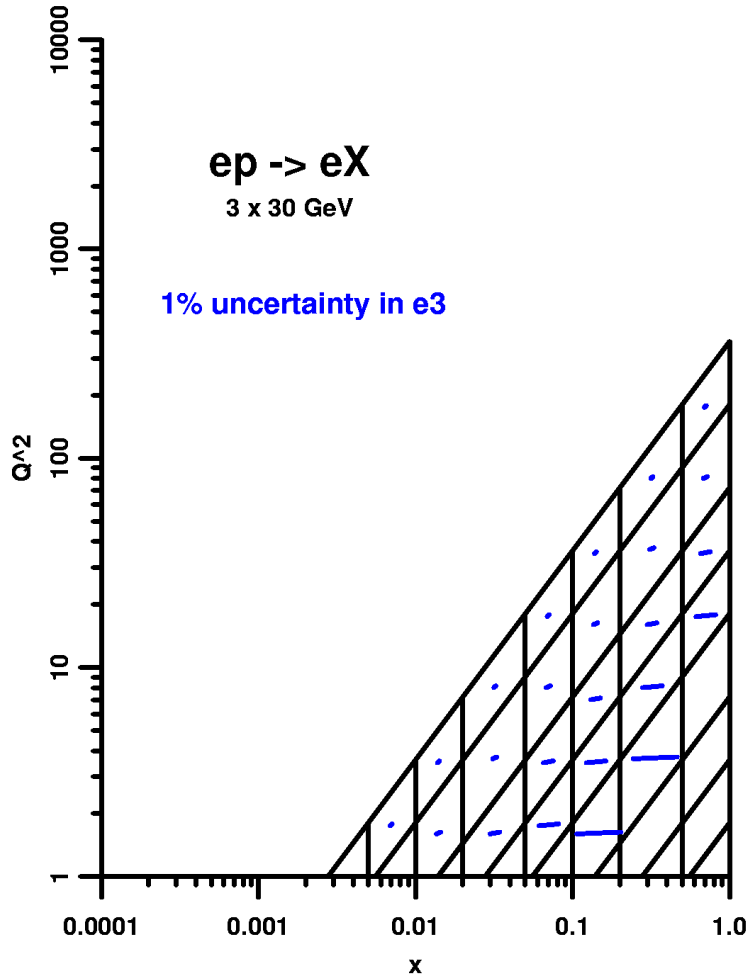
DIS Event Rates



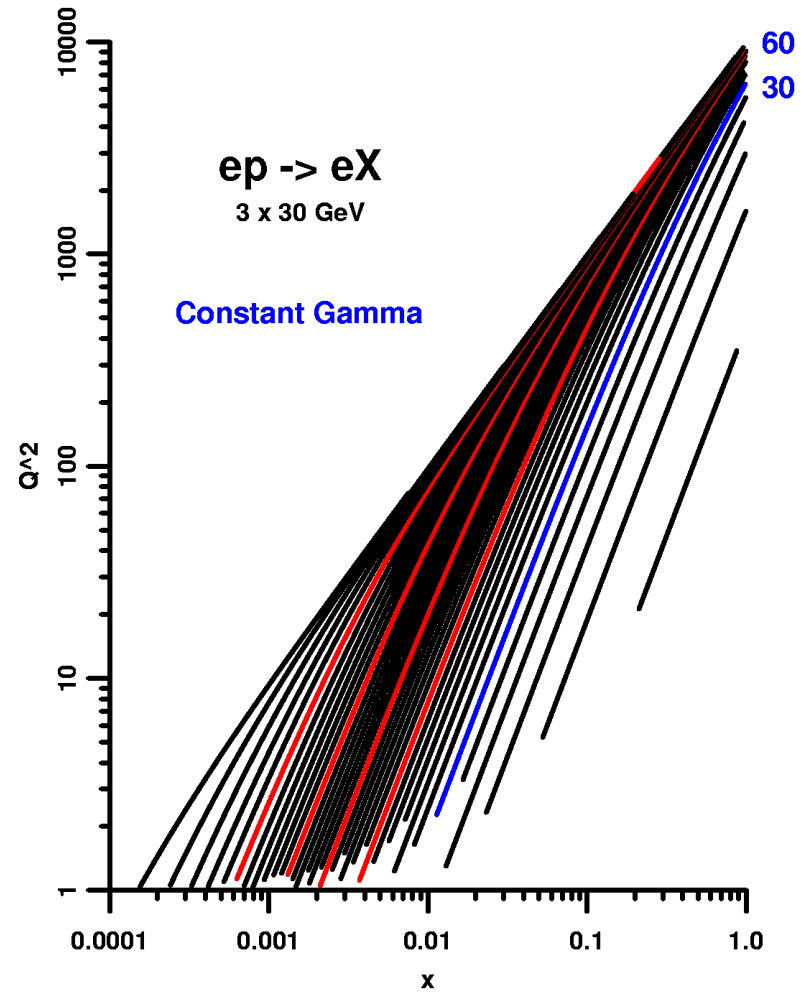
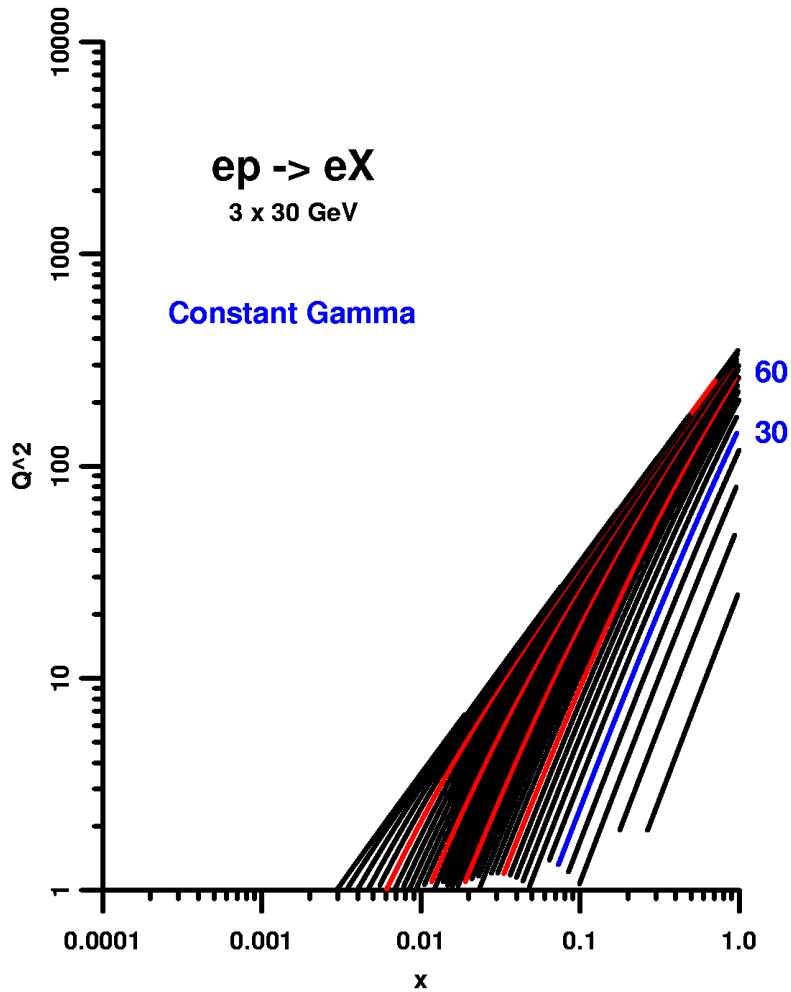
Uncertainty from Electron Angle



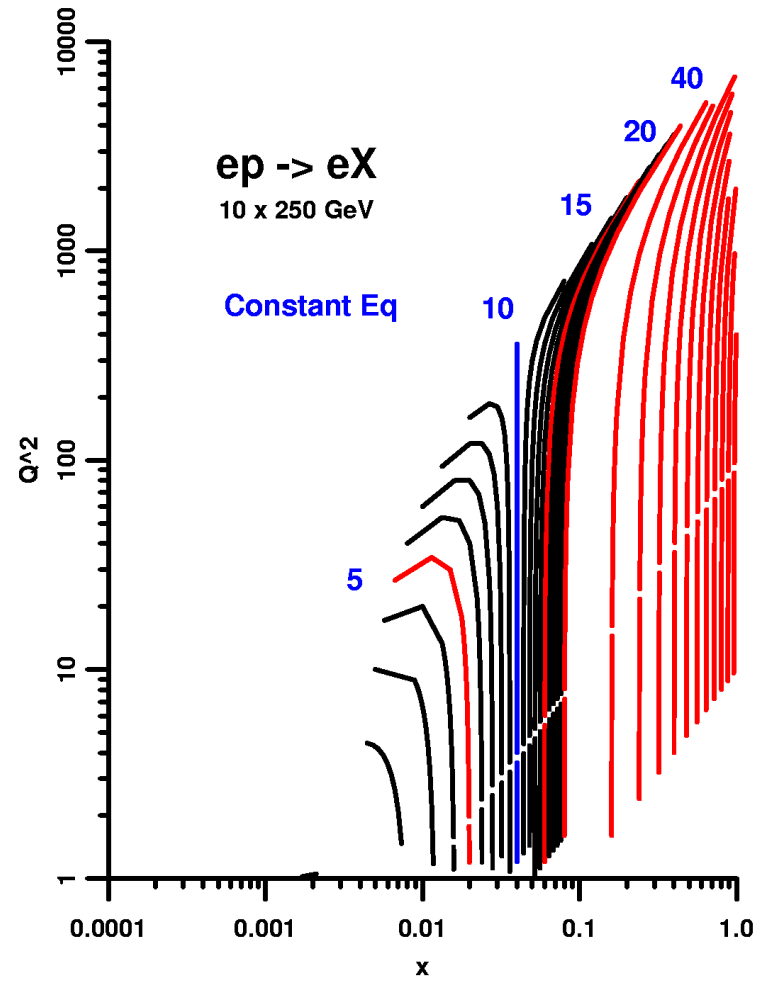
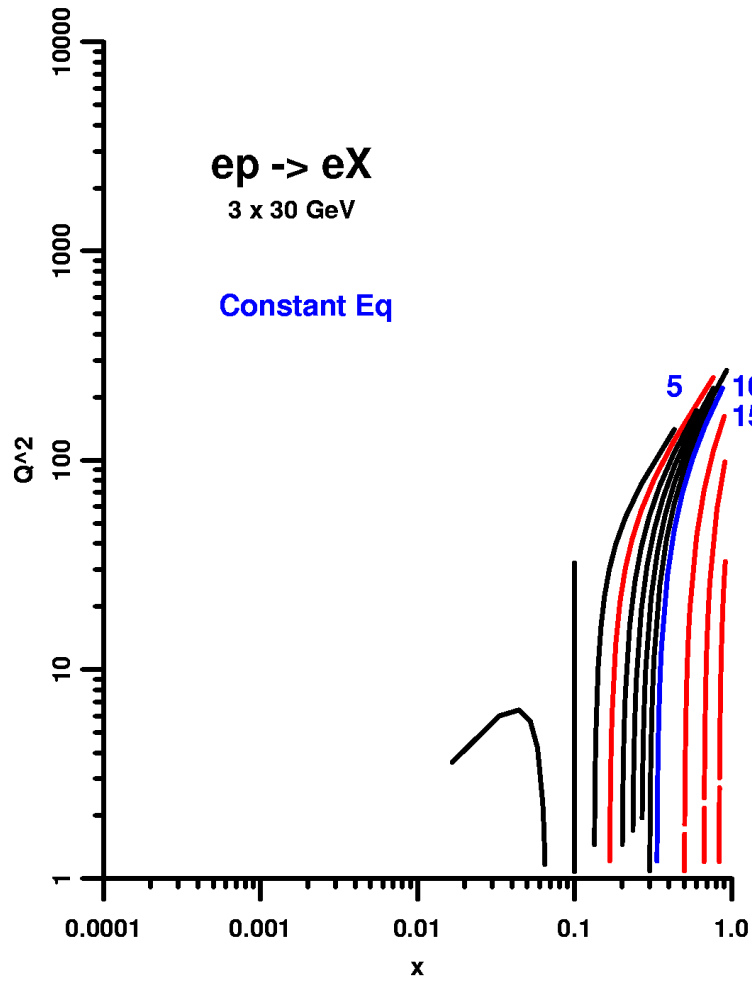
Uncertainty from Electron Energy



Current Scattering Angle



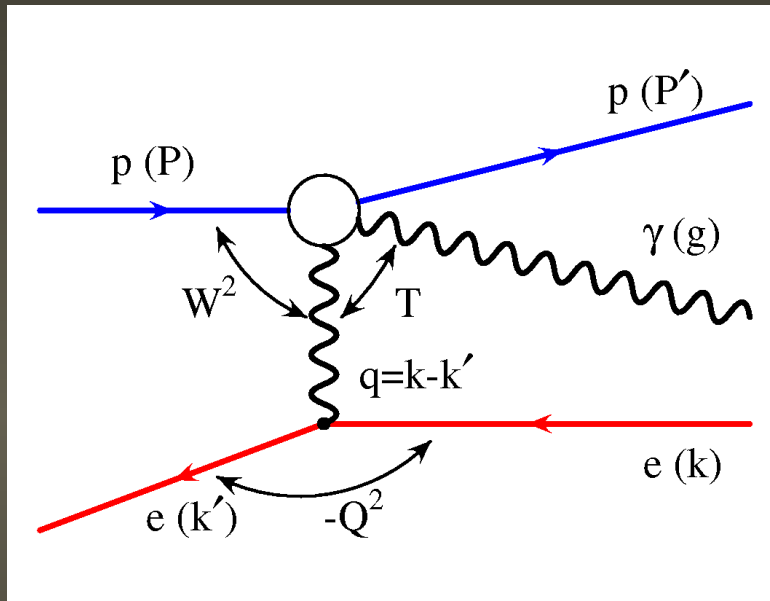
Current Energy



Summary from DIS

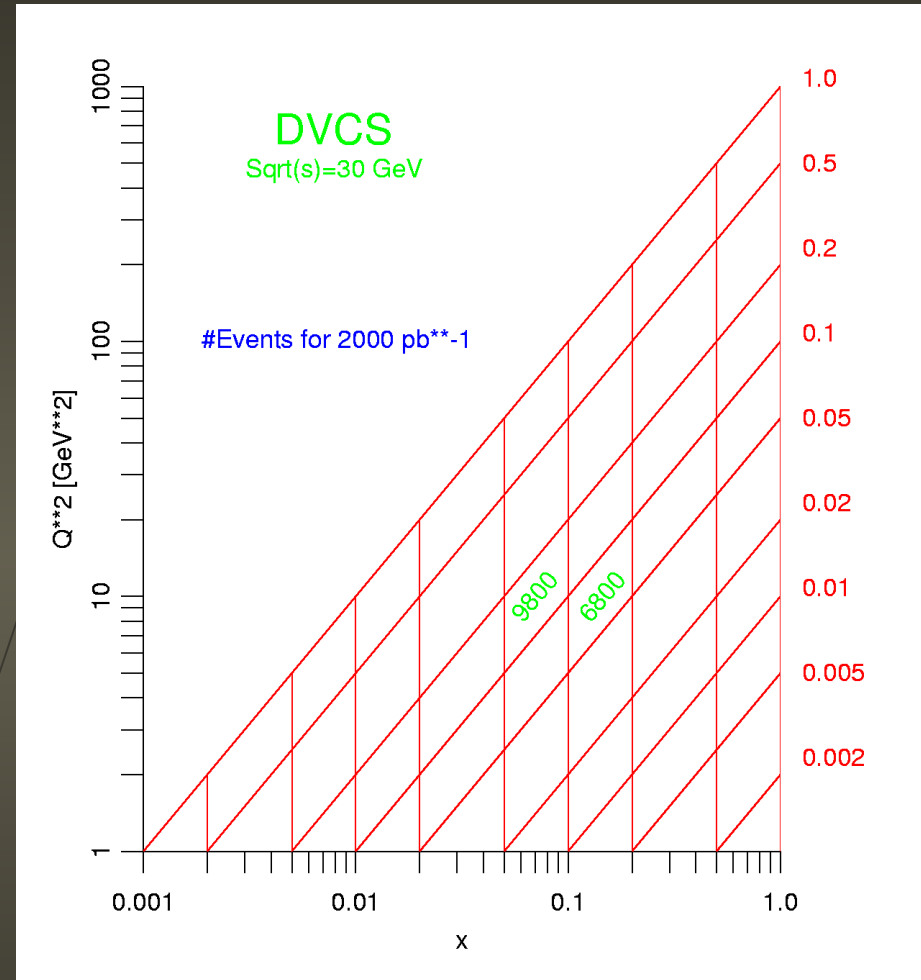
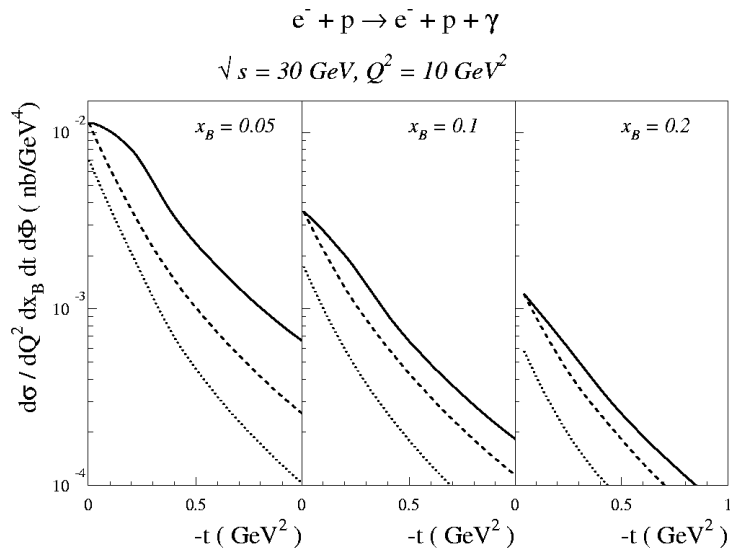
- variable CM energies give access to different regions of x and Q^{*2}
- to reach low Q^{*2} , low x at the higher CM energy need to detect particles near the beam
- rates at low CM energies significantly higher \rightarrow tune luminosity for highest CM and accept ~ 2 -10 lower luminosity at lowest CM
- range of CM energies allows Q^{*2} evolution \rightarrow QCD
- uncertainties in determining x , Q^{*2} define useful regions
 - improved by measuring current energy / angle
 - small angles for high x
 - larger angles for small x
- conceivable to have initially low luminosity and then upgrade to high luminosity
 - would design detector in anticipation
- range of CM energies allows “overlap” with Bates studies

DVCS



- important measurement in determining the generalized (skewed) structure functions
- sensitive to transverse components of spin dependent structure functions
- determine (x, Q^{*2}) from electron
- measure momentum transfer t from either photon or proton

DVCS Cross Section



cross section at $\text{sqrt}(s) = 3$ (eq $\sim 5 \times 50$)

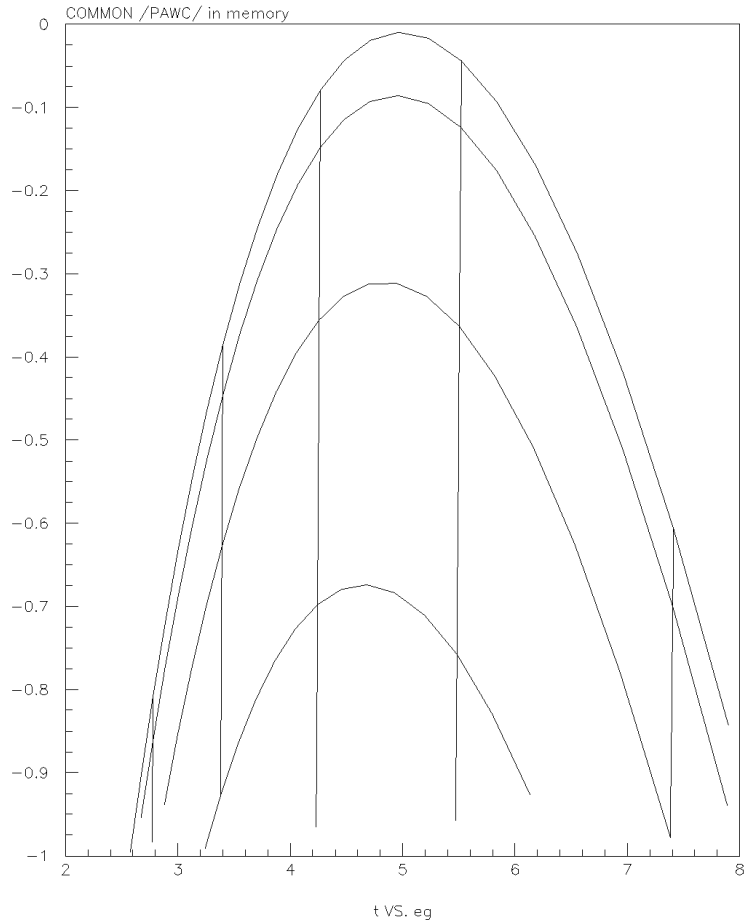
event rates for previous luminosity

1% statistics

DVCS Kinematics

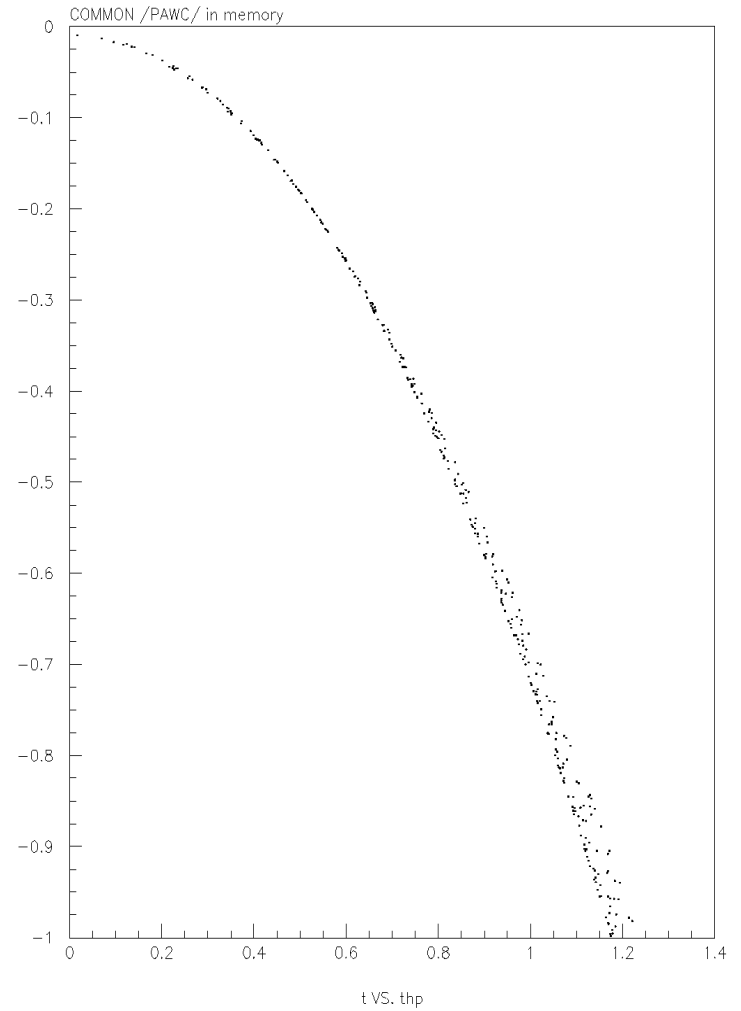
- 24 -

2000/11/03 17.45



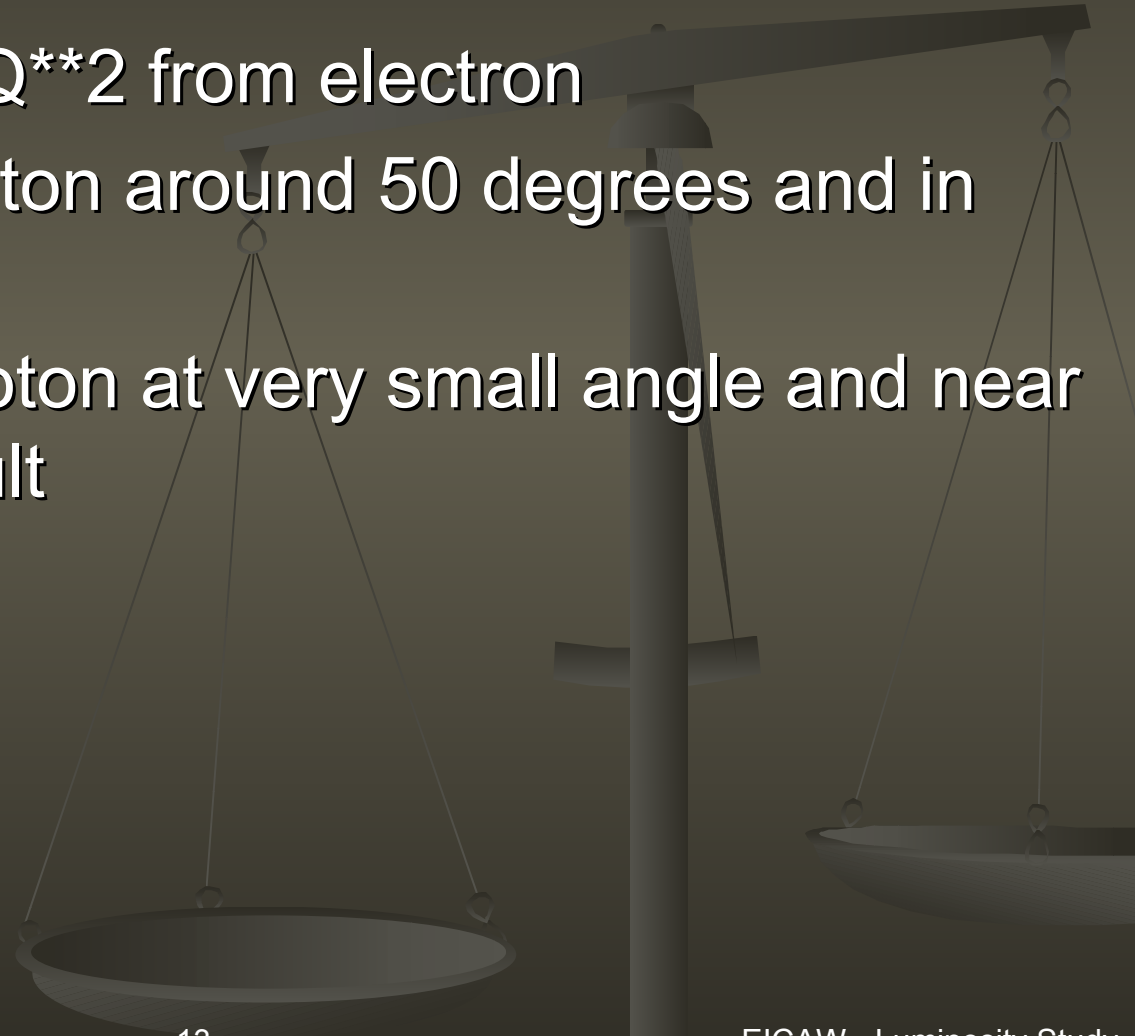
- 27 -

2000/11/03 18.12



Summary for DVCS

- interesting measurement
- need high luminosity to achieve statistics
- need to measure x , Q^{*2} from electron
- determine t from photon around 50 degrees and in plane with electron
- option to detector proton at very small angle and near beam energy - difficult



Polarization

- one of the main goals for EIC to measure spin dependent structure functions
 - longitudinal and (?) transverse polarizations
- quality factor varies as 4th ! power of polarization

$$Q_F = P_e^2 P_p^2$$

$$P_i \approx 70\% \longrightarrow Q_F = 0.25$$

$$P_i \approx 50\% \longrightarrow Q_F = 0.06$$

- going from 70% to 50% would require 4 x luminosity

Spin Dependent Structure Functions

- nucleon spin

$$A_L = D(A_1 + \eta A_2)$$

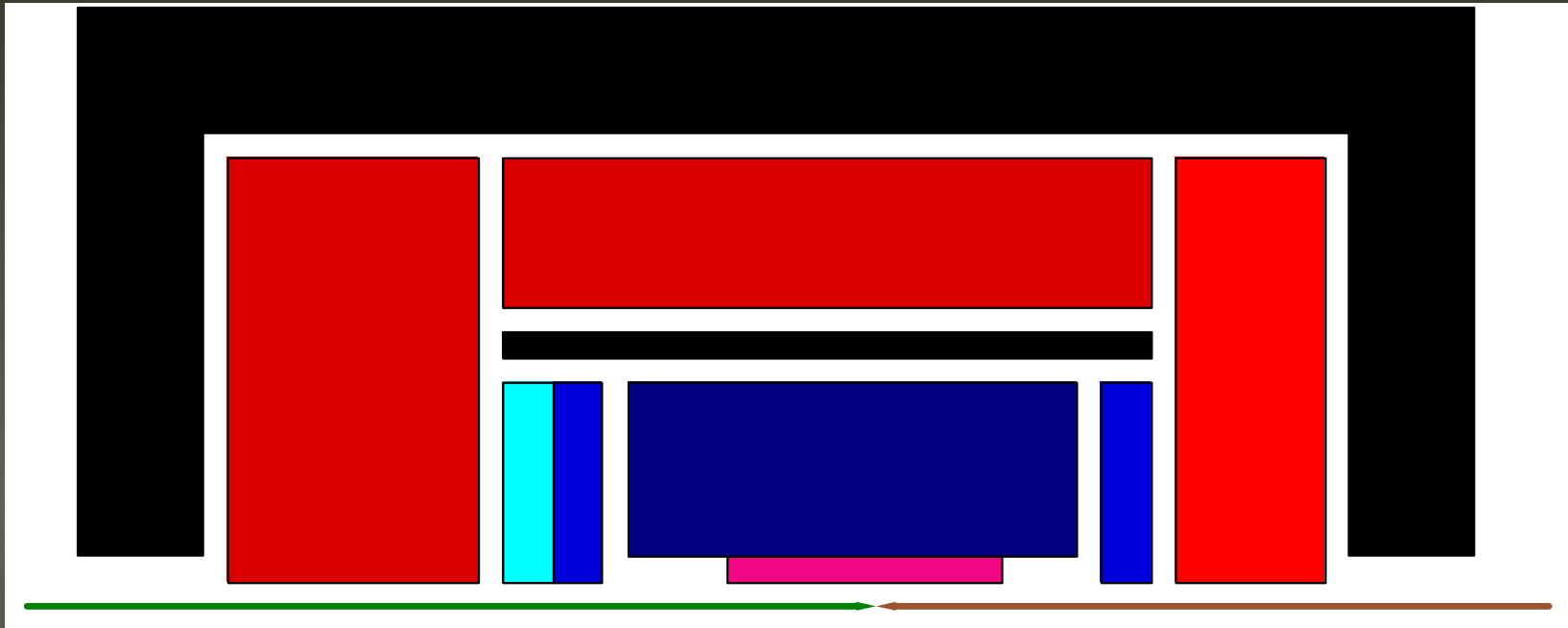
$$A_T = d(A_2 - \xi A_1)$$

$$A_1 = \frac{g_1 - \gamma^2 g_2}{F_1}$$

$$A_2 = \gamma \frac{g_1 + g_2}{F_1}$$

- the longitudinal and transverse asymmetries are measured to deduce the spin dependent structure functions g_1 and g_2
- but asymmetries typically $\sim 1.0-0.1\%$
 - need \sim one million events to get even 0.1% statistics
 - **high luminosity**

Toy Detector



~5 m long

micro-vertex, central, forward, and rear tracking

PID maybe only in forward direction

thin, superconducting solenoid with integral dipole at $r \sim 1$ m

calorimetry after solenoid

instrumented iron yoke

forward and rear spectrometers

Conclusions

- Basically we want it all
 - variable CM energies
 - high luminosity 10^{33}
 - high polarization 70%
 - +/- ~2 m for detector about IR



A 3 beams insertion preliminary considerations

A. Verdier

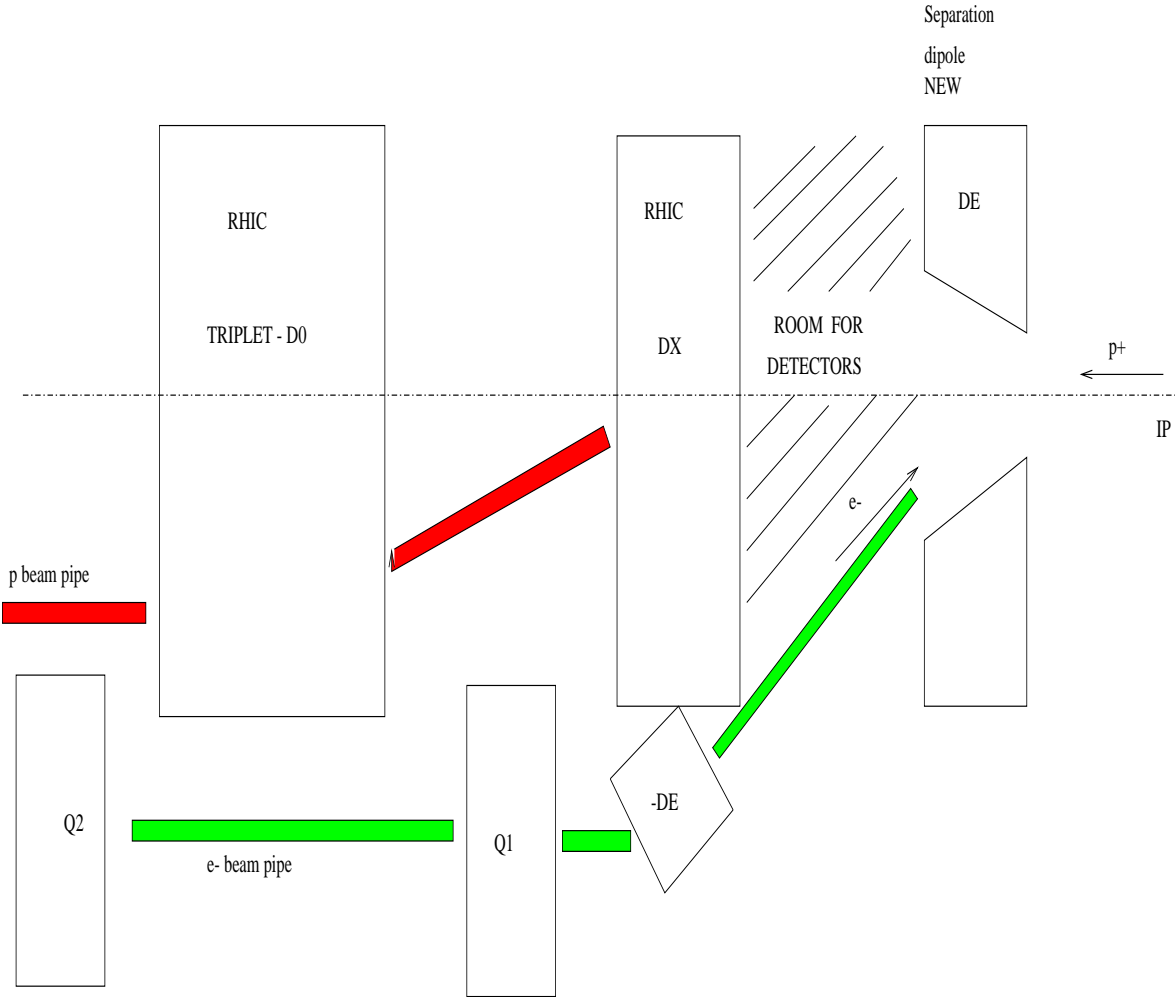
LBL Workshop February 2002

- Motivation
 - Run an e-A experiment simultaneously with the other RHIC experiments
 - switch from e-A to A-A
- Boundary conditions
- Optics : Doublet / Triplet
- Conclusion

Boundary conditions

- **Keep RHIC separation dipole DX**
(switch from e-A to A-A collisions)
 - First magnet 15m from IP
 - **Spin rotator ?**
 - lower limit on β^*
- Transverse space available for magnet installation : as in Note C-A/AP/14 (1m from the “green orbit”).
- **Negligible tune-shift from separated beam** (third beam)
 - standard values for ξ_{b-b}
 - e-p luminosity $\sim 10^{32} cm^{-2} s^{-1}$ with $\beta_e^* = 0.25m$ and upgraded RHIC beam.

Typical layout

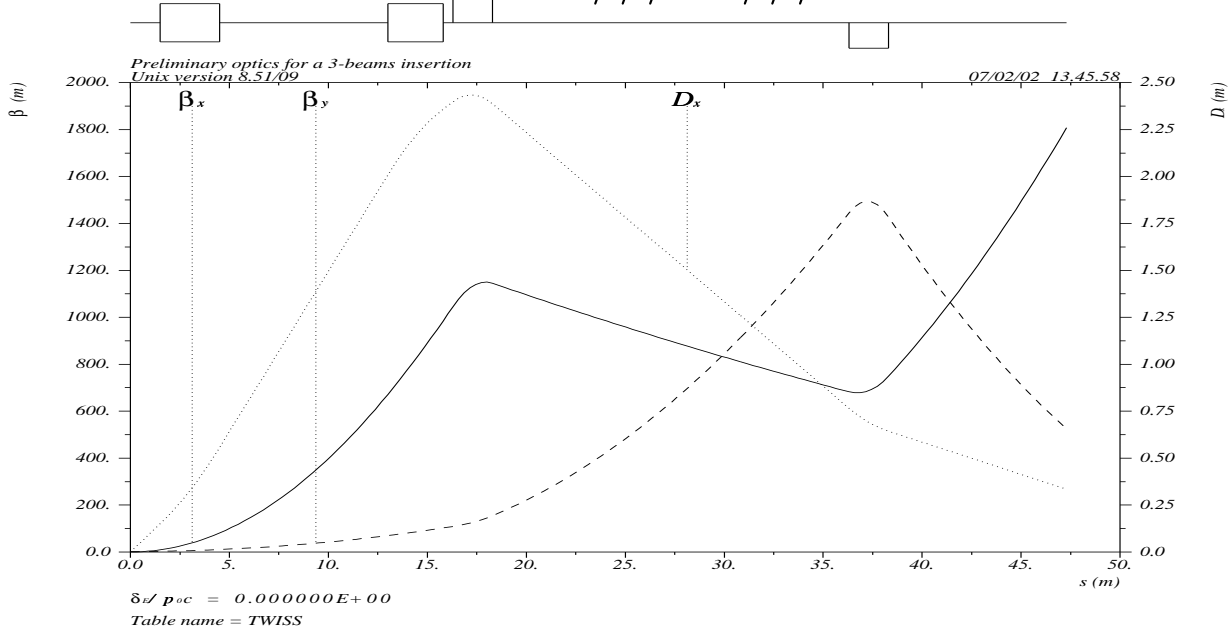


Optics functions (e-) / Doublet

No matching only “ β tracking”

Note : $D_x' = 0.1$, $\beta_x^* = 0.25m$, $\beta_y^* = 2.5m$

IP DE DX-DE Q1 ///D0/// Q2



DE : separator (KRASNY / Snowmass)

-DE : dipole to steer e-beam || RHIC. As close as possible to DX dipole.

Q1 first matching quadrupole.

Q2 second matching quadrupole, placed behind D0.

Optics problems / Doublet

- **Large D_x and β_x^* in Q1**

→ Contribution to ϵ_x ?

Presently : $\frac{\Delta\epsilon_x}{\epsilon_x} \sim$ some per mil.

→ $\sigma_x = 7\text{mm}$, large aperture quadrupoles.

- **Large Non-linear chromaticity.**

Limits the momentum acceptance :

off-momentum tune-shift scales with

$(\sigma_e D(Q1)/\beta_x^*)^2$ (AV in CAS 1995)

For LEP (4 PI's):

$\sigma_e D(Q1)/\beta_x^* = 0.57 * 4.7 / 0.05$

→ lower limit (safe) on β_x^* :

$(0.05 * 15 / 4.7) * (0.55 / 0.57) = 0.15\text{m}$.

(sextupole families)

$\xi_{y,bb}$ **10 times too large**

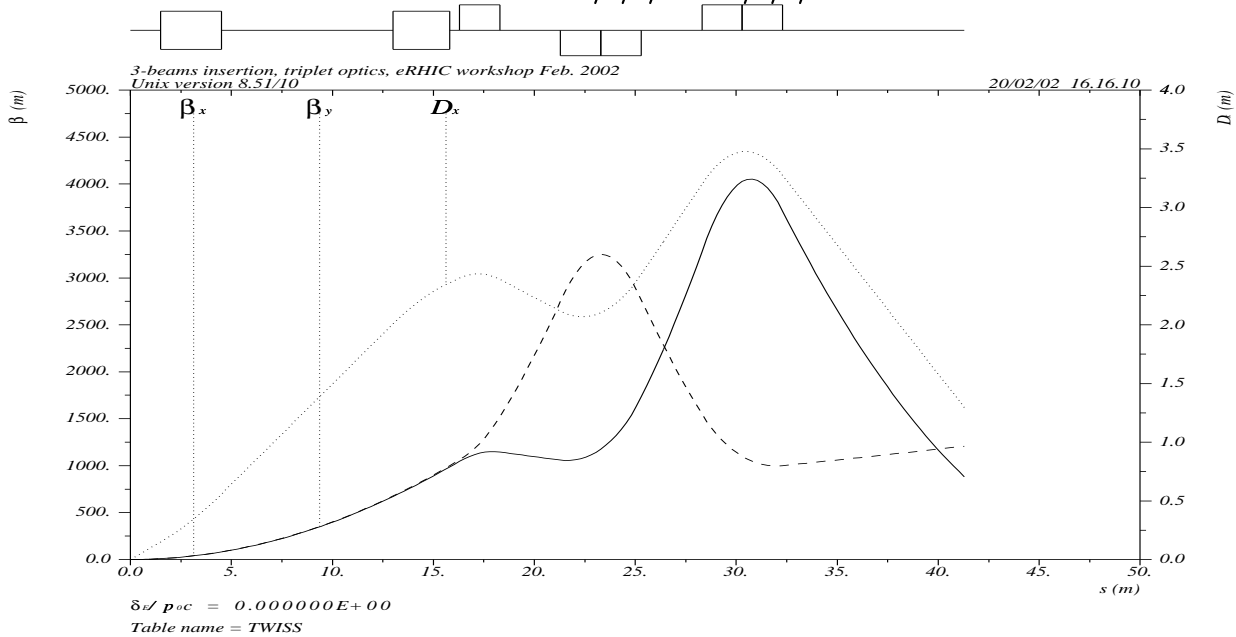
→ **triplet mandatory**

Optics functions (e-) / Triplet

No matching only “ β tracking”

Note : $Dx' = 0.1$, $\beta_x^* = \beta_y^* = 0.25m$

IP DE DX-DE Q1 ///D0///



DE : separator (KRASNY / Snowmass)

-DE : dipole to steer e-beam || RHIC. As close as possible to DX dipole.

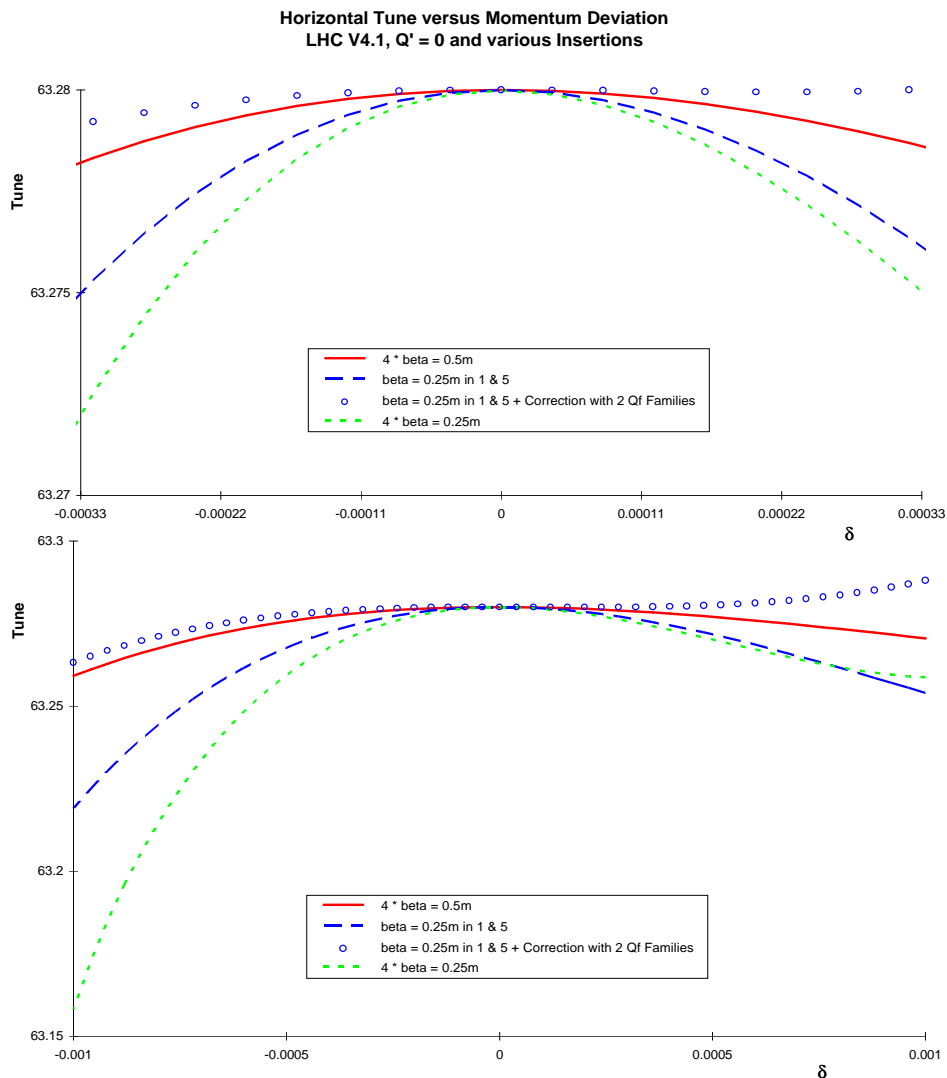
Q2 and Q3 doubled / previous Q2

Optics problems / Triplet

Non-linear chromaticity as in “ultimate LHC”.

Does not work for an electron machine :

Beam life-time due to cut in energy distribution.



From LHC Project Note 38 (F. Schmidt, 1994)

e-LINAC

Emittance buildup in the separator.

$$\Delta\epsilon = 2.04 \cdot 10^{-11} E^5 \mathcal{I}$$

$$\text{where } \mathcal{I} = \int_{dipole} [\gamma D_x^2 + 2\alpha D_x D'_x + \beta D_x'^2] \frac{ds}{\rho^3}$$

Most important contribution : -DE, 0.18nm.

Small compared with 3nm (LINAC emittance)

→ to be watched when matching.

$$\xi_{b-b} \times \sim 10$$

Limit to β -beating for beam recuperation.

The doublet solution can be used.

$$\beta^* \sim 2.5m \rightarrow \mathcal{L}_{e-p} \sim 10^{32} cm^{-2} s^{-1}$$

(same beam size as “nominal”)

Decrease β^* : likely possible (1/10 of CLIC ξ_{b-b}). Triplet to be tried.

CONCLUSION

e-Ring PROBLEMATIC :

- triplet mandatory / space + chromaticity ??
- ϵ_x (separation scheme)
- spin rotators : problematic because of space and contribution to emittance

Modify layout to have quads closer to IP ?

e-linac

PREFERRED SOLUTION :

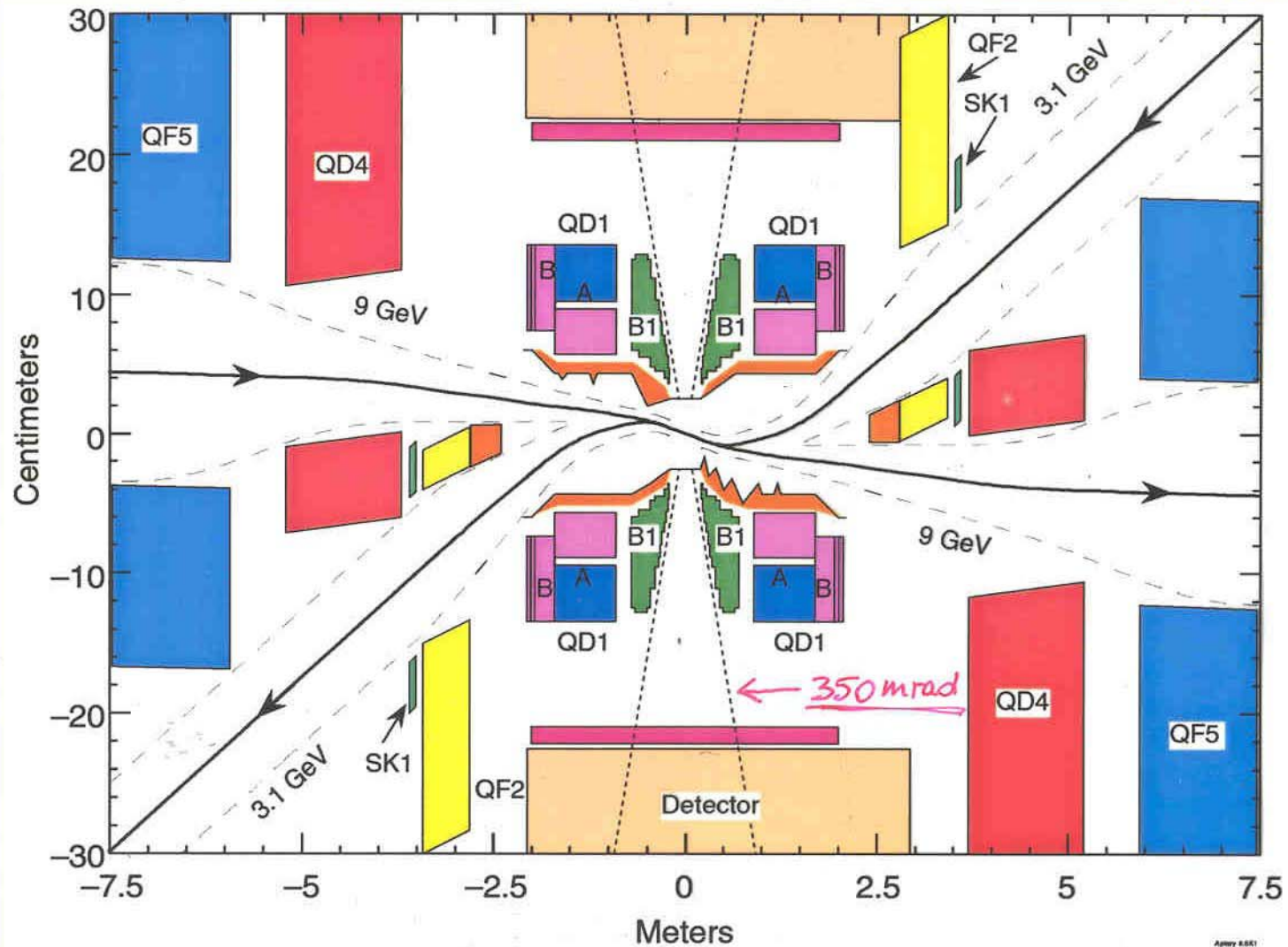
- simple matching with easy doublet
- ϵ_x increase from separation scheme is small (to be watched).
- $\xi_{b-b} \times \sim 10$: OK for energy recuperation
- Luminosity could be maximized further

IR group. Summary Talk

Witek Krasny

PEP-II IR Schematic

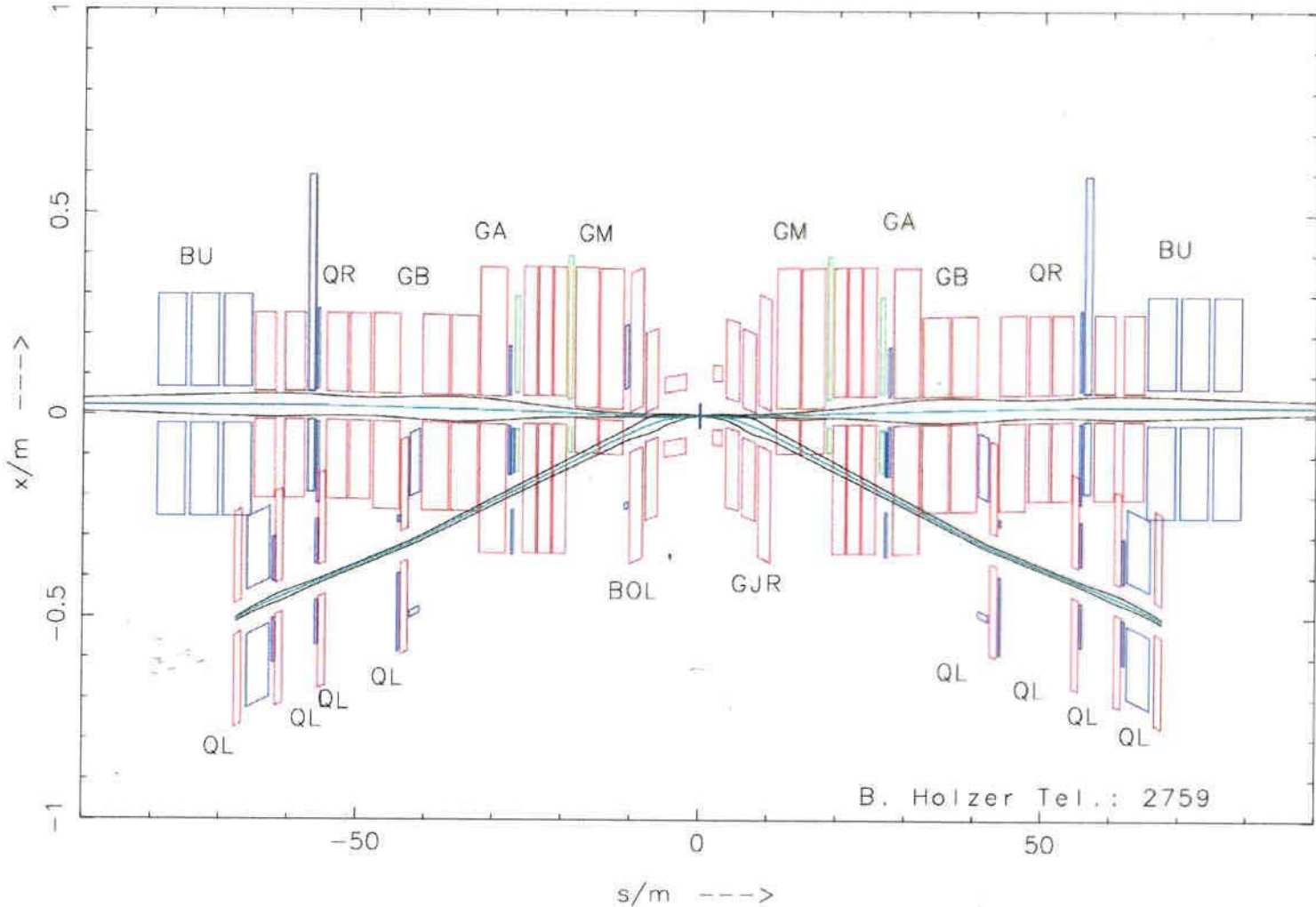
M. Sullivan



Amey A&E
MSullivan
Dec. 16, 1998

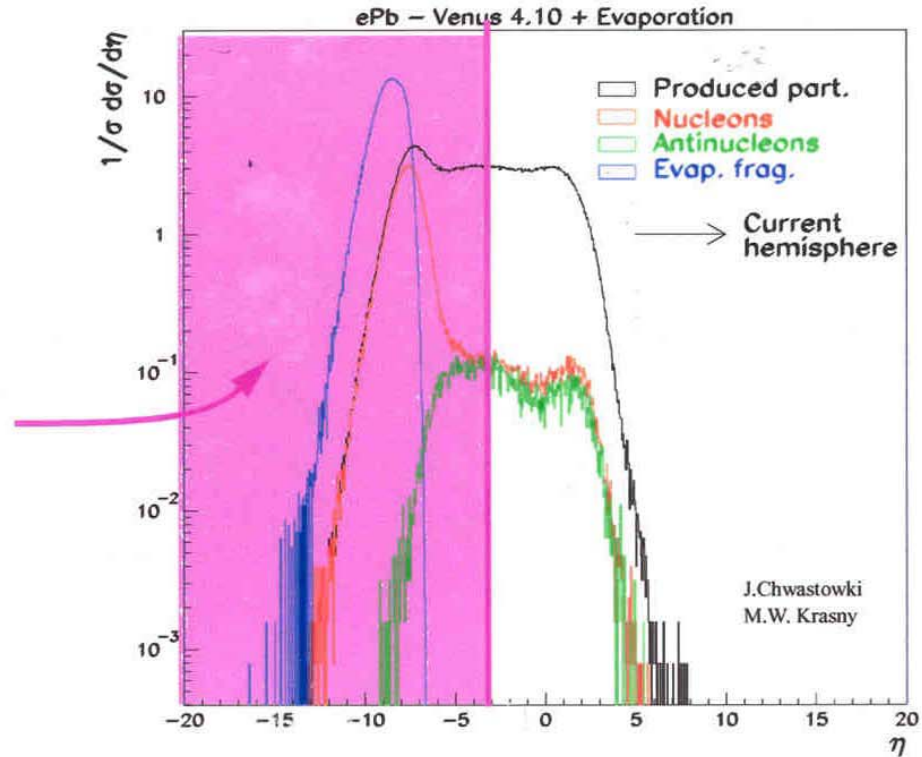
U. Wienands, SLAC-PEP-II
EICAW IR talk ppt, 26-Feb-02

Layout of HERA II IR

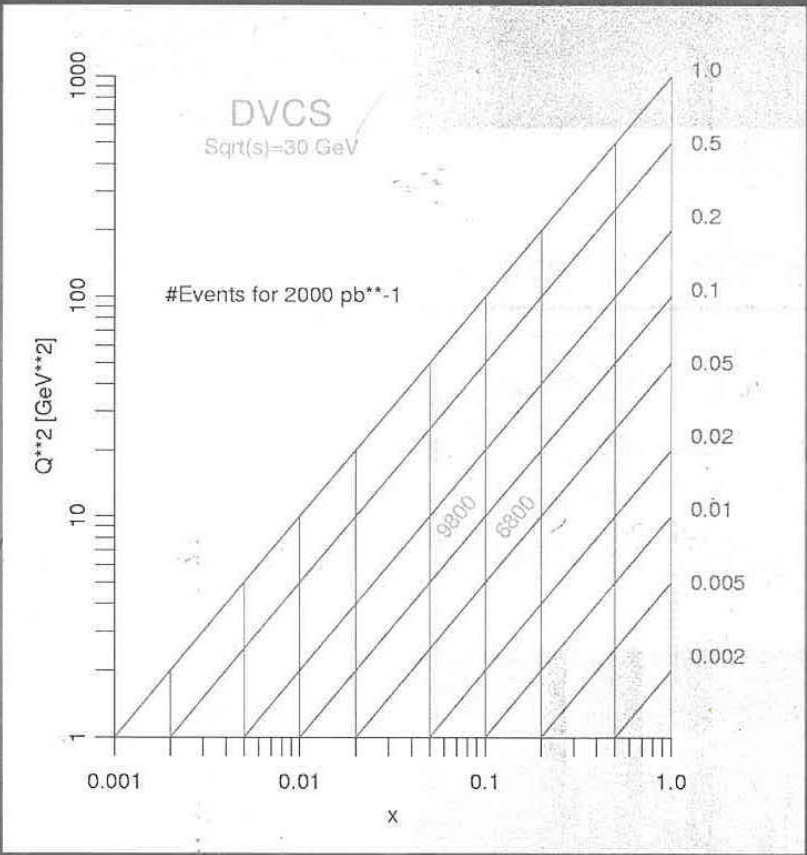
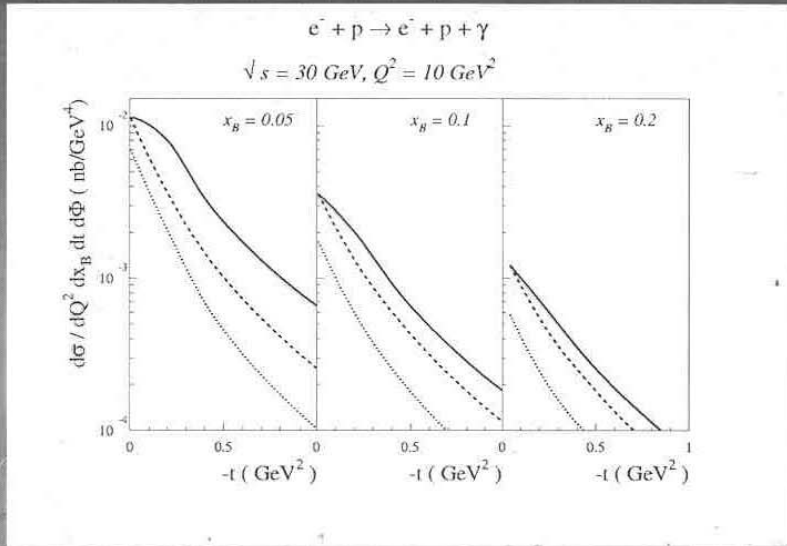


Measurement of produced particles

apart from leading neutron and leading proton tagging this kinematic domain is not covered at HERA



DVCS Cross Section



cross section at $\text{sqrt}(s) = 3$ (eq ~5 x 50)

event rates for previous luminosity

1% statistics

Detector Requirements

Hadron-side

-main functions (left to right):

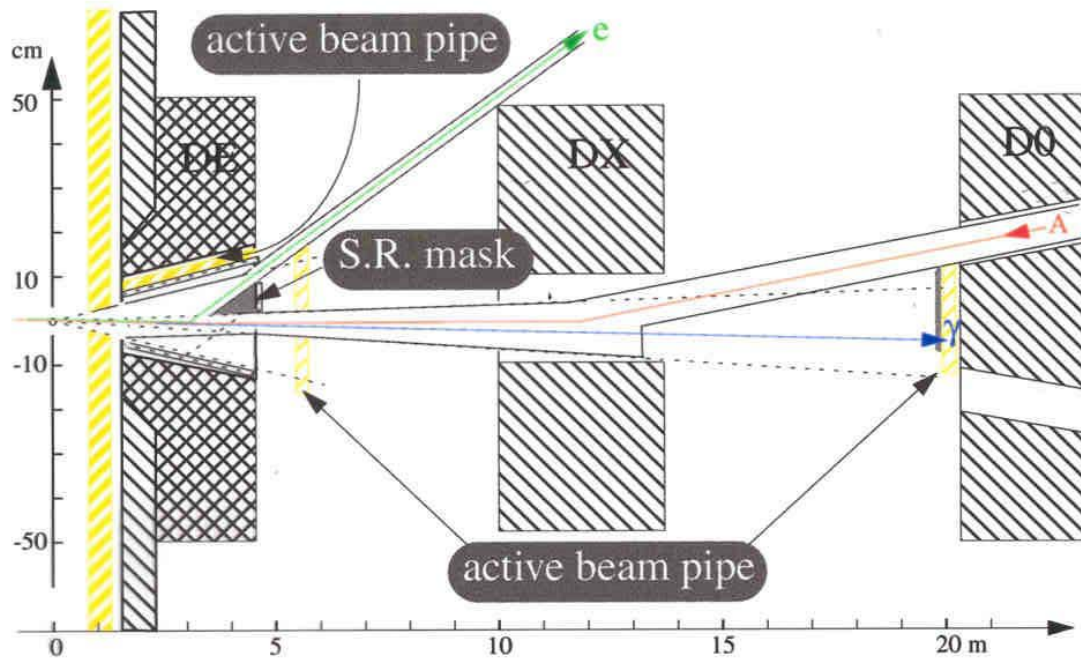
Roman pots (not on plan): diffractive scattering on beam (or same rigidity ion)

High rigidity spectrometer: EM calo for nuclear $\gamma(\pi^0)$; hadron calo for measuring evaporation neutrons and identifying p^+ & ions; tracking for measuring evaporation p^+ & ions

Medium rigidity spectrometer: EM calo for π^0 s; hadron calo for measuring wounded neutrons and identifying ions & wounded p ; tracking for measuring nuclear π^\pm , wounded p^+ and ions

Rapidity gap π -tagger: close the acceptance for charged particles emitted in the DIS process and tags diffractive events

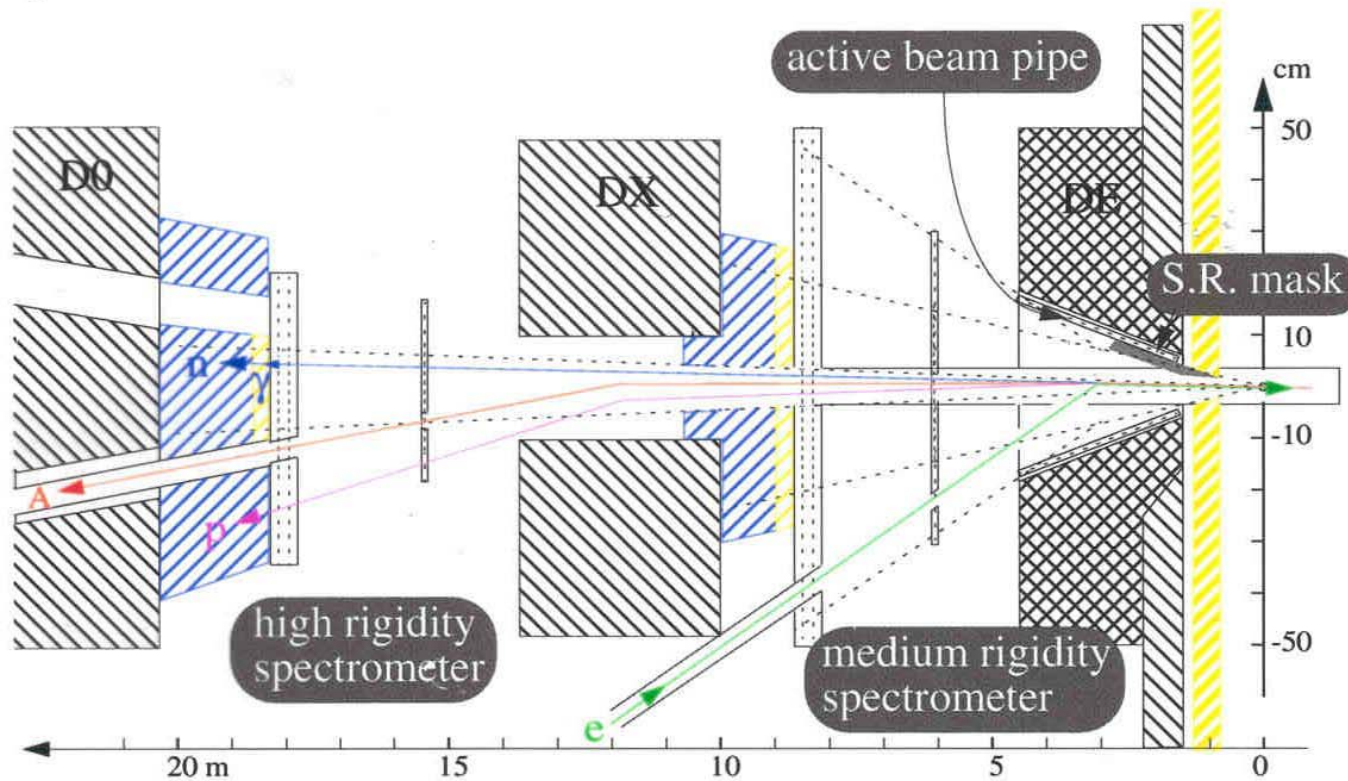
Toy model ~lepton-side~ (left to right):



electron tagger: tracker measure e^- up to 10 GeV (photoproduction or DIS tagging) and closes acceptance for π 's; backing EM calo confirms e^- tagging.

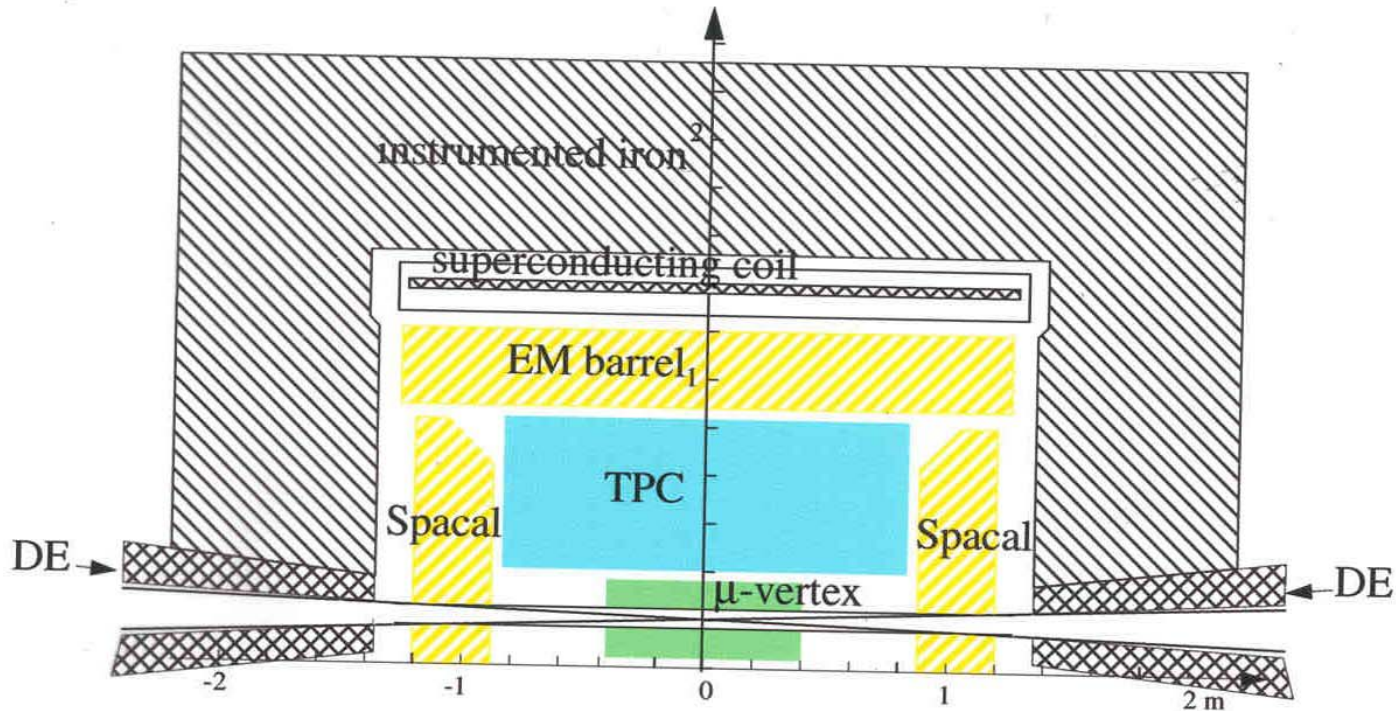
γ tagger: measure Bethe-Heitler spectrum and tags initial bremsstrahlung; receives copious synchrotron radiation.

Toy model ~hadron-side~:



- both spectrometer trackers using MWPC and drift chambers (or μ strips) at center.
- scintillating fiber calo for medium and high rigidity calorimeters (plastic or SiO_2 ?)
- scintillating fiber tracker (“active beam pipe”) for rapidity gap π -tagger

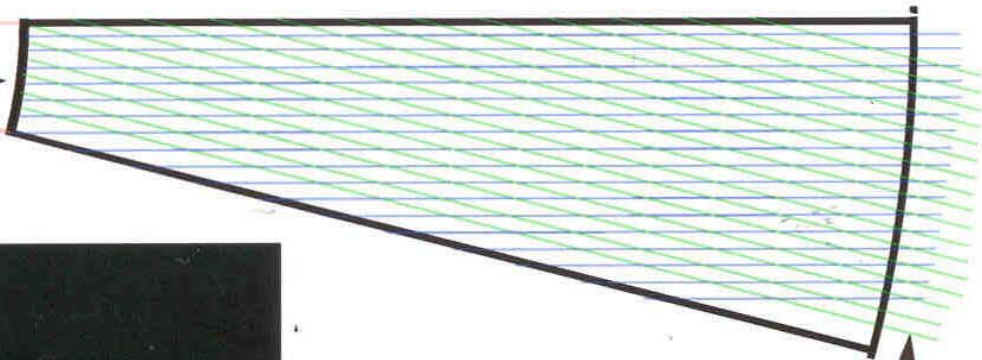
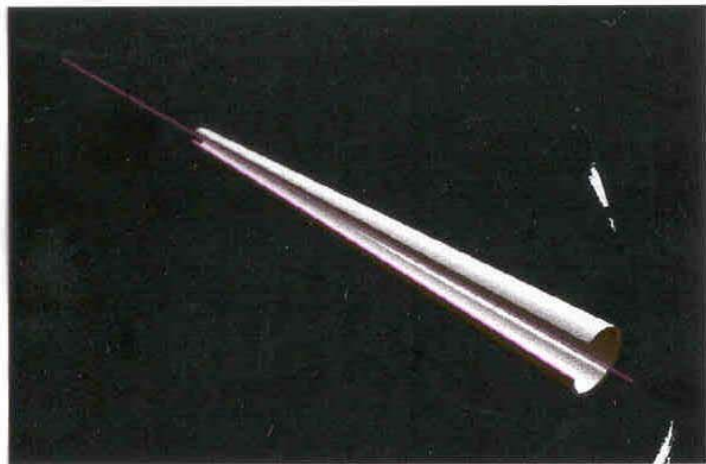
Toy model ~parton-side~ (good jet analysis, but not very high luminosities):



- Barrel is TPC backed by gas EM calorimeter inside magnet ($=\mathcal{N}/2^3$)
- Both endcaps are Spacal ($=H1$)
- μ -vertex provides small angle tracking

active beam pipe:

flattened pipe →



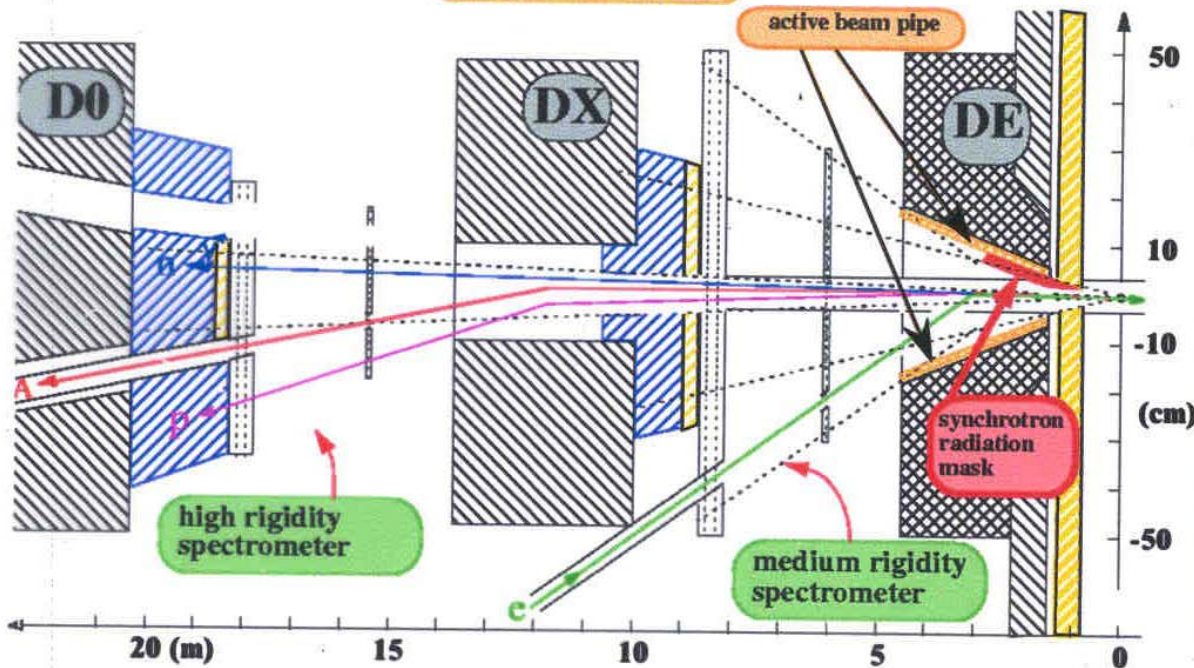
fiber layers

Experimental Physics Layout and Some Magnet Design Facts of Life.



W. Krasny 6/4/00 YALE Workshop

Hadron-side



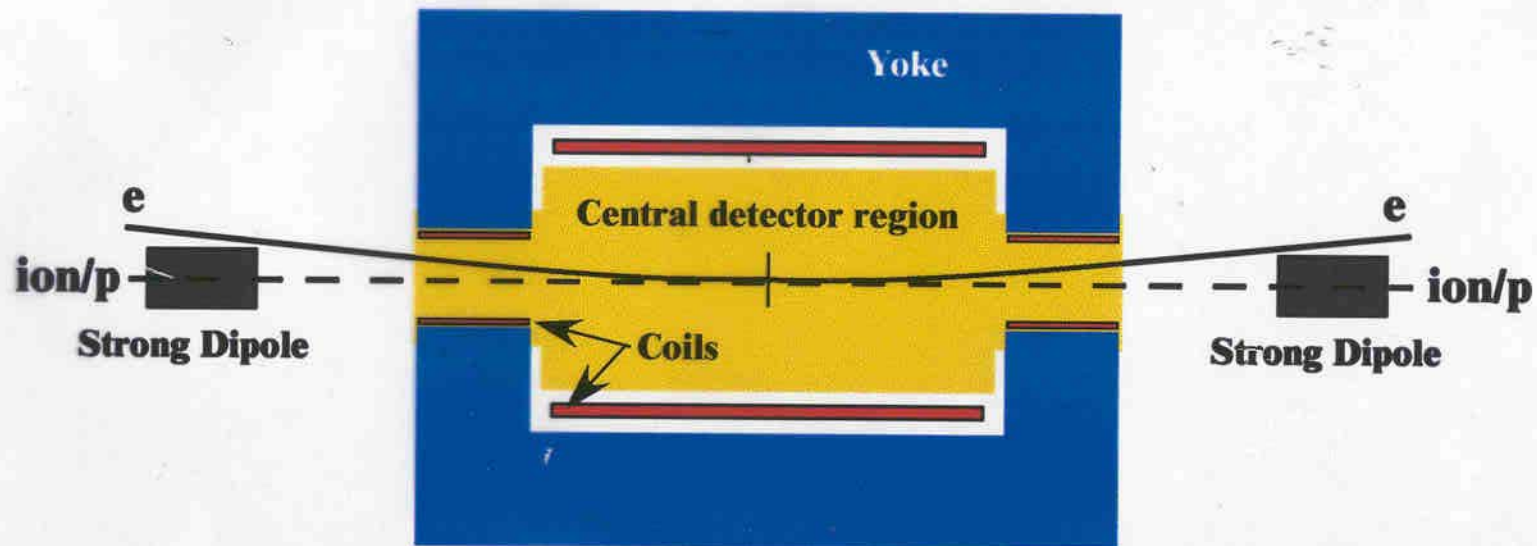
DE dipole, integrated with experimental detector, gives weak bend to get past superconducting DX magnet. DX then provides strong bend for high rigidity spectrometer.

Design Dilemma:

DE dipole field needed to clear DX is too high (synrad). Smaller field sends e-beam through DX yoke (leakage fields there are also too high).

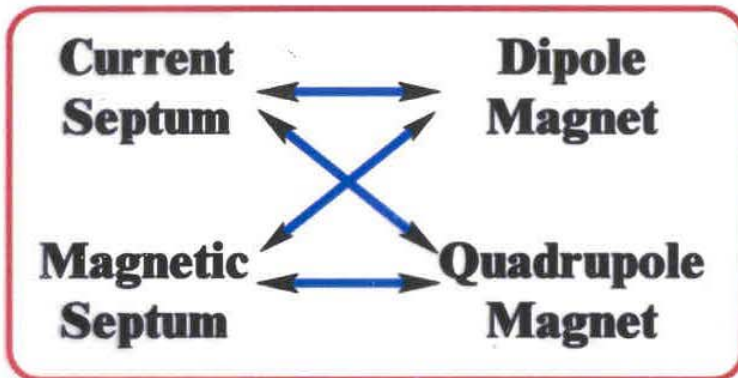
How can we improve upon this layout while keeping the advantages of a weak – strong bend geometry?

Design Principles, Tips and Tricks: Short list of EIC IR design suggestions.



- Weak dipole bend in the central region (e-beam synrad).
- Strong bend outside for protons/ions (e-beam shielded).
- Put quadrupole focusing in outer flux return yoke (β^*).
- Try to incorporate an antisolenoid close in (polarization).

Design Principles: Septum magnets provide a variety of fields for beams.



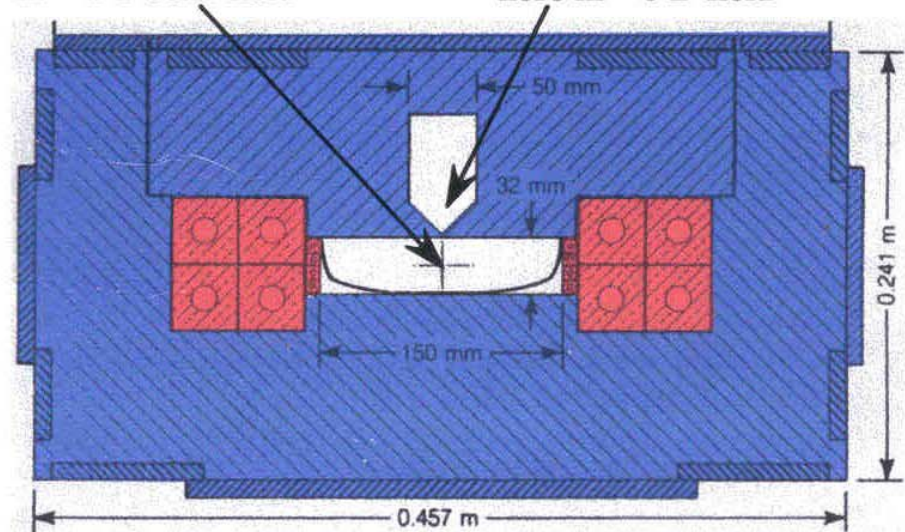
- Many septum magnet configurations are commonly used.
- Lambertson dipole, shown below, is typical for separating injected or extracted beams.

Proposal: Investigate using a septum dipole outside EIC detector to provide spectrometer functionality.

- Provide apertures for many beams.
- Instrument to integrate with detector.
- Easier to get close to a warm magnet.
 - ▲ Maintaining lever arm offsets lower field.
 - ▲ Get magnet close in for large solid angle.

Ion/p beams here in ≈ 1 T bend field

Electrons pass here in ≈ 0 B-field

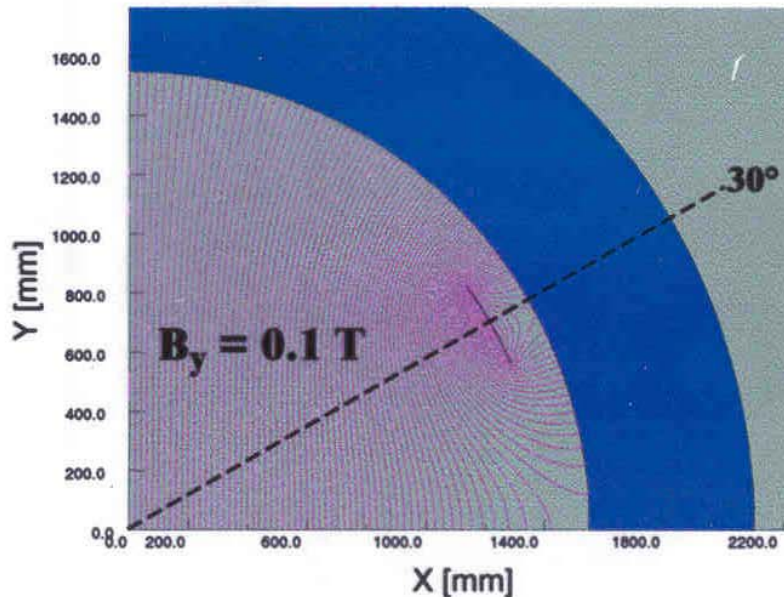


SSC Collider Ring Abort Lambertson Magnet

A cylindrical yoke is compatible with a low field strength dipole plus regular solenoid.



Dipole (1/4 Model + Boundary Conditions)



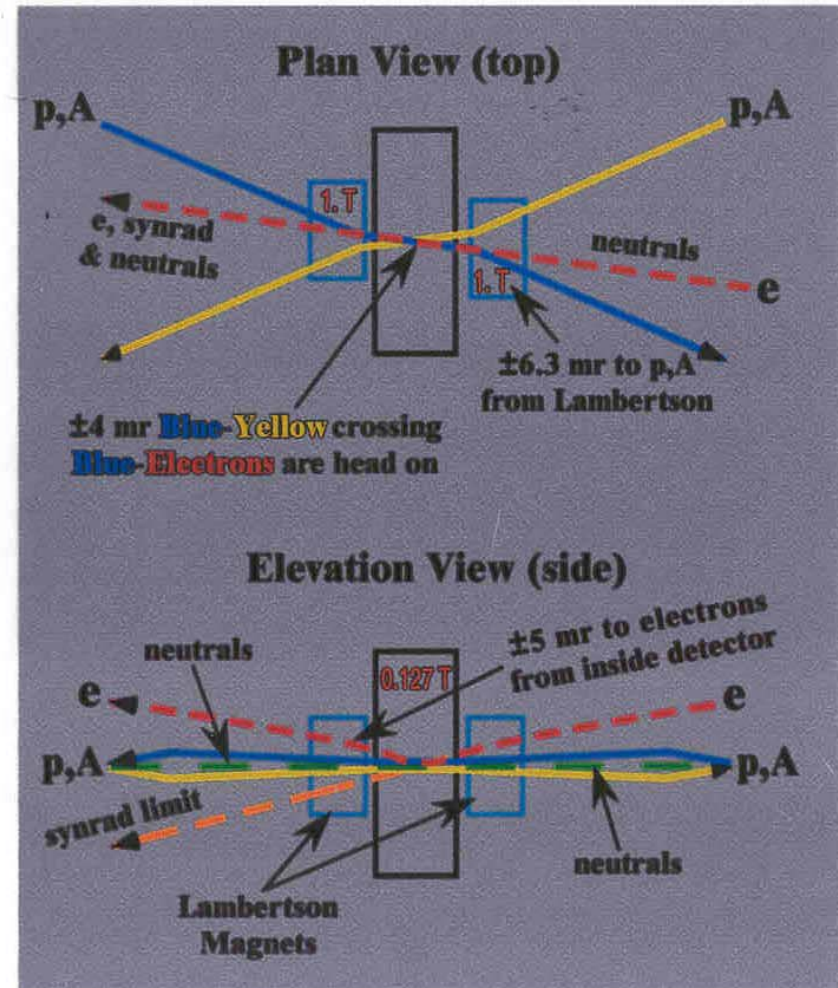
- ◆ Dipole with 0.1 T does not require excessive superconductor (even with $R_{\text{coil}} = 1.4$ m).
- ◆ Wind on top detector solenoid coil.
 - Avoid radiation length at small R.
 - Avoid issues with coil torques.
 - Even the partial coil shown at left, gives good field quality for beams.

Design shown has 10^{-5} field uniformity at $R = 80$ mm.

Proposal for hybrid eRHIC layout that is compatible with weak – strong bends.



- E-beam strikes head on with Blue at IP.
- A small vertical deflection inside detector separates electrons from circulating beams.
- Ions/p bent by 1 T field inside a Lambertson dipole (electrons in reduced B-field region).
- Long drift downstream of Lambertson gives spectrometer lever arm.
- Keep Lambertson short to pass synrad etc. via small Blue/Yellow crossing angle (but with reduced neutral separation).
- Small vertical kicks to Blue/Yellow beams compensated before triplets – proton spin should be ok.



Possibilities of Low Beta-star, Crab Crossing and Traveling Ion Focus for EIC

Ya. Derbenev, L.Merminga, Yu.Chao

Jefferson Laboratory

EIC Accelerator Workshop

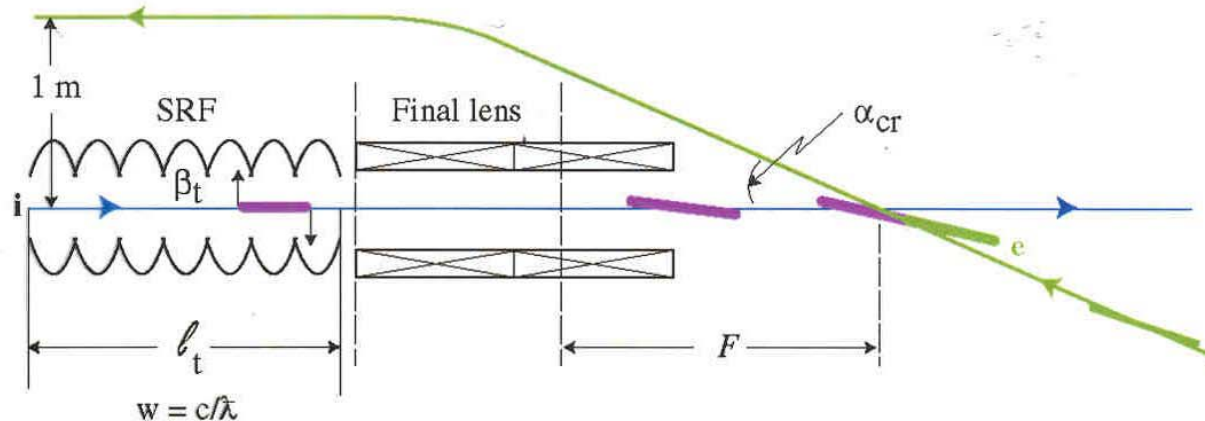
BNL

February 26-27, 2002



Crab Crossing for Interaction Point

- Short bunches also make feasible the Crab Crossing:
- SRF deflectors 1.5 GHz can be used to create a proper bunch tilt



$$\alpha_{cr} = 2\alpha_f = 2\theta_t \frac{F}{\lambda}$$

$$\theta_t = \frac{eB_t l_t}{E}$$

$$E = 100 \text{ GeV}$$

$$F = 3 \text{ m}$$

$$\lambda = 20 \text{ cm} \quad (1.5 \text{ GHz})$$

$$B_t = 600 \text{ G} \quad (= 20 \text{ MV/m})$$

$$l_t = 4 \text{ m}$$

$$\sigma_f = 1 \text{ mm}$$

$$\alpha_{cr} = 0.1$$

$$\theta_t = 5 \cdot 10^{-4}$$



Ring Ring
Working Group Summary
C. Tschalaer

Ring-Ring Version of the EIC

C. Tschalaer

The ring-ring proposal for the EIC consists of a small separate electron storage ring intersecting the RHIC ring at the 12 o'clock intersection region. A conceptual design for such a polarized electron ring of 5 to 10 GeV was presented by Y. Shatunov of BINP. Modeled on an earlier design for EPIC (3.5-7 GeV), it has a 950m circumference and is designed to reach a luminosity of 0.5 to $1 \cdot 10^{33}$ /cm²/s with a 10.65m bunch spacing. As a novel feature, its arcs are made up of so-called super bends containing a short high-field (2 Tesla) center magnet flanked by 2 to 5 Tesla variable magnets. This design reduces self-polarization times to 3-15 min (10-5 GeV) at acceptable RF power (max 10 MW).

Electron Cooling

To reach luminosities of order 10^{33} /cm²/s, electron cooling of the hadron beams is essential. Shatunov presented a concrete proposal for electron cooling of RHIC up to 100 GeV/? requiring 54 MeV electrons. Optimal electron bunch populations of $\sim 30 \cdot 10^{10}$ would bring a gain of about 10 in hadron emittance and thus luminosity. Y. Derbenev of Jefferson Lab. gave theoretical underpinning of electron cooling and corresponding luminosity limits. Finally Dong Wang (BNL) showed calculations for electron cooling beam dynamics and development of electron cooling tests at RHIC.

Spin Dynamics

The theory of spin dynamics in an electron ring was presented by D. Barber based on the invariant spin field \hat{n} . The variation of \hat{n} with particle energy (kinetic term) was shown to be of particular importance in self polarization and in the depolarizing effect of the interaction point (IP) straight sections where the polarization axis is near the horizontal plane. Exact modeling of spin propagation including non-linear beam-beam effects appear crucial in optimizing e-ring polarization.

The dynamic spin field term is largely untested today. A program for measuring its effect on polarization was presented by F. Wang and T. Zwart (MIT) using the MIT/Bates South Hall Ring which contains all necessary facilities (Siberian snakes, polarimeter, spin flipper). The low beam energy of 0.8 to 1.5 GeV provides clean test results uncluttered by strong betatron coupling of the spin. A cost-effective program using superconducting wigglers can test theory and tracking codes.

Outlook

With these elements, a logical and cost-effective path exists to a high-luminosity electron-ion collider:

- A 5-10 GeV "BINP-type" e-ring at RHIC is filled by a 2 GeV linac with unpolarized electrons (stacking), ramped to full energy, and allowed to self-polarize in 15 minutes. It collides with 10-100 GeV ions or 25-250 GeV polarized protons. With 0.45 A

circulating in each ring at 10.65m bunch spacing (360 pulses in RHIC), a luminosity of 0.5 to $1 \cdot 10^{33}/\text{cm}^2/\text{s}$ is expected.

- If self-polarization proves to be insufficient, the linac may be upgraded to full energy (10 GeV) and fitted with a polarized electron source. A full-energy polarized beam is then stacked and stored only as long as the polarization is maintained.
- If higher luminosities are required, an energy-recovering linac and much shorter storage (100 turns) as proposed by Jefferson Lab (Derbenev, Merminga) together with higher pulse repetition rates may be considered.
- A second IP may be established by a second e-ring at a neighboring IP site in RHIC using the same injector. For a relatively modest additional machine cost, this could provide for a fully independent collision experiment particularly if each e-ring would collide with alternate hadron beams which could conceivably be operated at different energies if no hadron-hadron collision experiments were run simultaneously.

Tasks Ahead

To prepare for an EIC construction proposal, a number of tasks need to be addressed as soon as possible. The most important ones are the following:

- Integrate the e-ring into the RHIC lattice;
- Develop detector concepts and integrate them into the collider;
- Develop polarized proton beams at RHIC;
- Realize electron cooling at RHIC;
- Develop spin tracking to optimize self polarization in the proposed e-ring;
- Test self polarization and tracking codes in the Bates SHR;
- Develop higher RHIC currents and pulse repetition rates.

With proper funding, a time frame of 3 years to accomplish this R&D seems ambitious but realistic.

- Spin Dynamics; Theory (Barber)
- Invariant spin field \hat{n} needs to be established properly, not just on closed orbit.
- Energy variation $d\hat{n}/d\eta$ (=kinetic term in S.T. self polarization) is large and important in IP straights.
- Exact modeling includes non-linear beam-beam terms crucial to assess and optimize obtainable ???
- Derbenev, Wang, Zwart
- Dynamic term $d\hat{n}/d\eta$ largely untested. Bates has ideal conditions for such tests
 - SHR
 - Siberian Snakes
 - Polarimeter
 - Spin flipper
 - “Brains”
- Low energy (0.8-1.5 GeV) gives “clean” test of $d\hat{n}/d\eta$ uncluttered by strong betatron coupling of spin at high energy.
- Cost-effective test program using super conducting wigglers (horizontal and vertical) to map $d\hat{n}/d\eta$ from 0.8 to 1.5 GeV

Ring-Ring EIC

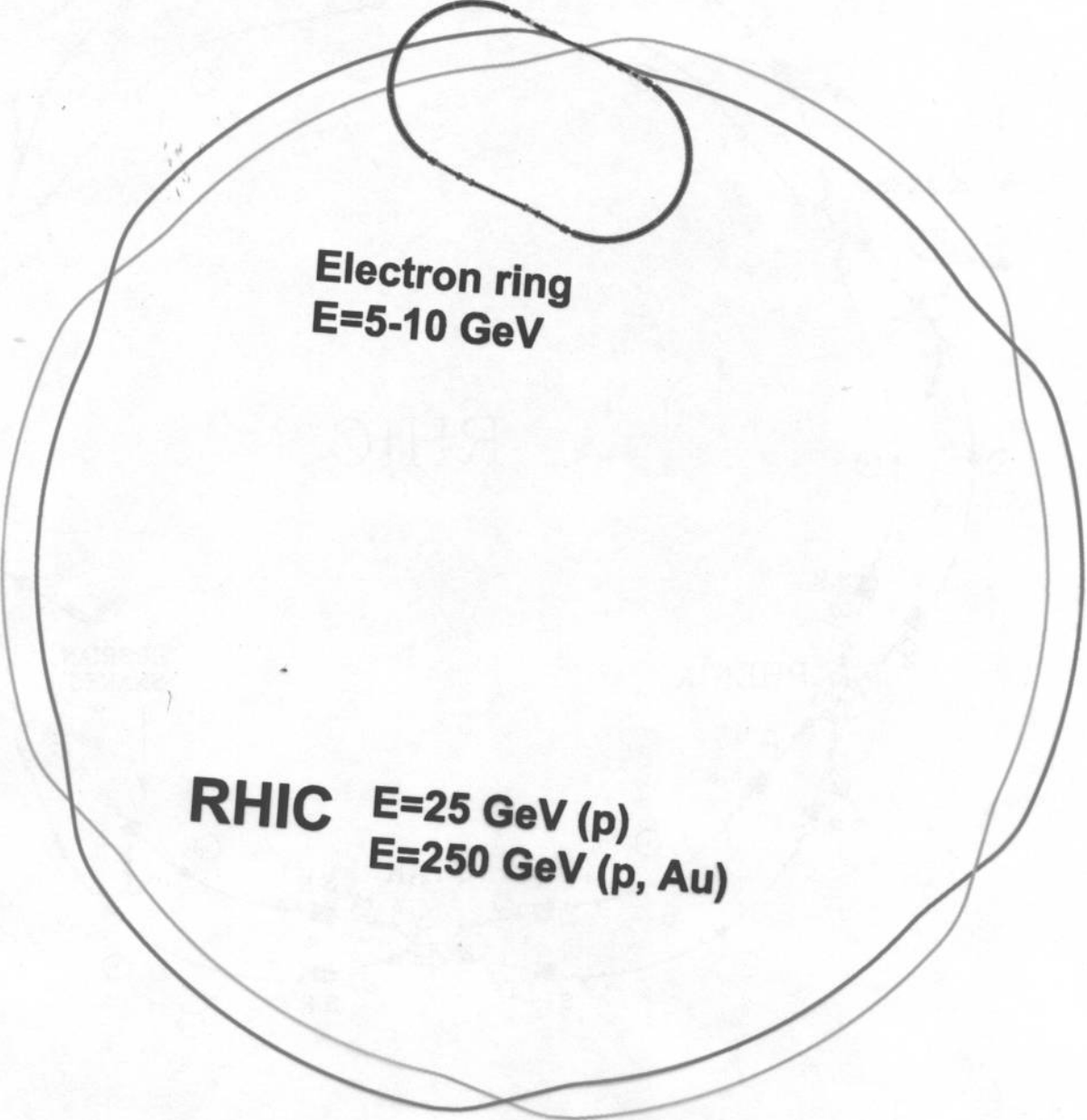
- **e-ring for eRHIC (Shatunov)**
 - eRHIC layout
 - Vertically spread hadron beams, 12 o'clock
 - e-ring plane below(?) RHIC plane, intersection at 12 o'clock point
 - 5-10 GeV; longitudinal polarization at IP at 7-5 GeV
 - 10.65 m bunch spacing (360 bunches)
 - $L=0.5$ to $1 \times 10^{33}/\text{cm}^2/\text{s}$ for 5 – 10 GeV
 - Special features
 - Super bend to speed up self polarization (15.3 min) at limited RF power (12.3-9.6 MW)
 - Spin transparent IPs straight → minimal depolarization
- **Electron Cooling**
 - **Shatunov:**
 - Conceptual e-cooling scheme for RHIC
 - Optimal electron bunch population of $\sim 3 \times 10^{33}$
 - Gain of ~ 10 in emittance → luminosity
 - **Derbenev:**
 - E-cooling theory → can increase tune shift tolerance by 10 to 0.1
 - **Wang:**
 - Calculation in progress to model e-cooling

Conclusions

Logical and Cost Effective Path Exists to eRHIC

- 5-10 GeV “Budker” e-ring with 2 GeV linac injector, inject unpolarized at 2 GeV → ramp to 5-10 GeV → self polarize in 15 min → collide with 10-100 GeV ions or 25-250 GeV proton with 10.7 m bunch spacing, 0.45 A in each ring for 0.5 to 1×10^{33} luminosity.
- To improve on self polarization: → upgrade linac to 10 GeV → inject polarized → stack → store for seconds or minutes before serious depolarization occurs.
- Install full energy recovery linac (ERL) boost RHIC rep. Rate, current, cooling → run e-ring as circulator → maximum luminosity.

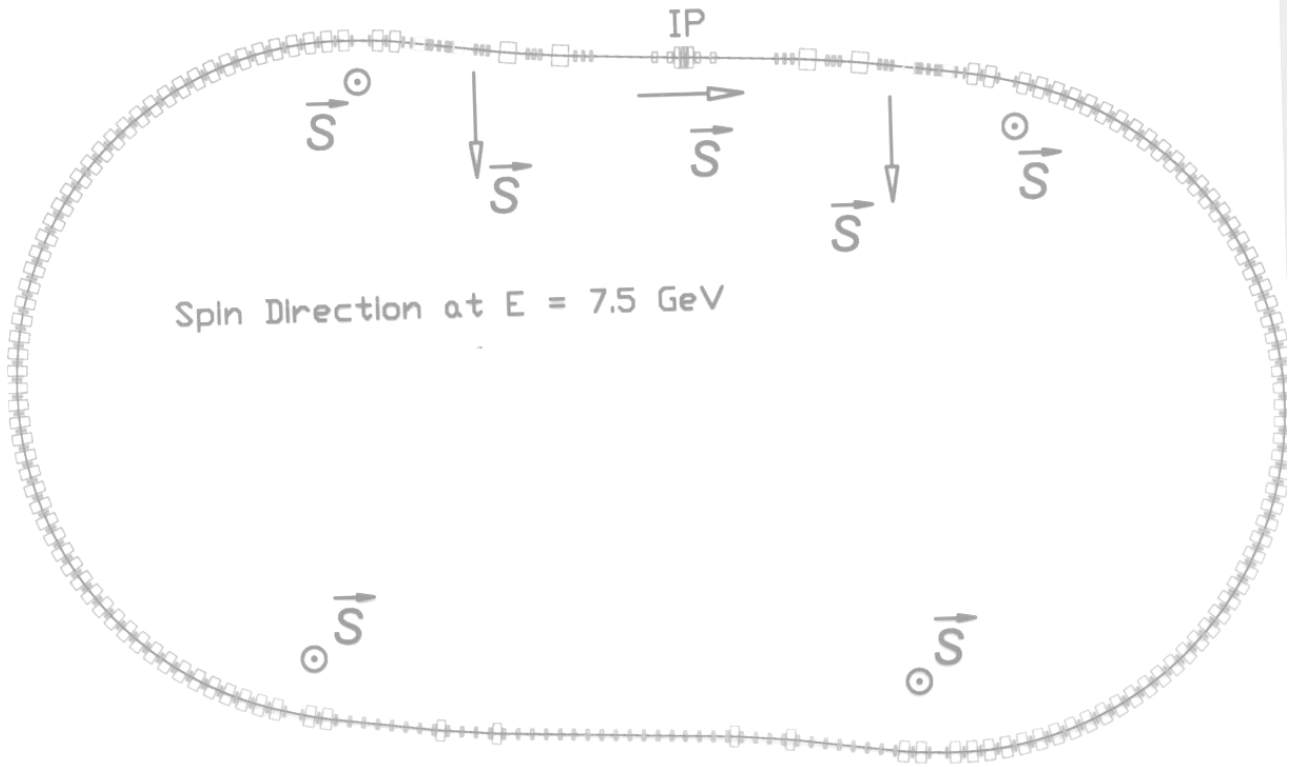
eRHIC



Electron ring
E=5-10 GeV

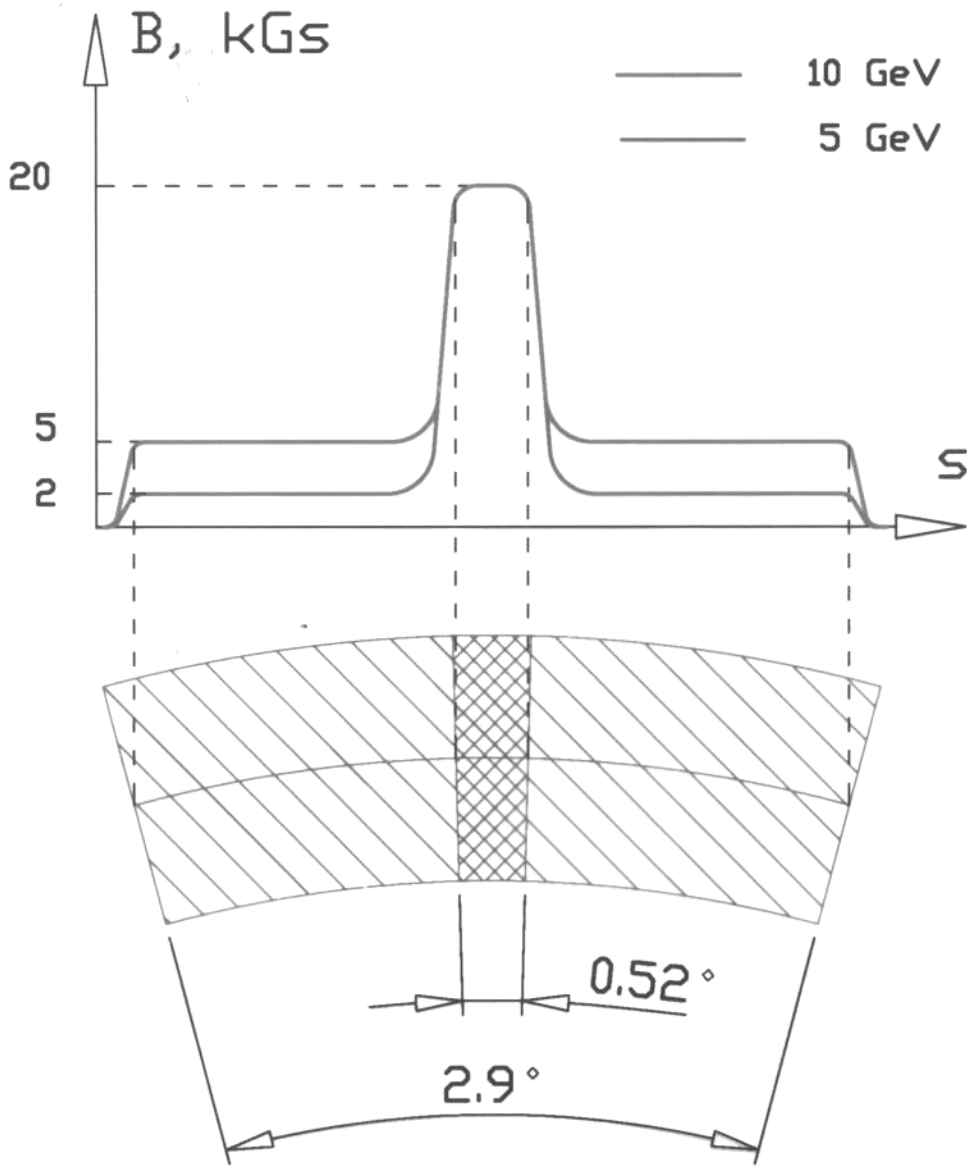
RHIC E=25 GeV (p)
E=250 GeV (p, Au)

Electron Ring E = 5-10 GeV



Spin Direction at E = 7.5 GeV

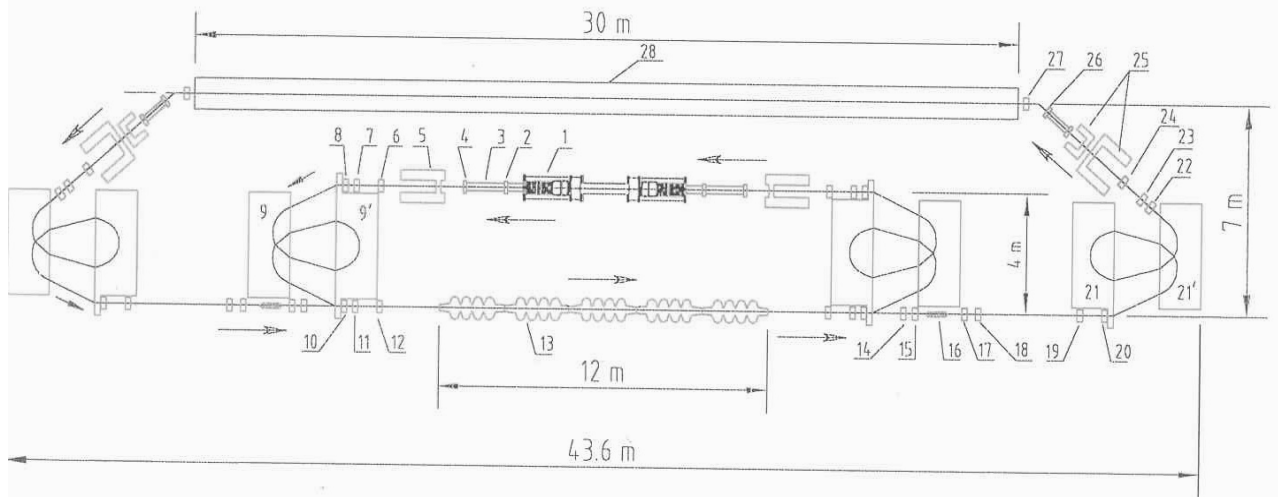
Super Bend

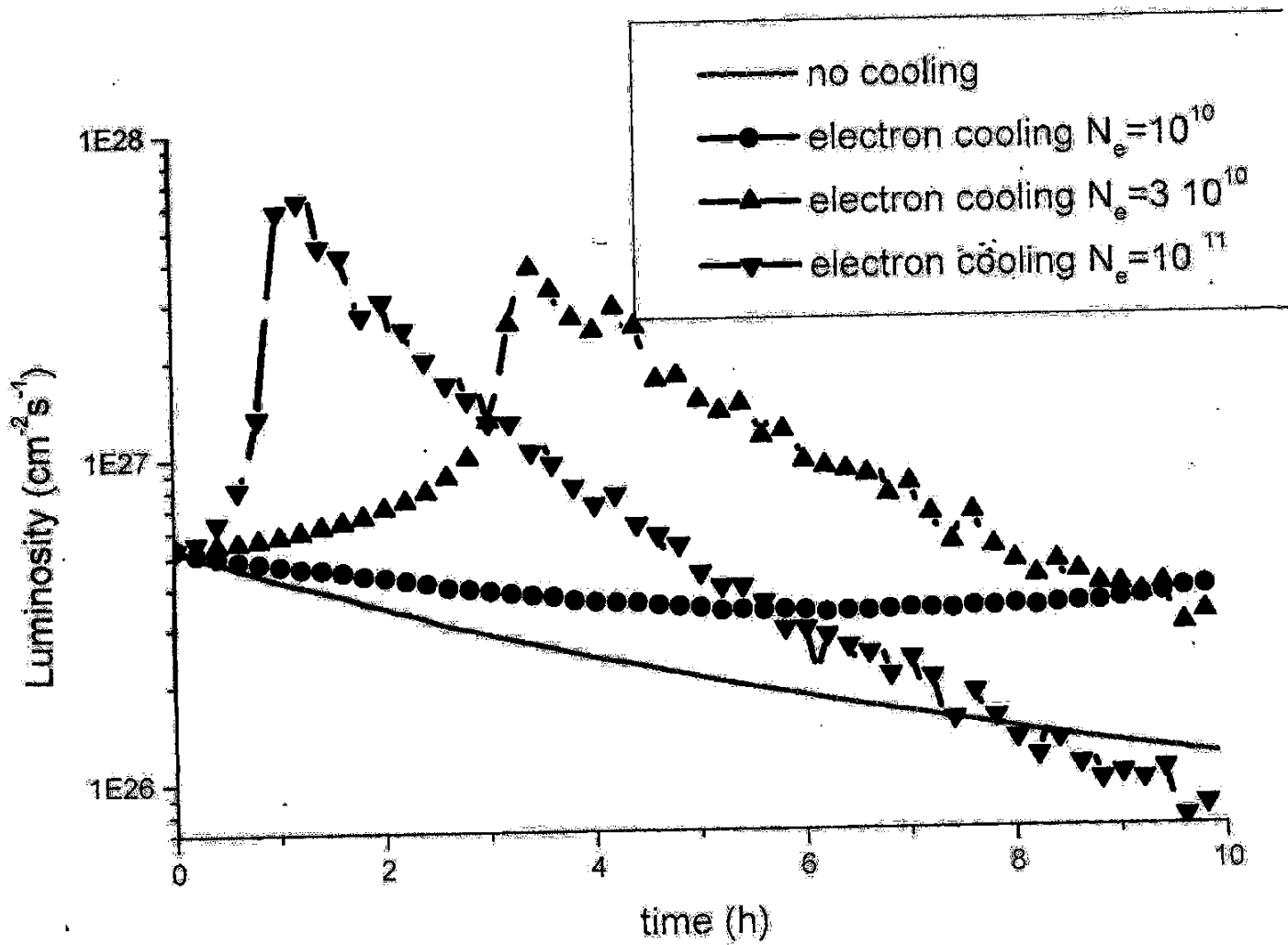


General parameters of the electron-proton collider

	Units	Electron ring	Proton ring
Circumferences	<i>m</i>	958.25	3833
Energy	<i>GeV</i>	5–10	25–200
Arc radius	<i>m</i>	97.98	610
Bending radius	<i>m</i>	63.59	243
Number of bunches		90	<u>360</u>
Bunch spacing	<i>m</i>	10.65	10.65
Bunch population		<u>$1 \cdot 10^{11}$</u>	$1 \cdot 10^{11}$
Beam currents	<i>A</i>	0.45	0.45
Harmonic number		1170	2520
RF frequency	<i>MHz</i>	365.7	196.9
Accelerating voltage	<i>MV</i>	30	1.5
Energy losses/turn	<i>MeV</i>	2.83– <u>21.26</u>	
Total radiated power	<i>MW</i>	1.27– <u>9.57</u>	
Beam emittances, $\epsilon_{x,z}$	$\mu\text{m} \cdot \text{mrad}$	43–65	48–6
Beta function at IP	<i>cm</i>	10	10
Beam size at IP, $\sigma_{x,z}^*$	μm	65–80	68–24
Momentum spread		$1.0\text{--}1.6 \cdot 10^{-3}$	$1.1\text{--}0.4 \cdot 10^{-3}$
Bunch length, σ_l	<i>cm</i>	1–2	10–5
Beam-beam parameter, ξ		0.046–0.023	0.009–0.002
Lasslett tune shift, $\Delta\nu$			0.2–0.009
Luminosity	$\text{cm}^{-2}\text{s}^{-1}$		0.45– $1 \cdot 10^{33}$

Electron Cooling System for RHIC collider (BNL)





Summary - Linac-Ring Working Group

Ilan Ben-Zvi (BNL) Working Group Convener.

The Linac-Ring (LR) working group considered the subject of a Linac-on-Ring Electron Ion Collider (EIC) with a large range in the center of mass energy for polarized electron-proton scattering, and electron-Ion (heavy ion) scattering with luminosity of $10^{33} \text{ cm}^{-2} \text{ sec}^{-1}$. The subject covers both a pure electron linac colliding with a hadron storage ring as well as a Linac with Circulating Ring (LCR) option.

The mission of the working group was to assess the LR potential performance and evaluate its technical risk. For practical reasons, the working group spent its efforts on the electron side of the EIC and the issues of electron – ion interactions, but not on the specific properties of the hadron ring. When hadron parameters were necessary for the discussion, RHIC parameters were assumed. Important issues that are specific to the subject of this working group are

- Luminosity as a function of energy
- Energy range that may be achieved
- Electron polarization as a function of energy
- R&D issues for the L-R EIC.

The advantages of a linac source (with or without a circulator ring) are as follows:

- The practically achievable electron polarization is very high. 80% polarization is common, but this is for typically low average currents. There is no experience with high average current (ca. 100 mA) polarized electron source.
- The polarization may be switched fast at will.
- There is no need for polarization rotators near the IP.
- The energy may be changed rapidly and over a large range without losing polarization.
- The linac maintains the high luminosity and polarization over a very large energy range.
- The linac can tolerate a much higher beam-beam parameter than a storage ring, leading to a potentially higher luminosity (if the number of ions in a bunch can be increased) or to the same luminosity with a lower current, thus less synchrotron radiation in the detector.
- The linac has a naturally round beam, small emittance. These are advantageous for beam-beam interactions and the IP design.

When the option of using a circulating ring to reduce the average current of the linac, the scheme has a low technical risk and no show stoppers, but requires a significant amount of R&D due to the lack of simulations of the system.

The Linac Circulator Ring (LCR), Y. Derbenev (JLAB).

This new approach to the Linac – Ring (LR) was proposed by Y. Derbenev and presented in a Plenary Talk as well as in the LR working group. This approach provides a continuous transition from a full Energy Recovery Linac (ERL) to regime where one uses only a fraction of the current (1/100 to 1/1000) in the linac. Therefore the LCR has the potential to ease up (by orders of magnitude) system demands on electron source and linac while preserving advantages of linac.

In the LCR approach, it is proposed to compliment the ERL by an electron circulator ring wherein the injected electron bunches will be kept in a temporary closed orbit to execute a large number of revolutions colliding with the ion beam. In this way, electron photo injector and linac operate in a pulse-current energy-recovery regime of a relatively low average current, while a high current circulates in collider. The polarization is still easily delivered and preserved. The number of revolutions in the

circulator ring can be adjusted over a wide range, and at the extreme this scheme can be naturally converted to the pure linac-ring scheme when beneficial.

The features of the LCR include:

- Easy maintenance of spin (no resonance crossings, no quantum depolarization).
- The emittance is determined by the photoinjector.
- Easily variable energy.
- Easier interaction point (no spin rotators next to IP, no depolarization from bends).
- Larger acceptable beam-beam parameters leading to higher luminosities.
- Much reduced (by orders of magnitude) requirements on the average current of the photoinjector.
- Reduction of BBU in SRF linac.
- Reduction of HOM power in SRF linac.

Issues to be investigated include

- The development of high quality kickers.
- Investigation of the microwave instability of short bunches in the circulator ring.
- Effects of CSR.

Electron Cooling

One issue that is critical for the performance of the EIC is electron cooling. This subject was discussed in a joint session of the Linac - Ring group and the Ring - Ring group. Electron cooling of the ions is a must in the ion ring, regardless of the approach to the electron machine. Electron cooling is well established at low energy, but for the high energy of the EIC machines, we face new developments:

- New accelerator technology (ERL) at high-energy (for a cooler) of ~50 MeV, 100 mA.
- Operation in a collider (some possible advantages for the collider)
- Bunched beams
- Electron bunch may be shorter than ion bunch

Other issues we encounter in the development of a high-energy electron cooler include:

- High-precision manufacturing and alignment of a long superconducting solenoid
- Generate, transport and match a “magnetized” beam without continuous magnetic field
- De-bunch (then re-bunch) the beam to obtain low energy spread
- Overcome recombination

Theory and New directions (Y. Derbenev, JLAB)

Realization of beam recovery in superconducting linear accelerators and new concepts of beam transport: discontinuous solenoid, circulator rings, flat to round beam adapters – made feasible the efficient electron cooling for hadron beams in colliders. The precision requirements to beam alignments are relaxed by use of dispersive cooling. Cooling with flattened beams (yet with round beams in the IP) allows one to decrease the critical electron current against IBS and minimize the non-linear beam-beam disruptive effects.

The start rate of electron cooling is limited usually by a large ion beam divergence caused by the Coulomb repulsion at beam forming in low energy part of ion facility. Halo beam gymnastics in phase space is proposed in order to overcome the space charge limit and maintain beam emittance at a level that delivered from a linac while stacking and accelerating the beam in a booster.

Electron cooling in cooperation with an intensive, high frequency superconducting field allows one to obtain very short heavy particle bunches, hence, raising the luminosity by making a stronger final focusing. Very short bunches also make feasible the crab crossing for hadron beams, that allows one to remove the parasitic beam-beam interactions and maximize the collision rate.

Summary of the BINP-BNL study of electron cooling of RHIC. (Y. Shatunov, BINP)

Electron cooling of RHIC has been investigated in collaboration between the Budker Institute of Nuclear Physics (BINP) and BNL. The PIs were V. Parkhomchuk (BINP) and I. Ben-Zvi (BNL). The study has been published as a Collider-Accelerator Department Accelerator Physics report. The report covers the performance of RHIC under electron cooling and includes simulations of the evolution of the beam parameters and luminosity as a function of time, the effect of starting parameters, ion-electron recombination, and dissociation of beam due to the collisions and various coherent effects of the electron-ion interaction. The design also analyses the accelerator hardware to be used in the cooler. An approach using a DC electron gun and an energy recovery linac has been analyzed in detail, including beam optics of the machine, the issue of magnetized electron transport and matching as well as de-bunching and re-bunching the beam to match longitudinal phase-space. The study estimates that 2×10^{10} electrons per bunch are sufficient to cool effectively a 100 GeV/A gold beam and achieve a luminosity increase of about a factor of 10 over the uncooled RHIC, with part of the gain coming for emittance decrease and part from the extension of the luminosity lifetime.

The primary conclusion of the study was that electron cooling of RHIC may be very effective, but there are many points left to resolve theoretically and experimentally.

- Need for 3-D simulations
- Need experiments to settle various hardware issues (electron source, linac energy spread...)

Electron cooling beam dynamics, (D. Wang, BNL)

Dong Wang described the current effort going on at the Collider-Accelerator Department on investigating electron cooling of RHIC. Electron cooling simulation software is being used, mostly the Simcool code written by V. Parkhomchuk BINP as part of the BINP-BNL study and the Betacool code developed at JINR, Dubna. A new code is being developed by Tech-X of Denver, Colorado to permit electron-cooling simulation using direct Coulomb interactions of the ions in an ensemble of electrons. The Betacool code upgrade is a subject of collaboration between JINR and BNL. Another effort is simulation of electron beam dynamics, leading towards end-to-end 3-D simulations of the cooler.

On the experimental side, an Electron Cooling Test Facility is planned, in which hardware will be tested, including:

- A superconducting and a room-temperature electron guns provided by Advanced Energy Systems (AES), (the superconducting gun also in collaboration with JLAB).
- A laser and photocathode system being developed by the BNL Instrumentation Division and C-AD.
- Superconducting ERL.
- Debunching and rebunching of the beam.
- Magnetized electron transport.
- A high-precision superconducting solenoid prototype.

Source theory, practice and lasers M. Farkhondeh (MIT)

A polarized electron source that could meet the requirements of a direct (no LCR) linac-ring electron-ion collider (EIC) is very challenging. The necessary highly polarized average current, 100-200 mA, is about three orders of magnitude above what is produced today.

At this point, the only practical method of producing high currents with a high degree of polarization is photoemission from negative electron affinity GaAs based photocathodes. Higher average currents may be achieved by a combination of increased laser power and/or higher quantum efficiencies of the photocathode. Higher degrees of polarization are routinely obtained when the four-fold degeneracy of the valance band is broken by adding uniaxial strain or super lattice structures. Quantum efficiency lifetimes at high average currents for existing polarized sources are primarily limited by ion back bombardment of the photocathodes, which is a function of the vacuum condition in the gun. The current state-of-the-art is 1/e lifetime of the cathode 10^5 Coul/cm². This translates to a lifetime of a couple of weeks at an area of 3 cm² and 0.2 A current. For the EIC currents, excellent UHV vacuum conditions approaching XHV (Extreme High Vacuum) will be required.

A laser system with the RF structure of EIC and sufficient power does not exist today and R&D will be required to develop such a laser. An attractive alternative may be the use of a CW high power fiber coupled diode array laser system that exists today. The 28 MHz microstructure must then be introduced to the electron beam using chopping and bunching with accelerating structures. Highly polarized beams with peak currents of about 100 mA and duty factors of 1% have been produced on a test setup at MIT-Bates. The duty factor has been limited by the source power supply.

R&D issues:

- Laser
- Surface-charge limit
- Demonstrate high-average current guns with large (~80%) polarization

Energy Recovering Linac Issues (L. Merminga, JLAB)

Energy recovery works in a users facility (5 mA, 50 MeV, the JLAB FEL facility). This is a good starting point to consider ERL issues. One of the recognized issues concerning very short electron bunches going through a superconducting linac at a high repetition rate is that of High-Order Mode (HOM) power (Merminga et. al., LINAC2000). At eRHIC, due to the relatively long (20 ps) pulse length, the amount deposited in the liquid helium cooled cavities is not a problem. However, there is still a significant amount of HOM power lost by the beam which couples to the beam pipes and it must be captured at room temperature to avoid heating of cold surfaces.

Multi-bunch, multi pass Beam Breakup (BBU) is a limit on the maximum beam current in an ERL, however the real limits are far from being explored. A study of BBU requires a good code. Such a code has been developed at JLAB (TDBBU) and benchmarked in experiments, showing a remarkable 40% agreement. Currently predicted threshold currents for this BBU are about ~100 to 200 mA, but With B-factory style feedback one expects a large improvement.

Experiments are planned (CEBAF@JLAB, Cornell, BNL) to address high ratios of final to injector energies and high current effects (200MeV/10mA to 50-100 MeV /50-100mA).

RF issues (J. Delayen, JLAB)

Superconducting RF (SRF) linac structures are extremely well known (JLAB, DESY, industry).

Energy recovery superconducting linacs are very efficient devices for certain applications. They can approach the electrical power usage efficiency of storage rings while preserving the beam properties of linacs. The concept has been fully demonstrated and is used routinely in a user facility. Studies have uncovered no fundamental show stoppers. The ultimate limits of the energy recovery concept have not been fully determined, on questions such as:

- What is the highest loaded Q factor for the cavities while maintaining phase and amplitude stability requirements.
- What is the highest current that can be accelerated and decelerated.
 - Preservation of rf stability
 - Avoidance of BBU instabilities
 - Extraction of HOM power
 - Control of beam loss

For the regime of operation of the EIC, using a 10 MeV injector, at a final energy of 7 GeV in the linac, the ratio of the beam energy to required linac RF power is between 200 to 400. With the current known level of acoustic noise on the cavities, resulting a 25 Hz rms frequency deviations, an external Q of 2×10^6 is appropriate for a 7 Cell CEBAF cavity at 20 MV/m, resulting a klystron power of about 5 kW per cavity.

Luminosity limitations in Linac-Ring Colliders (L. Merminga, JLAB)

The base luminosity of a Linac-Ring collider based on RHIC as the ion ring (running with 360 bunches) has been calculated at the top energy of the machine as given in the table below.

Species		P	Au
Luminosity	$\times 10^{31}$	100.0	1.0
sigma*	microns	32.0	32.0
Ion parameters			
# / bunch	1.00E+09	200.0	1.2
Emittance	microns	0.9	0.5
Laslett	$\times 0.001$	6.0	5.3
Beam-beam	$\times 0.001$	4.0	4.0
beta*	cm	31.0	21.0
Electron parameters			
# / bunch	1.00E+10	2.9	4.8
Emittance	nm	6.0	6.0
Beam-beam	$\times 0.001$	382.0	180.0
beta*	cm	17.0	19.0

This is not necessarily the maximum luminosity that can be obtained at such a machine. These numbers assume an angular acceptance of the IR quads at RHIC at about a quarter of a milliradian, a value restricted by the very large distance of these quads from the IP. Depending on the IP design, this angular

acceptance may be increased significantly and with it the luminosity. In addition, these numbers are not aggressive in the number of ions stored in the ring, in particular in view of the planned electron cooling. The behavior of the luminosity as a function of energy depends on several beam dynamical scenarios. At low energies the proton intensity is fundamentally limited by the intra-bunch space-charge forces, which impose a limit on the maximum attainable value of the Laslett tunes. For $\Delta\nu_L \sim 0.04$, the eRHIC luminosity is limited to about $10^{32} \text{ cm}^{-2} \text{ sec}^{-1}$ at 25 GeV and scales with the third power of the proton energy.

At intermediate energies, fundamental luminosity limits may arise either due to the beam-beam interaction or due to space charge forces. A simple model has been developed which calculates an optimum bunch length such that the two limits are equal at a chosen energy (assuming $\beta^* \approx \sigma_{z, \text{opt}}$). For eRHIC parameters the regime over which this analysis yields practical values for the optimum bunch length (20 cm to 1 cm) is from 75 GeV to 200 GeV proton beam energy. The optimized luminosity at 200 GeV is $4 \times 10^{34} \text{ cm}^{-2} \text{ sec}^{-1}$. Once the luminosity is optimized at a given energy E , it will be limited by beam-beam interaction for energies above E , and it will be limited by intra-bunch space charge for energies below E .

For proton energies above 200 GeV the luminosity is fundamentally limited by the beam-beam interaction. Assuming $\xi_e = 0.2$ (such as expected with the circulator ring), the maximum luminosity is $4 \times 10^{34} \text{ cm}^{-2} \text{ sec}^{-1}$. All the above estimates assume that the Laslett tunes is 0.04. Lower limits of the Laslett tunes will severely decrease the luminosity.

The beam-beam induced head-tail instability can also, in principle, limit the maximum attainable luminosity. Simple analytic models of this interaction based on a linear theory predict collective instabilities. These instabilities could be stabilized at some level by the nonlinear tunespread. Complete simulations must be done to quantitatively address the luminosity limitations due to this effect

The “head-tail” instability (R. Li, JLAB)

The relative high disruption of the electron beam during the beam-beam interaction makes its effect on the stability of the beam in the storage ring an important issue. The electron beam acts as an active impedance for the ion beam via the beam-beam interaction. A strong-strong beam-beam simulation based on the macroparticle model was developed for the linac-ring design, which has been benchmarked with results of flip-flop beam-beam instability in a ring-ring collider. For the earlier linac-ring B factory design study, this simulation revealed strong kink beam-beam instability with head-tail effect. Our analysis of this effect confirmed the numerical observation and provided further understanding of the process. For recently proposed linac-ring EIC designs, we used two-particle model and Vlasov approach to study this strong head-tail beam-beam instability based on linear beam-beam force approximation. Analytical and numerical studies of the full nonlinear beam-beam effects are still underway. For the time being one can use the two-particle model to estimate the effect of this instability on the EIC luminosity. The preliminary conclusion is that the kink instability will not limit the luminosity of the EIC operating at a luminosity level of $10^{33} \text{ cm}^{-2} \text{ sec}^{-1}$ over its proposed proton energy range.

R&D Issues

- High-Energy e Cooling --
 - Electron cooling Test Facility
- High-current polarized source, laser and cathode --
 - Polarized electron source R&D, including laser
- Linac current possibly too high --
 - Circulator ring option

Instabilities --

Detailed beam dynamics

HOM power in SRF linac: Development of on-line absorbers

BBU feedback: Simulations and design

Code development: BBU, beam dynamics, kink instability, electron cooling, spin dynamics in recirculator ring

Energy Recovery experiment (planned at CEBAF)

Test facilities to address the high current effects of ERLs

The Superconducting Electron Linac

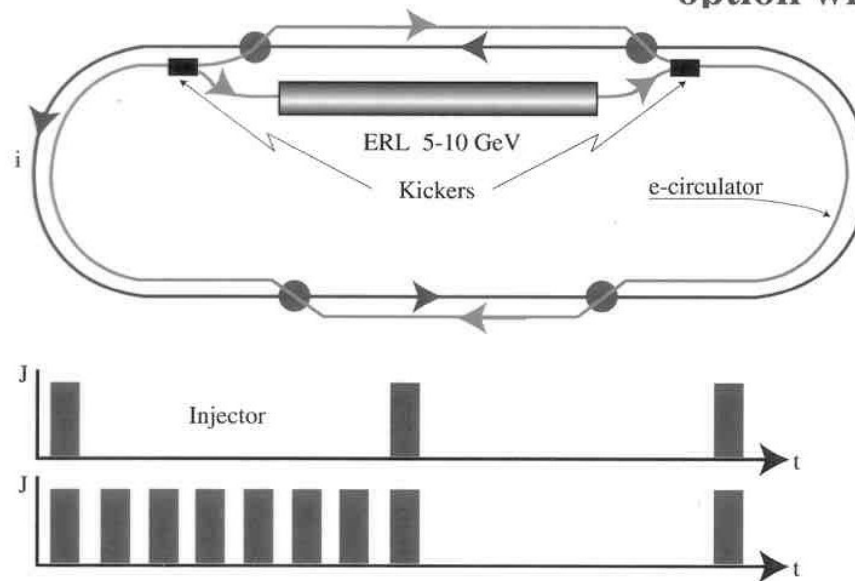
- Extremely well known (JLAB, DESY, industry)
- $R/Q=1036\Omega$, $L=1.038\text{m}$
- Take conservatively $Q_0=1.5\times 10^{10}$ at 2K, 20MV/m
- Refrigeration power 26 W/structure
- 500 cavities \rightarrow 13kW refrigeration
- HOM power: (Merminga et. al., LINAC2000) At eRHIC, due to the 20 ps pulse length, this is not a problem.

ERLs for EIC Colliders

- **No showstoppers have been found**
- **R&D topics have been identified**
- **HOM power: Development of on line absorbers (needed for electron cooling device)**
- **BBU feedback: Simulations, design**
- **Code Development/improvement: BBU beam dynamics, kink instability**
- **Energy recovery experiment at CEBAF to address high energy ratio of ERL-based colliders**
- **Jlab FEL (10/200) and Cornell (100/100)/BNL(50/50) prototype facility to address high current effects of ERLs**

Circulator Rings for LR Collider, or LCR option

- Macropulse source regime (high pulse / low average value)
- Number of revolutions in CR = macro-duty factor
- High circulating current = macropulse value
- Still ERL CW, although:
- Pulse SRF linac in alliance with CR as damping accumulator might be an interesting option
- Naturally convertible to pure LR option when beneficial



The recirculator ring option

- A suggestion by Derbenev (JLAB) to use a recirculator ring:
- Electron bunches are accelerated to full energy by a linac, stored a few hundred revolutions in a recirculating ring and dumped.
- All the advantages of the linac:
 - High polarization at any energy
 - Large beam-beam parameter
 - High luminosity at any energy
- Linac current is much lower.
- Needs to be studied!

Ilan Ben-Zvi
EICAW, L-R Working Group
BNL, February 26-27, 2002

LCR features

Respectively the RR option:

- Easy spin (no crossing resonances, no quantum depolarization)
- Emittance determined by the photoinjector (CR regime)
- Easily variable energy
- Easier interaction point (no depolarization of bends to appear)
- Larger admissible beam-beam tune shift (higher lumi)
- Larger accessible circulating current

Respectively the LR option:

- Photoinjector released of high average current
- Reduction of BBU in SRF linac
- Reduction of HOM

Issues:

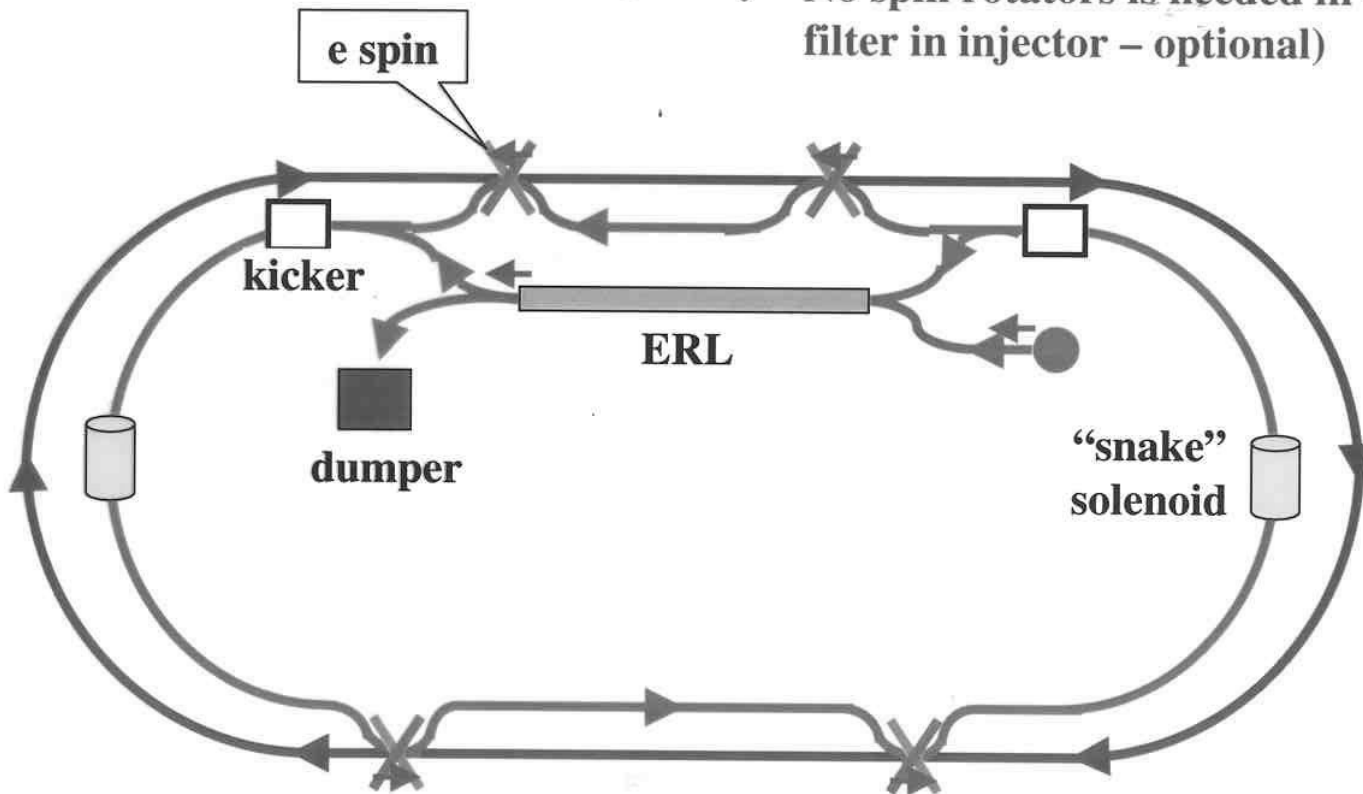
- Fast ejection-injection (develop best kickers)
- Microwave stability of short bunches in CR
- CSR effect
- SRF in CR to maintain short bunches



Spin Trends

- Solenoid Snakes for electrons in CR

- Full solenoid snake at 5 GeV: 60 TM
- 10 : 120
- No spin rotators is needed in CR (Wien filter in injector – optional)



Polarized Electron Source

- Farkhondeh – Source theory, practice and lasers.

- 135 mA, 80% polarization, require 200 W laser. Very challenging but feasible.
- Need R&D demonstrating high-current source (2 to 3 orders of magnitude higher average current than practiced today)
- Need R&D on laser
- Study issues such as surface-charge limit

QE 0.1-03 (%)

$\frac{1}{e}$ lifetime $10^5 \frac{\text{coul}}{\text{cm}^2}$
 $3 \text{ cm}^2, 200 \text{ mA} \Rightarrow$ Two weeks

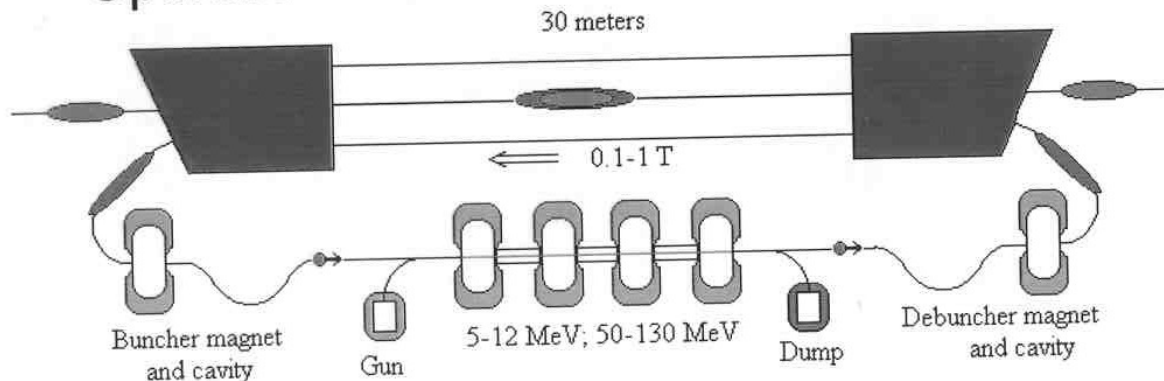
Parameters for Linac-Ring EIC at full energy

Species		P	Au
Luminosity	x10**31	100.0	1.0
sigma*	microns	32.0	32.0
Ion parameters			
# / bunch	1.00E+09	200.0	1.2
Emittance	microns	0.9	0.5
Laslett	x0.001	6.0	5.3
Beam-beam	x0.001	4.0	4.0
beta*	cm	31.0	21.0
Electron parameters			
# / bunch	1.00E+10	2.9	4.8
Emittance	nm	6.0	6.0
Beam-beam	x0.001	382.0	180.0
beta*	cm	17.0	19.0

Ilan Ben-Zvi
EICAW, L-R Working Group
BNL, February 26-27, 2002

EIC Electron Cooling

- Electron cooling is a must in the lower energy machines
- It is well established at low energy, but:
 - New accelerator technology (ERL)
 - Operation in a collider was not done



Ilan Ben-Zvi
EICAW, L-R Working Group
BNL, February 26-27, 2002

High-Energy Electron-Cooling Issues

- High-precision manufacturing and alignment of a long superconducting solenoid
- Operation of a high-current ERL (50 MeV, 100 mA)
- Generate, transport and match a “magnetised” beam without continuous magnetic field
- De-bunch (then re-bunch) the beam to obtain low energy spread
- Overcome recombination
- Bunched beam, electrons do not overlap hadrons

Ilan Ben-Zvi
EICAW, L-R Working Group
BNL, February 26-27, 2002

Electron Cooling

- Derbenev - Theory and new ideas
 - Recirculator ring for electron cooling
 - Improved cooling by equalizing cooling decrements
 - Generation and use of flat beams in rings (round at IP)
 - Generation and use of very short ion bunches

Electron Cooling and Luminosity

Optimizing the Electron Cooling

Measures to undertake:

- **Equalize cooling rates using the *dispersive mechanism***
- **This allows to avoid beam extension, hence, relax of the *alignment demands***
- ***Reduce x-y coupling outside the cooling section to a minimum***

Then, one gets a minimum critical electron current and ion equilibrium (flat beam) against IBS

Very Short Ion Bunches

- *Electron cooling in cooperation with a strong SRF allows to obtain very short ion bunches (1cm or even shorter)*

Circulators for Electron Cooling

- **Cooling of intense ion beams (up to a few Amps) requires a high electron current (hundreds of mA), in order to defeat the IBS**

This request can be satisfied at ERL incorporated with Circulator



Recent establishments and ideas

Optimization of EC and Colliding Beams:

Dispersive cooling

Cooling with flat beams (IBS criterion)

Cooling with electron fringe

Suppression of recombination of heavy ions

Flat to round colliding beams

Transport of Electron Beam:

Energy recovered linacs

Beam transport with discontinuous solenoid

Plane-vortex beam transformers

Hollow beams

Circulator rings

Electron Cooling (Continued)

- Shatunov - Summary of BINP-BNL study of electron cooling of RHIC.
 - Cooling very effective, but many points left to resolve theoretically and experimentally.
 - Need for 3-D simulations
 - Need experiments to settle various hardware issues (electron source, linac energy spread...)

Electron Cooling (Continued)

- Wang - Work at BNL on cooling
 - Cooling simulation software, BINP, JINR and Tech-X
 - Electron beam dynamics leading towards end-to-end 3-D simulations
 - Electron Cooling Test Facility:
 - Guns from AES, laser and photocathode
 - Superconducting ERL
 - Debunching and rebunching

Laser Systems (need > 200 W power)

- **Lasers with RF structure:**
 - **Electrons are produced in bunches at the laser frequency; challenging at 28 MHz. Existing systems provide at best a few Watts of power at of MHz (M. Poelker).**

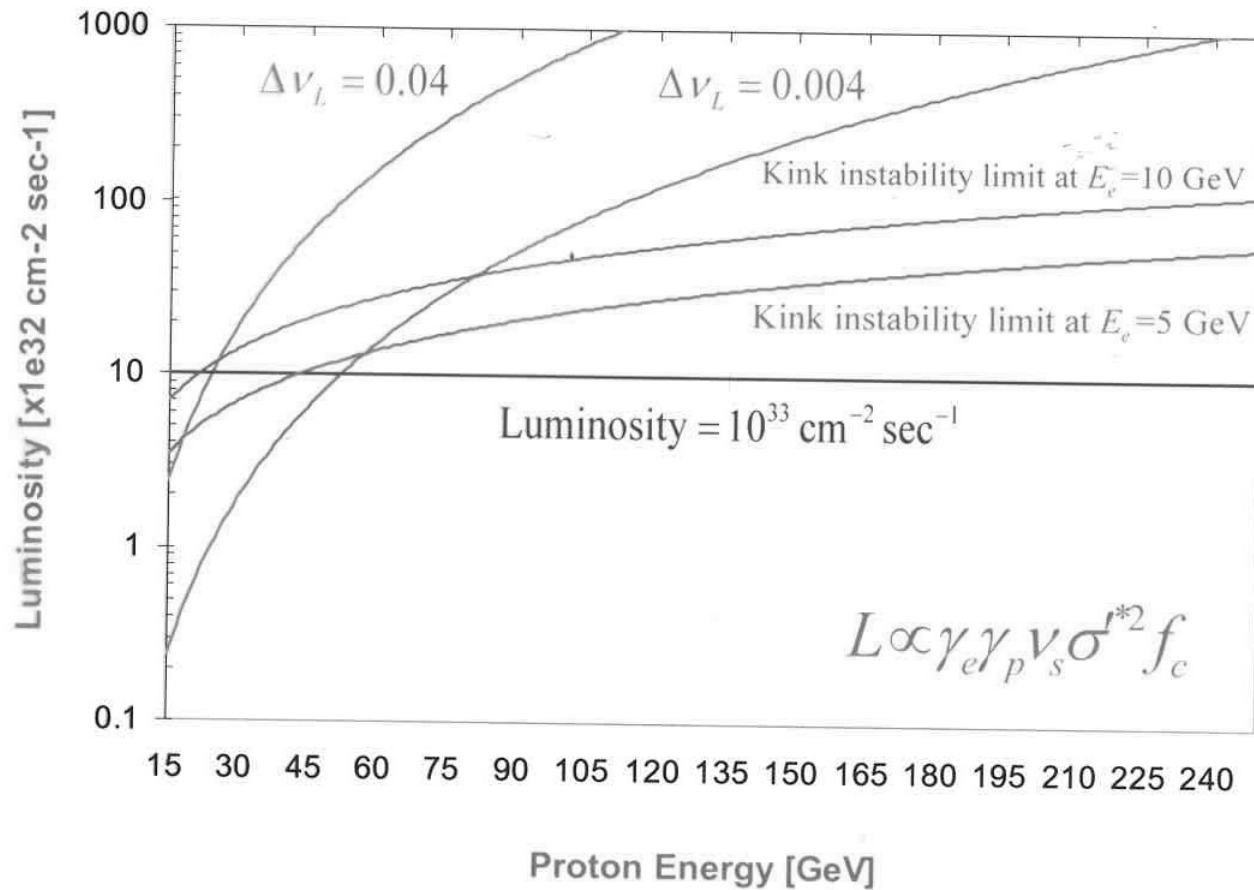
Do not exist for EIC current and frequency. Laser farm.

- **High power CW diode lasers**
 - **CW e-beams are produced and subsequently bunched with accelerator structure to the desired frequency; bunching may be difficult at 28 MHz. Today fiber coupled diode array lasers have power ~ 100 Watts.**

Issues: bunching and capture efficiencies at 28 MHz.

- **In linac-ring colliders, e-beam from linac acts as an active impedance to the ring beam via beam-beam interaction. Jitter of linac beam will influence ring-beam dynamics.**
- **For previous linac-ring e^-e^+ B factory study, strong-strong beam-beam simulation shows that relative offset of linac and ring beams will be amplified by beam-beam interaction (Kink instability with head-tail effect.) This is confirmed by analysis**
- **For linac-ring EIC, analysis based on linear beam-beam force shows head-tail and strong head-tail effect on ion beam due to beam-beam interaction with linac beam. Needs full nonlinear analysis. Full scale simulation for linac-ring EIC is on-going.**

Fundamental Luminosity Limitations (cont'd)



Conclusions

- Energy recovery superconducting linacs are very efficient devices for certain applications
 - They can approach the efficiency of storage rings while preserving the beam properties of linacs
- Concept has been fully demonstrated and is used routinely in a user facility
- Studies have uncovered no fundamental show stoppers
- The ultimate limits of the energy-recovering concept have not been fully determined
 - Highest Q_1 for the cavities while maintaining phase and amplitude stability requirements
 - Highest current that can be accelerated/decelerated
 - Preservation of rf stability
 - Avoidance BBU instabilities
 - Extraction of HOM power
 - Control of beam loss



RF to Beam Multiplication Factor for an ideal ERL

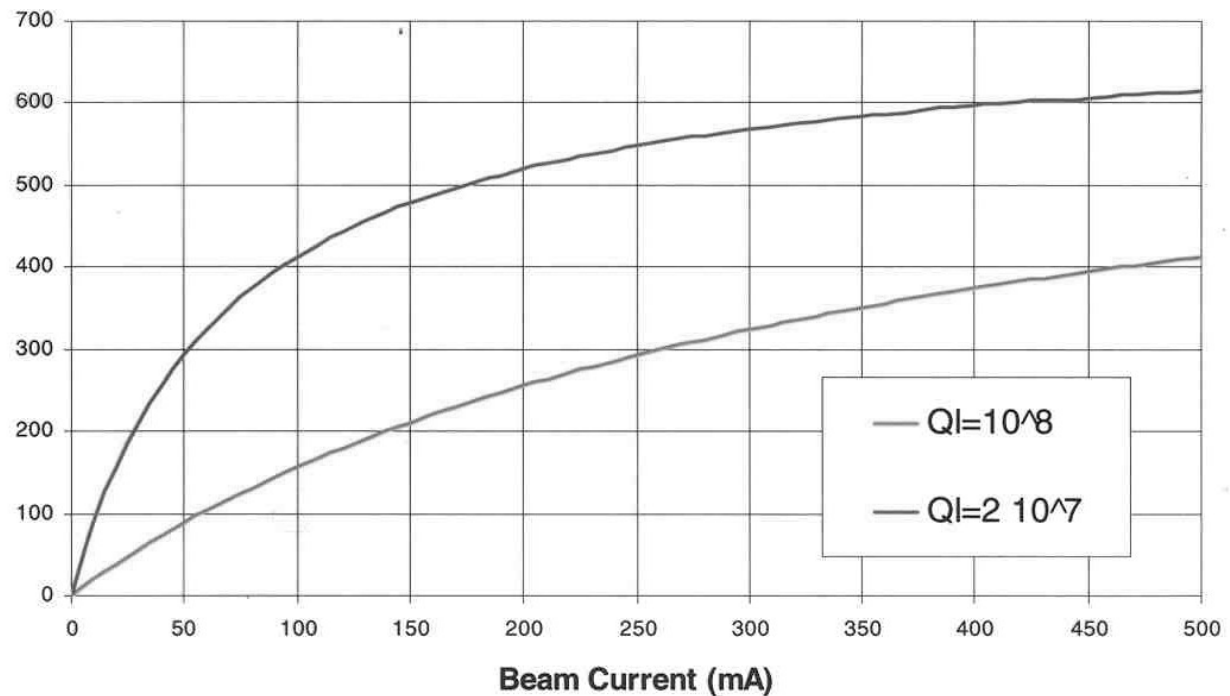
$$E_{acc} = 20 \text{ MV} / m$$

$$R/lQ = 1000 \Omega / m$$

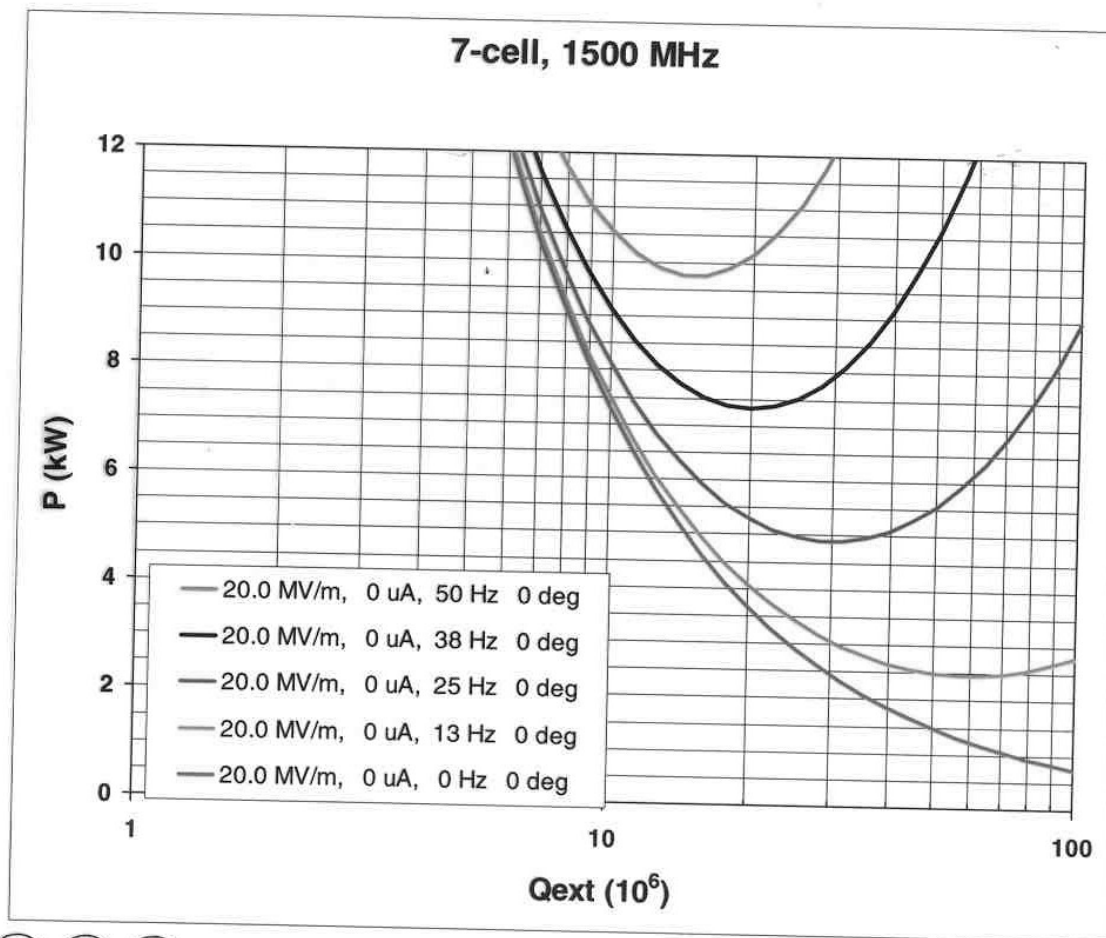
$$E_{inj} = 10 \text{ MeV}$$

$$E_f = 7 \text{ GeV}$$

RF to Beam Multiplication Factor



Generator Power vs. Loaded Q



Jefferson Lab

Thomas Jefferson National Accelerator Facility

EIC Accelerator Workshop, Jean Delayen 27 February 2002

Operated by the Southeastern Universities Research Association for the U. S. Department of Energy

THE EIC LINAC-RING OPTION

- A linac-ring collider can provide the same or greater luminosity and C.M. energy as a ring-ring collider. No positrons.
- Why use a linac?
 - The e^- polarization can be higher (R&D needed on both linac and ring polarization).
 - Polarization may be switched fast at will.
 - The energy may be changed rapidly and over a large range without losing polarization.
 - The linac maintains the high luminosity and polarization at lower energies, the ring not so.
 - The linac achieves the same luminosity with a lower current, thus less synchrotron radiation in the detector.
 - Naturally round beam, small emittance.

Ilan Ben-Zvi
EICAW, L-R Working Group
BNL, February 26-27, 2002

Participants
Electron Ion Collider Workshop
Accelerator Concepts

Last Name		Institution	email
Barber	Desmond	DESY	mpybar@mail.desy.de
Barrelet	Etienne	in2p3/lpnhe/cnrs	barrelet@in2p3.fr
Ben-Zvi	Ilan	BNL/C-AD	ilan@bnl.gov
Blum	Eric	Brookhaven National Laboratory	blum@bnl.gov
Botto	Tancredi	MIT/Bates	tancredi@mitlns.mit.edu
Chao	Yu-Chiu	TJNAF	chao@jlab.org
Chattopadhyay	Swapan	Jefferson Lab	swapan@jlab.org
Chwastowski	Janusz	Institute of Nuclear Physics	janusz@mail.desy.de
Courant	Ernest	BNL	ecourant@msn.com
Delayen	Jean	TJNAF	delayen@jlab.org
Derbenev	Yaroslav	TJNAF	derbenev@jlab.org
Dow	Karen	MIT Bates Linac	kdow@bates.mit.edu
Farkhondeh	Manouchehr	MIT-Bates	manouch@mit.edu
Franklin	Wilbur	M.I.T. - Bates	wafrankl@mit.edu
Hasell	Douglas	M.I.T.	hasell@mit.edu
Hseuh	Dick	BNL	hseuh@bnl.gov
Hughes	Vernon	Yale University	vernon.hughes@yale.edu
Kewisch	Jorg	BNL	jorg@bnl.gov
Krasny	Mieczyslaw Witold	CERN, Geneva	krasny@mail.cern.ch
Kruglov	Sergei	Petersburg Nuclear Physics Institute	kruglov@lnpi.spb.su
Li	Rui	Jefferson Lab	lir@jlab.org
Mackay	Waldo	BNL C-AD	waldo@bnl.gov
Merminga	Lia	Jefferson Laboratory	merminga@jlab.org
Milner	Richard	MIT-Bates	milner@mitlns.mit.edu
Montag	Christoph	BNL C-AD	montag@bnl.gov
Ozaki	Satoshi	Brookhaven National Laboratory	ozaki@bnl.gov
Parker	Brett	BNL	parker@bnl.gov
Peggs	Steve	BNL	peggs@bnl.gov
Pilat	Fulvia	BNL - CAD	pilat@bnl.gov
Pitzl	Daniel	DESY	pitzl@mail.desy.de
Ptitsyn	Vadim	BNL	vadimp@bnl.gov
Roser	Thomas	Brookhaven National Laboratory	roser@bnl.gov
Sandorfi	Andrew	Brookhaven National Lab	sandorfi@bnl.gov
Schneekloth	Uwe	DESY	uwe.schneekloth@desy.de
Schwandt	Peter	Indiana University Cyclotron Facility	schwandt@iucf.indiana.edu
Shatunov	Yuri	Budker Institute of Nuclear Physics	shatunov@inp.nsk.su
Trbojevic	Dejan	Brookhaven National Laboratory	dejan@bnl.gov
Tschalaer	Christoph	MIT/Bates	chris@bates.mit.edu
van der Laan	Jan	MIT-Bates	janvdl@mit.edu
Verdier	Andre	CERN	andre.verdier@cern.ch
Wang	Fuhua	MIT-BATES	fwang@rocko.mit.edu
Wang	Dong	Brookhaven National Lab	wangd@bnl.gov
Wang	Defa	Bates/MIT	DWANG@BATES.MIT.EDU
Wienands	Ulrich	Stanford Linear Accelerator Center	uli@slac.stanford.edu
Zhang	Yuhong	Jefferson Lab	yzhang@jlab.org
Zwart	Townsend	MIT Bates	zwart@bates.mit.edu